Clinical Ophthalmic Oncology

Orbital Tumors

Catherine J. Hwang
Bhupendra C. K. Patel
Arun D. Singh
Editors

Third Edition

Springer

Clinical Ophthalmic Oncology

Catherine J. Hwang
Bhupendra C. K. Patel
Arun D. Singh
Editors

Clinical Ophthalmic Oncology

Orbital Tumors

Third Edition

Springer

Editors
Catherine J. Hwang
Division of Orbital and Oculofacial Plastic Surgery, Cole Eye Institute
Cleveland Clinic Foundation
Cleveland, OH
USA

Bhupendra C. K. Patel
Division of Facial Cosmetic and Reconstructive Surgery
University of Utah
Salt Lake City, UT
USA

Arun D. Singh
Department of Ophthalmic Oncology,
Cole Eye Institute
Cleveland, OH
USA

ISBN 978-3-030-13557-7 ISBN 978-3-030-13558-4 (eBook)
https://doi.org/10.1007/978-3-030-13558-4

This Springer imprint is published by the registered company Springer Nature Switzerland AG
The registered company address is: Gewerbestrasse 11, 6330 Cham, Switzerland

Preface

Ophthalmic tumors are rare and diverse so their diagnosis can be quite complex. Treatment usually requires special expertise and equipment and in many instances is controversial. The field is advancing rapidly, because of accelerating progress in tumor biology, pharmacology, and instrumentation. Increasingly, the care of patients with an ocular or adnexal tumor is provided by a multidisciplinary team, consisting of ocular oncologists, general oncologists, radiotherapists, pathologists, psychologists, and other specialists.

For all these reasons, we felt there was a need for the new edition of the textbook providing a balanced view of current clinical practice. Although each section of *Clinical Ophthalmic Oncology* now represents a standalone volume, each chapter has a similar layout with boxes that highlight the key features, tables that provide comparison, and flow diagrams that outline therapeutic approaches. We gratefully acknowledge the contributions of Julian Perry, MD, for editing the previous two editions of the volume.

The enormous task of editing a multi-author, multi-volume textbook could not have been possible without support and guidance by the staff at Springer: Caitlin Prim, Melanie Zerah, ArulRonika Pathinathan, and Karthik Rajasekar. Michael D. Sova kept the pressure on to meet the production deadlines.

It is our sincere hope that our efforts will meet high expectation of the readers.

Cleveland, OH, USA — Catherine J. Hwang, MD
Salt Lake City, UT, USA — Bhupendra C. K. Patel, MD
Cleveland, OH, USA — Arun D. Singh, MD

Acknowledgments

To my husband, JD, my life partner and who edited the first and second editions of this book. To my parents, Steve and Nancy, who inspired me to be the person and surgeon I am today.

To my friends and family, for their undying support, laughter, and love (Catherine J. Hwang).

To she-who-must-be-obeyed, Mama Kelele, and the sprogs, Neel, Jay, and Tara, "who are the raison d'etre". To my parents, Chandu and Shanta, go immense gratitude for more than they will ever realize (Bhupendra C. K. Patel).

To my parents who educated me beyond their means, my wife Annapurna, and my children, Nakul and Rahul, who make all my efforts worthwhile (Arun D. Singh).

Contents

Contributors

Mary E. Aronow, MD Retina Service, Massachusetts Eye and Ear, Harvard Medical School, Boston, MA, USA

Elad Ben Artsi, MD Corneo-Plastic Unit, Queen Victoria Hospital, East Grinstead, England, UK

Alexander D. Blandford, MD Department of Ophthalmology and Oculofacial Plastic Surgery, Cole Eye Institute, Cleveland Clinic, Cleveland, OH, USA

Brian Chon, MD Department of Ophthalmology, Division of Orbital and Oculofacial Plastic Surgery, Cole Eye Institute, Cleveland Clinic, Cleveland, OH, USA

William T. Couldwell, MD, PhD Department of Neurosurgery, University of Utah, Salt Lake City, UT, USA

Patrick De Potter, MD, PhD Ocular Oncology Unit, Cliniques Universitaires St-Luc, Université Catholique de Louvain, Brussels, Belgium

Jonathan J. Dutton, MD, PhD Department of Ophthalmology, University of North Carolina, Chapel Hill, NC, USA

Aaron Fay, MD, FACS Harvard Medical School, Department of Ophthalmology, Boston, MA, USA

Jill A. Foster, MD Ophthalmic Surgeons and Consultants of Ohio, Eye Center of Columbus, The Ohio State University Wexner Medical Center, Columbus, OH, USA

Brian T. Hill, MD, PhD Hematology and Medical Oncology, Taussig Cancer Center, Cleveland Clinic, Cleveland, OH, USA

David R. Jordan, MD Department of Ophthalmology, University of Ottawa Eye Institute and the Ottawa Hospital, Ottawa, ON, Canada

Stephen R. Klapper, MD, FACS Klapper Eyelid and Facial Surgery, Carmel, IN, USA

Raman Malhotra, MBChB, FRCOphth Corneo-Plastic Unit, Queen Victoria Hospital, East Grinstead, UK

Alan A. McNab, FRANZCO, DMedSc Orbital Plastic and Lacrimal Clinic, Royal Victorian Eye and Ear Hospital, Melbourne, VIC, Australia

Ilse Mombaerts, MD, PhD Department of Ophthalmology, University Hospitals Leuven, Leuven, Belgium

Department of Neurosciences, Catholic University Leuven, Leuven, Belgium

Cameron B. Nabavi, MD Ophthalmic Surgeons and Consultants of Ohio, Eye Center of Columbus, The Ohio State University Wexner Medical Center, Columbus, OH, USA

Jacob Pe'er, MD Department of Ophthalmology, Hadassah-Hebrew University Medical Center, Jerusalem, Israel

Julian D. Perry, MD Department of Ophthalmology and Oculofacial Plastic Surgery, Cole Eye Institute, The Cleveland Clinic Foundation, Cleveland, OH, USA

Kuldeep Raizada, PhD International Prosthetic Eye Center, Hyderabad, Telangana State, India

Geoffrey E. Rose, DSc, FRCOphth Adnexal Service, Moorfields Eye Hospital, London, UK

NIHR Biomedical Centre, Institute of Ophthalmology, London, UK

Suresh Sagili, FRCOphth Ophthalmology Department, The Royal Shrewsbury Hospital, Shropshire, UK

Yvette Marie Santiago, MD Eye Institute, St. Luke's Medical Center, Quezon City, Metro Manila, Philippines

Paul Tanner, CCA Huntsman Cancer Hospital, University of Utah, Salt Lake City, UT, USA

David H. Verity, MD, MA, BM, BCh FRCOphth Adnexal Service, Moorfields Eye Hospital, London, UK

Editors

Catherine J. Hwang, MD Department of Ophthalmology, Division of Orbital and Oculofacial Plastic Surgery, Cleveland Clinic Foundation, Cole Eye Institute, Cleveland, OH, USA

Bhupendra C. K. Patel, MD, FRCS Division of Facial Cosmetic and Reconstructive Surgery, University of Utah, Salt Lake City, UT, USA

Arun D. Singh, MD Department of Cole Eye Institute, Cleveland Clinic, Cleveland, OH, USA

Examination Techniques

1

Catherine J. Hwang and Julian D. Perry

Introduction

Examination of a patient with orbital disease begins with a detailed history to discern the chronicity of symptoms, past medical history including systemic medical conditions or neoplasia, and past surgical history and review any corresponding imaging. Orbital examination techniques in the adult and child will help establish differential diagnoses and direct further studies.

History

The history aids in establishing a probable diagnosis and in guiding the initial workup and therapy. Important historical elements will be discussed in the following chapters of this section.

C. J. Hwang (✉) · J. D. Perry
Department of Ophthalmology, Division of Orbital and Oculofacial Plastic Surgery, Cole Eye Institute, Cleveland Clinic, Cleveland, OH, USA
e-mail: HWANGC2@ccf.org

Examination

External Examination

External examination with visual inspection is critical, assessing the position and symmetry of periocular structures, such as the brows, eyelids, canthi, surrounding soft tissues, and bony structures. Visual inspection should include observation for obvious globe deviation, including the direction. Grossly visible changes in the periocular skin and preauricular or submandibular lymph nodes and asymmetries are noted.

Pupils

All patients with suspected orbital disease should undergo a pupillary examination, to help aid in determining optic nerve function. The swinging flashlight test to determine the presence or absence of a relative afferent pupillary defect is helpful to ascertain possible compression of the optic nerve or disruption of the visual system between the optic nerve head and the apex of the orbit. Optic nerve function is further characterized by testing of visual acuity, color plates, and confrontational fields. The efferent pupillary pathway should be tested as well. Anisocoria should be recorded as worse in light (parasympa-

C. J. Hwang et al. (eds.), *Clinical Ophthalmic Oncology*,
https://doi.org/10.1007/978-3-030-13558-4_1

thetic defect) or in dark (sympathetic defect), and pharmacologic testing can be performed.

Tumors of the lateral orbit may impair ciliary ganglion function to produce a parasympathetic defect, whereas cavernous sinus or superior orbital fissure tumors may result in sympathetic dysfunction.

Extraocular Motility

Extraocular motility (EOM) should be tested in every patient, documenting restriction in motility as well as diplopia. EOM restriction can be documented in either a percentage from 1 to 100, with 100 being normal, or on a scale ranging from −4 to +4, with 0 being normal. If a phoria or tropia is found, the cover–uncover test can be useful to help measure deviations with the aid of prisms.

Reduction of EOM can either be a restrictive process or a palsy. To differentiate restriction versus a palsy, patients may undergo forced duction testing. Classically, after a drop of topical anesthetic is placed, a cotton-tipped applicator soaked in 4% lidocaine solution is applied to the muscle away from the direction of gaze limitation for approximately 1 min. The anesthetized muscle is then grasped firmly with toothed forceps and rotated toward the direction of gaze limitation. Resistance indicates a restrictive disorder; free movement is more likely a palsy. If the patient is not amenable to such testing while awake, one can discern restrictive disease from paresis by looking for a "floating" saccade or, basically, the relative speed and comparison of the simultaneous saccades between the two eyes. Standing approximately 3–4 ft directly in front of the patient, the examiner should ask the patient to look at the examiner's nose and then quickly look at his or her finger on an outstretched arm in the four main positions: left, right, up, and down. For example, if the patient has an abduction deficit on the right from 6th nerve paresis, he or she will have a saccade that "floats" to the right, when compared to the fast adducting saccade on the left. If the abduction deficit is due to restriction, the right eye abducting saccade will be limited by a sudden stop.

Fields of single vision and double vision can be mapped using a penlight; Finoff transilluminator, aka muscle light; or a kinetic perimeter.

Eyelid Position and Function

Eyelid position is characterized by marginal reflex distances (MRD). The MRD1 represents the distance from the center of the upper eyelid margin to the corneal light reflex measured in millimeters. The MRD2 represents the distance from the center of the lower eyelid margin to the corneal light reflex. The action of the levator muscle (levator function) is measured as the extent of upper eyelid excursion from downgaze to upgaze with the brows fixated. If present, scleral show is measured from each limbus to the corresponding eyelid margin with the eye in primary position. Upper eyelid ptosis (Fig. 1.1) may imply either mechanical involvement of the levator muscle or palsy, whereas eyelid retraction (Fig. 1.2) suggests proptosis, such as thyroid eye disease or CNS disorder. The upper eyelid may be everted to inspect the palpebral lobe of the lacrimal gland (Fig. 1.3) or by having the patient look down and in and lifting up the upper eyelid. An s-shaped deformity characterized by ptosis and edema laterally is usually associated with

Fig. 1.1 Right upper eyelid with ptosis. Note the right brow is also elevated due to the patient's use of the frontalis muscle in an attempt to lift the ptotic right upper eyelid. The left upper eyelid is also pseudo-retracted and would likely descend to a more normal position with ptosis correction on the right

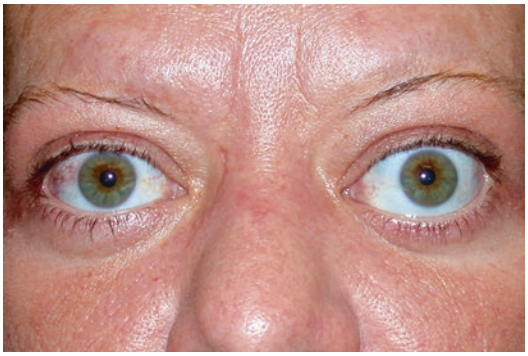

Fig. 1.2 Bilateral upper and lower eyelid retraction, left greater than right from thyroid eye disease

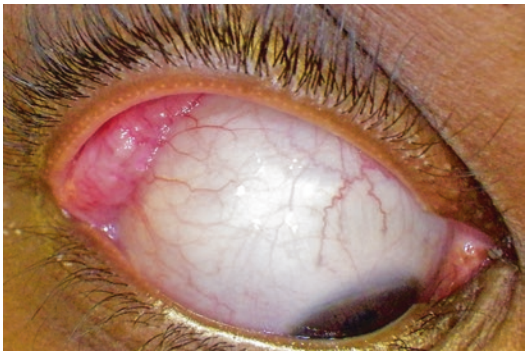

Fig. 1.3 Prominent palpebral lobe of lacrimal gland, visible beneath the upper eyelid

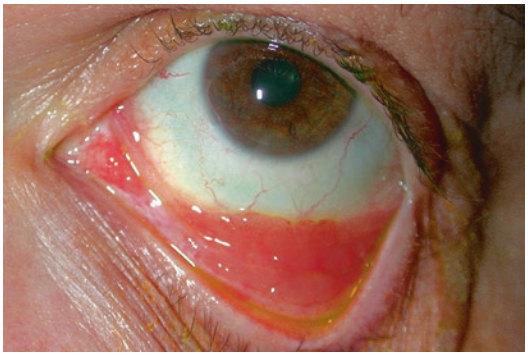

Fig. 1.4 Salmon-colored lymphoma in the inferior fornix

lacrimal gland enlargement. Lymphoma can result in a salmon-colored conjunctival mass that is visible upon inspection of the fornix (Fig. 1.4). Orbicularis strength, Bell's phenomenon, and lagophthalmos should also be evaluated as part of the cranial nerve exam detailed below.

Globe Position

Proptosis

By evaluating the patient in the submental view (chin-up position), the examiner can qualitatively look for globe protrusion or retrusion relative to the canthal angle and the nasion (Fig. 1.5). To quantify the degree, three common exophthalmometry tools exist: the Hertel, which is most commonly used (Fig. 1.6); the Naugle, which is useful for patients with abnormal lateral orbital rims (Fig. 1.7); and the Luedde, which is more feasible to use in children (Fig. 1.8).

The Hertel exophthalmometer quantifies the anterior protrusion of the eye by measuring the distance in millimeters from the anterior lateral orbital rim to the front surface of the cornea. The reading is taken with a base measurement of the separation of the positioning arms of the tool to help reference subsequent measurements on the same device. The Naugle exophthalmometer measures anterior globe position relative to the superior and inferior orbital rims. This method provides a more accurate assessment in those with lateral rim fractures, iatrogenic repositioning of the lateral rim, or orbital rim defects. The Luedde exophthalmometer measures globe protrusion unilaterally from the lateral orbital rim.

Fig. 1.5 Submental view of proptotic globes from Graves' disease (**a**). Child with left proptosis from orbital dermoid (**b**)

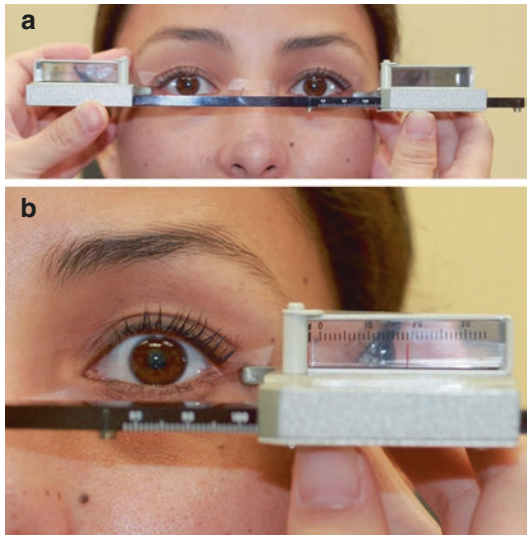

Fig. 1.6 Hertel exophthalmometer. While resting the Hertel instrument on both lateral rims, the base number is recorded on the ruler for consistency (**a**), and the amount of exophthalmos is measured by aligning the red bars then recording the number at which one sees the anterior surface of the cornea (**b**). The examiner and patient should be at eye level

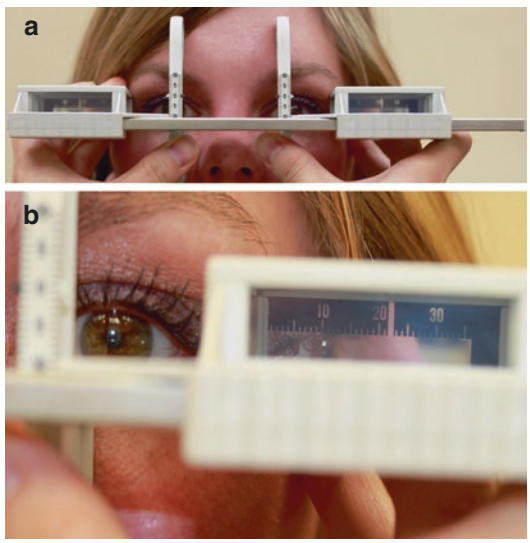

Fig. 1.7 Naugle exophthalmometer. In patients with lateral orbital rim defects, the Naugle can be used by resting the posts on the forehead and the maxillary prominence at the pupillary axis (**a**), aligning the red mark with the clear bar, and then recording the number at the anterior surface of the cornea (**b**)

Fig. 1.8 In children, the clear Luedde ruler is placed at the lateral orbital rim, and the distance to the anterior corneal surface is measured

It consists of a clear bar with millimeter markers. The anterior corneal surface can be visualized through the bar to determine the millimeters of protrusion. This can be positioned on the lateral orbital rim without a device in front of the eyes and is easier to use in children who reflexively more away and close their eyes with the other tools.

Hyperglobus or Hypoglobus

Orbital or periorbital neoplasms often displace the globe. Nonneoplastic conditions such as thyroid eye disease, trauma, and silent sinus syndrome may cause similar examination findings, and further imaging studies, such as computed tomography (CT) or magnetic resonance imaging (MRI), may be indicated.

Horizontal and vertical globe displacements are measured in millimeters from the central pupil to vertical midline and horizontal canthal line, respectively. For vertical displacement, one can draw an imaginary line horizontally across a patient's pupillary axis and determine if the pupil of the other eye is higher or lower, which could suggest hyperglobus (Fig. 1.9) or hypoglobus (Fig. 1.10), respectively. Care must be taken to ensure the patient's head is in primary position, without any tilt, and that the line is parallel to the ground.

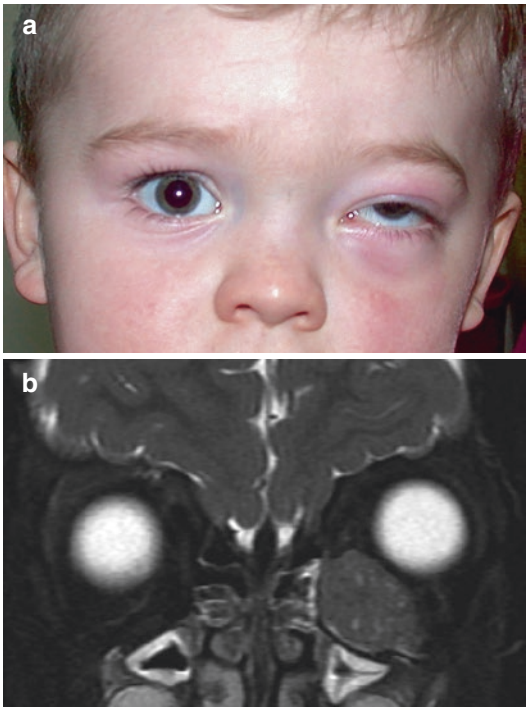

Fig. 1.9 A 23-month-old boy with left hyperglobus from desmoplastic small round cell tumor/round cell sarcoma, grade 3/3. Clinical appearance (**a**) and coronal MRI (**b**)

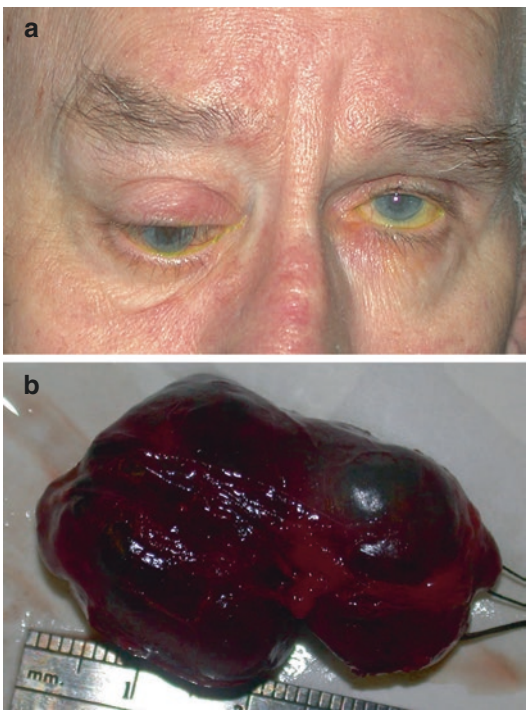

Fig. 1.10 Right hypoglobus from large cavernous hemangioma. Clinical appearance (**a**) and gross resected specimen (**b**)

Palpation

The examiner should palpate any abnormal areas for tenderness or a mass, assess the degree of resistance to retropulsion of each globe, and check for local adenopathy. The lacrimal gland area should be palpated for fullness and tenderness. Sensation to evaluate sensory nerve function is evaluated with tactile stimulation by touch. Areas of reduced sensation or hypesthesia are noted (see below CN V).

Resistance to Globe Retropulsion

The examiner places both forefingers over the anterior portion of the globe with the eyelids closed and gently pushes posteriorly on the globe. The degree of resistance is recorded on a relative scale. Orbital mass lesions often produce increased resistance to manual globe retrodisplacement.

Slit Lamp Examination

The slit lamp examination typically focuses on the corneal surface and the posterior pole in patients with a suspected orbital neoplasm. The corneal surface is evaluated for signs of exposure, and the posterior pole is evaluated for signs of ocular or optic nerve compression or congestion.

Fundus Examination

Orbital mass lesions may result in choroidal folds, optic disc edema, pallor, or shunt vessels (Fig. 1.11).

Cranial Nerves V and VII

Sensation to light touch in each dermatome of the trigeminal nerve, V1–V3, V2 may be tested using a tissue or wisp of cotton, including testing of the corneal blink reflex. Each motor branch of the facial nerve is also evaluated. Loss of muscle function may be graded on a relative scale comparing the weak side to the normal side. Bell's

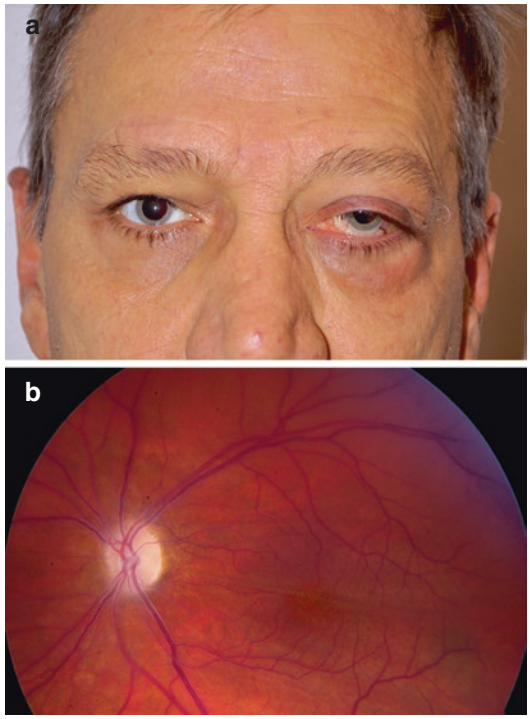

Fig. 1.11 Orbital mantle cell lymphoma. Clinical appearance with hyperglobus on the left (**a**). Note optic atrophy and choroidal folds (**b**)

phenomenon testing is performed in all patients with weak facial nerve function or lagophthalmos by asking the patient to squeeze his or her eyes shut, while the examiner tries to open them to evaluate if the eye supraducts sufficiently for corneal protection.

Lacrimal System

Attention should be directed to the superotemporal orbit to evaluate for fullness or tenderness of the lacrimal glands. The lacrimal secretory function can be measured using Schirmer's testing. This can be performed typically by placing a small strip of filter paper in the lateral conjunctival sac of bilateral lower eyelids for 5 min with the eyes closed. Basal tear secretion can be tested after placing topical anesthetic to prevent tearing from irritation. Normal wetting is 15 mm or more, mild dryness 9–14 mm, moderate 4–8, and severe less than 4 mm.

A tumor or malignancy may also involve the lacrimal drainage system and present as tearing. The excretory drainage patency is determined by irrigation of the lacrimal system with a cannula. Even in the absence of a tumor, lacrimal outflow obstruction alone can cause enlargement of the lacrimal sac and fullness in the medial canthal region. This more common benign lacrimal pathology usually begins below the medial canthus. If there is a lesion above the medial canthal tendon or presence of bloody tears, an imaging study evaluating for neoplasm should be performed. If there is a dacryocystitis, dacryocystorhinostomy (DCR) is usually indicated. Abnormal mucosa noted at the time of dacryocystorhinostomy is biopsied. If lymphoma is suspected, fresh tissue is sent to pathology for flow cytometry and lymphoma evaluation is performed.

Nasal Endoscopy

Intranasal examination using an endoscope can detect intranasal disease causing secondary orbital or lacrimal signs.

Special Issues in Examination of Children

The examination of the child with orbital pathology requires more creativity and adjustments depending on age of the patient and cooperation. Asking the parent to hold or feed an infant often facilitates the physical examination. Usage of small toys to attract the attention of the child is often critical in evaluating ductions and versions. Through observation alone, the evaluator may gather important information regarding eyelid and globe position, external periocular soft tissue changes, ocular motility, and vision. The examination should also include observation of any changes of globe position with crying, which may indicate a vascular malformation.

Patient cooperation, however, may limit the ability to perform a complete physical examination in the office. Thus, some children require sedation or general anesthesia to complete the

physical examination. Communication with the pediatrician regarding suspected etiology helps to determine the need for additional systemic evaluation. Systemic workup may include serologic testing, genetic studies, or imaging studies.

Complete Eye Examination

Orbital tumors can affect sensory visual function by producing compressive or glaucomatous optic neuropathy, refractive errors, or keratopathy. Any cause of visual dysfunction in the pediatric group may produce amblyopia. Detailed visual assessment can help localize an orbital tumor and determine whether amblyopia needs to be acutely addressed. In children, assessment requires a cycloplegic retinoscopy and refraction. Eyelid position and pupillary testing should be evaluated prior to placing drops for dilation. Versions, ductions, and strabismus measurements should be noted.

In older children, color plates and visual fields may help to better characterize optic nerve function, especially if the examiner is considering an underlying glioma. In younger children, measurement of visual evoked potential (VEP or VER) may be helpful in assessing optic nerve function. This test is one of many tools used to monitor optic nerve compression in fibrous dysplasia. Evaluation of stereopsis may help distinguish a long-standing tropia from strabismus due to a new orbital process. Comparison with old photos and history from the parents can be utilized.

A standard or portable slit lamp allows for the most detailed anterior segment evaluation. However, a penlight with or without a 20D lens for magnification may be used. Conditions such as lymphangioma, neurofibromatosis, or capillary hemangioma may present with anterior segment findings. Posterior pole examination follows and may reveal findings such as choroidal folds due to an orbital mass effect, optic disc pallor due to a glioma or other tumor compression, or orbital invasion from a primary intraocular tumor.

Orbital Examination

Globe Displacement

The examiner assesses globe position qualitatively with the child in the chin-up position. Although an exophthalmometer may provide an objective measure, patient cooperation may limit its accuracy. The Luedde device is particularly valuable for evaluation of globe position in children, who often find it less intimidating because it is smaller and placed on the side (Fig. 1.8). The Luedde instrument offers accurate measurements with the patient in the supine position and can be used during an examination under anesthesia.

Summary

Each step of the examination aids in disease localization and characterization to ultimately help formulate a treatment plan.

Classification of Orbital Tumors

2

Alexander D. Blandford and Julian D. Perry

Introduction

Orbital tumors represent approximately 0.1% of all body tumors and approximately one-fifth of all orbital diseases. Classification schemes vary and stratify orbital tumors based on demographics, site of origin, anatomic location within the orbit, histopathologic features, clinical course, and imaging findings. Defining orbital neoplasia presents difficulties, as choristomas, hamartomas, and inflammatory lesions can present as space-occupying lesions and behave as benign and even malignant, neoplasms. In general, neoplasms of the orbit may be classified as primary, secondary (infiltration from an adjacent structure), or metastatic (from distant structures). Orbital neoplasia can be divided into histological categories that include benign, benign but locally aggressive, and malignant. In some cases, especially lymphoproliferative lesions, a spectrum from benign to malignant exists.

This chapter aims to classify orbital tumors on clinical grounds in order to provide a framework to conceptualize space-occupying orbital lesions to determine an evaluation and treatment algorithm.

Differential Diagnosis of Orbital Tumors

Masquerading processes, such as infectious and inflammatory diseases, can resemble an orbital tumor and must be excluded during the workup of a space-occupying orbital lesion. Many non-neoplastic processes can be excluded based on a combination of demographic, clinical, and imaging characteristics (Box 2.1).

Box 2.1 Lesions that May Simulate an Orbital Neoplasm

- Infectious
  - Acute bacterial orbital cellulitis
  - Invasive fungal infection
  - Mycobacterial infection
- Inflammatory
  - Idiopathic orbital inflammation
  - Dysthyroid orbitopathy
  - Systemic vasculitides
- Other
  - Amyloidosis

A. D. Blandford (✉) · J. D. Perry
Department of Ophthalmology and Oculofacial Plastic Surgery, Cole Eye Institute, Cleveland Clinic, Cleveland, OH, USA
e-mail: blandfa@ccf.org

C. J. Hwang et al. (eds.), *Clinical Ophthalmic Oncology*,
https://doi.org/10.1007/978-3-030-13558-4_2

Clinicopathological Classification of Orbital Tumors

Cystic Lesions

Dermoid cysts are the most common cystic lesions of the orbit [1]. They represent congenital lesions that form from epithelial cells trapped beneath the surface epithelium during embryogenesis. They often occur along the orbital rim superotemporally at the zygomaticofrontal suture, but they can occur at other bony sutures or in deeper orbital tissues. Other orbital cystic lesions include colobomatous cyst, congenital cystic eye, meningocele, and teratoma. Several other orbital neoplasms may present with cystic components (Table 2.1).

Table 2.1 Orbital cystic tumors

Aneurysmal bone cyst	Meningoencephalocele
Colobomatous cyst	Mucocele
Congenital cystic eye	Optic nerve sheath cyst
Conjunctival epithelial cyst	Parasitic cysts (e.g., hydatid cyst)
Dermoid cyst	Respiratory cyst
Ductal cyst of the lacrimal gland	Teratoma
Meningocele	

Vascular Lesions

Vascular tumors include malformations of the arterial, venous, and lymphatic systems alone or in combination. Vascular tumors are classified by their hemodynamics as no-flow (type 1), low-flow (type 2), and high-flow (type 3) lesions. Significant overlap exists within these lesions depending on where in development the malformation occurred.

Low-flow malformations are divided into venous, lymphatic, and lymphaticovenous. Venous malformations are further classified as distensible or non-distensible based on a series of tests and maneuvers. Lymphatic malformations are further classified into macrocystic, microcystic, and mixed. Lymphaticovenous malformations are further divided by their hemodynamics and distensibility into venous dominant and lymphatic dominant. Venous dominant lymphaticovenous malformations demonstrate greater distensibility with Valsalva maneuver in clinic and on CT angiography. Lymphatic dominant lymphaticovenous malformations are non-distensible. The distensibility and clinical symptoms of low-flow malformations are directly related to the outflow channels of the lesion [2].

Table 2.2 Orbital vascular lesions

More common	Less common
Capillary hemangioma	Angiosarcoma
Cavernous hemangioma	Cholesterol granuloma
Hemangiopericytoma	Hemangioendothelioma
Lymphangioma (type 1)	Hemangiosarcoma
Varix (type 2)	Kaposi's sarcoma
AVM (type 3)	Kimura's disease
	Vascular leiomyoma
	Vascular leiomyosarcoma

High-flow malformations are divided into arteriovenous malformations, arteriovenous fistulas, and arterial aneurysms. Arteriovenous malformations may present with discomfort, pulsatile proptosis, acute swelling, or hemorrhage and gradually enlarge with time [2].

Treatment is based upon imaging and flow characteristics (Table 2.2).

Myogenic Tumors

Rhabdomyosarcoma represents the most common myogenic orbital tumor and the most common primary orbital malignant neoplasia of childhood. It accounts for 4% of all biopsied orbital masses in children [1]. Rhabdomyosarcoma is believed to arise from primitive orbital mesenchymal elements.

Lipomatous and Myxomatous Tumors

Lipomas are benign tumors of adipose tissue that occur only rarely within the orbit. Dermolipoma is a benign congenital lesion that often occurs as a

part of Goldenhar's syndrome. Liposarcoma, the most common soft tissue sarcoma in adults, has widespread distribution but occurs rarely in the orbit.

Primary Melanocytic Tumors

Primary melanocytic tumors of the orbit include melanoma, melanocytic hamartoma, and melanotic neuroectodermal tumor of infancy. Accounting for less than 1% of primary orbital neoplasms, primary orbital melanoma arises from native orbital melanocytes that are located along ciliary nerves, optic nerve leptomeninges, and scleral emissary vessels. Approximately one-half of primary orbital melanomas are associated with pigmentary disorders, including nevus of Ota, ocular melanocytosis, and blue nevi [3].

Tumors of the Lacrimal Gland

Classically, approximately one-half of all lacrimal gland tumors represent epithelial proliferations, and the remainder represents lymphoproliferative lesions. Of the epithelial proliferations, roughly half are pleomorphic adenomas (benign mixed tumors), and the remainder consists of malignant carcinomas, which include adenoid cystic carcinoma, malignant mixed cell tumor, and mucoepidermoid carcinoma. Nonepithelial lacrimal gland tumors consist of ductal cyst, lymphoma, and plasmacytoma (Table 2.3).

Table 2.3 Tumors of the lacrimal gland

Epithelial	Nonepithelial
Adenoid cystic carcinoma	Ductal cyst
Pleomorphic adenocarcinoma	Lymphoproliferative
Pleomorphic adenoma	Plasmacytoma
Mucoepidermoid carcinoma	
Myoepithelioma	
Oncocytoma	
Warthin's tumor	

Tumors of the Lacrimal Sac

Epithelial tumors are the most common neoplasms of the lacrimal sac The most common benign and malignant epithelial tumors of the lacrimal sac are the papilloma and squamous cell carcinoma, respectively [4]. Malignant tumors outnumber benign tumors in this region [4]. Other malignant tumors include transitional cell carcinoma, adenocarcinoma, oncocytic adenocarcinoma, mucoepidermoid carcinoma, adenoid cystic carcinoma, and melanoma [4].

Lymphoproliferative Tumors

Lymphoid and leukemic tumors represent a common group of orbital neoplasm, and they may arise anywhere within the orbit (Chap. 15).

Peripheral Nerve Tumors

Tumors arising from orbital peripheral nerves include neurilemmoma (schwannoma), neurofibroma, alveolar soft-part sarcoma, granular cell tumor, amputation neuroma, and malignant peripheral nerve sheath tumor. These tumors theoretically can arise from branches of orbital cranial nerves, sympathetic and parasympathetic fibers, and the ciliary ganglion, but most seem to arise from the ophthalmic division of the trigeminal nerve. The vast majority of orbital peripheral nerve sheath tumors are benign and either a neurilemmoma or neurofibroma. Patients typically present with non-axial globe displacement and proptosis [5]. Only a few well-documented cases of malignant peripheral nerve sheath tumors have been reported [5, 6].

Optic Nerve, Meningeal, and Other Neural Tumors

Optic nerve and meningeal tumors consist mainly of optic nerve glioma, malignant optic nerve astrocytoma, and meningioma. Optic nerve glioma presents with progressive visual loss and

axial proptosis in childhood. Neurofibromatosis (NF) affects children in up to 50% of cases. Conversely, only a minority of patients with NF develop optic nerve glioma.

Meningioma represents a benign neoplasm arising from the arachnoid layer of the meninges. Other neural tissue tumors include primitive neuroectodermal tumor, primary orbital neuroblastoma, and primary orbital carcinoid.

Fibrous Connective Tissue (Fibrohistiocytic Lesions)

These mass lesions, composed mainly of fibroblastic cells, may present with similar clinical and histological features. Examples include fibroma, fibrosarcoma, and fibrous histiocytoma.

Histiocytic Tumors

Proliferative disorders of histiocytes comprise a spectrum of disease ranging from solitary inflammatory lesions to widely disseminated lesions that may exhibit malignant behavior. Variants include Langerhans' cell histiocytosis, juvenile xanthogranuloma, Erdheim-Chester disease, sinus histiocytosis, and multinucleate cell angiohistiocytoma.

Langerhans' cell histiocytosis consists of three disorders formerly referred to as eosinophilic granuloma, Hand-Schuller-Christian disease, and Letterer-Siwe disease. Eosinophilic granuloma typically occurs in the orbital region as a solitary lesion of the bone.

Erdheim-Chester disease is a xanthogranulomatous disease that typically involves the long bones and visceral organs but can also involve the orbit. Patients may present with upper eyelid xanthelasma and can have diffuse orbital infiltration resulting in painless proptosis and ophthalmoplegia [7].

Primary Bone Tumors

Primary bone tumors of the orbit are a diverse group of conditions that account for 0.6%–2% of all orbital tumors [8]. Clinical presentation can range from gradual painless proptosis over many years to rapid proptosis with pain over a period of weeks.

Benign Fibro-osseous Lesions

Osteomas are benign proliferations of bony tissue that typically arise from the paranasal sinus bone, calvarium, and other facial bones. Orbital involvement is most commonly secondary to invasion from a tumor within the adjacent paranasal sinus bone and occurs most frequently in the ethmoidal, frontoethmoidal, and frontal regions. Patients typically present with gradual proptosis or globe displacement.

Fibrous dysplasia is an abnormal development of bony tissue that manifests as a benign proliferation of fibrous tissue and woven bone. It may involve one bone (monostotic) or multiple bones (polyostotic) or be a part of McCune-Albright syndrome. The triad of McCune-Albright syndrome consists of polyostotic fibrous dysplasia, precocious puberty, and cutaneous pigmentation occurring mainly in females. The majority of cases with orbital involvement occur in the setting of monostotic fibrous dysplasia, with the frontal bone followed by the sphenoid and ethmoid being bones most commonly affected. The disease presents with long-standing facial asymmetry, proptosis, and globe displacement. Depending on the orbital bones and foramina involved, patients may develop vision loss, numbness of the forehead and/or cheek, or nasolacrimal duct obstruction [9]. Slow growth often continues into adulthood, but may stabilize with bone maturation. Malignant transformation is very rare, but prior radiotherapy may increase this risk [8].

Ossifying fibroma is a benign fibro-osseous growth that rarely involves the orbit and is more commonly seen in the mandible of young females. When present in the orbit, patients present with gradual painless globe displacement, and CT shows a well-circumscribed round mass involving the frontal bone or less commonly the ethmoidal and maxillary bones. Treatment for symptomatic lesions is complete excision [8].

Benign Cartilaginous Tumors

While benign cartilaginous tumors within the orbit are exceedingly rare, chondromas are the most common. Other benign cartilaginous tumors include osteochondroma, enchondroma, and fibrochondroma.

Reactive Bone Lesions

Reactive bone lesions include cholesterol granuloma, aneurysmal bone cyst, giant cell granuloma, and brown tumor of hyperparathyroidism.

Cholesterol granulomas in the orbit are rare and typically develop after traumatic hemorrhage or bleeding from an underlying bony anomaly. The subsequent breakdown of the blood products leads to cholesterol deposition, and the granuloma formation represents a foreign body reaction. While more commonly seen in the middle ear and temporal bone, when cholesterol granulomas develop in the orbit, it is typically within the superotemporal frontal bone.

Aneurysmal bone cysts are more commonly found in the long bones or spine. Their presence in the orbit is rare and often secondary to other bone pathology.

Giant cell granulomas have rarely been reported in the orbit and are more commonly seen in the maxilla or mandible. The few reports or giant cell granulomas in the orbit typically present with subacute mass effect on the globe, but can be complicated by intralesional hemorrhage.

Brown tumors have also rarely been reported in the orbit, but when present are found in the maxilla or frontal bone of patients with hyperparathyroidism [8].

Bone Neoplasms

Primary orbital bone neoplasms include osteosarcoma and chondrosarcoma. Osteosarcoma rarely involves the orbit, but is the most common primary bone neoplasm. Typically there is a predilection for the maxilla and arises de novo. However, osteosarcoma may develop secondary to Paget's disease, fibrous dysplasia, radiotherapy, or patients with familial retinoblastoma. Chondrosarcoma usually arises from the nasal cavity or sinuses. When there is involvement of the orbit, patients may present with nasolacrimal duct obstruction or mass effect from a sinus mass.

Multiple myeloma and solitary plasmacytoma are hematopoietic lesions that may also involve the orbital bone. Typically patients over 50 years of age present with these lesions and complain of proptosis and pain. Patients with myeloma may also demonstrate systemic systems of fatigue or bone pain elsewhere.

Granular cell tumors may rarely involve the orbit, extraocular muscles, and periorbital and lacrimal sac [10]. Grossly, the lesions are well-encapsulated tumors composed of round- to oval-shaped cells with granular eosinophilic cytoplasm.

Bone Vascular Tumors

Orbital intraosseous hemangioma is extremely rare and presents as a slowly evolving painful mass typically involving the frontal bone [8]. Prior to excision, angiography with embolization should be considered to avoid profuse bleeding [11].

Miscellaneous Bone Tumors

Other neoplasms, including intramedullary lipoma, intraosseous myxomas, and cartilaginous hamartoma, can rarely affect the orbital bones.

Metastatic Tumors to the Orbit

Metastatic cancers to the orbit spread to the orbit hematogenously, as there are no significant lymphatics in the orbit. Metastatic orbital lesions account for approximately 12% of orbital neoplasms, depending on age, and up to 3.3% of all orbital lesions [12]. Nearly all systemic malignancies have been reported to metastasize to the orbit.

Adult Metastatic Disease

In adults, carcinomas that arise from the epithelial structures of organs most commonly metastasize to the orbit [12]. Breast cancer may account for 42% of all metastatic orbital lesions, followed by lung (11%), unknown pri-

mary (11%), prostate (8.3%), melanoma (5.2%), gastrointestinal tract (4.4%), and kidney (3.2%) [12]. Orbital metastatic disease may occur in the setting of both recognized and unrecognized systemic malignancy. In general, the more indolent systemic malignancies are diagnosed prior to orbital metastasis, whereas early orbital metastasis occurs in patients with more aggressive primaries. Orbital metastasis represents the presenting sign of systemic cancer in about 42% of cases of systemic malignancy affecting the orbit [12]. Average survival after orbital metastasis detection is approximately 9 months and even shorter for more aggressive primary malignancies, especially lung cancer [12]. Patients with orbital metastases frequently complain of diplopia, ptosis, proptosis, eyelid swelling, pain, and vision loss. Metastatic breast carcinoma may produce enophthalmos due to its scirrhous histological nature [13].

Metastatic Lesions in Children

In children, orbital metastases are more likely to arise from embryonal neural tumors, such as neuroblastoma and sarcomas. Metastatic neuroblastoma is second only to primary rhabdomyosarcoma as the most frequent orbital malignancy of childhood [14]. Patients develop rapidly progressive exophthalmos and eyelid ecchymosis. Isolated primary orbital neuroblastoma is exceedingly rare [15]. Other childhood tumors that metastasize to the orbit include Wilms' tumor, Ewing's tumor, and medulloblastoma [14].

Secondary Orbital Tumors

Secondary orbital tumors invade the orbital tissues from adjacent sites, including the eyelids (e.g., squamous cell carcinoma), conjunctiva (e.g., melanoma), lacrimal sac (e.g., adenoid cystic carcinoma), globe (e.g., retinoblastoma), paranasal sinuses (e.g., squamous cell carcinoma, sinonasal undifferentiated carcinoma), nasopharynx (e.g., esthesioneuroblastoma), and brain (e.g., glioblastoma) [16, 17].

Imaging Classification of Orbital Tumors

Orbital tumors can be differentiated based on imaging characteristics in order to determine their etiology and behavior. In general, benign orbital tumors present as well-circumscribed lesions, such as cavernous hemangioma, fibrous histiocytoma, hemangiopericytoma, lipoma, neurilemmoma, and pleomorphic adenoma. Diffuse (plexiform) neurofibroma represents a notable exception to this generalization, as this benign tumor presents as a poorly circumscribed, diffuse lesion.

Malignant orbital tumors can present as well-circumscribed or poorly circumscribed lesions. Examples of the former include mesenchymal chondrosarcoma, optic nerve glioma, optic nerve meningioma, and rhabdomyosarcoma. Examples of the latter include adenoid cystic carcinoma, fibrosarcoma, lymphoma, pleomorphic adenocarcinoma, primary orbital melanoma, and most metastatic lesions. Some metastatic lesions, such as melanoma and renal cell carcinoma, represent exceptions to this generalization and may present as well-circumscribed lesions.

Summary

Orbital tumors represent a heterogeneous group of neoplasms with varying classification schemes to provide a framework for clinical evaluation. A combination of imaging, clinical, and demographic data may be used to narrow the differential diagnosis and to determine the appropriate evaluation and treatment.

References

1. Shields JA, Bakewell B, Augsburger JJ, et al. Space-occupying orbital masses in children. A review of 250 consecutive biopsies. Ophthalmology. 1986;93(3):379–84.
2. Rootman J, Heran MK, Graeb DA. Vascular malformations of the orbit: classification and the role of imaging in diagnosis and treatment strategies*. Ophthal Plast Reconstr Surg. 2014;30(2):91–104.

3. Jakobiec FA, Ellsworth R, Tannenbaum M. Primary orbital melanoma. Am J Ophthalmol. 1974;78(1):24–39.
4. Stefanyszyn MA, Hidayat AA, Pe'er JJ, et al. Lacrimal sac tumors. Ophthal Plast Reconstr Surg. 1994;10(3):169–84.
5. Rose GE, Wright JE. Isolated peripheral nerve sheath tumours of the orbit. Eye (Lond). 1991;5(Pt 6):668–73.
6. Jakobiec FA, Font RL, Zimmerman LE. Malignant peripheral nerve sheath tumors of the orbit: a clinicopathologic study of eight cases. Trans Am Ophthalmol Soc. 1985;83:332–66.
7. Alper MG, Zimmerman LE, Piana FG. Orbital manifestations of Erdheim-Chester disease. Trans Am Ophthalmol Soc. 1983;81:64–85.
8. Selva D, White VA, O'Connell JX, et al. Primary bone tumors of the orbit. Surv Ophthalmol. 2004;49(3):328–42.
9. Goisis M, Biglioli F, Guareschi M, et al. Fibrous dysplasia of the orbital region: current clinical perspectives in ophthalmology and cranio-maxillofacial surgery. Ophthal Plast Reconstr Surg. 2006;22(5):383–7.
10. Jaeger MJ, Green WR, Miller NR, et al. Granular cell tumor of the orbit and ocular adnexae. Surv Ophthalmol. 1987;31(6):417–23.
11. Relf SJ, Bartley GB, Unni KK. Primary orbital intraosseous hemangioma. Ophthalmology. 1991;98(4):541–6; discussion 547.
12. Goldberg RA, Rootman J, Cline RA. Tumors metastatic to the orbit: a changing picture. Surv Ophthalmol. 1990;35(1):1–24.
13. Cline RA, Rootman J. Enophthalmos: a clinical review. Ophthalmology. 1984;91(3):229–37.
14. Albert DM, Rubenstein RA, Scheie HG. Tumor metastasis to the eye. II Clinical study in infants and children. Am J Ophthalmol. 1967;63(4):727–32.
15. Jakobiec FA, Klepach GL, Crissman JD, et al. Primary differentiated neuroblastoma of the orbit. Ophthalmology. 1987;94(3):255–66.
16. Reifler DM, Hornblass A. Squamous cell carcinoma of the eyelid. Surv Ophthalmol. 1986;30(6):349–65.
17. Howard GR, Nerad JA, Carter KD, et al. Clinical characteristics associated with orbital invasion of cutaneous basal cell and squamous cell tumors of the eyelid. Am J Ophthalmol. 1992;113(2):123–33.

3 Differential Diagnosis in Children

Catherine J. Hwang and Julian D. Perry

Introduction

There are many aspects of history, examination, and imaging that aid in the differential diagnosis of orbital lesions in children. Common etiologies of orbital tumors differ significantly between children and adults. For example, rhabdomyosarcoma, one of the most common primary pediatric orbital malignancies, rarely occurs in adults. The potential morbidity – and in some cases mortality – of pediatric orbital neoplasia requires an understanding of common findings and presentations to direct the evaluation. The history, physical examination, and diagnostic studies will help limit the differential diagnosis, which then determines the need for biopsy and initial therapy (Table 3.1).

History

As with adults, the history begins with a description of the symptoms, severity, onset, and rate of progression. However, obtaining a detailed history in the pediatric patient presents unique challenges. The direct history depends upon the age, maturity, and verbal skills of the child. In many cases, the bulk of the history requires input from the family. The evaluator should remember that a child may deny, forget, or embellish important historical facts that can confound the evaluation of an orbital tumor. For example, a child injured with a stick or toy may not disclose the cause, or a history of otherwise insignificant periorbital trauma may obscure the workup of true orbital neoplasia. Preverbal children cannot clearly communicate subjective findings such as pain, hypesthesia, diplopia, or diminished visual acuity. In these cases, the evaluator uses nonverbal clues and physical findings to focus the examination and develop the differential diagnosis.

Presenting Symptoms and Complaints

As with adults, pediatric orbital neoplasia presents with a wide spectrum of symptoms, but many may be underreported in the nonverbal child (Table 3.2). Tumor location and histology determine the presenting symptoms and signs, which can be divided into sensory, motor, and structural or functional.

C. J. Hwang (✉) · J. D. Perry
Department of Ophthalmology, Division of Orbital and Oculofacial Plastic Surgery, Cole Eye Institute, Cleveland Clinic, Cleveland, OH, USA
e-mail: HWANGC2@ccf.org

C. J. Hwang et al. (eds.), *Clinical Ophthalmic Oncology*,
https://doi.org/10.1007/978-3-030-13558-4_3

Table 3.1 Classification and differential diagnosis of orbital tumors in children

	Benign	Benign subtypes	Malignant
Developmental/ congenital	Dermoid	Superficial, deep	Retinoblastoma
	Plexiform neurofibroma		
	Teratoma		
	Microphthalmos with cyst and congenital cystic eye		
	Cranial orbital cephalocele	Dural meningocele, encephalic encephalocele	
	Rathke pouch cyst		
Acquired cystic	Mucocele		
	Lacrimal duct cyst		
Lacrimal	Pleomorphic adenoma (rare in children)		Adenoid cystic carcinoma (bimodal peak, 40s, and in first decade)
Inflammatory	Ruptured dermoid		
	Idiopathic lacrimal gland inflammation		
	Idiopathic orbital inflammatory syndrome		
Vascular	Venolymphatic malformations	Lymphangiomas, venous malformations, arteriovenous malformations (AVM)	
	Capillary malformations	Capillary hemangiomas	
Neural	Neurofibroma		
	Optic nerve glioma		
	Meningioma		
Mesenchymal	Leiomyoma		Rhabdomyosarcoma
Adipose	Lipoma		

Table 3.2 Presenting features of common orbital tumors in children

Category	Entity	Common symptoms and signs
Inflammatory	Ruptured dermoid	Acute onset, pain, proptosis if orbital
Congenital	Plexiform neurofibroma	Pulsating proptosis (absent sphenoid wing); painless, slow progression
	Dermoid	Proptosis with orbital lesions; painless, slow progression
	Teratoma	Progressive severe proptosis
Vascular	Capillary hemangioma	Slow progression, pain, and pulsation rare; blanches with palpation; proptosis if posterior
	Lymphangioma	Painless proptosis but pain with intralesional bleed or upper respiratory infection; conjunctival involvement may aid diagnosis
Benign	Optic nerve glioma	Axial proptosis, slow progression; usually painless
Malignant	Rhabdomyosarcoma	Rapid onset, painless proptosis; discoloration of overlying skin
Metastasis	Leukemia (chloroma)	Unilateral or bilateral painless proptosis; rapid progression
	Neuroblastoma	Abrupt progressive proptosis; bilateral eyelid ecchymoses

Rate of Onset

Pediatric orbital malignancies, such as rhabdomyosarcoma, often present with a subacute rate of onset that can be confused with orbital inflammation or trauma. Orbital lymphangioma may produce sudden findings due to intralesional bleeding and is sometimes precipitated

by trauma, which confounds the evaluation. Benign tumors, such as dermoid cysts, fibrous dysplasia, and gliomas, often present with slowly advancing symptoms. The growth rate of capillary hemangioma is highly variable, usually with an expansion phase and then possibly regression phase.

Past Medical History

The past medical history importantly relates to several pediatric orbital tumors. For example, proptosis that occurs predictably in conjunction with viral illness may indicate an underlying lymphangioma. Patients with lymphangioma may have airway or palatal lesions, and these may also increase during episodes of viral illness. Most patients with granulocytic sarcoma have a history of systemic leukemia. Large capillary hemangiomas are associated with Kasabach–Merritt syndrome and visceral lesions. Orbital neuroblastoma is most often metastatic from the thorax. Diseases that may simulate an orbital neoplasm in children may be associated with underlying medical conditions. For example, orbital cellulitis often occurs in the context of underlying sinusitis.

Examination

In addition to the systemic examination parameters detailed in Chap. 1, attention can also be paid to Krohel's six Ps of the orbital examination to help narrow the differential diagnosis (Box 3.1).

Box 3.1 The Six Ps of the Orbital Examination

- Proptosis
- Palpation
- Pulsation
- Periorbital changes
- Pain
- Progression

Based on data from Ref. [1].

Complete eye examination aids in the differential diagnosis as detailed in Chap. 1.

Orbital tumors frequently cause globe displacement in children. Proptosis may be quantified by using the Luedde method of exophthalmometry. Hyperglobus and hypoglobus should be noted (Chap. 1). Palpation yields information regarding tumor location, size, and shape. A dermoid cyst may feel firm, smooth, and rubbery; an orbital and eyelid neurofibroma may have a "bag of worms" consistency; and capillary hemangiomas are soft, spongy, and often blanch with palpation. Solid tissue malignancies may produce a high degree of resistance to globe retropulsion.

Pulsation and Bruits

Although rare, pulsations may occur with certain tumors in children, such as absence or hypoplasia of the sphenoid wing in the setting of neurofibromatosis. Bruits may be felt on palpation of arteriovenous malformations.

Periorbital Changes

The overlying tissues may show visible signs to suggest the etiology of an orbital neoplastic process. Neuroblastoma often presents with periorbital ecchymoses. Plexiform neurofibroma often presents with an S-shaped upper eyelid deformity with characteristic skin changes (Fig. 3.1).

Fig. 3.1 Plexiform neurofibroma with characteristic S-shaped upper eyelid deformity

Fig. 3.2 Orbital lymphangioma visible through the conjunctiva

Fig. 3.3 Rhabdomyosarcoma presenting with periorbital discoloration similar to inflammatory signs

Lymphangioma and capillary hemangioma can be visible through the conjunctiva or in the eyelid (Fig. 3.2). Rhabdomyosarcoma often presents with periorbital discoloration similar to inflammatory signs (Fig. 3.3).

Head and Neck Examination

Examination of the sinuses, nasopharynx, and adjacent lymphatic drainage areas also helps to limit the differential diagnosis. Vascular malformations sometimes involve the roof of the mouth.

Laboratory Evaluation

Laboratory analysis can augment the information gained from the history and physical examination and further narrow the differential diagnosis. Metastatic neuroblastoma often results in high levels of urine homovanillic acid (HVA) and vanillylmandelic acid (VMA). Peripheral blood smears may be useful in the evaluation of suspected granulocytic carcinoma with orbital presentation. Inflammatory markers such as erythrocyte sedimentation rate (ESR), c-reactive protein (CRP), antinuclear antibodies (p-ANCA/c-ANCA), lysozyme, angiotensin-converting enzyme (ACE), QuantiFERON gold antibodies, and serum levels of IgG4 may help distinguish inflammatory diseases involving the orbit.

Diagnostic Imaging

The evaluation of some pediatric orbital tumors, such as dermoid cyst and capillary hemangioma, may not require orbital imaging. In many cases, however, imaging is essential to solidify the diagnosis, clarify the extent of the disease, and determine the surgical approach.

Computed tomography (CT) and magnetic resonance imaging (MRI) studies represent the mainstay of current techniques. Orbital ultrasound may be of value in determining the size of an orbital lesion or to assess the homogeneity or flow characteristics of a lesion. CT provides the best views of the bone (Fig. 3.4), and MRI is better for evaluating soft tissue pathology (Fig. 3.5) and magnetic resonance venogram and angiogram (MRV/MRA) for blood flow.

Orbital ultrasonography may be helpful to evaluate an orbital vascular process. A capillary hemangioma with medium to high internal reflectivity may be differentiated from a solid tumor with low reflectivity [2]. Ultrasonography may also help guide fine-needle aspiration biopsy and can be used in conjunction with interventional radiology for sclerotherapy of orbital venolymphatic malformations [3].

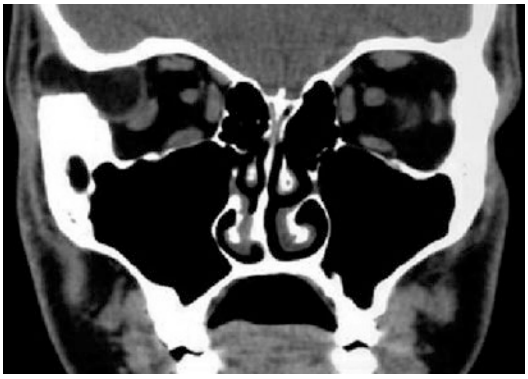

Fig. 3.4 CT scan shows bony changes associated with an orbital dermoid

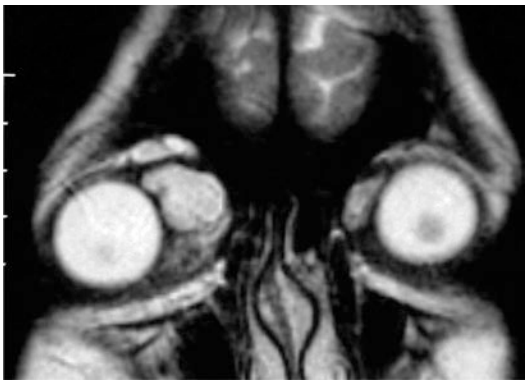

Fig. 3.5 MRI of an orbital lymphangioma

Biopsy

Confirmation of the diagnosis may require surgery. Surgical goals and planning are determined prior to surgery. Equipment and personnel are secured preoperatively for frozen section microscopy, microbiological studies, permanent biopsy specimens, ancillary testing, or other concomitant procedures that may be performed while the child is under anesthesia, such as bone marrow biopsy or venous port placement.

Suspected rhabdomyosarcoma often requires biopsy to establish the diagnosis (Fig. 3.6). Further chapters discuss specific surgical approaches, goals, and treatments. The differential diagnosis determines the need for frozen section or fresh specimens and the anticipated appropriate extent of surgical excision. If a frozen section or fresh specimen is needed, adequate specimen should, when possible, provide tissue for frozen or fresh processing and then additional tissue for further testing, including microbiological testing, cell marker studies, or electron microscopy. For evaluation of the tumor margins, marking sutures aid in specimen orientation.

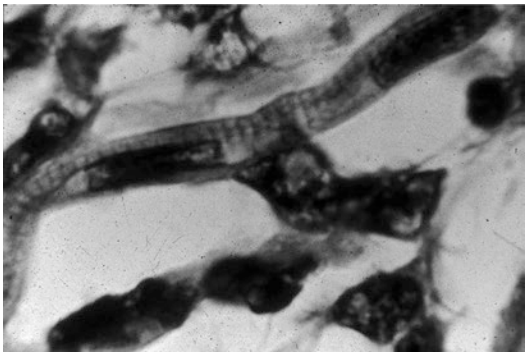

Fig. 3.6 Spindle-shaped cells containing striations in an embryonal rhabdomyosarcoma (hematoxylin and eosin)

Summary

A detailed knowledge of specific pediatric orbital disorders and their common presentations provides the framework for developing an appropriate differential diagnosis that in turn leads to appropriate workup and then management of orbital tumors in children. History, physical examination, laboratory studies, and diagnostic imaging studies are helpful in assessment and management. However, signs and symptoms of each tumor are not entirely specific, and the surgeon must be prepared to consider atypical presentations.

References

1. Krohel GB, Stewart WB, Chavis RM. Orbital disease. A practical approach. New York: Grune & Stratton; 1981. p. 9–20.
2. Byrne SF, Green RL. Ultrasound of the eye and orbit. 2nd ed. St. Louis: Mosby; 2002. p. 350–1.
3. Hill RH 3rd, Shiels WE 2nd, Foster JA, et al. Percutaneous drainage and ablation as first line therapy for macrocystic and microcystic orbital lymphatic malformations. Ophthal Plast Reconstr Surg. 2012;28(2):119–25.

Orbital Tumors: Differential Diagnosis in Adults

4

Cameron B. Nabavi, Julian D. Perry, and Jill A. Foster

Introduction

The variety of tissue types within the orbit and the spectrum of diseases leading to similar external signs can confound the diagnosis of an orbital neoplasm. The orbit contains all of the vital anterior visual pathway structures and the supporting elements that move and nurture the globe. An array of essential structures also surround the orbit, such as the anterior and middle cranial fossae; paranasal sinuses; high-flow vessels, including branches of the internal and external carotid arteries; and internal carotid artery itself. This astonishing variety and density of important tissues within and around the orbit can challenge even the experienced surgeon to determine the appropriate diagnostic and surgical plans. In order to treat orbital neoplasia, the surgeon must have a three-dimensional concept of orbital anatomy and then understand the spectrum of diseases that may affect structures within the orbit.

C. B. Nabavi · J. A. Foster (✉)
Ophthalmic Surgeons and Consultants of Ohio, Eye Center of Columbus, The Ohio State University Wexner Medical Center, Columbus, OH, USA
e-mail: fosterj@jillfoster.com

J. D. Perry
Department of Ophthalmology and Oculofacial Plastic Surgery, Cole Eye Institute, Cleveland Clinic, Cleveland, OH, USA

C. J. Hwang et al. (eds.), *Clinical Ophthalmic Oncology*,
https://doi.org/10.1007/978-3-030-13558-4_4

Even when a presentation strongly suggests a specific diagnosis, the results of biopsy may reveal a surprising tissue diagnosis. Although specific lesions often present in certain locations within the orbit, significant variation may occur. Similarly, while some neoplasms occur in certain age groups, age cannot be used to rule out any diagnosis. Even the histology of a particular lesion does not necessarily predict its benign or malignant clinical behavior. However, a focused differential diagnosis minimizes the morbidity and cost of the diagnostic workup and helps establish the diagnosis effectively and efficiently. A strong knowledge of the typical clinical and imaging features of orbital neoplasms as well as the spectra of possible presentations will allow the surgeon to create an effective differential diagnosis to begin the diagnostic algorithm (Table 4.1).

Although the etiologies of common orbital tumors differ significantly between children and adults, similar principles apply in developing a differential diagnosis. Similar to pediatric orbital tumors, specific elements of the history and the physical examination help establish a differential diagnosis, and the possible etiologies are further refined through appropriate imaging studies.

The advent of reliable and available imaging techniques over the past two decades has added granularity to the diagnostic algorithms employed for the workup of adult orbital neoplasia. This chapter will complement the chap-

Table 4.1 Common orbital lesions in adults. Anatomic location and appearance on imaging studies

Location	Lesion	Appearance
Optic nerve	Glioma	Fusiform +/− nerve kinking
	Meningioma	Circumferential enlargement "Tram-track" appearance
Intraconal space	Cavernous hemangioma	Well-defined Round or oval May remodel bone Does not destroy the bone
	Orbital cellulitis	Varies Well-defined, focal disease Diffuse inflammation May cause orbital abscess
	Idiopathic orbital inflammation	Varies Focal inflammation Diffuse inflammation Does not destroy the bone
	Lymphoproliferative disease	Varies Focal involvement Diffuse involvement May mimic other orbital neoplasms, infections, and inflammatory conditions May remodel the bone
	Metastasis	Varies Well-defined lesion Diffuse lesion May destroy the bone
Extraocular muscles	Thyroid eye disease	Diffuse enlargement of the EOM Spares the muscle tendon Bilateral but may be asymmetric
	Myositis due to idiopathic orbital inflammation	Focal or diffuse enlargement of the EOM Involves the muscle tendon May be unilateral or bilateral
	Metastasis	Focal or diffuse enlargement of one or more EOMs May be unilateral or bilateral
Extraconal space	Infection	Focal or diffuse
	Inflammation	Focal or diffuse
	Lymphoproliferative	Focal or diffuse
Lacrimal gland	Dacryoadenitis	Enlargement of the lacrimal gland May be viral, bacterial, or rheumatologic Bacterial infections may cause abscess formation
	Pleomorphic adenoma	Well-defined Round or oval mass May remodel the bone Does not destroy the bone
	Adenoid cystic carcinoma	Varies May be well- or poorly defined Often destroys the bone
Lacrimal sac	Dacryocystitis	Cystic cavity with surrounding inflammation
Orbital apex	Cavernous hemangioma	Low flow on gadolinium-enhanced MRI, discreet margins
	Metastasis	Feathery margins, increased blood flow, lytic bone changes
Orbital bones	Osteoma	Well-circumscribed with dense cortical sclerosis surrounding a more radiolucent center
	Sphenoid wing meningioma	Well-defined lesion May contain calcifications Hyperostosis of the associated bone
	Fibrous dysplasia	"Ground-glass" appearance on CT

Table 4.1 (continued)

Location	Lesion	Appearance
Extrinsic lesions	Mucocele	On CT, the affected sinus is completely opacified and the margins are expanded and the bone is usually thinned. Areas of complete bone resorption may be present resulting in bony defect and extension into adjacent tissues
Diffuse	Infection	On CT, poor definition of the orbital planes, edema of the extraocular muscles, diffuse edema
	Inflammatory	On CT, stranding of the orbital fat, enlargement of the extraocular muscles without preservation of the tendons

Table 4.2 Important history features

Appearance and anatomic site
Rate of onset
Nature of proptosis and dystopia
The presence of pain, hypesthesia
Changes in vision
Restriction of gaze

ter on "Differential Diagnosis in Children" (Chap. 3) by focusing on technological modalities to arrive at a focused differential diagnosis in adults.

History

While orbital imaging often represents a final common pathway for the workup of adult orbital tumors prior to obtaining a tissue diagnosis, several elements of the history may help to point toward a differential diagnosis and determine the proper imaging study to obtain (Table 4.2).

Pre-existing disease such as lung cancer, breast cancer, prostate cancer, or melanoma provides immediate direction when seeking the source of an orbital mass lesion, but 10% to 20% of those metastatic lesions may represent the initial manifestation of the disease.

Rate of Onset

Rate of onset and progression may help to direct initial investigations into the location and the source of the neoplasm (Table 4.3). In adults, most orbital tumors produce chronic signs and symptoms, while acute orbital signs typically result from causes other than neoplasia, such as infection, inflammation, trauma, and hemorrhage. However, an underlying neoplasm may also result in inflammation, trauma, or hemorrhage creating acute recognition of a more insidious cause. For example, an underlying vascular tumor may hemorrhage to produce an acute orbital compartment syndrome, a tumor within the lacrimal sac or lacrimal gland may result in secondary infection, mild trauma may rupture an underlying dermoid cyst to produce acute orbital signs, and metastatic and lymphoproliferative lesions may contain a significant inflammatory component.

Examination

Nature of Proptosis and Dystopia

Because the orbital bones limit orbital volume in each dimension except anteriorly, recognition of proptosis and evaluation with exophthalmometry help determine the presence of a space-occupying lesion. The pattern of the proptosis points to the lesion's location and aides in the formation of a differential diagnosis. Axial proptosis usually signifies an intraconal lesion, while non-axial anterior globe displacement typically suggests an extraconal process. However, posterior extraconal mass lesions may also cause axial proptosis.

Dystopia, or displacement of the globe in the coronal plane, results from extraconal lesions. The direction of globe displacement is typically

Table 4.3 Rate of onset of common orbital lesions

Hours	Days	Weeks	Months	Years
Trauma	Inflammatory	Inflammatory	Neoplastic	Neoplastic
Hemorrhage	Infection	Neoplastic	Lymphoid	Degenerative
Infection	Trauma	Trauma	Vascular	Lymphoid
Foreign body	Hemorrhage	Lymphoid	Inflammatory	Vascular
	Vascular	Vascular	Degenerative	Inflammatory

opposite to the location of the neoplasm. For example, inferonasal displacement of the globe is often due to a condition such as a lacrimal gland tumor in the superotemporal quadrant. Similarly, a process occurring in the superonasal quadrant of the orbit, such as a mucocele, will produce inferotemporal globe dystopia. Identifying the orbital surgical space and the quadrant of the lesion is useful in developing the differential diagnosis and surgical plan.

In contrast to the expected proptosis resulting from the mass of an orbital neoplasm displacing the globe, sclerosing conditions, such as metastatic breast carcinoma, colon cancer, pancreatic cancer, and stomach cancer, produce retrodisplacement of the globe resulting in enophthalmos.

The Presence of Pain

Pain in the absence of inflammation often signifies malignancy or other more serious processes. Slowly growing benign lesions may grow quite large without producing pain, unless from exposure keratopathy. On the other hand, malignancies, such as adenoid cystic carcinoma and squamous cell carcinoma, may display tendencies toward perineural invasion to produce pain.

Changes in Vision

Changes in vision as a result of orbital neoplasia may occur from exposure keratopathy, induced astigmatism, choroidal folds, or optic nerve infiltration or compression. These changes may occur in the setting of a benign or a malignant neoplasm and may occur acutely or chronically. Because of the protean causes and presentations of vision loss, vision loss alone does not often point to a particular diagnosis or group of diagnoses. Tumors residing in the orbital apex produce optic neuropathy more commonly than tumors occurring more anteriorly within the orbit. Compressive optic neuropathy often produces a central scotoma with breakout to the periphery, while infiltrative or vascular optic neuropathy may produce an altitudinal type defect. Static perimetry may occasionally be of value in determining a differential diagnosis, although characterization of optic nerve function is often more valuable as a way to follow tumor progression or treatment.

Gaze Restriction

Orbital tumors may occasionally present with diplopia as the first symptom. The motility disturbance may be due to direct involvement of one or more extraocular muscles by the tumor, motor neuron dysfunction, or displacement of the orbital contents. Examination can often determine the type of motility disturbance, which may assist in developing the differential diagnosis. Schwannomas or neurofibromas may involve CN III, IV, or VI. Malignant orbital neoplasms may infiltrate these nerves to produce dysfunction, or benign neoplasms may compress these motor nerves. Profound ophthalmoplegia and loss of vision may be caused by lesions at the orbital apex [1].

Diagnostic Imaging

Imaging studies show the location and tissue characteristics that ultimately refine the differential diagnosis (Chap. 5). The history and physical examination influence the choice of imaging modality. Magnetic resonance (MR) imaging

demonstrates soft tissue characteristics better, and is often the study of choice for evaluation of orbital lesions. However, computed tomographic (CT) imaging studies may show subtle bony changes better, take less time to obtain, and are less costly. Given the ubiquity of these imaging techniques, techniques with less resolution that are more difficult for the surgeon to interpret, such as B-scan ultrasonography, have assumed less importance in the workup to determine the differential diagnosis of orbital neoplasms. Doppler imaging, however, may provide useful information regarding flow characteristics of vascular lesions.

With respect to appearance on imaging, lesions may be broadly categorized as well-circumscribed (i.e., round or oval) or diffuse (infiltrative). In general, well-circumscribed lesions are more likely to be benign such as a cavernous hemangioma, fibrous histiocytoma, lipoma, neurofibroma, schwannoma or neurilemmoma, and pleomorphic adenoma. Conversely, malignancy more commonly presents with a diffuse infiltrative pattern such as adenoid cystic carcinoma, fibrosarcoma, lymphoma, pleomorphic adenocarcinoma, and most metastases.

However, important exceptions to this trend apply as some well-circumscribed lesions may be malignant, as with mesenchymal chondrosarcoma, optic nerve glioma, and some metastases (breast, renal cell, melanoma, and others). Lymphoma may also appear well-circumscribed on imaging, as may a benign mixed tumor with foci of malignant transformation. Conversely, benign tumors, such as lymphangioma and plexiform neurofibroma, may demonstrate a poorly circumscribed appearance. Nonneoplastic processes such as orbital cellulitis, idiopathic orbital inflammation, sarcoidosis, and Wegener granulomatosis may also appear poorly circumscribed on imaging and can be confused with malignancy. Finally, some entities such as orbital inflammatory disease can be either focal or diffuse.

In addition to demonstrating the boundaries of an orbital lesion, imaging can distinguish which orbital structures are involved to further refine the differential diagnosis. The locations within the orbit may also aid in creating the differential diagnosis. Specific neoplasms often localize to a particular structure or location within the orbit, such as the optic nerve, intraconal space, extraocular muscles, extraconal space, lacrimal gland or lacrimal gland fossa, nasolacrimal sac, orbital apex, orbital bones, areas extrinsic to the orbit, and multifocal orbital locations.

Imaging Location: Optic Nerve and Nerve Sheath

Lesions located in or around the optic nerve can represent glioma, meningioma, metastasis, lymphoma or a leukemic infiltrate, as well as inflammatory conditions or infection. Optic nerve gliomas often have a fusiform appearance on imaging and may cause kinking or bending of the optic nerve if the tumor outgrows its space. The optic canal limits the growth of intracanalicular gliomas, but expansion of the canal may be seen on coronal imaging in this case. Optic nerve meningiomas appear circumferentially enlarged on imaging and may exhibit a “tram-track” pattern of enhancement on CT and MR imaging studies when the tumor circumferentially surrounds the nerve without affecting the nerve itself, due to a lower central density and higher peripheral density. Orbital meningiomas may occur unrelated to the optic nerve and arise from the meninges near the orbital apex and superior orbital fissure. Less common lesions of the optic nerve include ganglioneuromas, ganglioglioma, medulloepithelioma, subarachnoid carcinomatosis, hemangioblastoma, hemangiopericytoma, and others [2].

Imaging Location: Intraconal Space

In the adult patient, lesions located within the muscle cone may represent infection (orbital cellulitis with or without abscess), inflammatory disease (idiopathic, sarcoidosis, Wegener’s granulomatosis), veno-lymphatic malformations, hamartomas (cavernous hemangioma), hemangiopericytoma, schwannoma, lymphoproliferative disease, angiosarcoma, metastases, and other

conditions. Cavernous hemangiomas appear as well-defined, oval, or round masses on CT imaging studies and typically reside within the intraconal space; however, larger lesions may extend extraconally. Bone remodeling may occur with long-standing lesions such as cavernous hemangiomas, but bony destruction should raise suspicion for malignancy.

Metastatic lesions, protean in appearance and location on imaging studies, occur commonly and factor into many differential diagnoses.

Infectious processes within the orbit range from diffuse inflammation of the orbital tissues to frank abscess formation, which can occur at any location within the orbit. The lacrimal gland and the areas adjacent to the sinuses are prone to abscess formation because of proximity to the entry site of the infectious agent. In the immunocompromised patient with a history of cancer, diffuse orbital disease may signal metastasis, but invasive fungal disease from organisms such as *Mucor*, *Aspergillus*, and *Rhizopus* should be kept in mind. Most orbital infection occurs in the context of underlying sinus disease, the presence of which helps determine the appropriate diagnostic technique.

Orbital inflammation represents a broad spectrum of disease, and the condition may appear focal or diffuse on imaging. Focal inflammation commonly involves the lacrimal gland or the extraocular muscles and may masquerade as malignancy. Diffuse inflammation may involve the intraconal or extraconal compartments and mimic lymphoproliferative disorders, lymphoma, or metastasis. Inflammatory disease rarely causes signs of bone destruction or globe indentation, and these imaging features should raise suspicion for a neoplastic etiology.

Retrobulbar hemorrhage may appear as a well-defined, hyperintense lesion on CT. Spontaneous orbital hemorrhages may occur with trauma, neoplasm, and bleeding disorders or can be idiopathic. MRI may be used to help distinguish blood from soft tissue. Orbital varices have a variety of appearances on imaging but are typically well-defined. A varix may be round, oval, tubular, and cone-shaped or have a tangled, "bag of worms" appearance, but they often enhance with IV contrast although filling can be partial due to thrombosis or phlebolith and a sedimentation level can be seen.

Imaging Location: Extraocular Muscles

Lesions of the extraocular muscles can appear focal or diffuse and may be caused by nonneoplastic conditions such as thyroid eye disease or other inflammatory diseases, trauma (intramuscular hematoma), and infection (extraocular muscle abscess). Neoplastic processes, such as lymphoproliferative disease, metastases, dermatolipoma, and schwannomas may appear to arise from an extraocular muscle on imaging studies. Myositis due to idiopathic inflammation may mimic extraocular muscle inflammation due to thyroid eye disease. However, in thyroid orbitopathy imaging typically demonstrates sparing of the muscle tendon, whereas in other inflammatory disorders, imaging shows tendon involvement. Metastasis and amyloidosis should also be considered in cases of bilateral enlargement of one or more extraocular muscles.

Imaging Location: Extraconal Space

Neoplastic lesions that may arise outside the muscle cone include metastasis, infection, lymphoproliferative disease, meningioma, and orbital schwannoma. Inflammatory diseases and hamartomas such as cavernous hemangioma may involve the extraconal space as well. Lymphoproliferative disorders, which range from benign reactive hyperplasia to lymphoma, may be focal or diffuse on imaging studies and may mimic other neoplasms, inflammatory, and infectious conditions.

Schwannomas can arise either within or around the muscle cone and appear as well-defined ovoid or fusiform masses. They are typically located in the superior orbit and run along the course of the affected nerve. Due to this tendency, these lesions often display elongation

along the anterior-posterior axis on imaging studies. Schwannomas may contain cystic cavities, probably due to degeneration, and should be included in the differential diagnosis of cystic orbital lesions.

As with schwannoma, a solitary neurofibroma may occur in the superior orbit and appear as a well-defined ovoid mass with elongation and anterior-posterior axis along the course of the affected nerve. The term "solitary" neurofibroma is used to differentiate this entity from multiple neurofibroma in which two or more neurofibromas occur in the same orbit.

Less common extraconal lesions include fibrous histiocytoma and solitary fibrous tumors, leiomyosarcoma, liposarcoma, epithelial cyst, conjunctival dermoid cyst, parasitic cysts, malignant peripheral nerve sheath tumor, and others. Orbital dermoids are tumors that begin in childhood but may present in adults because the findings are initially masked by slow tumor growth and orbital volume expansion due to bone remodeling.

Imaging Location: Lacrimal Gland and Lacrimal Gland Fossa

Nonneoplastic lesions of the lacrimal gland occur much more commonly than tumors but can mimic a tumor on imaging studies. These nonneoplastic lesions of the lacrimal gland and lacrimal gland fossa include infectious and inflammatory dacryoadenitis. While most cases of inflammatory dacryoadenitis remain idiopathic, IgG4-related orbital inflammation may be responsible in approximately one-quarter of cases [3]. Infiltrative etiologies include the spectrum of lymphoproliferative disorders – from benign reactive lymphoid hyperplasia to lymphoma, as well as amyloidosis, Wegener granulomatosis, Sjögren syndrome, and sarcoidosis [4].

Neoplasms of the lacrimal gland in the adult include benign lesions such as benign mixed tumor or pleomorphic adenoma, monomorphic adenoma, and oncocytomas. Malignant tumors include adenoid cystic carcinoma, pleomorphic adenocarcinoma, squamous cell carcinoma, mucoepidermoid carcinoma, and lymphoma [5]. Schwannomas of the lacrimal gland fossa may also occur and may be mistaken for an epithelial tumor on imaging.

Adenoid cystic carcinoma may vary in appearance on CT from a poorly defined entity to a well-defined round or oval mass, but bone destruction is often present. Imaging studies of lacrimal gland tumors can help point to an epithelial malignancy when bone erosion is present. Indenting of the globe, with bone remodeling, is more commonly seen in benign epithelial neoplasms.

Imaging Location: Lacrimal Sac

Lesions of the lacrimal sac include infectious dacryocystitis; papillomas; granulomatous conditions such as Wegener granulomatosis and sarcoidosis; lymphoproliferative disorders; and epithelial neoplasms. In this location, benign lesions far outnumber malignant lesions [6]. Although inverted papilloma of the lacrimal sac is a benign tumor, its invasive and highly recurrent nature usually indicates more aggressive surgical excision.

Imaging Location: Orbital Apex

Lesions located at the orbital apex may be challenging to distinguish based on imaging studies. Both neoplastic and non-neoplastic conditions may affect this region and include metastases, inflammation, granulomatous inflammation (Tolosa-Hunt syndrome), hamartomas, venous and venous lymphatic malformations, arteriovenous malformations, fibrous dysplasia, and sphenoid wing meningioma [1]. Disease processes involving the bones of the orbital apex include fibrous dysplasia, which may be monostotic or polyostotic, and Paget's disease, which can rarely involve the greater and lesser wings of the sphenoid as well as the clinoid process. In the orbital apex, both CT and MRI may be indicated to assess both the bone and the soft tissue to identify characteristics of the lesions.

Imaging Location: Orbital Bones

Evaluation of the orbital bones on imaging studies provides important information regarding the behavior and extent of an orbital neoplasm. The bone itself may give rise to a tumor, or it may be involved secondarily with indentation, bone molding, erosion, infiltration, or hyperostosis.

Primary orbital bone tumors include benign conditions such as osteoma, osteoblastoma, ossifying fibroma, aneurysmal bone cyst, brown tumor, cholesterol granulomas, fibrous dysplasia, and fibrous histiocytoma as well as malignancies, such as osteosarcoma, chondrosarcoma, Ewing sarcoma, Paget's disease, multiple myeloma, and plasmacytoma. Cavernous hemangiomas may arise within the sphenoid bone of the orbit or other orbital bones, giving a distinct appearance on imaging studies.

Fibrous dysplasia appears as an amorphous hyperdense type of bone that has a "ground-glass" appearance. On computed tomographic imaging studies, orbital bone osteomas appear as well-defined, round, or lobulated masses arising from the bone, and the fibrous subtype of the tumor may have a ground-glass appearance reminiscent of fibrous dysplasia. Bone destruction is not typical. A long-standing mucocele can also present with similar bony changes.

Osteosarcoma, on the other hand, appears irregular in appearance with bone destruction along with increased areas of calcium representing deposition of new albeit neoplastic bone. Osteosarcomas vary widely in amount of osseus, cartilaginous, and fibrous tissues present, and the appearance of the tumor on imaging studies will vary accordingly.

Sphenoid wing meningiomas appear as relatively well-defined lesions, which may contain areas of calcification. While computed tomographic imaging studies may show thickened, hyperostotic sphenoid bone, MR imaging better shows cavernous sinus and intracranial involvement. Ewing sarcoma, which rarely occurs past the age of thirty, appears as an irregular cystic mass with bone destruction on CT imaging studies. Fibrosarcomas of the orbit appear as lytic bone lesions on CT imaging studies and may erode through the paranasal sinuses and orbital walls.

Orbital bones may also be secondarily involved in certain inflammatory conditions such as Wegener's granulomatosis. Orbital intraosseous hemangioma and malignant vascular tumors of the orbital bones exist but are rare. Orbital tumors of cartilaginous origin include chondromas, osteochondromas, enchondroma, and fibrochondroma. Orbital dermoids that occur deeper in the orbit usually present later in life and may produce significant bony changes, especially in the trigone region of the greater wing of the sphenoid.

Imaging Location: Eyelid, Globe, Sinus, and Brain

Invasion of the orbit by neighboring periorbital pathologies is less common than intraorbital metastasis and primary orbital lesions. Neoplasms of the cranial vault, paranasal sinuses, eyelids, and globe may all secondarily extend into the orbit.

In adults, ocular tumor extension into the orbit is uncommon due to the conspicuous effects on visual function and cosmesis, as well as the time course required for such lesions to extend into the orbit. Malignant melanoma may grow through the emissary vessels or into the optic nerve to produce microscopic or limited orbital disease, but significant orbital extension in ocular melanoma typically only occurs in neglected cases.

Cutaneous and conjunctival neoplasia around the eye can invade the orbit in neglected cases but also in cases where appropriate patient and physician vigilance has occurred. Tumors arising in the medial canthus are more likely to result in orbital extension due to the less robust orbital septum in this region. Certain aggressive tumors, such as sebaceous cell carcinoma, dermatofibrosarcoma protuberans, and undifferentiated squamous cell carcinoma have a higher predilection for orbital invasion. Recurrent basal cell carcinoma or basal cell carcinoma occurring in the medial canthus or in the setting of Gorlin's syndrome may also grow to involve the orbit.

Orbital invasion from tumors of the paranasal sinuses occurs relatively commonly [7]. Tumors in this region often produce few symptoms, so both benign and malignant tumors may achieve significant size prior to presentation. It is not

uncommon for such tumors to grow unnoticed until they produce orbital signs and symptoms. Mucoceles and mucopyoceles may occupy an entire sinus cavity with intracranial extension prior to presentation. Mucoceles appear as relatively well-defined cystic masses within an opacified paranasal sinus, often with adjacent bone erosion and remolding. Sinonasal carcinomas, including squamous cell carcinoma, nonkeratinizing carcinoma, and sinonasal undifferentiated carcinoma, may erode into the orbit and through the medial canthal skin prior to presentation. Imaging studies reveal significant bone destruction. Inverted papillomas of the paranasal sinuses, and even the lacrimal sac, may behave aggressively to produce orbital signs and bone destruction on imaging studies. Less commonly, ossifying fibroma, sinonasal fibrosarcoma, and schwannoma may arise primarily from a paranasal sinus and erode into the orbit.

Neoplasms arising within the nasopharynx, such as esthesioneuroblastoma and nasopharyngeal carcinoma, can also extend into the orbit, as can lesions from the cranial cavity, including meningocele, encephalocele, trigeminal schwannoma, and glioblastomas.

Imaging Location: Diffuse Lesions

Several entities can involve contiguous orbital structures and may arise from any location within the orbit (Table 4.4). The more common conditions that can present with this multifocal or diffuse pattern include lymphoproliferative disease, idiopathic orbital inflammation, amyloidosis, IgG4-related orbital disease, and metastasis [8]. Imaging studies may not differentiate these entities, but each has a typical anatomic predilection and constellation of imaging findings.

Table 4.4 Well-circumscribed lesions vs. diffuse lesions in the adult

Well-defined appearance	Diffuse appearance
Cavernous hemangioma	Orbital inflammation
Fibrous histiocytoma	Metastatic lesions
Dermoid	Primary malignant tumor
Neurofibroma	Lymphoproliferative disorders
Schwannoma	Veno-lymphatic malformations
Pleomorphic adenoma	

Conclusion

Specific elements of the history and the physical examination begin the process of formulating a differential diagnosis. These elements also determine appropriate imaging studies to further refine the list of possible etiologies. The imaging studies help guide the surgical plan for diagnosis and treatment.

References

1. Vohra ST, Escott EJ, Stevens D, et al. Categorization and characterization of lesions of the orbital apex. Neuroradiology. 2011;53(2):89–107.
2. Kralik SF, Kersten R, Glastonbury CM. Evaluation of orbital disorders and cranial nerve innervation of the extraocular muscles. Magn Reson Imaging Clin N Am. 2012 Aug;20(3):413–34.
3. Okazaki K, Umehara H. Are classification criteria for IgG4-RD now possible? The concept of IgG4-related disease and proposal of comprehensive diagnostic criteria in Japan. Int J Rheumatolol. 2012;2012:357071.
4. Soheilian M, Bagheri A, Aletaha M. Dacryoadenitis as the earliest presenting manifestation of systemic Wegener granulomatosis. Eur J Ophthalmol. 2002;12(3):241–3.
5. Wang XN, Qian J, Yuan YF, et al. Space-occupying lesions of the lacrimal gland at one tertiary eye center in China: a retrospective clinical study of 95 patients. Int J Ophthlamol. 2012;5(2):208–11.
6. Demirci H, Christianson MD. Orbital and adnexal involvement in sarcoidosis: analysis of clinical features and systemic disease in 30 cases. Am J Ophthalmol. 2011 Jun;151(6):1074–80.
7. Chu Y, Liu HG, Yu ZK. Patterns and incidence of sinonasal malignancy with orbital invasion. Chin Med J. 2012 May;125(9):1638–42.
8. Shields JA, Shields CL, Brotman HK, et al. Cancer metastatic to the orbit: the 2000 Robert M. Curts Lecture. Ophthal Plast Reconstr Surg. 2001;17(5):346–54.

Imaging Techniques

5

Brian Chon, Patrick De Potter, and Arun D. Singh

Introduction

Ultrasonography, color Doppler imaging, CT, and MR imaging are the most important imaging tools for the clinician in the field of orbital oncology. Catheter diagnostic angiography has a limited role in the diagnostic approach of orbit lesions except for evaluating vascular abnormalities suggesting the diagnosis of carotid-cavernous fistula. The role of positron emission tomography with fluoro-2-deoxy-D-glucose (FDG) in evaluation of orbital tumors is limited because FDG accumulates in extraocular muscles in proportion to their contractile activities and decreases lesion conspicuity in regions with high physiological tracer uptake.

B. Chon
Department of Ophthalmology, Division of Orbital and Oculofacial Plastic Surgery, Cole Eye Institute, Cleveland Clinic, Cleveland, OH, USA

P. De Potter
Ocular Oncology Unit, Cliniques Universitaires St-Luc, Université Catholique de Louvain, Brussels, Belgium

A. D. Singh (✉)
Department of Ophthalmic Oncology, Cole Eye Institute, Cleveland Clinic, Cleveland, OH, USA
e-mail: singha@ccf.org

C. J. Hwang et al. (eds.), *Clinical Ophthalmic Oncology*,
https://doi.org/10.1007/978-3-030-13558-4_5

Techniques of Orbital Imaging

Ultrasonography

Ultrasonography is a noninvasive, simple, fast, and economical imaging technique allowing detection of an orbital lesion before deciding if further evaluation with CT or MR imaging is necessary. However, it is limited by the requirement of skilled operators and by limited penetration of the deeper regions of the orbit at energy levels acceptable for the retina.

Although A- and B-mode orbital ultrasonography may provide good information about acoustic inner texture of an orbital lesion, it is difficult to differentiate normal from abnormal tissues, and it remains a semiquantitative approach for tissue characterization (reflectivity and sound attenuation, Table 5.1). Dynamic or real-time information represents one of the advantages of ultrasonography over CT and MRI. The relationships of a pathologic process to the normal anatomic structures can be easily shown by evaluating the same section with different gaze directions, particularly in cases of intraconal lesions. Extension to the orbital walls, especially when associated with erosion or destruction of bone, however, is better appreciated by CT. There are no studies of the relationship between reflectivity and histopathology in the orbit, but most orbital lesions display less coarse and heterogeneous structures with lower reflectivity than the normal orbital tissues (Fig. 5.1) [1].

Table 5.1 Acoustic tissue properties in various orbital diseases

Tissue/disease	Acoustic properties		
	Reflectivity at tissue sensitivity	Attenuation	Associated features
Normal orbital fat	Very high (95–100%)	Medium	Multiple interfaces
Orbital inflammation	High (60–95%)	High	
Neurofibroma		Medium to high	Low reflectivity areas indicate mucoid spaces
Schwannoma			
Cavernous malformation			Phleboliths
Hemangiopericytoma			
Hematoma – abscess (acute)	Medium (40–60%)	Low	
Lymphatic malformation		Low	Cystic spaces
Optic nerve glioma		High or medium	
Optic nerve sheath meningioma		High or medium	
Mucocele	Low (5–40%)	Low	
Dermoid			High and low reflectivity areas (fine hair, cartilaginous remnants)
Hematoma – abscess (chronic)			
Lymphoma			Homogeneous at high sensitivity
Malignant tumor	Variable	Variable	

Based on data from Ref. [1]

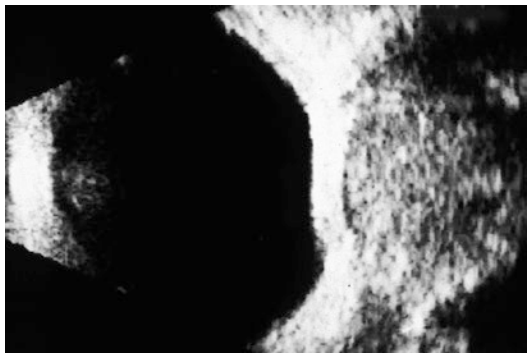

Fig. 5.1 B-scan ultrasound of cavernous malformation displays a well-defined oval echogenic lesion deforming the globe

Color Doppler Imaging (CDI)

CDI allows Doppler evaluation of blood flow and has proved effective in displaying the normal orbital and intraocular vasculature, tumor vascularization, and echographic differentiation of tumors from subretinal hemorrhage [2]. In patients with carotid-cavernous fistula or dural cavernous arteriovenous malformations, CDI clearly demonstrates the dilated, arterialized superior ophthalmic vein with high-velocity blood flow toward the transducer [3]. In addition, CDI may be able to differentiate meningioma from glioma of the optic nerve. It may also be effective in confirming the diagnosis of orbital varices by showing the dynamic changes throughout inspiration and expiration [4].

Computed Tomography

The basis of computed tomography (CT) is the measurement of different tissue absorption values (Hounsfield units, HU) of a given tissue to neighboring structures, following exposure to X-rays.

Conventional Computed Tomography

Conventional CT provides excellent detail of the eye, orbital soft tissues, and bony orbit and has an established role in the evaluation of orbital

trauma and orbital diseases (Box 5.1). However, there are several drawbacks, including relatively long exposures times and increased radiation exposure (approximately 75 mGy of radiation). Moreover, reconstructions in the sagittal and coronal planes can be obtained from conventional CT data. (Table 5.2).

Box 5.1 Indications of Orbital CT as a First Imaging Step

- Evaluation of patient with proptosis with suspicion of osseous, fibro-osseous, and fibrous lesions
- Evaluation of patient with clinical diagnosis of lacrimal gland lesion
- Evaluation of orbital trauma
- Detection of calcification
- Contraindication for MRI (claustrophobia, metallic implants, allergy to contrast agent)

Helical Computed Tomography

Most CT studies have evolved to a spiral (helical) technique with multiple detectors or a rotating detector system. Helical CT, also known as spiral or volume acquisition CT, acquires data in a continuous fashion. With the use of image-reconstruction algorithms, multiple, very thin-sectioned, and multiplanar computer-reformatted images can be produced that are superior to those obtained from standard incremental axial CT images. By producing planar and three-dimensional reformations with less motion artifact than conventional CT, helical CT provides useful information in almost any plane. If bony involvement is clinically suspected, bone algorithm reconstruction (bone window) should be used (Fig. 5.2) [5–7]. In addition, acquisition time is reduced, a great advantage with children and unstable patients [5, 6, 8].

Three-Dimensional (3D) Computed Tomography

Three-dimensional imaging, a computerized post-processing technique, allows unique topographic

Table 5.2 Comparison of various imaging techniques

Technique	Comparison	
Ultrasonography	Advantages	Disadvantages
	Inexpensive	Requirement for skilled operator
	Tissue characterization	
	Dynamic information	
	Evaluation of anterior orbital lesions	
Computed tomography	Availability	Ionizing radiation
	Short examination time	Allergic reaction with contrast agents
		Artifacts:
		High-density foreign body
		Positioning
		Partial voluming
		Beam hardening
Magnetic resonance imaging	High soft tissue contrast	Slow acquisition
	Large imaging depth	Claustrophobia
	No ionizing radiation	Obesity
	Paramagnetic effects by:	Missile and thermal injuries
	Methemoglobin	
	Protein	
	Melanin	Artifacts:
	Gadopentetate dimeglumine	Motion
		Wrap around
		Bioinhomogeneity
		Chemical shifts
		Partial volume
		Flow or pulsation

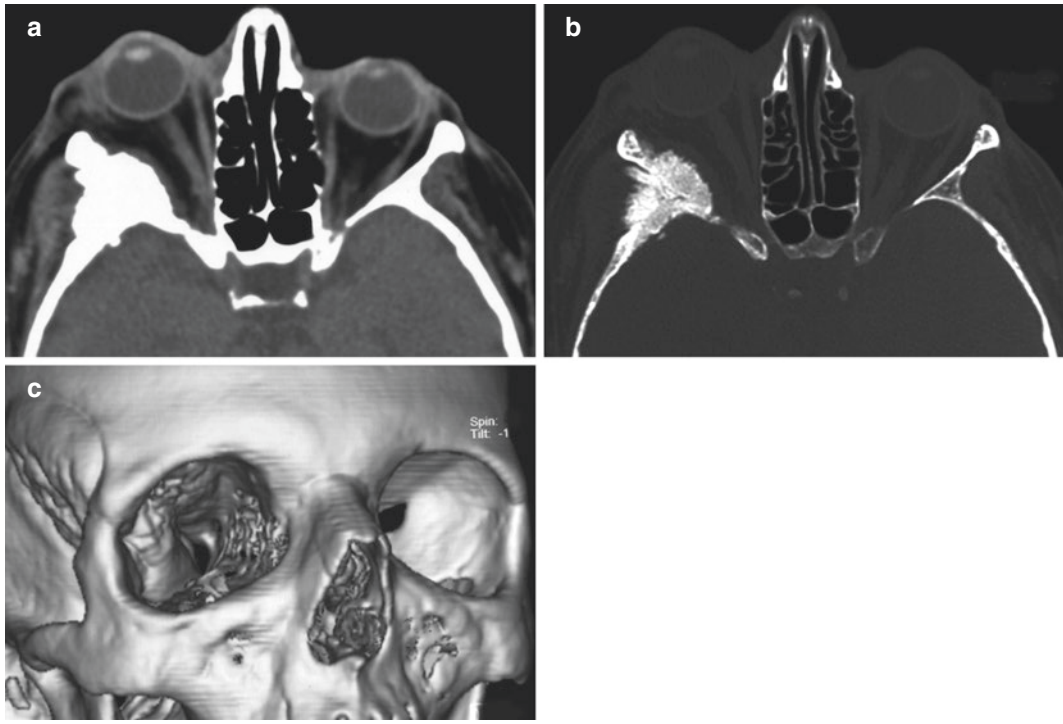

Fig. 5.2 Axial CT images of a right sphenoid wing meningioma. Helical CT showing a right hyperostotic sphenoid wing (**a**), bone windows (**b**), and three-dimensional scan (**c**)

overview of selected anatomic or pathologic structures that have been isolated (a process called segmentation) from the image tissue volume [9]. For 3D CT imaging of the head and orbits, scanning technique with either 1.5-mm contiguous slices or 1-mm slices at 1.5-mm slice incrementation is recommended. Due to partial volume averaging, the thin medial wall, the orbital floor, and the anterior wall of the maxillary sinuses are not visualized, causing artificial holes often referred as pseudoforamina. Special processing techniques and sophisticated edge detection algorithms may be used to avoid these imaging artifacts. Low-contrast tissue segmentation like in tumor-muscle or tumor-neural tissue interfaces requires visual identification and manual separation [9]. Three-dimensional imaging of the orbit is a perfect technique to illustrate a wide variety of teratogenic (particularly craniofacial dysplasia and synostosis), pathogenic, traumatogenic, and iatrogenic orbital abnormalities and to comprehend the extent and location of the pathology in order to plan the surgical approach and facilitate comparison between preoperative and postoperative changes (Fig. 5.2). Computed tomography, while excellent for bony detail of the lacrimal drainage system, provides a limited soft tissue detail compared to MRI and suffers from image degradation in out-of-plane images.

Magnetic Resonance Imaging

Magnetic resonance (MR) imaging is based on a physical phenomenon called nuclear magnetic resonance effect on the atomic nuclei, primarily hydrogen atoms of water molecules in human tissues. MR images of patients are obtained by inducing electromagnetic signals from the magnetic dipole movements of ^{1}H nuclei and then converting these signals into cross-sectional images.

Diffusion-weighted imaging (DWI) is an additional sequence that can be generated and evaluated on MRI. DWI sequences are from signal contrast based on the random motion of particles. In tissue, water diffusion is limited by cellular membranes and tissue characteristics. Restricted diffusion shows on DWI as high

signal, indicating restricted diffusion. An apparent diffusion coefficient (ADC) can be calculated from the DWI analysis and displayed as an ADC map. For orbital imaging, studies utilizing DWI and ADC imaging have shown potential benefit in differentiating lymphoma from inflammation [7], diagnosing venous malformations [9], differentiating orbital infantile hemangioma from rhabdomyosarcoma [10], and evaluating uveal melanoma response to therapy [11].

Although CT and MR studies are complementary, MR imaging provides superior soft tissue contrast. Its multiplanar capability with outstanding tissue contrast and the absence of ionizing radiation make MR imaging an especially suitable technique for imaging orbital structures (Box 5.2) [5]. Moreover, the superficial location of the eye and eyelids permits the use of surface coils which improve the display of anatomic details. Current MRI is often performed using 1.5 T units of magnetic strength. The overall scan time can be shortened by fast spin-echo sequences. Fat suppression techniques are used to eliminate the extremely strong bright signal intensity from orbital fat which may overwhelm high signal intensities of enhancing surrounding lesions.

Box 5.2 Indications of Orbital MRI as a First Imaging Step

- Location and extent of orbital lesion
- Evaluation of orbital, intracanalicular, and prechiasmal optic pathways
- Evaluation of patient with proptosis (hemorrhagic, neoplastic, fibrosclerotic, mucinoid/cystic degeneration)
- Evaluation of patient with progressive bluish lid swelling (capillary hemangioma versus lymphatic malformation)
- Evaluation of tumor response after radiotherapy or chemotherapy
- Evaluation of anophthalmic socket when orbital tumor recurrence is suspected
- Orbital trauma when ferromagnetic material is excluded
- Identification of fibrovascular ingrowth within biocompatible implant

Interpretation of Imaging Studies

Interpretation of imaging studies is facilitated by evaluating radiological characteristics such as anatomic location, appearance, content, post-contrast enhancement features, and bone characteristics [5, 12–15].

Location

CT provides similar information to MR imaging on the location and extent of a lesion in the anterior orbital space, the globe, the intraconal-extraconal space, orbital fat, extraocular muscles, cavernous sinus, and temporal fossa. CT remains the imaging modality of choice in the evaluation of lesions located in the lacrimal gland fossa, the paranasal sinuses, and the adjacent bony orbit. Due to superior soft tissue contrast resolution by MR imaging, it is the study of choice for lesions infiltrating the optic nerve, optic nerve sheath, and orbital apex.

Appearance

An orbital lesion may be described as having a regular (round or oval) or irregular (infiltrative) configuration. Its margin characteristics may be well circumscribed or diffuse. In general, benign lesions tend to be well circumscribed, malignant lesions tend to have irregular shape, and inflammatory lesions are more typically diffuse and irregular [15].

Content

Information on the content of the lesion (cystic or solid, homogeneous or heterogeneous) could be obtained by both CT and MR imaging techniques. Both imaging techniques also detect presence of fluid/fluid or fluid/air levels. When lesion density is higher than that of the vitreous, CT images identify a lesion as solid. As a wide range of tissue densities on CT scans or signal intensities on MR images relate to the internal architecture and the presence of proteinaceous or blood products,

it is not always possible to differentiate a solid from a cystic orbital lesion. MR images identify tissue compounds such as melanin, methemoglobin, deoxyhemoglobin, ferritin, and proteinaceous material. Punctate or conglomerate increased densities on CT scans or foci of signal void on MR scans may be seen in trauma, vascular tumors, optic nerve sheath tumors (meningioma), epithelial lacrimal gland tumor, and malignant osseous tumors (osteosarcoma). In general, MR images provide more information about the content of the lesion than the CT images. However, CT is best suited for the detection of calcification.

Contrast Enhancement

The pattern of contrast enhancement (present or absent, homogeneous or heterogeneous) of orbital lesions guides in forming a differential diagnosis. Enhancement characteristics of an orbital lesion are best identified on post-contrast fat-suppressed T1-weighted images. No enhancement is documented in hemorrhagic process, dense scar tissue, collection of fluid, or necrotic portion of tumors. Minimal contrast enhancement suggests a chronic or sclerosing orbital inflammation, tissue fibrosis, or post-therapeutic scar tissue. Moderate to marked contrast enhancement is usually noticed in solid tumors as well as in acute inflammatory orbital lesions. Linear enhancement surrounding a non-enhancing well-delineated lesion suggests the cystic nature of the lesion. Well-defined linear or void of signal within an enhancing lesion may suggest air, high blood flow vessels (artery or vein), fragments of cortical bone, or foreign body. Gadolinium-enhanced MR imaging has proven as the best-suited imaging modality for assessing the fibrovascularization tissue progression into porous orbital implants (hydroxyapatite and porous polyethylene).

Bone Characteristics

Bone changes induced by an orbital lesion include cortical bony indentation and molding, bone erosion, bone lysis, bone infiltration, and hyperostosis. The destruction of cortical bone is seen on CT as a loss of the highly dense cortical bone and on MR scans as a discontinuity of the linear signal void produced by the normal cortical bone. CT with bone windows or 3D CT is almost always preferred over MRI to assess orbital disorder suspected to affect the bony orbit.

Bone Molding

Molding of the bone by a well-circumscribed orbital mass highly suggests a congenital lesion (dermoid cyst, lymphatic malformation) or a slowly growing benign tumor (cavernous malformation, neurofibroma, schwannoma, and benign lacrimal gland tumor).

Bone Erosion

Bone erosion is usually seen with more aggressive inflammatory lesions, primary tumors, and secondary tumors.

Bone Lysis

Bone destruction or lysis is observed in very aggressive primary tumors, secondary malignant tumors, and inflammatory lesions (idiopathic orbital inflammation, eosinophilic granuloma).

Bone Infiltration

Tumor infiltration of the bony orbit is best seen on CT with bone algorithm reconstruction and identified on MR imaging as a discontinuity of cortical signal void and loss of high signal intensity of the fat in the bone marrow.

Hyperostosis

Hyperostosis is observed with benign osseous tumors (meningioma), malignant bone tumors (osteosarcoma), and metastatic tumors such as from prostate carcinoma. In general, osseous

spiculation and heterogeneous density are findings suggestive of a malignant tumor.

Radiological Differential Diagnosis

To obtain a reliable differential diagnosis, orbital tumors can be classified into one of seven radiological patterns: well-circumscribed solid, ill-defined solid, circumscribed cystic, enlarged optic nerve, enlarged lacrimal gland, enlarged extraocular muscles, and anomalies of the bony orbit (Box 5.3).

Box 5.3 Seven Radiological Patterns of Orbital Tumors

- Well-circumscribed solid tumor
- Ill-defined solid tumor
- Circumscribed cystic tumor
- Enlarged optic nerve
- Enlarged lacrimal gland
- Enlarged extraocular muscles
- Anomalies of the bony orbit

Well-Circumscribed Solid Orbital Lesions

The most frequent well-circumscribed orbital tumors are cavernous malformation (Chap. 8), schwannoma, neurofibroma, fibrous histiocytoma, and solitary fibrous tumor (Chap. 9) [14–19]. These tumors usually present as a well-defined, oval-to-round intraconal orbital mass on MR imaging (Table 5.3).

Cavernous malformation shows increasing homogeneous enhancement on delayed images owing to the pooling of the contrast material within the tumor. The early areas of contrast enhancement of cavernous malformation on CT start from focal points or patchy areas and on MRI start from patchy or geographical areas. Later images show less heterogeneous and more homogeneous enhancement. These differences may be due to different acquisition times of CT and MRI, as well as hemodynamic variability among cavernous malformations between patients [16]. Heterogenicity in tumor signal may be related to the presence of calcified phleboliths which produce signal void on T1- and T2-weighted images.

Table 5.3 Magnetic resonance imaging features of well-circumscribed orbital tumors on spin-echo sequences

	Lesion appearance		
	Signal intensity[a]		Degree of enhancement with Gd-DTPA
Tumor	T1-WI	T2-WI	
Cavernous malformation	Homo	Hetero/homo (late)	Homo
	Iso/hyper	Iso/hypo	+++
Schwannoma	Hetero	Hetero	Hetero
	Iso/hyper	Iso/hypo	+/+++
Neurofibroma	Hetero	Hetero	Hetero
	Iso/hyper	Iso/hypo	+/+++
Fibrous histiocytoma	Hetero	Hetero	Hetero
	Hyper/hypo	Hyper/hypo	++++
Solitary fibrous Tumor	Homo	Homo	Hetero
	Iso/hyper	Iso/hypo	++++
Orbital varix	Homo/hetero	Homo/hetero	Homo/hetero
	Iso/hyper	Iso/hypo	++++
Thrombosed varix	Hetero	Hetero	Hetero
	Iso/hyper	Iso/hypo	–/+
Orbital metastasis (skin melanoma, carcinoid)	Homo	Homo	Homo
	Iso/hyper	Iso/hypo	+/+++

Iso isointense, *Hyper* hyperintense, *Hypo* hypointense, *Homo* homogeneous, *Hetero* heterogeneous
[a]With respect to vitreous

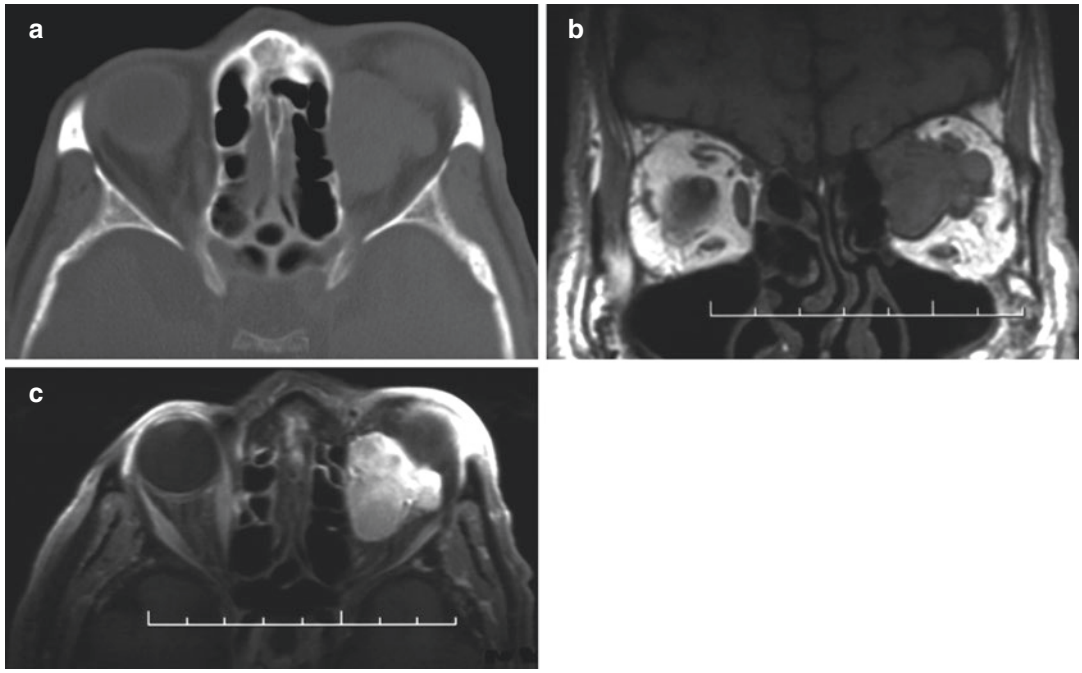

Fig. 5.3 Left orbital schwannoma. Axial CT image showing a well-circumscribed orbital mass (**a**). Coronal pre-contrast T1-weighted image. The lesion shows slight heterogeneous appearance (**b**). Axial post-contrast T1-weighted image displaying heterogeneous enhancement (**c**)

On both CT and MR, schwannomas tend to show smooth expansion of neural foramina, osseous remodeling, a disproportionately small amount of edema, and deformation of adjacent tissue [17]. On T2-weighted MRI imaging, schwannomas may be heterogeneously hyperintense, and this can be due to a variable mixture of compactly arranged cells, Antoni A, and more loosely arranged cells, Antoni B [18]. Schwannoma, neurofibroma, fibrous histiocytoma, and hemangiopericytoma may conceivably have identical non-enhancing MR characteristics of less common well-circumscribed orbital lesions such as lymphoproliferative disorder, metastasis from skin melanoma or carcinoid tumor, capillary hemangioma, orbital varix, and rhabdomyosarcoma (Fig. 5.3).

Ill-Defined Solid Orbital Lesions

The radiological differential diagnosis of common solid ill-defined orbital lesions in children includes capillary hemangioma, lymphatic malformation, plexiform neurofibroma, idiopathic orbital inflammation, and metastasis [12, 13, 15]. In adults idiopathic orbital inflammation (Chap. 7), lymphoproliferative disorder (Chap. 15), metastasis (Chap. 16), and primary orbital tumor are more frequent causes.

There are no specific CT features of ill-defined orbital lesions, but CT provides clues regarding the malignant nature or chronic behavior of an orbital mass if bone changes (molding, erosion, lysis, and hyperostosis) are identified on bone window scans. Radiolucency areas within the tumor may suggest necrotic changes.

The increased signal of an inflammatory process is related to its acute stage and its high concentration of free water (Table 5.4). By studying T2 relaxation times, it may be possible to differentiate muscle enlargement caused by inflammatory edema from infiltrative process. Malignant tumors and occasionally inflammatory lesions may produce bone changes which appear as disruption of the regular signal void of the adjacent cortical bone or as a loss of the high signal of the marrow fat.

Table 5.4 Magnetic resonance imaging features of ill-defined orbital tumors on spin-echo sequences

Tumor	Lesion appearance		Degree of enhancement with Gd-DTPA
	Signal intensity[a]		
	T1-WI	T2-WI	
Orbital metastasis	Homo/hetero	Homo/hetero	Homo/hetero
	Hyper/hypo +/+++	Iso/hypo	+/+++
Capillary hemangioma	Homo/hetero	Homo/hetero	Homo/hetero
	Iso/hyper	Iso/hypo	+++
Lymphoid proliferative disorder	Homo	Homo	Homo
	Hyper	Hypo	+++
Primary orbital tumor	Homo/hetero	Homo/hetero	Homo/hetero
	Hyper	Hypo	+/+++
Acute idiopathic inflammation	Homo	Homo	Homo
	Iso/hyper	Iso/hypo	+++
Chronic idiopathic inflammation (sclerosing type)	Homo	Homo	Homo/hetero
	Iso/hyper	Hypo	–/+

Iso isointense, *Hyper* hyperintense, *Hypo* hypointense, *Homo* homogeneous, *Hetero* heterogeneous
[a]With respect to vitreous

Table 5.5 Magnetic resonance imaging features of cystic orbital tumors on spin-echo sequences

Tumor	Lesion appearance		Degree of enhancement with Gd-DTPA
	Signal intensity[a]		
	T1-WI	T2-WI	
Dermoid cyst	Hetero	Hetero	Lumen –
	Iso/hyper	Iso/hypo	Capsule, septa +
Epithelial cyst	Homo	Homo	Lumen –
	Iso/hyper	Iso/hypo	Capsule, septa +
Mucocele	Homo	Homo	Lumen –
	Iso/hyper	Iso/hypo/hyper	Capsule, septa +
Hemorrhagic cyst/lymphatic malformation	Hetero	Hetero	Lumen –
	Iso/hyper	Iso/hypo/hyper	Capsule, septa +

Iso isointense, *Hyper* hyperintense, *Hypo* hypointense, *Homo* homogeneous, *Hetero* heterogeneous
[a]With respect to vitreous

Minimal and heterogeneous enhancement is usually observed in the sclerosing type of orbital inflammation, and marked enhancement is observed in the acute type making their radiological differentiation easier. However, MRI does not provide sufficient histologic tissue specificity to allow reliable differentiation between idiopathic orbital pseudotumor, benign reactive lymphoid hyperplasia, atypical lymphoid hyperplasia, and lymphoma.

Well-Circumscribed Cystic Lesions

The differential diagnosis of cystic orbital lesions includes dermoid cyst, colobomatous cyst, teratoma, meningoencephalocele, lymphatic malformation, acquired inclusion cyst, chronic hematic cyst (cholesterol granuloma), mucocele, subperiosteal hematoma, parasitic cyst, and orbital abscess (Chap. 9) [12, 13, 15, 19].

Orbital CT offers excellent information regarding the cystic features of the lesion as its density is similar to that of the vitreous. However, cystic lesions with higher density (high content of protein, keratinaceous material, blood products) may simulate solid well-circumscribed orbital tumor. MR studies are more specific than CT in identifying tissue component within the cystic mass as well as the linear enhancement of the capsule surrounding the non-enhancing lumen of the cyst. On MR imaging the cystic lesions appear as well-defined, round-to-oval lesions with variable signal intensities depending upon the composition of their content (Table 5.5). Dermoid cysts are typically located at the frontozygomatic suture or frontomaxillary

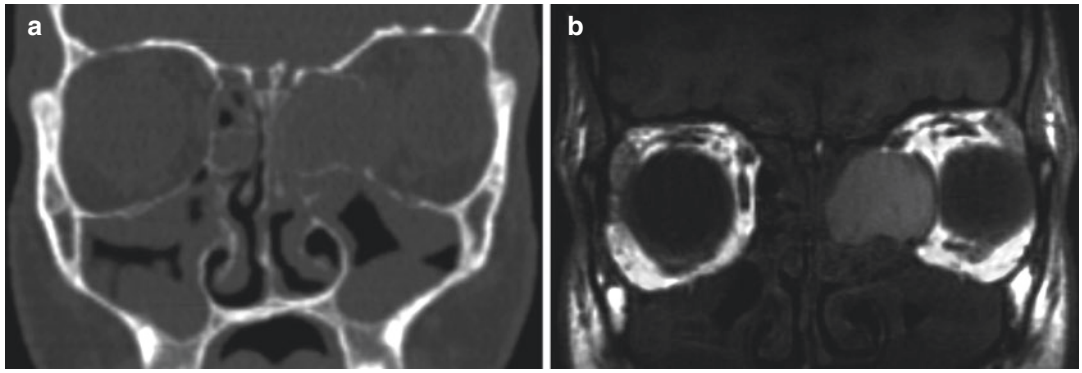

Fig. 5.4 Left ethmoidal mucocele with bilateral pansinusitis. Coronal CT with bone window suggesting the erosion of the medial orbital wall (**a**). Coronal pre-contrast T1-weighted image. The cystic lumen shows high signal intensity due to the high proteinaceous content (**b**)

suture, and may have a characteristic dumbbell configuration. A fat-filled cyst is highly characteristic of dermoid cysts. A fluid-fluid level is suggestive of subacute hemorrhagic lymphatic malformation or hemorrhagic cyst with the superior aspect of the cyst containing the methemoglobin released from the lysed erythrocytes and the dependent portion containing the settled cellular elements of the hemorrhage with intracellular methemoglobin. The increasing concentration of proteinaceous secretions in a mucocele produces a higher signal intensity of the lesion (Fig. 5.4).

Enlarged Optic Nerve

The differential diagnosis of an enlarged optic nerve includes optic nerve glioma, malignant glioma, secondary tumor from intraocular tumor (retinoblastoma, uveal melanoma, melanocytoma), CNS lymphoma or systemic metastatic disease, and optic neuritis (Chap. 11) [12, 13, 15, 20]. In all these diseases, the optic nerve may assume a tubular, fusiform, or lobular configuration. The differential diagnosis of an enlarged optic nerve sheath includes meningioma, meningeal spread of tumor, meningitis, arachnoidal cyst, hemorrhage, and CSF expansion as seen with pseudotumor cerebri or orbital apex compression.

The pattern of enhancement of an enlarged optic nerve allows differentiation between an optic nerve lesion and an optic nerve sheath

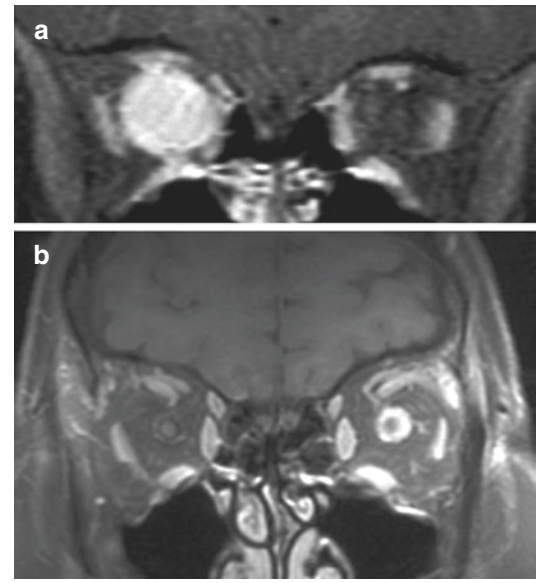

Fig. 5.5 Enlarged optic nerve on coronal post-contrast T1-weighted images. Enhancing pattern of juvenile pilocytic astrocytoma within the right optic nerve (**a**). Rim-like enhancing left optic nerve sheath meningioma (**b**)

lesion. In optic nerve lesions, the enhancement is within the optic nerve, whereas in optic nerve sheath lesions, the enhancement is eccentric surrounding a hypointense optic nerve. The characteristic kinking and buckling of the enlarged optic nerve is highly suggestive of juvenile pilocytic astrocytoma (optic nerve glioma). On pre-contrast T1-weighted images, juvenile pilocytic astrocytoma (JPA) appears isointense with respect to the cerebral gray matter (Fig. 5.5). The

tumor may be surrounded by reactive arachnoid hyperplasia which shows a slightly hypointense signal. On T2-weighted images, fusiform JPA demonstrates relatively high signal intensity, whereas large lobulated tumors tend to show a more heterogeneous signal. The peripheral hyperintense portion (perineural arachnoid gliomatosis or arachnoidal hyperplasia or CSF accumulation) surrounds a central linear core of lower signal intensity (compact proliferation of glial cells). On post-contrast studies, JPA shows variable enhancement which can be traced through the optic canal to the chiasm and optic tracts when it involves the intracranial portion of the optic nerve. The non-enhancing peripheral portion of the tumor, which is hyperintense on T2-weighted images, probably represents arachnoidal hyperplasia or an ectatic subarachnoid space around the optic nerve. The perineural arachnoid gliomatosis shows enhancement. Involvement of the optic nerve with retinoblastoma or melanoma cells, lymphoproliferative tissue, and metastatic process are best detected on post-contrast MR studies. In these cases, the pattern of enhancement within the optic nerve may be localized or diffuse.

The intensity pattern of optic nerve sheath meningioma on pre-contrast MR studies is variable, and the tumor may appear isointense, hypointense, or hyperintense with respect to the optic nerve on T1- and T2-weighted images. On post-contrast films, the tumor shows marked enhancement which characteristically take a rim or eccentric pattern surrounding the non-enhancing optic nerve. A small intracanalicular or intracranial extension of the tumor is best identified on post-contrast T1-weighted images with fat suppression techniques. Calcification shows a low signal intensity on T1- and T2-weighted images without enhancement with Gd-DTPA. Calcification is better appreciated on CT than MRI.

On CT, the tubular or globular enlargement seen with an optic nerve sheath meningioma is nonspecific. Tram track, sign in which the denser and thicker involved optic nerve sheath outlines a central lucency, which represents the residual optic nerve, is characteristic but is not specific to optic nerve sheath meningioma.

Enlarged Lacrimal Gland

Lacrimal gland lesions may be classified as non-epithelial and epithelial (Chap. 13). The non-epithelial lacrimal gland lesions include inflammation and lymphoid tumors, whereas the epithelial lesions included dacryops, pleomorphic adenoma, and malignant epithelial tumors (adenoid cystic carcinoma) [21].

Orbital CT is more specific than MRI in the detection of calcification within the enlarged lacrimal gland and in the evaluation of bone destruction in the lacrimal gland fossa. On MRI, among the non-epithelial lesion of the lacrimal gland, the inflammatory process (dacryoadenitis) usually appears more ill-defined than a lymphoid infiltrate which can mold to the globe (Table 5.6). In 40% of lymphoid tumors, the lacrimal gland is involved [22]. Typically, lymphoid tumors mold to surrounding structures rather than displacing them. At the time of imaging, lymphoid tumors may either have a smooth, circumscribed appearance or a diffuse and ill-defined appearance. The epithelial tumor of the lacrimal gland usually presents as a well-circumscribed mass in the lacrimal gland fossa, homogeneous and produces smooth bone remodeling or bone scalloping of the frontal bone. Adenoid cystic carcinoma may have an irregular, relatively well-defined, or infiltrative pattern with possible evidence of bone destruction. Malignant epithelial tumors of the lacrimal gland are more likely to have a tail or wedge sign, indicating posterior extension into the orbit [23].

Calcification within the enlarged lacrimal gland is suggestive of adenoid cystic carcinoma and appears as hypointense areas on T1- and T2-weighted images without enhancement on post-contrast scans [23].

Enlarged Extraocular Muscles

The extraocular muscles can be enlarged by infectious, inflammatory, neoplastic, vascular, and degenerative processes (Table 5.7). Such involvement is usually best seen on post-contrast coronal CT and MR images [13–16]. In thyroid-associated

Table 5.6 Magnetic resonance imaging features of lacrimal gland lesions on spin-echo sequences

Tumor	Lesion appearance		Degree of enhancement with Gd-DTPA
	Signal intensity[a]		
	T1-WI	T2-WI	
Dacryops	Homo	Homo	–
	Iso/hyper	Iso/hypo	
Lymphoid proliferative disorder	Homo	Homo	Homo
	Hyper	Hypo	+/+++
Acute idiopathic inflammation (dacryoadenitis)	Homo	Homo	Homo
	Iso/hyper	Iso/hypo	+++
Chronic idiopathic inflammation (sclerosing type)	Homo	Homo	Homo/hetero
	Iso/hyper	Hypo	–/+
Pleomorphic adenoma (Benign mixed tumor)	Homo	Homo	Homo
	Iso/hyper	Iso/hypo	+++
Adenoid cystic carcinoma	Homo/hetero	Homo/hetero	Homo/hetero
	Hyper	Hypo	+/+++

Iso isointense, *Hyper* hyperintense, *Hypo* hypointense, *Homo* homogeneous, *Hetero* heterogeneous
[a]With respect to vitreous

Table 5.7 Magnetic resonance imaging features of enlarged extraocular muscles on spin-echo sequences

Entity/tumor	Extent of involvement	Lesion appearance		Degree of enhancement with Gd-DTPA
		Signal intensity[a]		
		T1-WI	T2-WI	
Thyroid orbitopathy	Uni/bilateral	Homo	Homo	Homo
	Single/multiple	Hyper	Iso/hypo	+/+++
	Tendon (+)			
Idiopathic myositis	Uni/bilateral	Homo	Homo	Homo
	Single/multiple	Hyper	Iso/hypo	+/+++
	Tendon (+)			
Rhabdomyosarcoma	Unilateral	Homo/hetero	Homo/hetero	Homo/hetero
	Single/multiple	Iso/hyper	Iso/hypo	
	Tendon (+/–)			
Metastasis	Uni/bilateral	Homo/hyper	Homo/hetero	Homo/hetero
	Single/multiple	Hyper	Hypo	–/+++
	Tendon (+/–)			
Lymphoma	Uni/bilateral	Homo	Homo	Homo
	Single/multiple	Hyper	Hypo	+++
	Tendon (+/–)			
Carotid-cavernous fistula	Unilateral	Homo	Homo	Homo
	Multiple	Hyper	Hypo	+++
	Tendon (–)			

Iso isointense, *Hyper* hyperintense, *Hypo* hypointense, *Homo* homogeneous, *Hetero* heterogeneous
[a]With respect to vitreous

orbitopathy, the belly of the extraocular muscles is expanded, and unlike idiopathic myositis, the tendinous attachment to the globe is usually spared [19]. In thyroid-associated orbitopathy, the rectus muscle most commonly involved is the inferior rectus, followed by the medial, superior, and lateral rectus. In contrast, in idiopathic myositis, all muscles are nearly equally involved, except for perhaps slightly less involvement of the inferior rectus [24]. Neoplastic infiltration (rhabdomyosarcoma, metastasis, lymphoma) may involve the extraocular muscle focally or diffusely with occasional sparing of the inserting tendon. Tumor necrosis may produce heterogeneous signal

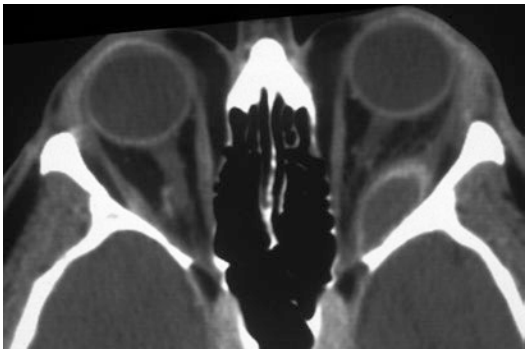

Fig. 5.6 Focal enlargement of the left lateral rectus muscle by metastatic carcinoid from the lung

intensities. Focal or multifocal nodularity of the extraocular muscle(s) is highly suggestive of metastatic disease (Fig. 5.6) [24].

Anomalies of Bony Orbit

CT remains the imaging modality of choice for the evaluation of bone abnormalities (scalloping, deformity, hyperostosis, expansion, and bone marrow invasion) as well as osseous, fibro-osseous, and fibrous tumors [25]. The fact that cortical bone has a signal void permits bone to be demarcated from adjacent tissues on MR imaging. Good contrast is therefore available between the bone and orbital fat, muscle, and brain. However, cortical bone may not be clearly defined when it lies adjacent to structures in which signal is not generated such as air, rapidly flowing blood, dura, or calcification.

Osteosarcoma appears as an ill-defined mass with a heterogeneous, hyperintense signal with respect to the vitreous and gray matter on T1-weighted scans. On T2-weighted images, the tumor has a heterogeneous lower signal intensity. After Gd-DTPA injection, osteogenic sarcoma demonstrates heterogeneous enhancement. Replacement of the cortical bone and fat marrow and orbital and cranial extension are best identified on post-contrast fat-suppressed T1-weighted images. CT scans demonstrate an irregular, invasive, and destructive tumor with lytic and sclerotic changes associated with focal areas of calcification.

Fibrous dysplasia displays sclerotic, homogeneous, dense, and ground-glass appearance on CT, but alternate areas of lucency and increased density can also be identified. On MR imaging fibrous dysplasia shows very low signal intensity on T1- and T2-weighted images.

Aneurysmal bone cysts of the orbit appear as multicystic, loculated masses associated with bone destruction and possible extension to the adjacent sinuses. These tumors have heterogeneous signal intensities and fluid-fluid levels reflecting the various stages of evolution of the hemorrhagic content. Orbital CT scans show irregular expansion and destruction of bone associated with a mildly enhancing loculated cystic mass.

The major role of MR in evaluation of secondary orbital tumors from the paranasal sinuses is to delineate the extent of the infiltrative tumor process within the orbit, the sinuses, and the brain. These malignant tumors are fairly cellular and usually show a low signal intensity on T1-weighted images and increased signal on T2-weighted images with respect to orbital fat.

Summary

Ultrasonography, color Doppler imaging, CT, and MR imaging are the most important imaging tools for the clinician in the field of orbital oncology. Although orbital ultrasonography may provide good information about acoustic inner texture of an orbital lesion, it is difficult to differentiate normal from abnormal tissues and has an issue with deeper visualization. CT provides excellent detail of the eye, orbital soft tissues, and bony orbit and has an established role in the evaluation of orbital trauma and orbital diseases. Although CT and MR studies are complementary, MR imaging provides superior soft tissue contrast. Interpretation of imaging studies is facilitated by evaluating radiological characteristics such as anatomic location, appearance, content, post-contrast enhancement features, and bone characteristics. Moreover, orbital tumors can be classified into one of seven radiological patterns (well-circumscribed solid, ill-defined solid, circumscribed cystic, enlarged optic nerve,

enlarged lacrimal gland, enlarged extraocular muscles, and anomalies of the bony orbit) to obtain reliable differential diagnosis.

References

1. Nasr AM, Chacra GIA. Ultrasonography in orbital differential diagnosis. In: Karcioglu Z, editor. Orbital tumors. New York: Springer; 2015.
2. Lieb WE. Color Doppler imaging of the eye and orbit. Radiol Clin N Am. 1998;36(6):1059–71. Epub 1999/01/13. PubMed PMID: 9884688
3. Karam EZ, Destarac L, Hedges TR, et al. Abnormal ophthalmic veins: Differential diagnosis and management using color Doppler imaging. Neuro-Ophthalmology. 2009;22:87–96. https://doi.org/10.1076/noph.22.2.87.3732.
4. Jacquemin C, Bosley T, Mullaney P. Orbital color Doppler imaging of optic nerve tumors. Int Ophthalmol. 1999;23(1):11–5. https://doi.org/10.1023/A:1006492631341.
5. Ornan D, Donahue J. The basics of orbital imaging. In: Karcioglu ZA, editor. Orbital tumors: diagnosis and treatment. New York: Springer; 2015. p. 83–95.
6. Klevansky A. The efficacy of multiplanar reconstructions of helical CT of the paranasal sinuses. AJR Am J Roentgenol. 1999;173(2):493–5. Epub 1999/08/03. PubMed PMID: 10430160. https://doi.org/10.2214/ajr.173.2.10430160.
7. Hiwatashi A, Togao O, Yamashita K, et al. Diffusivity of intraorbital lymphoma vs. inflammation: comparison of single shot turbo spin echo and multishot echo planar imaging techniques. Eur Radiol. 2018;28(1):325–30. Epub 2017/08/06. PubMed PMID: 28779398. https://doi.org/10.1007/s00330-017-4995-5.
8. Rhea JT, Rao PM, Novelline RA. Helical CT and three-dimensional CT of facial and orbital injury. Radiol Clin N Am. 1999;37(3):489–513. Epub 1999/06/11. PubMed PMID: 10361543
9. Kalin-Hajdu E, Colby JB, Idowu O, et al. Diagnosing distensible venous malformations of the orbit with diffusion-weighted magnetic resonance imaging. Am J Ophthalmol. 2018;189:146–54. Epub 2018/02/20. PubMed PMID: 29458038. https://doi.org/10.1016/j.ajo.2018.02.005.
10. Kralik SF, Haider KM, Lobo RR, et al. Orbital infantile hemangioma and rhabdomyosarcoma in children: differentiation using diffusion-weighted magnetic resonance imaging. J AAPOS. 2018;22(1):27–31. Epub 2017/11/09. PubMed PMID: 29113884. https://doi.org/10.1016/j.jaapos.2017.09.002.
11. Foti PV, Longo A, Reibaldi M, et al. Uveal melanoma: quantitative evaluation of diffusion-weighted MR imaging in the response assessment after proton-beam therapy, long-term follow-up. Radiol Med. 2017;122(2):131–9. Epub 2016/10/19. PubMed PMID: 27752969. https://doi.org/10.1007/s11547-016-0697-3.
12. De Potter P, Shields JA, Shields CL. MRI of the eye and orbit. Philadelphia: Lippincott; 1995.
13. Müller-Forell W, Pitz S. Orbital pathology. In: Baert AL, Sartor K, Müller-Forell WS, editors. Imaging of orbital and visual pathway pathology. Berlin/Heidelberg: Springer; 2002. p. 147–340.
14. Lee WW, Erickson BP. Imaging in orbital differential diagnosis. In: Karcioglu ZA, editor. Orbital tumors: diagnosis and treatment. New York: Springer; 2015. p. 97–109.
15. Ben Simon GJ, Annunziata CC, Fink J, et al. Rethinking orbital imaging establishing guidelines for interpreting orbital imaging studies and evaluating their predictive value in patients with orbital tumors. Ophthalmology. 2005;112(12):2196–207. Epub 2005/12/06. PubMed PMID: 16325712. https://doi.org/10.1016/j.ophtha.2005.09.013.
16. Young SM, Kim YD, Lee JH, et al. Radiological analysis of orbital cavernous hemangiomas: a review and comparison between computed tomography and magnetic resonance imaging. J Craniofac Surg. 2018;29(3):712–6. Epub 2018/01/31. PubMed PMID: 29381625. https://doi.org/10.1097/SCS.0000000000004291.
17. Skolnik AD, Loevner LA, Sampathu DM, et al. Cranial nerve schwannomas: diagnostic imaging approach. Radiographics. 2016;36(5):1463–77. Epub 2016/08/20. PubMed PMID: 27541436. https://doi.org/10.1148/rg.2016150199.
18. Pointdujour-Lim R, Lally SE, Shields JA, et al. Orbital schwannoma: radiographic and histopathologic correlation in 15 cases. Ophthalmic Plast Reconstr Surg. 2018;34(2):162–7. Epub 2017/03/30. PubMed PMID: 28353472. https://doi.org/10.1097/IOP.0000000000000900.
19. Bond JB, Haik BG, Taveras JL, et al. Magnetic resonance imaging of orbital lymphangioma with and without gadolinium contrast enhancement. Ophthalmology. 1992;99(8):1318–24. Epub 1992/08/01. PubMed PMID: 1513586
20. Saeed P, Rootman J, Nugent RA, et al. Optic nerve sheath meningiomas. Ophthalmology. 2003;110(10):2019–30. Epub 2003/10/03. PubMed PMID: 14522782. https://doi.org/10.1016/S0161-6420(03)00787-5.
21. Ben Simon GJ, Syed HM, Douglas R, et al. Extraocular muscle enlargement with tendon involvement in thyroid-associated orbitopathy. Am J Ophthalmol. 2004;137(6):1145–7. Epub 2004/06/09. PubMed PMID: 15183812. https://doi.org/10.1016/j.ajo.2004.01.033.
22. Demirci H, Shields CL, Karatza EC, et al. Orbital lymphoproliferative tumors: analysis of clinical features and systemic involvement in 160 cases. Ophthalmology. 2008;115(9):1626–31, 31 e1–3. Epub 2008/04/29. PubMed PMID: 18440641. https://doi.org/10.1016/j.ophtha.2008.02.004.

23. Young SM, Kim YD, Shin HJ, et al. Lacrimal gland pleomorphic adenoma and malignant epithelial tumours: clinical and imaging differences. Br J Ophthalmol. 2018. Epub 2018/04/24. PubMed PMID: 29680804. https://doi.org/10.1136/bjophthalmol-2017-311538.
24. Lacey B, Chang W, Rootman J. Nonthyroid causes of extraocular muscle disease. Surv Ophthalmol. 1999;44(3):187–213. Epub 1999/12/10. PubMed PMID: 10588439
25. Wenig BM, Mafee MF, Ghosh L. Fibro-osseous, osseous, and cartilaginous lesions of the orbit and paraorbital region. Correlative clinicopathologic and radiographic features, including the diagnostic role of CT and MR imaging. Radiol Clin N Am. 1998;36(6):1241–59, xii. Epub 1999/01/13. PubMed PMID: 9884700.

6 Specific Orbital Inflammatory Diseases

Alan A. McNab

Introduction

Orbital inflammatory processes form a very large proportion of orbital disease in clinical practice. They can be divided into infective (bacterial cellulitis, viral, and parasitic infections) and non-infective. Non-infective inflammation can in turn be divided into specific forms of inflammation and non-specific, the latter sometimes termed idiopathic orbital inflammation (IOI) or, in the past, orbital pseudotumor. IOI should be a diagnosis of exclusion, and in order to exclude a more specific disease process, appropriate investigations should be undertaken rather than simply assuming a diagnosis based on clinical and imaging features and treating the patient with the blunt instrument of systemic corticosteroids. Every effort should be made to establish a diagnosis, and this will require appropriate blood tests and in most instances, a tissue diagnosis (biopsy), which is then examined appropriately by a pathologist knowledgeable in the field of orbital pathology.

Of the specific forms of orbital inflammation, Graves' orbitopathy (or thyroid-related orbitopathy, or thyroid eye disease, etc.) is by far the commonest. The group of idiopathic orbital inflammations (non-specific inflammation) is covered elsewhere. This chapter will focus on the specific orbital inflammatory processes, most of which are in a sense "idiopathic" also, but they do have specific clinical (local and systemic) and pathological features and increasingly more targeted therapies, which makes the establishment of as precise a diagnosis as possible all the more important.

The group of specific orbital inflammatory diseases has enlarged in recent years with the recognition of IgG4-related disease. This has reduced the proportion of cases of non-infective orbital inflammation which is idiopathic (IOI). It seems likely that as investigative tools become more sophisticated, the pool of patients with IOI will become smaller still (Table 6.1).

Table 6.1 Specific orbital inflammatory diseases

1. Granulomatous inflammations
Sarcoidosis
Xanthogranulomatous disorders
Adult-onset xanthogranuloma (AOX)
Adult-onset asthma and periocular xanthogranuloma (AAPOX)
Necrobiotic xanthogranuloma (NBX)
Erdheim-Chester disease (ECD)
2. Sjögren's syndrome
3. Vasculitic diseases
Granulomatosis with polyangiitis (GPA, previously called Wegener's granulomatosis)
Eosinophilic granulomatosis with polyangiitis (Churg-Strauss syndrome)
4. IgG4-related disease

A. A. McNab (✉)
Orbital Plastic and Lacrimal Clinic, Royal Victorian Eye and Ear Hospital, Melbourne, VIC, Australia

C. J. Hwang et al. (eds.), *Clinical Ophthalmic Oncology*,
https://doi.org/10.1007/978-3-030-13558-4_6

Granulomatous Orbital Diseases

Granulomatous inflammation is a very specific form of inflammation characterized by the formation of granulomas with giant cells and macrophages or histiocytes. Sarcoidosis is the commonest cause of granulomatous inflammation in the orbit, and the granulomatous inflammation in sarcoidosis is non-necrotizing. Other causes of granulomatous inflammation such as mycobacterial infection (tuberculosis or atypical mycobacterial infection), in which there is classically necrotizing granulomatous inflammation, fungal infection, or foreign bodies, must all be excluded by the use of appropriate histopathological stains and in some cases by microbiological culture of tissue. Granulomatous inflammation occurs also as part of the vasculitides which affect the orbit (granulomatosis with polyangiitis (GPA or Wegener's granulomatosis) and eosinophilic granulomatosis with polyangiitis or Churg-Strauss syndrome), but these disorders also have vasculitis as a critical part of their disease process and are therefore discussed under the heading of vasculitis.

Sarcoidosis

Sarcoidosis is most commonly a multisystem disease, with the lung, lymph nodes, and skin being common sites of involvement. Its cause remains unknown. In ophthalmic practice, sarcoidosis is more commonly encountered as a cause for uveitis, and ocular adnexal sarcoidosis is much less common. Unexpectedly, the two are often not seen together. The commonest orbital or ocular adnexal tissue to be involved is the lacrimal gland (42–63%), which may be unilateral or bilateral (Fig. 6.1) [1–3]. This is followed by the anterior orbit, where mass lesions may occur, more commonly in the inferior orbit (13–38%) and the eyelid (11–17%) (Fig. 6.2). Less commonly the

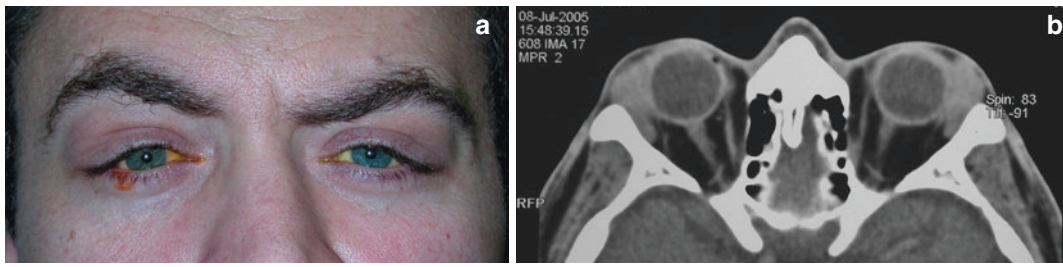

Fig. 6.1 (**a**) A young adult male presented with bilateral painless lacrimal gland enlargement over some months. (**b**) An axial CT scan shows bilateral lacrimal gland enlargement which on biopsy showed non-necrotizing inflammation consistent with sarcoidosis

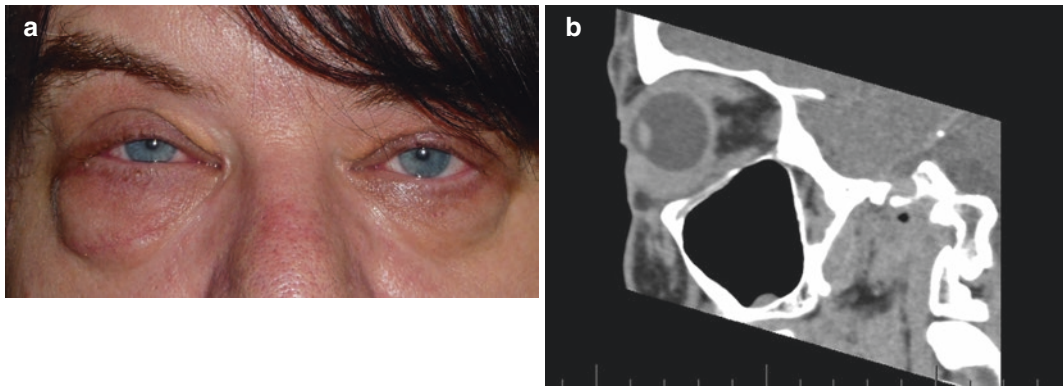

Fig. 6.2 (**a**) A middle-aged male presented with bilateral mostly inferior orbital masses, larger on the right. (**b**) A sagittal CT scan shows an infiltrative mostly in the anterior inferior orbit, shown to be sarcoidosis on biopsy

lacrimal sac and nasolacrimal duct may be involved, often in association with sarcoidosis causing rhinosinusitis. The optic nerve and sheath may also be involved as a manifestation of neurosarcoid, and this may mimic optic nerve sheath meningioma.

Angiotensin-converting enzyme levels are not commonly elevated in ocular adnexal sarcoidosis (20% in one series) [2]. Concurrent systemic disease is common at presentation (50%) [2], with the diagnosis already known (37%) [3] or found on testing (a further 27%) [3]. It may never be found (30%) or develop after some years [3].

Diagnosis can be made by finding the typical changes on biopsy specimens of non-necrotizing granulomatous inflammation, with other causes such as fungal infections and mycobacterial infection excluded by the use of appropriate histochemical stains and in some instances by tissue culture. Supportive evidence in the form of mediastinal and lung disease on chest X-ray or computerized tomography (CT) and elevated angiotensin-converting enzyme or serum calcium can be sought.

Treatment of the ocular adnexal disease, if required, is usually with oral or local injection of steroids or steroid-sparing agents such as methotrexate, and response rates are good.

Xanthogranulomatous Disease

This group of diseases is rare and in adults comprises four entities: adult-onset xanthogranuloma (AOX), adult-onset asthma and periocular xanthogranuloma (AAPOX), necrobiotic xanthogranuloma (NBX), and Erdheim-Chester disease (ECD) [4]. These diseases are non-Langerhans cell histiocytic disorders and have characteristic foamy or lipid-laden macrophages, and Touton giant cells present. Additionally, there is usually a lymphocytic infiltrate, often dominated by CD-20-positive B-cells and some fibrosis.

AOX, AAPOX, and NBX tend to involve the eyelids and anterior orbits, with swelling, erythema, and yellowish discoloration of tissues, sometimes with xanthelasma-like changes in the skin of the eyelids (Fig. 6.3a). The yellowish discoloration extends more deeply into the tissues of the eyelids and anterior orbits. AOX and AAPOX are usually bilateral and symmetrical, although unilateral cases may also occur. Although the lids and anterior orbits are mostly involved, changes can extend along the walls of the orbit, most usually the lateral wall and orbital roof behind the lacrimal gland (Fig. 6.3b). Extraocular muscles can sometimes be enlarged also.

AAPOX and AOX may present similarly in terms of the ocular adnexal features, but in AAPOX, there is adult-onset asthma, usually present for some years prior to the development of the ocular adnexal disease, often along with paranasal sinusitis and reactive lymphadenopathy.

NBX has additional features on histopathology of geographic areas of necrosis often surrounded by palisaded histiocytes. NBX has a strong association with paraproteinemia, either as a monoclonal gammopathy of uncertain

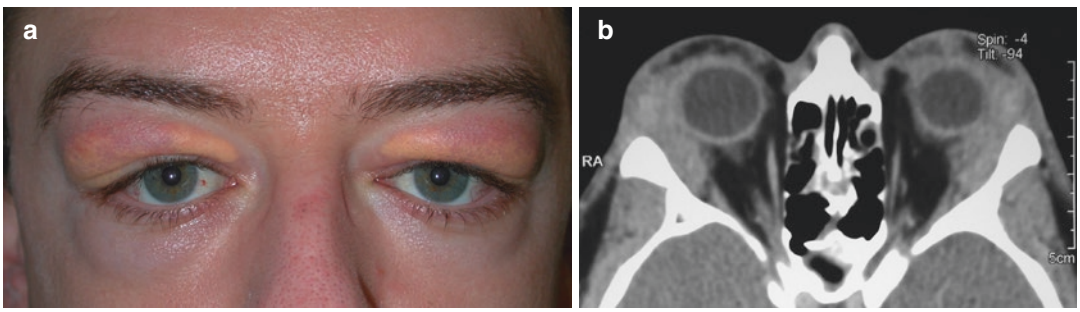

Fig. 6.3 (**a**) A young adult male with yellowish-red swelling of the upper eyelids and anterior orbits, increasing over a year. (**b**) An axial CT scan shows preseptal swelling plus lacrimal gland enlargement bilaterally with disease extending along the posterior lateral orbital walls. Biopsy identified adult-onset xanthogranulomatous (AOX) disease without systemic involvement

significance or multiple myeloma, and occasionally other hematological malignancies.

The treatment of AOX and AAPOX has been usually with oral corticosteroids and other immunosuppressants, with a variable response [4]. Recent reports have shown AOX, AAPOX, and NBX respond very well to rituximab, often with very long periods of complete remission [5, 6].

ECD, although showing features of xanthogranulomatous inflammation, is quite different in many aspects to AOX, AAPOX, and NBX. It usually involves both posterior orbits symmetrically and widely and is a systemic disease often affecting the retroperitoneum, kidney, lung, long bones, pericardium, or meninges and is the only member of this group with an identified *BRAF* gene mutation [7], making it amenable to treatment with monoclonal antibodies such as vemurafenib. Prior to this form of treatment becoming available, it carried a high mortality rate.

Xanthogranulomatous ocular adnexal disease may show significant numbers of IgG4+ plasma cells, sometimes enough to reach the threshold of published diagnostic criteria for IgG4-related disease [7]. However, the presence of other features of xanthogranulomatous inflammation should make the diagnosis obvious. There have however been occasional cases published where features of both diseases have occurred in the same patient, and it may be that there is an overlap of these disease processes, at least in a small proportion of patients [7].

Sjögren's Syndrome

Primary Sjögren's syndrome (pSS), described in 1933 by the Swedish ophthalmologist Henrik Sjögren, is a common systemic autoimmune rheumatic disease causing sicca syndrome (dry mouth, nose, and eyes), swollen salivary glands (and sometimes lacrimal glands), and in some patients, joint, skin, lung, and other disease [8]. Secondary Sjögren's syndrome occurs when similar sicca symptoms occur in patients with other connective or autoimmune conditions.

Depending on the duration of the disease, the lacrimal glands may be swollen [9], normal in size, or atrophic. If swollen, biopsy should be undertaken to help establish the diagnosis and also to exclude the possibility of lymphoma. Usually the lacrimal gland enlargement will be bilateral and relatively symmetrical. Diagnosis without tissue specimens can be difficult and relies on clinical features and serology (anti-Ro and anti-La autoantibodies). Labial salivary gland biopsies can be helpful. Dry eye is usual but is non-specific. Many cases previously diagnosed as "atypical Sjögren's syndrome" (negative serology) were probably IgG4-related disease.

Sjögren's syndrome carries an increased risk of the development of non-Hodgkin's lymphoma, most commonly marginal lymphoma of MALT type, and this has been quantified as a 14-fold increase compared to the normal population [10]. For this reason alone, enlarged lacrimal glands in these patients should be biopsied to exclude lymphoma [11]. Lymphoma tends to occur in sites affected by the Sjögren's syndrome (salivary glands, lacrimal glands, and mucosal surfaces) [11]. Very rarely, a large cystic expansion may occur within the orbital lobe of the lacrimal gland, and in a small reported series, two of three cases also had marginal zone lymphoma within the wall of the cyst [12].

Vasculitic Diseases

The commonest vasculitic disease to affect the orbit is granulomatosis with polyangiitis (GPA, formerly known as Wegener's granulomatosis). Churg-Strauss disease, or eosinophilic granulomatosis with polyangiitis, and polyarteritis nodosa rarely affect the orbit. Giant cell (or temporal) arteritis commonly affects the optic nerve but very rarely other orbital tissues.

Granulomatosis with Polyangiitis

GPA is a rare multisystem disease characterized by granulomatous and sometimes necrotizing small vessel vasculitic disease, which commonly affects the kidneys, lungs, and upper airways (generalized GPA). If untreated it is fatal, but

with modern immunosuppressive therapy and targeted monoclonal antibodies, the morbidity and mortality of this disease are markedly diminished.

Up to 60% of patients with generalized GPA will have orbital or ocular adnexal disease at some point [13]. Conversely, many patients with orbital disease present with a more localized form of the disease without systemic involvement, although a proportion of these patients may develop systemic disease over time [14, 15]. In this group of patients with the so-called limited form of the disease, the diagnosis may be difficult because of atypical biopsy findings (the classic triad of vasculitis, granulomatous inflammation, and tissue necrosis may be absent in 50–75% of cases) and because c-ANCA is negative in about half the cases with orbital and paranasal sinus disease alone and in two-thirds of those with orbital disease alone [14, 15]. If patients present with purely orbital disease, the risk of transformation to systemic disease in the longer term is small [16].

Patients often present with orbital mass lesions, which are usually adjacent to the paranasal sinuses (Fig. 6.4). Pain, erythema, and edema of the eyelids are commonly seen. If the lesion is large or involves the posterior orbit, then optic neuropathy may occur. Restrictive strabismus from extraocular muscle involvement is also common (Fig. 6.4). Lacrimal gland disease, unilateral or bilateral, may be the presenting feature, being the sole feature in some, but more than half the patients presenting with lacrimal gland involvement will have features of disease elsewhere in the orbit and paranasal sinuses, again often with loss of bone in the orbital walls or within the nasal cavity and paranasal sinuses (Fig. 6.4) [17]. Many patients will have also ocular features such as scleritis, sclerokeratitis, or retinal vasculitis in addition to their orbital and ocular adnexal disease.

The presence of nasal and paranasal sinus disease, often with associated bone destruction, is very suggestive of GPA (Fig. 6.4) [16, 17]. Up to half of patients with orbital and ocular adnexal GPA will have lacrimal obstruction as part of their symptomatology [15]. Disease of the nasal cavity and paranasal sinuses can affect the nasolacrimal duct, or orbital disease, which is often in the inferomedial orbit, can involve the lacrimal sac. If surgery for lacrimal obstruction is performed, ideally

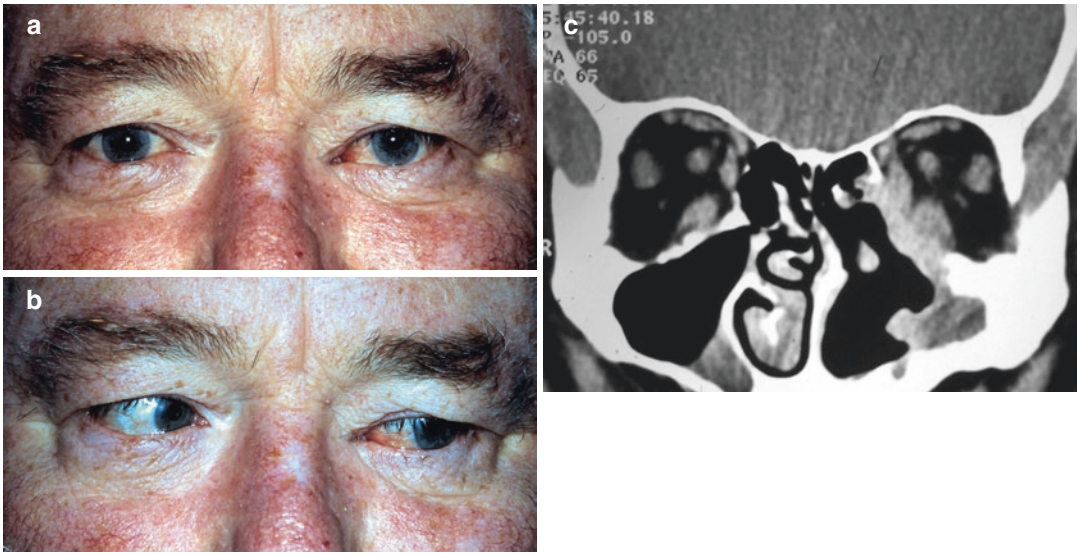

Fig. 6.4 (**a**) An elderly male complained of left epiphora and diplopia on left gaze. (**b**) He had limited left eye abduction and a hard mass in the inferomedial orbit, with complete lacrimal obstruction. (**c**) A coronal CT scan shows a mass in the inferomedial orbit with loss of bone in the medial orbital wall as well as destruction of normal intranasal structures on that side due to granulomatosis with polyangiitis, without renal or pulmonary disease

the patient should have the disease controlled with appropriate immunosuppression at the time of surgery. Care should be taken to make sure there is an adequate nasal airway medial to the lacrimal sac fossa in which to open the rhinostomy. Patients with more advanced nasal disease may have nasal collapse and dense fibrosis between the lateral nasal wall and nasal septum making a dacryocystorhinostomy impossible. However, if the disease is controlled and the nasal anatomy satisfactory, then high rates of success can be achieved with lacrimal bypass surgery in patients with GPA [18], either as an external or endonasal dacryocystorhinostomy.

A proportion of patients previously diagnosed with idiopathic orbital inflammation may have limited GPA. This stresses the importance of obtaining tissue samples in patients with orbital inflammatory disease, considering repeat biopsies and also repeating imaging and serology over time to see if features of GPA develop or the patient develops a positive c-ANCA. A recent study of pooled orbital biopsy specimens in patients with idiopathic orbital inflammation found a small proportion had gene expression profiles matching those with established GPA [19].

Before immunosuppressive therapy became available for the treatment of GPA in the 1970s, the disease had a high mortality rate, with a median survival of 5 months and a greater than 80% mortality in the first year after diagnosis [20]. Treatment with corticosteroids and cyclophosphamide, or other agents such as methotrexate or azathioprine, transformed the outlook for GPA patients, with 95% survival at 5 years. Treatment is aimed at inducing remission and maintaining remission, but patients usually need to stay on maintenance treatment disease of steroids and other immunosuppressants. More recently, the anti-CD20 monoclonal antibody rituximab has been shown to be very effective in GPA, with remission rates similar to steroids and cyclophosphamide, but with a lesser side effect profile [21].

Surgery has a limited role in the management of orbital GPA. Apart from obtaining tissue for diagnostic purposes and lacrimal bypass surgery, occasionally patients will benefit from debulking surgery for large orbital masses, or decompression of the orbit, or exceptionally exenteration for control of severe orbital disease with blindness and pain not responsive to other treatments. Care should be taken in embarking on surgery in patients with vasculitis, however, as tissue healing is often poor and surgery may lead to further tissue breakdown or fistula formation.

Eosinophilic Granulomatosis with Polyangiitis (Churg-Strauss Syndrome)

Churg-Strauss syndrome is characterized by the triad of asthma, eosinophilia, and vasculitis. Histopathologically, there is granulomatous inflammation with abundant eosinophils and vasculitis. Asthma and rhinosinusitis often precedes the development of eosinophilia and then vasculitis. Churg-Strauss syndrome very rarely affects the orbit and has more commonly produced retinal vasculitis and occlusions, uveitis, optic neuropathy, scleritis and episcleritis, and granulomatous conjunctivitis. However, cases of dacryoadenitis [22], orbital inflammatory masses [23], and diffuse bilateral orbital inflammation [24] have been described.

IgG4-Related Disease

IgG4-related disease (IgG4-RD) is a recently recognized entity characterized by tumefactive lesions with dense lymphoplasmacytic infiltration, rich in IgG4-positive plasma cells, fibrosis, usually of a storiform pattern, and in some organs, an obliterative phlebitis. Serum IgG4 levels may be elevated or normal. The orbit is a frequently involved site (when the preferred term is IgG4-related ophthalmic disease or IgG4-ROD), and the majority of patients with orbital disease will have disease elsewhere, making the establishment of the diagnosis of increased importance.

The disease was first hinted at by the Japanese in 2001, in a group of patients with autoimmune pancreatitis (AIP) who had elevated serum IgG4

levels [25]. It was soon recognized that extrapancreatic fibro-inflammatory lesions, rich in IgG4+ plasma cells, were common in patients with AIP. Since then, the condition has been described in almost all organs, with lacrimal gland being one of the earliest recognized. Other commonly involved sites include the biliary tree, retroperitoneum, salivary glands, orbit, lymph nodes, kidneys, lungs, meninges, aorta, breast, prostate, thyroid, pericardium, and skin. A number of diseases have now been recognized as part of the spectrum of IgG4-RD, and these include sclerosing cholangitis, Mikulicz's disease, Küttner's tumor (sclerosing sialadenitis), Riedel's thyroiditis, multifocal fibrosis, Ormond's disease (idiopathic retroperitoneal fibrosis), and others.

IgG4 is the fourth and smallest subclass of IgG, and the exact role, if any, of the IgG4+ plasma cells and IgG4 itself in the disease process remains unknown, and it may have either a primary or secondary role. While the pathogenesis remains unknown, a useful analogy is with sarcoidosis, in which there is a well-defined pathological change in multiple organs, also of unknown pathogenesis.

Diagnostic criteria for IgG4-RD (both clinical and pathological) and IgG4-ROD have been published. For the histopathological criteria, a consensus statement [26] suggests a three-tier diagnostic terminology:

1. Highly suggestive histologically of IgG4-RD
2. Probable histological features of IgG4-RD
3. Insufficient histological evidence of IgG4-RD

The first category requires at least two of the characteristic features (dense lymphoplasmacytic infiltrates, storiform fibrosis, and obliterative phlebitis) except in lacrimal gland where the latter two findings are usually absent. The IgG4+ plasma cell counts required for different organs vary from 10 to 200/hpf. An elevated IgG4+/IgG+ plasma cell ratio of >40% is also required. The second category, probable histological features of IgG4-RD, usually involves cases with a single histological feature and required numbers of IgG4+ plasma cells.

Umehara et al. attempted to define comprehensive diagnostic criteria for IgG4-RD, combining clinical and pathological features [27]. They used three criteria:

1. Clinical examination showing characteristic diffuse/localized swelling or masses in single or multiple organs
2. Serum IgG4 levels ≥ 135 mg/dl
3. Histopathology showing:
   (a) Marked lymphocytic and plasmacytic infiltration and fibrosis
   (b) Infiltration of IgG4+ plasma cells, with the ratio of IgG4+/IgG+ cells >40% and > 10 IgG4+ plasma cells/hpf

They defined three categories of patients:

- Definite IgG4-RD: 1 + 2 + 3
- Probable IgG4-RD: 1 + 3
- Possible IgG4-RD: 1 + 2

A Japanese ophthalmological study group later published criteria for IgG4-ROD [28]:

1. Imaging studies show enlargement of the lacrimal gland, trigeminal nerve, or extraocular muscle as well as masses, enlargement, or hypertrophic lesions in various ophthalmic tissues.
2. Histopathological examination shows marked lymphocyte and plasma cell infiltration and sometimes fibrosis. A germinal center is frequently observed. IgG4+ plasma cells are found and satisfy the following criteria: ratio of IgG4+ cells to IgG+ cells of 40% or above or more than 50 IgG4+ cells per high-power field (X400).
3. Blood tests show elevated serum IgG4 (>135 mg/dl).

The diagnosis is classified as "definitive" if 1, 2, and 3 are satisfied, "probable" when 1 and 2 are satisfied, and "possible" when 1 and 3 are satisfied.

It is important to recognize that IgG4+ plasma cells and an elevated serum IgG4 level can be found in a variety of other pathological processes

including inflammatory diseases (granulomatosis with polyangiitis or Wegener's granulomatosis [29] as well as xanthogranulomatous diseases [30]) and neoplasms, and it is important to exercise caution in making the diagnosis of IgG4-RD.

Much of the published literature on IgG4-RD is from Asia (Japan, Korea, and Hong Kong), but there is no evidence that IgG4-RD is commoner there [30]. AIP (IgG4-related pancreatitis) has a strong male predominance (2.8–7.5:1), the opposite for most other autoimmune diseases. Head and neck IgG4-RD however has a more even male/female ratio. The mean age of onset for IgG4-ROD is 55 years (slightly younger than for AIP – mean 58–69). Rare cases have been reported in children.

Between 39% and 48% of patients with AIP will have or develop lacrimal or salivary gland lesions [31]. Patients presenting with IgG4-ROD will have systemic disease (disease elsewhere) at presentation about 50% of the time. Between 25% and 40% of cases, historically labeled idiopathic orbital inflammation or reactive lymphoid hyperplasia has been shown to be IgG4-ROD.

Most patients have an indolent, chronic disease without an obvious acute inflammatory process at any time. Symptoms of inflammation such as pain, redness, and swelling are rarely seen. IgG4-ROD may present in many ways, but commoner patterns include:

- Lacrimal gland swelling, usually bilateral, and sometimes associated with symmetrically enlarged salivary glands (submandibular and parotid, previously called Mikulicz's disease) (Fig. 6.5)
- Enlargement of the infraorbital nerve(s) (IONE) (Fig. 6.6) or frontal nerve(s) (Fig. 6.7) associated with lacrimal gland disease, extraocular muscle disease, patchy orbital fat involvement, paranasal sinusitis, and often peripheral eosinophilia
- Sclerosing orbital inflammation, sometimes with adjacent lacrimal drainage apparatus and nasal involvement
- Rarely, scleritis and mild anterior uveitis, exceptionally, conjunctival disease associated with scleritis [31] or even isolated conjunctival involvement [32]

Some reports have shown a proportion of periocular xanthogranulomatous disease have numbers of IgG4+ plasma cells which reach IgG4-ROD diagnostic levels, but the relationship between IgG4-ROD and xanthogranulomatous disease remains unknown. It may be that there is a small overlap between the two groups of conditions [7].

IONE, unilateral or bilateral, is a strong marker for IgG4-ROD. Interestingly, patients with AIP have been shown to have statistically larger infraorbital nerves than controls [33]. Despite the sometimes grossly enlarged nerves, sensory loss in the distribution of the involved nerves is rare [34]. Other nerves may be affected, including perioptic nerve lesions. Bony expansion of the infraorbital canal is often seen.

Patients may have symptomatic or asymptomatic IgG4-related disease elsewhere, with the salivary gland, pancreas, hepatobiliary tree, lymph nodes, retroperitoneum, kidneys, and aorta being commoner, but almost any organ can be affected. Disease elsewhere may be present at the same time, or develop later, often after many years [31].

In common with a number of other chronic inflammatory diseases, IgG4-RD appears to predispose to the development of lymphoma, which is usually low-grade marginal zone lymphoma of MALT type [35]. Reports suggest this risk is about 10%.

Establishing the diagnosis requires the integration of clinical features, blood tests, imaging, and histopathology. Histopathology is the key to the diagnosis with classic features being:

(a) An often dense lymphoplasmacytic infiltrate
(b) Fibrosis, classically in a storiform pattern (not usually seen in the lacrimal gland)
(c) Obliterative phlebitis (more usually seen in pancreas and larger organs, not in the lacrimal gland)
(d) The presence of significant numbers of IgG4+ plasma cells (the numbers required to reach published diagnostic criteria have varied, minimum 10/high-power field, up to 100/hpf)

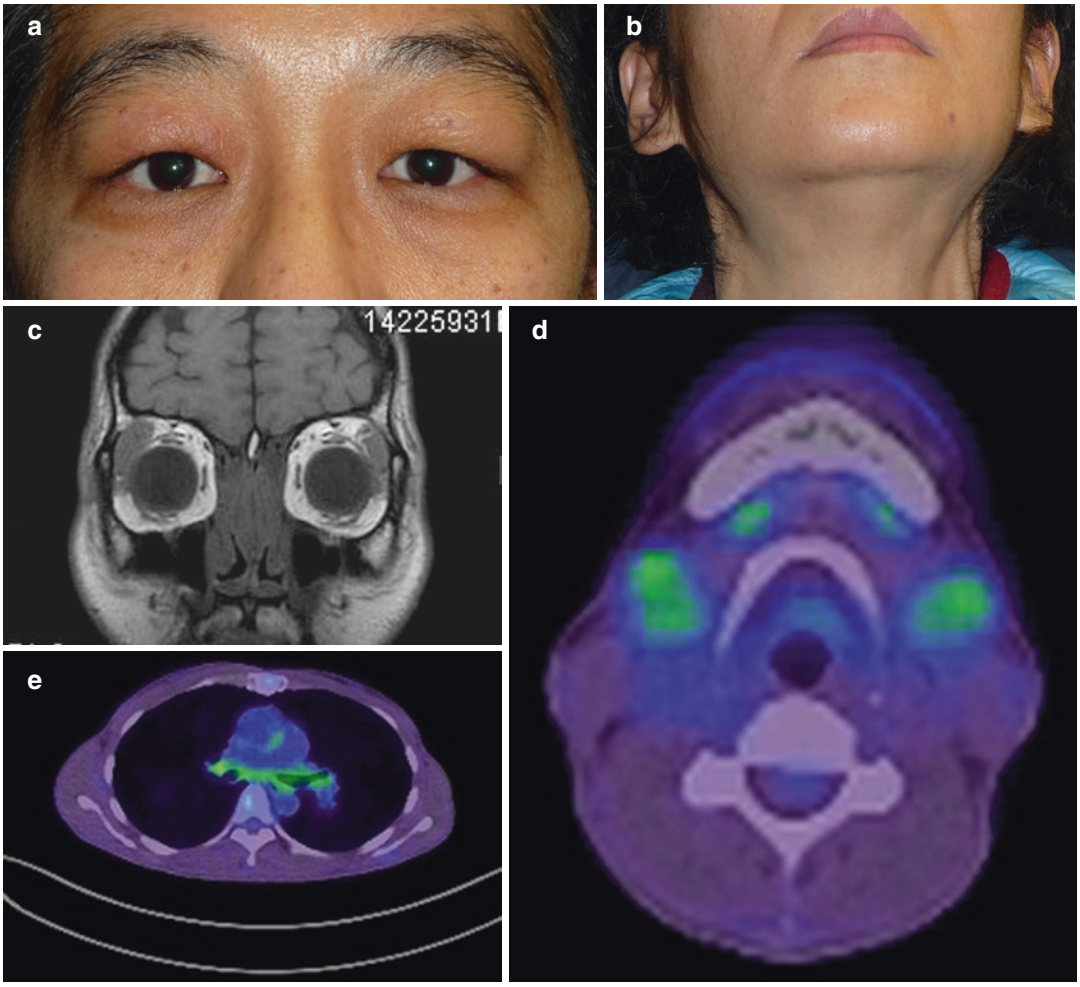

Fig. 6.5 (**a**) A middle-aged female presented with several months of painless bilateral upper outer eyelid swelling, nasal obstruction, and reduced exercise tolerance. (**b**) She also had enlarged submandibular glands. (**c**) MRI showed symmetrical enlargement of both lacrimal glands, which on biopsy showed features consistent with Ig4-related disease, as well as rhinosinusitis. (**d**) PET-CT scans showed uptake in the submandibular glands. (**e**) There was also uptake on PET-CT in the main bronchi of both lungs

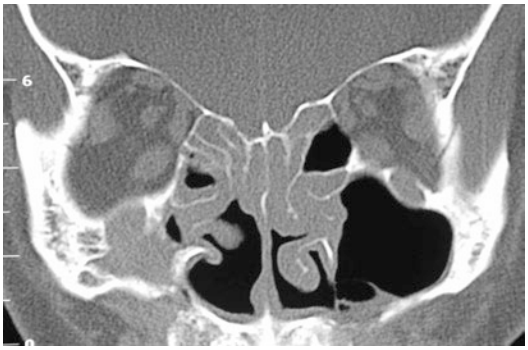

Fig. 6.6 A coronal CT of a patient with long-standing definite IgG4-related disease, with chronic sinus disease and bilateral enlargement of the infraorbital nerves and bony canals

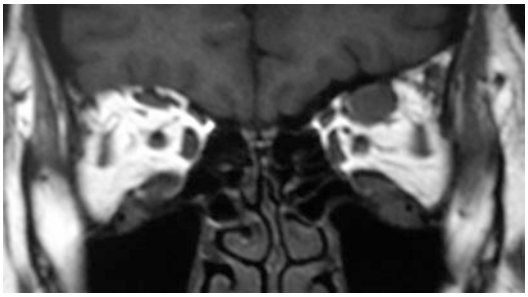

Fig. 6.7 A coronal MRI of a patient with definite IgG4-related disease has enlargement of both infraorbital nerves but also the left frontal nerve (biopsy proven). She also has sclerosing cholangitis, cervical lymphadenopathy, and lacrimal and salivary gland enlargement

(e) A ratio of IgG4+ plasma cells to IgG+ plasma cells of at least 40% (this is probably more important than absolute numbers)
(f) Large numbers of eosinophils [30]

Caution should be exercised in making the diagnosis when features such as granulomatous inflammation, infiltration with polymorphs, or necrosis are present. Many other diseases can have significant numbers of IgG4+ plasma cells present. While serum IgG4 elevation may be helpful, it is not diagnostic. Levels above 135 mg/dl form part of the diagnostic criteria of IgG4-related disease, but on their own, are not diagnostic. Recent studies have suggested that elevated numbers of IgG4+ circulating plasmablasts may be a more useful marker for disease and disease activity and response to treatment [36].

To determine whether IgG4-related disease is present in other anatomical sites, the first step is a thorough clinical history and examination. This might be best performed by a physician such as a rheumatologist or immunologist. Blood tests to look for other organ involvement might include liver function tests, renal function, renal ultrasound (to exclude obstructive nephropathy from retroperitoneal fibrosis), and serum IgG4 levels. Imaging by either CT or MRI from the head and neck to the pelvis should detect other tumefactive lesions and retroperitoneal disease. PET-CT scanning may be very useful in detecting disease activity in all anatomical sites, including the retroperitoneum, aorta, and other difficult-to-image sites. PET-CT may also be useful in monitoring response to treatment [37].

IgG4-ROD is generally an indolent, chronic process, and it may progress slowly over many years and evolve from single organ to multiple organ involvement. This evolution can be seen in the orbit also where patients may present initially with bilateral lacrimal and other gland enlargement and then over time (years) may develop IONE enlargement, extraocular muscle disease, and paranasal sinus disease [31].

The disease process can lead to organ damage and loss of function, and IgG4-ROD can lead to visual loss in a small number of cases, usually by optic nerve compression. These are good reasons to establish the diagnosis by appropriate tissue biopsy, careful histopathological examination, and disease staging. The risk of developing lymphoma is also to be borne in mind.

Treatment of IgG4 disease is usually with corticosteroids with or without other immunosuppressants. It should be borne in mind that spontaneous resolution of IgG4-RD has been noted occasionally. Corticosteroids are the mainstay of treatment. No benefit for IV-steroids over oral steroids has been shown. The optimal initial dose is unknown, but patients are often started on 0.6 mg/kg/day and tapered by 5 mg every 1–2 weeks. A maintenance dosage of 5 mg has been shown to reduce the rate of recurrence in AIP, and it may be prudent to do the same for patients with IgG4-ROD, particularly as a significant proportion will initially respond to corticosteroids then relapse on a taper. Other immunosuppressants such as methotrexate, mycophenolate, and cyclophosphamide have been used, but the most dramatic responses have been recorded with the use of the anti-CD20 antibody rituximab [38].

A very small number of cases of IgG4-ROD treated with low-dose radiotherapy have been reported, with variable response. The rationale for radiotherapy is based on the response of reactive lymphoid lesions and low-grade lymphomas to this modality [31].

The main and essential role for surgery is in obtaining biopsy material. Rarely bulky nonfunctioning lacrimal glands may be excised. Rare cases of optic nerve compromise due to compression that do not respond to medical treatment may benefit from orbital decompression.

As already noted, many patients respond to corticosteroids but with relapse on tapering or ceasing treatment. Nonsteroid immunosuppressants offer an alternative, including rituximab. Reduction in mass lesions gives a good indication of response in IgG4-ROD, as does lowering of serum IgG4, lower IgG4+ plasmablast counts, and loss of positivity of PET-CT scanning of previously involved sites.

Clinical monitoring of orbital disease long-term is advisable because of the risk of relapse or transformation to low-grade lymphoma. Other organ involvement should be monitored by the appropriate specialist.

References

1. Prabhakaran VC, Saeed P, Esmaeli B, et al. Orbital and adnexal sarcoidosis. Arch Ophthalmol. 2007;125:1657–62.
2. Mavrikakis I, Rootman J. Diverse clinical presentations of orbital sarcoid. Am J Ophthalmol. 2007;144:760–75.
3. Demirci H, Christianson MD. Orbital and adnexal involvement in sarcoidosis: analysis of clinical features and systemic disease in 30 cases. Am J Ophthalmol. 2011;151:1074–80.
4. Sivak-Calcott JA, Rootman J, Rasmussen SL, et al. Adult xanthogranulomatous disease of the orbit and ocular adnexa: new immunohistochemical findings and clinical review. Br J Ophthalmol. 2006;90:602–8.
5. Satchi K, McNab AA, Godfrey T, et al. Adult orbital xanthogranuloma successfully treated with rituximab. Ophthalmology. 2014;121:1664–5.
6. Sagiv O, Thakar SD, Morell G, et al. Rituximab monotherapy is effective in treating orbital necrobiotic xanthogranuloma. Ophthal Plast Reconstr Surg. 2018;34:e24–7.
7. McKelvie P, McNab AA, Hardy TG, et al. Comparative study of clinical, pathological, radiological, and genetic features of patients with adult ocular adnexal xanthogranulomatous disease, Erdheim-Chester disease, and IgG4-related disease of the orbit/ocular adnexa. Ophthal Plast Reconstr Surg. 2017;33:112–9.
8. Rischmueller M, Tieu J, Lester S. Primary Sjögren's syndrome. Best Pract Res Clin Rheumatol. 2016;30:189–220.
9. Parkin B, Chew JB, White VA, et al. Lymphocytic infiltration and enlargement of the lacrimal glands. A new subtype of primary Sjögren's syndrome? Ophthalmology. 2005;112:2040–7.
10. Liang Y, Yang Z, Qin B, Zhong R. Primary Sjögren's syndrome and malignancy risk: a systematic review and meta-analysis. Ann Rheum Dis. 2014;73:1151–6.
11. Tonami H, Matoba M, Yokata H, et al. Mucosa-associated lymphoid tissue lymphoma in Sjögren's syndrome. Am J Roentgenol. 2002;179:485–9.
12. Cassidy DT, McKelvie P, Harris GJ, et al. Lacrimal gland orbital lobe cysts associated with MALT lymphoma and primary Sjögren's syndrome. Orbit. 2005;24:257–63.
13. Muller K, Lin JH. Orbital granulomatosis with polyangiitis (Wegener granulomatosis). Arch Pathol Lab Med. 2014;138:1110–4.
14. Harman LE, Margo CE. Wegener's granulomatosis. Surv Ophthal. 1998;42:458–80.
15. Woo TL, Francis IC, Wilcsek GA. Australasian orbital and adnexal Wegener's granulomatosis. Ophthalmology. 2001;108:1535–43.
16. Tan LT, Davagnanam I, Isa H, et al. Clinical and imaging features of orbital granulomatosis with polyangiitis and the risk of systemic involvement. Ophthalmology. 2014;121:1304–9.
17. Tan LT, Davagnanam I, Isa H, et al. Clinical and imaging features of lacrimal gland involvement in granulomatosis with polyangiitis. Ophthalmology. 2015;122:2125–9.
18. Lee BJ, Nelson CC, Lewis CD, et al. External dacryocystorhinostomy in patients with Wegener granulomatosis. Ophthal Plast Reconstr Surg. 2012;28:389–92.
19. Rosenbaum JT, Choi D, Wilson DJ, et al. Orbital pseudotumor can be a localized form of granulomatosis with polyangiitis as revealed by gene expression profiling. Exp Mol Pathol. 2015;99:271–8.
20. Pakrou N, Selva D, Leibovitch I. Wegener's granulomatosis: ophthalmic manifestations and management. Semin Arthritis Rheum. 2006;35:284–92.
21. Taylor SR, Salama AD, Joshi L, et al. Rituximab is effective in the treatment of refractory ophthalmic Wegener's granulomatosis. Arthritis Rheum. 2009;60:1540–7.
22. McNab AA. Orbital inflammation in Churg-Strauss syndrome. Orbit. 1998;17:203–5.
23. Heine A, Beck R, Stropahi G, et al. Inflammatory pseudotumour of the anterior orbit. A symptom in allergic granulomatous angiitis (Churg-Strauss syndrome). Ophthalmologe. 1995;92:870–3.
24. Pradeep TG, Prabhakaran VC, McNab A, et al. Diffuse orbital inflammation in Churg-Strauss syndrome. Ophthal Plast Reconstr Surg. 2010;26:57–9.
25. Hamano H, Kawa S, Horiuchi A, et al. High serum IgG4 concentrations in patients with sclerosing pancreatitis. N Engl J Med. 2001;344:732–8.
26. Deshpande V, Zen Y, Chan JKC, et al. Consensus statement on the pathology of IgG4-related disease. Hum Pathol. 2012;25:1181–92.
27. Umehara H, Okazaki K, Masaki Y, et al. Comprehensive diagnostic criteria for IgG4-related disease (IgG4-RD), 2011. Mod Rheumatol. 2012;22:21–30.
28. Goto H, Takahira M, Azumi A, Japanese Study Group for IgG4-Related Ophthalmic Disease. Diagnostic criteria for IgG4-related ophthalmic disease. Jpn J Ophthalmol. 2015;59:1–7.
29. Chang SY, Keogh KA, Lewis JE, et al. IgG4-positive plasma cells in granulomatosis with polyangiitis (Wegener's): a clinicopathological and immunohistochemical study on 43 granulomatosis with polyangiitis and 20 control cases. Hum Pathol. 2013;44:2432–7.
30. McNab AA, McKelvie P. IgG4-related ophthalmic disease. Part I: background and pathology. Ophthal Plast Reconstr Surg. 2015;31:83–8.
31. McNab AA, McKelvie P. IgG4-related ophthalmic disease. Part II: clinical aspects. Ophthal Plast Reconstr Surg. 2015;31:167–78.
32. Aziz HA, Villa-Forte A, Plesec TP, et al. Isolated conjunctival inflammation suggestive of IgG4-related disease. Ocul Oncol Pathol. 2015;2:51–3.
33. Watanabe T, Fujinaga Y, Kawakami S, et al. Infraorbital nerve swelling associated with autoimmune pancreatitis. Jpn J Radiol. 2011;29:194–201.
34. Hardy TG, McNab AA, Rose GE. Enlargement of the infraorbital nerve: an important sign associated with orbital reactive lymphoid hyperplasia or IgG4-related inflammation. Ophthalmology. 2014;121:1297–303.

35. Cheuk W, Yuen HKL, Chan ACL, et al. Ocular adnexal lymphoma associated with IgG4+ chronic sclerosing dacryoadenitis: a previously undescribed complication of IgG4-related sclerosing disease. Am J Surg Pathol. 2008;32:1159–67.
36. Wallace ZS, Mattoo H, Carruthers M, et al. Plasmablasts as a biomarker for IgG4-related disease, independent of serum IgG4 concentrations. Ann Rheum Dis. 2015;74:190–5.
37. Ebbo M, Grados A, Guedj E, et al. Usefulness of 2-[18F]-flouro-2-deoxy-D-glucose-positron emission tomography/computed tomography for staging and evaluation of treatment response in IgG4-related disease: a retrospective multicenter study. Arthritis Care Res (Hoboken). 2014;66:86–96.
38. Khosroshahi A, Bloch DB, Deshpande V, et al. Rituximab therapy leads to rapid decline of serum IgG4 levels and prompt clinical improvement in IgG4-related systemic disease. Arthritis Rheum. 2010;62:1755–62.

Idiopathic Orbital Inflammation

7

Ilse Mombaerts

Introduction

Idiopathic orbital inflammation (IOI) is a term applied to a poorly understood orbit-specific disorder characterized by an enlarged orbital structure or mass consisting of nonspecific inflammation without identifiable local or systemic cause [1]. Based on the primary involvement of anatomic structures, IOI is anatomically categorized into *idiopathic dacryoadenitis* (lacrimal gland) and *idiopathic orbital myositis* (extraocular muscles). When located in the orbital fibrofatty matrix or involving several structures, it is grossly referred to as – diffuse – IOI. Myositis represents a specific subentity and is segregated as *myositic* IOI, with the other lesions (i.e., idiopathic dacryoadenitis, orbital fat IOI) as *nonmyositic* IOI. Depending on histologic findings, nonmyositic IOI is further subdivided into *sclerosing* and *nonslerosing* IOI (Table 7.1) [2].

Table 7.1 Idiopathic orbital inflammation: clinical and histopathological categories

Clinical category	Predominant involvement	Histopathological categories
Orbital myositis	Extraocular muscles	
Dacryoadenitis	Lacrimal gland	Sclerosing
		Nonsclerosing
Diffuse orbital inflammation	Fibrofatty matrix or involving several structures	Sclerosing
		Nonsclerosing

Historical Perspective and Terminology

In Victorian and Edwardian times, space-occupying lesions were commonly considered malignant until proven otherwise, relying on surgical exploration, histological examination and observation. The earliest reported possible case of IOI can be traced back to 1850, describing the illustrious patient Austrian Field Marshal Count Radetzky sufferring from a clinically suspected malignant orbital tumor who was cured with homeopathic treatment [3]. In 1895, Panas coined the French term *pseudoplasm malin* to describe lesions presenting as a malignant tumor but appearing to be benign on follow-up. The recognition of idiopathic orbital myositis dates back to 1903, when Gleason described a patient with the clinical symptoms of a rapid onset, aggressive

I. Mombaerts (✉)
Department of Ophthalmology, University Hospitals Leuven, Leuven, Belgium

Department of Neurosciences, Catholic University Leuven, Leuven, Belgium
e-mail: ilse.mombaerts@uzleuven.be

C. J. Hwang et al. (eds.), *Clinical Ophthalmic Oncology*,
https://doi.org/10.1007/978-3-030-13558-4_7

bilateral orbital tumor which displayed on histopathological examination inflamed extraocular muscles. In 1905, Birch-Hirschfeld, the son to a pathologist, introduced the concept of *inflammatory orbital pseudotumor* for patients with a clinical presentation of an orbital tumor, and recognized a subset of patients in whom surgery and histopathology revealed a mass composed of chronic nonspecific inflammation with lymphoid follicles. Unfortunately, the term pseudotumor became accepted as a working diagnosis for patients with orbital inflammatory syndrome and unexplained space-occupying lesions. In the 1980s, orbital pseudotumor became erroneously synonymous with orbital inflammation or mass lesions promptly responding to high-dose systemic corticosteroids, despite their low diagnostic yield. This largely contributed to a confusing literature confounded by the inclusion of non-pseudotumoral conditions.

With advanced identification and classification of orbital disorders, the concept of orbital pseudotumor was gradually reduced back to its original definition, i.e., denoting an orbital mass of nonspecific inflammation of unknown cause. For its irrational use, the term orbital pseudotumor fell into disgrace, and alternative names related to histology and presumed pathogenesis were suggested. Of these, IOI, introduced by Jacobiec and Font, and *nonspecific orbital inflammation*, proposed by Rootman, became adopted in the current lexicon.

Pathogenesis

The etiopathogenesis of IOI remains to be defined. Based on its heterogeneous phenotype with unpredictable course, IOI may be considered as an inflammatory process rather than a specific disease [4]. An infectious antigenic precursor has been postulated, which is supported by molecular identifications of an aberrant cell-mediated type 1 helper T-cell (T_H1) pathway, particularly in sclerotic idiopathic dacryoadenitis, and Toll-like receptors of the innate immune system [5–7]. In keeping with the infectious theory, there is reported genetic evidence for Epstein-Barr virus in nonsclerotic IOI [8]. T_H2-B-cell humoral immunity has been implicated in the pathogenesis of nonsclerotic idiopathic dacryadenitis [7]. Mast cells have been linked to the fibrogenesis in IOI, with evidence for a role of fibrocytes, which have features of both immune cells and fibroblasts [9, 10].

In patients with myositic IOI, there is an increased prevalence of autoimmune comorbidity, particularly regional enteritis (Crohn's disease) and ulcerative colitis [11–13]. Specimens of presumed IOI share gene expression profiling with those of granulomatosis with polyangiitis (GPA), and, in the lacrimal gland, of sarcoidosis, underscoring the weak concept of a diagnosis of IOI [14, 15].

Epidemiology

IOI affects any age group, with a peak incidence at 50 years in dacryoadenitis and 30 years in myositis. Although patient age has no absolute limit, younger (<10 years) and older (>75 years for nonmyositic and >60 years for myositic IOI) patients are more likely to be classified as having another disease [16]. It is slightly more prevalent in females, without racial preferences. IOI, particularly myositis, may arise during or after pregnancy, although a causal relationship has not been established [17].

Clinical Features

Depending on the orbital tissue involved, degree of inflammation, associated fibrosis, and mass effect, symptoms of IOI vary and can include eyelid swelling, redness and ptosis, proptosis, limited ocular motility, corneal dryness, and visual dysfunction. The onset of presentation is typically acute (within days) or subacute (within weeks), with a subsequent slow rate of progression.

Clinical Subtypes

Idiopathic Dacryoadenitis

Idiopathic dacryoadenitis is featured by acute to subacute onset of upper eyelid swelling, ptosis, and redness and, in 70% of cases, associated with pain, which varies from discomfort and tenderness to severe pain referred to the periorbital region (Fig. 7.1) [18, 19]. Half of the patients with idiopathic dacryoadenitis present with a dry eye and 20% with episcleritis in the superolateral quadrant [19]. Usually only one gland is affected, but bilateral disease, either simultaneously or sequentially, occurs with an incidence of 16–20% [18, 19].

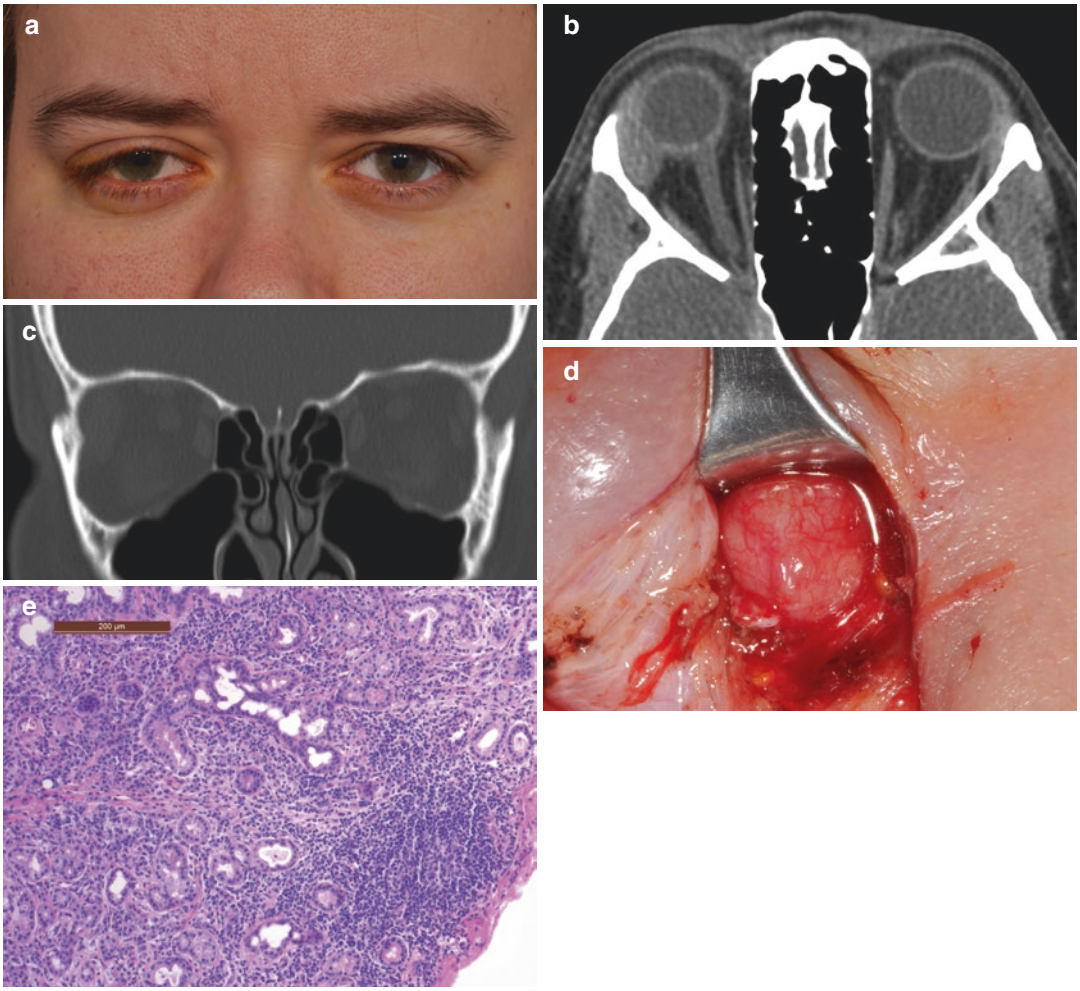

Fig. 7.1 Idiopathic dacryoadenitis. (**a**, *top left*) S-shaped deformity of the right upper eyelid with ptosis and mild swelling. (**b**, *top right*) Axial and (**c**, *middle left*) coronal computerized tomography scan showing diffuse enlargement of the lacrimal gland which appears "almond-shaped." (**d**, *middle right*) Intraoperative view of the lacrimal gland mass, exposed through translid anterior orbitotomy under local anesthesia. (**e**, *bottom left*) Histopathology showing lymphoplasmacytic infiltration with lymphoid follicle formation and acinar and ductal atrophy (hematoxylin and eosin staining, original magnification ×100). The patient recovered uneventfully from debulking surgery without use of anti-inflammatory drugs

Idiopathic Orbital Myositis

Idiopathic orbital myositis typically presents with acute or subacute onset of conjunctival redness, eyelid swelling, orbital pain – which is usually severe, diplopia, and mild proptosis [11]. The feature of acute onset of severe orbital pain distinguishes it from thyroid eye disease. The involved muscle can be clinically identified by episcleral redness at the site of its insertion. Examination of eye motility shows a weakened action of the muscle (Fig. 7.2). The pain is exacerbated on eye movement, particularly on gaze away from the action of the involved muscle, which should not be interpreted as restrictive motility. Bilateral myositis can occur simultaneously or sequentially, with an incidence of 50% [11].

Any extraocular muscle can be affected, but more commonly the horizontal rectus muscles are involved. Idiopathic myositis tends to relapse, in which case the same or contralateral muscle is commonly affected [11]. When different muscles in the same orbit or in the contralateral orbit become involved during recurrences, it is referred to as *migratory idiopathic myositis* [20].

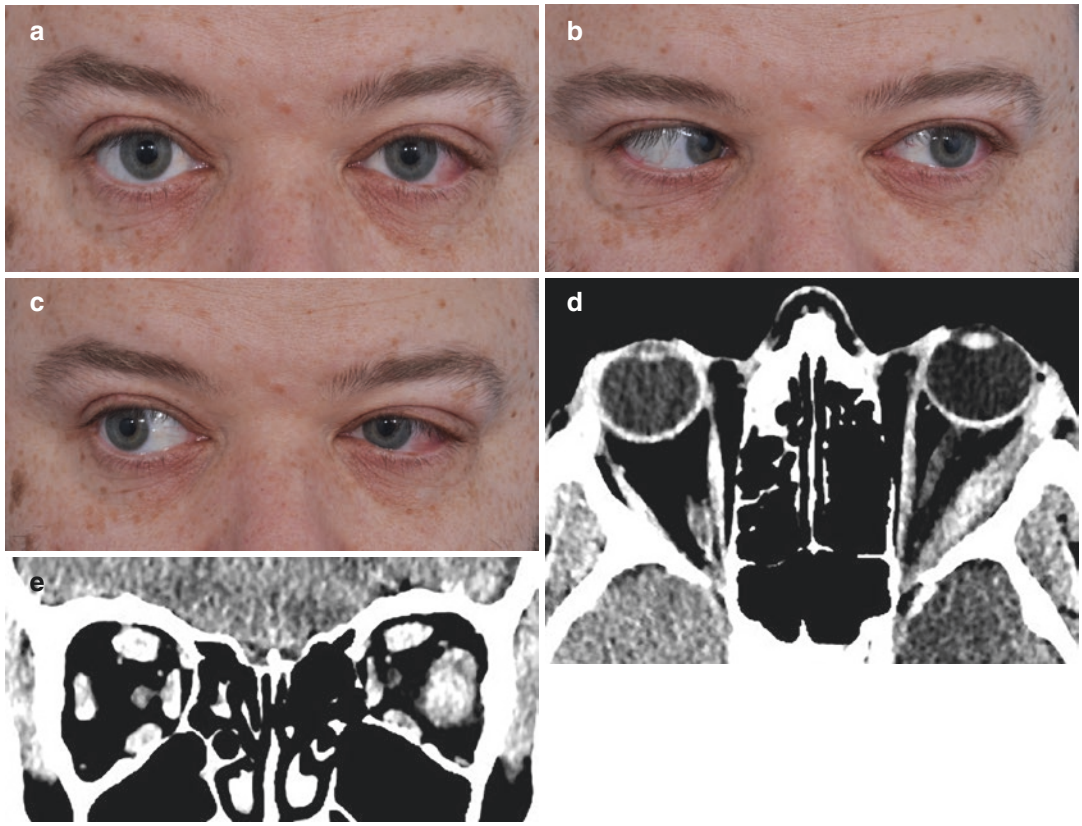

Fig. 7.2 Idiopathic orbital myositis. (**a**, *top left*) Episcleral redness in the lateral sector of the left eye (**b**, *top right*) Limitation on abduction of the left eye. (**c**, *middle left*) Full but painful adduction of the left eye. (**d**, *middle right*) Axial and (**e**, *bottom left*) coronal computerized tomography scan showing diffuse enlargement of the lateral rectus muscle with sparing of the anterior tendon. The patient promptly responded to high-dose corticosteroid treatment with full recovery of the eye motility during the weeks of slow taper of corticosteroids

Orbital Fat IOI

Symptoms of orbital fat IOI include pain, double vision, proptosis, eyelid swelling, and, where the orbital apex is involved, compressive optic neuropathy. Often, the lesions are highly sclerotic on histology, in which case they tend to involve the superolateral, mid-, or apical/posterior orbit, of which 25% extend outside the orbit [21].

Diagnostic Evaluation

Given the variability of the clinical phenotype and lack of robust distinguishing features, making a diagnosis of IOI is difficult. By recent consensus, the diagnosis of nonmyositic IOI should be supported by tissue biopsy, and, of myositic IOI, by responsiveness to high-dose corticosteroids (Fig. 7.3) [16]. This differs from commonly taught practice, in which the diagnostic corticosteroid trial is used for all anatomical subgroups, and biopsies only in the cases of corticosteroid unresponse, or which recur on tapering or ceasing of corticosteroids.

Imaging

CT is as useful as MRI in the evaluation of IOI. The lesions enhance with contrast and, on MRI, may display bright fat-suppressed T2-weighted image signals depending on the amount of tissue edema. Idiopathic dacryoadenitis is marked by a diffuse enlargement of the orbital and palpebral lobe of the gland, which appears as "almond-shaped" (Fig. 7.1). Occasionally, the glandular mass extends into the surrounding orbital structures such as the upper eyelid, lateral and superior rectus muscle, and orbital fat [19].

Idiopathic orbital myositis is featured by diffuse and smooth enlargement of one or several extraocular muscles, with the horizontal recti being most commonly affected (Fig. 7.2). In addition to the muscle belly enlargement, anterior ten-

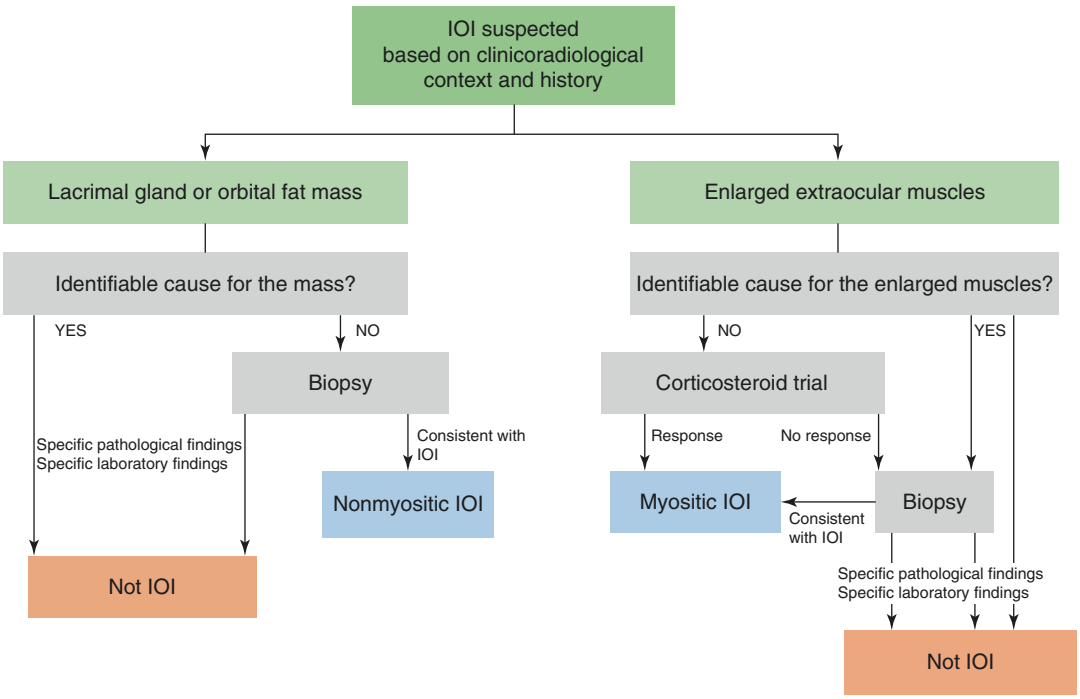

Fig. 7.3 Algorithm for the diagnosis of IOI

don thickening occurs in approximately half of the cases. The feature of tendon enlargement, however, is not pathognomic nor conclusive for a diagnosis of idiopathic myositis, as it is also observed in orbital lymphoma, orbital granulomatous giant cell myositis and thyroid eye disease [22, 23].

Orbital fat IOI presents as an ill-defined infiltrative mass incorporating several orbital structures, often localized in the superolateral orbit [24]. It may spread outside the orbit, via the superior orbital fissure into the cavernous sinus and the middle cranial space or via the inferior orbital fissure into the pterygopalatine and infratemporal fossa [25]. In 36% of cases, extraorbital extension is associated with bone changes, such as erosion, destruction, sclerosis, or remodeling [25]. The association of bony and mucosal changes of the adjacent paranasal sinuses, however, should raise suspicion of other causes such as GPA, lymphoproliferative tumors, malignancy, and immunoglobulin G4-related disease (IgG4-RD).

Laboratory Testing

In patients with suspected IOI, inflammatory and autoimmune markers are measured to eliminate sarcoidosis, GPA, Sjögren's disease, IgG4-RD, and thyroid eye disease as possible cause of the orbital inflammatory lesion [26, 27]. The comprehensive laboratory panel should include [16]:

- White blood cell count with differential, platelet count, calcium, liver function erythrocyte sedimentation rate, C-reactive protein
- Antineutrophil cytoplasmic antibody/proteinase-3, IgG, IgG2, IgG4, angiotensin-converting enzyme, lysozyme
- *In solitary lacrimal gland involvement*
  Add anti-Ro (Sjögren syndrome-A), anti-La (Sjögren syndrome-B), rheumatoid factor, anti-cyclic citrullinated peptide antibody, anti-citrullinated protein antibody, and anti-nuclear antibody titer and pattern.
- *In solitary extraocular muscles involvement*
  Add triiodothyronine (T_3), thyroxine (T_4), thyroid-stimulating hormone, thyroid-stimulating hormone receptor antibody.

In the investigation of systemic diseases, however, inflammatory markers are not diagnostic as they reflect inflammation disregarding the etiology, and normal laboratory findings can be deceptive. Biomarkers and autoantibodies are associated with the burden of disease and thus are frequently false-negative in limited (e.g., orbit-only) or mild systemic disease, and they also confer a likelihood of false-positive results [27, 28].

Known History of Orbital-Related Systemic Disease

The diagnosis of IOI is unlikely in patients with a known history of systemic disease such as sarcoidosis, GPA, Sjögren's disease, IgG4-RD, lymphoproliferative and histiocytic disorders, xanthogranulomatous disease, and metastatic disease. This exclusion criterion is less strict for thyroid disease, as comorbidity of nonmyositic IOI with thyroid eye disease is possible [29]. It is ambiguous if myositic IOI with coexisting Crohn's disease or ulcerative colitis represents a distinct entity or simple coincidence. In the absence of clinical evidence of systemic disease, an internal medicine work-up is not routinely performed, but can be useful in selected cases.

Biopsy

Tissue biopsy is a critical diagnostic step in nonmyositic IOI. Adequate (i.e., large) and representative (i.e., from various involved sites and depths) tissue specimens are obtained by open biopsy. Where corticosteroids or other immunosuppressants are used, they should be stopped several weeks before biopsy to ensure lymphocytic representivity of the tissue. The lesions are accessed through translid or lateral canthotomy orbitotomy without the need to mobilize bone, which are minimally disruptive procedures and can often be performed under local anesthesia [30]. Fine needle aspiration biopsy is not favored as it entails a low diagnostic yield in lesions solid in consistency, as in IOI, and the complete morphological picture cannot be assessed. Biopsy

may be deferred where surgical morbidity is expected to be high, such as in mass lesions confined to the orbital apex or around the optic nerve.

In typical myositic IOI, biopsies are not routinely taken. Atypical myositic cases are suspected of other distinct disease and may warrant muscle biopsy after exclusion of thyroid eye disease. These include painless presentation, all extraocular muscles affected, nodular muscle enlargement, extremely enlarged single muscle, history of primary malignancy, and unresponsiveness to corticosteroids (Fig. 7.3) [31].

Histopathology

IOI is characterized by a mixed polymorphous infiltrate of small, well-differentiated lymphocytes with T-cells outnumbering the B-cells, plasma cells, and neutrophil and eosinophil granulocytes [1]. Other findings include the presence of histiocytes and macrophages. The infiltrate can be focally organized in lymphoid follicles with reactive germinal centers. Presence of granulomas, granulomatous inflammation, vasculitis, and necrosis generally excludes the diagnosis of IOI. In the lacrimal gland, varied degrees of glandular destruction are observed, with the acini early destroyed, followed by the ductules. In the muscle, rhabdomyolysis is seen with loss of normal striations and degeneration of the myofibers.

Connective tissue is often increased with fibrosis, which is not associated with duration of the disease. Where fibrosis is disproportionally prominent and the inflammatory infiltrate paucicellular, the lesion is defined as sclerosing IOI [32]. The finding of sclerotic IOI should prompt investigation to rule out systemic disease such as IgG4-RD and multifocal fibrosclerosis [33, 34]. The finding of fibrosis, lymphoplasmacytic infiltration, and glandular atrophy, however, should not be confused with the intrinsic connective tissue and immunoarchitecture and involutional atrophy of a normal and aging lacrimal gland [35].

The histopathological findings of IOI, particularly where fibrosis is predominant, resemble those of IgG4-RD. The differentiation between the disorders is based on immunohistochemical identification of tissue IgG4-positive plasma cells [36]. In IOI, tissue plasma cell IgG4 positivity is not a prominent finding. With a ratio of IgG4-positive to IgG-positive plasma cells of 40% or less, up to 30 IgG4-positive cells/high-power field for any orbital tissue may be seen in IOI [16]. Notably, similar positive tissue IgG4 stains have been observed in autoimmune and other orbital inflammatory disorders that are unrelated to IgG4-RD. [27, 37]

There is recent evidence that tissue IgG2-positive plasma cells, along with serum IgG2, may represent more specific diagnostic parameters for IgG4-RD. [27]

The Corticosteroid Trial

Patients with orbital inflammatory disease may show dramatic improvement of their signs and symptoms within 48 hours after administration of systemic prednisolone (1 mg/kg/day), referred to as *the corticosteroid trial*. Myositic IOI is characterized by such a dramatic response. In nonmyositic IOI, however, the trial confers a lower positive predictive value, with only 44–79% of cases responding, and has a poor diagnostic specificity since a response is observed in several conditions with an inflammatory component, among which are B- and T-cell lymphoma, metastatic disease, fungal infections, GPA, and sarcoidosis [24, 38–41]. Regrettably, the clinical practice of a corticosteroid trial without biopsy or adequate investigation has introduced unacceptable long delays in a definitive diagnosis of these conditions. Additionally, it is essential to differentiate a lack of response from a frequently encountered rebound of symptoms after tapering of the corticosteroids.

Treatment

Treatment of IOI is tailored to severity of disease to prevent destruction and fibrosis of the orbital structures and to minimize morbidity, such as

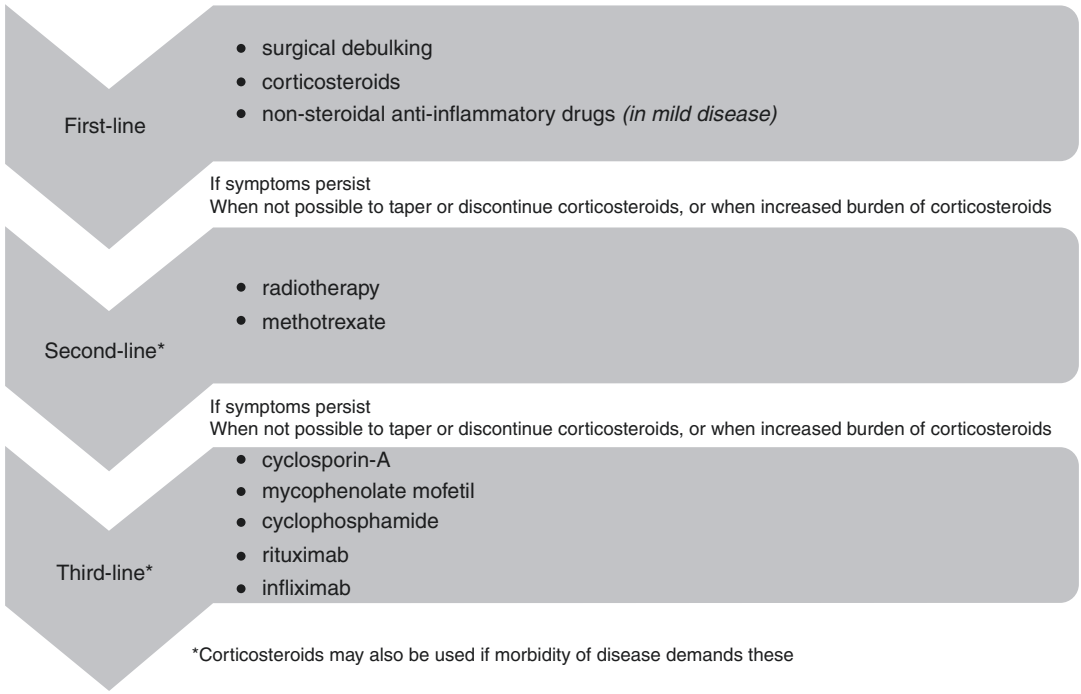

Fig. 7.4 Treatment algorithm for IOI. The order of treatment options in each line does not reflect preference

pain, double vision, and visual dysfunction. In selected cases with mild disease and low morbidity, nonsteroidal anti-inflammatory drugs are given as first choice [11]. In severe cases, therapeutic strategies depend on the orbital structures involved and include surgical debulking, corticosteroids, radiation therapy, and immunomodulators (Fig. 7.4).

Surgical Debulking

Surgical debulking is part of the biopsy procedure, in which generous biopsies are taken and fibrotic tissue is removed. In idiopathic dacryoadenitis, debulking offers a very low relapse rate (8%) and is curative in the majority of cases (74%) [19]. Debulking may be the only effective measure in IOI with established fibrosis [21, 24, 36, 37]. After initial increase of swelling, a gradual relief of symptoms can be anticipated within 2 months postoperatively. Lesions not amenable to debulking include myositic and apical masses.

Corticosteroids

High-dose (60–80 mg) systemic corticosteroids initially relieve clinical symptoms in most myositic cases and in about 80% of nonmyositic nonsclerotic cases and are useful in 92% of cases with combined compressive optic neuropathy [39]. However, they require a slow taper over several months, and roughly half of cases relapse on tapering or ceasing, rendering a 37% efficacy to corticosteroids as a long-term cure [39, 41]. In sclerosing IOI, corticosteroids are less effective with only 33% of cases responding [24].

To reduce side effects from systemic use, corticosteroids injected intralesionally can be favorable as first-line or adjunctive treatment in lesions localized in the anterior orbit such as the lacrimal gland [42, 43].

Radiation Therapy

External beam radiation, in doses between 20 and 30 Gray, has been demonstrated with modest

efficacy as a second-line adjunctive therapy in patients who are corticodependent, fail to respond to corticosteroids, or recur. In nonmyositic nonsclerotic IOI, symptoms improve in 85% of cases and 45% achieved complete discontinuing of corticosteroids [44]. On the other hand, sclerotic and myositic cases have a low radiosensitivity, although, in the latter group, radiation may delay the next recurrence [2, 11, 24].

Immunomodulatory Drugs

Traditional nonspecific immunosuppressive and newer specific biologic agents have been employed as second- and third-line therapy to control the inflammatory process in corticodependent and recalcitrant IOI, with varying degrees of success. They should be given for prolonged times.

The antimetabolite methotrexate is reportedly moderately successful and well tolerated as corticosteroid-sparing agent in IOI [45, 46]. There is anecdotal evidence of clinical benefit with cyclosporin-A (T-cell inhibitor), mycophenolate mofetil (antimetabolite), cyclophosphamide (alkylating agent), and rituximab (B-cell inhibitor) [46]. Infliximab, a biologic antitumor necrosis factor-alpha agent, has anti-inflammatory potential in cases which are severe, recurrent, or recalcitrant to corticosteroids and methotrexate [13]. In view of their systemic toxicity profile and the costs inherent in newer biologic agents, these drugs are reserved as third-line strategy for aggressive lesions with severe symptomatology, such as the sclerotic IOIs.

Conclusion

IOI is a diagnosis of exclusion. With management tailored to the clinicoradiological findings, surgery plays an important role both in diagnosis and treatment of nonmyositic IOI. The sole evidence of an adequate response to a trial of systemic corticosteroids, as well as IgG4 negativity on tissue immunostaining, is not diagnostic of IOI. It should be emphasized that IOI is not a sound long-term diagnosis. When new findings manifest, reevaluation is necessary for the possibility of other distinct – possibly systemic – disease.

IOI is a disease with an unknown natural course and unpredictable outcome. There is no consensus on treatment protocol. Surgical debulking following the biopsy procedure can be efficacious as first-line treatment. In view of the high recurrence rate, corticosteroids are less attractive as first choice therapy but remain useful in patients with significant morbidity such as combined optic neuropathy. Although evidence is limited, additional treatment options comprise radiotherapy and immunomodulators in severe refractory and recurrent disease.

References

1. Mombaerts I, Goldschmeding R, Schlingemann RO, et al. What is orbital pseudotumor? Surv Ophthalmol. 1996;41(1):66–78.
2. Rootman J, McCarthy M, White V, et al. Idiopathic sclerosing inflammation of the orbit. A distinct clinicopathologic entity. Ophthalmology. 1994;101(3):570–84.
3. Mombaerts I. Orbital pseudotumor. Amsterdam: Kugler Publications; 1996.
4. Harris GJ. Idiopathic orbital inflammation: a pathogenetic construct and treatment strategy: the 2005 ASOPRS Foundation Lecture. Ophthal Plast Reconstr Surg. 2006;22(2):79–86.
5. Wladis EJ, Iglesias BV, Gosselin EJ. Characterization of the molecular biologic milieu of idiopathic orbital inflammation. Ophthal Plast Reconstr Surg. 2011;27(4):251–4.
6. Wladis EJ, Iglesias BV, Adam AP, et al. Toll-like receptors in idiopathic orbital inflammation. Ophthal Plast Reconstr Surg. 2012;28(4):273–6.
7. Guo J, Qian J, Zhang R. Histopathology and immunohistochemical profile in idiopathic dacryoadenitis. Curr Eye Res. 2012;37(5):365–71.
8. Ren MW, Du Y, Ren S, et al. Epstein-Barr virus-encoded small RNAs in idiopathic orbital inflammatory pseudotumor tissues: a comparative case series. Int J Ophthalmol. 2017;10(8):1268–72.
9. Yan J, Li Y, Qiu H, et al. Immunohistochemical study of the presence of mast cells in idiopathic orbital inflammatory pseudotumor: possible role of mast cells in the course of its pathogenesis. Int Ophthalmol. 2007;27(4):235–9.
10. Lee BJ, Atkins S, Ginter A, et al. Increased CD40+ fibrocytes in patients with idiopathic orbital inflammation. Ophthal Plast Reconstr Surg. 2015;31(3):202–6.

11. Mombaerts I, Koornneef L. Current status in the treatment of orbital myositis. Ophthalmology. 1997;104(3):402–8.
12. Culver EL, Salmon JF, Frith P, et al. Recurrent posterior scleritis and orbital myositis as extra-intestinal manifestations of Crohn's disease: case report and systematic literature review. J Crohns Colitis. 2008;2(4):337–42.
13. Garrity JA, Coleman AW, Matteson EL, et al. Treatment of recalcitrant idiopathic orbital inflammation (chronic orbital myositis) with infliximab. Am J Ophthalmol. 2004;138(6):925–30.
14. Rosenbaum JT, Choi D, Wilson DJ, et al. Orbital pseudotumor can be a localized form of granulomatosis with polyangiitis as revealed by gene expression profiling. Exp Mol Pathol. 2015;99(2):271–8.
15. Rosenbaum JT, Choi D, Harrington CA, et al. Gene expression profiling and heterogeneity of nonspecific orbital inflammation affecting the lacrimal gland. JAMA Ophthalmol. 2017;135(11):1156–62.
16. Mombaerts I, Bilyk JR, Rose GE, et al. Consensus on diagnostic criteria of idiopathic orbital inflammation using a modified delphi approach. JAMA Ophthalmol. 2017;135(7):769–76.
17. Jakobiec FA, Syed ZA, Stagner AM, et al. Orbital inflammation in pregnant women. Am J Ophthalmol. 2016;166:91–102.
18. Andrew NH, Kearney D, Sladden N, et al. Idiopathic dacryoadenitis: clinical features, histopathology, and treatment outcomes. Am J Ophthalmol. 2016;163:148–53 e141.
19. Mombaerts I, Cameron JD, Chanlalit W, et al. Surgical debulking for idiopathic dacryoadenitis: a diagnosis and a cure. Ophthalmology. 2014;121(2):603–9.
20. Avni-Zauberman N, Tripathy D, Rosen N, et al. Relapsing migratory idiopathic orbital inflammation: six new cases and review of the literature. Br J Ophthalmol. 2012;96(2):276–80.
21. Pemberton JD, Fay A. Idiopathic sclerosing orbital inflammation: a review of demographics, clinical presentation, imaging, pathology, treatment, and outcome. Ophthal Plast Reconstr Surg. 2012;28(1):79–83.
22. Mombaerts I, Tousseyn T, Van Limbergen E, et al. Clinically recognizing enlarged extraocular muscles from lymphoid origin. Ophthalmology. 2015;122(1):217–8.
23. Ben Simon GJ, Syed HM, Douglas R, et al. Extraocular muscle enlargement with tendon involvement in thyroid-associated orbitopathy. Am J Ophthalmol. 2004;137(6):1145–7.
24. Hsuan JD, Selva D, McNab AA, et al. Idiopathic sclerosing orbital inflammation. Arch Ophthalmol. 2006;124(9):1244–50.
25. Zborowska B, Ghabrial R, Selva D, et al. Idiopathic orbital inflammation with extraorbital extension: case series and review. Eye. 2006;20(21):107–13.
26. Srinivasan A, Kleinberg TT, Murchison AP, et al. Laboratory investigations for diagnosis of autoimmune and inflammatory periocular disease: part II. Ophthal Plast Reconstr Surg. 2016;32:321.
27. Chan ASY, Mudhar H, Shen SY, et al. Serum IgG2 and tissue IgG2 plasma cell elevation in orbital IgG4-related disease (IgG4-RD): potential use in IgG4-RD assessment. Br J Ophthalmol. 2017;101(11):1576–82.
28. Rabinowitz MP, Halfpenny CP, Bedrossian EH Jr. The frequency of granulomatous lacrimal gland inflammation as a cause of lacrimal gland enlargement in patients without a diagnosis of systemic sarcoidosis. Orbit. 2013;32(3):151–5.
29. Bijlsma WR, Kalmann R. Idiopathic orbital inflammation and Graves ophthalmopathy. Arch Ophthalmol. 2010;128(1):131–2.
30. Hamed-Azzam S, Verity DH, Rose GE. Lateral canthotomy orbitotomy: a rapid approach to the orbit. Eye (Lond). 2018;32(2):333–7.
31. Mombaerts I, Rose GE, Verity DH. Diagnosis of enlarged extraocular muscles: when and how to biopsy. Curr Opin Ophthalmol. 2017;28(5):514–21.
32. McCarthy JM, White VA, Harris G, et al. Idiopathic sclerosing inflammation of the orbit: immunohistologic analysis and comparison with retroperitoneal fibrosis. Mod Pathol. 1993;6(5):581–7.
33. Andrew NH, Sladden N, Kearney DJ, et al. An analysis of IgG4-related disease (IgG4-RD) among idiopathic orbital inflammations and benign lymphoid hyperplasias using two consensus-based diagnostic criteria for IgG4-RD. Br J Ophthalmol. 2015;99(3):376–81.
34. Winn BJ, Rootman J. Sclerosing orbital inflammation and systemic disease. Ophthal Plast Reconstr Surg. 2012;28(22):107–18.
35. Mombaerts I. The many facets of dacryoadenitis. Curr Opin Ophthalmol. 2015;26(5):399–407.
36. Deshpande V, Zen Y, Chan JK, et al. Consensus statement on the pathology of IgG4-related disease. Mod Pathol. 2012;25:1181–92.
37. Wong AJ, Planck SR, Choi D, et al. IgG4 immunostaining and its implications in orbital inflammatory disease. PLoS One. 2014;9(10):e109847.
38. Mombaerts I, Schlingemann RO, Goldschmeding R, et al. The surgical management of lacrimal gland pseudotumors. Ophthalmology. 1996;103(10):1619–27.
39. Mombaerts I, Schlingemann RO, Goldschmeding R, et al. Are systemic corticosteroids useful in the management of orbital pseudotumors? Ophthalmology. 1996;103(3):521–8.
40. Mombaerts I, Rose GE, Garrity JA. Orbital inflammation: biopsy first. Surv Ophthalmol. 2016;61:664.
41. Swamy BN, McCluskey P, Nemet A, et al. Idiopathic orbital inflammatory syndrome: clinical features and treatment outcomes. Br J Ophthalmol. 2007;91(12):1667–70.
42. Leibovitch I, Prabhakaran VC, Davis G, et al. Intraorbital injection of triamcinolone acetonide in patients with idiopathic orbital inflammation. Arch Ophthalmol. 2007;125(12):1647–51.
43. Reggie S, Neimkin M, Holds J. Intralesional corticosteroid injections as treatment for non-infectious orbital inflammation. Orbit. 2018;37(1):41–7.
44. Prabhu RS, Kandula S, Liebman L, et al. Association of clinical response and long-term outcome among

patients with biopsied orbital pseudotumor receiving modern radiation therapy. Int J Radiat Oncol Biol Phys. 2013;85(3):643–9.
45. Smith JR, Rosenbaum JT. A role for methotrexate in the management of non-infectious orbital inflammatory disease. Br J Ophthalmol. 2001;85(10):1220–4.
46. Carruth BP, Wladis EJ. Inflammatory modulators and biologic agents in the treatment of idiopathic orbital inflammation. Curr Opin Ophthalmol. 2012;23(5):420–6.

Orbital Vascular Anomalies

8

Yvette Marie Santiago and Aaron Fay

Introduction

Vascular anomalies are a group of disorders of blood vessel growth that leads to identifiable vascular lesions and their associated deformities. For many years, understanding this group of diseases was vague due to inconsistencies in nomenclature and classification. In 2014, the ISSVA, a multispecialty interest group in diagnosis, management, and investigation of vascular anomalies, adopted a revised binary classification scheme based on the initial grouping suggested by Mulliken and Glowacki in 1982 [1]. Vascular tumors/neoplasms, like hemangiomas, that result from active cell proliferation of endothelial cells are differentiated from vascular malformations which are congenital defects in vessel morphogenesis. These two types exhibit different clinical behaviors and require different diagnostic and treatment plans (Table 8.1).

Vascular anomalies frequently occur in children, and when these lesions appear in the periocular region, they can affect visual, eyelid, and orbital development.

Y. M. Santiago (✉)
Eye Institute, St. Luke's Medical Center,
Quezon City, Metro Manila, Philippines

A. Fay
Harvard Medical School,
Department of Ophthalmology, Boston, MA, USA

C. J. Hwang et al. (eds.), *Clinical Ophthalmic Oncology*,
https://doi.org/10.1007/978-3-030-13558-4_8

Orbital Vascular Tumors

Orbital vascular tumors are actively proliferating neoplasms that are either benign, locally aggressive, or malignant (Table 8.1). The most common benign vascular tumor in children is infantile hemangioma followed by pyogenic granuloma. Congenital hemangioma is a rare vascular tumor that mimics IH but presents differently. Kaposiform hemangioendothelioma is a locally aggressive vascular tumor often associated with Kasabach-Merritt syndrome. It is rarely seen in the orbital region and will not be discussed here. Angiosarcoma is a rare malignant vascular tumor that has been reported to occur in the eyelid.

Infantile Hemangioma

Infantile hemangiomas (IH) are unique vascular neoplasms that exhibit peculiar biological behavior and more commonly appear in the head and neck. They are distinguished from vascular malformations by age at presentation, clinical behavior, histopathology, and response to treatment (Table 8.2). Incidence is higher in females, low-birthweight premature infants, and children subjected to chorionic venous sampling [2]. IH has a unique immunohistochemical profile, expressing glucose transport protein (glut-1) that is otherwise expressed only in placenta and blood-brain barrier tissues [3].

Table 8.1 Summary of ISSVA classification of vascular anomalies

Vascular anomalies		
Vascular tumors		
Benign	**Locally aggressive or borderline**	**Malignant**
Infantile hemangioma/hemangioma of infancy	Kaposiform hemangioendothelioma	Angiosarcoma
Congenital hemangioma	Retiform hemangioendothelioma	Epithelioid hemangioendothelioma
Tufted angioma	Papillary intralymphatic angioendothelioma	Others
Spindle cell hemangioma	Composite hemangioendothelioma Kaposi sarcoma	
Epithelioid hemangioma	Others	
Pyogenic granuloma		
Others		
Vascular malformations		
Simple	**Combined**	**Others**
Capillary malformations (CM) Cutaneous and/or mucosal Telangiectasia Cutis marmorata telangiectatica congenita Nevus simplex/salmon patch/"angel kiss," "stork bite" Others	Capillary-venous malformation	Vascular malformations associated with other anomalies Klippel-Trenaunay syndrome Parkes Weber syndrome Servelle-Martorell syndrome Sturge-Weber syndrome Maffucci syndrome
Lymphatic malformations (LM) Common (cystic) LM (macrocystic/microcystic/mixed cystic LM) Generalized lymphatic anomaly (GLA) LM in Gorham-Stout disease Channel type LM Primary lymphedema Others	Capillary-lymphatic malformation	Anomalies of major named vessels (aka "hannel type" or "truncal" vascular malformations)
Venous malformations (VM) Common VM Familial VM cutaneo-mucosal (VMCM) Blue rubber-bleb nevus (Bean) syndrome VM Glomuvenous malformation (GVM) Cerebral cavernous malformation (CCM) (different types) Others	Capillary-arteriovenous malformation	Others
Arteriovenous malformations (AVM)	Lymphatic-venous malformation	
Arteriovenous fistula (AVF)	Capillary-lymphatic-venous malformation	
	Capillary-lymphatic-arteriovenous malformation	
	Capillary-venous-arteriovenous malformation	
	Capillary-lymphatic-venous-arteriovenous malformation	

Table 8.2 Comparison between infantile hemangioma and vascular malformations

	Infantile hemangiomas	Malformations
Presentation	Absent at birth	Present at birth
Behavior	Independent life cycle	Relentless progression
Progression	Rapid proliferation (+ mitosis)	Slow expansion (hypertrophy)
Clinical course	Slow involution	Non-involuting
Gender predilection	Female>male	Female = male
Race predilection	Caucasians	No race predilection
Histopathology	Varies with stage	Consistent
Immunohistochemical staining	GLUT-1 positive	GLUT-1 negative

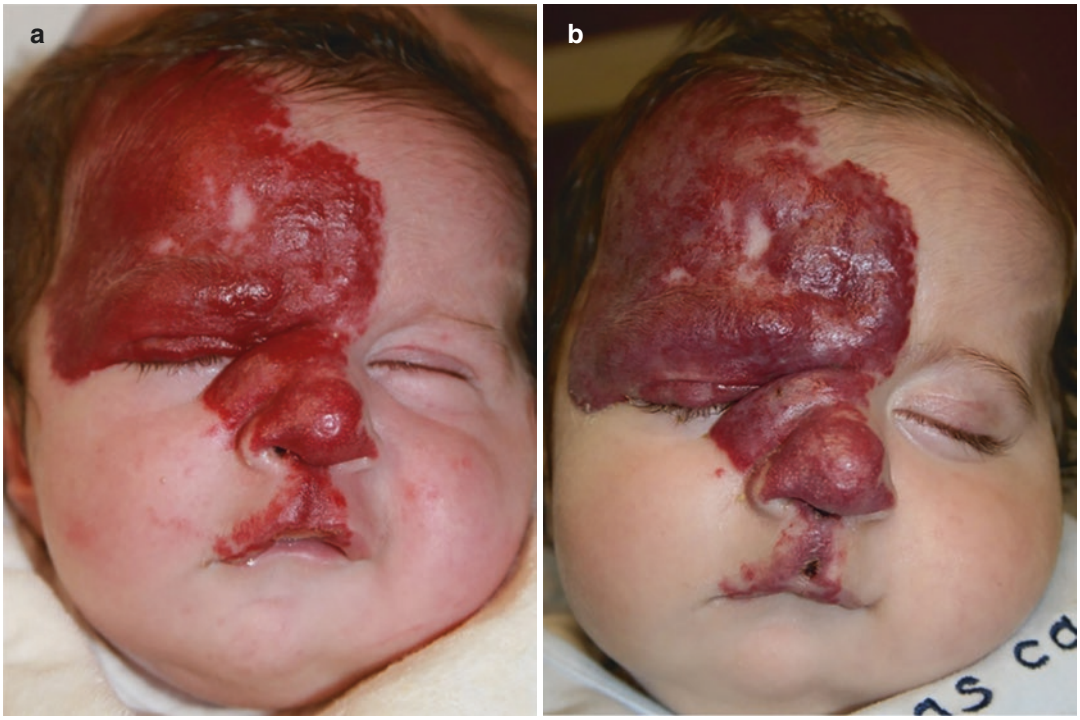

Fig. 8.1 (**a**, **b**) Demonstrating progression of hemangioma during the proliferation phase. (Courtesy of Milton Waner, MD)

Clinical Features

The unique biological behavior of IH can easily distinguish it from other vascular anomalies. They are usually absent or small at birth, generally growing rapidly in the first months of life, followed by a variable period of involution that spans months to years. Majority of these tumors are seen by the fourth week of life, while some show clinical evidence at birth, often with a paradoxically hypovascular blanch. In many cases, a pale halo, area of erythema, or cluster of telangiectatic vessels can be the initial presenting sign (Fig. 8.1).

The life cycle of IH is predictable. It starts with a proliferative phase characterized by rapid expansion and endothelial hyperplasia within the first year. This phase is often biphasic; most of the growth occurs within the first month of life, and then a second rapid growth phase happens at 6 months. The subsequent involutional phase is characterized by spontaneous, steady regression with histologic fibrosis and fat deposition. It has been observed that lesions whose involution commenced earlier tended to resolve more thoroughly [4]. However, there is no reliable method

of predicting which hemangiomas will involute, how long the regression will continue, or how completely a given hemangioma will resolve [5].

More than half of hemangiomas occur in the head-and-neck region, with clear sites of predilection within the head and neck [6]. Two subtypes of superficial IH that occur in these areas have been recognized, namely, focal IH and segmental IH. Focal IH are discrete hemangiomas that occur along lines of fusion between embryological facial placodes (Fig. 8.2) [7]. Segmental IH, on the other hand, form large plaque-like lesions overlying individual or multiple facial placodes. Each subtype varies in behavior, systemic disease association, and treatment options.

Focal periocular IH can cause significant functional and cosmetic deformity. Visual development is affected when IH of the eyelids exert pressure on the cornea and sclera to cause astigmatism resulting in subsequent amblyopia [8]. Tumor growth within the eyelid can lead to ptosis with obstruction of the visual axis resulting in deprivational amblyopia [9].

With orbital involvement, IH can produce rapid proptosis, exposure keratopathy, compressive optic neuropathy, globe displacement, and strabismic amblyopia [10]. If left untreated, large intraorbital IH can produce orbital expansion with considerable increase in orbital volume and subsequent enophthalmos or inferior displacement of the globe.

Soft tissue ulceration can occur in segmental IH and can be extremely painful. This also increases the risk of infection and may result in cutaneous scarring. The naso-jugal and V2 distributions tend to be at highest risk for ulceration in the periocular region (Fig. 8.3).

Infants with greater than four cutaneous hemangiomas are at increased risk of visceral hemangiomatosis, most commonly involving the liver, and should undergo further screening with abdominal ultrasound. Segmental IH associates more with systemic diseases than focal IH. It is

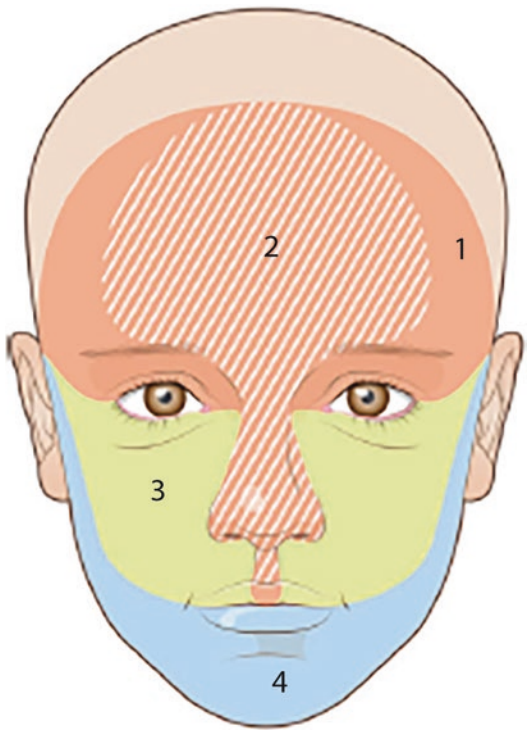

Fig. 8.2 Composition of facial placodes. Lateral optic vesicle area (1), frontonasal prominence (2), maxillary prominence (3), and mandibular prominence (4). (Modified from Zallmann et al. [7]. With permission from John Wiley & Sons]

Fig. 8.3 Segmental infantile hemangioma with ulceration. (Courtesy of Milton Waner, MD)

one of the features of a neurocutaneous syndrome known as PHACE (*p*osterior fossa malformations; segmental infantile *h*emangioma of the head, neck, or face; and anomalies of cerebral *a*rteries, *c*ardiac, and *e*ye) syndrome [10].

Diagnostic Evaluation

Currently there are no laboratory investigations in clinical use for evaluation of IH. Ancillary tests that will help diagnose suspected IH are ultrasound (US), radiographic imaging, and biopsy. US can be used for screening of small, superficial periocular tumors. Grayscale and color Doppler US evaluates vascularity and type of vessels present. IH may appear as a well-defined mass with variable echogenicity on grayscale US and show high-flow vascularity on color Doppler. Computed tomography (CT) scan reveals a well-delineated, uniformly enhancing tumor. Magnetic resonance imaging (MRI) provides a detailed view of soft tissues and determines the extent of large lesions. T1-weighted contrast study shows an enhancing iso-to intermediate intensity mass that is hyperintense on T2-weighted images. Smaller lesions are more likely to be homogenous in signal and enhancement, whereas larger lesions tend to be more heterogeneous. Enhancement patterns are nonspecific in IH, and as involution occurs, gradual replacement by fibrofatty tissue causes MRI features to vary accordingly [11].

Histopathological evaluation of hemangioma tissue reveals characteristic findings in each phase of the life cycle. In the proliferative phase, the lesions appear as well-defined, nonencapsulated masses of plump, proliferating endothelial cells and attendant pericytes that focally form small, rounded red blood cell-containing lumens. Numerous mitotic figures and apoptotic bodies demonstrating nuclear fragmentation are simultaneously present in the tumor. The involution phase can be detected microscopically before the lesion begins to regress clinically. Apoptotic bodies and increased numbers of mast cells remain, while mitotic figures diminish. The endothelium begins to flatten as the lumen enlarges. As involution proceeds, loose fibrous or fibro-adipose tissue begins to separate vessels both within and between lobules as the number of proliferating vessels decrease. End-stage lesions show a fibrofatty background with a mast cell count comparable to that of normal skin, studded by a few residual vessels similar to normal capillaries or venules and scattered larger vessels with fibrotic walls. No endothelial or pericytic mitotic activity remains [12].

The most important immunohistochemical marker that is not demonstrated in other orbital vascular anomalies is the expression of GLUT-1 in IH. This important discovery has improved the accuracy of diagnosing IH. Other immunohistochemical biomarkers that are expressed by IH are CD31, CD34, Lewis Y antigen, merosin, and FC-γ RII. These markers are not specific to IH, but their presence helps provide an immunohistochemical profile that is unique to vascular tumors.

Differential Diagnosis

IH has a great variety of presentations depending on the stage and location, so differential diagnosis is extensive. Early in presentation, IH may be confused with benign venular midline malformation, also known as "nevus flammeus neonatorum," "stork bite," "angel kiss," or "salmon patch." Benign venular midline malformation occurs in up to 40% of newborns and most often disappears by the first year of life [13].

Focal IH with cutaneous components may mimic venous malformations, particularly when mucosal surfaces are involved. Deep focal lesions may resemble childhood mass lesions like rhabdomyosarcoma, metastatic neuroblastoma, hemangiopericytoma, mucocele, meningocele, etc. Small focal IH on the eyelid may look like pyogenic granulomas. Segmental hemangiomas can be easily confused with port wine stain or other cutaneous vascular malformations that also tend to follow dermatomal patterns. Lastly, the involuted cutaneous hemangioma can appear like a lipoma or may leave scarring that appears like the cicatrix of trauma, chemical injury, or thermal burns.

Treatment

Treating IH has been controversial for decades because of its high rate and unique characteristic

of spontaneous involution. Therefore, IH was popularly managed by simple "watchful waiting." The modern approach to IH was fundamentally revolutionized when the beta-blocker effect on infantile hemangiomas was discovered in 2008 [14]. Additional advances in pharmacologic treatment, laser technology, and surgical technique gave rise to the establishment of multidisciplinary clinics that are devoted to the management of vascular anomalies. These clinics offer a vast array of treatment possibilities to their patients.

Two distinct decision processes are involved in the rational approach to managing IH that must answer these questions: (1) Is treatment necessary or beneficial? (2) What is the appropriate treatment modality? [15] The first decision takes into consideration anatomic location, lesion size, and age of the child. Each of these aspects determine whether it is necessary to intervene or more prudent to postpone treatment. For instance, small lesions in the eyelid or orbit of infants that are significant enough to cause ptosis, astigmatism, and subsequent amblyopia would benefit from early treatment compared to relatively larger lesions in other locations that do not affect visual development and may be conservatively observed. Similarly, an infant may tolerate a significantly sized lesion on the face but as self-image begins to develop, an older child may start to become self-conscious even if spontaneous involution is still anticipated.

Indications for treatment of orbital and periocular IH include astigmatism, globe deformity, occlusion of visual axis, ptosis and eyelid distortion, proptosis, strabismus, corneal exposure, optic nerve compression, and orbital bone deformity. Dermatologic indications are skin and soft tissue hypertrophy and ulceration. Psychosocial implications associated with large facial deformities require treatment before self-awareness of body image develops in a child [16].

Once treatment is deemed necessary, the second decision is to determine which of the many treatment modalities is most advantageous: pharmacologic treatment, laser, surgery, or any combination of the three. Additional factors that weigh in this decision are subtype, depth, and stage of the tumor.

Pharmacologic Treatment

Localized intralesional corticosteroid injection has been popularly used in the past to promote involution of IH. It aims to deliver a high concentration of medication directly to the tumor while minimizing systemic absorption and potential side effects of systemic corticosteroids. A variety of formulations use a mixture of triamcinolone and betamethasone with great success. Although effective, serious ocular complications have been reported including ophthalmic artery occlusion, retinal embolization, and central retinal artery occlusion. These occur as a result of high pressure during intralesional injection that promotes particle embolization [9, 17–19]. Therefore, slow injection under low pressure may prevent retrograde arterial flow and minimize these potential problems. Other complications are eyelid hypopigmentation, subcutaneous fat atrophy, sclerodermiform linear atrophy, eyelid necrosis, periocular calcification, retrobulbar hemorrhage, and inadvertent ocular penetration [20, 21]. In light of newer, safer treatment options, and the risks mentioned above, periocular steroid injection should be avoided in hemangioma patients.

Steroid-resistant IH have reportedly been treated effectively with immunosuppressants like interferon-alpha, vincristine, cyclophosphamide, and imiquimod. Use of these agents are now extremely limited after the discovery of safer alternatives.

Propranolol, a nonselective beta-blocker, was serendipitously found to inhibit hemangioma proliferation in pediatric patients that were concomitantly being treated for congenital cardiac disorders [14]. Leaute-Labreze observed that severe hemangiomas in these patients stabilized or regressed after being treated with systemic propranolol of 2 milligrams per kilogram body weight per day (mg/kg/day) for up to 9 months with no systemic side effects reported. Subsequent case reports and case series validated the dramatic efficacy of propranolol in treating primarily segmental hemangiomas [22, 23]. The effect on focal hemangiomas has been less dramatic. Rare complications of systemic propranolol are transient hypoglycemia, bradycardia, and hypoten-

sion; bronchospasm can be seen in patients with underlying reactive airway. These risks can be managed anticipatorily by obtaining a pediatric pretherapy evaluation, by monitoring vital signs and blood glucose levels at initiation and throughout therapy, and by maintaining frequent pediatric follow-ups. Doses of propranolol can be administered intravenously or orally. Propranolol has also clearly emerged as the preferred medical treatment for deep orbital and other inaccessible infantile hemangiomas.

The best protocol for administering propranolol to infants as young as 1 week of age has not been clearly determined. Several protocols have been suggested. A recent randomized clinical trial recommended a safe and effective regimen of 3 mg/kg/day in two or three divided doses [24]. Some authors recommend pretreatment cardiac workup for infants younger than 6 weeks of age, while others believe there is no indication for additional evaluation in otherwise healthy infants; the latter starts the medication on an outpatient basis.

Laser Photocoagulation

Laser treatment is utilized for cutaneous IH [24]. Pulsed dye laser (PDL) has become the standard for treating superficial proliferative hemangiomas, reaching up to a depth of 1.2 mm. Adjunctive treatment with propranolol, intralesional steroid injection, or surgery may be used for deeper lesions. A typical treatment regimen consists of PDL, 585–595 μm, with fluences of 5–12 J/cm^2, pulse duration 300–450 μs, spot size 5–7 mm, and concomitant surface cooling device. The desired purpuric response is produced by two to three passes with overlapping spots over the lesion. Up to eight treatments may be necessary to produce the desired endpoint, with 6–8 weeks interval between treatments, depending on response. Complications include minor temporary blistering, ulceration, crusting, textural changes, scarring, and skin pigmentary changes.

CO2 laser resurfacing CO_2 and non-ablative fractional photothermolysis are now used to improve the skin texture of atrophic scars from involuted IH and to revise surgical scars.

Surgery

The effect of surgical excision of IH is rapid and definitive. Furthermore, proliferating subcutaneous IH has a tissue-expanding effect that is advantageous during early surgery, making skin closure and reconstruction easier and minimizing surgical scars. Unfortunately, surgery is still only considered by many centers for vision- and life-threatening cases, and end-stage reconstruction, emphasizing the higher risk compared to medical management. Current advances in pediatric anesthesia and new surgical technologies and techniques have narrowed the gap between these risks, allowing for a more balanced treatment planning.

Hemorrhage is the most significant risk factor that limits surgery and requires strategies to manage intraoperative and postoperative bleeding. Bloodless dissection techniques continue to improve with the use of fine electrocautery dissecting needles. Adjunctive use of chemical and mechanical hemostatic agents such as topical thrombin, gelatin and cellulose coagulants, fibrin tissue adhesives, etc., during surgery, have allowed better control of intraoperative bleeding especially in previously inaccessible areas like the deep orbit. As more options for controlling intraoperative hemorrhage become available, surgeons have been able to dissect in hard to reach areas with relative safety. Surgical excision has been recommended as primary treatment for periocular IH and for lesions refractory to medical treatment.

Prognosis

Correct timing and proper mode and execution of treatment can prevent the plausible periocular complications that may otherwise cause visual impairment, physical deformity, and psychological damage to children with IH.

Congenital Hemangioma (CH)

Congenital hemangioma is a benign vascular neoplasm that grossly resembles IH but appears fully developed at birth and does not express the

GLUT-1 protein. Since CH undergoes the proliferative phase in utero, some can be identified during prenatal screening [11, 25]. It is further classified into rapidly involuting congenital hemangioma (RICH), when it spontaneously regresses from a few weeks after birth up to 2 years of age, and non-involuting congenital hemangioma (NICH), when it does not undergo involution but, instead, grows proportionately with the child.

Clinical Features

The presentation of CH greatly varies and can grossly appear just like IH. It could present as elevated, violaceous lesions with ectatic veins, raised grayish tumors with multiple telangiectasias surrounded by a pale halo, or flat infiltrative tumor with violaceous overlying skin (Fig. 8.4). They can also occur as variable shades of pink to purple, round to ovoid lesions with telangiectasia, and central or peripheral pallor. NICH are generally larger that RICH, and some lesions demonstrate high flow on Doppler ultrasonography.

Fig. 8.4 Congenital hemangioma present at birth

Diagnostic Evaluation

Imaging features of CH overlap with IH in terms of heterogeneity, visible vessels, and calcifications. Therefore, the radiologist must be aware of the age at presentation and clinical findings, in order to suggest a congenital hemangioma.

Histopathological examination of congenital hemangiomas reveals lobular collections of capillaries with prominent endothelial cells. Dilated dysplastic veins within interlobular areas and increased mast cells may be seen in NICH. The main differentiating feature between CH and IH is the absence of GLUT-1 in immunohistochemical staining of CH. Additionally, D2-40 and Wilms' tumor 1 can be expressed in lobular areas of NICH.

Differential Diagnosis

CH can mimic the same lesions that resemble IH in the proliferative and involutional phases, respectively.

Treatment

RICH behaves almost similarly to IH in terms of its ability to spontaneously resolve while also potentially causing visual, physical, and psychological complications. Therefore, the same principles in decision-making process apply when managing these cases. On the other hand, NICH often needs to be excised with or without selective embolization [26].

Pyogenic Granuloma

Pyogenic granuloma (PG) or lobular capillary hemangioma is the second most common benign vascular tumor. It also resembles infantile hemangioma. PG can appear at any age, with a predilection for females. It has been postulated that female sex hormones may play a role in the pathogenesis of this tumor. In the periocular region, it may arise in response to various stimuli such as minor trauma or surgery and has been reported as a complication of pterygium surgery, chalazia, anophthalmic sockets, and punctal plug use in dry eye treatment.

Fig. 8.5 Pyogenic granuloma of the eyelid

Clinical Features

PG presents as a pink, red, or purple lesion that is often pedunculated and may bleed recurrently (Fig. 8.5). It usually grows in mucosal tissue and is more common in the oral and nasal cavities. Periocular tumors involve conjunctiva, eyelids and, rarely, the cornea.

Diagnostic Evaluation

Laboratory and ancillary testing are often not necessary to diagnose this lesion. Surgical biopsy best confirms diagnosis.

The term pyogenic granuloma is a misnomer because it suggests a pus-forming lesion that contains epithelioid giant cells that are universally seen in granulomatous inflammation.

Histopathologically, however, PG is composed of acute and chronic inflammatory cells interspersed between fibroblasts, fibrocytes, and lobules of proliferating capillaries. Lobular capillary hemangioma is, therefore, a more apt descriptive term.

Treatment

Management of PG includes surgical excision and removal of the known inciting agent or irritant. Electrocautery, laser photocoagulation, and medical management with topical or oral beta-blockers have also been reported as effective for managing PG. Further studies are necessary to establish their advantages.

Prognosis

Prognosis is good after proper surgical resection and removal of known inciting agent.

Angiosarcoma

Angiosarcoma is a rare malignant vascular tumor that occurs in the head and neck. It accounts for less than 0.1% of malignancies in this area [27]. It rarely grows in the periocular region. There are a few case reports and series in literature of angiosarcoma developing in the eyelid, either as an isolated tumor or as part of a more diffuse malignant process [28].

Clinical Features

Eyelid angiosarcoma is a painless mass that may appear like any of the following: erythematous nodule, erythematous-to-violaceous maculopapular lesion, red-to-violaceous plaque or infiltrative lesion, yellow plaque or infiltrative lesion, or yellow nodule. Many occur with diffuse eyelid swelling.

Diagnostic Evaluation

The main modality for the diagnosis of angiosarcoma is surgical biopsy. Its histological features range from well- to poorly differentiated lesions, but the hallmark finding is abnormal pleomorphic malignant endothelial cells [29]. Atypical endothelial cells line anastomosing dissecting sinusoids with either diffuse epithelioid or spindle cell proliferation [30]. Immunohistochemical staining may show expression of factor VIII-related antigen, CD31, and CD34 in angiosarcoma cells [29].

Differential Diagnosis

Eyelid angiosarcoma may resemble a chalazion and malignancies of the eyelid such as squamous cell carcinoma, basal cell carcinoma, and sebaceous gland carcinoma.

Treatment

Due to its rarity, there is no generally accepted treatment guideline for angiosarcomas. The popular standard of care is wide excision surgery followed by external beam radiotherapy (EBRT). The invasiveness and multifocal nature of angiosarcoma make complete resections difficult. Therefore, adjuvant treatment with doxorubicin or paclitaxel and docetaxel has been utilized.

Prognosis

Prognosis is poor in spite of aggressive treatment of angiosarcoma. In Dermici and Christanson's review of 22 patients, those who underwent excisional biopsy with EBRT or chemotherapy had the best outcome, but the reported treatment successes were all within less than 5 years [28]. In angiosarcoma of the head and neck, tumor size, depth of invasion, and completeness of surgical resection are more reliable prognostic indicators than histologic grading. These are aggressive tumors that can recur locally and metastasize in spite of multimodal treatment. Angiosarcoma can spread to the lungs, liver, cervical lymph nodes, spleen, heart, and brain with a mean survival time of 4 months after metastasis. Death can occur from 15 to 24 months of presentation, either from local extension or metastasis.

Orbital Vascular Malformations

Vascular malformations are lesions that result from inborn morphogenesis defects of various vessels. Vascular development occurs during the retiform stage of embryogenesis, beginning at approximately day 48 of development, and vascular malformations, therefore, result from errors beginning at this stage. Examples include isolated lesions as well as numerous congenital syndromes: Sturge-Weber, Osler-Weber-Rendu, Wyburn-Mason, Klippel-Trénaunay, and blue rubber-bleb nevus (BLEB) syndrome. Vascular malformations grow with age and never involute. They are comprised of ectatic venules, veins, arterioles, arteries, and lymphatic vessels, all with flat (normal appearing) endothelial cells. The most common malformations that present in the orbit are venous and lymphatic malformations or a combination of the two (Table 8.1).

In 1999 the Orbital Society published a classification concept unique to orbital lesions and based entirely on clinical and radiographic hemodynamics. Lesions were classified by flow characteristics: no flow, slow flow, and rapid flow [31]. The emphasis on flow, rather than tissue type, was felt to help guide treatment planning (Table 8.3).

Unlike vascular neoplasms, vascular malformations usually grow in proportion with the child and can be exaggerated by hormonal changes during puberty or pregnancy or as a result of thrombosis or infection.

Lymphatic Malformations

Lymphatic malformations (LM), formerly called lymphangiomas, are benign malformations of the lymphatic system representing up to 8% of all orbital masses. Since these are not proliferative lesions, the "-oma" nomenclature is inap-

Table 8.3 Diagnostic features of orbital vascular lesions

Type	Flow	Imaging		Treatment
		Doppler US angiography	CT MRI	
Lymphangioma (type I)	No flow	No flow	No enhancement Fluid levels	Debulking
Varix (type II)	Venous flow	Venous flow	Contrast enhancement Flow voids	Sclerotherapy, ligation, and excision
AV malformation (type III)	Arterial flow	Arterial flow	Contrast enhancement Flow voids	Embolization then debulking

Fig. 8.6 Venous malformation on the eyelid, midface, and scalp of a 7-year-old boy (**a**) distention of the upper eyelid and cheek on upright position, (**b**) swelling subsides in supine position, and distention moves to the scalp

propriate. The specific etiology has not been fully elucidated. It has no gender predilection and typically involves subconjunctival and periocular tissues. LM contain tissue pockets that can range from microscopic to greater than 1 cm in diameter [32]. Lymphatic malformations would be classified as "no-flow" lesions in the flow-based scheme.

Clinical Features

Patients with LM may present with swelling, sudden proptosis, intraorbital hemorrhage, and ptosis. Unilateral proptosis or swelling is the primary symptom in 76% of patients [33]. When lymphatic malformations are combined with venous components, known as venolymphatic malformations, they present with soft, compressible bluish masses that may swell in dependent positions or with Valsalva (Fig. 8.6).

Orbital LM has the tendency to slip through extraconal and intraconal spaces, violating normal anatomic boundaries. Deep orbital LM that do not have superficial subconjunctival or eyelid extensions may be asymptomatic until there is an infection and sudden swelling ensues. Fluctuations in size are a typical feature of LM with upper respiratory tract infections. The lesion suddenly expands after intralesional hemorrhage. This sudden increase in size poses a risk for optic nerve compression that can lead to permanent visual impairment. In such cases, the need for treatment becomes urgent.

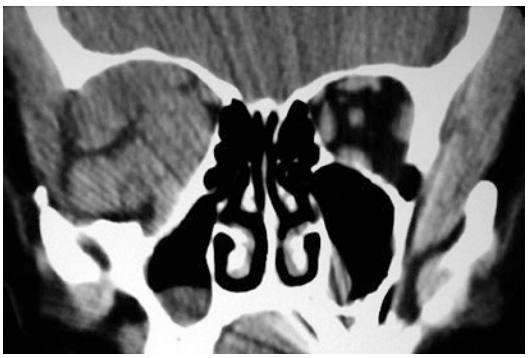

Fig. 8.7 Coronal CT imaging study shows lobulated appearance of lymphangioma (type 1 vascular lesion). Note surgical absence of lateral wall

Diagnostic Evaluation

The extent of orbital LM is best demonstrated by MR or CT imaging (Fig. 8.7). (CT scanning is typically avoided in young children.) LM appear as multilobulated, septated masses with intermediate to hypointensity on T1-weighted studies and hyperinsity on T2-weighted images. Internal fluid-fluid levels are commonly seen when intralesional hemorrhage is present manifesting as hyperintensity on T1-weighted studies in contrast to the intermediately intense cystic fluid.

Differential Diagnosis

Lymphatic malformations can present like other orbital masses depending on its extent and location of tumors. Differentials include other orbital vascular malformations, and hemangiomas, and orbital mass lesions like rhabdomyosarcoma, lymphoma, meningioma, and neurofibroma.

Treatment

The standard of care for LM is total resection of the lesion because of its high recurrence rate. However, involvement of deeper orbit and extension around major neurovascular structures make complete removal challenging. Ablative treatment with sclerosing agents have been utilized to decrease the impact and complications of surgery. Sclerosing agents induce collapse of these channels by destroying the endothelial lining and inciting an inflammatory reaction and fibrosis that occurs over several weeks. Doxycycline and bleomycin have been effectively used as sclerotherapeutic agents but can cause perilesional fibrosis that makes subsequent surgical excision more difficult. Other sclerosing agents such as alcohols and OK-432 that are useful in most anatomic regions should be avoided in the orbit due to intense inflammation and iatrogenic compartment syndrome [34]. OK-432 is a lyophilized biologic product that contains a mixture of a low virulence strain of *Staphylococcus pyogenes* that has been inactivated with penicillin G [34]. Intralesional pingyangmycin (a close analog of bleomycin) is another effective agent with sequelae of only mild inflammation and fibrosis [35].

Acute enlargement and swelling of LM often results from upper respiratory infection, hormonal shifts surrounding puberty, as well as other systemic stressors. These patients, who often present to unsuspecting emergency room staff, should receive systemic corticosteroids.

When complete surgical resection seems implausible, the goal of partial resection surgery or tumor debulking is to remove sight-threatening and cosmetically disfiguring lesions. Alternatively, patients with very large, recurrent, and incompletely resectable LM may benefit from orbital decompression. However, medial wall decompression can potentially cause spread of the lesion into the nasal cavity and sinuses, causing sinus-related complications. Other alternative, yet less effective and limited, options are aspiration, radiofrequency ablation, and laser treatment. Sirolimus, a systemic immunosuppressant used to prevent transplant rejection, is another alternative treatment that shows promising effects for treating unresectable, life-threatening lymphatic malformations. Efficacy of sildenafil for the treatment of LM remains to be assessed in large series of patients [36, 37].

Prognosis

Prognosis is excellent when complete surgical excision of LM is possible. However, when it is located in the deep orbit adjacent to vital orbital structures, complete resection becomes unlikely, and a high recurrence rate is expected.

Venous Malformations

Venous malformations (VM), formerly called cavernous hemangioma, consist of venous channels that are connected, albeit unpredictably, to normal veins and sinuses. Histopathology reveals large, thin-walled vessels within fibrous stroma. These channels are endothelial lined and contain smooth muscle. According to the flow-based scheme, lesions that behave this way are defined in the "slow-flow" category. Venous and lymphatic malformations can occasionally contain substantial proportions of both tissue types. This is generally where the flow classification and the tissue classification diverge.

Clinical Features

Venous malformations, like all malformations, are present at birth. A blue hue may be seen subcutaneously when the eyelids, temple, nose, or cheek are involved. Hemifacial VM involving the orbit is not uncommon. Purely orbital lesions may remain clinically dormant for some years but tend to come to attention during puberty. Symptoms include positional pain or exercise intolerance. Symptoms are sometimes worse in the morning,

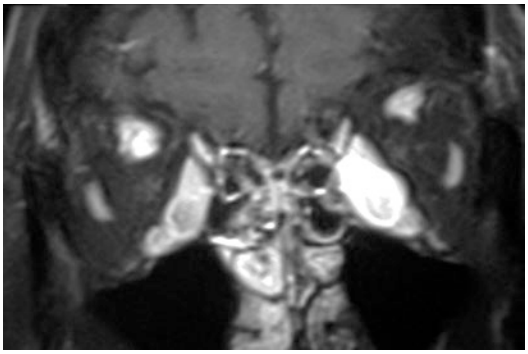

Fig. 8.8 Coronal Gd-DTPA-enhanced MRI shows bilateral contrast-enhancing lesions consistent with type 2 vascular lesions

presumably due to nocturnal distension in the recumbent position. Later in life, patients may complain of pain when upright that correlates with impressive enophthalmos. The long-standing lesion evidently compresses and eventually replaces normal orbital fat. Increased venous pressure will cause VMs to distend, producing pathognomonic positional exophthalmos when located in the orbit.

Diagnostic Evaluation

Color Doppler and directional ultrasound detect venous flow in venous malformations that are not thrombosed. CT and MRI reveal diffuse contrast enhancement (Fig. 8.8). CT scans may reveal pathognomonic calcified phleboliths, bony hypertrophy, or intraosseous extension. MR imaging best delineates these lesions and may reveal thrombosed areas. MR taken without raised intravenous pressure may miss the lesion entirely. MR angiography often detects the venous flow through distensible lesions. Percutaneous or remote access angiography remains the most comprehensive imaging method, allowing precise evaluation of drainage routes and rates.

Treatment

Surgery

Surgical management for orbital venous malformations is notoriously difficult. Surgical excision of venous malformations carries a high risk of complications, including hemorrhage, orbital compartment syndrome, and vision loss. Complete excision is difficult because these lesions often encase critical neuromuscular structures. Certain precautions can minimize intraoperative bleeding. Both preoperative thrombotherapy and fibrin sealant intraoperative injection (prior to excision) may significantly reduce flow. Maintaining normothermia and regional venous hypotension further reduces risk. Matched blood and platelet donor products may be needed when operating on small infants.

Sclerotherapy

Intralesional sclerotherapy that has revolutionized treatment of lymphatic malformations has been less useful for venous malformations. The flow found in VMs can recanalize these lesions 2–3 years or more after seemingly successful sclerotherapy. Furthermore, sclerotherapy for venous malformations requires careful assessment of the lesion's outflow so as to avoid inadvertent damage in the cavernous sinus. This assessment can be done with percutaneous or endovascular fluoroscopy. Newer methods include CT image fusion and frameless stereotactic guidance in combination with x-ray fluoroscopic monitoring of the injection [38].

Sclerotherapy of venous malformations not only may produce transient effects but also may induce catastrophic visual loss. Needle puncture of the delicate vessel wall may lead to intraoperative or delayed rupture resulting in orbital hemorrhage, compartment syndrome, and compressive optic neuropathy. For these reasons, many venous malformations ultimately require surgical treatment [39].

Other Methods

Venous malformations respond well to Nd:YAG laser, delivered percutaneously or by optical fiber, but have not been used extensively in the orbit where collateral heat and fibrosis cannot be well controlled [40]. Other treatment options include electrocoagulation and cryotherapy. These techniques may be used alone or preoperatively in order to reduce hemorrhagic complications.

Arteriovenous Malformations

Orbital arteriovenous malformations (AVM), like all AVMs, shunt blood from the high-pressure arterial vasculature, across an absent or defective capillary network, to the venous circulation. These are "high-flow" vascular malformations that are present at birth but may not manifest until childhood or adulthood. Like other vascular malformations, these lesions generally grow proportionately with the child and may be influenced by hormonal changes, thrombosis, infection, or trauma. In contrast to venous and lymphatic malformations, AVMs may enlarge very rapidly over months or years and destroy large regions or previously normal tissue. Congenital AVM is embryologically derived from the arterial or venous systems or both. These are characterized by progressively enlarging communications between arteries and veins that bypass normal capillary beds usually with numerous feeder arteries, a central low-resistance nidus, and multiple draining veins. Often, both internal and external carotid branches act as feeder vessels. Histologically, the muscularis layer of the involved arteries and veins appears abnormal.

Arteriovenous fistulae usually occur within the brain, a phenomenon in which arteries and veinous sinuses communicate directly [41]. The arteriovenous fistula known to ophthalmologists is the carotid artery-cavernous sinus communication in which carotid blood enters the venous sinus and superior ophthalmic vein causing orbital and ocular congestion. These lesions, typically seen in older adults, can occur spontaneously or as a result of trauma.

Clinical Features

AVM may manifest as a red pulsatile, warm mass that may cause proptosis, periorbital pain, increased intraocular pressure, pulsation, and bruit. Prolonged ocular ischemia may cause glaucoma and vision loss via progressive venous hypertension or diminished peak retinal arterial pressure from shunting. Venous hypertension may cause arterialization of conjunctival vessels reminiscent of changes seen with carotid-cavernous fistula (Fig. 8.9). A combination of cutaneous angiomas and retinal, orbital, and cerebral AVMs is known as Wyburn-Mason syndrome.

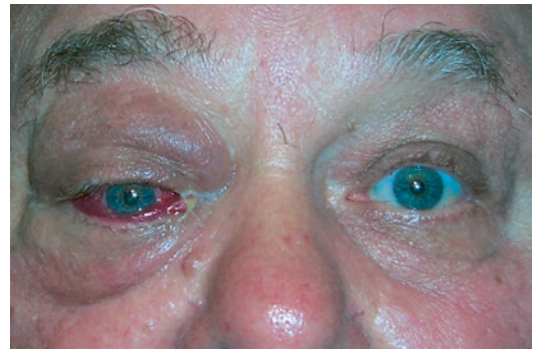

Fig. 8.9 External photograph demonstrates severe arterialization and proptosis of the right eye in a patient with type 3 orbital vascular lesion

Although these malformations typically display slow growth, acute aggravation of symptoms may occur after spontaneous orbital hemorrhage, and this presentation may mimic an acquired AV shunt. The older demographic and certain angiographic characteristics may help to distinguish acquired shunts from congenital malformations.

Diagnostic Evaluation

Noninvasive tests that can help diagnose high-flow malformations are ultrasonography and radiographic imaging to delineate the extent of the malformation. They are often multispacial and hypervascular on color Doppler US. MRI of the orbit may not show a discrete mass lesion but can reveal a dilated superior orbital vein and signs of congestion of intraocular soft tissue. Angiography is the main basis for diagnosis AVM, showing an engorged rapidly filling proximal arterial system, malformation, and distal venous drainage (Fig. 8.10). Histologically, the affected vessels show irregularities in the thickness of the muscularis layer and a partial elastica in some vessels.

Differential Diagnosis

Orbital lesions that have similar characteristics as orbital AVM are carotid-cavernous fistulas, dural cavernous fistulas, and cerebral AVM.

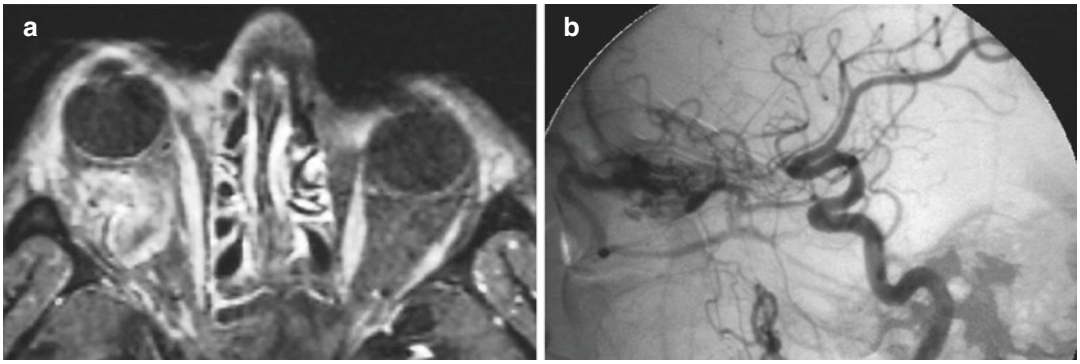

Fig. 8.10 MRI of orbital AVM shows enhancing lesion with flow voids (**a**). Angiography of orbital AVM demonstrates communication to the internal and external carotid arteries (**b**)

Treatment

Management of AVM follows a multidisciplinary approach, involving the orbit specialist, interventional radiologist, and other relevant specialists [39, 42, 43]. Asymptomatic lesions may be observed. Treatment is indicated when there is visual compromise, lesion-related patient discomfort, and/or deformity.

The main mode of treatment is surgery usually requiring preoperative embolization.

Surgical excision of any arterial-flow lesion risks intraoperative bleeding. Preoperative endovascular embolization of the lesion significantly reduces the risks incurred during surgical debulking. Surgery should be planned within 24 h after embolization. Incomplete excision may result in rapid recurrence through recruitment of collateral vessels.

Prognosis

The risk of recurrence is high when incomplete resection and only partial embolization is done. These lesions have a tendency to recruit new feeder vessels when their supply is partially reduced. Outcomes after a multidisciplinary approach can be surprisingly good.

Orbital Cavernous Venous Malformations

Orbital cavernous venous malformation (CVM) is the most common benign vascular tumor in adults [44]. It used to be called cavernous hemangioma. However, further understanding of the composition and behavior of this lesion makes the use of "hemangioma" in its name obsolete [45]. The term, "hemangioma," is reserved for neoplastic lesions that undergo active proliferation and mitosis with increased endothelial cell turnover. CVM exhibits normal endothelial turnover and is formed merely as a result of structural abnormalities of the venous system. Lesions previously described as "intraosseous hemangiomas" are also now pathologically known as venous malformations due to their histopathologic presentation and lack of GLUT-1 expression [46].

Clinical Features

CVMs present an etiologic conundrum because while they show low proliferative tendencies, they are not generally seen in children. They contradict theories of both neoplasm and malformation! Nevertheless, tissue studies and clinical behavior favor the classification into malformations. It is more common in women between the 2nd and 6th decades of life, presenting as slow painless, progressive proptosis [47]. Often they are detected incidentally when imaging studies are performed for unrelated headache or trauma (Fig. 8.11). Vision may be diminished due to compressive optic neuropathy or an induced hyperopic shift. Some patients complain of diplopia or pain.

Previously quiescent lesions may grow significantly during pregnancy as a result of hormonal shifts. When large enough, it may induce

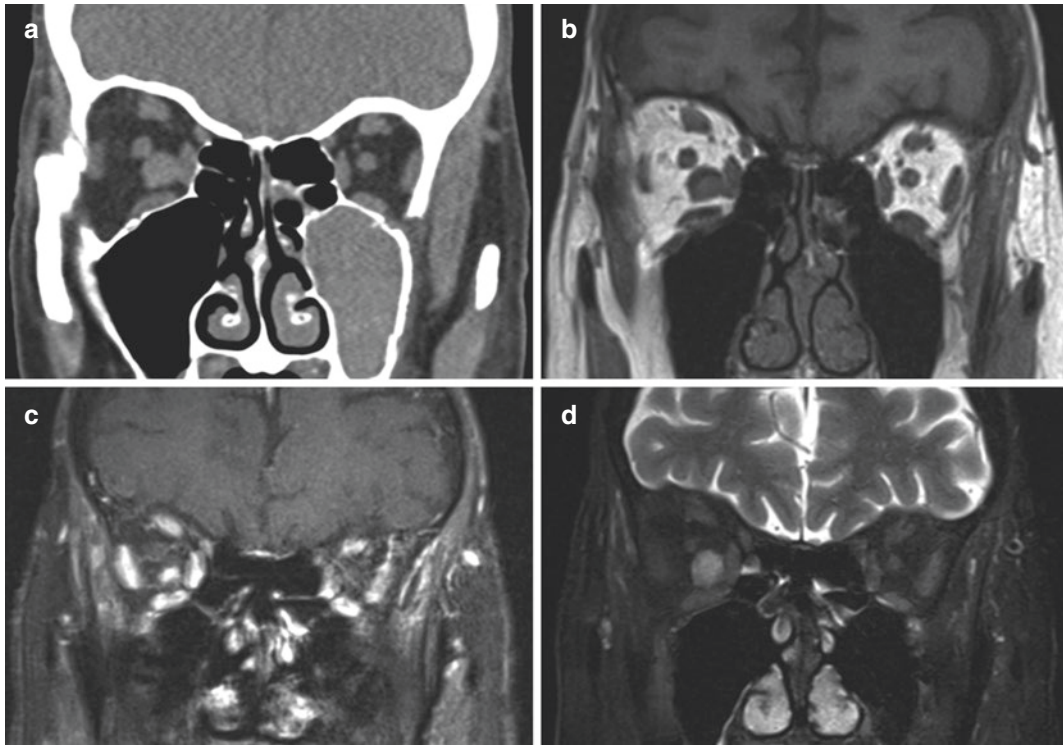

Fig. 8.11 Cavernous hemangioma. A 69-year-old woman underwent CT of the head following a bicycle accident. Incidental intraconal orbital mass was identified (**a**) in addition to opacified left maxillary sinus. Patient had no orbital signs on examination with visual acuity of 20/20. MRI revealed an intraconal circumscribed mass inferonasal to the optic nerve without signs of compression (**b**, T1). The lesion enhanced following administration of contrast (**c**, T1 fat suppressed and **d**, T2 fast suppressed)

hyperopia or optic nerve compression leading to decreased vision. Other clinical findings may include axial proptosis, elevated intraocular pressure, extraocular muscle (EOM) motility defects + diplopia, relative afferent pupillary defect, and other signs of optic nerve compression.

Diagnostics

Ancillary tests than can support a clinical diagnosis of CVM are ultrasonography and CT or MRI imaging. B-scan can show a well-delineated round retrobulbar mass with iso- to hyper-echogenicity. CT scan typically reveals a well-circumscribed, moderately enhancing intraconal lesion that is hyperdense to EOM. Coronal views are helpful in assessing the position of the tumor in relation to the optic nerve. MRI may show a mass that is isointense to muscle on T1-weighted study and hyperintense on T2-weighted study, exhibiting contrast enhancement that is patchy in the early phase and then later becomes homogenous [48]. Phleboliths are also characteristically seen in radiographic images of venous malformations.

Histologically, CVM contains abnormally formed and dilated deep and superficial veins with thin walls that lack smooth muscle. The pseudocapsule is formed by progressively condensed collagen as the lesion slowly enlarges.

Differential Diagnosis

CVM may clinically resemble other well-circumscribed solid orbital tumors such as schwannoma, neurofibroma, solitary fibrous tumor, hemangiopericytoma, and melanoma.

Treatment

The decision to treat CVM depends on the presence or absence of symptoms. Small, asymptomatic lesions may be found incidentally in patients who undergo radiographic imaging for other indications. These lesions may be observed. Large lesions that cause visual impairment and diplopia are surgically removed. Careful dissection is done especially in large intraconal lesions to prevent damage to the optic nerve, EOMs, and surrounding adnexa. However, attempts to resect a tumor at or near orbital apex can be associated with visual morbidity. Therefore, use of stereotactic radiation therapy has been explored. Gamma Knife radiation (GKR) used in multiple treatment sessions is reported to show promising results (Fig. 8.12) [49, 50]. In a study of five patients, use of multisession GKR with a marginal dose of 5 Gy and 50% isodose in four sessions seems to be an effective management strategy for circumscribed tumors at orbital apex tumors [50]. Outcome in larger series of patients is expected to be published soon [51]. Alternatively, orbital apex CVM respond well to sclerotherapy, orbital apex decompression, or, when medially or inferiorly located, endonasal resection [52].

Prognosis

Complete resection of CVM results in cure for symptomatic lesions [53, 54].

Orbital Hemangiopericytoma

Hemangiopericytomas are characterized by a spectrum of pericyte proliferation. Histopathology often shows a mixed pattern of ovoid cells and sinusoidal space formations creating the classic "staghorn" vascular pattern (Fig. 8.13) [55]. Varying levels of cellular atypia underlie the less benign nature of this lesion, which may malignantly transform or metastasize. In 2002, controversy in its classification arose when the WHO considered solitary fibrous tumor, giant cell angiofibromas, and hemangiopericytoma as part of a spectrum of spindle cell neoplasms, rather than unique diagnostic entities. The 2013 WHO Classification of Tumors of Soft Tissue and Bone, Fourth Edition no longer recognizes hemangiopericytoma as a distinct pathologic diagnosis [56].

Clinical Features

Hemangiopericytoma typically presents in middle-aged adults as slowly progressing unilateral proptosis, often with pain and vision loss [57, 58]. Other signs and symptoms depend on tumor location (Fig. 8.13). Frequent intracranial extension and invasion into sinus cavities may produce additional associated symptoms.

Hemangiopericytomas are characterized by a spectrum of pericyte proliferation. Histopathology often shows a mixed pattern of ovoid cells and sinusoidal space formations creating the classic "staghorn" vascular pattern. Varying levels of cellular atypia underlie the less benign nature of this lesion, which may malignantly transform or metastasize [55, 59].

Diagnostic Evaluation

Ultrasound reveals an encapsulated and well-defined solid mass with low internal reflectivity. Orbital hemangiopericytoma has been reported to undergo cystic changes within necrotic zones and may resemble the echographic appearance of lymphangiomas. On MRI, T1-weighted images reveal a well-defined hypointense mass to fat. T2-weighted studies show less lesion definition. CT imaging often detects bony changes around these contrast-enhancing lesions. Angiography typically reveals early tumor blush with rapid washout of contrast. Diagnosis of this lesion requires histologic confirmation.

Differential Diagnosis

The differential diagnosis for hemangiopericytoma includes meningiomas, lymphangioma, orbital venous malformation, and schwannoma.

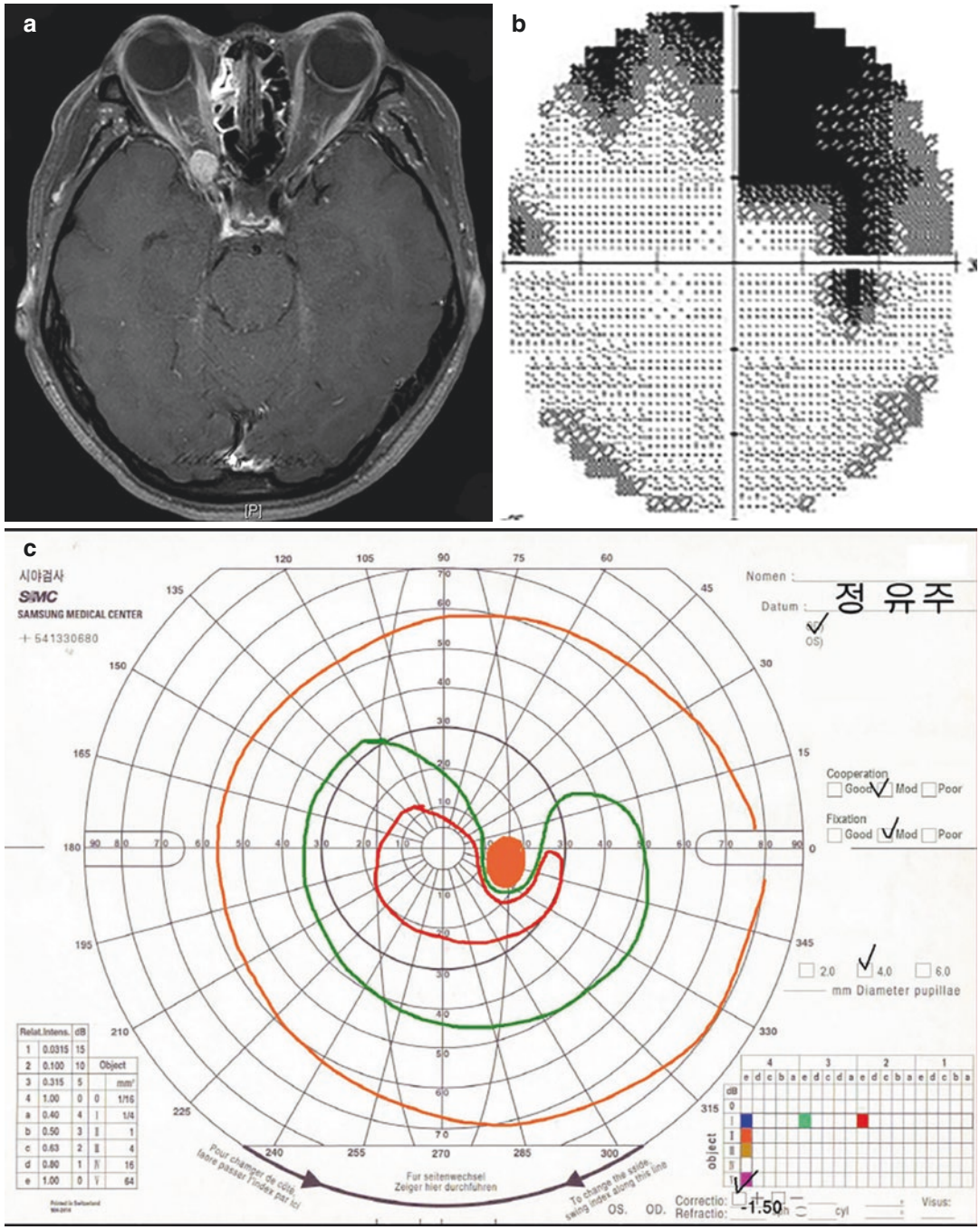

Fig. 8.12 A 34-year-old woman presented with headache and eye pain. Enhancing circumscribed mass was observed at orbital apex (**a**, MR Gd-enhanced). Visual field deficit was observed on visual field testing (**b**, Humphey; **c** Goldmann). Following fractionated Gamma Knife radiosurgery, the mass has become smaller (**d**), and visual fields have become normalized (**e**, Humphey; **f**, Goldmann). (Courtesy of Yoon-Duck Kim, MD)

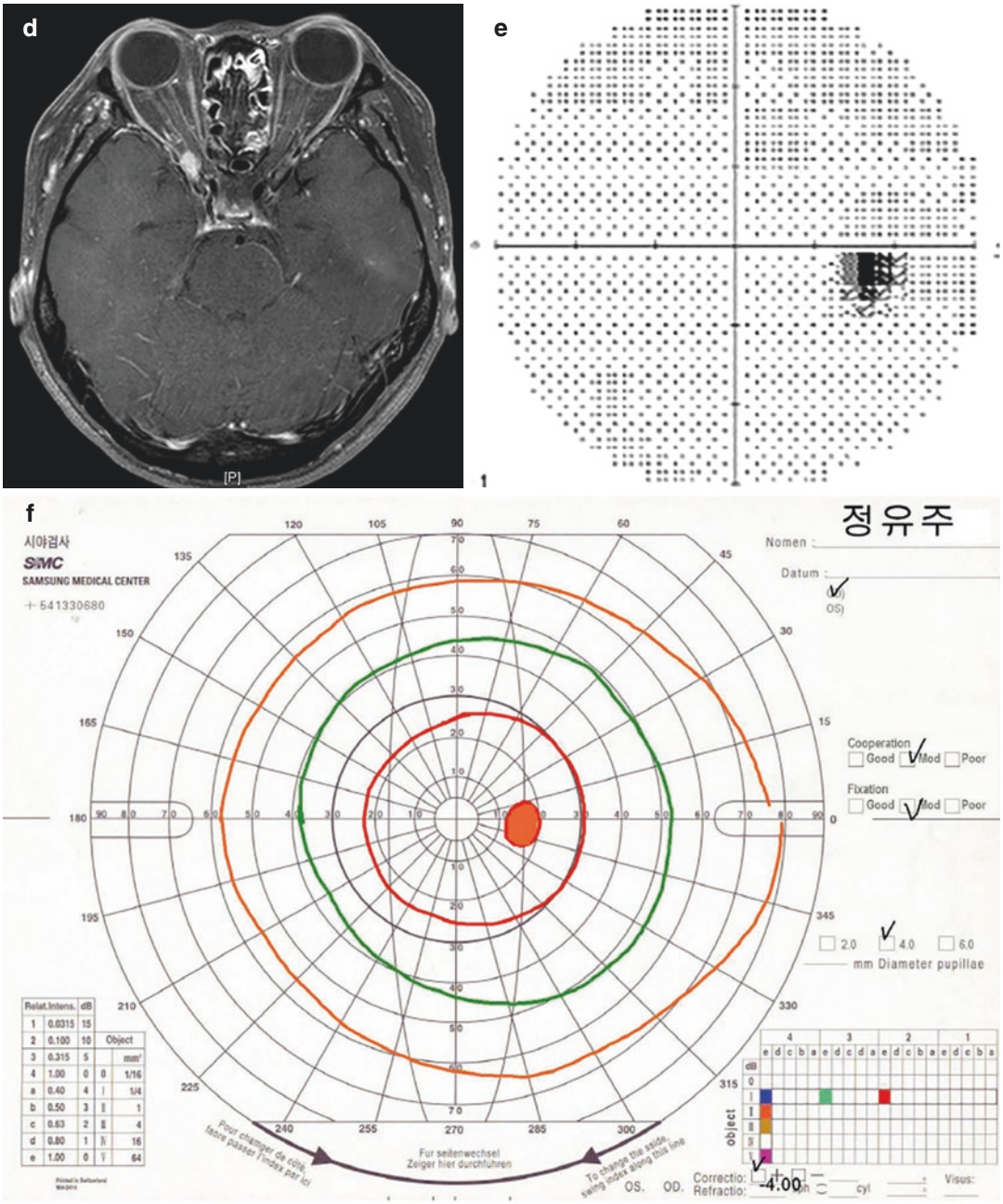

Fig. 8.12 (continued)

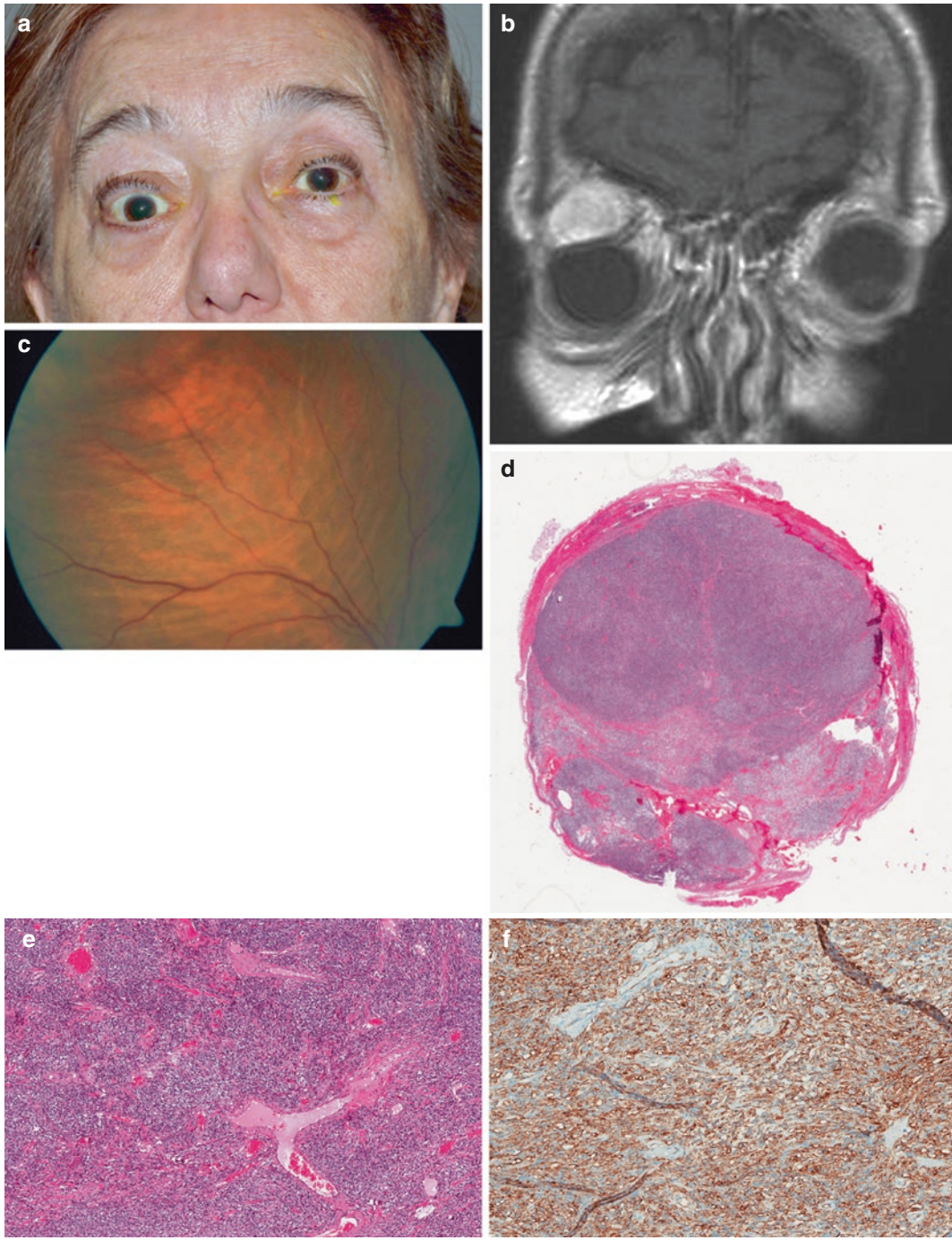

Fig. 8.13 Hemangiopericytoma. Clinical appearance of proptosis and hypoglobus (**a**). Coronal (**b**) MRI showing a circumscribed enhancing mass. Funduscopic examination revealed choroidal folds (**c**). Low-power photomicrograph demonstrating a well-circumscribed cellular lesion (**d**). Medium-power photomicrograph revealing relatively uniform spindle cells without a recognizable growth pattern. Small areas of densely pink "ropey" collagen are seen, as is a branched "staghorn" blood vessel (**e**). CD34 stain is diffusely and strongly positive in the spindle cells (**f**). (**d**–**f** Courtesy of Thomas Plesec, MD, Cleveland, Ohio, USA)

Treatment

Although the majority of these lesions are benign, the high rate of malignant transformation and recurrent disease mandates aggressive en bloc excision with wide margins. Adjunctive radiation therapy may be of benefit although conclusive studies are difficult due to the rarity of this tumor [55, 57].

Prognosis

The spectrum of aggressiveness of a particular lesion is difficult to predict as even more histologically benign lesions may result in clinically invasive disease or malignant transformation. The elusive nature of this entity warrants aggressive surgery and often adjuvant therapy.

References

1. Mulliken JB, Glowacki J. Hemangiomas and vascular malformations in infants and children: a classification based on endothelial characteristics. Plast Reconstr Surg. 1982;69(3):412–22.
2. Haggstrom AN, Drolet BA, Baselga E, et al. Hemangioma Investigator Group. Prospective study of infantile hemangiomas: demographic, prenatal, and perinatal characteristics. J Pediatr. 2007;150(3):291–4.
3. North PE, Waner M, Mizeracki A, et al. GLUT1: a newly discovered immunohistochemical marker for juvenile hemangiomas. Hum Pathol. 2000;31(1):11–22.
4. Finn MC, Glowacki J, Mulliken JB. Congenital vascular lesions: clinical application of a new classification. J Pediatr Surg. 1983;18(6):894–900.
5. Fay A, Santiago YM, Waner M. Infantile hemangiomas and other vascular neoplasms. In: Fay A, Dolman P. Diseases and disorders of the orbit and ocular adnexa. Elsevier. 2018.
6. Margileth AM, Museles M. Cutaneous hemangiomas in children. Diagnosis and conservative management. JAMA. 1965;194(5):523–6.
7. Zallmann M, Leventer RJ, Mackay MT, et al. Screening for Sturge-Weber syndrome: a state-of-the-art review. Pediatr Dermatol. 2018;35(1):30–42.
8. Robb RM. Refractive errors associated with hemangiomas of the eyelids and orbit in infancy. Am J Ophthalmol. 1977;83(1):52–8.
9. Schwartz SR, Blei F, Ceisler E, et al. Risk factors for amblyopia in children with capillary hemangiomas of the eyelids and orbit. J AAPOS. 2006;10(3):262–8.
10. Haik BG, Karcioglu ZA, Gordon RA, et al. Capillary hemangioma (infantile periocular hemangioma). Surv Ophthalmol. 1994;38(5):399–426.
11. Lowe LH, Marchant TC, Rivard DC, et al. Vascular malformations: classification and terminology the radiologist needs to know. Semin Roentgenol. 2012;47(2):106–17.
12. Waner M, Suen JY. A classification of congenital vascular lesions. . In: Waner M, Suen JY, eds. Hemangiomas and vascular malformations of the head and neck New York: J: Wiley-Liss, 1999.
13. Pratt AG. Birthmarks in infants. AMA Arch Derm Syphilol. 1953;67(3):302–5.
14. Leaute-Labreze C, Dumas de la Roque E, Hubiche T, et al. Propranolol for severe hemangiomas of infancy. N Engl J Med. 2008;358(24):2649–51.
15. Fay A, Nguyen J, Waner M. Conceptual approach to the management of infantile hemangiomas. J Pediatr. 2010;157(6):881–8 e1-5.
16. Dieterich-Miller CA, Cohen BA, Liggett J. Behavioral adjustment and self-concept of young children with hemangiomas. Pediatr Dermatol. 1992;9(3):241–5.
17. Ruttum MS, Abrams GW, Harris GJ, et al. Bilateral retinal embolization associated with intralesional corticosteroid injection for capillary hemangioma of infancy. J Pediatr Ophthalmol Strabismus. 1993;30(1):4–7.
18. Shorr N, Seiff SR. Central retinal artery occlusion associated with periocular corticosteroid injection for juvenile hemangioma. Ophthalmic Surg. 1986;17(4):229–31.
19. Egbert JE, Schwartz GS, Walsh AW. Diagnosis and treatment of an ophthalmic artery occlusion during an intralesional injection of corticosteroid into an eyelid capillary hemangioma. Am J Ophthalmol. 1996;121(6):638–42.
20. Droste PJ, Ellis FD, Sondhi N, et al. Linear subcutaneous fat atrophy after corticosteroid injection of periocular hemangiomas. Am J Ophthalmol. 1988;105(1):65–9.
21. Sutula FC, Glover AT. Eyelid necrosis following intralesional corticosteroid injection for capillary hemangioma. Ophthalmic Surg. 1987;18(2):103–5.
22. Sagi L, Zvulunov A, Lapidoth M, et al. Efficacy and safety of propranolol for the treatment of infantile hemangioma: a presentation of ninety-nine cases. Dermatology. 2014;228(2):136–44.
23. Lou Y, Peng WJ, Cao Y, et al. The effectiveness of propranolol in treating infantile haemangiomas: a meta-analysis including 35 studies. Br J Clin Pharmacol. 2014;78(1):44–57.
24. Bauman NM, McCarter RJ, Guzzetta PC, et al. Propranolol vs prednisolone for symptomatic proliferating infantile hemangiomas: a randomized clinical trial. JAMA Otolaryngol Head Neck Surg. 2014;140(4):323–30.
25. Boon LM, Enjolras O, Mulliken JB. Congenital hemangioma: evidence of accelerated involution. J Pediatr. 1996;128(3):329–35.

26. Ooi KG, Wenderoth JD, Francis IC, et al. Selective embolization and resection of a large noninvoluting congenital hemangioma of the lower eyelid. Ophthalmic Plast Reconstr Surg. 2009;25(2):111–4.
27. Sturgis EM, Potter BO. Sarcomas of the head and neck region. Curr Opin Oncol. 2003;15(3):239–52.
28. Demirci H, Christanson MD. Eyelid angiosarcoma: a case report and review of the literature. Middle East Afr J Ophthalmol. 2013;20(3):259–62.
29. Young RJ, Brown NJ, Reed MW, et al. Angiosarcoma. Lancet Oncol. 2010;11(10):983–91.
30. Morgan MB, Swann M, Somach S, et al. Cutaneous angiosarcoma: a case series with prognostic correlation. J Am Acad Dermatol. 2004;50(6):867–74.
31. Harris GJ. Orbital vascular malformations: a consensus statement on terminology and its clinical implications. Orbital society. Am J Ophthalmol. 1999;127(4):453–5.
32. Wiegand S, Eivazi B, Bloch LM, et al. Lymphatic malformations of the orbit. Clin Exp Otorhinolaryngol. 2013;6(1):30–5.
33. Greene AK, Burrows PE, Smith L, et al. Periorbital lymphatic malformation: clinical course and management in 42 patients. Plast Reconstr Surg. 2005;115(1):22–30.
34. Hall N, Ade-Ajayi N, Brewis C, et al. Is intralesional injection of OK-432 effective in the treatment of lymphangioma in children? Surgery. 2003;133(3):238–42.
35. Yue H, Qian J, Elner VM, et al. Treatment of orbital vascular malformations with intralesional injection of pingyangmycin. Br J Ophthalmol. 2013;97(6):739–45.
36. Gandhi NG, Lin LK, O'Hara M. Sildenafil for pediatric orbital lymphangioma. JAMA Ophthalmol. 2013;131(9):1228–30.
37. Swetman GL, Berk DR, Vasanawala SS, et al. Sildenafil for severe lymphatic malformations. N Engl J Med. 2012;366(4):384–6.
38. Ernemann U, Westendorff C, Troitzsch D, et al. Navigation-assisted sclerotherapy of orbital venolymphatic malformation: a new guidance technique for percutaneous treatment of low-flow vascular malformations. AJNR Am J Neuroradiol. 2004;25(10):1792–5.
39. Goldberg RA, Garcia GH, Duckwiler GR. Combined embolization and surgical treatment of arteriovenous malformation of the orbit. Am J Ophthalmol. 1993;116(1):17–25.
40. Werner JA, Dunne AA, Folz BJ, et al. Current concepts in the classification, diagnosis and treatment of hemangiomas and vascular malformations of the head and neck. Eur Arch Otorhinolaryngol. 2001;258(3):141–9.
41. Osaki T, Fay A, Waner M. Vascular malformations. In: Fay A, Dolman P, editors. Diseases and disorders of the orbit and ocular adnexa. Edinburgh: Elsevier; 2018.
42. Multimodal management of arteriovenous malformations of the basal ganglia and thalamus: factors affecting obliteration and outcome. J Neurosurg. 2018:1–10.
43. Chelliah MP, Do HM, Zinn Z, et al. Management of complex arteriovenous malformations using a novel combination therapeutic algorithm. JAMA Dermatol. 2018;154(11):1316–9.
44. Calandriello L, Grimaldi G, Petrone G, et al. Cavernous venous malformation (cavernous hemangioma) of the orbit: current concepts and a review of the literature. Surv Ophthalmol. 2017;62(4):393–403.
45. Osaki TH, Jakobiec FA, Mendoza PR, et al. Immunohistochemical investigations of orbital infantile hemangiomas and adult encapsulated cavernous venous lesions (malformation versus hemangioma). Ophthalmic Plast Reconstr Surg. 2013;29(3):183–95.
46. Bruder E, Perez-Atayde AR, Jundt G, et al. Vascular lesions of bone in children, adolescents, and young adults. A clinicopathologic reappraisal and application of the ISSVA classification. Virchows Arch. 2009;454(2):161–79.
47. McNab AA, Wright JE. Cavernous haemangiomas of the orbit. Aust N Z J Ophthalmol. 1989;17(4):337–45.
48. Xian J, Zhang Z, Wang Z, et al. Evaluation of MR imaging findings differentiating cavernous haemangiomas from schwannomas in the orbit. Eur Radiol. 2010;20(9):2221–8.
49. Kim JW, Im YS, Nam DH, et al. Preliminary report of multisession gamma knife radiosurgery for benign perioptic lesions: visual outcome in 22 patients. J Korean Neurosurg Soc. 2008;44(2):67–71.
50. Goh ASC, Kim YD, Woo KI, Lee JI. Benign orbital apex tumors treated with multisession gamma knife radiosurgery. Ophthalmology. 2013;120(3):635–41.
51. Young SM, Kim KH, Kim Y-D, et al. Orbital apex venous cavernous malformation with optic neuropathy – treatment with multisession Gamma knife radiosurgery. Br J Ophthalmol. 2019;. epub ahead of print
52. Chhabra N, Wu AW, Fay A, et al. Endoscopic resection of orbital hemangiomas. Int Forum Allergy Rhinol. 2014;4(3):251–5.
53. Kiratli H, Bulur B, Bilgic S. Transconjunctival approach for retrobulbar intraconal orbital cavernous hemangiomas. Orbital surgeon's perspective. Surg Neurol. 2005;64(1):71–4.
54. Brusati R, Goisis M, Biglioli F, et al. Surgical approaches to cavernous haemangiomas of the orbit. Br J Oral Maxillofac Surg. 2007;45(6):457–62.
55. Croxatto JO, Font RL. Hemangiopericytoma of the orbit: a clinicopathologic study of 30 cases. Hum Pathol. 1982;13:210218.
56. Fletcher CDM, Bridge JA, Hogendoorn P, et al. WHO classification of tumours. In: WHO classification of tumours of soft tissue and bone, vol. 5. 4th ed: IARC; Geneva, Switzerland, 2013. http://apps.who.int/bookorders/anglais/detart1.jsp?codlan=1&codcol=70&codcch=4005#
57. Karcioglu ZA, Nasr AM, Haik BG. Orbital hemangiopericytoma: clinical and morphologic features. Am J Ophthalmol. 1997;124(5):661–72.
58. Bernardini FP, de Conciliis C, Schneider S, et al. Solitary fibrous tumor of the orbit: is it rare? Report of a case series and review of the literature. Ophthalmology. 2003;110(7):1442–8.
59. Girnita L, Sahlin S, Orrego A, et al. Malignant solitary fibrous tumour of the orbit. Acta Ophthalmol. 2009;87(4):464–7.

Benign Orbital Tumors

9

Bhupendra C. K. Patel and Arun D. Singh

Introduction

Benign orbital tumors represent a broad spectrum of tumors (Chap. 2). In addition, orbital inflammation and infection may clinically simulate an orbital neoplasm (Chap. 7). In a recent survey of 1264 consecutive patients with suspected orbital tumor referred to an ophthalmic oncology center, 64% of the lesions were benign [1].

Benign orbital tumors may be congenital or, more frequently, acquired. Benign tumors more commonly are of vascular (Chap. 8), neural (Chap. 11), meningeal, fibrolytic, and osseous origin. Benign tumors may also arise from the lacrimal gland (Chap. 13) and lacrimal sac (Chap. 14). The details of clinical examination (Chap. 1) and imaging techniques (Chap. 5) supplement contents of this review. Benign orbital tumors not covered under other chapters are reviewed herein.

B. C. K. Patel (✉)
Division of Facial Cosmetic and Reconstructive Surgery, University of Utah, Salt Lake City, UT, USA
e-mail: bhupendra.patel@hsc.utah.edu

A. D. Singh
Department of Ophthalmic Oncology, Cole Eye Institute, Cleveland Clinic, Cleveland, OH, USA

C. J. Hwang et al. (eds.), *Clinical Ophthalmic Oncology*,
https://doi.org/10.1007/978-3-030-13558-4_9

Conjunctival Epithelial Cysts

Introduction

Conjunctival orbital cysts are usually secondary to previous trauma or surgery and are generally observed in adults, even when they are primary in nature. Rarely, they may present in neonates [1].

Clinical Features

Non-pulsatile proptosis is the usual manifestation in adults and in children, although worsening of the proptosis on crying has been noted in a neonate with an orbital cyst [1].

Differential Diagnosis

In adults, the differential diagnosis includes dermoids and lymphangiomas. In neonates and children, the differential diagnosis includes orbital teratoma, colobomatous cyst, lymphatic malformations, dacryoceles, and meningocele/encephalocele.

Diagnostic Evaluation

With improvement in image resolution of routine prenatal ultrasonography and ultrafast fetal

magnetic resonance imaging, it is possible to detect a wide range of fetal ocular abnormalities such as cataract, microphthalmos, dacryocele, and retinoblastoma. Orbital cysts have similarly been detected during routine prenatal ultrasonography (Figs. 9.1 and 9.2). MRI will show no solid component or calcification within the lesion.

Treatment

Surgical removal of the whole of the cyst or partial removal is usually curative.

Dermoid and Epidermoid Cysts

Introduction

Dermoid cysts are the most common orbital cysts, representing up to 5% of all orbital tumors [2]. Epidermoid cysts have a single layer of keratinized or nonkeratinized epithelium without evidence of adnexal structures. Most epidermoid cysts are traumatic in origin [3]. Dermoids, on the other hand, are choristomas with adnexal structures such as hair, sebaceous glands, and lipid. They arise from ectodermal nests pinched off at suture lines. Clinically, dermoid and epidermoid cysts may present very similarly and so are now usually differentiated by location: superficial or deep. Histopathology of dermoids may show hair, keratin, sebaceous glands, macrophages, lipid globules, multinucleated giant cells, and calcium.

Clinical Features

Most dermoid cysts are present in infancy with a well-defined, round periorbital mass. Approximately 60% of all dermoids arise

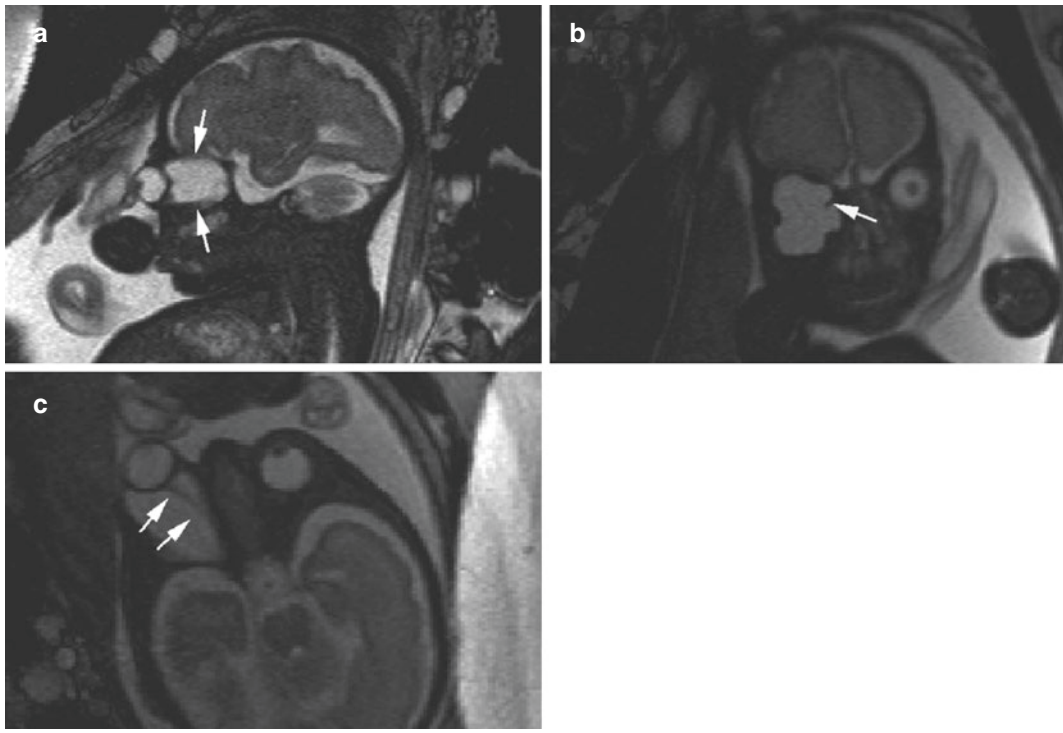

Fig. 9.1 Ultrafast magnetic resonance imaging image of the fetus. Right parasagittal view shows an orbital cyst (arrows) resulting in marked proptosis (**a**). Coronal (**b**) and axial (**c**) views show an orbital cyst resulting in attenuation of the optic nerve. Note absence of any solid component. The globe is of normal size and shape. (Reprinted from Singh et al. [1]. with permission from Elsevier)

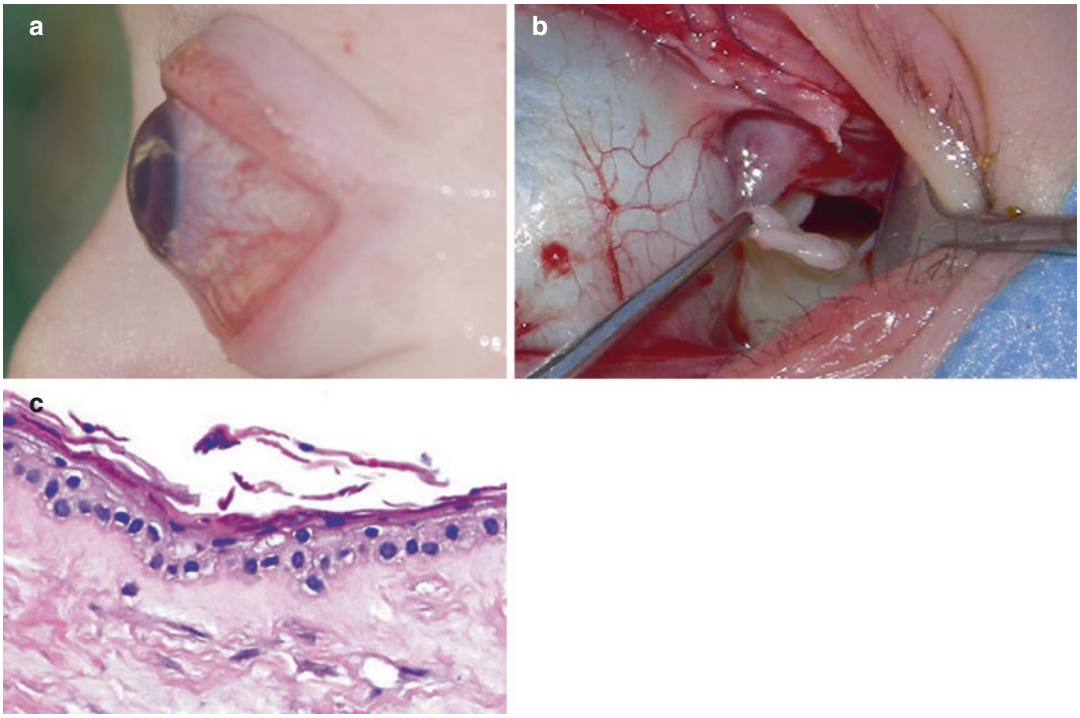

Fig. 9.2 Marked proptosis of the right globe at birth (**a**). A 5 × 4 mm rectangular piece of the cyst wall was removed via anterior transconjunctival orbitotomy (**b**). Histopathologic examination revealed cyst wall lined by squamous epithelium with mild focal keratinization (**c** hematoxylin and eosin original magnification ×40). Subsequent orbital excision and biopsy of the orbital cyst/mass revealed teratoma. (Reprinted from Singh et al. [1]. with permission from Elsevier)

superotemporally from the frontozygomatic suture; 25% arise superomedially from the frontolacrimal suture (Fig. 9.3) [4]. Others may arise from frontoethmoidal sutures and in the deep temporalis fossa [5]. A few may arise from the sphenozygomatic suture.

The cysts are usually less than 2 cm in diameter and cause little ocular displacement. They are smooth, firm, nontender, and nonfluctuant. Many are not intraorbital but sit on the frontozygomatic suture or just behind the orbital rim. Mild lateral upper eyelid ptosis is often seen. Deeper dermoids may be seen along the medial and lateral orbital walls. These deeper dermoids remodel bone over many years. They may cause extraorbital expansion of the cyst into the temporal fossa or into the intracranial cavity [6]. Such patients may present with proptosis on mastication [7]. Deeper cysts often present later, in the third or fourth decade. Other presentations of deep cysts include proptosis and displacement of the eye opposite to the site of the cyst. Most patients will not have diplopia or visual problems as the cysts are of long duration [8].

Patients may present with discomfort because of leakage. Asymptomatic leakage of lipid and keratin may lead to inflammation and adherence of the dermoid cyst to neighboring structures. Intermittent lid swelling with localized redness and pain may be seen. Chronic inflammation may be seen even in asymptomatic patients. Ruptured dermoids may present with a fistula to the skin [9].

Differential Diagnosis

Superomedial lesions may be confused with retention cysts and orbitofrontal mucoceles. Medial dermoids must be differentiated from encephaloceles. Deep midline intranasal dermoid

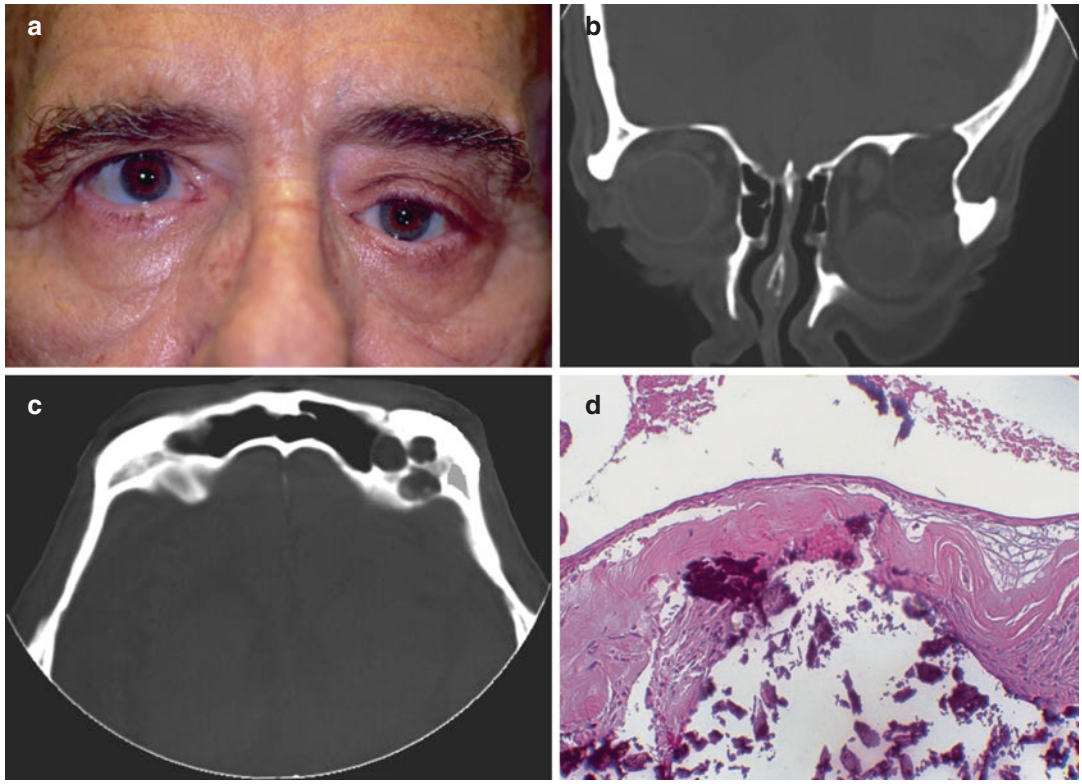

Fig. 9.3 Dermoid cyst. A 75-year-old male presented with left proptosis and hypoglobus with double vision of several months' duration (**a**). CT scan demonstrated thinning of the superotemporal orbital wall (**b** coronal view) and a cystic lesion (**c** axial view). The cyst wall is lined with stratified epithelium and there is keratin within the lumen (**d**)

cysts may present like discharging lacrimal sac mucoceles in children. Unlike mucoceles, the dermoids present with a central cutaneous dimple.

Deep superotemporal dermoids should be differentiated from lacrimal gland tumors radiographically, as dermoids often are isodense to fat and produce bony changes only in proximity to the frontozygomatic suture. Ultrasound may help confirm the cystic nature of the dermoid, although debris within the cyst may make the distinction difficult.

Diagnostic Evaluation

On CT scans, the majority of orbital dermoids have some adjacent bony changes, which are rounded and well defined (Fig. 9.3). A well-defined wall is seen with a center of fat density. Some will show calcification and fluid levels. In the presence of previous rupture, the margins may be irregular. The presence of a tunnel, channel, or cleft through the adjacent wall is noted in as many as a third of cases [10]. Many patients have a blind pit or cleft in the bone. Irregular bony margins suggest rupture with granulomatous distribution of the adjacent bone. Posterior masses may show bony pressure effects. Ultrasonography may be used for an anterior cyst.

Treatment

The surgical aim is to completely remove the dermoid. Dermoids presenting in childhood are removed soon after presentation to avoid traumatic rupture. Most can be safely removed via an

anterior or anterolateral orbitotomy. An upper eyelid skin crease approach with appropriate distraction of the incision can be used for removal of most superolateral dermoids. The cryoprobe may be used to provide traction during the dissection around the wall. While the plane of dissection is easier to follow if the cyst is intact, sometimes, especially for large cysts, decompression of the cyst is necessary to allow complete excision. If an inadvertent rupture of the cyst should occur, the area should be irrigated with an antibiotic solution, and the contents and lining should be meticulously removed.

Deeper superotemporal and inferotemporal cysts can be accessed via a lateral orbitotomy with removal of the lateral orbital wall [11]. A transfrontal craniotomy approach is used when cysts extend intracranially and for cysts at the apex of the orbit. Dumbbell tumors with extension into the temporal fossa are removed first from the orbit. The temporal component and the bony canal are subsequently removed. The bony tunnel should be cored out to remove the connecting stalk in dumbbell tumors.

Intradiploic Arachnoid Cyst

Introduction

Arachnoid cysts are congenital outpouchings within the arachnoid membrane filled with cerebrospinal fluid (CSF). Occasionally, these cysts occur in the intracranial intradiploic space, the majority of which have been reported following head trauma and associated with posttraumatic skull fractures in children. While the majority of intradiploic arachnoid cysts described in the literature have been traumatic in origin, there have been several reported nontraumatic cases. These nontraumatic cystic lesions are presumed to be congenital, with CSF pulsating through a dural defect into the intradiploic space and leading to gradual enlargement with thinning of the inner and outer tables of bone. Given the low pressure of CSF pulsations, Thomas and Rout have speculated that the lesions must be initiated before ossification of the cranium since normal CSF pressure would not likely cause intradiploic expansion in otherwise intact bone. Although these nontraumatic cases are presumed to be congenital, these cysts are generally identified in older patients.

Clinical Features

Patients may present with local pain or diffuse headache or proptosis. Sometimes, these lesions are identified as incidental findings when imaging is performed for nonassociated symptoms. The majority of these lesions have been identified in the occipital bone and the frontotemporal region. Figure 9.4 illustrates a case in a child where the sphenoid bone was involved.

Differential Diagnosis

In the pediatric population, the differential for calvarial lesions includes epidermoid or dermoid cyst, eosinophilic granuloma, aneurysmal bone cyst, lymphatic or vascular malformations, cystic fibrous dysplasia, multiple myeloma, giant cell tumor, metastatic disease, rhabdomyosarcoma, Ewing sarcoma, osteogenic carcinoma, and osteogenic sarcoma.

Diagnostic Evaluation

On CT scans, osseous expansion and remodeling is seen. MRI scans show no enhancement and no solid component of the mass and will follow CSF signal intensity on all pulse sequences [12].

Treatment

Surgical treatment of these lesions consists of craniectomy or craniotomy with fenestration of the cyst, excision of its pedicle, and repair of the dural defect, sometimes combined with implants to replace bony defects.

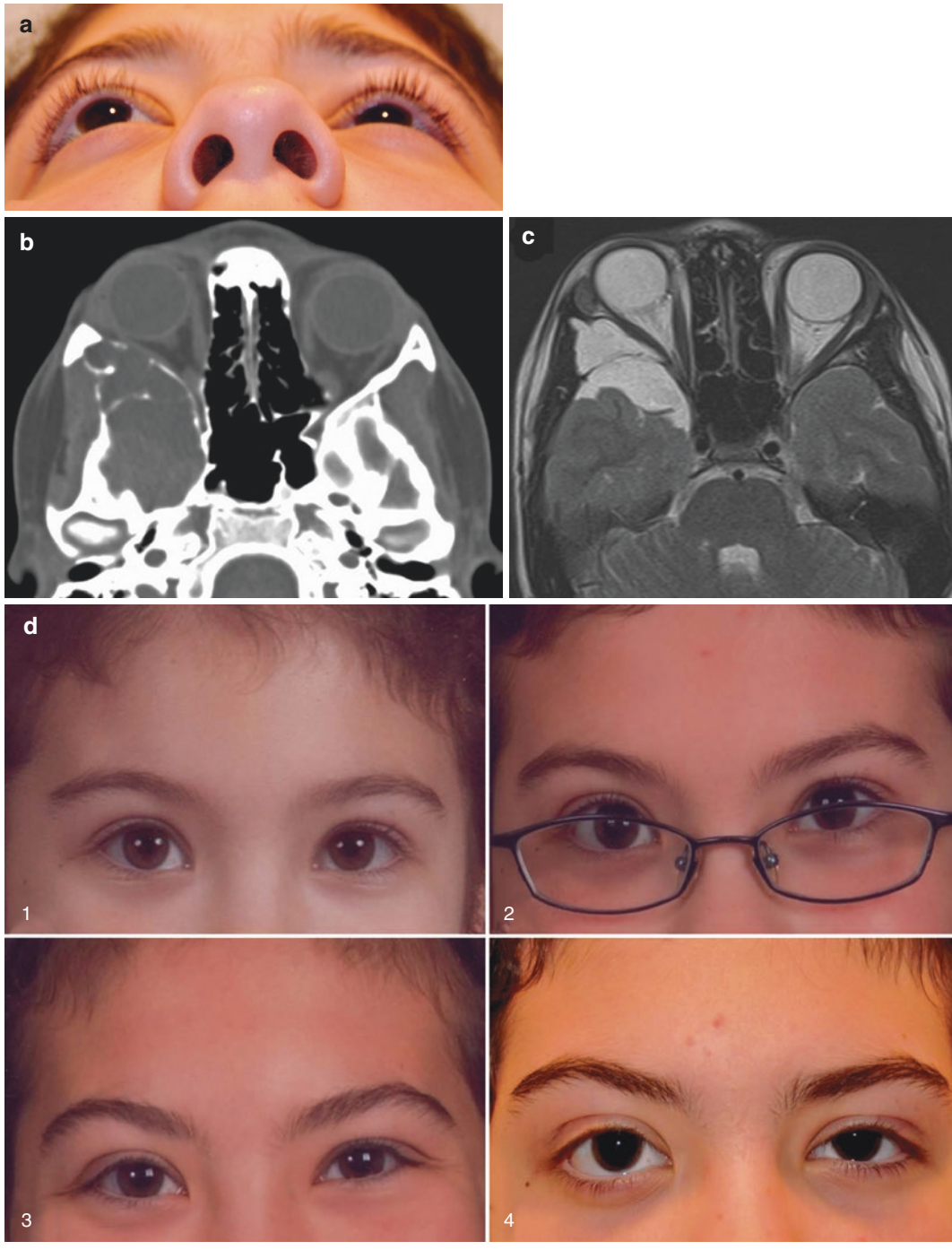

Fig. 9.4 Intradiploic cyst. External chin-up photograph demonstrates gross axial proptosis of the right eye (**a**). The eye otherwise appears normal. Axial non-contrast CT image demonstrates marked expansion and remodeling centered in the greater wing of the sphenoid. There is also an immediately adjacent arachnoid cyst overlying the right temporal lobe (**b**). Axial T2-weighted image confirms the presence of a middle cranial fossa arachnoid cyst and demonstrates fluid signal intensity in the cyst similar to that within the remodeled and expanded greater wing of sphenoid (**c**). External photographs show progressive right orbital fullness, most evidently superior to the lateral brow, dating 2006 (d-1), 2008 (d-2), 2010 (d-3), and current 2011 (d-4)

Mucocele

Introduction

Mucoceles occur mostly in adults; 60% affect the frontal sinus, while 30% occur in the ethmoid sinus, and 10% occur in the maxillary sinus. They result secondary to an obstruction of the ostium of the affected sinus. Mucoceles may result from facial fractures, nasal or sinus surgery, paranasal osteomas, chronic polyposis, or congenital abnormalities [13]. Mucoceles in childhood suggest underlying cystic fibrosis.

Clinical Features

Obstruction of the normal sinus ostia will create entrapment of the secretory epithelium, accumulation of mucous, pressure on the surrounding bony structures, thinning of the bony walls, and extension through the wall into the adjacent orbit, nasopharynx, or cranial cavity [14]. Mucocele may develop slowly with subacute exacerbations mimicking orbital cellulitis. Extension of the mucocele into the orbit will result in proptosis or other globe displacement, ptosis, a palpable superonasal mass, diplopia, headache, orbital pain, or visual impairment (Fig. 9.5). Orbital apex involvement may lead to orbital apex syndrome with deep orbital pain, headache, and visual impairment.

Frontoethmoid Mucocele

Clinical features are dependent upon the location of the sinus involved. Frontoethmoid mucocele may present with superomedial fullness, inferolateral displacement, epiphora, hypertelorism, or fistula [15]. Hypertelorism, seen more often in bilateral mucoceles, may be associated with cystic fibrosis.

Sphenoid and Posterior Ethmoid Sinus Mucocele

Sphenoid and posterior ethmoid sinus mucocele may cause visual changes and proptosis.

Maxillary Mucocele

A maxillary mucocele usually causes proptosis but may cause enophthalmos secondary to erosion of the floor of the orbit [16].

Diagnostic Evaluation

CT scans show a well-defined homogenous mass isodense with brain. Cystic contents completely fill the enlarged sinus and displace, rather than destroy, the bony margins (Fig. 9.5). The bone thins and the mucocele becomes part of the orbit.

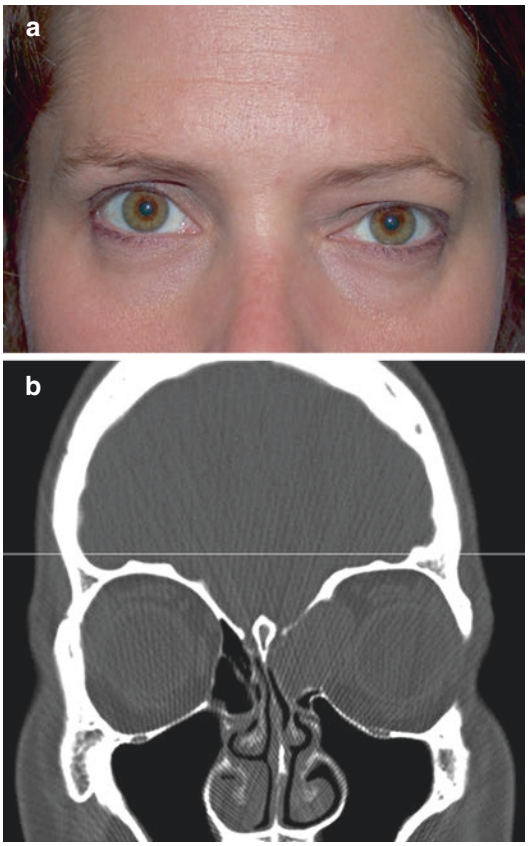

Fig. 9.5 Frontal mucocele. A 38-year-old female with a 2-week history of left periorbital pain and diplopia on upgaze (**a**). CT scan demonstrating left frontal mucocele with opacification of the frontal sinus and erosion of the superomedial orbital wall (**b**). The orbital component is well defined and rounded. The orbital structures are displaced inferiorly and laterally

Treatment

Management involves complete surgical removal of the lining and reestablishment of normal drainage or obliteration of the sinus. The optimal obliteration technique remains controversial. Methods include the use of muscle, fat, and alloplastic materials. Repair of the bony defect is rarely required. Displacement of the globe often improves after effective treatment [17].

Sinonasal Inverted Papilloma

Introduction

Primary inverted papilloma of the lacrimal system is unusual; most inverted papillomas arise from the lateral nasal wall and the maxillary and ethmoid sinuses and rarely from the frontal and sphenoid sinuses.

Clinical Features

Primary nasolacrimal system papillomas and secondarily invading sinonasal inverted papillomas present with epiphora and a medial canthal mass. Orbital extension of inverted papilloma occurs in 2–3% of cases.

Diagnostic Evaluation

CT scans reveal soft tissue attenuation in the lacrimal sac and nasolacrimal duct with bone remodeling and thinning and expansion of the nasolacrimal duct (Fig. 9.6). Associated changes will be seen in the adjoining sinuses when the primary origin is from the sinus. The lesion is a benign polypoid proliferation of the sinonasal mucosa, but the behavior is locally aggressive. Bony destruction with intraorbital and intracranial extension may be seen [18].

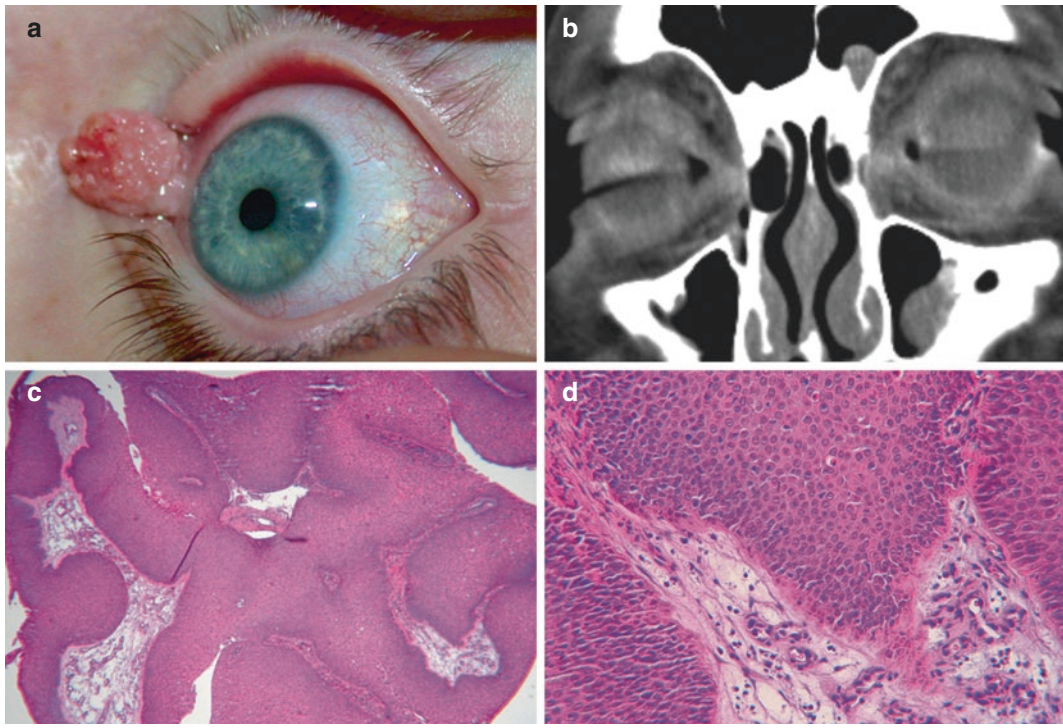

Fig. 9.6 Inverted papilloma. A large exophytic tumor at the caruncle (**a**). CT scan showing a diffuse mass in the caruncular region and the nasolacrimal duct (**b**). Ribbons of respiratory epithelium enclosed by basement membrane which grows into the subjacent stroma with micromucous cysts (**c**, **d**)

Treatment

The etiology of inverted papilloma is not well characterized: DNA viruses such as human papilloma virus (HPV) types 6 and 11 and the Epstein-Barr virus have been identified in the lesions. HPV presence indicates a higher likelihood of both malignancy and recurrence. Traditionally, these lesions have been approached via a medial maxillectomy through a lateral rhinotomy incision or midface degloving. Total resection with adequate margins has been the standard of care. Many cases are now effectively treated using endoscopic approaches, avoiding external incisions [19]. Recurrence of the tumor has been reported to range from 27 to 71%. Malignant transformation into carcinoma occurs in about 10% of cases.

Cholesterol Granuloma

Introduction

Nomenclature for cholesterol granuloma has changed from previous terms, including hematic cyst, hematoma, hematocele, chocolate cyst, blood cyst, subperiosteal hemorrhage, and orbital cholesteatoma. A cholesterol granuloma is not a true cyst, as it lacks an epithelial lining.

Cholesterol granulomas are seen mostly in men in their fourth or fifth decade in the superotemporal orbital wall and sometimes in the zygoma. Although factors causing elevated venous pressure, blood clotting diseases, and other causes have been invoked, it is now recognized that most cholesterol granulomas are caused by previous trauma [20]. Hematogenous debris accumulation creates an osmotic gradient with resultant absorption of fluid and increased volume. An anticoagulant effect caused by high concentrations of fibrinogen degradation products may also result in recurrent hemorrhage.

Clinical Features

The patient usually presents with a superolateral mass developing over weeks to years, causing inferior globe displacement, proptosis, and limited upgaze with diplopia in upgaze (Fig. 9.7). The patient may rarely have blurred vision. Headache or pain in the region of the mass may also occur.

Diagnostic Evaluation

CT scans reveal a well-defined, nonenhancing osteolytic lesion with bone erosion and sometimes intralesional bone fragments. The mass is usually homogenous and isodense with the brain [21]. The smooth margins contrast with the moth-eaten appearance seen with malignant tumors such as plasma cell myeloma. These lesions do not transgress the frontozygomatic suture. The differential diagnosis includes dermoid cyst and lacrimal gland carcinoma.

Treatment

Surgical evacuation of the lesion via a percutaneous approach is usually curative. There is usually a yellow-brown viscous material within the cavity containing friable tissue and loose bone. The bone itself may be yellow. The fluid is altered blood in various stages of degeneration and organization. Bone wax may be used to control oozing that occurs from the bony lining. Occasionally, a drain may be necessary at the end of the procedure. It is not necessary to pack the cavity. Recurrence is rare and when seen usually indicates subtotal curettage [22].

Orbital Cephalocele

Introduction

Cephaloceles are protrusions of brain tissue through bony defects. An encephalocele is a protrusion of the parenchymal brain. A meningocele has protrusion of dura, while a mixture of brain and meninges is a meningoencephalocele. All cephaloceles retain some attachment to the brain by a cord or stalk of tissue. These are often associated with other congenital facial anomalies involving the midline structures.

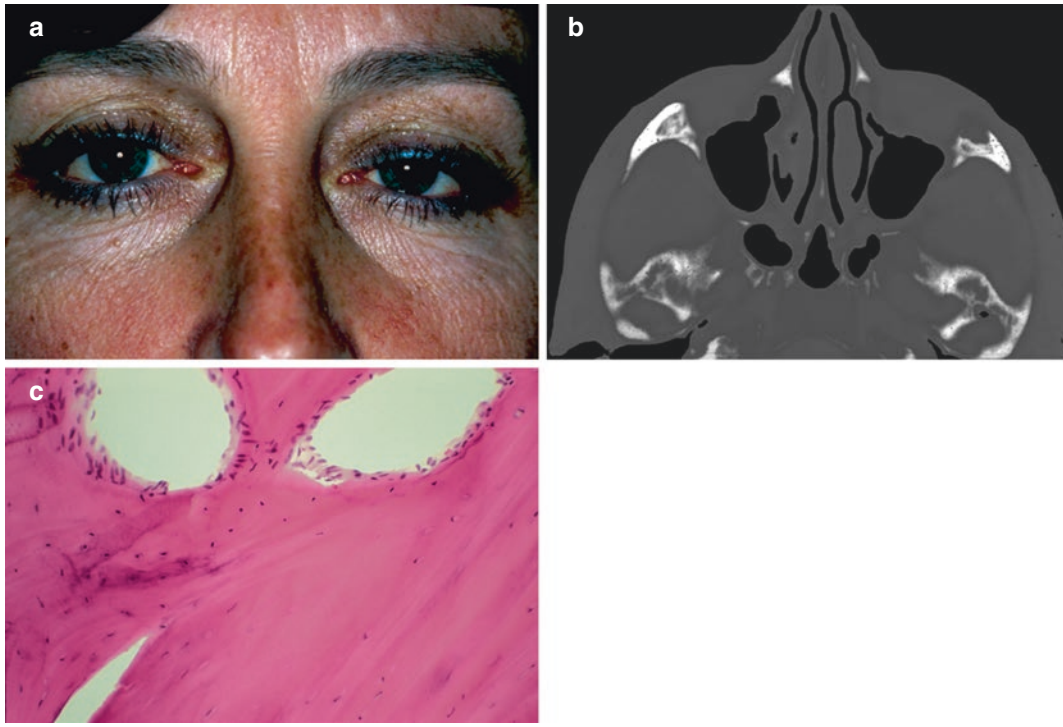

Fig. 9.7 Cholesterol granuloma. A 42-year-old female presents with left hypoglobus and a tender mass over the superolateral left orbital rim. History of trauma to the left orbit 6 months previously (**a**). Expansion of the diploic space of the left frontal bone is seen (**b**). Osteoid material with vascular channels (**c**). Older cholesterol granulomas would show frank cholesterol granulomas and lipid-laden histiocytes

Clinical Features

Cephaloceles may be anterior, basal, or posterior.

Anterior Cephalocele

Anterior cephalocele is the commonest, presenting as a paranasal mass located at the nasofrontal-orbital junction. The lesion may be soft or firm and is usually painless.

Basal Cephalocele

Basal cephalocele is associated with a defect in the cribriform plate and presents with a midline mass. The patient may have a broad nasal root, hypertelorism, and inferolateral globe displacement. The basal cephalocele may be confused with a mucocele and may also present as bilateral nasolacrimal duct obstructions [23].

Posterior Cephalocele

Posterior orbital cephalocele is less common; it herniates through a foramen or a dehiscence in the sphenoid bone and may present with pulsatile proptosis, optic nerve atrophy, and strabismus [24].

Diagnostic Evaluation

CT scans show a homogenous lesion, isodense with the brain. Dermoid and teratoma show more

fluid content. Mucocele is usually present below the medial canthal tendon, while cephalocele is located above the tendon.

Treatment

Management involves excision of the extracranial extension and stalk and repair of the dural and bony defect. Surgical repair involves a combined craniofacial and neurosurgical approach with correction of other facial deformities [25].

Neurofibroma and Neurilemmoma (Schwannoma)

Introduction

Neurofibromas are twice as common as schwannomas in the orbit and, together, constitute 4% of all orbital tumors. Isolated, solitary neurofibromas usually present in middle age and are in 90% of instances unassociated with neurofibromatosis. Plexiform neurofibromas may involve any of the cranial, sympathetic, and parasympathetic nerves in the orbit. Schwannomas are well-defined, encapsulated, slowly growing tumors that develop as eccentric growths from peripheral nerves. They are usually solitary and may also be associated with neurofibromatosis.

Clinical Features

Most neurofibroma and neurilemmoma manifest as a solitary mass, frequently in the upper quadrants. They are solid, isolated, circumscribed, slow-growing masses leading to displacement and local expansion of the orbit with associated anesthesia, paresthesia, and hypesthesia [26, 27]. In more superficial locations, the tortuous enlarged nerves produce a characteristic "bag of worms" feel, and the overlying skin may be thickened (elephantiasis neuromatosa). When intraconal, the tumor presents with proptosis, lid swelling, posterior indentation of the globe, and diplopia in extremes of gaze (Fig. 9.8). Apical tumors may extend through the superior and inferior orbital fissure. Defects in the greater wing of sphenoid may be seen.

Diagnostic Evaluation

Neurofibroma and neurilemmoma are homogenous, well-circumscribed tumors with a density similar to brain on CT scans with contrast enhancement. CT scans demonstrate bony expansion and may show superior orbital fissure expansion [28]. MRI shows isointensity to vitreous on T1-accentuated images and hypointensity to vitreous on T2-weighted sequences (Fig. 9.8).

Differential Diagnosis

The differential diagnosis of neurofibroma includes all causes for slowly progressing axial proptosis: meningioma, lymphangioma, fibrous histiocytoma, hemangiopericytoma, and cavernous hemangioma. On MR imaging, the lesion is indistinguishable from cavernous hemangioma, fibrous histiocytoma, and hemangiopericytoma.

Treatment

Although solitary orbital neurofibroma and neurilemmoma may be easily excised, the involved nerve is, by necessity, sacrificed. Therefore, care should be taken to identify the involved nerve as a sensory nerve rather than a motor nerve. Solitary neurofibroma and neurilemmoma are seen during surgery as well-defined, firm, circumscribed, rubbery, gray masses with little vascularity. Plexiform neurofibroma is vascular and diffusely intertwined with normal tissues. Complete surgical resection is rarely possible. When indicated, resection of plexiform neurofibroma is best approached through transfrontal craniotomy. Bleeding is always a problem. Repair of bony defects is necessary in the presence of

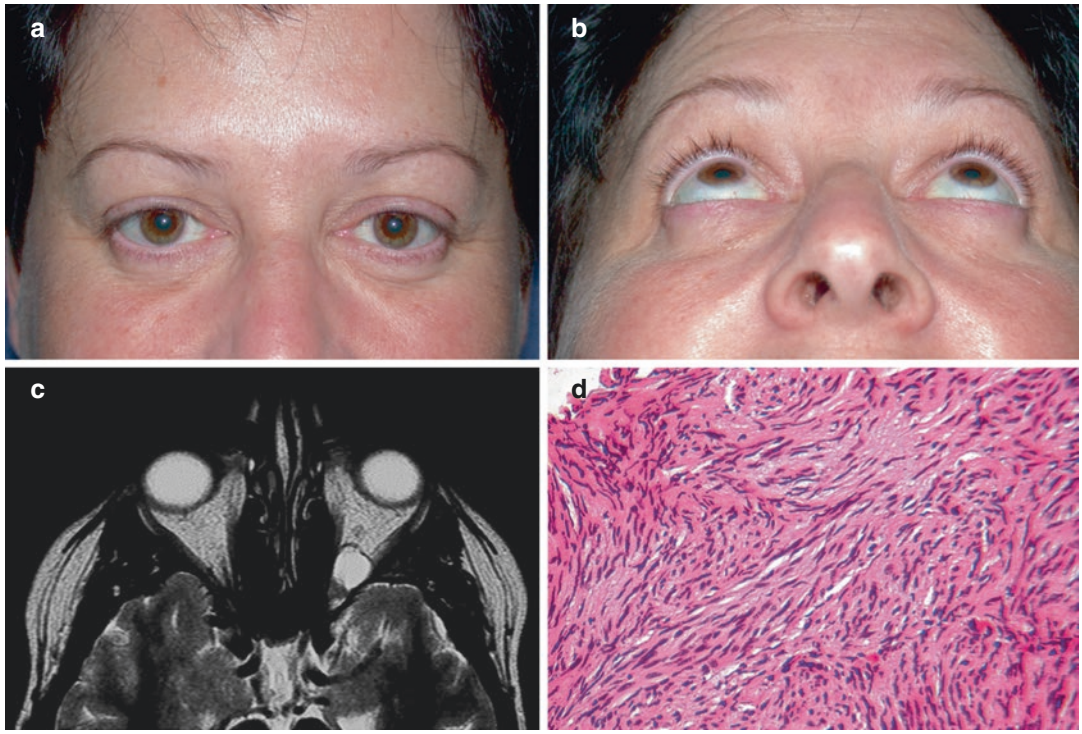

Fig. 9.8 Schwannoma. A 51-year-old female presents with left blurred vision, hypoglobus (**a**), and proptosis (**b**). MRI (T2-weighted image) shows a well-circumscribed apical superior orbital mass hyperintense to fat (**c**). Note spindle-shaped nuclei in whirling or fascicular pattern within eosinophilic glassy cytoplasm (**d**, H&E original magnification ×200)

pulsating proptosis. Complications can include bleeding, hematoma, cerebral edema, recurrence of pulsating proptosis and secondary socket, and orbital deformities.

Solitary Fibrous Tumor

Introduction

Solitary fibrous tumor (SFT) is a spindle cell tumor which arises most commonly from the pleura. The first case of SFT was described as recently as 1994 [29].

Clinical Features

Clinical presentation is like that of a hemangioma or hemangiopericytoma with proptosis, globe displacement, double vision, and vision changes (Fig. 9.9). Although orbital SFT typically follows a benign course, evidence of local invasion and malignancy may be seen. Although usually confined to the orbit, extraorbital extension has been described [30].

Diagnostic Evaluation

On imaging, the lesions usually appear well defined and may appear encapsulated with mild to moderate enhancement. Clinically, they are difficult to distinguish from hemangiopericytomas. Generally, there is no bony erosion although a few cases of bony erosion and extension of the tumors have been described. T2-weighted MRI images may reveal a hypointense or a hyperintense mass, depending upon the density of the fibrous matrix. Ultrasonically, SFTs have low reflectivity with

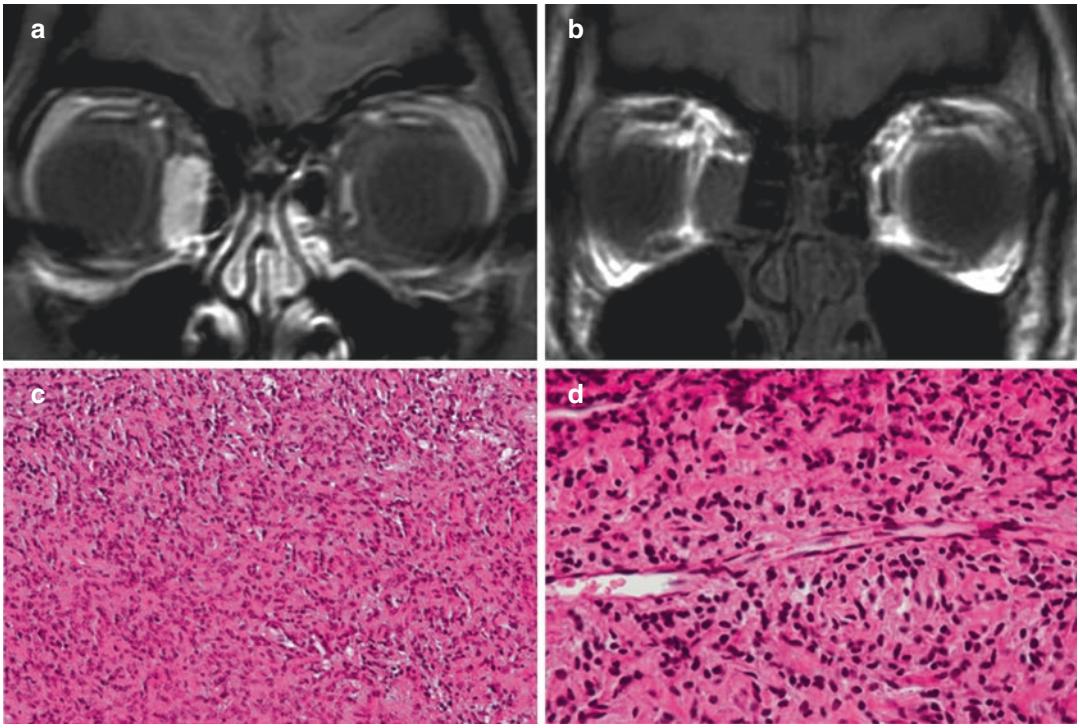

Fig. 9.9 Solitary fibrous tumor. A 37-year-old male who presents with a 3-week history of pressure behind the right eye with right proptosis and a headache. MRI showing an enhanced right medial orbital tumor (**a**, **b**). Tumor marked by cellularity and multiple small slit-like staghorn spaces (**c**). Benign-appearing vascular endothelial cells with some oval to spindle-shaped cells consistent with pericytes. No dysplastic features noted (**d**)

moderate sound attenuation. There has been controversy regarding the classification of SFT and orbital hemangiopericytoma as discrete entities due to overlapping histologic characteristics. Immunohistochemical studies help to distinguish SFT from other tumors, as it generally displays positivity for CD34, CD99, and bcl-2. Although hemangiopericytomas may also be positive for CD34, CD99, and bcl-2, hemangiopericytomas are usually focally or less intensely immunopositive. Staghorn vascular patterns are often seen in SFT and in hemangiopericytoma. Epithelial membrane antigen and smooth muscle actin may occasionally be expressed, while SFT is usually negative for S-100 and cytokeratins [31]. Histologic features suggestive of aggressive behavior include a high mitotic rate of more than four mitoses per ten high-powered fields, necrosis, hypercellularity, nuclear pleomorphism, and high MIB-1 labelling.

Treatment

Definitive management of SFT of the orbit is complete removal. In the presence of subtotal excision, close follow-up is indicated. Recurrence is usually seen in the presence of subtotal resection.

Meningioma

Introduction

Meningiomas constitute 20% of adult and 2% of childhood intracranial tumors. Primary meningioma, which affects a younger age group, arises within the orbit and may arise from the optic nerve sheath or the orbital surface of the sphenoid bone. The secondary type extends into the orbit from an intracranial source. These secondary tumors arise

from the sphenoid ridge, the basofrontal region, the suprasellar area, the olfactory groove, and the paranasal sinuses [32]. Most adult meningiomas are seen in the fifth decade with females being affected 75% of the time. Previous ionizing radiation and neurofibromatosis type 2 are predisposing factors. Only primary optic nerve sheath meningioma is discussed in this chapter.

Clinical Features

Patients may present with proptosis, decreased visual acuity, disc pallor, eyelid edema, disturbance of ocular motility, headaches or orbital pain, and seizures (Fig. 9.10). Chemosis is often seen. Some patients will have "boggy edema" of the eyelids. The more medial sphenoidal ridge tumors cause cranial nerve palsies, visual deficits, and venous obstructive signs. Proptosis is less prevalent in secondary meningiomas. A mass may be palpable in the temporal fossa when lateral expansion of meningiomas of the greater wing of the sphenoid bone occurs. Occasional bilateral meningiomas have been reported. Visual field testing as well as CT or MR imaging may help to judge progression of the tumor.

Diagnostic Evaluation

CT and MRI are both useful imaging modalities [33]. CT imaging often shows hyperostosis, and calcification is seen in 25% of the cases (Fig. 9.10). MRI shows a hyperintensity lesion against the isointense brain on T1-weighted sequences allowing delineation of intracranial meningiomas, especially when gadolinium enhancement is used.

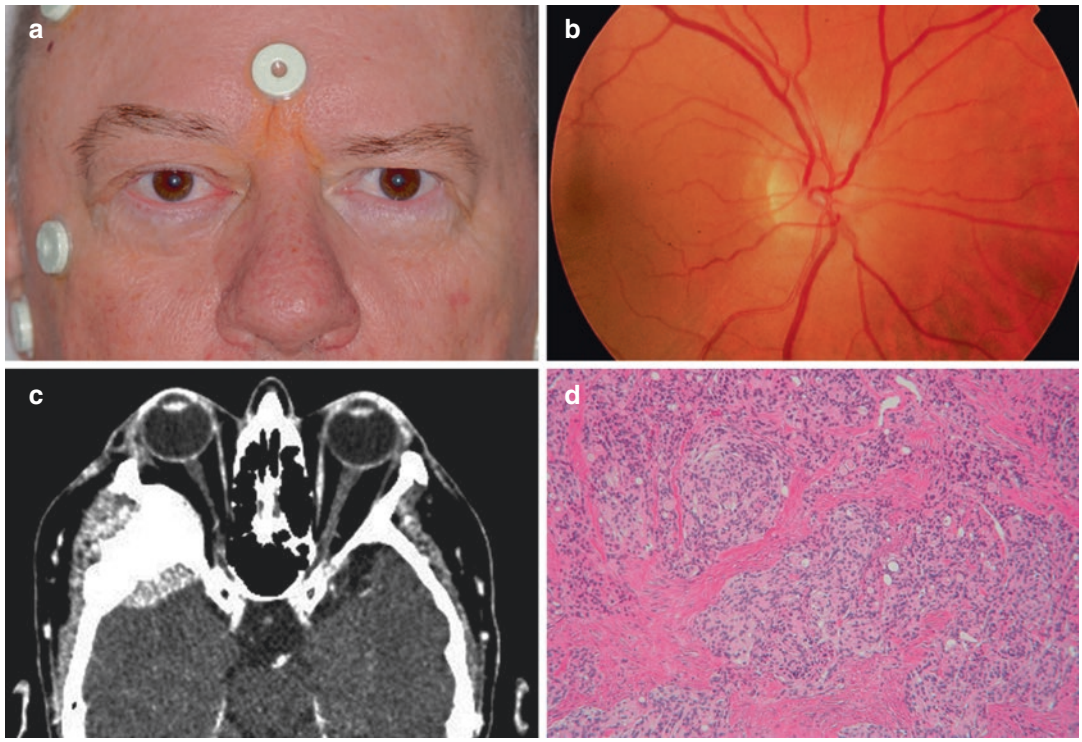

Fig. 9.10 Sphenoidal wing meningioma invading orbit. A 58-year-old male presented with bump on temple, decreased vision, and right-sided headaches (**a**). Right optic disc was edematous (**b**). CT scan demonstrated a right sphenoidal wing hyperostosis with a well-defined and homogenous soft tissue mass extending into the orbit (**c**). Histopathology shows parallel interlacing bundles of elongated cells. Whorled meningothelial cells are also present (**d**)

Treatment

It is believed that meningioma in patients younger than 20 years is more aggressive and requires earlier surgical intervention. Observation is warranted in older patients and where vision is not at risk. Observation is particularly warranted in meningiomas of the optic nerve where surgical resection is associated with high morbidity due to injury to the vascular supply of the optic nerve with 94% of patients reporting worsened vision postoperatively [34]. When the tumor is close to or abuts the globe, local radiation delivery may be difficult. In such cases, observation is also indicated (Fig. 9.11).

Major indications for surgery are disfiguring or severe proptosis, temporal fullness, orbital congestion, and impaired vision [35]. Aggressive

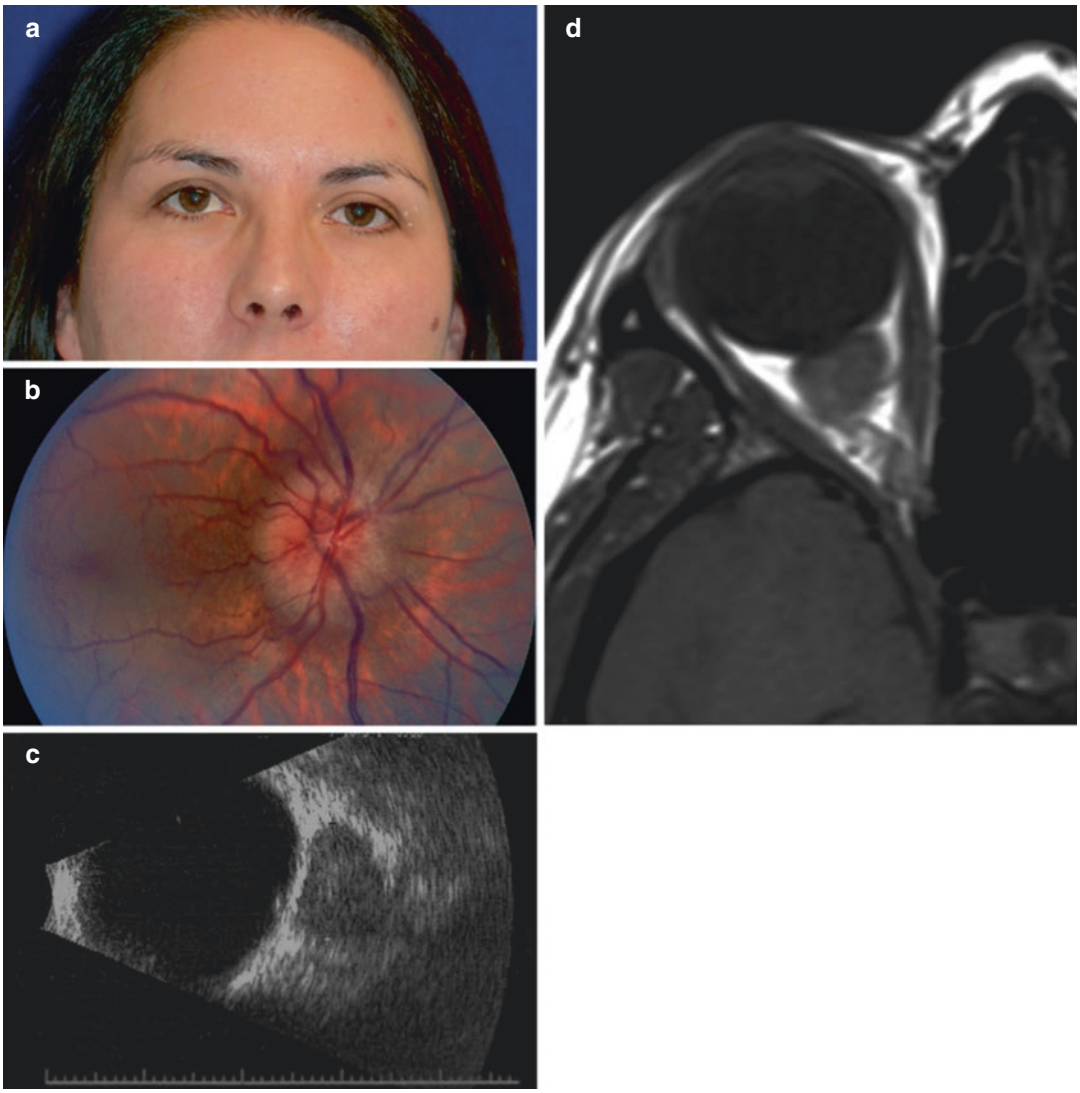

Fig. 9.11 Optic nerve sheath meningioma. A 38-year-old female presents with left proptosis and left hypoglobus (**a**). Fundus shows disc swelling (**b**). Ultrasonography shows an orbital mass abutting the globe (**c**). MRI shows mass involving the optic nerve, but the optic nerve cannot be made out distinctly from the mass (**d**, T1 and **e**, T2). CT scan shows absence of calcification in the mass (**f**). Histopathology shows a characteristic pattern of meningothelial meningioma. Note the whorls and nests of tumor cells (**g**, H&E 100×). Meningothelial cells have round to oval nuclei with intranuclear vacuoles. Mitotic activity is low (**h**, H&E 400×)

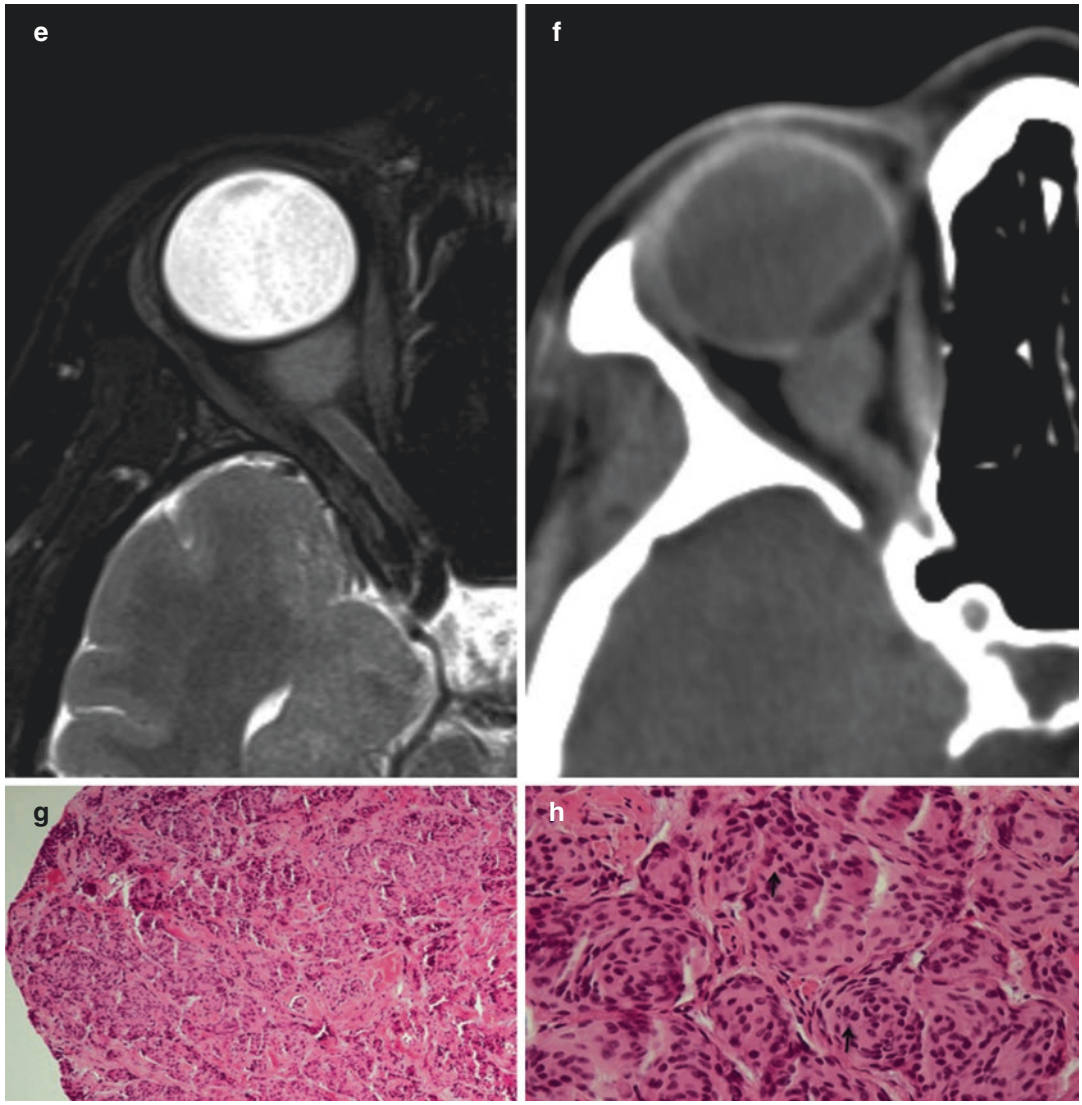

Fig. 9.11 (continued)

excision or debulking of sphenoid wing tumors may allow improvement in cosmesis, alleviate compressive symptoms, and postpone visual loss [36]. Most patients undergoing surgical resection of sphenoidal ridge meningioma develop recurrences over several years requiring further surgery. Recurrent, residual, and cavernous sinus disease may be treated with radiotherapy [37]. Stereotactic radiosurgical techniques allow more accurate delivery of radiation.

Teratoma

Introduction

Teratoma, formerly called teratoid cysts or teratoid tumors, is a tumor composed of tissues derived from more than one germ layer and usually from all three. They are rare tumors, usually seen at birth or in the neonatal period. Rarely, they may be seen in adolescents and adults [38].

Clinical Features

A typical teratoma presents as a rapidly bulging eye with marked orbital distortion in an infant. The mass may be soft or solid. The tumor enlarges rapidly and may present with marked orbital and facial changes. The persistent enlargement of this neoplasm is attributed to mucus secretion from the embryonic intestinal tissue. While malignant teratomas are seen, most teratomas are benign [39, 40].

Diagnostic Evaluation

The differential diagnosis includes orbital hemangioma, lymphangioma, rhabdomyosarcoma, retinoblastoma, metastatic tumors (neuroblastoma and leukemia), microphthalmos with cyst, congenital cystic eyeball, unilateral congenital glaucoma, cephalocele, and plexiform neurofibroma (Table 9.1). CT imaging shows orbital enlargement with focal calcification in the lumen of the tumor. Erosion of the greater wing of sphenoid bone may be seen. The definitive diagnosis of an orbital teratoma is made by histopathology which shows gut-like structures, the sine qua non for diagnosis of a teratoma.

Treatment

Although vision preservation is rare, surgery should remove the tumor but retain the eye if possible to encourage orbitofacial development. In more severe tumors, enucleation is necessary. Recurrent teratomas may undergo malignant degeneration. Therefore, close follow-up is necessary.

Table 9.1 The differential diagnosis of orbital teratoma

Category	Subcategory	Diagnosis
Congenital anomaly of the globe		Congenital cystic eyeball
		Microphthalmos with cyst
		Congenital glaucoma
Congenital anomaly of the orbit		Cephalocele
Orbital tumor	Primary	Hemangioma
		Lymphangioma
		Rhabdomyosarcoma
		Plexiform neurofibroma
	Secondary	Retinoblastoma
	Metastatic	Neuroblastoma
		Leukemia

Fibrous Histiocytoma

Introduction

Fibrous histiocytoma is the most common mesenchymal orbital tumor in adults, seen most commonly in middle-aged adults. They may be benign, locally aggressive, or malignant. Fibrous histiocytoma is defined as a proliferating, complex admixture of fibroblasts and histiocytic-like cells of biphasic nature in a fibrous or collagenous matrix of varying proportion, associated with minor contents of lymphocytes, macrophages, capillaries, lipid, and reticulin [41].

Clinical Features

These tumors, presenting most commonly with an upper nasal quadrant mass, are seen mostly in middle adult life. They are slow-growing, relatively firm masses. Patients present with proptosis, a mass effect, decreased vision, double vision, pain, eyelid swelling, and ptosis.

Diagnostic Evaluation

CT scans show a well-defined, irregular mass of uniform density. Bony erosion and enlargement of the orbit are seen with recurrent or malignant tumors. Ultrasound shows a well-defined mass with a smooth round or oval contour. Cystic cavities may be identified within the tumor.

Differential Diagnosis

Superotemporal tumors may mimic a lacrimal gland tumor. CT scan appearance of the tumor may resemble neurofibromas, schwannomas, or cavernous

hemangiomas. Histopathologically, benign fibrous histiocytoma must be differentiated from locally aggressive and malignant variant [42].

Treatment

Surgical excision via an orbitotomy is indicated. Complete excision is recommended as complete resection of the tumor results in a high rate of recurrence. Grossly, the tumor appears as a lobulated, well-circumscribed, firm, grayish white to yellow tan mass. Histopathology shows cartwheel bundles of elongated fibroblasts with spindle-shaped uniformly staining nuclei set in a dense fibrous stroma. The majority of tumors fall in the benign or intermediate group. However, aggressive tumors may spread locally some years after initial diagnosis. Malignant change may occur (Chap. 16).

Osteoma

Introduction

Primary osteomas of the orbit, although rare, are the most common bony tumor of the orbit. They are well-defined benign tumors of bone. Most are seen in the superonasal orbit and arise secondarily from the frontal sinus, ethmoidal sinus, and junctions [43].

Clinical Features

Osteoma is essentially an overgrowth of bone and presents as rock hard mass without pain. Most are solitary and asymptomatic (Fig. 9.12). However, larger lesions may cause proptosis and globe displacement. The patient may present

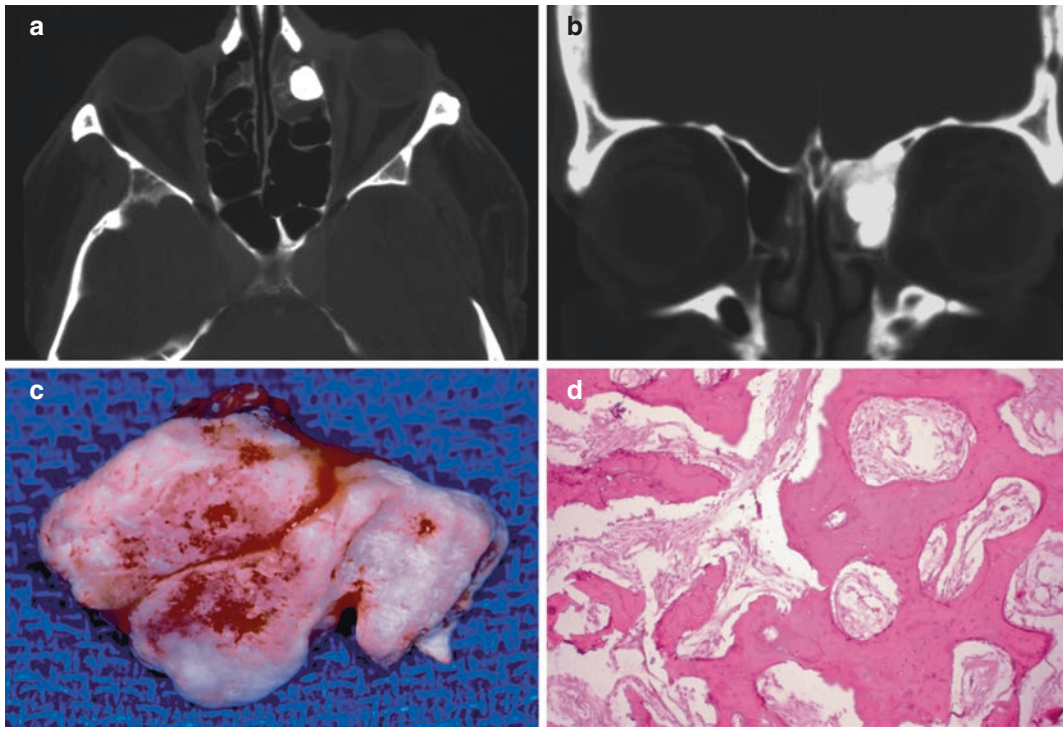

Fig. 9.12 Osteoma. CT scan showing a well-circumscribed radiodense mass in the medial wall of the left orbit (**a**, axial view) (**b**, coronal view). Typical appearance of the resected osteoma (**c**). Osteoma is composed of compact bone devoid of fibrovascular stroma (**d**)

with headaches. Chronic sinusitis or mucocele may result in frontal or frontoethmoid lesions. Frontal sinus osteoma presents with proptosis and downward displacement of the eye; ethmoidal osteomas produce a more lateral shift of the eye. Gardner syndrome is an autosomal dominant familial polyposis of the large bowel associated with osteoma of the skull or jaws and epidermal and sebaceous cysts of the subcutaneous tissues [44]. Some osteoma present with gaze-induced visual loss.

Diagnostic Evaluation

CT scans show a sharply circumscribed, very dense, rounded, or lobulated mass arising from bone (Fig. 9.12). Fibrous osteoma has a low-density, ground-glass appearance similar to fibrous dysplasia or ossifying fibroma. The adjacent paranasal sinus may be opacified from secondary drainage obstruction.

Treatment

If osteoma is symptomless, it may be followed [45]. Resection is indicated when secondary complications arise. Sphenoidal mass is resected endoscopically to prevent encroachment of the optic canal [46]. Recurrence is rare. Histologically, osteoma may be classified as compact, cancellous, and fibrous.

Fibrous Dysplasia

Introduction

Fibrous dysplasia is a benign, developmental disorder characterized by proliferation of fibrous tissue. It is a hamartomatous malformation thought to be an arrest of bone maturation at the woven bone stage. The fibrous tissue replaces and distorts medullary bones. Three forms have been described: monostotic, polyostotic, and McCune-Albright syndrome.

Monostotic Fibrous Dysplasia

Monostotic fibrous dysplasia usually involves one bone around the orbit. The monostotic type accounts for 80% of cases. The frontal bone is most frequently affected, followed by the sphenoid and ethmoid [47].

Polyostotic Fibrous Dysplasia

Polyostotic fibrous dysplasia involves multiple bones.

McCune-Albright Syndrome

McCune-Albright syndrome is a constellation of polyostotic fibrous dysplasia, sexual precocity, and cutaneous pigmentation [48].

Clinical Features

Although fibrous dysplasia progresses slowly, sudden exacerbation of disfigurement may be seen over weeks. Symptoms depend upon the anatomic site of the affected bone, the number of bones affected, the rate and duration of tumor growth, and the soft tissues compressed or displaced or distorted. Anterior tumors affecting the frontal, ethmoid, or maxillary bones displace the globe in the direction opposite to the involved bone. Unilateral progressive proptosis and globe displacement sometimes occur with limitation of ocular movement and diplopia (Fig. 9.13). Nasolacrimal duct obstruction may be seen. Patients may also present with persistent headaches or discomfort and compression at the orbital apex with involvement of III, IV, and VI and visual loss [49]. The optic chiasm may also be affected.

Secondary sphenoid sinus mucoceles may occur with sudden loss of vision because of compression of the optic nerve. Patients may develop an intralesional hemorrhage or a secondary aneurysmal bone cyst, both of which can cause compression of the optic nerve. Slow compression of the optic canal or at the chiasm may also result in chronic visual loss. Malignant transformation (in less than 1% of cases) to osteogenic sarcoma, fibrosarcoma, or chondrosarcoma may occur if prior radiotherapy has been administered [50].

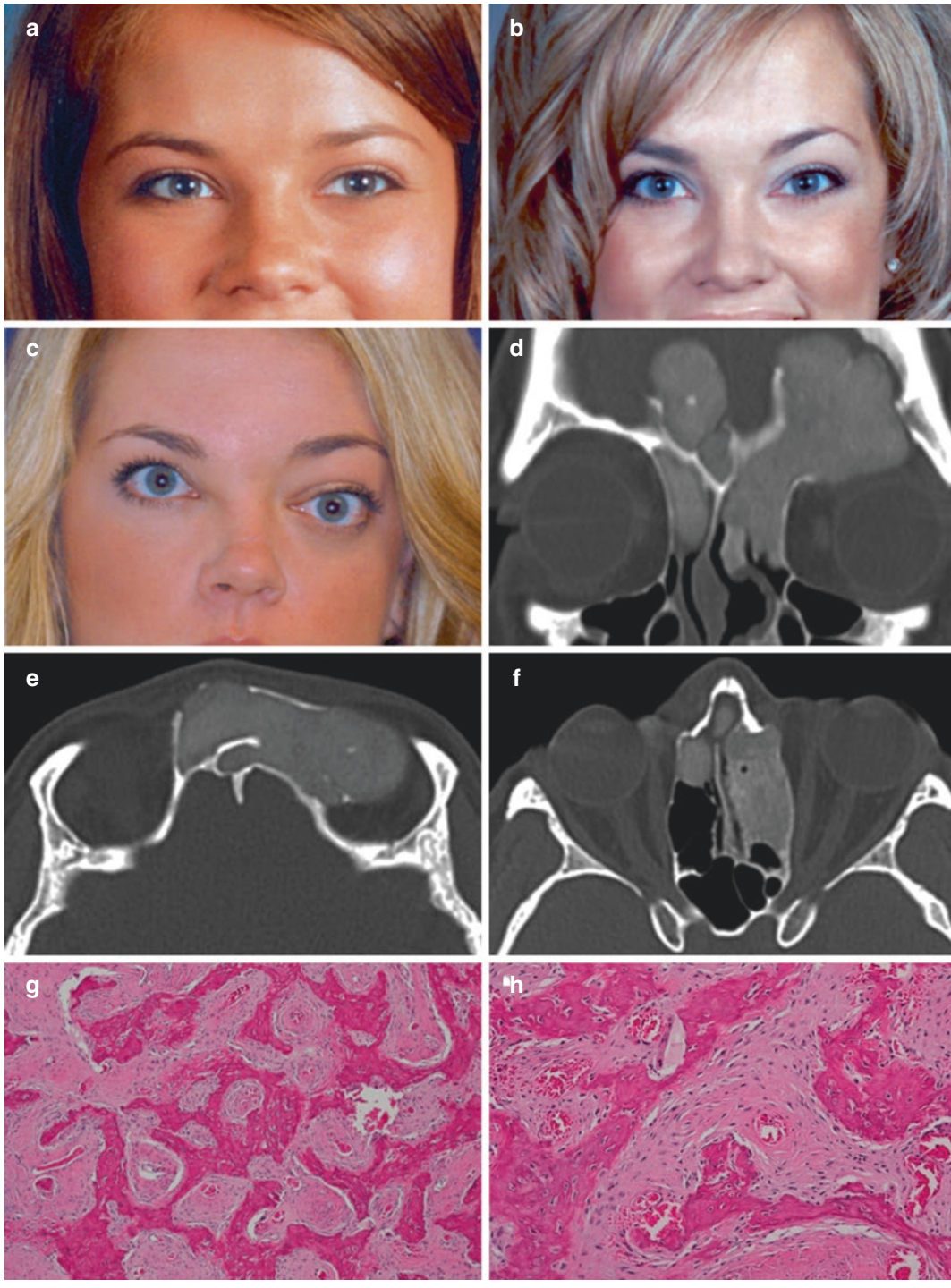

Fig. 9.13 Fibrous dysplasia. Clinical appearance at age 14 years (**a**), 18 years (**b**), and 21 years (**c**). Bone-window CT showing typical ground-glass appearance of fibrous dysplasia (**d**–**f**). Pattern of dense fibrous connective tissue in between spicules of woven bone (**g**, H&E 40×). The light pink is the fibrous connective tissue – it contains immature osteoprogenitor cells. The dark pink is immature woven bone. At higher magnification you can easily make out chondrocytes in the immature osseous structure. Of note, there are no osteoblasts (**h**, H&E 200×)

Diagnostic Evaluation

CT scans show increased bone thickness. Increased fibrous content makes the bone look more lucent in appearance and may show a cystic appearance; a more prominent osseous component gives a ground-glass or sclerotic character. Mixed pattern of alternating sclerosis and radiolucency is often seen. The orbital contour is narrowed and adjacent sinuses are replaced with dense bone.

Differential Diagnosis

Differential diagnosis includes hyperostotic meningioma which will show an associated enhancing soft tissue component (best visualized on MRI). Other conditions to be considered include Paget's disease and cystic bone lesions, such as Langerhans cell histiocytosis. Although juvenile ossifying fibromas have been distinguished from fibrous dysplasia, such fibromas may occur in the presence of fibrous dysplasia (Fig. 9.14) [51].

Treatment

There has been much debate about whether surgical intervention before the patient is symptomatic is useful. As the complications of major craniofacial surgical intervention are significant, surgery is only indicated for gross deformity, functional deficits, pain, or sarcomatous transformation. In the presence of optic canal compression, resection and reconstruction are indicated. However, as most patients with fibrous dysplasia will remain asymptomatic during long-term follow-up, expectant management has been recommended in asymptomatic patients even in the presence of radiological evidence of apical compression of the optic nerve [52].

Aneurysmal Bone Cyst

Introduction

Aneurysmal bone cyst is a reactive lesion of bone. Aneurysmal bone cyst may arise in the orbit secondary to trauma or as a result of local vascular disturbance. In 30% of cases, the cyst is associated with an underlying bone lesion, such as fibrous dysplasia, non-ossifying fibroma, or giant cell tumor [53]. The orbital roof is most commonly involved.

Clinical Features

Patients present with proptosis, displacement of the globe, and diplopia secondary to cranial nerve palsy (Fig. 9.15). There may be pain and local swelling. The patient may present with refractive changes. Compressive optic neuropathy and visual loss are rare.

Diagnostic Evaluation

CT scans show an irregular lytic bone lesion with cortical destruction (Fig. 9.15). A fluid level may be seen within the cavities due to hemorrhage with settled blood products. The margins of the tumor may show calcification. MRI scans show a multicystic mass with associated bone destruction. Fluid-filled levels may be seen with varying levels of signal intensity, depending upon the state of the blood within the cyst [54].

Treatment

Complete surgical curettage is usually curative. The prognosis is usually excellent. Visual compromise is very rare. Radiation, used in the past, is inadvisable because of potential risk of radiation-induced sarcoma.

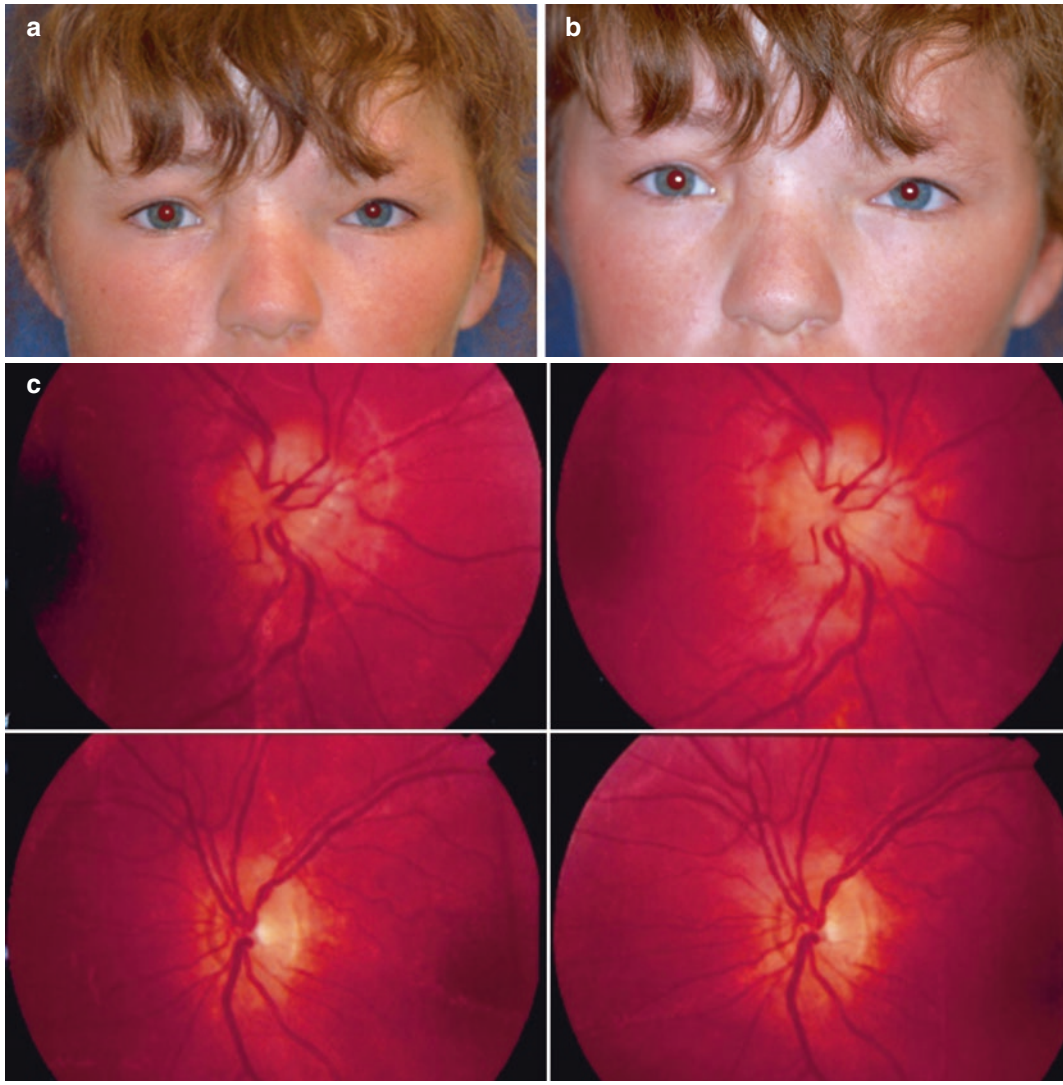

Fig. 9.14 Fibroma arising from fibrous dysplasia. Left hypoglobus and proptosis with superonasal mass at age 15 years (**a**, **b**). Right optic nerve swelling with evidence of compression of the right optic nerve (**c**). T1-weighted MRI scan shows typical low signal in the ethmoid and sphenoid sinus, typical of fibrous dysplasia (**d**). At low magnification you can see fascicles of dense irregular fibrous connective tissue (**e**, 40× and **f**, 200×). These findings are consistent with a dense fibroma. Normal bone is seen on the far left with marrow space, osteoblasts, and vessels. Fibrous dysplastic bone is on the right (**g**, 40×)

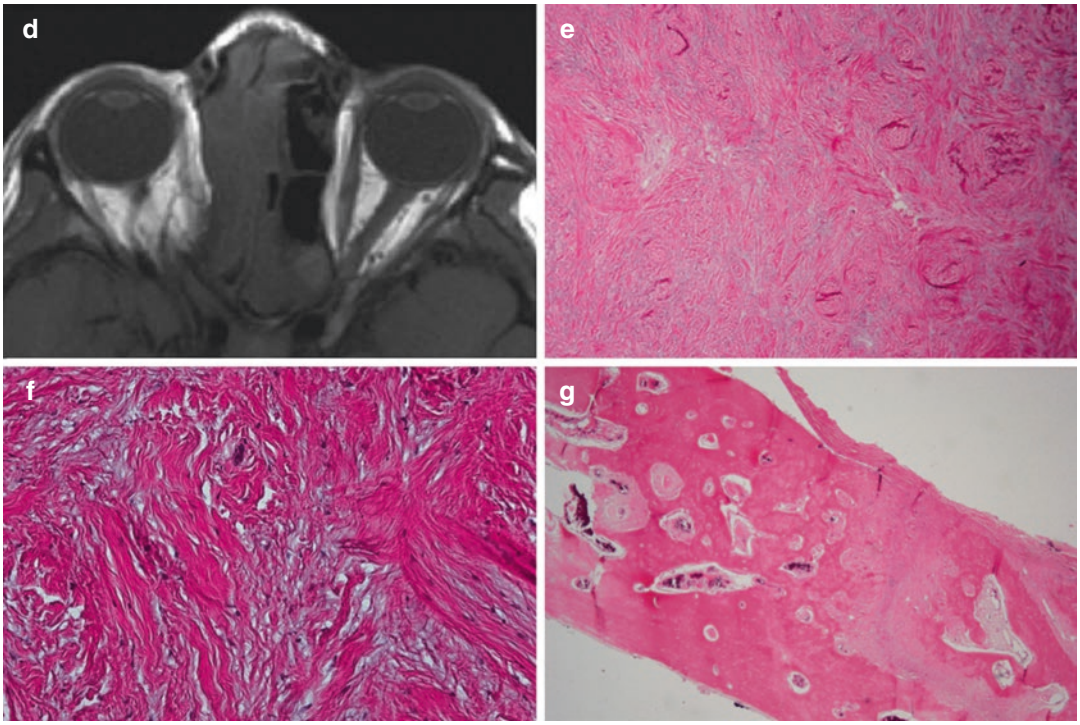

Fig. 9.14 (continued)

Leiomyoma

Introduction

Orbital leiomyoma is a rare, benign tumor of well-differentiated striated muscle which may present anywhere in the orbit [55].

Clinical Features

Slowly progressive proptosis is the commonest presentation without evidence of inflammation or pain. Extraocular muscle involvement with motility problems may be seen. Rhabdomyomas are divided into five types: adult type, fetal type, genital type, rhabdomyomatous mesenchymal hamartoma of skin, and cardiac type.

Diagnostic Evaluation

CT and MRI scans will show diffuse lesions with no specific features to aid with the diagnosis. Histology shows no nuclear pleomorphism, giant cells, or mitotic figures which helps distinguish this from a leiomyosarcoma. There is lack of nuclear atypia; the tumor is S-100 negative and actin and desmin positive. The differential diagnosis is vast and includes leiomyosarcoma, infiltrative processes, rhabdomyosarcoma, lymphoma, granular cell myoblastoma, reticulohistiocytoma, and meningioma.

Treatment

Complete surgical resection is desirable. Because the tumors are diffuse, incomplete resection is more

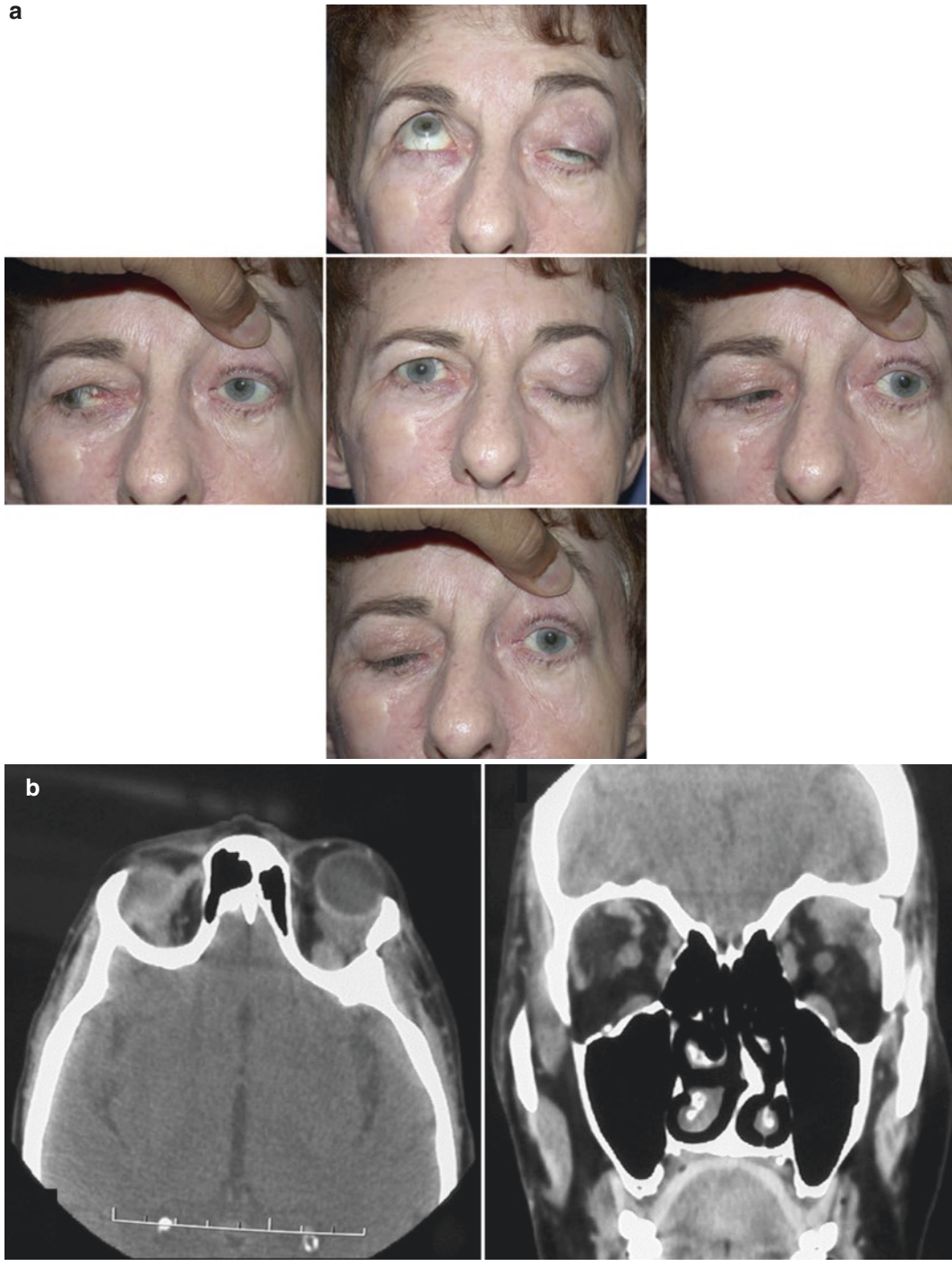

Fig. 9.15 Leiomyoma. A 68-year-old female had a left orbital tumor removed elsewhere without a definitive diagnosis. She was left with a complete left ophthalmoplegia and complete left ptosis following surgery. She presented for a diagnostic evaluation. Her vision was 20/25 right and 20/50 left with no afferent pupillary defect and full color vision (**a**). CT shows an ill-defined left orbital mass involving the superior rectus and lateral rectus and possibly the lacrimal gland. Abnormal enhancement was seen through the bony defect which was the site of the prior lateral bony orbitotomy (**b**).On H&E, pathology shows well-striated muscles with a collagenous stroma, lack of nuclear atypia, and centrally placed nuclei indicating immature striated muscle cells (**c**). Negative for S-100 stain except for a few cells (**d**). Positive for smooth muscle actin (**e**) and desmin (**f**)

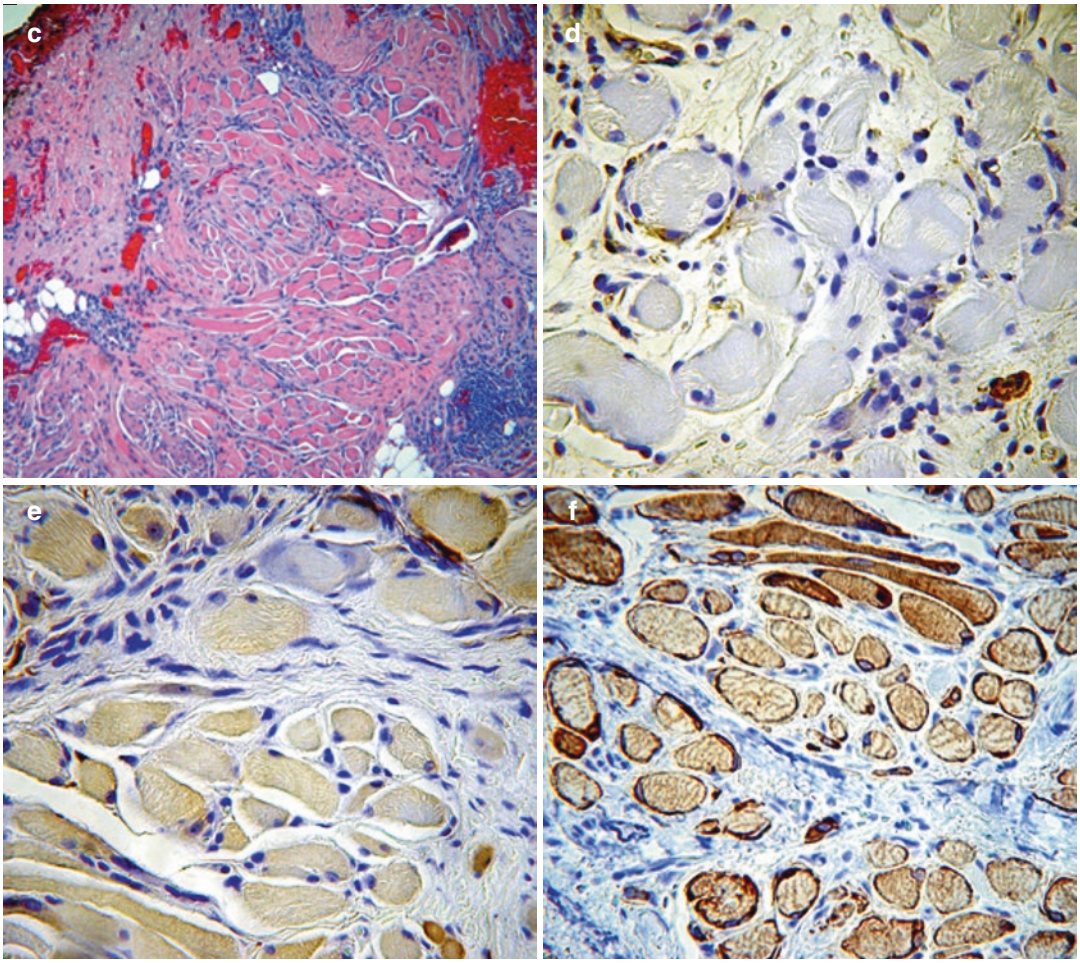

Fig. 9.15 (continued)

common. The patient will need to be followed for further growth. These tumors are radioresistant and can transform into sarcomas with irradiation.

References

1. Singh AD, Traboulsi EI, Reid J, Patno D, Chapa J, Rodriguez R, Iben S, Schoenfield L. Orbital cyst: prenatal diagnosis. Ophthalmology. 2009;116(10):2042–42.e2.
2. Shields JA, Shields CL, Scartozzi R. Survey of 1264 patients with orbital tumors and simulating lesions: the 2002 Montgomery lecture. part 1 Ophthalmology. 2004;111(5):997–1008.
3. Shields JA, Kaden IH, Eagle RC Jr, Shields CL. Orbital dermoid cysts: clinicopathologic correlations, classification and management. Ophthal Plast Reconstr Surg. 1997;13:265–76.
4. Bonavolonta G, Tranfa G, de Conciliis C, et al. Dermoid cysts: 16-year survey. Ophthal Plast Reconstr Surg. 1995;11:187–92.
5. Meyer DR, Lessner AM, Yeatts RP, et al. Primary temporal fossa dermoid cysts. Characterization and surgical management. Ophthalmology. 1999;106(2):342–9.
6. Perry JD, Tuthill R. Simultaneous ipsilateral temporal fossa and orbital dermoid cysts. Am J Ophthalmol. 2003;135(3):413–5.
7. Emerick GT, Shields CL, Shields JA, et al. Chewing-induced visual impairment from a dumbbell dermoid cyst. Ophthal Plast Reconstr Surg. 1997;13:57–61.
8. Sherman RP, Rootman J, Lapointe JS. Orbital dermoids: clinical presentation and management. Br J Ophthalmol. 1984;68:642–52.
9. Wells TS, Harris GJ. Orbital dermoid cyst and sinus tract presenting with acute infection. Ophthal Plast Reconstr Surg. 2004;20(6):465–7.

10. Sathananthan N, Moseley IF, Rose GE, et al. The frequency and clinical significance of bone involvement in outer canthus dermoid cysts. Br J Ophthalmol. 1993;77(12):789–94.
11. Yuen HK, Chong YH, Chan SK, et al. Modified lateral orbitotomy for intact removal of orbital dumbbell dermoid cyst. Ophthal Plast Reconstr Surg. 2004;20(4):327–9.
12. Thomas TA, Rout D. Non-traumatic intraosseous cerebrospinal fluid cyst with associated craniovertebral anomalies: a case report and suggested mechanism of formation. Neurol India. 2010;58:122–4.
13. Illiff CE. Mucoceles in the orbit. Arch Ophthalmol. 1973;89:392–5.
14. Delfini R, Missori P, Iannetti G, et al. Mucoceles of the paranasal sinuses with intracranial and intraorbital extension: report of 28 cases. Neurosurgery. 1993;32:901–6.
15. Lund VJ, Rolfe ME. Ophthalmic considerations in fronto-ethmoidal mucoceles. J Laryngol Otol. 1989;103:667–9.
16. Garber PF, Abramson AL, Stallman PT, et al. Globe ptosis secondary to maxillary sinus mucocele. Ophthal Plast Reconstr Surg. 1995;11:254–60.
17. Benninger MS, Marks S. The endoscopic management of sphenoid and ethmoid mucoceles with orbital and intranasal extension. Rhinology. 1995;33:157–61.
18. Golub JS, Parikh SL, Budnick SD, et al. Inverted papilloma of the nasolacrimal system invading the orbit. Ophthal Plast Reconstr Surg. 2007;23(2):151–3.
19. Nakamaru Y, Furuta Y, Takagi D, et al. Preservation of the nasolacrimal duct during endoscopic medial maxillectomy for sinonasal inverted papilloma. Rhinology. 2010;48(4):452–6.
20. McNab AA, Wright GE. Orbitofrontal cholesterol granuloma. Ophthalmology. 1990;97:28–32.
21. Hill CA, Moseley IF. Imaging of orbitofrontal cholesterol granuloma. Clin Radiol. 1992;46:237–42.
22. Sia DI, Davis G, Selva D. Recurrent orbitofrontal cholesterol granuloma: a case report. Orbit. 2012;31(3):184–6.
23. Bagheri A, Naghibozakerin J, Yazdani S. Cerebrospinal fluid leakage during dacryocystorhinostomy in a patient with meningoencephalocele. Eur J Ophthalmol. 2005;15(4):500–3.
24. Strandberg B. Cephalocele of posterior part of orbi. General survey, with report of caset. Arch Ophthal. 1949;42:254–65.
25. Songur E, Mutluer S, Gurler T, et al. Management of frontoethmoidal (sincipital) encephalocele. J Craniofac Surg. 1999;10:135–9.
26. Rose GE, Wright JE. Isolated peripheral nerve sheath tumours of the orbit. Eye. 1991;5:668–73.
27. Rootman J, Goldberg C, Robertson W. Primary orbital schwannomas. Br J Ophthalmol. 1982;66:194–204.
28. Dervin JE, Beaconsfield M, Wright JE, et al. CT findings in orbital tumors of nerve sheath origin. Clin Radiol. 1989;40:475–9.
29. Tam ES, Chen EC, Nijhawan N, et al. Solitary fibrous tumor of the orbit: a case series. Orbit. 2008;27(6):426–31.
30. Young TK, Hardy TG. Solitary fibrous tumor of the orbit with intracranial involvement. Ophthal Plast Reconstr Surg. 2011;27(3):e74–6.
31. Gengler C, Guillou L. Solitary fibrous tumour and haemangiopericytoma: evolution of a concept. Histopathology. 2006;48:63–74.
32. Honeybul S, Neil-Dwyer G, Lang DA, et al. Sphenoid wing meningioma en plaque: a clinical review. Acta Neurochir. 2001;143(8):749–57.
33. Ehlers N, Malmros R. The suprasellar meningioma. A review of the literature and presentation of a series of 31 cases. Acta Ophthalmol Suppl. 1973;121:1–74.
34. Bloch O, Matthew S, Gurvinder K, et al. Fractionated radiotherapy for optic nerve sheath meningiomas. J Clin Neurosci. 2012;19:1210–5.
35. Shrivastava RK, Sen C, Costantino PD, et al. Sphenoorbital meningiomas: surgical limitations and lessons learned in their long-term management. J Neurosurg. 2005;103(3):491–7.
36. Sandalcioglu IE, Gasser T, Mohr C, et al. Sphenoorbital meningiomas: interdisciplinary surgical approach, resectability and long-term results. J Craniomaxillofac Surg. 2005;33(4):260–6.
37. Peele KA, Kennerdell JS, Maroon JC, et al. The role of postoperative irradiation in the management of sphenoid wing meningiomas. A preliminary report. Ophthalmology. 1996;103:1761–7.
38. Mamalis N, Garland PE, Argyle JC, et al. Congenital orbital teratoma: a review and report of two cases. Surv Ophthalmol. 1985;30:41–6.
39. Gnanaraj L, Skibell BC, Coret-Simon J, et al. Massive congenital orbital teratoma. Ophthal Plast Reconstr Surg. 2005;21(6):445–7.
40. Mahesh L, Krishnakumar S, Subramanian N, et al. Malignant teratoma of the orbit: a clinicopathological study of a case. Orbit. 2003;22(4):305–9.
41. Jacobiec FA, Howard GM, Jones IS, et al. Fibrous histiocytomas of the orbit. Am J Ophthalmol. 1974;77:333–45.
42. Font RL, Hidayat AA. Fibrous histiocytoma of the orbit. A clinicopathologic study of 150 cases. Hum Pathol. 1982;13:199–209.
43. Grove AS Jr. Osteoma of the orbit. Ophthalmic Surg. 1978;9:23–39.
44. McNab AA. Orbital osteoma in Gardner's syndrome. Aust N Z J Ophthalmol. 1998;26:169–70.
45. Ciappetta P, Delfini R, Iannetti G, et al. Surgical strategies in the treatment of symptomatic osteomas of the orbital walls. Neurosurgery. 1992;31:628–35.
46. Naraghi M, Kashfi A. Endonasal endoscopic resection of ethmoido-orbital osteoma compressing the optic nerve. Am J Otolaryngol. 2003;24(6):408–12.
47. Bibby K, McFadzean R. Fibrous dysplasia of the orbit. Br J Ophthalmol. 1994;78:266–70.

48. Albright F, Butler AM, Hampton AO, et al. Syndrome characterized by osteitis fibrosa disseminata, areas of pigmentation and endocrine dysfunction with precocious puberty in females. N Engl J Med. 1937;216:727–46.
49. Osguthorpe JD, Gudeman SK. Orbital complications of fibrous dysplasia. Otolaryngol Head Neck Surg. 1987;97:403–5.
50. Yabut SM, Kenan S, Sissons HA. Malignant transformation of fibrous dysplasia. A case report and review of the literature. Clin Orthop. 1988;228:281–9.
51. Linhares P, Pires E, Carvalho B, et al. Juvenile psammomatoid ossifying fibroma of the orbit and paranasal sinuses. A case report. Acta Neurochir. 2011;153(10):1983–8.
52. Amit M, Collins MT, FitzGibbon EJ, et al. Surgery versus watchful waiting in patients with craniofacial fibrous dysplasia–a meta-analysis. PLoS One. 2011;6(9):e25179.
53. Lucarelli MJ, Bilyk JR, Shore JW, et al. Aneurysmal bone cyst of the orbit associated with fibrous dysplasia. Plast Reconstr Surg. 1995;96:440–5.
54. Patel BC, Sabir DI, Flaharty PM, et al. Aneurysmal bone cyst of the orbit and ethmoid sinus. Arch Ophthalmol. 1993;111:586–7.
55. Fernandes BF, Castiglione E, Belfort RN, et al. Orbital leiomyoma: histopathologic and immunohistochemical findings of a rare tumor. Ophthal Plast Reconstr Surg. 2009;25(1):59–61.

Orbital Meningioma

10

Bhupendra C. K. Patel and William T. Couldwell

Introduction

Meningiomas arise from meningothelial cells (arachnoid cap cells) with the tumors being attached to the inner surface of the dura. Meningiomas arise wherever meninges exist: the commonest sites are the parasagittal region, skull base, cerebral convexities, and the falx. Felix Plater first described the features of a meningioma in 1614 at an autopsy. Cushing coined the term "meningioma" in 1922 [1].

Meningiomas are the most common primary brain tumors comprising 13%–20% of all brain tumors and 34–36% of all primary brain tumors [2]. Meningiomas make up 4% of all orbital tumors. Meningioma surgery has been described as the single procedure that has most advanced in neurosurgery [3].

Orbital meningiomas are divided into:

- Primary orbital meningiomas
- Optic nerve meningiomas
- Sphenoidal wing meningioma with orbital involvement

Primary Orbital Meningioma

Primary orbital meningiomas, also termed intraorbital ectopic meningioma, are thought to arise without any discernible optic nerve sheath or meningeal connection. These are rare tumors that present around 30 years of age, and it has been suggested that they arise from ectopic arachnoid tissue. Most of the described cases have tumors superomedially, medially, or inferomedially in the orbit. Trauma is thought to be responsible for some of these tumors, but a history of trauma has usually not been present in the cases described to date. It has been suggested that with advanced radiological imaging, many of these will be found to have connections to the olfactory groove or have other subtle skull base lesions which may be missed [4]. The cases that have been described have been mostly meningotheliomatous (syncytial) or transitional meningioma, locally invasive but with a good prognosis with complete removal of the tumor.

Optic Nerve Sheath Meningioma

A brief overview is given here as these tumors are discussed in more detail in the chapter on optic nerve tumors (Chap. 11).

Optic nerve sheath meningiomas (ONSM) arise from the optic nerve sheath arachnoid layer and make up 2% percent of all orbital tumors and

B. C. K. Patel (✉)
Division of Facial Cosmetic and Reconstructive Surgery, University of Utah, Salt Lake City, UT, USA
e-mail: bhupendra.patel@hsc.utah.edu

W. T. Couldwell
Department of Neurosurgery, University of Utah, Salt Lake City, UT, USA

C. J. Hwang et al. (eds.), *Clinical Ophthalmic Oncology*,
https://doi.org/10.1007/978-3-030-13558-4_10

1–2% of all meningiomas [5, 6]. ONSM are the second most common optic nerve tumors after gliomas and can be associated with neurofibramosis type 2.

Patients present with proptosis and visual complaints and can demonstrate the classic triad of vision loss, optic atrophy, and optociliary shunt vessels. Five percent of cases are bilateral. The tumors envelop the optic nerve in tubular fashion and slowly progress leading to vision loss. CT scans show classic tram-track appearance. Most cases are managed conservatively as the growth tends to be slow. Adherence to the pial vessels by the tumor makes surgical resection risky and results in loss of vision. Fractionated radiotherapy is usually the first line of treatment for tumor control when growth is seen [7]. Stereotactic surgery and Gamma Knife radiosurgery are being assessed currently [8].

Sphenoid Wing Meningioma with Orbital Involvement

Sphenoid wing meningiomas represent 15%–20% of all supratentorial meningiomas. Sphenoid wing meningioma with orbital involvement is termed spheno-orbital meningiomas (SOM), although they are also known as orbitosphenoid meningiomas, meningiomas en plaque of the sphenoid wing and sphenoid wing meningiomas with osseous involvement. Sphenoidal wing meningioma makes up 9% of all intracranial meningiomas [9].

Sphenoidal wing meningiomas are often associated with sphenoidal wing hyperostosis, are often invasive, and spread to the dura in the frontal, temporal, and orbital regions. Meningiomas have two growth patterns: meningioma en masse which forms a space-occupying lesion and meningioma en plaque, which is a flat spreading tumor. Anterior skull base meningiomas are tumors that arise anterior to the chiasmatic sulcus which separates the middle cranial fossa from the anterior cranial fossa. These sphenoidal wing meningiomas may expand medially into the cavernous sinus wall, anteriorly into the orbit, and laterally into the temporal bone. They are divided into lateral, middle, and medial (clinoidal) tumors [10]. Clinoidal (medial) meningiomas are further subclassified (Table 10.1).

Table 10.1 Clinoidal meningiomas

Type I originate from the inferomedial clinoidal process proximal to the distal carotid ring. These tumors are difficult to resect because of the adherence of the tumor to the internal carotid artery
Type II originate from the superolateral surface, widening the Sylvian fissure, and are not difficult to remove
Type III originate at the optic foramen and extend into the optic canal
Frontal skull base meningiomas can also arise from the olfactory groove (from where they may invade the orbit and 15–30% grow into the ethmoid sinuses) or the planum sphenoidale which arise 2 cm posterior to olfactory groove meningiomas. The rest of this chapter will discuss spheno-orbital meningiomas

Pathophysiology

Ionized Radiation

Radiation exposure is the commonest known risk factor for meningiomas [11]. Children with tinea capitis treated with doses of 1.5 Gy have a relative 9.5% risk of developing meningioma [12]. After a full-mouth series of dental radiography exposure, the risk of meningioma is double. Radiation-induced tumors may also develop after previous radiation treatment of other lesions.

Cahan et al. [13] proposed the criteria necessary to identify radiation-induced tumors: these criteria have now been applied to radiation-induced meningiomas. Radiation-induced tumors are defined as lesions that arise after a latency period (4 years was initially proposed) within a field of prior irradiation and have histopathology that is different from the treated tumor. With other modifications since the first description, the full set of criteria that apply to radiation-induced meningiomas are shown in Table 10.2.

The most commonly reported radiation-induced tumor is meningioma. Radiation-induced meningiomas develop more frequently over the convexities than the skull base, at a ratio of 1.9:1 for both high-dose and low-dose radiation.

Table 10.2 Criteria for radiation-induced meningiomas

The tumor must arise in the field of irradiation
The histological features must differ from any prior neoplasm in the treated region
There should be an interval sufficient to ensure the neoplasm did not exist prior to irradiation (formerly 4 years was proposed but now accepted as "several years"
Tumor type must occur frequently enough after irradiation to suggest a causal relationship
It should be known that the incidence of the type of tumor is significantly higher in irradiated patients compared to an adequate control group
There must be no family history of a phacomatosis

Radiation-induced meningiomas are more likely to be multiple and present at a younger age than spontaneous meningiomas [14]. These tumors exhibit more malignant behavior, as indicated histologically by high cellularity, pleomorphism, multinucleation, and giant cell pseudoinclusions, although these findings have not yet been confirmed by others.

The latency period for the development of radiation-induced meningiomas varies: higher doses of radiation, not surprisingly, have a shorter latency. The latency period can be as short as 14 months and as long as 63 years, although the average latency period is 30–40 years in most cases [14].

Genetic Abnormalities

In cytogenetic studies, the most commonly reported genetic abnormality is the loss of *NF2* tumor suppressor gene on the long arm of chromosome 22 (monosomy 22). This genetic alteration leads to loss of expression of NF2 protein product (neurofibromin) and has been reported in 40%–70% of meningiomas [15]. Other commonly reported genetic alterations in meningioma include deletion of the short arm of chromosome 1; loss of chromosomes 6, 10, 14, 18, and 19; and gain of 1q, 9q, 12q, 15q, 17q, and 20q [16]. Abnormalities of chromosome 22 have been associated with type II neurofibromatosis; 75% of patients with type II neurofibromatosis develop meningioma during their lifetime. Ten percent of these are multiple lesions.

Hormonal Factors

There is a striking predominance of meningiomas in women; the female-to-male ratio is 2:1 for intracranial tumors and 10:1 for spinal meningiomas. Therefore, hormonal factors (e.g., estrogen, progesterone, androgen, steroid) have been studied extensively as risk factors for meningiomas. Other evidence to substantiate the implication of sex-specific hormones comes from data showing increased growth of meningiomas during pregnancy and hormonal replacement therapy. Estrogen receptor (ER) has been found in 30% of meningiomas in one series, predominantly the ER-beta receptor isoform [17].

The progesterone receptor is the best candidate among the sex-specific factors as a cause for meningiomas. Progesterone receptors have been shown to be expressed in 81% of women and 40% of men with meningiomas [18]. Other studies indicate that progesterone binds to meningiomas in 50%–100% of tested specimens. Although progesterone receptor expression has been observed more frequently in benign meningioma (96%) than the malignant type (40%), no relation has been found between progesterone receptor status and age, sex, location of tumor, or menopausal state [18]. These findings have prompted researchers to develop antiprogesterone medications, such as mifepristone (RU-486), which appears to inhibit tumor growth in vitro and in vivo.

Androgen receptors have also been found in approximately 50% of meningiomas, but their receptor expression is variable, making them less likely candidates in the pathophysiology of meningiomas. Meningiomas also vary in expression of receptors for other hormones (e.g., vascular endothelial growth factor receptor [VEGFR], epidermal growth factor [EGF], platelet-derived growth factor [PDGF], fibroblast growth factor, insulin-like growth factor-1 [IGF-1]), making them less likely candidates for oncogenesis of meningiomas. It has been suggested that the direct stimulatory effect of EGF on PDGF or PDGF itself may be partially responsible for angiogenesis and even oncogenesis in meningiomas. PDGF is a particularly attractive candidate

because it has structural homology with the product of c-sis oncogene on chromosome 22.

Viruses

Some viruses have been found within meningiomas, including polyoma virus, simian vacuolating virus 40 (SV-40), and adenovirus. A suggested role for these viruses or parts of viruses is related to the proteins involved in the induction or maintenance of tumor growth and transformation. However, this association has not been proven.

Head Injury and Electromagnetic Fields

Among the other potential factors for inducing meningiomas that have not been proven are head trauma and electromagnetic field exposure. Head trauma and skull fractures have been suggested as a risk factor for meningioma development by some authors [19]. However, a large population-based 2014 study from Taiwan found no association between head injury and meningioma development in two cohorts of patient with and without head injury [20].

Similarly, electromagnetic field exposure, especially with the widespread use of cell phones, has generated interest in relation to the pathophysiology of brain tumors. Many studies suggest that little, if any, evidence supports the implications of cell phone use on meningioma development, although there is generally a lack of well-conducted studies to date and a significant amount of debate in this regard [2].

Epidemiology

The average age at onset is 63 years. The incidence of meningiomas increases with age [21]. The annual incidence of meningiomas can be as low as 0.74 per 100,000 individuals younger than 34 years and as high as 18.86 per 100,000 individuals older than 85 years. It is 2.5 times more common in females than in males (10.87 per 100,000 population in females vs 4.98 per 100,000 population males) [22]. In children, meningioma accounts for 4.6% of all primary brain tumors. Incidental meningioma is found in 0.52%–0.9% of brain images [23].

Previous studies reported variability in the prevalence of meningiomas among whites, Africans, African-Americans, and Asians and greater incidence among blacks than whites. However, the 2015 CBTRUS report showed that the rates among whites, blacks, and Hispanics were similar [22].

Natural History

Meningiomas are generally slow growing. Growth patterns of meningioma in a 2011 series of incidentally diagnosed meningioma included no growth, linear growth, or exponential growth. The presence of calcification, T2-weighted MRI tumor hypointensity, and older age at onset were associated with slower growth rate [24]. In a large series of 603 asymptomatic meningiomas, 63% did not increase in size, and only 6% of patients eventually experienced symptoms over a mean follow-up of 3.9 years [25].

True metastases are extremely uncommon, and dissemination is usually believed to occur hematogenously, with the lungs as the most common site. Bony invasion is not evidence of malignancy in meningiomas, and invasion of mesenchymal components (e.g., bone, muscle, dura) can occur with benign meningiomas [26].

Clinical Features

Cushing and Eisenhardt's 1938 description of the clinical presentation has not changed. The classic triad of SOM is proptosis (86%), which is usually painless; visual impairment (78%) which is usually gradual but acute in up to 12% of cases; and ocular paresis (20%) with double vision [27, 28]. Papilledema and eventual optic atrophy may ensue. Headache is also a common manifestation [27], in addition to nausea if there is raised intracranial pressure. Ptosis may be neurological or mechanical. Transient ischemic attack-like presentation has also been reported. Involvement of

the superior orbital fissure and foraminal encroachment will lead to involvement of cranial nerves.

Wright noted that vision loss was the commonest initial symptom and then proptosis and double vision [29]. Afferent pupillary defect will be detected together with optic nerve head changes and shunt vessels which are optociliary shunt vessels on the disc surface: these are collateral vessels between the central retinal vein and the choroidal venous system. Other variants of clinical presentation also occur (Table 10.3).

Differential Diagnosis

Depending on the radiological features and clinical manifestations, the following differential diagnoses of sphenoid wing meningioma should be considered: (Table 10.4).

Table 10.3 Variants of clinical presentation of meningiomas

Eye swelling and hearing loss secondary to compression of the eustachian tube
Blindness and optic atrophy in one eye, sometimes with papilledema of the other (Foster Kennedy syndrome)
Mental changes
Increased intracranial pressure and intracranial hemorrhage secondary to bony hyperostosis and stretching of underlying venous structures

Table 10.4 Differential diagnosis of meningioma

Fibrous dysplasia
Paget disease
Brown tumor
Osteogenic sarcoma
Eosinophilic granuloma
Aneurysmal bone cyst
Osteoma
Hemangioma
Hemangiopericytoma
Epidermoid tumor and dermoid
Multiple myeloma
Plasmacytoma
Giant cell tumor
Metastatic cancer
Exuberant arachnoid hyperplasia
Fibrous histiocytoma
Juvenile ossifying fibroma
Solitary fibrous tumor/hemangiopericytoma

Diagnostic Evaluation

Laboratory Studies

Laboratory studies may be indicated to rule out other differential diagnoses (e.g., metabolic panel including calcium, bone-specific alkaline phosphatase, urine hydroxyproline).

Imaging (Figs. 10.1 and 10.2)

Plain radiography of the skull: Abnormalities have been found in 30%–60% of patients with sphenoid wing meningioma. Hyperostosis, thinning of bone, and irregular foci of calcification can be seen [30].

CT scanning: CT scanning with bone windows typically shows a thick, hyperdense, intradiploic lesion expanding the calvaria and destroying the cortical layers of the skull. The bony expansion and ground-glass appearance of sphenoid wing meningioma complicates differentiation from fibrous dysplasia [31]; however, the inner table of the skull looks smooth in fibrous dysplasia, whereas sphenoid wing meningiomas often demonstrate irregularity of the inner table associated with a dural reaction. Clinically, fibrous dysplasia usually presents in younger individuals and stops growing after puberty, in contrast to meningioma, which typically develops in older individuals. Among sphenoid wing meningiomas, 59% are osteoblastic, 10%–35% are osteolytic, and 6% are a mixed picture of both osteolytic and hyperostosis[32].

MRI allows better delineation of the soft tissue component of the tumor and dural involvement, as well as delineation of intraorbital extension. A dural tail in sphenoid wing meningioma is typically identified but can be absent especially in the en plaque variant.

Angiography is not necessary in sphenoid wing meningioma. When performed, it usually shows tumor blush of the en masse component and tortuous external carotid artery feeders.

C-PiB and F-FDG positron-emission tomography scanning: two patients who had undergone contrast-enhanced MRI scans that revealed extra-axial tumors next to the sphe-

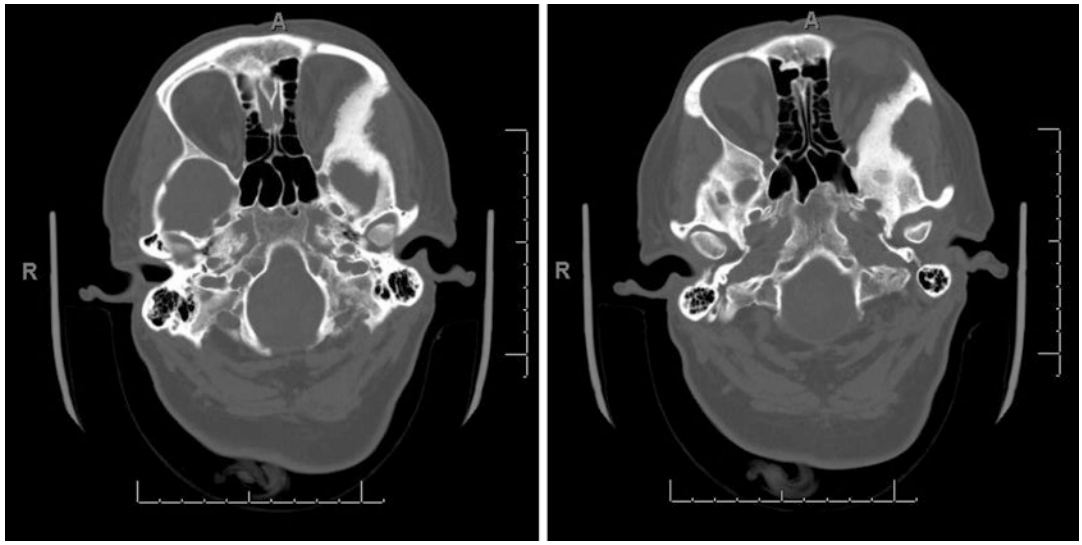

Fig. 10.1 CT scan with bone window shows intraosseous meningioma involving left sphenoid wing, lateral orbital, superior orbital fissure, and the anterior part of the middle fossa floor

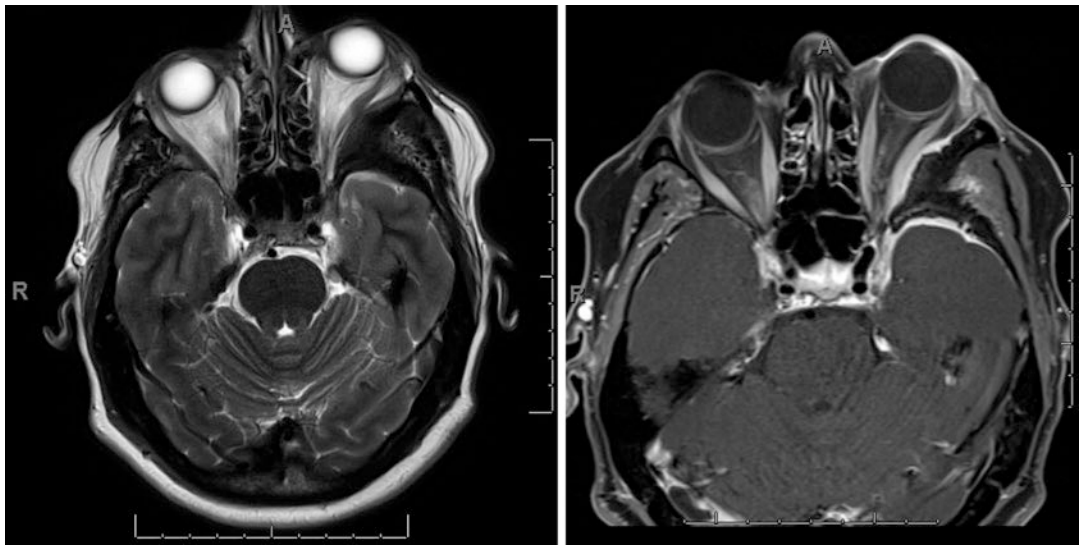

Fig. 10.2 MRI brain T2W (left) and T1W Fat-Sat (right) sequences showing involvement of the left sphenoid wing associated with dural thickening and the periorbita. Notice proptosis of the left globe secondary to left orbital wall involvement with meningioma

noid wing were examined using C-PiB and F-FDG positron-emission tomography (PET) scanning. The researchers concluded that C-PiB could be used as a meningioma marker [33].

Other Tests

Preoperative evaluation of patients with anterior basal meningiomas includes formal visual field and acuity testing. Metastatic work-up includes

CT scanning of the chest, abdomen and pelvis, skeletal survey, radionuclide scanning and PET scanning. Intraoperative radiodetection of somatostatin receptors is feasible, especially in bone-invasive meningiomas using the gamma probe.

Management

Most meningiomas that involve the orbit progress and eventual neurological involvement and compression of the optic nerve may occur. If there is no neurological involvement, it is reasonable to follow the tumors with sequential examination and scanning. If there is progression and neurological involvement, the best option is total surgical resection.

Surgery (Figs. 10.1, 10.2, and 10.3)

Total microsurgical resection of sphenoid wing meningioma is usually curative however difficult to achieve. A recurrence risk approaching 30% has been reported when there is incomplete resection [34, 35]. Depending on the bony involvement and the soft tissue component of the tumor, the principles of resecting a sphenoid wing en plaque meningioma are complete removal of all the involved bone, including the sphenoid wing, orbital roof, and orbital lateral wall. Decompression of optic nerve, superior orbital fissure, and maxillary branch of the trigeminal nerve posteriorly to foramen rotundum should be accomplished.

The skin incision is made 0.5–1 cm anterior to the tragus at the level of the zygomatic arch and extended behind the hairline toward the widow's peak. It can be curved back across the midline toward the contralateral superior temporal line, if needed. Care must be taken not to injure the temporal branch of the facial nerve. The temporalis muscle, along with the superficial and the deep fascial layers, is incised in similar fashion from the skin down to the bone. The musculocutaneous flap is reflected anteriorly using a periosteal elevator. Avoid cauterizing the blood supply and innervation to the temporalis muscle to prevent future muscle atrophy.

Once the muscle is elevated and reflected anteriorly, lateral sphenoid wing hyperostosis is usually apparent, and any noticed during elevation of the temporal muscle is excised. Multiple bur holes are then made around the invaded or hyperostotic bone to prevent excessive bleeding and dural tear. The drill is then used to connect

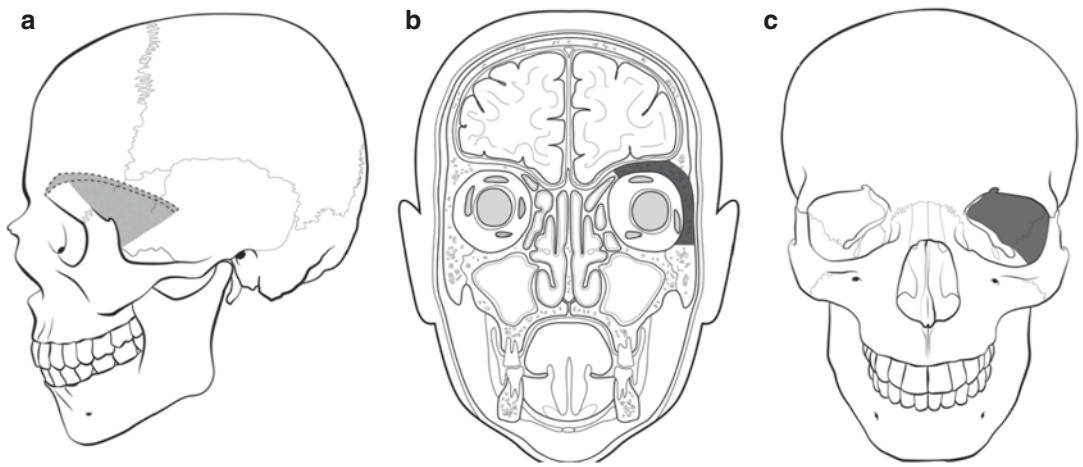

Fig. 10.3 An approach to spheno-orbital meningiomas with orbital involvement. Shading demonstrates the area of bone removal from an external lateral view (**a**), inset coronal view (**b**), and coronal external view (**c**). The shaded areas include the lateral wall, superior wall, optic canal, and clinoid process. We preserve the orbital rim

the bur holes and to remove the invaded bone. This process continues until all hyperostotic tissue is removed from the sphenoid wing down to the meningo-orbital band.

The meningo-orbital band is then coagulated and cut sharply, followed by dural stripping from the superior orbital fissure and the anterior part of the lateral wall of the cavernous sinus, exposing the middle fossa floor laterally to the foramen spinosum and posteriorly to the foramen rotundum. Hyperostotic tissue is then removed in a similar manner from the orbital roof and lateral walls of the orbit.

The superior orbital fissure is completely decompressed. The optic nerve in the canal is unroofed, and anterior clinoidectomy is performed. Once the bone removal is complete, attention is focused on resecting the intradural portion of the tumor, and the dura is resected beyond the enhanced dural tail. The intraorbital extension with involvement of the periorbital and extraocular muscles should also be removed.

Abdominal fat or temporalis fascia with or without a pericranial flap can be used to repair the frontal, maxillary, and ethmoid sinuses if they have been opened to prevent postoperative development of a CSF leak and rhinorrhea. A duraplasty is performed using a dural substitute. There is no clear consensus in the literature regarding whether to reconstruct the orbit. Orbital wall reconstruction has been recommended whenever the orbital floor or more than one wall has been resected or the periorbita was resected to prevent occurrence of pulsatile enophthalmos postoperatively [36]. However, studies have concluded that this complication is uncommon, and that orbital reconstruction is unnecessary except in rare occasions when the orbital rim is resected [37]. When orbital reconstruction is needed, the area can be reconstructed using mesh, dural substitute, or split bone if only the superior and lateral walls of the orbit have been removed. The cranial flap is placed back if it was not involved by the tumor, or a piece of Medpor can be used to cover the cranial defect, making sure to cover the keyhole area. The temporal muscle is then reattached, and the skin is closed in two layers (Figs. 10.4 and 10.5).

Medical Treatment

Anecdotal reports have described using antihormonal agents in the treatment of meningiomas. Medical treatment is reserved for atypical and malignant meningiomas as an adjunct to surgery.

Tamoxifen, an antiestrogen hormone, inhibits the effects of estrogen by competitively binding to estrogen receptor, producing a nuclear complex that decreases DNA synthesis and inhibits estrogen effects. Its use has been reported in small series of patients with refractory or unresectable meningiomas; in one study, 19 patients were included in a phase II trial. Results showed partial MRI response in three patients, six patients remained stable for a median duration of 31 months, and ten patients had progression [38].

Mifepristone, RU-486 (Mifeprex), is an antiprogesterone agent. A 2015 systematic review of all studies reporting on this medication did not provide any evidence for benefit beyond preclinical uses [39]. Hydroxyurea is a chemotherapeutic agent that selectively inhibits ribonucleoside diphosphate reductase and induces apoptosis. Small case series of patients with recurrent grade II and III meningiomas have been published. Some of the studies suggest clinical stabilization of the disease with radiological response.

Radiotherapy

Radiotherapy is usually reserved for atypical meningiomas and as adjuvant treatment postsurgical resection. Radiotherapy as a primary treatment is usually not indicated unless surgical resection is not possible, e.g., cavernous sinus.

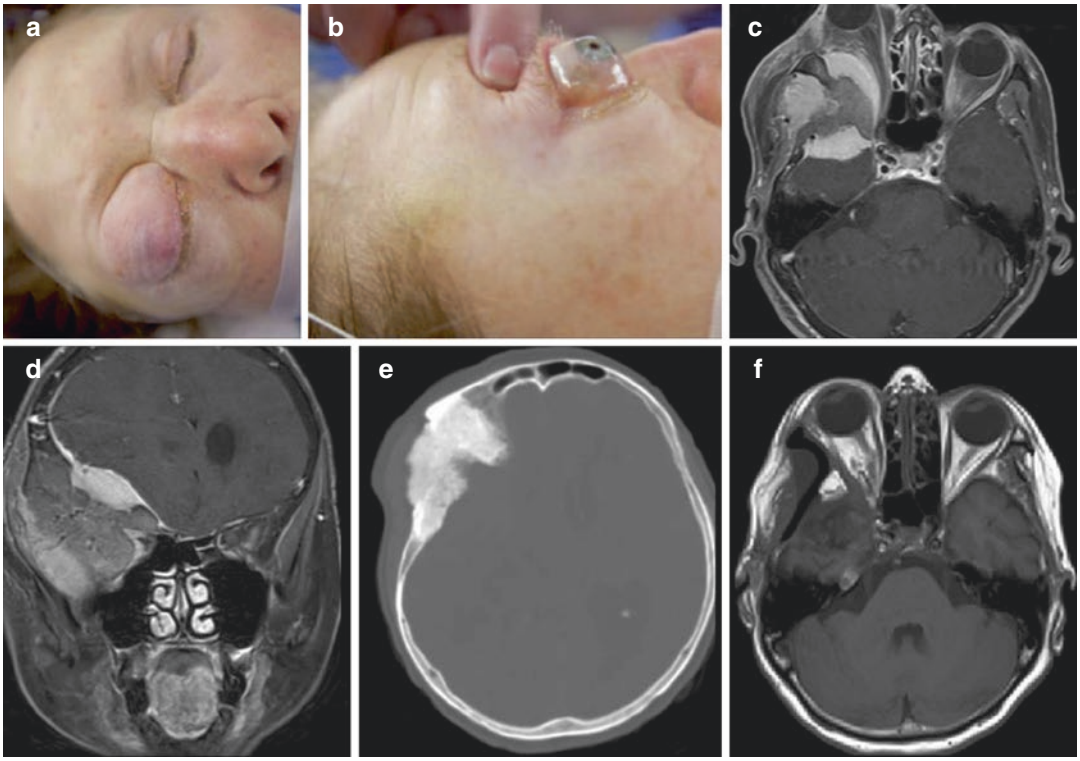

Fig. 10.4 (**a**, **b**)-Preoperative photographs demonstrating significant right eye proptosis. (**c**) Preoperative Axial T2 MRI demonstrating the significant proptosis and extent of optic nerve compression. (**d**) Coronal T2 MRI showing the significant width of tumor infiltration in the sphenoorbital region. (**e**) Preoperative axial CT scan demonstrating the reactive hyperostosis and extent of bony involvement with this tumor. (**f**) Postoperative axial T1 MRI demonstrating the excellent proptosis resolution

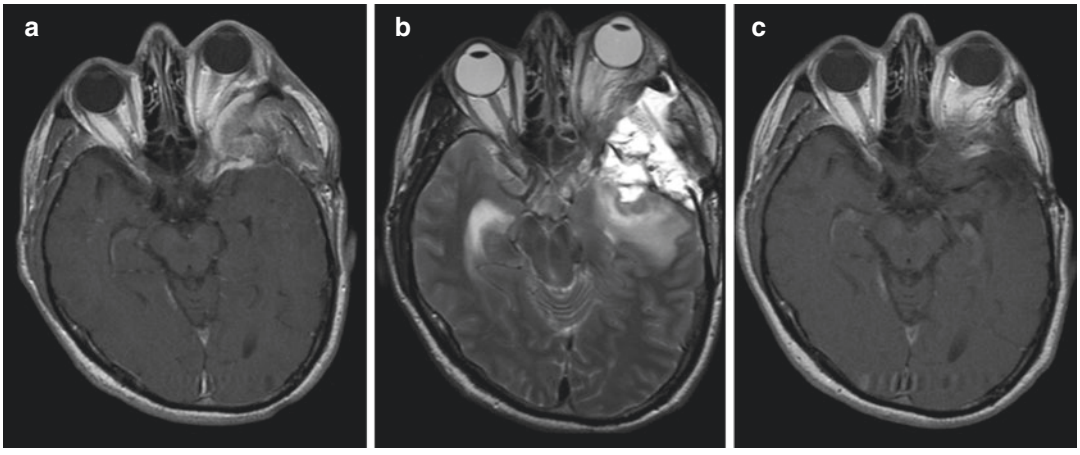

Fig. 10.5 (**a**) Pre-op T1 with GAD MRI brain. (**b**) Pre-op T2 MRI brain. (**c**) Post-op T1 with Gad MRI brain demonstrating the significant proptosis reduction

Histology

Virchow first described the classic pathological feature found in meningiomas in 1847, the psammoma body, which means "sand-like" alluding to the tumor granules [40]. According to the WHO, in 2007 and 2016, the following three types of meningiomas exist based on malignant behavior [41, 42]:

- Grade I (benign), with a recurrence rate of 7%–25%, does not meet atypical or malignant meningioma criteria. Despite involvement of the adjacent bony structures, grade I meningiomas do not invade the brain parenchyma. Grade I meningiomas include nine histological subtypes: meningothelial, fibrous, transitional, psammomatous, angiomatous, macrocystic, secretory, lymphoplasmacyte-rich, and metaplastic.
- Grade II (atypical), with a recurrence rate of 29%–52%, includes atypical, clear cell, and chordoid histological subtype or increased mitotic activity (4–19 mitoses per 10 high-powered fields) or brain invasion, or 3 or more of the following features: increased cellularity, small cells with a high nuclear/cytoplasmic ratio, prominent nucleoli, uninterrupted patternless or sheetlike growth, or foci of spontaneous or geographic necrosis.
- Grade III (malignant), with a recurrence rate of 50%–94%, includes anaplastic, papillary, and rhabdoid histological subtypes. Anaplastic meningiomas have 20 or more mitoses per 10 high-powered fields or malignant characteristics resembling carcinoma, sarcoma, or melanoma.

Malignant transformation is rare. Originally, malignancy was seen in anaplastic tumors, but they may arise from any of the meningioma variants or atypical meningiomas. Papillary histopathology is associated with local aggressiveness and an increased incidence of late distant metastasis. The papillary type is considered malignant by definition and is encountered more frequently in children.

Earlier classification schemes used the term angioblastic meningioma for what is now considered to be a hemangiopericytoma. This neoplasm is distinctly separate from a meningioma, and it shows extremely high propensity for recurrence and metastasis. Hemangiopericytoma is a sarcoma in the new WHO classification.

Mortality and Morbidity

The complexity of skull base approaches, proximity of the cranial nerves, poor accessibility, dural attachments, and involvement of the extracranial compartment, especially the nasal sinuses and orbit for skull base meningiomas, makes the complication frequency for these lesions higher than with other locations [43].

For medial sphenoid wing meningiomas, visual loss and abnormalities of cranial nerves III, IV, VI, V1, and V2 may occur because the meningioma may have some degree of encasement of these structures as they pass through the cavernous sinus. Seizures, paresis, and sensory loss may occur, depending on potential damage to adjacent brain parenchyma among patients with lateral sphenoid wing meningiomas.

Among patients with skull base meningiomas, a 2016 study reported the overall mortality rate was 5%, with transient cranial nerve deficits occurring in 32% of cases, definite cranial nerve lesions in 18%, and cerebrospinal fluid (CSF) leak in 14% [44]. Another study reported an overall mortality rate of 5.8%, transient cranial nerve deficit rate of 11.7%, definitive morbidity of 5.8%, and second recurrence rate of 5.8% [45].

Potential complications include bleeding, deep venous thrombosis and embolism, air embolism, venous infract, wound-healing deficits, paresis, sensory deficits, cranial nerve palsy, aphasia, seizures, brain edema, hygroma, CSF fistula hydrocephalus, ischemia, and pituitary insufficiency. These complications vary depending on preoperative morbid conditions, age, and tumor size and location.

Prognosis

A 1983 study showed that recurrence-free survival rates after complete surgical removal in 114 patients (60% of which were sphenoid wing meningioma) at 5, 10, and 20 years were 80%, 70%, 50%, respectively [46]. The extent of surgical resection and histological grade are very important prognostic factors.

In 1957, Simpson classified meningiomas based on the extent of resection as follows [47]:

- Grade I – Macroscopically complete removal of the tumor with excision of its dural attachment and of any abnormal bone
- Grade II – Macroscopically complete removal of the tumor and of its visible extensions with endothermy coagulation of its dural attachment
- Grade III – Macroscopically complete removal of the intradural tumor without removal or coagulation of its dural attachment or extradural extensions
- Grade IV – Partial removal of the tumor
- Grade V – Simple decompression with or without biopsy

The 10-year risk of recurrence for grades I through IV were 9%, 19%, 29%, and 44%, respectively.

When WHO histological grading of meningiomas is considered regarding survival, a 2016 study of 905 patients demonstrated that the 5-year overall survival rate was 85%–90% for WHO grade I, 75%–78% for WHO grade II, and 30%–35% for WHO grade III tumors [20]. Recurrence rates of tumors graded according to the 2007 WHO classification of tumors of the central nervous system were 7%–25% for WHO grade I, 29%–52% for WHO grade II, and 50%–94% for WHO grade III [48].

Studies on the prognosis of sphenoid wing meningioma and spheno-orbital meningioma have generally showed good outcomes. In a series of 67 patients with spheno-orbital meningioma who underwent surgical resection with orbital wall reconstruction, a total removal was achieved in 14 cases (82.3%), with only 1 recurrence (7.1%) over a mean follow-up period of 36 months. Proptosis was corrected in all cases, and visual acuity improved in seven (70%) of ten cases. Radical resection was followed by cranio-orbital reconstruction to prevent enophthalmos and to obtain good cosmetic results. No deaths or serious complications occurred in association with surgery. Revision of the orbital reconstruction was required because of postoperative enophthalmos (two cases) or restricted postoperative ocular movement (one case) [28]. A 2016 series of 33 patients with spheno-orbital meningioma who underwent resection without formal orbital wall reconstruction (mean follow-up, 4.5 years) showed improved proptosis in all patients, and only 2 patients had tumor recurrence at the orbit that required surgery [36]. The authors of these studies emphasize aggressive removal of the hyperostotic bone to achieve satisfactory results and to decrease the risk of recurrence. However, patients should be followed closely for recurrence as long-term recurrence rates can be as high as 27.7% [49]. Neurosurgical procedures invariably carry significant risks. Minimally invasive techniques have been explored with good initial success in controlling disease with decreased morbidity [50, 51]. Long-term follow-up will be necessary to compare these approaches to traditional techniques.

Conclusion

SOM can be treated with careful orbital and neurosurgical techniques. Careful clinical and radiological assessment is necessary to detect progression and neurological involvement. SOM should be followed long term due to risk of recurrence.

References

1. Cushing H. The meningiomas (dural endotheliomas): their source, and favoured seats of origin. Brain. 1922;45:282–316.
2. Claus EB, Bondy ML, Schildkraut JM, et al. Epidemiology of intracranial meningioma. Neurosurgery. 2005;57(6):1088–95.

3. MacCarty CS, Piepgras DG, Ebersold MJ. Meningeal tumors of the brain. In: Youmans JR, editor. Neurological surgery, vol. 5. 2nd ed. Philadelphia: WB Saunders; 1982. p. 2936–66.
4. Tan LT, Stewart CM, Sheerin F, et al. Ectopic orbital meningioma: fact or fiction? Orbit. 2017;36(3):144–6.
5. Eddleman CS, Liu JK. Optic nerve sheath meningioma: current diagnosis and treatment. Neurosurg Focus. 2007;23(5):E4.
6. Dutton JJ. Optic nerve sheath meningiomas. Surv Ophthalmol. 1992;37(3):167–83.
7. Pandit R, Paris L, Rudich DS, et al. Long-term efficacy of fractionated conformal radiotherapy for the management of primary optic nerve sheath meningioma.Br J Ophthalmol. 2018. pii: bjophthalmol-2018-313135. https://doi.org/10.1136/bjophthalmol-2018-313135. [Epub ahead of print].
8. Parker RT, Ovens CA, Fraser CL, et al. Optic nerve sheath meningiomas: prevalence, impact, and management strategies. Eye Brain. 2018;10:85–99. https://doi.org/10.2147/EB.S144345. eCollection 2018.
9. Cannon PS, Rutherford SA, Richardson PL, et al. The surgical management and outcomes for spheno-orbital meningiomas: a 7-year review of multi-disciplinary practice. Orbit. 2009;28:371–6.
10. MacCarty CS. Meningiomas of the sphenoidal ridge. J Neurosurg. 1972;36(1):114–20.
11. Morgenstern PF, Shah K, Dunkel IJ, et al. Meningioma after radiotherapy for malignancy. J Clin Neurosci. 2016;30:93–7.
12. Sadetzki S, Flint-Richter P, Ben-Tal T, et al. Radiation-induced meningioma: a descriptive study of 253 cases. J Neurosurg. 2002;97(5):1078–82.
13. Cahan WG, Woodard HQ. Sarcoma arising in irradiated bone; report of 11 cases. Cancer. 1948;1(1):3–29.
14. Godlewski B, Drummond KJ, Kaye AH. Radiation-induced meningiomas after high-dose cranial irradiation. J Clin Neurosci. 2012;19(12):1627–35.
15. Mawrin C, Chung C, Preusser M. Biology and clinical management challenges in meningioma. Am Soc Clin Oncol Educ Book. 2015;35:e106–15.
16. Pećina-Šlaus N, Kafka A, Lechpammer M. Molecular genetics of intracranial meningiomas with emphasis on canonical Wnt signalling. Cancers (Basel). 2016;8(7). pii: E67.
17. Carroll RS, Zhang J, Black PM. Expression of estrogen receptors alpha and beta in human meningiomas. J Neuro-Oncol. 1999;42(2):109–16.
18. Hsu DW, Efird JT, Hedley-Whyte ET. Progesterone and estrogen receptors in meningiomas: prognostic considerations. J Neurosurg. 1997;86(1):113–20.
19. Preston-Martin S. Descriptive epidemiology of primary tumors of the brain, cranial nerves and cranial meninges in Los Angeles County. Neuroepidemiology. 1989;8(6):283–95.
20. Kuan AS, Chen YT, Teng CJ, et al. Risk of meningioma in patients with head injury: a nationwide population-based study. J Chin Med Assoc. 2014;77(9):457–62.
21. Linsler S, Keller C, Urbschat S, et al. Prognosis of meningiomas in the early 1970s and today. Clin Neurol Neurosurg. 2016;149:98–103.
22. Ostrom QT, Gittleman H, Fulop J, et al. CBTRUS statistical report: primary brain and central nervous system tumors diagnosed in the United States in 2008-2012. Neuro-Oncology. 2015;17(Suppl 4):iv1–iv62.
23. Yue NC, Longstreth WT Jr, Elster AD, et al. Clinically serious abnormalities found incidentally at MR imaging of the brain: data from the Cardiovascular Health Study. Radiology. 1997;202(1):41–6.
24. Chamoun R, Krisht KM, Couldwell WT. Incidental meningiomas. Neurosurg Focus. 2011;31(6):E19. http://reference.medscape.com/medline/abstract/22133182.
25. Yano S, Kuratsu J, Kumamoto Brain Tumor Research Group. Indications for surgery in patients with asymptomatic meningiomas based on an extensive experience. J Neurosurg. 2006;105(4):538–43.
26. Velnar T, Pregelj R, Limbaeck-Stokin C. Brain meningioma invading and destructing the skull bone: replacement of the missing bone in vivo. Radiol Oncol. 2011;45(4):304–9.
27. Shrivastava RK, Sen C, Costantino PD, et al. Sphenoorbital meningiomas: surgical limitations and lessons learned in their long-term management. J Neurosurg. 2005;103(3):491–7. http://reference.medscape.com/medline/abstract/16235682.
28. Bikmaz K, Mrak R, Al-Mefty O. Management of bone-invasive, hyperostotic sphenoid wing meningiomas. J Neurosurg. 2007;107(5):905–12.
29. Wright JE. Primary optic nerve meningiomas: clinical presentation and management. Trans Am Acad Ophthalmol Otolaryngol. 1977;83:617–25.
30. Changhong L, Naiyin C, Yuehuan G, et al. Primary intraosseous meningiomas of the skull. Clin Radiol. 1997;52(7):546–9.
31. Chen TC. Primary intraosseous meningioma. Neurosurg Clin N Am. 2016;27(2):189–93.
32. Crawford TS, Kleinschmidt-DeMasters BK, Lillehei KO. Primary intraosseous meningioma. Case report. J Neurosurg. 1995. Nov.;83(5):912–5.
33. Chaves H, Bergamo Y, Paz S, et al. Sphenoid wing meningioma behavior on 11C-PiB and 18F-FDG PET. Clin Nucl Med. 2015;40(1):e81–2.
34. Talacchi A, De Carlo A, D'Agostino A, et al. Surgical management of ocular symptoms in spheno-orbital meningiomas. Is orbital reconstruction really necessary? Neurosurg Rev. 2014;37(2):301–9; discussion 309–10.
35. Simas NM, Farias JP. Sphenoid wing en plaque meningiomas: surgical results and recurrence rates. Surg Neurol Int. 2013;4:86.
36. DeMonte F, Tabrizi P, Culpepper SA, et al. Ophthalmological outcome after orbital entry during anterior and anterolateral skull base surgery. J Neurosurg. 2002;97(4):851–6.

37. Bowers CA, Sorour M, Patel BC, et al. Outcomes after surgical treatment of meningioma-associated proptosis. J Neurosurg. 2016;125(3):544–50.
38. Goodwin JW, Crowley J, Eyre HJ, et al. A phase II evaluation of tamoxifen in unresectable or refractory meningiomas: a Southwest Oncology Group study. J Neuro-Oncol. 1993;15(1):75–7.
39. Cossu G, Levivier M, Daniel RT, et al. The role of mifepristone in meningiomas management: a systematic review of the literature. Biomed Res Int. 2015;2015:267831.
40. Virchow R. Entwickelungsgescichte des Krebes. Virchows Arch. 1847;1:94.
41. Backer-Grøndahl T, Moen BH, Torp SH. The histopathological spectrum of human meningiomas. Int J Clin Exp Pathol. 2012;5(3):231–42.
42. Louis DN, Perry A, Reifenberger G, et al. The 2016 World Health Organization classification of tumors of the central nervous system: a summary. Acta Neuropathol. 2016;131(6):803–20.
43. Kotecha RS, Jacoby P, Cole CH, et al. Morbidity in survivors of child and adolescent meningioma. Cancer. 2013;119(24):4350–7.
44. da Silva CE, de Freitas PE. Large and giant skull base meningiomas: the role of radical surgical removal. Surg Neurol Int. 2015;6:113.
45. da Silva CE, Peixoto de Freitas PE. Recurrence of skull base meningiomas: the role of aggressive removal in surgical treatment. J Neurol Surg B Skull Base. 2016;77(3):219–25.
46. Adegbite AB, Khan MI, Paine KW, et al. The recurrence of intracranial meningiomas after surgical treatment. J Neurosurg. 1983;58(1):51–6.
47. Simpson D. The recurrence of intracranial meningiomas after surgical treatment. J Neurol Neurosurg Psychiatry. 1957;20(1):22–39.
48. Louis DN, Ohgaki H, Wiestler OD, et al. The 2007 WHO classification of tumours of the central nervous system. Acta Neuropathol. 2007;114(2):97–109.
49. Terrier LM, Bernard F, Fournier HD, et al. Sphenoorbital meningiomas surgery: multicenter management study for complex extensive tumors. World Neurosurg. 2018;112:e145–56.
50. Altay T, Patel BC, Couldwell WT. Lateral orbital wall approach to the cavernous sinus. J Neurosurg. 2012;116(4):755–63.
51. Almeida JP, Omay SB, Shetty SR, et al. Transorbital endoscopic eyelid approach for resection of sphenoorbital meningiomas with predominant hyperostosis: report of 2 cases. J Neurosurg. 2018;128(6):1885–95.

Tumors of the Optic Nerve

11

Jonathan J. Dutton

Introduction

Primary tumors of the optic nerve include anterior visual pathway gliomas and optic nerve sheath meningiomas. Both are relatively rare lesions that result in significant visual morbidity. Together they account for less than 4% of all orbital tumors. There has been controversy about the natural history and appropriate management of these lesions, often resulting from small sample sizes and short follow-up periods. Other tumors, such as gangliogliomas and primary lymphomas, have also been described but are extremely rare (Table 11.1).

Anterior Visual Pathway Glioma

Optic pathway gliomas (OPG) are uncommon benign lesions classified as pilocytic astrocytomas. They represent 1.5–4% of all orbital tumors and 50–55% of all primary optic nerve tumors [1, 2].

Association with Neurofibromatosis Type 1

Optic pathway gliomas may be sporadic or syndromic, the latter mostly associated with neurofibromatosis type 1 (NF1). The reported incidence of NF1 among patients with optic gliomas varies from 10% to 70%, with an overall incidence of 29% [1]. Although some reports have shown no difference in the course and prognosis of optic pathway gliomas with and without NF1, others have shown a more indolent course and a better visual prognosis in patients with OPG and NF1 [3–5].

When associated with NF1, the glioma may present at a somewhat later age and show progression for a long time, justifying regular ophthalmological monitoring of this population over a long period [6, 7]. OPG occur in 15–20% of children with NF1, even though visual symptoms are seen in less than half of these individuals. Reliable visual evaluation can be challenging in young children making it difficult to determine if, and when, intervention is warranted. A combination of ophthalmic, electrophysiologic, and imaging biomarkers has been proposed as a guideline for initiating therapy [8].

J. J. Dutton (✉)
Department of Ophthalmology,
University of North Carolina, Chapel Hill, NC, USA
e-mail: Jonathan_dutton@med.unc.edu

C. J. Hwang et al. (eds.), *Clinical Ophthalmic Oncology*,
https://doi.org/10.1007/978-3-030-13558-4_11

Table 11.1 Diagnostic features of optic nerve tumors

Lesion	Mean age	Sex	Location	Prognosis
Optic nerve glioma	8.8 years	F = M	ON, OC, MB	Vision = fair to good
				Life = 36% mortality
Malignant optic glioma	42.5 years	65% M	OC +/− ON	Vision = blindness
				Life = 100% mortality
Optic sheath meningioma	41 years	60% F	ON	Vision = poor
				Life = 0% mortality

ON optic nerve, *OC* optic chiasm, *MB* midbrain

Clinical Features

Age Distribution

Gliomas have been described in patients from birth to 79 years of age. However, 71% of cases occur in children in the first decade of life and 90% within the first two decades. The overall mean age at presentation is 8.8 years for all optic gliomas [1].

Sex Distribution

The sexual distribution for all optic pathway gliomas shows approximately equal numbers of males and females [1]. For gliomas confined to the optic nerve, 65% occur in females, compared to 35% for males. For tumors involving the optic chiasm, there is no sex predilection.

Location

About 20–25% of optic gliomas are confined to the optic nerve alone, but in three-quarters of cases, the chiasm is involved [9, 10]. Of the tumors that involve the chiasm, 40% eventually extend into the adjacent hypothalamus or third ventricle. Several studies have shown that the orbital optic nerve is involved more frequently in patients with NF1 (21.5%) than in those without NF1 (5.5%) [11].

Signs and Symptoms

The specific findings of optic pathway gliomas depend principally on the location of the tumor. Regardless of location, 85% of patients lose some vision, with about 25% retaining good vision between 20/20 and 20/40. About 60% of patients show vision of 20/300 or worse.

Fig. 11.1 External photograph of a child with a left orbital optic nerve glioma showing axial proptosis

Proptosis is a presenting sign in 95% of patients with gliomas involving the orbital optic nerve (Fig. 11.1). With gliomas of the optic chiasm, proptosis is much less common, seen in fewer than 20% of patients, and all with concomitant involvement of at least one intraorbital optic nerve. Limitation of ocular motility is seen infrequently with optic gliomas. It is reported in 30% of intraorbital lesions and 20% of gliomas involving the chiasm. Pain and headache are present in up to 30% of patients with chiasmal tumors. Other rare symptoms seen with CNS invasion include nystagmus, spasmus nutans, and seizures. Hydrocephalus and hypothalamic-pituitary dysfunction can include precocious puberty and deficiency of growth hormone, gonadotropin, TSH, and ACTH. On funduscopic examination, 60% of patients demonstrate some degree of optic atrophy. Disc edema, primarily associated with intraorbital gliomas, is seen in half of such cases. With chiasmal tumors, disc edema is noted in only 20% of patients, and in these, the tumor is

usually contiguous with the intraorbital optic nerve (Box 11.1).

Box 11.1 Optic Pathway Glioma

- Early visual loss 88%
- Optic disc swelling 35%
- Optic disc atrophy 59%
- Proptosis, orbital tumors 94%; chiasmal tumors 22%
- Nystagmus 24%
- Hypothalamic signs 26%
- Increased intracranial pressure 27%

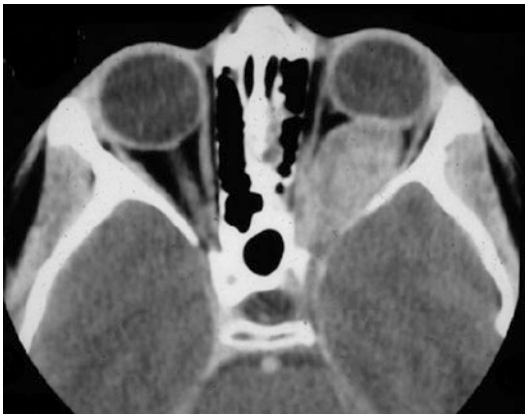

Fig. 11.2 Axial CT scan shows a fusiform glioma of the left optic nerve

Diagnostic Evaluation

Imaging studies reveal that enlargement of the optic canal is demonstrated in up to 80% of patients with a glioma involving the optic nerves. Enlargement and J-shaped excavation of the sella turcica may be associated with chiasmal gliomas but are reported in only 25% of patients.

Neuroimaging

Computed Tomography (CT)

CT imaging typically demonstrates enlargement of the optic nerve and/or chiasm. Contrast enhancement ranges from imperceptible to moderate but generally is less than with sheath meningiomas. Typical optic gliomas show a well-outlined fusiform swelling of the optic nerve (Fig. 11.2), but occasionally they may be more rounded or even exophytic. Calcification occurs only occasionally.

Magnetic Resonance Imaging (MRI)

MRI has proved superior to CT for evaluation of chiasmal, hypothalamic, and optic tract lesions. Gliomas demonstrate normal to slightly prolonged T1 relaxation times, which image isointense to slightly hypointense compared to normal optic nerve. The T2 relaxation time is prolonged, giving a hyperintense image on T2-weighted sequences.

Histopathology

Although optic gliomas were formerly believed to be congenital nonneoplastic hamartomas with self-limiting growth, their histologic features, rates of growth, rare malignant potential, and a clear tendency to invade the leptomeninges show that these tumors are true neoplasms that have the ability to invade locally.

Optic gliomas arise from supporting astrocytes of the optic nerve and along the visual pathway. Most are classified as benign pilocytic astrocytomas in which proliferating neoplastic astrocytic cells predominate. Proliferating astrocytes may extend through the pia mater into the arachnoid and subarachnoid space, where they provoke an exuberant reactive proliferation of fibrovascular tissue and meningothelial cells. This so-called arachnoidal hyperplasia may extend beyond the limits of the tumor itself, simulating tumor extension. Enlargement of optic gliomas may occur as a result of proliferation of neoplastic cells, reactive arachnoidal proliferation, or an accumulation of extracellular PAS-positive mucosubstance secreted by the astrocytes.

Treatment Options

Anterior visual pathway gliomas are neoplasms with the potential to spread into contiguous areas of the optic nerve, chiasm, and adjacent brain. They appear at an early age and grow slowly for a few years, and vision generally stabilizes in most cases. However, indolent growth can be seen in up to 40% of cases. Although the best treatment options are still evolving, an algorithm for the management of patients with optic pathway gliomas is suggested in Fig. 11.3. As with most medical decisions, treatment must be individualized based on patient symptoms, nature and extent of the lesion, visual function, clinical course, and side effect profile of the proposed treatment [12, 13].

Observation

Long-term survival shows a good prognosis even in patients followed conservatively without intervention [14–17]. After an initial period of deterioration, vision tends to stabilize in nearly 80% of cases. There is little difference in visual outcome or survival in patients undergoing treatment versus observation alone [1]. However, significant progression of tumor can occur in some patients despite clinically stable visual acuity for many years.

Surgery

Until recently, surgery was considered the treatment of choice for optic nerve gliomas. Today most authorities limit the indications for surgery to biopsy or to resect tumors involving the orbital or intracranial optic nerves that threaten posterior extension toward the optic chiasm [18]. Once vision is lost, surgery can be beneficial for reduction of severe proptosis or for control of orbital pain. Where vision is present, surgical intervention carries a very significant risk of further visual morbidity.

Radiotherapy

The role of radiotherapy has been a subject of debate for decades. Some studies have failed to show any benefit of radiotherapy on long-term survival, visual acuity, or both [1]. However,

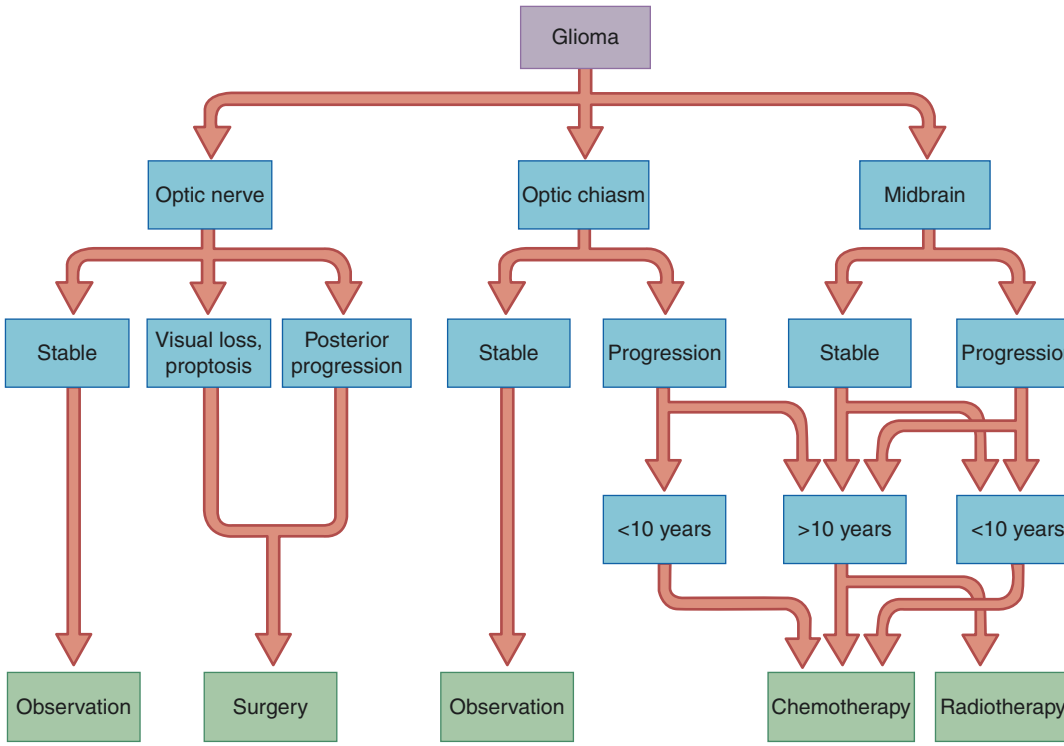

Fig. 11.3 Proposed management algorithm for treatment of anterior visual pathway glioma

more recent studies showed improvement or stability in visual acuity after treatment and a better progression-free survival interval [19, 20]. Overall, the data suggest a possible benefit. Any potential benefit must also be tempered by the adverse effects of radiotherapy on the central nervous system in younger children. Several cases of malignant transformation have been reported following radiotherapy.

Chemotherapy

While some recent studies question the benefit of chemotherapy for OPG [21], others have suggested a positive role for chemotherapy in the management of optic pathway gliomas. Most studies show stabilization of vision and/or tumor regression in 50–65% of treated patients [22–27]. Although this is not much better than for tumors observed conservatively, chemotherapy may be useful for young children with progressive lesions in order to delay the potential complications of radiotherapy.

Prognosis

A review of the literature shows that for all patients with optic pathway gliomas in all locations and with all forms of treatment, including observation, tumor recurrence or progression occurs in 38% of cases [1]. The overall tumor-related mortality is 36% with a mean follow-up of 11 years. However, with longer follow-up intervals of 25–30 years, the prognosis for survival may be considerably worse. The outlook for vision is actually rather good. About 55% of patients retain stable vision or show some improvement. Only 45% show progressive loss of vision. Spontaneous regression of optic gliomas have been documented [28], and one case has been reported of malignant transformation [29].

Glioma Confined to the Optic Nerve

For gliomas initially confined to the optic nerve and treated conservatively or incompletely excised, recurrence or progression is seen in 17% [1]. The mortality rate is 12%, typically from intracranial extension. The prognosis for vision, however, is good, with over 90% remaining stable over many years. With optic nerve tumors treated by complete surgical excision or partial excision plus radiotherapy, the mortality rate drops to near zero. The same is true for tumors that progress but remain confined to the optic nerve. Obviously, the prognosis for vision in such cases is poor after surgery.

Gliomas with Extension to the Chiasm

Gliomas that extend to the chiasm but that do not invade the adjacent hypothalamus or third ventricle show results similar to those for untreated optic nerve tumors. Chiasmal gliomas left untreated or that are partially excised show a mortality rate of 17% over a mean follow-up period of 10 years. As with optic nerve tumors, death usually follows from extension into the hypothalamus or third ventricle. Recurrence or progression of tumor after partial excision is seen in 64% of cases. Visual prognosis in this group is good, with 80% remaining stable. In patients with chiasmal tumors, radiotherapy may delay progression to some extent. Mortality in this group is 22%, and recurrence or progression of tumor is seen in 43% of cases. Prognosis for vision is similar to that of untreated patients, with 68% remaining stable or demonstrating a slight improvement.

Gliomas with Extension to the Chiasm and with Invasion of the Hypothalamus

In patients with chiasmal tumors plus hypothalamic or third ventricle involvement at the time of presentation, the prognosis for life is markedly reduced. The mortality rate is 50% or more over 15 years [1]. For patients who receive radiotherapy, recurrence or progression is noted in 52%, but the mortality rate is somewhat better, at 43%.

Malignant Optic Nerve Glioma

In 1973 Hoyt et al. [30] described five cases of optic pathway glioma in adults which had an aggressive behavior and a uniformly fatal outcome. To date about 60 additional cases have been reported in the literature, all confirming the original concept of the disease.

Clinical Features

Age Distribution

Malignant optic pathway gliomas have been seen in patients from 6 to 79 years old but occur most commonly in middle age. The mean age at presentation is 48 years [1].

Sex Distribution

This disease has a distinct sexual predilection, with 65% occurring in males and 35% in females.

Location

In all described cases, the optic chiasm is the major site of origin. In all cases except one [31], the disease is bilateral with both optic nerves involved. In only 23% of cases does the tumor extend to the intraorbital portion of the nerve. In nearly half of affected patients, the tumor extends posterior to the chiasm along the optic tracts and into the hypothalamus or temporal lobe [1].

Signs and Symptoms

All patients present with rapidly progressive loss of vision, first in one and then in the second eye. In 63% of cases, both eyes may already be involved at presentation. Initially the condition is usually misdiagnosed as optic neuritis or anterior ischemic optic neuropathy [32]. Bilateral blindness typically results within a matter of months. Optic disc edema is seen in most patients, and if they survive long enough, optic atrophy results. Orbital signs are uncommon, as most tumors are confined to the intracranial compartment. Proptosis and ophthalmoplegia are seen in only 20–25% of cases (Box 11.2).

Box 11.2 Malignant Optic Glioma

- Very rapid loss of vision to blindness over weeks to months
- Optic disc swelling 43%
- Optic disc atrophy 31%
- Proptosis 23%
- Ophthalmoplegia 19%
- Other neurologic signs 35%

Diagnostic Evaluation

Enlargement and enhancement of the optic chiasm on CT or MRI is the most common finding, seen in 80% of cases. One or both optic nerves may also be involved along their intracranial portions. The final diagnosis is usually made only after tissue biopsy.

Histopathology

Malignant optic gliomas present as anaplastic astrocytomas (WHO grade III) or glioblastomas (WHO grade IV). Histopathology shows malignant astrocytes with pleomorphic nuclei and areas of vascular proliferation and necrosis. Subpial extension along the optic pathways is seen. There is invasion into the optic chiasm and nerve and into adjacent areas of the brain.

Treatment

To date no treatment has proven effective in slowing the progression of this disease. Neither surgery nor radiotherapy up to 60 Gy has significantly altered the prognosis. Combination of chemotherapy and radiotherapy, with or without prior surgery, improves survival but only for several months [33].

Prognosis

Prognosis for vision is dismal, with all patients progressing to profound bilateral visual loss within months of initial presentation. The prognosis for life is equally dismal, with a nearly 100% mortality rate. The mean survival rate is typically less than 1 year.

Optic Nerve Sheath Meningioma

Meningiomas are the second most common brain neoplasms after gliomas. They represent 15–20% of all intracranial tumors in adults and 2% of

intracranial tumors in children [34]. Most orbital meningiomas are secondary extensions from intracranial sites, including the sphenoid wing, olfactory groove, and tuberculum sellae. Primary orbital meningiomas arise from the optic nerve sheath, and account for 1.3% of all meningiomas, and 10% of orbital meningiomas. The remaining 90% arise from teh sphenoid wing.

Association with Neurofibromatosis Type 1

The incidence of NF1 in patients with sheath meningiomas is unclear because most studies in the past failed to mention the occurrence. Of the studies that specifically examined for NF, 9% of patients were affected. This is considerably lower than the 29% association with optic gliomas but still significantly higher than the 0.3–0.5% incidence of NF in the general population.

Clinical Features

Age Distribution

Despite several reports of orbital meningiomas occurring with high frequency in young individuals, most series confirm that this is a disease primarily of middle age. On imaging studies, meningiomas may be confused with arachnoid proliferation associated with optic gliomas in young patients. The mean age for presentation of optic sheath meningioma is 41 years, and only 4% of patients are under 20 [34, 35].

Sex Distribution

It has long been recognized that meningiomas occur more frequently in females. When large series are examined, the ratio has tended to equalize, but there does appear to be a slight female preponderance of approximately 60%.

Laterality

A slight predilection for the right optic nerve has been reported in several studies. Others have not confirmed these findings. However, when larger series are examined among unilateral cases, 52% of sheath meningiomas occur in the right optic nerve, 48% in the left. Overall, 6% are bilateral [34]. Interestingly, among bilateral cases 60% are canalicular meningiomas, compared to all sheath meningiomas together, where canalicular tumors account for only 8%.

Sites of Origin

For optic sheath meningiomas, 94% are unilateral and 6% bilateral. In about 8% of cases, the meningioma is confined to the optic canal. Among canalicular tumors there is a significant propensity toward bilaterality, 65% being unilateral and 35% bilateral. About 4% of optic sheath meningiomas show focal tumor invasion of the optic disc, sclera, choroid, and retina. Tumor may enter the globe along penetrating vascular channels. Dutton [34] noted that 18 of 475 cases of primary orbital meningioma arose ectopic to the optic nerve sheath. Since then another 13 cases have been described [36, 37]. The exact etiology of such lesions remains uncertain, and it is possible that in some cases they represent other lesions mistaken for meningiomas.

Signs and Symptoms

The most frequent presenting symptom of optic sheath meningioma is loss of vision, seen in 96% of cases (Box 11.3). In about 45% visual acuity is 20/20 to 20/40, and in only 25% is it counting fingers or worse. Visual loss usually takes place over several years. In bilateral cases, visual loss in the two eyes may be separated in time by 2–30 years. Visual field defects are noted in 83% of patients. Most commonly these include peripheral constriction; central, centrocecal, and paracentral scotomas; altitudinal defects; and increased size of the blind spot. Proptosis is found on initial examination in 59% of patients (Fig. 11.4). It is seen less frequently in patients with canalicular lesions, as they typically have significant visual loss while the tumor is still very small. Limitation of ocular motility is variable but may be seen in nearly half of patients. Upgaze is commonly severely impaired, possibly because of stiffening of the optic nerve from the relatively firm tumor.

Fig. 11.4 External photograph of a patient with a right orbital optic nerve sheath meningioma demonstrating proptosis

Box 11.3 Optic Nerve Sheath Meningioma

- Slowly progressive visual loss 96%
- Decreased visual field 83%
- Optic disc swelling 48%
- Optic disc atrophy 49%
- Proptosis 59%
- Decreased ocular motility 47%
- Optociliary shunt vessels 30%
- Increased intracranial pressure 27%

Chronic disc edema is an early finding in 48% of patients. Optic atrophy, which may be subtle, is a somewhat later finding, noted in nearly half of cases at presentation. Both edema and atrophy may be seen together, and overall 98% of patients will show one or the other of these two findings. The association between optic sheath meningiomas and optociliary shunt vessels has long been considered a key finding suggestive of optic sheath meningiomas. However, chronic disc edema and congestion of the central retinal vein usually precede the first appearance of shunts by several years, and the shunts usually disappear as optic atrophy becomes complete. In fact, optociliary shunt vessels are relatively infrequent with sheath meningiomas, being seen in only 30% of reported cases. Because shunts tend to appear some years after symptoms begin and involute as optic atrophy is complete, this probably does not indicate their true incidence.

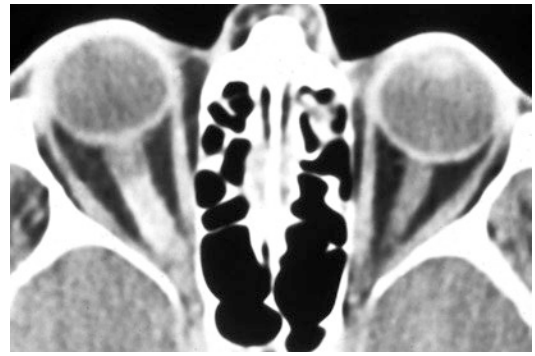

Fig. 11.5 Axial CT scan shows a tubular optic nerve sheath meningioma with tram-tracking. The involved sheath enhances brightly, with the uninvolved optic nerve centrally

Diagnostic Evaluation

Computed Tomography

Plain orbital radiographs and computed tomography through the optic canals demonstrate enlargement of the optic foramen in less than 30% of cases. CT scanning demonstrates enlargement of the optic nerve in 97% of examinations. The most common pattern is diffuse tubular enlargement, but a globular or fusiform shape may be seen also. Tram-tracking, a radiographic sign in which the denser and thickened optic nerve sheath outlines a central lucency representing the residual optic nerve, is a characteristic of sheath meningioma (Fig. 11.5). Contrast studies generally show moderate to marked enhancement. Calcification, an important finding, may help differentiate meningiomas from optic gliomas. It is seen in 20–50% of patients.

Magnetic Resonance Imaging

MRI shows a thickening of the nerve and sheath contrasted against orbital fat, and there is increased signal intensity compared to normal nerve on both the T1- and T2-weighted sequences.

Histopathology

Optic meningiomas arise from meningothelial cap cells of the arachnoid villi that lie along the

intraorbital optic nerve. Two histologic patterns are seen. In the meningothelial or syncytial pattern, polygonal cells are arranged in sheets separated by vascular trabeculae. In the transitional pattern, spindle-shaped or oval cells are arranged in a concentric whorl formation. Psammoma bodies are seen more commonly in the transitional pattern and contain the calcifications noted on radiologic studies. Optic nerve meningiomas typically remain indolent over many years. As the tumor grows within the subarachnoid space, it commonly encircles the optic nerve. Compression results in obstruction of axoplasmic flow, disc edema, dilatation of optociliary shunt channels, and eventually demyelinization and optic atrophy. Tumor cells may also invade through the dura and into surrounding orbital tissues. Although they can invade along the intracranial optic nerve to the chiasm, meningiomas usually do not invade the brain.

Treatment

The most appropriate therapy for optic sheath meningiomas has been a matter of some controversy. For sheath meningiomas that extend to the intracanalicular or intracranial portions of the optic nerve, the decision regarding treatment becomes less complex. The major rationale for treatment is the perceived risk of spread to the contralateral optic nerve. The actual risk of tumor spread from one optic nerve to the other remains unknown, but based on the high incidence of bilaterality with canalicular tumors and on documented unilateral tumors with progressive posterior extension, it may be very real. Because vision in such cases will eventually be lost, treatment to prevent possible extension to the contralateral side is justified. In most cases radiotherapy may slow or halt tumor progression. However, in cases of treatment failure, surgical excision should be considered. Newer treatment options have gained considerable support over the past decade, and these are changing the approach to management. A proposed treatment algorithm is shown in Fig. 11.6.

Observation

For meningiomas confined to the intraorbital optic nerve, when vision remains and symptoms and radiographic findings are stable, observation without treatment is appropriate [38]. The only possible exceptions that justify surgery are small anterior tumors and cases in young children, where biopsy for diagnosis may be indicated. Progressive visual loss is expected in most cases, but some patients may remain stable for many years. The prognosis for life is excellent, and there have been no tumor-related deaths reported for this disease.

Surgery

Some have considered surgical excision necessary to prevent intracranial extension. This may be possible for some small anterior orbital lesions [39] or even with some posterior tumors [40, 41], but in general the morbidity is high and loss of vision is a very common sequela due to disruption of vascular supply to the optic nerve. Once blindness results, surgical extirpation may be necessary for relief of disfiguring proptosis, orbital pain, or intraocular complications. Prechiasmal transection of the optic nerve has been proposed as an option to prevent tumor growth and to preserve vision in the contralateral eye [42]. Incomplete excision has been associated with diffuse orbital invasion and intracranial spread to the chiasm. The risk of such spread outweighs the potential benefit of attempted resection. Attempts to decompress the optic nerve by opening the dural sheath have proved disappointing and have resulted in massive orbital invasion requiring exenteration following surgical decompression. For lesions in the optic canal, canal decompression with dural sheath release may preserve sight in some cases [43].

Radiotherapy

For lesions that show progression by worsening symptoms or radiographic findings, radiotherapy would be an appropriate option. In the past radiotherapy was considered ineffective; however, more recent reports using newer techniques suggest that in appropriate doses radiotherapy can be

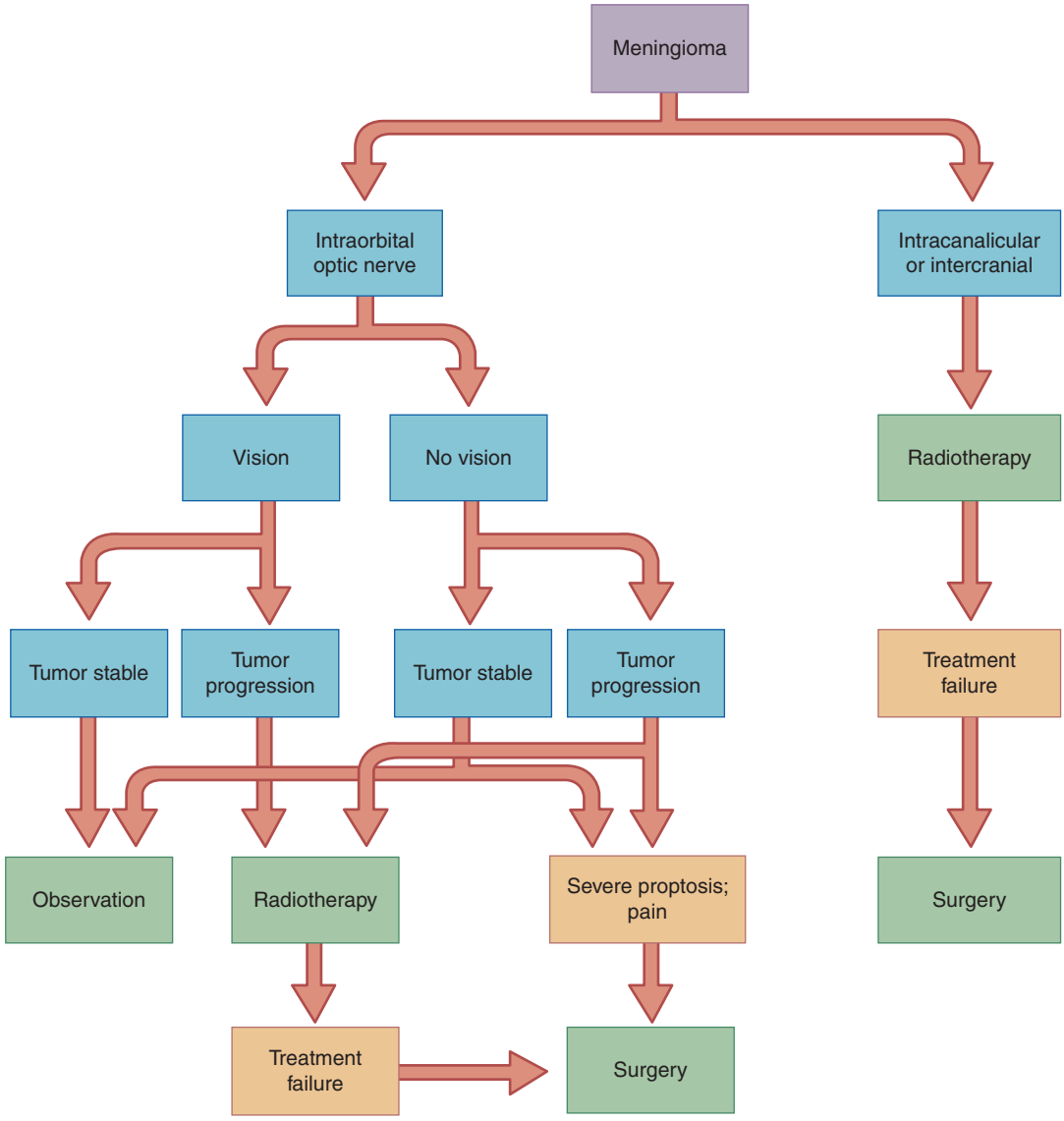

Fig. 11.6 Proposed management algorithm for treatment of uninvolved optic nerve centrally, sheath meningioma

effective [44]. Fractionated stereotactic radiotherapy may offer a promising refinement with fewer complications [45]. The optimum total dose appears to be in the range of 50–55 Gy. Stability or improvement of vision has been reported in 50–95% of cases. Similar results are being reported with the use of three-dimensional conformal fractionated radiation [46]. Complications of radiotherapy are reported in up to 15% of cases and include new visual field defects, central retinal artery occlusion, and encephalopathy. More recently, staged fractionated robotic CyberKnife radiosurgery with 20 Gy has given local control with visual improvement in 80% of patients [47].

Prognosis

Patients with optic sheath meningiomas have an excellent prognosis for life. There are few, if any, documented cases of tumor-related death.

The prognosis for vision, however, is poor. Without treatment, in most patients visual loss progresses slowly but inexorably to blindness in the affected eye. However, in some cases a spontaneous improvement in vision or visual field has been reported. Surgery offers little additional benefit and in most cases accelerates the process of visual loss. Rarely, a small anteriorly situated tumor may be excised with preservation or improvement of vision. Radiotherapy may stabilize or improve visual symptoms in some cases.

References

1. Dutton JJ. Gliomas of the anterior visual pathway. Surv Ophthalmol. 1994;38:427–52.
2. Shields JA, Shields CL, Scartozzi R. Survey of 1264 patients with orbital tumors and simulating lesions: the 2002 Montgomery Lecture, part I. Ophthalmology. 2004;111:997–1008.
3. Thiagalingam S, Flaherty M, Billson F, et al. Neurofibromatosis type 1 and optic pathway gliomas: follow-up of 54 patients. Ophthalmology. 2004;111:568–77.
4. Singhal D, Birch JM, Kerr B, et al. Neurofibromatosis type 1 and sporadic gliomas. Arch Dis Child. 2002;87:65–70.
5. Shamji MF, Benoit BG. Syndromic and sporadic pediatric optic pathway gliomas: review of clinical and histopathological differences and treatment implications. Neurosurg Focus. 2007;23:E3.
6. Thiagalingam S, Flaharty M, Billson F, et al. Neurofibromatosis type 1 and optic pathway gliomas: follow-up of 54 patients. Ophthalmology. 2004;111:568–77.
7. Segal L, Darvish-Zargar M, Dilenge ME, et al. Optic pathway gliomas in patients neurofibromatosis type 1: follow-up of 44 patients. JAAPOS. 2010;14:155–8.
8. de Blank PMK, Fisher MJ, Liu GT, et al. Optic pathway gliomas in neurofibromatosis type 1: an update: surveillance, treatment indications, and biomarkers of vision. J Neuroophthalmol. 2017;37(Suppl 1):S23–32.
9. Binning MJ, Liu JK, Kestle JR, et al. Optic pathway gliomas: a review. Neurosurg Focus. 2007;23:E2.
10. Astrup J. Natural history and clinical management of optic pathway gliomas. Br J Neurosurg. 2003;17:327–35.
11. Czyzyk E, Jozwiak S, Roszkowski M, et al. Optic pathway gliomas in children with and without neurofibromatosis 1. J Child Neurol. 2003;18:471–8.
12. Grill J, Laithier V, Raquin MA. When do children with optic pathway tumors need treatment? An oncological perspective in 106 patients treated in a single center. Eur J Pediatr. 2000;q59:692–6.
13. Lee AG, Dutton JJ. A practice pathway for the management of gliomas of the anterior visual pathway: an update ad an evidenced-based approach. Neuro-Ophthalmology. 1999;22:139–55.
14. Glaser JS, Hoyt WF, Corbett J. Visual morbidity with chiasmal glioma. Long-term studies of visual fields in untreated and irradiated cases. Arch Ophthalmol. 1971;85:3–12.
15. Hoyt WF, Bagdassarian SA. Optic gliomas of childhood: natural history and rationale for conservative management. Br J Ophthalmol. 1969;53:793–8.
16. Tow SL, Chandela S, Miller NR, et al. Long-term outcome in children with gliomas of the anterior visual pathway. Pediatr Neurol. 2003;28:262–70.
17. Mikaeloff Y, Chaix Y, Grill J, et al. Optic pathway gliomas in neurofibromatosis type 1. Longitudinal study of 30 cases in two multidisciplinary practices. Arch Pediatr. 2002;9:797–804.
18. Borghei-Razavi H, Shibao S, Schick U. Prechiasmatic transection of the optic nerve in optic nerve glioma: technical description and surgical outcome. Neurosurg Rev. 2017;40:135–41.
19. Khafaga Y, Hassounah M, Kandil A, et al. Optic gliomas: a retrospective analysis of 50 cases. Int J Radiat Oncol Biol Phys. 2003;56:807–12.
20. Combs SE, Schulz-Ertner D, Moschos D, et al. Fractionated stereotactic radiotherapy of optic pathway gliomas: tolerance and long-term outcome. Int J Radiat Oncol Biol Phys. 2005;62:814–9.
21. Kalin-Hajdu E, Décarie JC, Marzouki M, et al. Visual acuity of children treated with chemotherapy for optic pathway gliomas. Pediatr Blood Cancer. 2014;61:223–7.
22. Aquno VM, Fort DW, Kamen BA. Carboplatin for the treatment of children with newly diagnosed optic chiasm gliomas: a phase II study. J Neuro-Oncol. 1999;41:255–9.
23. Silva MM, Goldman S, Keating G, et al. Optic pathway hypothalamic gliomas in children under three years of age: the role of chemotherapy. Pediatr Neurosurg. 2000;33:151–8.
24. Hsu TR, Wong TT, Chang FC, et al. Responsiveness of progressive optic pathway tumors to cisplatin-based chemotherapy in children. Childs Nerv Syst. 2008;24:1457–61.
25. Kelly JP, Leary S, Khanna P, et al. Longitudinal measures of visual function, tumor volume, and prediction of visual outcomes after treatment of optic pathway gliomas. Ophthalmology. 2012;119:1231–7.
26. Doganis D, Pourtsidis A, Tsakiris K, et al. Optic pathway glioma in children: 10 years of experience in a single institution. Pediatr Hematol Oncol. 2016;33:102–8.
27. Dodgshun AJ, Elder JE, Hansford JR, et al. Long-term visual outcome after chemotherapy for optic pathway glioma in children: site and age are strongly predictive. Cancer. 2015;121:4190–6.
28. Zoeller GK, Brathwaite CD, Sandberg DI. Malignant transformation of an optic pathway glioma without prior radiation therapy. J Neurosurg Pediatr. 2010;5:507–10.

29. Parsa CF, Hoyt CS, Lesser RL, et al. Spontaneous regression of optic gliomas: thirteen cases documented by serial neuroimaging. Arch Ophthalmol. 2001;119:516–29.
30. Hoyt WF, Meshel LG, Lessell S, et al. Malignant optic glioma of adulthood. Brain. 1973;96:121–32.
31. Wabbels B, Demmier A, Seitz J, et al. Unilateral adult malignant optic nerve glioma. Graefes Arch Clin Exp. 2004;242:741–8.
32. Traber GL, Pangalu A, Neumann M, et al. Malignant optic glioma – the spectrum of disease in a case series. Graefes Arch Clin Exp Ophthalmol. 2015;253:1187–94.
33. Alireza M, Amelot A, Chauvet D, et al. Poor prognosis and challenging treatment of optic nerve malignant gliomas: literature review and case report series. World Neurosurg. 2017;97:751.e1–6.
34. Dutton JJ. Optic nerve sheath meningiomas. Surv Ophthalmol. 1992;37:167–83.
35. Saeed P, Rootman J, Nugent RA, et al. Optic nerve sheath meningiomas. Ophthalmology. 2003;110:2019–30.
36. Tendler I, Belinsky I, Abranson DH, et al. Primary extradural ectopic orbital meningioma. Ophthal Plast Reconstr Surg. 2017;33(Suppl):S99–S101.
37. Gündüz K, Kurt RA, Erden E. Ectpic orbital meningioma: report of two cases and literature review. Surv Ophthalmol. 2014;59:643–8.
38. Miller NR. New concepts in the diagnosis and management of optic nerve sheath meningioma. J Neuroophthalmol. 2006;26:200–8.
39. Yuceer N, Erdogan A, Ziya H. Primary optic nerve sheath meningiomas. Report of seven cases (clinical neuroradiological, pathological and surgical considerations in seven cases). J Neurosurg Sci. 1994;38:155–9.
40. Cristante L. Surgical treatment of meningiomas of the orbit and optic canal: a retrospective study with particular attention to the visual outcome. Acta Neurol (Wien). 1994;126:27–32.
41. Hunt PJ, DeMonte F, Tang RA, et al. Surgical resection of an optic nerve sheath meningioma: relevance of endoscopic endonasal approaches to the optic canal. J Neurol Surg Rep. 2017;78:e81–5.
42. Norris JH, Norris JS, Akinwunmi J, et al. Optic canal decompression with dural sheath release: a combined orbito-cranial approach to preserving sigh from tumours invading the optic canal. Orbit. 2010;31:34–43.
43. Pacelli R, Cella L, Conson M, et al. Fractionated stereotactic radiation therapy for orbital optic nerve sheath meningioma – a single institution experience and a short review of the literature. J Radiat Res. 2011;52:82–7.
44. Abouaf L, Girard N, Lefort T, et al. Standard-fractionated radiotherapy for optic nerve sheath meningioma: visual outcome is predicted by mean eye dose. Int J Radiat Oncol Biol Phys. 2012;82:1268–77.
45. Zweckberger K, Unterberg AW, Schick U. Prechiasmatic transection of the optic nerve can save contralateral vision in patients with optic nerve sheath meningiomas. Clin Neural Neurosurg. 2013;115:2426–31.
46. Narayan S, Cornblath WT, Sandler HM, et al. Preliminary visual outcomes after three-dimensional conformal radiation therapy for optic nerve sheath meningioma. Int J Radiat Oncol Biol Phys. 2003;56:537–43.
47. Romanelli P, Bianchi L, Muacevic A, et al. Staged image guided robotic radiosurgery for optic nerve sheath meningiomas. Comput Aided Surg. 2011;16:257–66.

Optic Nerve Sheath Fenestration and Optic Nerve Biopsy

12

Bhupendra C. K. Patel

Introduction

The medial and superior intraconal space, just posterior to the globe and next to the optic nerve, presents a challenge to the orbital surgeon: the tetrahedral shape of the orbit and the presence of the globe make access to this area difficult. Traditionally, tumors in this space have been approached via a transcranial route or with lateral out-fracturing of the lateral bony orbit and a medial transconjunctival approach. Both these approaches carry significant risks. We developed a surgical approach to this space which is relatively quick and can be performed efficiently and safely. This technique is useful for performing ONSF, obtaining optic nerve biopsies, and removing lesions in the medial and superior intraconal space [1].

Definition of ONSF

Optic nerve sheath fenestration is the opening of the optic nerve sheath with the removal of a window of the sheath. It is usually performed on the orbital portion of the optic nerve, with the aim of releasing the cerebrospinal fluid from the subarachnoid space, which normally extends forward to just behind the optic disc.

Mechanism of ONSF

ONSF is thought to reduce the pressure on the optic nerve head by reducing the subarachnoid pressure. It has been theorized that a cerebrospinal fluid (CSF) filter from the subarachnoid space of the optic nerve into the orbital tissue continues to give a sustained reduction of pressure at the optic nerve head. MRI and ultrasound studies have demonstrated fluid collection around the fenestration site after surgery. The other theory of fibrous tissue proliferation at the incisional site, preventing transmission of elevated CSF pressure to the optic nerve head, seems less likely as one sees the improvement in the visual field within a few days of surgery. However, such fibrosis may well contribute to a sustained improvement in the transmission of pressure to the optic nerve head over the following months [2].

Indications for ONSF

The commonest indication for ONSF is to release pressure around the optic nerve in IIH where there is progressive visual loss which is resistant to medical therapy. In approximately 10% of patients with untreated IIH, visual loss will

B. C. K. Patel (✉)
Division of Facial Cosmetic and Reconstructive Surgery, University of Utah, Salt Lake City, UT, USA
e-mail: bhupendra.patel@hsc.utah.edu

C. J. Hwang et al. (eds.), *Clinical Ophthalmic Oncology*,
https://doi.org/10.1007/978-3-030-13558-4_12

Table 12.1 Indications for optic nerve sheath fenestration

BIH with progressive visual loss, resistant to medical therapy
Dural sinus thrombosis
Radiation-induced optic neuropathy with progressive visual loss
Post-decompression blindness: syndrome of visual loss due to a compartment syndrome after removal of a CNS lesion
Osteopetrosis
Optic nerve glioma
Unresectable CNS mass causing cerebral venous system obstruction and chronic papilledema
Arteriovascular malformation of the vein of Galen
Papilledema and vision loss in cryptococcal meningitis
Chronic inflammatory demyelinating polyneuropathy
Subarachnoid hemorrhage of the optic nerve
Optic nerve sheath arachnoid cyst
Idiopathic papilledema with visual loss

progress to the point of meeting the legal criteria for blindness [3]. Numerous other conditions have been reported in the literature to have been helped with ONSF (Table 12.1). It should be noted that the second commonest indication for ONSF used to be ischemic optic neuropathy, but the ischemic optic neuropathy trial has shown that not only does ONSF not help but (the medial approach) technique itself may lead to more harm [4]. Certain other indications for ONSF like central vein occlusion and for normal tension glaucoma are reflected in isolated reports but the efficacy has not been.

History of ONSF

It is remarkable that the first optic nerve sheath fenestration (ONSF) was presented as early as 1872 by the renowned Parisian ophthalmologist De Wecker at the International Ophthalmic Congress in London for the treatment of "neuroretinitis" [5]. He described a transconjunctival approach between the lateral and inferior rectus muscles with the fenestrations being performed with longitudinal incisions and being done blindly under the guidance of a finger threaded back to the optic nerve without anesthesia! Henry Power (who became the first ophthalmic surgeon at St. Bartholomew's Hospital in 1870) used this approach in a 13-year-old girl whose vision was improved from no vision to hand movements.

Carter of London (who helped establish the Nottingham Eye Hospital in 1959) split the lateral rectus longitudinally to perform fenestration of the optic nerve under direct vision and presented four of his cases [6].

Muller in 1916 performed what amounted to a Kronlein procedure with removal of the lateral orbital rim for better exposure of the optic nerve [7]. As is often the case, this was presented as a new procedure with failure to acknowledge the previous techniques. Therefore, this procedure was called "Muller's operation for nerve sheath trepanation."

Gomez-Marquez of Barcelona performed a lateral canthotomy and detached the lateral rectus to gain access to the optic nerve in 1935 [8].

Interest in optic nerve sheath surgery was revived by Professor Hayreh's investigations into the pathogenesis of optic nerve edema. He demonstrated the reversal of papilledema with ONSF and also showed that papilledema could be prevented with ONSF. He was the first to show bilateral improvement after unilateral ONSF and also showed decreased intracranial pressure following ONSF [9, 10].

Smith et al., in 1969, used a Kronlein approach with lateral retraction of the eye and a medial approach to ONSF on a patient with field changes, visual obscurations, and disc swelling caused by an arachnoidal cyst of the optic nerve sheath [11]. The patient recovered her vision.

Sydney Davidson of Liverpool presented results of ONSF in five patients with unresectable intracranial tumor in 1969 [12]. He showed reduction of headaches and disc edema in all his patients and vision improvement in four. He used Berke's 1953 modification of Kronlein's 1888 lateral approach [13] which improved upon the semicircular temporal scar by performing a lateral canthotomy, undermining and cantholysis of the common canthal attachment to the lateral orbital rim. Berke's modification [14] was a major advance in orbital surgery. Davidson, however, described the dissection to expose the optic nerve "difficult and tedious." I participated in this

approach with Mr. Davidson in the mid-1980s in Liverpool, and, true enough, each procedure took us around 3 hours. I have a distinct memory of the consultant taking a couple of breaks during the procedures while the senior house officer continued to mind the patient. We even performed two fenestrations with the help of neurosurgeons at Walton Hospital via a transcranial approach, which, not surprisingly, took us several hours.

The next major advance was by Galbraith and Sullivan in 1973 when they described their medial trans-conjunctival approach with detachment of the medial rectus muscle [15]. This approach, which is familiar to ophthalmologists, continues to be the most commonly used one for ONSF although other techniques (see below) are beginning to get accepted as they reduce morbidity and surgical time.

Tse et al. in 1988 described the lateral approach to the optic nerve via a lateral orbitotomy and removal of the lateral orbital rim [16]. This is similar to Mr. Davidson's Berke modification and removal of the lateral orbital rim. In their approach, a large skin incision with bone removal and manipulation of the temporalis muscle was needed.

Kersten and Kulwin in 1993 [17] described a lateral canthotomy and cantholysis approach to the optic nerve without removal of the lateral orbital rim, which was similar to that of Gomez-Marquez in 1935 except they did not detach the lateral rectus muscle.

Patel and Anderson in 1994 described a lateral upper eyelid approach to the optic nerve without a canthotomy and without detachment of the lateral rectus muscle [18]. Their procedure allowed better exposure of the optic nerve with reduced complications and was quicker to perform than other procedures described until then. They entered the muscle cone via the periosteum and between the superior rectus and lateral rectus muscles.

Blessing and Tse have recently described a modified lateral transconjunctival approach to the optic nerve performed in combination with a lateral canthotomy and retraction of the lateral rectus without detachment of the muscle [19].

We presented our superomedial approach to the optic nerve and intraconal space in 2000 but have been using it since 1995 [1].

Development of the Superomedial Approach to the Optic Nerve

The development of the superomedial approach to the optic nerve, as with some advances in medicine, was based upon a fortuitous observation. When my kids were messing about in a hot tub, as kids are wont to do, I heard a scream. My daughter had a hand over her right eye: she complained that her brother had poked her in the eye. An abrasion was present over the superomedial upper eyelid where a bruise was developing but of greater concern was her claim that she could not see. She could see my hand moving but she claimed she could not see as well as with the opposite eye. I dilated her and examined the optic nerve and the fundus and found nothing untoward. By this time, she had an impressive bruise on the upper eyelid, and her vision was back to what she called normal. There was no limitation of ocular movement and no proptosis. This reminded me of a case of bilateral auto-enucleation that I had seen in London, where the patient had enucleated both her globes with impressive lengths of optic nerves attached to the globes by insinuating a finger under the upper eyelid medially. The upper and lower eyelids were intact, and the sockets almost looked like there had been surgical enucleations, except for the bleeding that was present. Finally, while performing fat decompressions with or without bone removal for thyroid-related proptosis, I had regularly made upper eyelid incisions not only to access the levator aponeurosis and Müller's muscle but also to remove intraconal orbital fat. I had often commented on the impressive view of the optic nerve that I obtained during this dissection. Based upon these observations, I went on to use this approach to obtain optic nerve biopsies, perform optic nerve sheath fenestration, and remove intraconal orbital tumors from 1995. In 1999, we carried out cadaver studies to measure the angles, the exposure, and the distance to the optic nerve of the four commonly used approaches for optic nerve fenestrations. These studies clearly showed the superiority of the superomedial approach to the optic nerve for fenestration but also for obtaining biopsies and for removing medial, superomedial,

and superior intraconal tumors. We reviewed our results of fenestrations and removal of intraconal tumors which we published together with details of the surgical technique [1].

Anatomy

The superomedial orbit is a "busy" area but with natural planes which allow relatively easy access to the medial and superior intraconal orbital space. The medial eyelid skin and orbicularis muscle make the anterior wall of the superomedial space. Superiorly behind the orbicularis lies the trochlea and the superior oblique tendon which traverses medially and posteriorly to the superior globe. The superior rectus muscle marks the inferolateral aspect of the space. The medial rectus marks the inferior boundary, while the medial levator aponeurosis and the superomedial globe mark the inferior border of the entry to the superomedial space. The medial border is composed of the nasal and ethmoid bones (Fig. 12.1). The supraorbital, the supratrochlear, and infratrochlear vessels and nerves are along the roof and the medial wall of this space. The space behind the medial orbital septum leads to the intraconal fat which is divided by major and minor fascial planes of Koornneef [20]. The superior ophthalmic vein is in the superior part of this space and can be traced by following branches of the supraorbital vein. The superior ophthalmic vein will generally be superior to the plane of dissection and is rarely encountered during the dissection. Moving through the orbital fat between the medial rectus and superior rectus, one gets to the space medial to the optic nerve where one finds the medial posterior ciliary arteries as they enter the globe. A variable vortex vein may be encountered along the superomedial globe. The short and long posterior ciliary nerves enter the globe usually at the 3 and 9 o'clock positions. The Tenon capsule covers the posterior globe separating the globe from the intraconal fat. Posterior ciliary arteries and short posterior ciliary arteries mostly enter the sclera medial and lateral to the optic nerve with only 9% of eyes showing a superior posterior ciliary artery [21]. The central retinal artery enters the optic nerve 8–15 mm behind the globe, inferior, inferolateral, or lateral to the optic nerve.

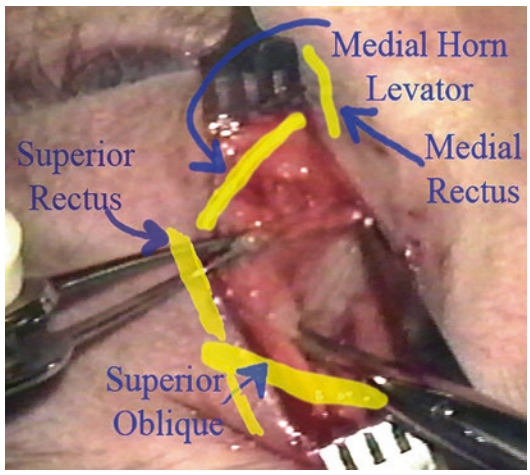

Fig. 12.1 The anatomical borders of the superomedial space used for the approach to the optic nerve and the superomedial intraconal orbit

The orbital surgeon needs to be familiar with the different sections of the optic nerve: it is divided into four sections.

A. The optic nerve head (also called the optic disc) is where the nerve inserts into the eye. 1.2 million retinal ganglion cells converge to form the optic nerve head, which is 1.5 mm in diameter and 1 mm in length. Blood supply is from the circle of Zinn-Haller and the posterior ciliary arteries (branches of the ophthalmic artery).
B. The intraorbital optic nerve which is 28 mm long (the distance from the back of the eye to the orbital apex is 15 mm, which allows proptosis of the globe without affecting the optic nerve, up to a certain point): the retinal nerve fiber layer exits the eye at the lamina cribrosa, which is a portion of the sclera made up of sheets of elastic fibers with fenestrations. The axons are covered by myelin after exiting the lamina cribrosa which increases the diameter of the optic nerve to 3 mm. The nerve acquires a covering of pia mater, arachnoid mater, and dural sheath. The pial vessels derived from the ophthalmic artery provide the blood supply to the orbital optic nerve.

C. Intracanalicular optic nerve: the periorbita of the orbit and the dura mater of the optic nerve fuse at the orbital apex, where the nerve is also encircled by the annulus of Zinn which is made up of the insertions of the four rectus muscles. The intracanalicular optic nerve is relatively fixed within the optic canal which measures 8–10 mm in length and 5–7 mm in width. Anteriorly, the nerve is supplied by the ophthalmic artery, posteriorly from the internal carotid artery branches.
D. Intracranial optic nerve: measures 8–12 mm before joining the optic chiasm. The nerve exits the canal under the anterior clinoid process with the ophthalmic artery under it. The internal carotid artery, the superior hypophyseal artery, the anterior cerebral artery, and the anterior communicating artery supply this portion of the optic nerve.

The subarachnoid space of the optic nerve is continuous with the subarachnoid space of the brain. The CSF circulates freely between the optic nerve and the brain. Raised intracranial pressure is transmitted to the subarachnoidal space within the optic nerve sheath, leading to optic nerve head edema (papilledema). The axoplasmic transport system is disturbed, leading to axonal swelling at the optic nerve head, leading to nerve fiber function loss: loss of central vision, peripheral vision, and eventual optic atrophy occur. It has been shown that with raised intracranial pressure, sequestration of CSF at the optic nerve head may cause optic neuropathy [22, 23].

Preparation

Instruments (Fig. 12.2)

Besides the basic plastic surgery instrument set with the standard orbital instruments, certain additional instruments are needed for this procedure. Yasargil and Rhoton bayonet scissors come in various lengths and may be straight or curved. We keep several different lengths and curves available. Rhoton style micro dissectors come in a set with round, curved, angled, sharp, blunt, and small, medium, and large tips: these are useful when accessing the optic nerve sheath, for picking up the sheath prior to fenestration and to undermine the dura when necessary. Neurosurgical cottonoids are useful to keep the orbital fat away from the optic nerve once exposure has been obtained. Sewell orbital retractors are essential for exposing the optic nerve.

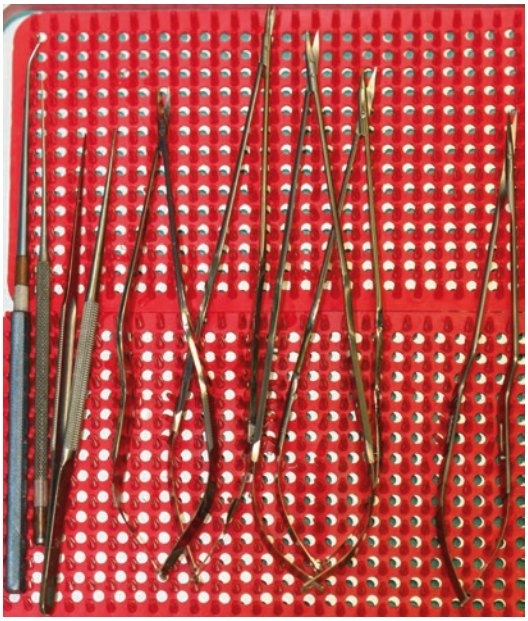

Fig. 12.2 Yasargil curved and straight bayonet microscissors, Rhoton sharp, and blunt picks and dissectors

Patient Positioning

We place the patient in a moderate Trendelenburg position as this allows a better angle of approach to the optic nerve and the medial intraconal space. We use this position when operating with operating loupes with a surgical headlight (our preferred technique), or with an operating microscope (which we use when teaching).

Anesthesia

Although we have performed several of these procedures under sedation anesthesia and local anesthesia, general anesthesia with endotracheal

intubation is preferred. 1 cc of 0.5% bupivacaine hydrochloride with 1:100,000 epinephrine solution is injected subcutaneously with a 30-gauge 1 cm needle. The injection is administered immediately after anesthesia has been induced and prior to sterile preparation of the surgical area to give time for vasoconstriction.

Surgical Technique (Figs. 12.3a, b and 12.4)

Incision

An incision between 6 and 10 mm is made at or just above the medial upper eyelid skin crease. We make the incision through the skin and use Stevens scissors to separate the orbicularis fibers. There will be oozing from the skin edges and from just under the orbicularis muscle: it is important to control this oozing with bipolar cautery at this point to prevent the blood from obscuring the view posteriorly as we dissect further.

Surgical Dissection

The orbital septum is opened medially to expose the medial horn of the levator aponeurosis inferiorly and medially and the medial fat pad centrally. Stevens scissors are used to make an opening in the medial fat pad by using an opening dissection technique only. The scissors are aimed inferiorly, posteriorly, and only slightly laterally. When teaching, we find surgeons aim too far posteriorly. It is best to aim for the back of the globe at this stage. Sewall retractors are used to separate the tissues medially and laterally. If the superior ophthalmic vein is encountered (which is uncommon), it is gently teased superiorly. The retractors which are inserted are placed so that the tips allow for separation of the deeper orbital tissues with little tension placed at the incision. The orbital septae will be encountered which are opened, again using a blunt "scissor-opening" technique. It is sometimes necessary to reposition the retractors and bluntly open the fascial planes several times. A surgical aid at this point is to aim as if one is dissecting toward the medial rectus muscle. This will expose the vortex vein, and a number of posterior wiggly ciliary vessels which are usually medial to the optic nerve but may be in the superomedial quadrant. If such vessels are encountered, long Q-tips or a beaded neurosurgical probe are used to gently push them out of the way. Sharp dissection is not used nor is any electrocautery. If one encounters any gentle oozing (again, this is rare), simple pressure with a moist Q-tip is applied.

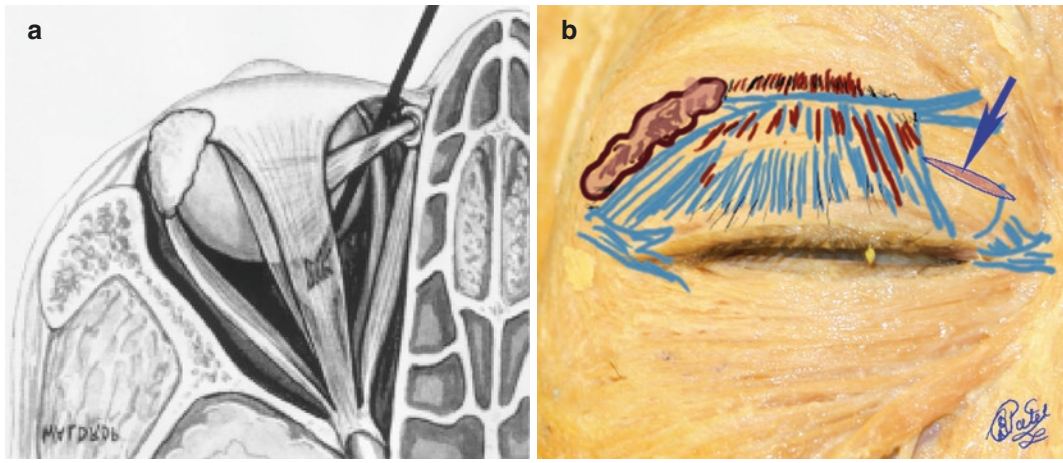

Fig. 12.3 (**a**, **b**) Surgical approach is via a natural space that exists between the superior oblique tendon, the medial levator and medial levator horn, and the superomedial orbital rim. The dissection direction is below the superior oblique, above the medial canthal tendon and lateral to the superior rectus muscle and above the medial rectus muscle. (**a**: Reprinted from Pelton and Patel [1]. With permission from Wolters Kluwer Health, Inc. **b**: Courtesy of Bhupendra C. K. Patel)

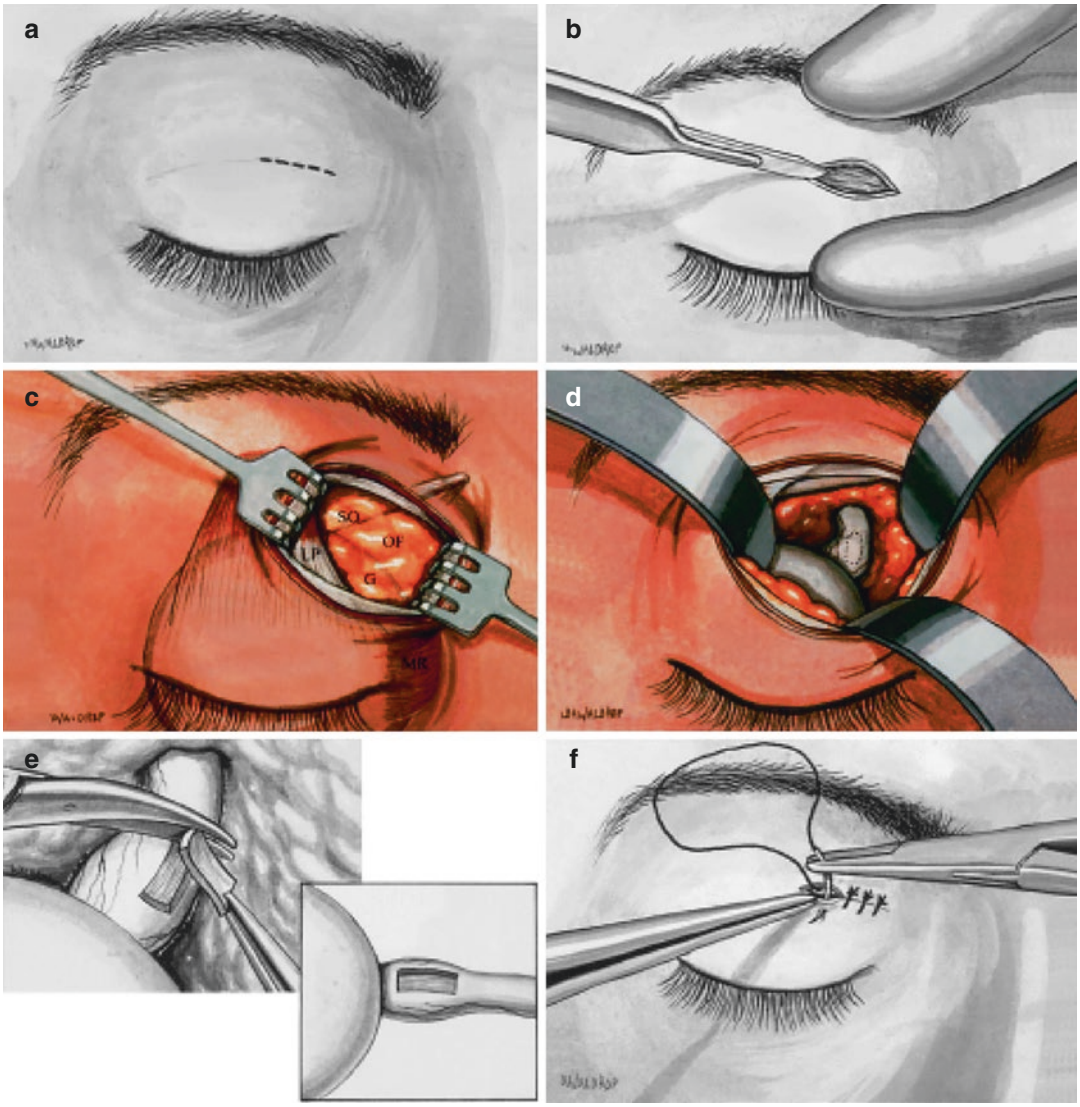

Fig. 12.4 Surgical sequence (**a**) incision marked over the medial third of the upper eyelid skin crease or just above it (**b**) blunt dissection through the orbicularis oculi muscle after the skin incision is made (**c**). SO is superior oblique, OF is orbital fat, G is globe and LP is medial levator palpebrae aponeurosis. This is the entry point. (**d**). Exposure of the optic nerve with Sewell retractors (**e**). Fenestration of the optic nerve sheath with removal of a rectangle of the sheath 2 × 3 mm (**f**). Closure with interrupted 6–0 catgut sutures. (Reprinted from Pelton and Patel [1]. With permission from Wolters Kluwer Health, Inc.)

Overweight patients have "fat orbits." If one is fenestrating an optic nerve sheath in benign intracranial hypertension, one may encounter a surfeit of fat at this stage. A good technique is to insert mildly moist neurosurgical cottonoids and use the Sewell retractors over these cottonoids to hold the fat out of the way. This will allow about 6–10 mm of the optic nerve to be exposed quite effectively (Fig. 12.5a–c).

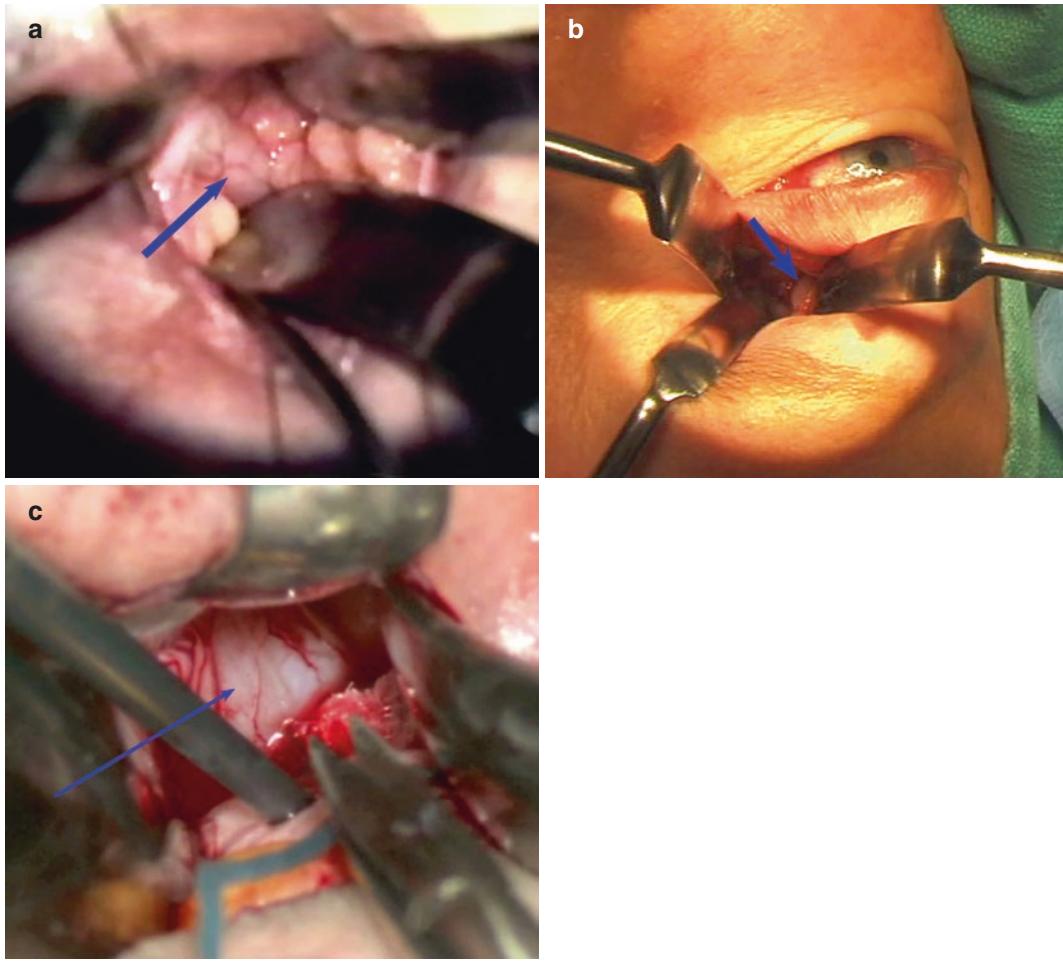

Fig. 12.5 (**a**–**c**) Three examples of the optic nerves being exposed (blue arrows) to varying distances. Note the epidural vessels in Fig. 12.5c: these can be gently moved with a moist Q-tip or a blunt Rhoton hook

Fenestration of the Optic Nerve Sheath (Fig. 12.6a, b)

Because the nerve sheath is bulbous just behind the globe, we used to, when we first designed this surgical approach, use neurosurgical forceps to pick up the sheath and then fenestrate it with bayonet curved microscissors. A safer approach is to use a neurosurgical pick which allows the sheath to be tented: a safe incision is made with the microscissors (when egress of the cerebrospinal fluid is seen) and extended, all the while keeping the sheath tented. About 3 mm × 2 mm of the dural sheath is resected to make a window. We have recently designed punches ("Patel Punches"), which allow the surgeon to safely remove a portion of the optic nerve sheath with minimal risk. Although we do bluntly "dissect" the tissue under the sheath with a blunt probe, we have not noted any adhesions in the subdural space.

Effect of Unilateral ONSF

Although it has been observed that the unoperated eye may also show an improvement in the papilledema and vision with unilateral ONSF, this is variable [3]. Some patients show an excellent response, others a partial response, and a significant number will show no improvement

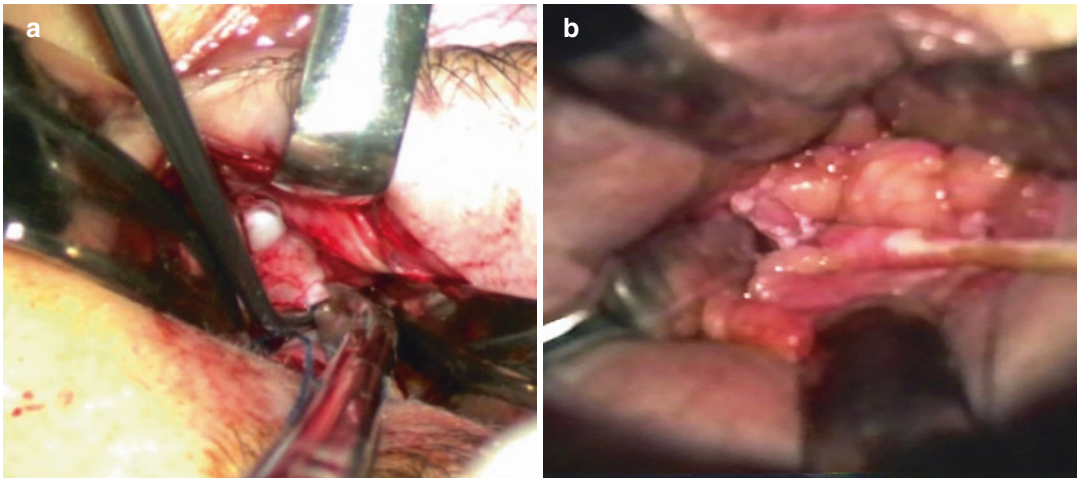

Fig. 12.6 (**a**) The dural sheath is being lifted with a sharp, angled Rhoton pick which allows the sheath to be tented whilst a Yasargil curved microscissors is used to fenestrate the sheath. (**b**) The optic nerve is visible under the sheath fenestration

at all. Trabeculations in the arachnoid space are thought to reduce the transmission of pressure along the nerve, which explains why only some patients will get an improvement in the eye opposite to the one that is fenestrated. We generally follow the request of the neuro-ophthalmologists who determine if they want unilateral or bilateral surgery, based upon the severity of the disease and urgency for intervention.

Removal of Intraconal Tumors

Medial, superomedial, and superior intraconal tumors have traditionally been approached via a medial conjunctival approach and without fracturing of the lateral orbital wall to allow displacement of the globe. Neurosurgeons often access these tumors that are between the globe and the medial optic nerve via a transcranial approach through the orbital roof.

Once the intraconal space is reached and the tumor identified, traction on tumors may be provided with a 4-0 silk or the use of a cryoprobe. Gentle "Ngorongoro Crater" circular dissection with a freer elevator which gently circles the tumor while separating any surrounding attachments is performed. Patience is needed here to continue this careful circular dissection as this leads to a gentle delivery of tumors like hemangiomas, hemangiopericytomas, and lymphangiomas with minimal traction being applied to the surrounding structures. If a cryoprobe is used, it is not used to apply strong traction but just a gentle hold on the tumor while this dissection is performed. This principle should apply to the removal of any orbital tumors as injury to surrounding structures is caused by blind dissection, aggressive manipulation, severe traction, and sharp dissection. Even large intraconal tumors can be safely delivered with excellent cosmetic and functional results (Figs. 12.7a–g and12.8).

Bleeding

Other than cauterizing the oozing at the incision site, we generally never use any bipolar cautery within the orbit with these procedures. If ciliary vessels are encountered, the retractors and the orbital cottonoids can be removed and replaced: this will generally move the vessels out of the way. Otherwise, gentle teasing of the vessels away from the optic nerve can be performed with a moist Q-tip or blunt Rhoton dissectors. Neither cryotherapy nor cautery should be used on or close to the optic nerve.

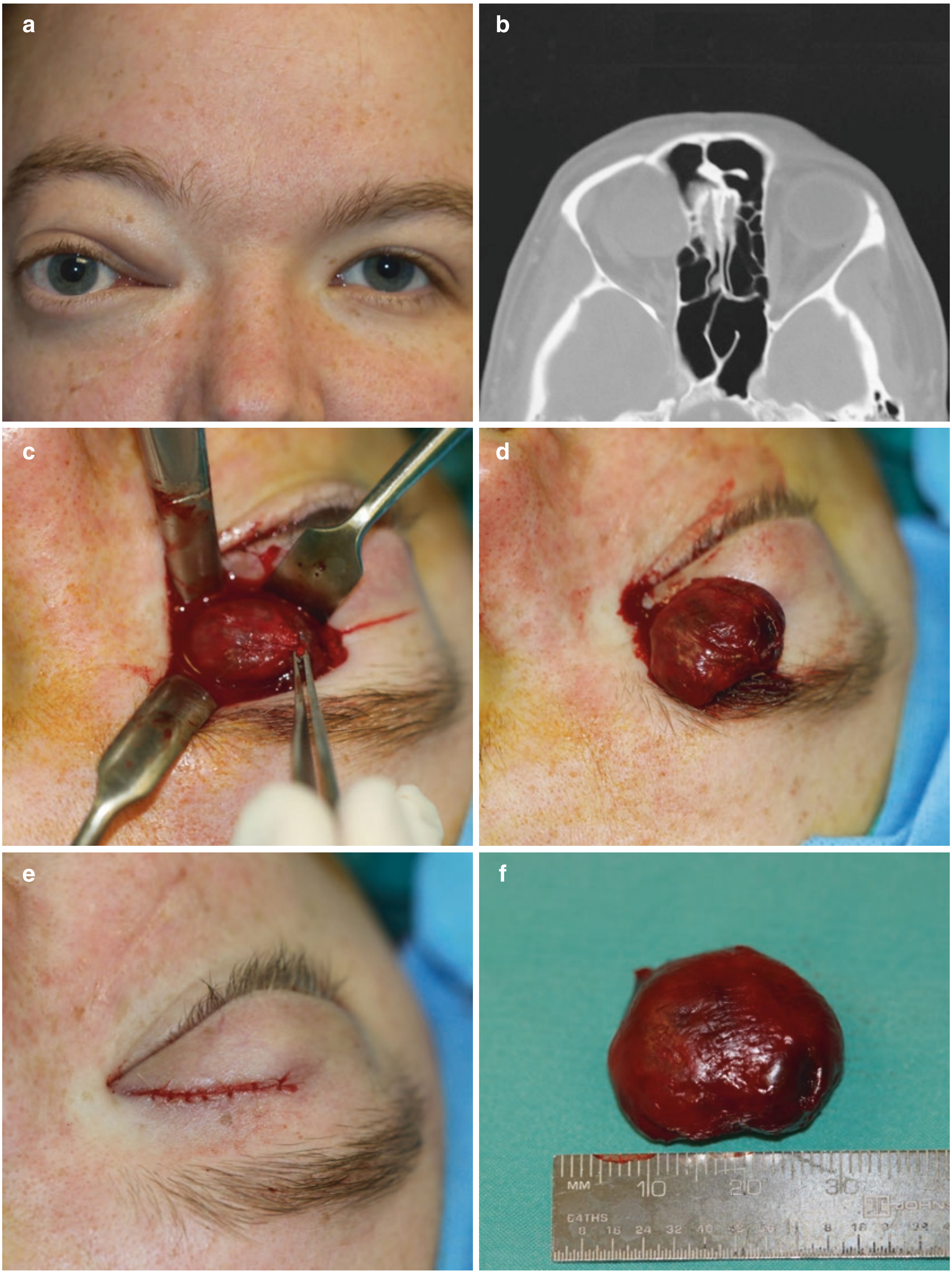

Fig. 12.7 (**a**) 23-year-old female presents with an 18-month history of worsening double vision, pressure, and pain on movement of the right eye. Patients have right proptosis, hypoglobus, and exoglobus. Vision is 20/20 with no visual field defect (**b**). Evidence of a large slow-growing superomedial orbital mass with molding of the medial wall of the orbit (**c**). Superomedial skin incision approach with gentle dissection around the tumor (**d**). Delivery of a large tumor via this incision (**e**). Appearance of the closed incision at the end of the procedure (**f**). Tumor measures 26 mm in diameter. Histopathology shows it to be a cavernous hemangioma (**g**). Six months after surgery. No residual ptosis, double vision, or globe malposition. Vision is 20/20

Fig. 12.7 (continued)

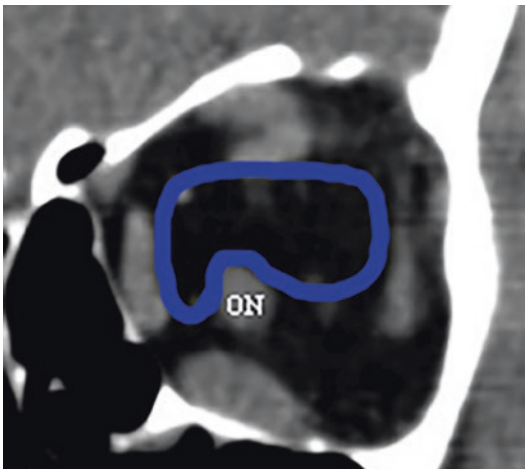

Fig. 12.8 The superomedial approach allows the removal of tumors in the medial, superomedial, and superior intraconal space as marked. ON: optic nerve

Closure

The cottonoids are removed, and a simple skin closure is performed with interrupted 6-0 catgut sutures. Local anesthesia is administered around the incision site at the end of the procedure. Most of our patients do not need prescription pain medication after these operations.

Postoperative Care

Immediately after surgery, the eye and vision are examined. Pain is usually mild. Prescription opiates are rarely required. We generally do not apply a patch on the operated eye. Erythromycin eye ointment is applied twice a day for a week.

Complications

Complications have been minor with this surgical approach. This report is based upon 168 optic nerve sheath fenestrations and 27 medial, superomedial, or superolateral tumor removals by the author. Vertical diplopia was noticed in the immediate postoperative period in a few patients, which did not last more than a few days except in seven patients who had vertical diplopia for up to 2 months, but none had permanent double vision. Mild medial ptosis for 7–14 days is common because of the surgical approach. To date, we have not had to perform ptosis surgery on any of the patients. It is possible that mild residual ptosis may remain in some patients, but, again, we have not had occasion to address this in any of the patients. A tonic pupil developed in six patients.

There were no cases of hematoma, vision loss, permanent ptosis, or permanent strabismus.

Comparison to Other Surgical Approaches to ONSF (Boxes 12.1, 12.2, and 12.3)

Box 12.1 Complications seen with medial transconjunctival ONSF (reported in 4.8% to 45% of cases with a mean of 12.9%)

Pupillary dysfunction (16.3%), strabismus, lost medial rectus muscle, damage to third nerve branch to medial rectus, conjunctival bleb, globe perforation, chemosis, Tenon's cyst, dellen formation, corneal ulcer, microhyphema, angle closure glaucoma, pupil dysfunction, chorioretinal scar from globe traction, branch arterial obstruction, central artery occlusion, choroidal ischemia, traumatic optic neuropathy, optic nerve cyst formation, orbital apex syndrome, orbital infection, orbital hemorrhage, lost muscle, conjunctival abscess, optic disc hemorrhage. Cilioretinal and long posterior ciliary retinal artery occlusions

Based on data from Ref. [24]

Box 12.2 Complications seen with superomedial ONSF

Medial ptosis (usually transient), vertical diplopia (always transient), pupillary dysfunction (less than 2%), visible upper eyelid scar (rare)

Based on data from Ref. [1]

Box 12.3 Complications seen with lateral ONSF

Pupillary dysfunction (up to 50%), vision loss, retrobulbar hemorrhage, double vision, ptosis

Based on data from Ref. [25]

The immediate retrobulbar optic nerve is bulbous because of the larger subarachnoidal space and the loose arachnoidal attachments in this region. This makes this portion of the optic nerve the safest to fenestrate. In cadaver studies, we showed that the angle of access to this portion of the optic nerve through the medial transconjunctival approach is acute (25 degrees) as compared to the superomedial approach which had an average of 38 degrees. Although the angle was larger via the lateral approach without a bone flap (54 degrees) and largest with a bone flap (72 degrees), the lateral approach encounters the ciliary ganglion and the associated ciliary nerves. Indeed, Henry Stallard, in his description of the Stallard lateral orbitotomy approach, noted that "...most of the important blood vessels and nerves lie on the lateral side of the optic nerve."

In the medial transconjunctival approach, traction must be placed on the globe to move it laterally to allow the nerve to be fenestrated, especially now that the medial approach is generally used without out-fracturing the lateral orbital wall.

The average distance from the skin incision to the nerve in the superomedial approached was 25 mm. Although the distance was shorter with the medial transconjunctival approach 20 mm, this distance of 25 mm is only slightly longer and allows the surgeon to work safely in the confines of limited space. The increased horizontal space available to the surgeon with gentle traction in the superomedial approach makes this extra 5 mm of little significance.

Medial Transconjunctival Approach (Galbraith and Sullivan Procedure)

The main disadvantage of this approach is the acute angle of approach to the optic nerve and the need to disinsert the medial rectus muscle. Whereas the distance to the optic nerve is the shortest (20 mm), there is risk to the extraocular muscle, potential for pupil dysfunction and need for substantial traction to the globe. In our hands, these procedures took 45–60 minutes of operating time.

Lateral Orbital Approach with Bone Flap (Tse et al. Procedure) (Fig. 12.9)

This approach gives the most en face approach to the optic nerve, but the distance to the optic nerve is the longest at 36 mm. There needs to be significant traction applied to the lateral rectus muscle and extensive dissection of intraorbital tissues to reach the optic nerve. There is also a very high chance of pupil dysfunction. The width of the surgical field is good. Operating times are about 45–60 minutes.

Lateral Orbital Approach Without Bone Flap (Patel and Anderson Procedure)

This approach has the same advantages and disadvantages as the lateral orbital approach with a bone flap, except the distance to the optic nerve is a little shorter at 30 mm. The exposure of the optic nerve is more limited, and significant traction needs to be applied. Pupil abnormalities are common with this approach. The surgical time with this technique was 15–30 minutes. Even though we were able to reduce the surgical time by designing a lateral eyelid crease approach to the optic nerve without a canthotomy or bone removal, we realized that the lateral approach to the optic nerve for fenestration is just unwise because of the many important structures that crowd this surface of the optic nerve: central retinal artery, ciliary ganglion, short posterior ciliary nerves, and short posterior ciliary vessels. We abandoned this approach because of the high incidence of pupillary abnormalities and the potential for more severe complications. Pupillary abnormalities, whether full-blown Adie's pupils or just sectorial iris involvement, should be taken

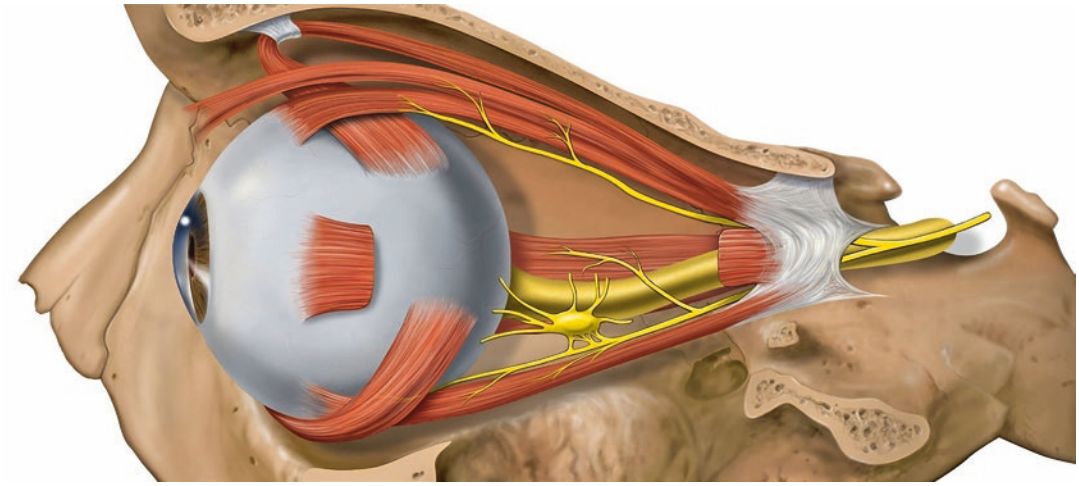

Fig. 12.9 Access to the lateral portion of the optic nerve is hindered by the short posterior ciliary vessels, nerves, and ciliary ganglion, and the retinal artery also enters the optic nerve inferolaterally. This increases the risk of complications with this approach

seriously as most of these patients that we operate upon are young and such pupillary abnormalities cause visual problems.

Advantages of the Superomedial Approach to the Optic Nerve and Intraconal Tumors

In all the other procedures, there is significant manipulation of one or more extraocular muscles with resultant potential problems. The superomedial approach, on the other hand, allows access to the intraconal space anterior and below the superior oblique tendon, medial to the superior rectus, and superior and medial to the medial rectus muscle. Mild retraction needs to be applied to the region of the medial horn of the levator aponeurosis only. With the understanding that the retraction is provided deeper within the wound with angling of the Sewell retractors, little traction needs to be applied to the aponeurosis. Inevitable postoperative swelling does give temporary double vision in a small number of patients, but this resolves within a few days.

The posterior ciliary nerves and vessels enter the globe at the 3 o'clock and the 9 o'clock positions. Therefore these structures are most vulnerable using the medial and lateral approaches. Adie's pupil is a significant risk with the lateral approach. The superomedial approach, by contrast, allows the surgeon to approach the optic nerve at the 11 to 2 o'clock positions where there are the least number of vessels and nerves.

Other advantages of the superomedial approach include very little bleeding, a wider surgical view, little pressure on the globe, an excellent cosmetic outcome, and minimal surgical time. The eyelid anatomy is very familiar to oculoplastic and orbital surgeons. Lastly, no cutting of normal tissues is needed as the approach is more of a "star wars" gliding through anatomical planes. It is a truism about orbital surgery that the risk of complications rises with increased surgical dissection and with longer surgeries. Certainly, speed alone should never be a reason to choose a particular surgical approach. However, with experience comes efficiency, and our average skin-to-skin operating time over the last 50 cases for ONSF is just under 10 minutes (with the fastest being 3 minutes 40 seconds, a little quicker than the world mile record).

Surgical Tips for Successful ONSF with the Superomedial Approach

Whenever a new surgical procedure is introduced into the literature, the usefulness of the procedure is judged by how successfully the technique is performed by surgeons other than the inventors. To that end, after presenting the procedure at major meetings and after publishing it, I received multiple calls from experienced orbital surgeons. Based upon these calls and also upon the experience of teaching the technique to fellows and residents, the following surgical tips may be useful.

The simple advice of ensuring that the surgeon had absolute hemostasis before entering the orbital space cannot be stressed enough. If there is a continuous ooze from the vessels at the edge of the incision and below the orbicularis muscle, this will spread into the surgical site, which, being effectively at the end of a tunnel, will make it difficult to know where the blood is coming from.

When performing orbital dissection once the orbital septum has been opened, only blunt dissection with the opening of Stevens scissors should be employed. There should be little, if any, cutting of tissues. The sequence is blunt separation of the fat lobules and Koornneef's septae followed by repositioning of the Sewell retractors. This has to be done several times.

Several surgeons called saying they had a hard time finding the optic nerve. The commonest mistake was pointing the dissection too posteriorly. It is surprising how anteriorly and inferiorly the dissection needs to be to reach the optic nerve within a few seconds. A good technique that our fellows have found useful is to pretend that you are aiming for the medial rectus muscle.

Initially, we used to lift the sheath with neurosurgical microforceps to allow us to fenestrate the sheath. Of course, patients do not always have a large amount of CSF around the nerve which carries the risk of causing injury to the optic

nerve. A much better approach is to tent up the sheath with an angled Rhoton sharp-tipped pick and cut the sheath with curved Yasargil bayonet microscissors. Once the opening is made and CSF has been released, a blunt hook may be used to tent up the sheath, thereby allowing one to create a fenestration. It is easy to create a fenestration measuring 2–4 mm square. In order to create fenestrations easily, we have designed modified surgical punches (Patel Punch, 1 mm and 2 mm in diameter) which have been used successfully on a few patients.

As has been discussed, "fat orbits" will allow floppy orbital fat to tumble into your surgical site. Mildly moist cottonoids are very useful. Dry cottonoids are sticky to the orbital fat. We usually place two, one superolaterally and the other inferomedially, and use the Sewell retractors to hold these cottonoids and fat back.

A good assistant is essential. We designed some self-retaining retractors for this operation but found that there needs to be dynamic retraction, and the use of Sewell retractors and a good assistant are better than any self-retaining retractors. I have learned to resist the temptation to be too helpful.

Conclusion

A review of the current preference of orbital surgeons for optic nerve sheath fenestration has shown a rapid increase in the uptake of the superomedial approach, although the medial approach is still the procedure most familiar to surgeons and used most often [26]. We believe that with careful study of the orbital anatomy will allow most surgeons to successfully undertake this approach for fenestration as well as for the removal of orbital tumors.

References

1. Pelton RW, Patel BCK. Superomedial lid crease approach to the medial intraconal space: a new technique for access to the optic nerve and central space. Ophthal Plast Reconstr Surg. 2001;17(4):241–53.
2. Mukherjee N, Bhatti MT. Update on the surgical management of idiopathic intracranial hypertension. Curr Neurol Neurosci Rep. 2014;13(3):438.
3. Vaidya NS, Mahmoud AM, Buzzacco D, et al. Visual outcomes following optic nerve sheath fenestration via the medial transconjunctival approach. Orbit. 2016;35(5):271–7.
4. The Ischemic Optic Neuropathy Decompression Trial Research Group. Optic decompression surgery for nonarteritic anterior ischemic optic neuropathy (NAION) is not effective and may be harmful. JAMA. 1995;273:625–32.
5. DeWecker L. On incision of the optic nerve in cases of neuroretinitis. Int Ophthalmol Cong Rep. 1872;4:11–4.
6. Carter RB. Case of swollen optic disc, in which the sheath of the optic nerve was incised behind the eyeball. Proc Med Soc London. 1887;10:290.
7. Müller L. Die Trepanation der Optikusscheide: Eine neue Operation zur Heilung der Stauungspapille. Wien Klin Wochenschr. 1916;29:1001–3.
8. Gomez-Marquez M. Traitement chirurgical local de la stase papullaire. Bull Soc Ophthalmol Paris. 1935;5:814–27.
9. Hayreh SS. Optic disc edema in raised intracranial pressure. V pathogenesis. Arch Ophthalmol. 1977;95(9):1553–65.
10. Hayreh MS, Hayreh SS. Optic disc edema in raised intracranial pressure. i. Evolution and resolution. Arch Ophthalmol. 1977;95(7):1237–44.
11. Smith JL, Hoyt WF, Newton TH. Optic nerve sheath decompression for relief of chronic monocular choked discs. Am J Ophthalmol. 1969;68:633–9.
12. Si D. A surgical approach to plerocephalic disc oedema. Trans Ophthalmol Soc U K. 1969;89:669–90.
13. Krönlein RU. Zur pathologie und behandlung der dermoidcysten der orbita. Beitr Klin Chir. 1888;4:149.
14. Berke RN. A modified Krönlein operation. Arch Ophthalmol. 1945;51:609–32.
15. Galbraith JE, Sullivan JH. Decompression of the perioptic meninges for relief of papilledema. Am J Ophthalmol. 1973;76(5):687–92.
16. Tse DT, Nerad JA, Anderson RL, et al. Optic nerve sheath fenestration in pseudotumor cerebri. A lateral orbitotomy approach. Arch Ophthalmol. 1988;106(10):1458–62.
17. Kersten RC, Kulwin DR. Optic nerve sheath fenestration through a lateral canthotomy incision. Arch Ophthalmol. Jun 1993;111(6):870–4.
18. Patel BCK, Anderson RL. Lateral eyelid optic nerve sheath fenestration. In: Naugle TC, editor. Diagnosis and management of oculoplastic and orbital disorders. Amsterdam/New York: Kugler Publications; 1996. p. 355–67.
19. Blessing NW, Tse DT. Optic nerve sheath fenestration: a revised lateral approach for nerve access. Orbit. 2018;22:1–7.
20. Koornneef L. Orbital septa: anatomy and function. Ophthalmology. 1979;86(5):876–80.

21. Hayreh SS. Posterior ciliary artery circulation in health and disease: the Weisenfeld lecture. Invest Ophthalmol Vis Sci. 2004;45:749–57.
22. Killer HE, Jaggi GP, Flammer J, et al. Cerebrospinal fluid dynamics between the intracranial and the subarachnoid space of the optic nerve. is it always bidirectional? Brain. 2007;130(pt 2):514–20.
23. Killer HE, Jaggi GP, Miller NR, et al. Cerebrospinal fluid dynamics between the basal cisterns and the subarachnoid space of the optic nerve in patients with papilloedema. Br J Ophthalmol. 2011;95(6):822–7.
24. Friedman DI, Jacobson DM. Idiopathic intracranial hypertension. J Neuroophthalmol. 2004;24(2):138–45.
25. Corbett JJ, Nerad JA, Tse DT, et al. Results of optic nerve sheath fenestration for pseudotumor cerebri. The lateral orbitotomy approach. Arch Ophthalmol. 1988;106(10):1391–7.
26. Sobel RK, Syed NA, Carter KD, et al. Optic nerve sheath fenestration; current preferences in surgical approach and biopsy. Ophthalmic Plast Reconstr Surg. 2015;31(4):310–2.

Lacrimal Gland Tumors

13

David H. Verity and Geoffrey E. Rose

Introduction

While 9–15% of orbital tumors arise in lacrimal gland, inflammatory or infiltrative diseases – such as sarcoidosis, Wegener's granulomatosis, IgG4 disease, or other (nonspecific) dacryoadenitis – comprise two-thirds of lacrimal gland masses and can present with signs and symptoms similar to tumors [1, 2]. Often a firm diagnosis can be reached only with tissue biopsy.

Inflammatory lesions typically present with acute or subacute symptoms that can include a painful, tender swelling in the lacrimal gland area, an "S-shaped" deformity of the upper eyelid, or conjunctival redness and injection (Fig. 13.1). Lymphomas tend to produce chronic, painless globe displacement, although some present with inflammatory features, which portend a worse prognosis [3].

Benign or malignant tumors can present similarly, and both enter the differential diagnosis for many lacrimal masses. About a half of primary tumors of the lacrimal gland are benign, most being of epithelial in origin; however, other very rare benign tumors – such as hemangiopericytoma, neurilemmoma, neurofibroma, lymphangioma, and other vascular malformations – can be centered on the gland. In addition to a thorough history and examination, high-resolution imaging plays a key role in establishing an appropriate treatment plan.

Epidemiology

Almost all benign lacrimal gland tumors are pleomorphic adenomas (Table 13.1) [4], and adenoid cystic carcinoma is the commonest malignant epithelial tumor [5]. Carcinoma arising in prior pleomorphic adenoma ("malignant mixed tumor") represents the second most common lacrimal gland malignancy [1, 5, 6], whereas mucoepidermoid carcinomas, primary adenocarcinomas, and squamous carcinomas are rare. Lymphoma, associated with systemic disease in a minority, accounts for about 10–14% of all lacrimal gland masses [1, 2], while metastases to the lacrimal gland are very uncommon; the latter tend to mimic the primary lesion, most such masses being fast growing and associated with a poor prognosis.

Clinical Features

Pleomorphic adenomas present from childhood [7] to old age, with a peak incidence in middle age and without a significant gender bias [4].

D. H. Verity
Adnexal Service, Moorfields Eye Hospital, London, UK

G. E. Rose (✉)
Adnexal Service, Moorfields Eye Hospital, London, UK

NIHR Biomedical Centre, Institute of Ophthalmology, London, UK
e-mail: geoff.rose1@nhs.net

C. J. Hwang et al. (eds.), *Clinical Ophthalmic Oncology*,
https://doi.org/10.1007/978-3-030-13558-4_13

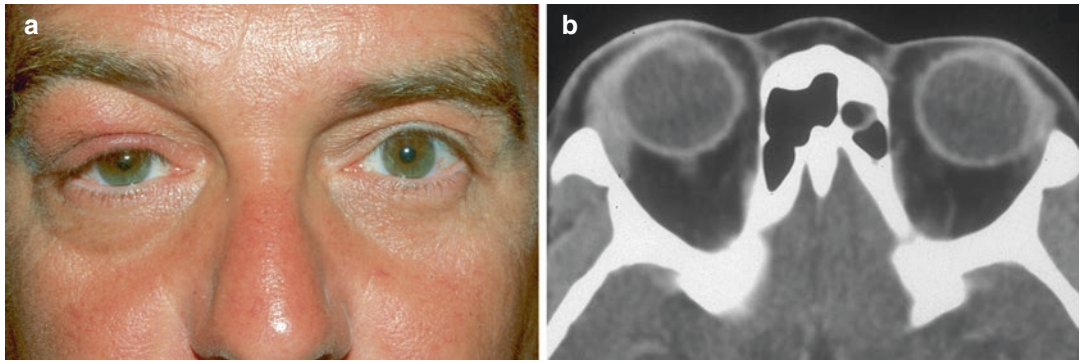

Fig. 13.1 S-shaped deformity of the right upper lid caused by subacute dacryoadenitis (**a**). CT showing right lacrimal gland enlargement with molding around the globe (**b**)

Table 13.1 Common primary lacrimal gland tumors

Types	Nomenclature
Benign tumors	Pleomorphic adenoma
	Myoepithelioma[a]
Malignant tumors	Adenoid cystic carcinoma
	Malignant mixed tumor (usually adenocarcinoma arising in pleomorphic adenoma)
	Mucoepidermoid carcinoma
	Adenocarcinoma

[a]Rare

Likewise, malignant epithelial tumors, present at a similar age to pleomorphic adenomas, have a peak incidence in the fourth decade and do not have a gender bias [5].

Symptoms

Patients with lacrimal gland tumors typically present with upper eyelid swelling or mass, but other features depend on the size, site, and nature of the lesion. Tumors in the palpebral lobe are rarer than orbital lobe tumors and, because of the anterior location, tend to present earlier with a palpable upper eyelid mass or an alteration in lid contour [8]. Patients with pleomorphic adenomas generally have a slowly progressive, uninflamed mass that has been present for over a year or have a facial asymmetry noted by others (Fig. 13.2). Larger tumors may also cause limitation of eye movements with diplopia or visual disturbances due to distortion of the globe by the firm tumor mass, with or without choroidal folds [4, 5].

Pain occurs rarely with pleomorphic adenoma or lacrimal lymphoma, but primary malignant tumors of the lacrimal gland are characterized by a short history and persistent pain. Lacrimal gland carcinoma tends to spread posteriorly along the lateral orbital wall, displacing the lateral rectus inferomedially [9], with microscopic invasion of the orbital fat and a propensity for perineural spread. Later in the disease, it tends to breach orbital periosteum, with spread to the bone and temporalis fossa, or extends through the superior orbital fissure into the middle cranial fossa.

Signs

Anterior enlargement of the gland occurs primarily with adenomas of the palpebral lobe: such adenomas are palpable in the lateral aspect of the upper lid and tend to be very hard in consistency – like a "chickpea." Occasionally palpebral lobe enlargement presents as a prominent gland in the upper fornix [8]. In contrast, orbital lobe tumors are often difficult to palpate – being set deep in the lacrimal fossa posterior to the orbital rim – and are characterized by progressive hypoglobus and relatively little proptosis, often passing unnoticed by the patient or relatives for years [4].

Malignant infiltration of cranial nerves at the superior orbital fissure or in the cavernous sinus

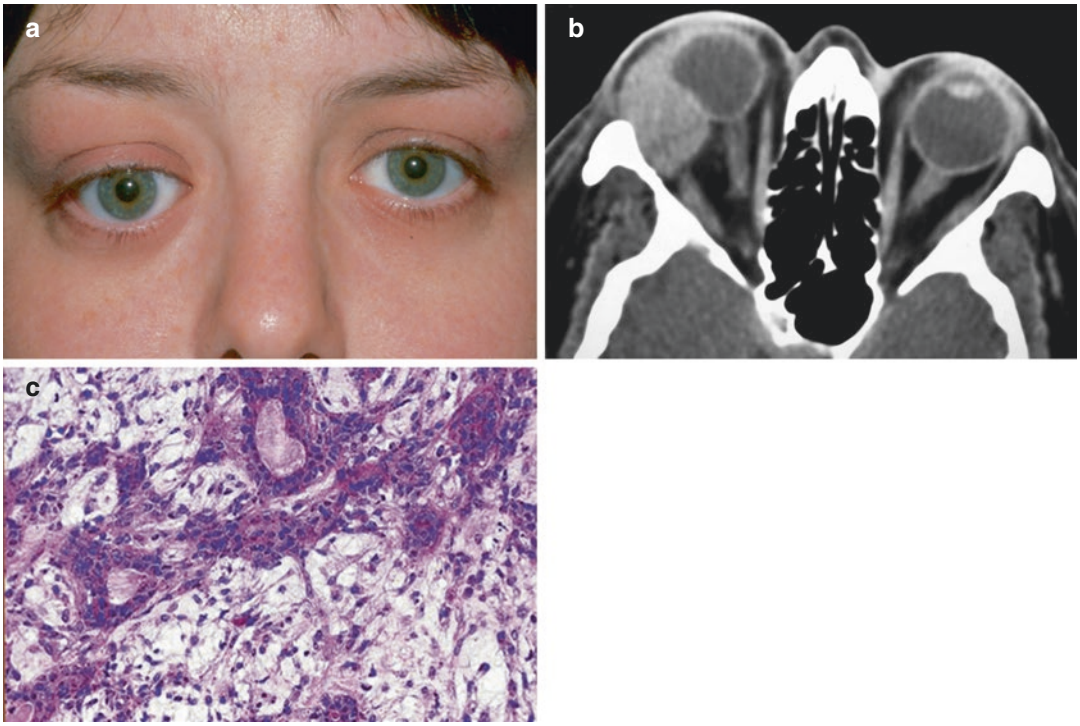

Fig. 13.2 Facial asymmetry due to pleomorphic adenoma of the right lacrimal gland (**a**). CT showing marked enlargement of the right lacrimal gland with indentation of the globe (**b**). Epithelial cells centrally with eosinophilic cytoplasm and myoepithelial cells surrounding ducts showing clear lumen (**c**, hematoxylin and eosin)

causes episcleral congestion, ptosis, diplopia, and periorbital sensory disturbance; indeed, in the presence of a lacrimal gland mass, persistent pain and sensory disturbance are strong predictors of malignancy. The rate of growth, although faster than for benign tumors, varies among different malignancies: adenocarcinomas progress rapidly, well-differentiated mucoepidermoid carcinomas have a relatively slow course, and the relentless growth of adenoid cystic carcinoma varies from extremely slow to slowly progressive [5]. Lacrimal gland metastases tend to follow the course of the parent tumors, while the generally indolent lymphomas may be primary orbital disease or part of a systemic condition [3].

Diagnostic Evaluation

Multi-slice or helical computed X-ray tomography (CT), the prime technique for providing high-resolution orbital images free of motion artifact, is invaluable in the differentiation of lacrimal gland masses. Bone changes are poorly shown on magnetic resonance imaging, and this modality is less useful than CT with lacrimal gland lesions, where an appreciation of the contour and quality of the adjacent lateral orbital wall is essential [10].

Benign Tumors

Pleomorphic adenomas appear as well-defined, but sometimes nodular and nonhomogeneous, lesions that show moderate enhancement with intravenous contrast (Fig. 13.2). Palpebral lobe tumors lie anterior to the orbital rim, whereas expansion of the lacrimal fossa with preservation of intact cortical bone is seen in many cases of orbital lobe adenomas; the latter frequently flatten the globe, and discrete flecks of calcification are distinctly rare [4].

Malignant Tumors

Malignant lesions are less defined, with infiltration into surrounding tissues, and "pitting" erosion of the cortical bone within the fossa is not uncommon (Fig. 13.3). Calcification occurs in about one-third of carcinomas [5] but is diffuse as compared to pleomorphic adenomas; lymphomas and metastases are only very rarely calcified. In contrast to hard adenomas that flatten the globe, rapidly growing and softer lesions (such as carcinomas and lymphomas) mold around the globe, and carcinomas also tend to respect the intermuscular septum and displace the lateral rectus inferomedially, as they extend backward along the lateral orbital wall in a "wedge" configuration [9].

Pathology

As pleomorphic adenomas and adenoid cystic carcinomas account for most lacrimal gland tumors, only their features will be discussed; details of other tumors can be found elsewhere in the literature [6].

Pleomorphic Adenoma

Pleomorphic adenomas are typically solitary, lobulated, firm, grayish-white masses; microscopic examination shows sheets, cords, or masses of epithelial cells that are of ductal origin (Fig. 13.2c). The "pleomorphic" appearance arises from epithelial metaplasia giving myxoid and pseudocartilaginous areas. Tiny tumor buds lie within the "pseudocapsule" of compressed neighboring tissues, and this probably accounts for tumor recurrence where the resection margin is insufficient.

Adenoid Cystic Carcinoma

Adenoid cystic carcinomas are gray-white, somewhat soft lesions that, although often showing

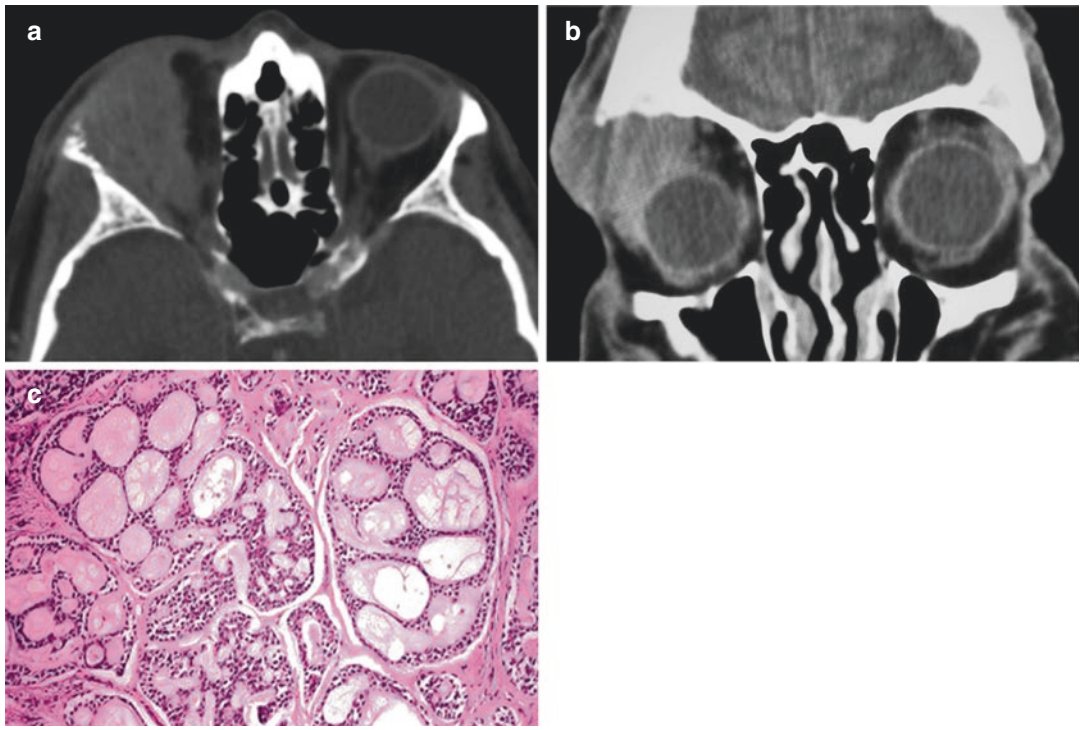

Fig. 13.3 Adenoid cystic carcinoma of the right lacrimal gland with destruction of the lateral orbital wall bone (**a**, bone window). Soft tissue invasion of the right temporalis fossa through lateral wall defect (**b**). Typical cribriform appearance (**c**, hematoxylin and eosin)

macroscopic sparing of muscles and bone, will often have some areas of adherence to orbital fat or Tenon's fascia. Microscopic examination shows small hyperchromatic, basophilic cells with varying amount of stroma (Fig. 13.3c), and five subtypes have been described: cribriform (most common), tubular, solid (basaloid), sclerosing, and comedo-carcinomatous. The basaloid pattern is least common but associated with the most aggressive behavior [5].

Differential Diagnosis

The sudden onset of a painful, swollen, and tender lacrimal gland is likely to be of inflammatory or infectious origin (bacterial or viral), rather than a tumor. Lacrimal gland swelling persisting for more than a few weeks and poorly responding to nonsteroidal anti-inflammatory agents might, however, suggest underlying carcinoma and should be further investigated with orbital imaging and, if appropriate, biopsy.

Differentiation of benign adenoma from primary malignancy is the key to appropriate surgical planning, as pleomorphic adenoma requires intact excision, whereas malignancy necessitates incisional biopsy [11]. Prior to high-resolution imaging, a clinical scoring was proposed to differentiate the two groups (Table 13.2) [4] – this being based on duration of symptoms and the presence of pain; painless lesions of over 10 months' duration were typically pleomorphic adenomas (although the differential diagnosis included lymphoma, sarcoidosis, and chronic mild dacryoadenitis), whereas malignant tumors had a shorter history relative to their size, as well as persistent pain and paresthesia. Although this algorithm results in a minority of glands (having been thought to be adenomas) being excised intact [12], this result – the inadvertent, but intact, excision of a nonfunctioning gland – is a mere inconvenience as compared with the problems of dealing with pervasively recurrent pleomorphic adenoma [11]. Although fine-needle aspiration biopsy, widely used for salivary tumors, can reliably diagnose pleomorphic adenoma [13], such foreknowledge has limited practical value in the final clinical management.

The advent of high-resolution CT has now become the major determinant in the management of lacrimal gland masses: a well-circumscribed tumor should be treated like a pleomorphic adenoma, whereas incisional biopsy should be carried out if the mass molds to the globe, where the mass forms a "wedge" sign along the lateral orbital wall [9] or where there is radiologic evidence of bone invasion or intraorbital extension. A diagnosis of malignant transformation within a pleomorphic adenoma (malignant mixed tumor)

Table 13.2 Management plan for a mass within the lacrimal gland

Characteristics		Score	
		−1	+1
Clinical	Duration of acute symptoms	<10 months	>10 months
	Persistent pain	Present	Absent
	Sensory loss	Present	Absent
Radiologic (features on thin-slice CT images)	Well-defined mass	Present	Absent
	Mass molding to globe or along lateral orbital wall	Present	Absent
	Tumor calcification	Present	Absent
	Invasion of bone	Present	Absent
	Duration of symptoms in relation to tumor size	Present	Absent
Therapeutic recommendation	Total score	Probable diagnosis	Type of biopsy
	−8 to +2	Carcinoma	Incisional
	−6 to +2	Malignant mixed tumor	Incisional or excisional
	+3 to +8	Pleomorphic adenoma	Total excision *without* prior biopsy

Adapted from Rose and Wright [4]. With permission from BMJ Publishing Group, Ltd

should be considered when a patient with long-standing symptoms develops a dramatic acceleration of symptoms, especially if accompanied by recent pain [14].

It has recently been shown that leptins are present at increased concentration in the tear films of patients with lacrimal gland adenoid cystic carcinoma, as compared to those with pleomorphic adenomas, but this is not yet available as a clinical test [15].

Treatment

Pleomorphic Adenoma

Pleomorphic adenomas should be excised intact with a cuff of normal tissue, and handling with sharp instruments should be avoided. Palpebral lobe tumors are readily resected through an upper lid skin crease incision, although some tumors may be accessible through the upper conjunctival fornix. Orbital lobe tumors can be resected through a skin crease incision, which can be extended into the lateral canthal rhytids where lateral osteotomy is required. Avoidance of capsular breach, with tumor mobilization on an island of periosteum and a buffer of normal tissue at the isthmus between the orbital and palpebral gland, gives an excellent chance of long-term cure [16]. If intraoperative spillage of cells occurs, the breach should be treated by surgical isolation, cautery of the capsular breach, and lavage of the operative field; cyanoacrylate glue may be applied to minor capsular breaches during surgery. Excision of the orbital lobe alone, with preservation of palpebral lobe, reduces the incidence of dry eye and secondary corneal disease [4].

If a pleomorphic adenoma has been inadvertently biopsied, which is distinctly rare with contemporary imaging, the biopsy tract and the tumor should be meticulously excised as recurrence of pleomorphic adenoma is typically multinodular and infiltrative, which may necessitate later extensive tissue resection or even exenteration [11, 17, 18].

Adenoid Cystic Carcinoma

In 1992 it was reported that patients with adenoid cystic carcinoma who – having very localized tumors – had been selected for craniofacial resection fared no better than another group judged unsuitable for major surgery [5]; indeed, it may well be that disruption of the orbital walls actually seeded tumor into cranial bone and thereby worsened the outlook for this aggressive tumor. Since that time, several reports from other centers support this contention, and there has been a significant shift toward globe-sparing surgery with adjunctive radiotherapy [19–25]. Current evidence therefore favors tumor debulking followed by about 55–60 Gy of fractionated external beam irradiation, this probably delaying tumor recurrence and improving survival [5]; the areas irradiated should include the superolateral soft tissues of the orbit, the lacrimal gland fossa, lateral orbital wall, and the orbital apex to include the superior orbital fissure as well as anterior cavernous sinus. This radiotherapy regime does have ocular morbidity in a minority of patients but preserves a long-term vision of 20/80 or better in many [26]. Although brachytherapy with locally implanted radioactive plaques or seeds might give local disease control, it fails to treat the superior orbital fissure and cavernous sinus where recurrences from perineural spread tend to arise and for this reason has little or no role in the management of malignant lacrimal gland disease.

Chemotherapy alongside exenteration and radiotherapy delays tumor recurrence and improves survival [27–29], although it remains unclear which parts of the regime carry efficacy [30]. Two or three cycles of intra-arterial cisplatin (delivered via the external carotid artery – with concomitant intravenous doxorubicin) are given over a few weeks prior to orbital exenteration, leading to a marked reduction in tumor size and, thereby, facilitation of surgery [27–29]. External beam radiotherapy is administered after orbital exenteration and, where tolerated, the intravenous chemotherapy consolidated to a total of six cycles.

Malignant Mixed Tumor

Malignant mixed tumors (Fig. 13.4) – that is, malignancy (generally adenocarcinomas) arising within a preexisting pleomorphic adenoma – can be treated by local excision followed by irradiation. Primary adenocarcinomas of the lacrimal gland are very rare and progress rapidly to involve other orbital tissues, the temporalis fossa, and the cranium and are generally treated with resection followed by radiotherapy [5, 21, 31, 32].

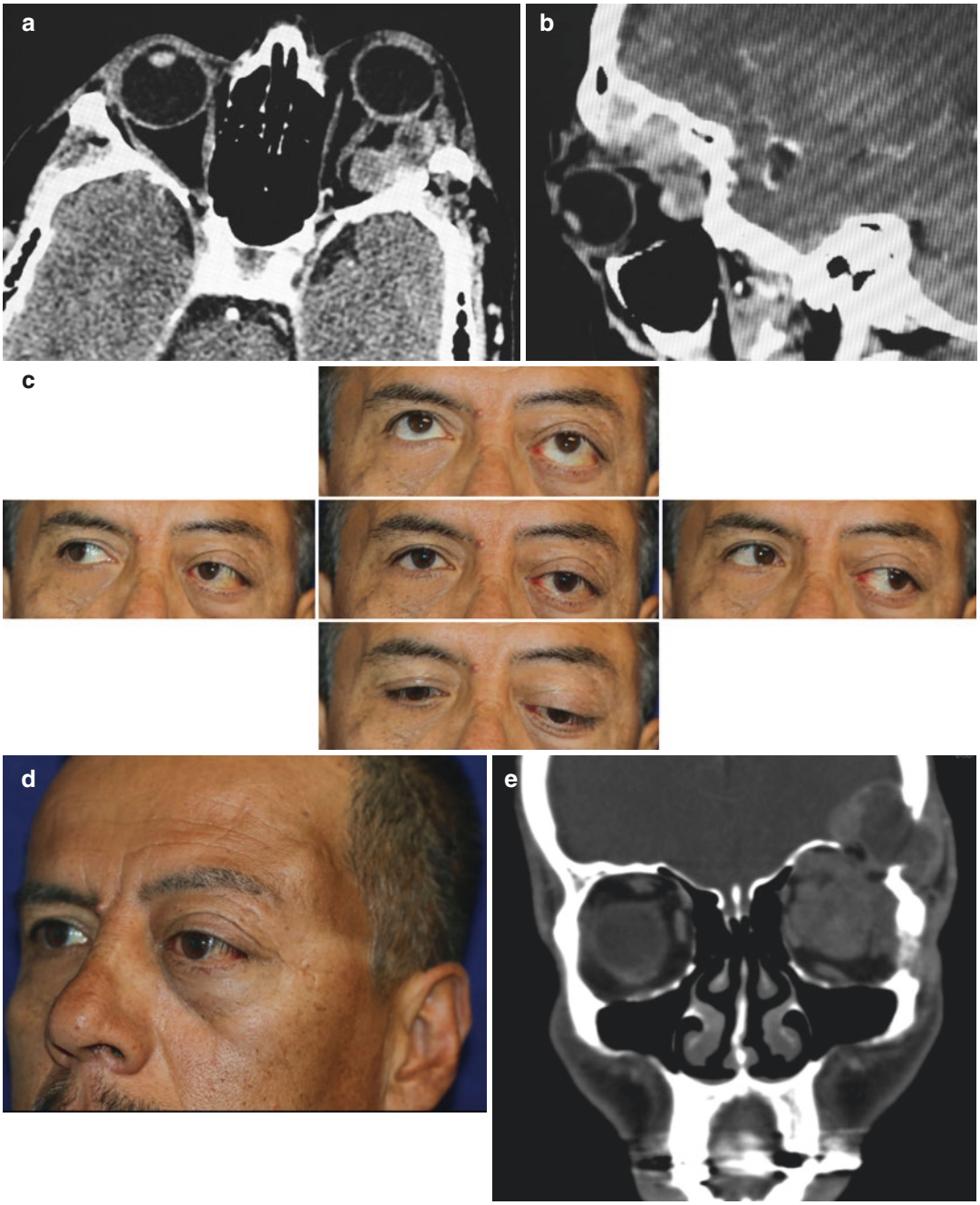

Fig. 13.4 (**a–j**) Carcinoma developing in a previous pleomorphic adenoma of the lacrimal gland

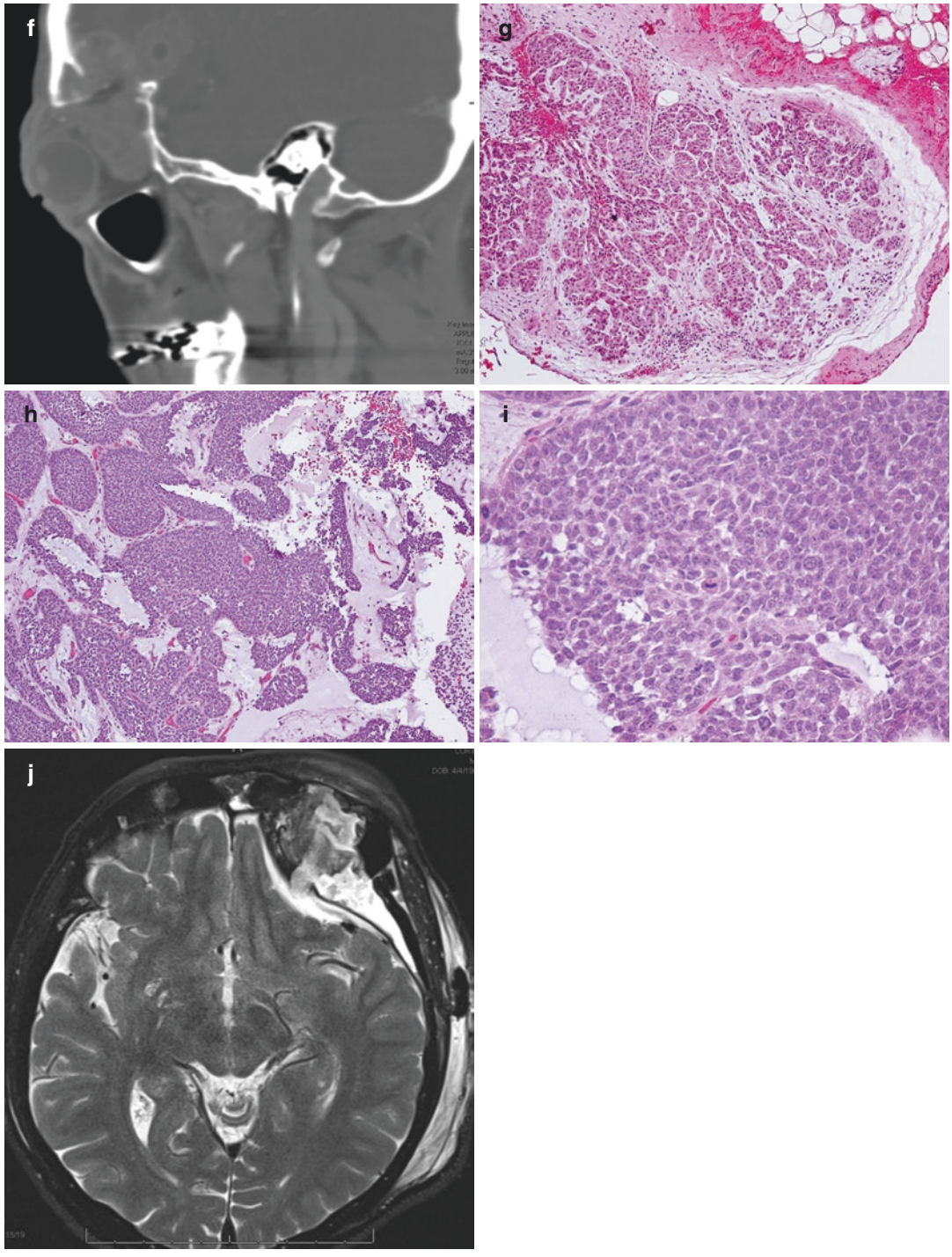

Fig. 13.4 (continued)

A 52-year-old patient had had three resections of his left orbital tumor: 2007, 2013, and March 2017. Exact details of his surgeries were not available. He presented for an opinion.

The scans that he brought taken just prior to his third operation (Fig. 13.4a, b) show an irregular lobulated supero-temporal mass with bony contouring superiorly.

When he presented to us, 7 months after his last surgery, he complained of a rapid increase in a bump on his left temple, pressure behind his left eye, some discomfort, and intermittent double vision. He had (Fig. 13.4c, d) left proptosis of 6 mm, hypoglobus, esoglobus, and limitation of movement of the left eye in all fields of gaze. The globe was firm to retropulsion.

Coronal and sagittal CT scans (Fig. 13.4e, f) show extension of the superior and superolateral orbital mass through the orbital roof and through the temporal bone into the temporal fossa. There was also extension through the lateral orbital wall, presumably through an area of weakness created by removal of the lateral orbital wall during one or more of the surgeries.

A review of the outside pathology of tissue (H&E ×100) obtained after the third operation (Fig. 13.4g) showed a benign pleomorphic adenoma mixture of glandular tissue and myoepithelial cells. No obvious dysplastic change noted with no nucleoli, pleomorphism, or mitotic figures.

The patient underwent an extensive resection via a frontotemporal approach. Because of the extent of the disease, an exenteration was discussed with the patient, but he declined. Therefore a resection of the tumor was performed with preservation of the globe. Histopathology (Fig. 13.4h-H&E ×100) and (Fig. 13.4i- H&E ×400) showed a malignant mixed tumor (carcinoma ex pleomorphic adenoma) with a mixture of glandular tissue and myoepithelial cells. Nodules of dysplastic tumor cells with large nuclear-to-cytoplasmic ratios and an occasional mitotic figure.

An MRI scan taken a week later (Fig. 13.4j) shows concern for residual tumor in the left supra-zygomatic masticator space, lateral orbit, and left supraorbital region. The patient is undergoing irradiation and will need follow-up scans.

This case illustrates the importance of complete and intact removal of a pleomorphic adenoma during the initial surgery. As can be seen, even 10 years after his initial two surgeries, the pathology revealed a benign mixed tumor (pleomorphic adenoma). However, it grew more aggressively after the third intervention, and the cellular nature turned into a carcinoma ex pleomorphic adenoma.

Metastatic Tumors

Metastatic deposits in the lacrimal gland carry a poor prognosis, and their treatment, generally palliative, reflects that of the primary tumor and generally necessitates palliative orbital irradiation and, where appropriate, chemotherapy.

Prognosis

Pleomorphic Adenoma

Intact excision of lacrimal gland pleomorphic adenomas would appear curative [16] and imperative in most cases, as these benign tumors undergo malignant transformation in up to 20% of cases after 20 years – especially after incomplete excision [33].

Carcinomas

The prognosis for primary epithelial carcinomas of the lacrimal gland is guarded and is determined by the cell type. Adenoid cystic carcinomas are characterized by late recurrence, often with distant metastasis, but perineural spread and direct seeding into the cranial diploe are thought to be responsible for intracranial recurrence after extensive local resections [5]. The median disease-free period is about 2–4 years after treatment [5, 21, 31], and the basaloid variant carries a particularly poor prognosis [5, 21, 34]. Although addition of chemotherapy might improve this poor prognosis [27–29] and render some larger tumors amenable to surgery, the assessment of

"cure" for this tumor is very difficult as late recurrence is common – being reported up to 24 years after presentation [6].

Systemic and Metastatic Tumors

The prognosis for lacrimal gland lymphoma depends on multiple factors: systemic dissemination is more likely in patients with orbital or lacrimal gland involvement as well as patients with prior systemic disease [3]. Where ophthalmic symptoms have been present for more than a year, systemic dissemination is less likely [3]. Histologic classification of infiltrating cells is a further determinant for morbidity, the 5-year mortality rate varying from 12% for marginal zone lymphoma to 53% for diffuse large B cell lymphoma [35].

Genomics

Genetic anomalies have been demonstrated in many patients with adenoid cystic carcinoma of lacrimal gland, including mutations in the *KRAS*, *NRAS*, *MET*, *NOTCH1*, and *NOTCH2* oncogenes [36–39]. Recent investigations have also shown adenoid cystic carcinoma in this and other sites to have a fusion oncogene between MYB and NFIB, with a translocation between chromosome 6q22-23 and chromosome 9p23-24 [39–41]. This fusion oncogene possibly leads to an overexpression of MYB target proteins – these being associated with modulation of cellular apoptosis, cell cycle control, cell growth and adhesion, and angiogenesis – and future therapeutic options could be aimed at altering these responses.

Conclusion

High-resolution CT scanning has improved the ability to differentiate between pleomorphic adenoma and other lacrimal gland masses, but the prognosis for lacrimal gland carcinoma remains poor, despite advances in diagnosis and treatment of other malignancies. If malignancy is suspected in the lacrimal gland, it is important not to move the bone (osteotomies, etc.), as lacrimal gland cancers have a propensity to spread through the weakness thereby created. Orbital irradiation after debulking of lacrimal malignancies seems to give the best disease-free interval, while combined intra-arterial and intravenous chemotherapy might improve the outcome for some of these tumors. Cranio-orbital resection does not appear to prolong life, probably because of the propensity of adenoid cystic carcinoma for perineural spread or micrometastasis.

References

1. Shields JA, Shields CL, Epstein JA, et al. Primary epithelial malignancies of the lacrimal gland: the 2003 Ramon L. Font Lecture. Ophthalmic Plast Reconstr J. 2004;20:10–21.
2. Shields JA, Shields CL, Scartozzi R. Survey of 1264 patients with orbital tumors and simulating lesions: the 2002 Montgomery Lecture, part 1. Ophthalmology. 2004;111:997–1008.
3. Jenkins C, Rose GE, Bunce C, et al. Clinical features associated with survival of patients with lymphoma of the ocular adnexa. Eye. 2003;17:809–20.
4. Rose GE, Wright JE. Pleomorphic adenoma of the lacrimal gland. Br J Ophthalmol. 1992;76:395–400.
5. Wright JE, Rose GE, Garner A. Primary malignant neoplasms of the lacrimal gland. Br J Ophthalmol. 1992;76:401–7.
6. Rootman J, White V, Hind A. Tumors of the lacrimal gland. In: Rootman J, editor. Disease of the orbit. A multidisciplinary approach. 2nd ed. Philadelphia: Lippincott Williams & Wilkins; 2003.
7. Cates CA, Manners RM, Rose GE. Pleomorphic adenoma of the lacrimal gland in a 10 year old girl. Br J Ophthalmol. 2002;86:249–50.
8. Vangveeravong S, Katz SE, Rootman J, White V. Tumors arising in the palpebral lobe of the lacrimal gland. Ophthalmology. 1996;103:1606–12.
9. Lorenzano D, Rose GE. The "wedge sign": an imaging sign for aggressive lacrimal gland disease. Ophthalmology. 2017;124:1081–3.
10. Aviv RI, Miszkiel K. Orbital imaging: part 2. Intraorbital pathology. Clin Radiol. 2005;60:288–307.
11. Rose GE. To crash or not to crash? Probability in the management of benign lacrimal gland tumours. Eye. 2009;23:1625–8.
12. Prabhakaran VC, Cannon PS, McNab A, et al. Lesions mimicking lacrimal gland pleomorphic adenoma. Br J Ophthalmol. 2010;94:1509–12.
13. Kopp ED, Sahlin S, Tani E, et al. Fine- needle aspiration biopsy in lacrimal gland pleomorphic adenoma. Eye. 2010;24:386–9.

14. Perzin KH, Jakobiec FA, Livolsi VA, et al. Lacrimal gland malignant mixed tumors (carcinomas arising in benign mixed tumors): a clinico-pathologic study. Cancer. 1980;45:2593–606.
15. Kim YJ, Kim YS, Chin S, et al. Cytoplasmic and nuclear leptin expression in lacrimal gland tumours: a pilot study. Br J Ophthalmol. 2015;99:1306–10.
16. Currie ZI, Rose GE. Long-term risk of recurrence after intact excision of pleomorphic adenomas of the lacrimal gland. Arch Ophthalmol. 2007;125:1643–6.
17. Ni C, Kuo PK, Dryja TP. Histopathological classification of 272 primary epithelial tumors of the lacrimal gland. Chin Med J. 1992;105:481–5.
18. Rose GE, Wright JE. Exenteration for benign orbital disease. Br J Ophthalmol. 1994;78:14–8.
19. Polito E, Leccisotti A. Epithelial malignancies of the lacrimal gland: survival rates after extensive and conservative therapy. Ann Ophthalmol. 1993;25:422–6.
20. Ahmad SM, Esmaeli B, Williams M, et al. American Joint Committee on Cancer classification predicts outcome of patients with lacrimal gland adenoid cystic carcinoma. Ophthalmology. 2009;116:1210–5.
21. Skinner HD, Garden AS, Rosenthal DI, et al. Outcomes of malignant tumors of the lacrimal apparatus. Cancer. 2011;117:2801–10.
22. Esmaeli B, Yin V, Hanna E, et al. Eye-sparing multidisciplinary approach for the management of lacrimal gland carcinoma. Head Neck. 2014;38:1258–62.
23. Woo KI, Kim YD, Sa HS, et al. Current treatment of lacrimal gland carcinoma. Curr Opin Ophthalmol. 2016;27:449–56.
24. Han J, Kim YD, Woo KI, et al. Long-term outcomes of eye-sparing surgery for adenoid cystic carcinoma of lacrimal gland. Ophthal Plast Reconstr Surg. 2018;34:74–8.
25. Woo KI, Sagiv O, Han J, et al. Eye-preserving surgery followed by adjuvant radiotherapy for lacrimal gland carcinoma: outcomes in 37 patients. Ophthal Plast Reconstr Surg. 2018;34(6):570–4.
26. Gore SK, Plowman NP, Dharmasena A, et al. Corneal complications after orbital radiotherapy for primary epithelial malignancies of the lacrimal gland. Br J Ophthalmol. 2018;102(7):882–4.
27. Meldrum ML, Tse DT, Benedetto P. Neoadjuvant intracarotid chemotherapy for treatment of advanced adenocystic carcinoma of the lacrimal gland. Arch Ophthalmol. 1998;116:315–21.
28. Tse DT, Benedetto P, Dubovy S, et al. Clinical analysis of the effect of intraarterial cytoreductive chemotherapy in the treatment of lacrimal gland adenoid cystic carcinoma. Am J Ophthalmol. 2006;141:44–53.
29. Tse DT, Kossler AL, Feuer WJ, et al. Long-term outcomes of neoadjuvant intraarterial cytoreductive chemotherapy for lacrimal gland adenoid cystic carcinoma. Ophthalmology. 2013;120:1313–23.
30. Le Tourneau C, Razak ARA, Levy C, et al. Role of chemotherapy and molecularly targeted agents in the treatment of adenoid cystic carcinoma of the lacrimal gland. Br J Ophthalmol. 2011;95:1483–9.
31. Esmaeli B, Ahmadi MA, Youssef A, et al. Outcomes in patients with adenoid cystic carcinoma of the lacrimal gland. Ophthal Plast Reconstr Surg. 2004;20:22–6.
32. Heaps RS, Miller NR, Albert DM, et al. Primary adenocarcinoma of the lacrimal gland. A retrospective study. Ophthalmology. 1993;100:1856–60.
33. Font RL, Gamel JW. Epithelial tumors of the lacrimal gland: an analysis of 265 cases. In: Jakobiec FA, editor. Ocular and adnexal tumors. Birmingham: Aesculapius; 1978. p. 787–805.
34. El-Sawy T, Savar A, Williams MD, et al. Prognostic accuracy of the seventh edition vs sixth edition of the American Joint Committee on cancer tumor classification for adenoid cystic carcinoma of the lacrimal gland. Arch Ophthalmol. 2012;130:664–6.
35. Jenkins C, Rose GE, Bunce C, et al. Histological features of ocular adnexal lymphoma (REAL classification) and their association with patient morbidity and survival. Br J Ophthalmol. 2000;84:907–13.
36. Tse D. Clinical and microdissection genotyping analyses of the effect of intra-arterial cytoreductive chemotherapy in the treatment of lacrimal gland adenoid cystic carcinoma. Trans Am Ophthalmol Soc. 2005;103:337–67.
37. Bell D, Sniegowski MC, Wani K, et al. Mutational landscape of lacrimal gland carcinomas and implications for treatment. Head Neck. 2016;38:E724–9.
38. Sant DW, Tao W, Field MG, et al. Whole exome sequencing of lacrimal gland adenoid cystic carcinoma. Invest Ophthalmol Vis Sci. 2017;58:BIO240–6.
39. von Holstein SL, Fehr A, Persson M, et al. Adenoid cystic carcinoma of the lacrimal gland: MYB gene activation, genomic imbalances, and clinical characteristics. Ophthalmology. 2013;120:2130–8.
40. Chen TY, Keeney MG, Chintakuntlawar AV, et al. Adenoid cystic carcinoma of the lacrimal gland is frequently characterized by MYB rearrangement. Eye (Lond). 2017;31:720–5.
41. Persson M, Andren Y, Mark J, et al. Recurrent fusion of MYB and NFIB transcription factor genes in carcinomas of the breast and head and neck. Proc Natl Acad Sci. 2009;106:18740–4.

Lacrimal Sac Tumors

14

Jacob Pe'er and Bhupendra C. K. Patel

Introduction

Tumors of the lacrimal drainage system, especially the lacrimal sac, are rare; since the first publications reporting such tumors by Spratt, Duke-Elder, Radnot and Gall, and others [1–7], only about 800 cases have been reported in the medical literature in the last 120 years. Despite their rarity, physicians should be aware of the clinical features of lacrimal sac tumors, as many are life-threatening and early diagnosis and appropriate treatment can save lives. These tumors often masquerade as a chronic inflammatory process. Due to the rarity of lacrimal sac tumors, large clinical studies with statistically meaningful data are unavailable, and we learn about the biological behavior, management, and prognosis of these tumors only from case series and case reports.

J. Pe'er (✉)
Department of Ophthalmology, Hadassah-Hebrew University Medical Center, Jerusalem, Israel
e-mail: peer@hadassad.org.il

B. C. K. Patel
Division of Facial Cosmetic and Reconstructive Surgery, University of Utah, Salt Lake City, UT, USA

C. J. Hwang et al. (eds.), *Clinical Ophthalmic Oncology*,
https://doi.org/10.1007/978-3-030-13558-4_14

Clinical Features

Lacrimal sac tumors are usually diagnosed in adults, with the average age in the 50s, with benign tumors appearing about a decade earlier than malignant tumors [1–9]. Tumors in the lacrimal sac have also been reported in children and infants [9–11]. Although a series from China reported that men are more commonly affected [8, 12], most series show no significant gender difference in the incidence of lacrimal sac tumors [1–7, 9, 13]. Various series report malignancy in 50–95% of lacrimal sac tumors and an epithelial origin in about three-quarters of tumors [1–9, 12, 13].

Most lacrimal sac tumors present with symptoms of dacryostenosis and/or dacryocystitis due to obstruction or partial obstruction of the drainage [8, 9, 14]. Thus, most patients complain of epiphora as well as redness, swelling, and purulent discharge [15]. Due to the similarity of symptoms, lacrimal sac tumors are often found inadvertently at the time of dacryocystorhinostomy (DCR) for presumed dacryostenosis [16]. This is the reason that it has been suggested by some authors that DCR specimens should always be submitted for pathologic evaluation [17, 18].

The main sign of lacrimal sac tumors is the development of a mass in the area of the lacrimal sac (Fig. 14.1); the appearance of a mass above the medial canthal tendon level is most typical. In benign tumors the typical mass grows slowly and is elastic in consistency, with distinct margins,

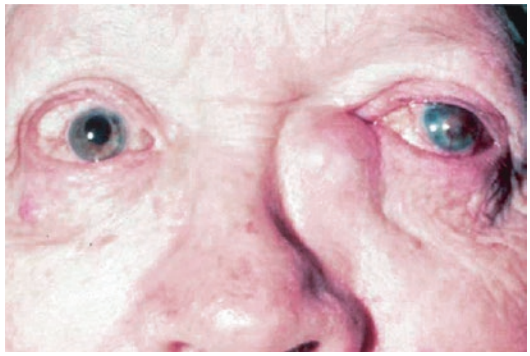

Fig. 14.1 A man with a transitional cell carcinoma of the lacrimal sac of the left eye presenting with a mass that reaches a level above the medial canthal tendon. (Courtesy of Dr. Mary A. Stefanyszyn)

Fig. 14.2 A CT scan shows a mass over the left lacrimal sac area. (Courtesy of Dr. Mary A. Stefanyszyn)

and is freely movable under the skin. On the other hand, most malignant tumors grow faster, and the mass is firm, noncompressible, and fixed to the underlying tissue. Fistulous tracts can develop. Bleeding from the puncta, either spontaneously or on applying pressure to the lacrimal sac, epistaxis, or dark bloody nasal discharge, may occur in some patients, especially those with epithelial tumors [9]. Some patients with a malignant tumor complain of pain [7].

In advanced cases of malignancy, ulceration over the mass can be seen and involvement of the preauricular, submandibular, and cervical lymph nodes can be diagnosed. In some cases, regional lymph node involvement appears before discovery of the primary tumor. When a tumor grows significantly to involve the orbit, proptosis and limitation of ocular motility may develop. Local invasion of the face, nose, ethmoid and maxillary sinuses, and palate, as well as intracranial extension, can occur [2].

Diagnostic Evaluation

In one series of 377 DCR specimens [15], lacrimal sac neoplasms resulting in chronic lacrimal drainage obstruction occurred in 4.6% of cases; in 2.1% they were not suspected before surgery. Therefore, in every case of a mass in the lacrimal sac area that causes obstruction, lacrimal sac tumor should be suspected. Inflammatory response in this area does not rule out the diagnosis of a tumor. In such patients, history of blood-stained tears or epistaxis should increase the suspicion.

Imaging studies are important in evaluation of lacrimal sac tumors [2, 3, 8, 9, 19]. CT scan shows a solid mass over the lacrimal sac area and may display expansion of the lacrimal fossa and/or bony erosion or destruction of the lacrimal fossa and, in advanced cases, invasion into neighboring structures (Fig. 14.2). Dacryocystography may reveal a filling defect of the sac lumen or a distended sac with uneven or mottled contrast media or delay in draining of the contrast material (Fig. 14.3). In cases of benign tumor or early stages of tumor, the lacrimal drainage system may be patent, such that negative results do not rule out a tumor. Ultrasound of the lacrimal sac area can also be used, and some experts have found magnetic resonance imaging (MRI) to be superior to computed tomography for imaging of the lacrimal sac, as MRI provides better tumor definition and determination of the cystic or solid nature of the mass [11].

Since most patients with lacrimal sac tumors present with symptoms and signs of dacryocystitis, the main differential diagnosis includes acute or chronic dacryocystitis. Inflammatory disorders of the lacrimal sac, such as granulomas or granulation tissue, or infectious processes due to tuberculosis or fungus, should also be included in the differential diagnosis.

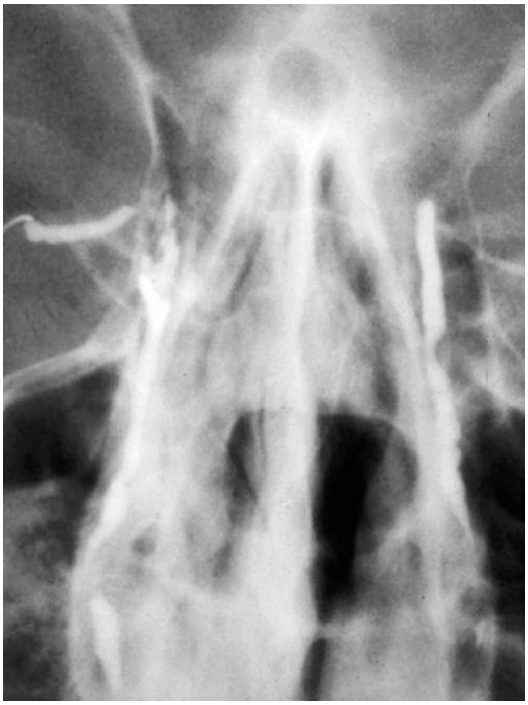

Fig. 14.3 Dacryocystogram reveals a mottled defect in the right lacrimal sac as compared to the smooth outline of the left lacrimal sac. (Courtesy of Dr. Mary A. Stefanyszyn)

Table 14.1 Histopathological classification of epithelial tumors of the lacrimal sac

Benign
Papilloma
Squamous papilloma
Transitional cell papilloma
Mixed-cell papilloma Schneiderian papilloma
Papilloma unspecified
Oncocytoma
Pleomorphic adenoma (mixed tumor)
Mucocele
Cysts
Cylindroma
Malignant
Papilloma with carcinoma
Carcinoma
Squamous cell carcinoma
Transitional cell carcinoma
Mixed squamous/transitional carcinoma
Oncocytic adenocarcinoma
Mucoepidermoid carcinoma
Adenoid cystic carcinoma
Adenocarcinoma
Adenocarcinoma ex pleomorphic adenoma
Eccrine adenocarcinoma Basal cell carcinoma
Undifferentiated carcinoma
Secondary tumors

The final diagnosis can be ascertained only by histopathological examination, for which excisional biopsy is preferred. If the entire tumor cannot be removed, deep incisional biopsy is essential since the tumor periphery may show only inflammatory response, leading to misdiagnosis. When a patient with suspected lacrimal sac tumor has involvement of the nasal cavity, biopsy via the nasal route is possible.

Histopathological Classification

Lacrimal sac tumors are divided into two major groups: epithelial tumors, which constitute the majority of the lacrimal sac tumors, accounting for about 75% of all reported cases, and non-epithelial tumors, which account for the remaining 25% [8, 9, 17, 20–22]. All types of reported lacrimal sac tumors, common and rare, are listed in Tables 14.1 and 14.2.

Often it is difficult to establish whether a tumor arises primarily in the lacrimal sac, rather than from other parts of the nasolacrimal system, nose, paranasal sinuses, cutaneous adnexa, conjunctiva, or caruncle, with subsequent spread to the sac [7]. The lacrimal sac tumors, epithelial and non-epithelial, reported in the literature are believed to arise primarily in the lacrimal sac.

The lacrimal drainage system is composed of the canaliculus, which is lined by nonkeratinized stratified squamous epithelium, and the lacrimal sac and nasolacrimal duct, which are lined by stratified columnar (transitional) epithelium. The transitional epithelium contains mucous glands and is histologically similar to the epithelium lining the nasal passages and paranasal sinuses.

The origin of most benign and malignant epithelial tumors is in the epithelial lining of the lacrimal sac and therefore can be either squamous or transitional type [5, 7, 9]. The papilloma may exhibit an exophytic growth pattern, growing

Table 14.2 Histopathological classification of non-epithelial tumors of the lacrimal sac

Mesenchymal—fibrous tissue tumors
Benign
Fibrous histiocytoma
Lipoma
Juvenile xanthogranuloma
Malignant
Malignant fibrous histiocytoma
Mesenchymal—vascular tumors
Benign
Hemangiopericytoma
Cavernous hemangioma
Capillary hemangioma
Angiofibroma
Hemangioendothelioma
Glomus tumor
Solitary fibrous tumor
Malignant
Kaposi's sarcoma
Rhabdomyosarcoma
Melanocytic tumors
Benign
Nevi
Malignant
Melanoma primary of lacrimal sac
Melanoma: seeding from conjunctival melanoma
Lymphoproliferative tumors
Benign reactive lymphoid hyperplasia
Lymphoma
Leukemic infiltrate (granulocytic sarcoma)
Plasmacytoma
Neural tumors
Neurofibroma
Neurilemmoma (schwannoma)
Inflammatory pseudotumors
Secondary tumors
Nose, paranasal sinuses, orbit, conjunctiva, skin
Metastases
Melanoma, hepatocellular carcinoma, renal cell carcinoma

toward the sac lumen, or an inverted pattern, growing toward the stroma. The latter tends, more than the former, to be more invasive, to recur, and sometimes to undergo malignant change. Some of the papillomas may show foci of carcinoma, evidence that they may be the source for the development of carcinomas. Marked inflammation is often seen in the stroma of the papillomas. Human papilloma viruses (HPV) type 6 or 11 have been found in lacrimal sac papillomas and carcinomas [23, 24].

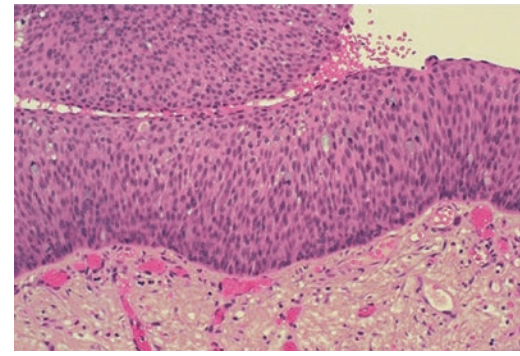

Fig. 14.4 Histological picture of transitional cell carcinoma of the lacrimal sac, showing cylindrical epithelial cells. Some goblet cells are seen among the epithelial cells (hematoxylin and eosin, original magnification ×40). (Courtesy of Dr. Mary A. Stefanyszyn)

Squamous cell carcinomas may range from well-differentiated tumors with keratin pearls and intercellular bridges to poorly differentiated tumors. Transitional cell carcinoma may show a papillary pattern and be composed of cylindrical epithelial cells (Fig. 14.4). Goblet cells may be seen. Both types of carcinomas invade the lacrimal sac wall and produce a hard mass.

Most other epithelial tumors of the lacrimal sac, benign and malignant, are of glandular origin and are similar to those found in glands such as the lacrimal and salivary glands. The most common benign tumors in this group are the oncocytoma and pleomorphic adenoma and, among the malignant tumors, oncocytic adenocarcinoma and adenoid cystic carcinoma. Epithelial tumors with a basal cell component were also reported [25]. The existing mixed glands with serous and mucous cells in the lacrimal sac as well as in the nasolacrimal duct wall are the origin of these tumors [20].

Non-epithelial tumors of the lacrimal sac constitute about one-quarter of the lacrimal sac tumors; of these, about half are mesenchymal tumors, one-quarter melanomas, and one-quarter lymphoproliferative tumors. Only a few neural tumors were reported [21]. The mesenchymal tumors appear at a relatively young age, compared to other groups of lacrimal sac tumors.

In the recent literature, fibrous histiocytoma is the most common mesenchymal tumor of the

lacrimal sac, but it does not appear in the earlier literature, probably because it was recognized only in the past 40 years. These tumors are composed of cells resembling fibroblasts and histiocytes and contain xanthomatous cells and multinucleated giant cells. Most fibrous histiocytomas that were described in the lacrimal sac are benign, and some are locally aggressive. No malignant fibrous histiocytomas of the lacrimal sac were reported.

Among the very rare vascular tumors of the lacrimal sac, the most commonly reported is hemangiopericytoma, which shows a vascular pattern of sinusoidal spaces, among which are solid areas of spindle-shaped cells. Even benign-appearing lesions have the potential to metastasize. Other types of hemangiomas are reported as individual cases and include capillary hemangioma, cavernous hemangioma, angiofibroma, hemangioendothelioma, and Kaposi's sarcoma.

It is difficult to classify the lymphoproliferative tumors of the lacrimal sac reported in the literature, due to their rarity and frequent classification system changes. In recent publications it appears that most lymphomas in this region are of the non-Hodgkin's B-cell type [10, 11, 14] (Table 14.3). The common types are diffuse large B-cell lymphoma (DLBCL) and MALT lymphoma [26]. Leukemic infiltrates in the lacrimal drainage system are probably more frequent than reported [10, 27]. Multiple myeloma of the lacrimal sac may also occur.

Table 14.3 Primary lacrimal sac lymphoma

Diffuse large B-cell lymphoma (non-Hodgkin's lymphoma) 33%
Extranodal marginal zone B-cell lymphoma (mucosa-associated lymphoid tissue, MALT lymphoma 53%)
"Transitional MALT lymphomas" 20%[a]
Unclassified B-cell lymphomas 13%

Reprinted from Sjö et al. [26]. With permission from BMJ Publishing Group Ltd.

[a]Classified as "transitional MALT lymphoma" as these tumors consisted of centrocyte-like cells admixed with a larger number of large B cells than found in a classic MALT lymphoma. The large cells were scattered among the centrocytes as single cells or, less frequently, as small clusters of up to ten cells, but sheets of large B cells were not present. These tumors were designated MALT lymphoma in transition, assuming that the presence of increased numbers of large cells reflected incipient transformation to DLBCL.

Melanoma of the lacrimal sac, like melanomas of other mucous membranes, has a poor prognosis and is probably the most malignant tumor of the lacrimal sac [21]. It originates in melanocytes in and under the epithelial lining of the lacrimal sac; most are composed of epithelioid melanoma cells.

Neural tumors of the lacrimal sac are extremely rare. They originate from adjacent neural elements and invade the lacrimal sac wall. The medical literature contains reports of two neurilemmomas and two neurofibromas.

Secondary tumors of the lacrimal sac may originate either from adjacent structures such as the nose, paranasal sinuses, orbit, conjunctiva, and skin or as metastases, although the latter are rarely confined to the lacrimal sac alone.

Treatment

The treatment of lacrimal sac tumors depends on the histological typing, malignancy, and the extent of its invasion through the lacrimal sac to adjacent tissue [2, 8–14, 28–30]. The treatment of choice is complete surgical removal of the tumor. When epithelial and mesenchymal tumors are confined to the lacrimal sac, dacryocystectomy is performed, and this usually suffices for benign tumors. Intact excision of the tumor with the periosteum of the fossa and supplemental external irradiation can be added if the tumor is malignant. Deep incisional biopsy, with or without frozen section, is performed when the mass is found, by imaging, to extend beyond the lacrimal fossa, or when lacrimal sac malignancy is clinically obvious. The definitive therapy is determined according to the histopathological diagnosis. In some cases, biopsy can be taken through nasal endoscopy.

Extension of tumors, mainly premalignant and malignant, down the nasolacrimal duct accounts for recurrences and failure of therapy; therefore, lateral rhinotomy, which offers a greater chance of cure, should be performed. More extensive surgical excision of the cana-

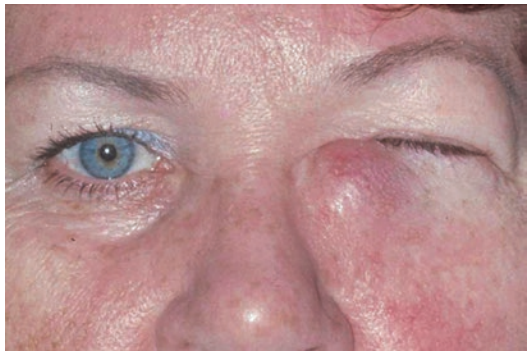

Fig. 14.5 A woman with squamous cell carcinoma of the left lacrimal sac presenting with irreducible hard mass and a history of chronic dacryocystitis. (Courtesy of Dr. Mary A. Stefanyszyn)

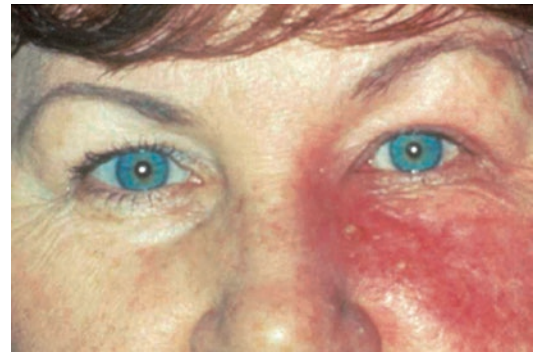

Fig. 14.6 The same woman of Fig. 14.5 following extensive surgical resection of the tumor and postoperative radiation, soon after the radiation. Tumor is not seen but redness, dryness, and scaling skin are evident. (Courtesy of Dr. Mary A. Stefanyszyn)

liculi and nasolacrimal duct, together with the sac, may be needed in certain cases. When the tumor extends beyond the lacrimal drainage system to adjacent tissue, more radical surgery is needed. This may include exenteration of the orbital tissue, paranasal sinus resection, and cervical lymph node dissection. A combined medial maxillectomy and medial orbitotomy for en bloc resection of the lacrimal sac tumor followed by reconstruction with a tailored contoured titanium mesh to support the globe and eyelid was reported to achieve optimal tumor clearance in the advanced cases [29]. Postoperative radiotherapy is recommended for malignant epithelial tumors, with a suggested tumor dose of approximately 60 Gy [28]. Orbital-sparing treatment approach that included proton therapy successfully achieved disease control [30]. Chemotherapy, either concurrent with radiation therapy, as neoadjuvant treatment, or for progressive or metastatic disease, is used as needed [28, 30]. Recurrent lesions may be treated with further surgery or radiotherapy (Figs. 14.5 and 14.6).

The primary treatment of lacrimal sac lymphoma, after incisional or excisional biopsy, consists of radiotherapy with or without chemotherapy, with a favorable response in most patients. Malignant melanoma of the lacrimal sac has a poor prognosis, and various treatments such as extensive surgical resection, radiotherapy, or chemotherapy may delay recurrence but usually do not improve survival.

Clinical Course

The outcome in cases of lacrimal sac tumor depends on the stage at the time of diagnosis, the histopathological features of the tumor including its growth pattern, and the appropriateness of treatment. Ni and his colleagues [8] offered four stages for the evolution of lacrimal sac tumors: Stage 1, in which there are symptoms and signs but no definite tumor mass is seen or palpable; Stage 2, in which obvious tumor formation is confined to the sac; Stage 3, in which the tumor extends beyond the lacrimal sac to adjacent structures such as the orbit or paranasal sinuses; and Stage 4, which is marked by evident metastases.

Malignant tumors of the lacrimal sac display three types of growth [8]: along the surface of the epithelium, protruding toward the lumen as papillary growth, and infiltrating the wall of the sac as solid cell nests. There are three main modes of tumor spread [8]: direct extension is the most common, to adjacent structures such as the orbit, nasolacrimal duct, paranasal sinuses, and the skull; lymphatic metastases mainly to the submandibular, preauricular, and cervical glands; and remote, most probably hematogenous spread—the most common site is to the lung.

Benign papillomas of the lacrimal sac often recur, especially those with an inverted pattern, which show recurrence rates of 10–40% [14]. Most of the papillomas that recur do not reveal malignant changes [7]. Low-grade carcinomas

have variable cure rates depending on the extent of the disease and the treatment. Recurrence rate of invasive squamous cell and transitional cell carcinoma appears to be about 50% with up to 50% of those being fatal, although some series reported a much better outcome.

Recurrence and mortality rates of non-epithelial lacrimal sac tumors vary [9, 14, 21]. Benign fibrous histiocytoma has a good prognosis if completely excised, while the malignant potential of hemangiopericytoma can be unpredictable. Lymphoid lesions respond to radiotherapy and chemotherapy and have variable prognosis depending on the extent of the disease and the type of the tumor. The most dismal prognosis is that of malignant melanoma, which is often fatal in a short period of time in spite of aggressive treatment.

Lacrimal sac tumors are often silent tumors: as preoperatively unsuspected lacrimal sac tumor may be found during routine DCR, some authors have argued for obtaining routine lacrimal sac biopsies during DCR surgeries. Many lacrimal surgeons do not subscribe to the view that routine lacrimal sac biopsies are necessary. Instead, they use certain criteria to indicate the need for obtaining biopsies. One such approach is presented in Table 14.4. This table also advocates good clinical practice when assessing patients with symptoms and signs of acquired nasolacrimal duct obstruction.

Table 14.4 Avoidance of surprises during dacryocystorhinostomy

Maintain a high level of suspicion
Examine the reflux from irrigation of the lacrimal system for blood or discoloration
Press on the lacrimal sac: beware of firm, incompressible, immobile masses
Press on the lacrimal sac: examine for any blood-stained or discolored discharge from the puncta
Beware of a mass above the medial canthal tendon: always biopsy these
Peroperatively, if the lacrimal sac look like anything other than an inflamed sac, obtain a biopsy
Perform a nasal examination looking for bloody discharge, ulceration, mass, or erosion
Beware of skin ulceration or telangiectasia
In the presence of a lacrimal sac mass, examine for regional lymphadenopathy
If in doubt about the appearance of the lacrimal sac, biopsy
In the presence of a DCR being performed on a patient with a history of lymphoma or leukemia, always biopsy

References

1. Spratt CN. Primary carcinoma of the lacrimal sac. Arch Ophthalmol. 1937;18:267–73.
2. Duke-Elder S. Diseases of the lacrimal passages—tumours and pseudo-tumours. In: Duke Elder S, editor. Textbook of ophthalmology, vol. 13, pt. II. St. Louis: CV Mosby; 1974. p. 735–59.
3. Jones IS. Tumors of the lacrimal sac. Am J Ophthalmol. 1956;42:561–6.
4. Radnot M, Gall J. Tumoren des Traensackes. Ophthalmologica. 1966;151:1–22.
5. Harry J, Ashton N. The pathology of tumours of the lacrimal sac. Trans Ophthalmol Soc UK. 1968;88:19–35.
6. Schenck NL, Ogura JH, Pratt LL. Cancer of the lacrimal sac. Ann Otol Rhinol Laryngol. 1973;82:153–61.
7. Ryan SJ, Font RL. Primary epithelial neoplasms of the lacrimal sac. Am J Ophthalmol. 1973;76:73–88.
8. Ni C, D'Amico DJ, Fan CQ, et al. Tumors of the lacrimal sac: a clinicopathological analysis of 82 cases. Int Ophthalmol Clin. 1982;22:121–40.
9. Stefanyszyn MA, Hidayat AA, Pe'er JJ, et al. Lacrimal sac tumors. Ophthal Plast Reconstr Surg. 1994;10:169–84.
10. Yip CC, Bartley GB, Habermann JM, et al. Involvement of the lacrimal drainage system by leukemia and lymphoma. Ophthal Plast Reconstr Surg. 2002;18:242–6.
11. Schefler AC, Shields CL, Shields JA, et al. Lacrimal sac lymphoma in a child. Arch Ophthalmol. 2003;121:1330–3.
12. Bi YW, Chen RJ, Li XP. Clinical and pathological analysis of primary lacrimal sac tumors. Zhonghua Yan Ke Za Zhi. 2007;43:499–504. article in Chinese
13. Kroll J, Busse H. Tumours of the lacrimal passages. Klin Monatsbl Augenheilkd. 2008;225:91–5.
14. Parmar D, Rose GE. Management of lacrimal sac tumours. Eye (Lond). 2003;17:599–606.
15. Bewes T, Sacks R, Sacks PL, et al. Incidence of neoplasia in patients with unilateral epiphora. J Laryngol Otol. 2015;129(Suppl 3):S53–7.
16. Tanweer F, Mahkamova K, Harkness P. Nasolacrimal duct tumours in the era of endoscopic dacryocystorhinostomy: literature review. Laryngol Otol. 2013;127:670–5.
17. Anderson NG, Wojno TH, Grossniklaus HE. Clinicopathologic findings from lacrimal sac biopsy specimens obtained during dacryocystorhinostomy. Ophthal Plast Reconstr Surg. 2003;19:173–6.
18. Koturović Z, Knežević M, Rašić DM. Clinical significance of routine lacrimal sac biopsy during dacryocystorhinostomy: A comprehensive review of literature. Bosn J Basic Med Sci. 2017;17:1–8.

19. Kumar VA, Esmaeli B, Ahmed S, et al. Imaging features of malignant lacrimal sac and nasolacrimal duct tumors. AJNR Am J Neuroradiol. 2016;. Epub ahead of print
20. Pe'er J, Hidayat AA, Ilsar M, et al. Glandular tumors of the lacrimal sac. Their histologic patterns and possible origins. Ophthalmology. 1996;103:1601–5.
21. Pe'er JJ, Stefanyszyn M, Hidayat AA. Nonepithelial tumors of the lacrimal sac. Am J Ophthalmol. 1994;118:650–8.
22. Campbell RJ, Sobin LH. Tumours of the lacrimal drainage system. In: Histological typing of tumours of the eye and its adnexa. 2nd ed. World Health Organization international histological classification of tumors. Berlin: Springer; 1998. p. 25–6.
23. Sjo NC, von Buchwald C, Cassonnet P, et al. Human papillomavirus: cause of epithelial lacrimal sac neoplasia? Acta Ophthalmol Scand. 2007;85:551–6.
24. Afrogheh AH, Jakobiec FA, Hammon R, et al. Evaluation for High-risk HPV in Squamous Cell Carcinomas and Precursor Lesions Arising in the Conjunctiva and Lacrimal Sac. Am J Surg Pathol. 2016;40:5519–28.
25. Katircioglu YA, Yildiz EH, Kocaoglu FA, et al. Basal cell carcinoma in lacrimal sac. Orbit. 2006;26:303–7.
26. Sjo LD, Ralfkiaer E, Jul BR, et al. Primary lymphoma of the lacrimal sac: an ORTC ophthalmic oncology task force study. Br J Ophthalmol. 2006;90:1004–9.
27. Krishna Y, Irion LD, Karim S, et al. Chronic Lymphocytic Leukaemia/ Small-Cell Lymphocytic Lymphoma of the Lacrimal Sac: A Case Series. Ocul Oncol Pathol. 2017;3:224–8.
28. El-Sawy T, Frank SJ, Hanna E, et al. Multidisciplinary management of lacrimal sac/nasolacrimal duct carcinomas. Opthal Plast Reconstr Surg. 2013;29:454–7.
29. Alabiad CR, Weed DT, Walker TJ, et al. En bloc resection of lacrimal sac tumors and simultaneous orbital reconstruction: surgical and functional outcomes. Opthal Plast Reconstr Surg. 2014;30:459–67.
30. Holliday EB, Esmaeli B, Pinckard J, et al. A Multidisciplinary Orbit-Sparing Treatment Approach That Includes Proton Therapy for Epithelial Tumors of the Orbit and Ocular Adnexa. Int J Radiat Oncol Biol Phys. 2016;95:344–52.

Orbital and Adnexal Lymphoma

15

Mary E. Aronow, Brian T. Hill, and Arun D. Singh

Introduction

Orbital and adnexal lymphoma (OAL) encompasses a broad spectrum of lymphomas that involve the orbit and adnexal structures including the eyelids, conjunctiva, lacrimal apparatus, and the extraocular muscles. Involvement may be unilateral or bilateral, limited to a single site, or overlapping multiple adnexal structures. Furthermore, disease can be localized to the ocular adnexal region, or it can affect regional, central, and peripheral lymph nodes, as well as distant, extranodal sites. Depending upon the lymphoma subtype and pattern of involvement, there are multiple focal and systemic therapies that will be discussed within the chapter. While there is potential for disease-related morbidity, the 10-year over disease-specific mortality is as low as 5–10% [1].

Epidemiological Aspects

OAL represents approximately 8% of all extranodal non-Hodgkin's lymphoma (NHL). This is a rare disease with an incidence of 0.2 per 100,000 [2]. Most clinical series have demonstrated a slight female predilection (60% of cases) [3, 4]. OAL can affect individuals from all ethnic backgrounds. In contrast, Caucasians account for the highest proportion of individuals with systemic lymphoma in the United States. The incidence of systemic lymphoma appears to be increasing, while corresponding trends for OAL do not exist due to the paucity of cases.

Of all ophthalmic neoplasms, OAL accounts for 6–8% of orbital and 10–15% of adnexal tumors [5, 6]. Localized, ocular-only disease is present at diagnosis in 60–80% of cases, while the remainder have evidence of systemic involvement at the time of ophthalmic presentation. Bilateral involvement is observed in 10–15% of individuals with ocular-only lymphoma [7]. Among affected ocular sites, the frequency of involvement is as follows: conjunctiva 20–33%, orbit/lacrimal gland 46–74%, and eyelid 5–20% [1, 8]. In some cases, distinction between sites can be difficult to determine; therefore involvement of overlapping sites may be underreported.

M. E. Aronow (✉)
Retina Service, Massachusetts Eye and Ear, Harvard Medical School, Boston, MA, USA
e-mail: mary_aronow@meei.harvard.edu

B. T. Hill
Hematology and Medical Oncology, Taussig Cancer Center, Cleveland Clinic, Cleveland, OH, USA

A. D. Singh
Department of Ophthalmic Oncology, Cole Eye Institute, Cleveland Clinic, Cleveland, OH, USA

C. J. Hwang et al. (eds.), *Clinical Ophthalmic Oncology*,
https://doi.org/10.1007/978-3-030-13558-4_15

Etiology and Pathogenesis: B-cell Biology and Lymphomagenesis

Lymphoma arises from germinal centers (follicular lymphoma), the mantle zone (mantle cell lymphoma), or memory B cells (extranodal marginal zone lymphoma). Each lymphoma subtype demonstrates a unique immunophenotypic expression profile (Table 15.1). During normal lymphocyte maturation, errors may occur in which an antigen-receptor-gene region is juxtaposed to an oncogene region, resulting in dysregulation of the oncogenic region. Less often, a novel oncogenic protein is formed by fusion of two other genes. Chromosomal translocations underlying these alterations are well-described in as many as 90% of systemic lymphoma [9]. Limited data suggests that such translocations are less common in OAL [10].

The infection/inflammation/mutation (IMM) model of lymphomagenesis refers to the theory that lymphoma develops due to errors in normal lymphocyte response to infection or inflammation. This has been corroborated by the recognized association between lymphoma and infection as well as autoimmune disease. A classic example is the known association between gastric extranodal marginal zone lymphoma (EMZL) of mucosal-associated lymphoid tissue (MALT) which develops in response to chronic *H. pylori* infection. For OAL, studies have demonstrated the presence of DNA from both *C. psittaci* and *H. pylori* in lymphoma tissue samples [11, 12]. While infectious agents are implicated in etiology, there is wide variation of this association between geographic regions as well as within different series in the same geographic location [11]. This has important implications for therapy, where antibiotics may be minimally effective in regions where infection plays a small role in lymphomagenesis [13].

Classification

OAL represents the malignant end of the spectrum of ocular adnexal lymphoproliferative disorders. Reactive lymphoid hyperplasia (RLH) represents the benign end of the spectrum of lymphoproliferative disorders. With advances in molecular diagnosis, the vast majority of RLH have been reclassified as low-grade malignant lymphoma. OAL is a localized form of lymphoma which has been integrated into the schema of lymphoproliferative diseases described in two major classification systems, the Revised European American Lymphoma classification [14] and the World Health Organization (WHO) Classification of Tumors of Hematopoietic and Lymphoid Tissue [15].

OAL can be divided by the type and site(s) of tissue involvement. The vast majority of OAL are of the non-Hodgkin's B-cell type. Despite the multitude of systemic lymphoma subtypes, most OAL belong to one of five subtypes: EMZL (or MALT lymphoma), follicular lymphoma, (FL), diffuse large B-cell lymphoma (DLBCL), mantle cell lymphoma (MCL), and lymphoplasmacytic lymphoma (LPL) (Table 15.2) [16]. Most OAL, approximately 75%, are of the EMZL/MALT subtype [17]. OAL is termed solitary if limited to the ocular adnexa, secondary when contiguous

Table 15.1 Immunophenotypic expression of OAL

Type	Precursor cell	CD3	CD5	CD10	CD20	CD23	CD43	CD79	Bcl-2	Bcl-6	Cyclin D1
EMZL	Memory B cell	–	–	–	+	–	+	+	–	–	–
FL	Centrocyte	–	–	+	+	±	–		+	+	–
MCL	Mantle cell	–	+	–	+				–		+
LPL	Memory B cell	–	+	–	+	+					
DLBCL	Centroblast	–	–	+	+			+			

EMZL extranodal marginal zone lymphoma, *FL* follicular lymphoma, *MCL* mantle cell lymphoma, *LPL* lymphoplasmacytic lymphoma, *DLBCL* diffuse large B-cell lymphoma

Table 15.2 Distribution of various types of OAL

Author	Year	Patients	EMZL (%)	FL (%)	MCL (%)	LPL (%)	DLBC (%)	Plasmacytoma (%)	T cell (%)
Nakata	1999	44	77	–	4	2	14	–	–
Jenkins	2000	192	54	11	2	24	8	–	<1
Stafford	2001	48	60	–	–	–	4	–	–
McKelvie	2001	70	63	17	3	–	11	–	1
Mannami	2001	43	86	–	2	–	12	–	–
Bhatia	2001	47	17	53	–	–	26	–	–
Coupland	2003	230	59	12	3	4	13	4	3
Fung	2003	98	57	18	4		7	–	–
Sharara	2003	17	47	12	18	6	18	–	–
Cho	2003	57	98		2			–	–
Sullivan	2005	69	35	22	1	4	7	3	6
Rosado	2006	62	89	–	–	–	<1	–	–
Ferry	2007	353	52	23	5	1	8	–	<1
Oh	2007	128	75	–	3	1	5	1	4
Yun	2007	69	87	–	–	–	–	3	–
Hatef	2007	43	44	21	1	–	21	–	<1
Rootman	2011	122	60	12	1	4	4	–	–
Watkins	2011	57	28	2	5	–	4	4	5
Zanni	2012	41	63	10	5	5	17	–	–
Parikh	2015	79	75	25	–	–	–	–	
Woolf	2015	81	88	6	–	–	–	–	1
Konig	2016	52	52	14	–	–	–	–	–
Total		2002	17–98	2–53	1–18	1–24	1–26	1–4	1–6

EMZL extranodal marginal zone lymphoma, *FL* follicular lymphoma, *MCL* mantle cell lymphoma, *LPL* lymphoplasmacytic lymphoma, *DLBCL* diffuse large B-cell lymphoma

sites are involved, and systemic if remote involvement is present. OAL is solitary in 60–80% of cases at presentation [18, 19].

Clinical Features

Symptoms

Subjective complaints in OAL are broad and may include a visible mass, exophthalmos, pain, pressure, tearing, or diplopia. If the lacrimal gland is involved, dry eye symptoms may occur. Many lesions are asymptomatic.

Fig. 15.1 Conjunctival lymphoma with typical salmon patch appearance

Signs

OAL have site-specific presentations which affect diagnosis. In the conjunctiva, lesions are characteristically a salmon-pink color (Fig. 15.1). Clinical appearance does not allow distinction of benign from malignant lymphoproliferative disease. In the orbit, lacrimal gland, and eyelid, the disease often presents as a mass. If palpable, these masses are typically firm.

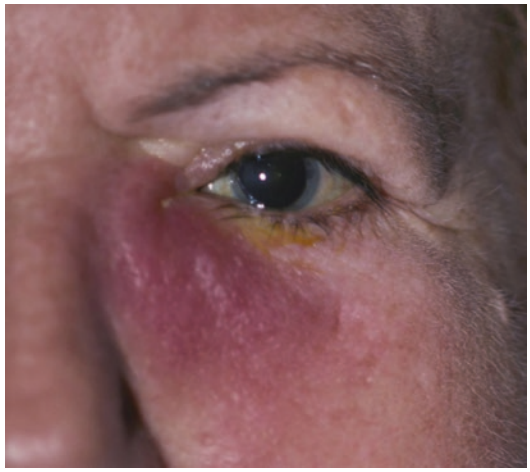

Fig. 15.2 Clinical appearance of lymphoma involving the nasolacrimal sac

Mobility is variable depending upon attachment to other structures. Diplopia may occur depending upon size and timeframe over which the mass develops. Exophthalmos and decreased retropulsion of the globe may be the only clinical signs. Secondary ptosis can also occur. Orbital lymphoma when visualized at the time of biopsy appears as a whitish pink mass reflecting its leukocytic and vascular characteristics. Involvement of the nasolacrimal drainage system can result in epiphora (Fig. 15.2). Compression or invasion of the optic nerve can lead to neuropathy and vision loss.

Diagnostic Evaluation

Evaluation of OAL involves characterization of the lesion and staging. Biopsy should ideally be obtained by open methods (incisional or excisional biopsy, rather than fine-needle aspiration biopsy) to allow sufficient material for multiple special studies: histopathology, lymphocyte immunophenotypical analysis, and molecular genetics studies to identify gene rearrangements indicative of clonality and/or translocations.

While there is variability in biopsy technique, several general principles apply. If lymphoma is suspected, specimens should be sent fresh and kept moist. Wrapping tissue in gauze soaked in saline is preferable to immersing samples in saline (tissue should not be left to dry or immersed in a fixative). When sending fresh samples, it is advisable to communicate with the pathology team ahead of time and to deliver samples from the operating room within 60 minutes of collection. Samples should be obtained with as minimal trauma as possible, being careful not to induce crush artifact. Cautery should be used sparingly and preferably after an adequately sized biopsy has been obtained. Specimens should be oriented and labeled with the site and exact location in order to facilitate the pathologist in their analysis. It is also helpful to provide the pathologist with a brief patient history as well as any relevant prior biopsy reports.

Local Imaging Studies

Imaging studies of the orbit play an important role in OAL but are performed at different times depending on the presentation. With conjunctival disease, the lesion is frequently biopsied first, and imaging of the orbit follows to assess for the possibility of orbital involvement. For orbital and eyelid disease, the orbit is usually imaged up front to optimize the biopsy approach. Contrast enhanced CT and MRI of the orbits will show enhancing lesions which can be discrete or diffuse (Figs. 15.3 and 15.4). Lymphoid lesions typically mold to structures such as the globe or bony orbit. Neuroimaging will reveal occult orbital involvement in up to 50% of clinically unsuspected cases [20]. Paranasal sinus involvement is not uncommon.

It is important to emphasize the relatively high rate of overlap that occurs between OAL and uveal lymphoma [21, 22]. Dilated fundus examination and ancillary imaging studies such as B-scan ultrasonography and angiography are useful for characterizing disease extent and laterality. This is particularly important in cases with subtle extra-scleral extension (ESE) or occult involvement of the fellow eye. B-scan ultrasonography is a sensitive modality for detecting ESE. The pattern of ESE may be crescentic thickening, a discrete mass (often adja-

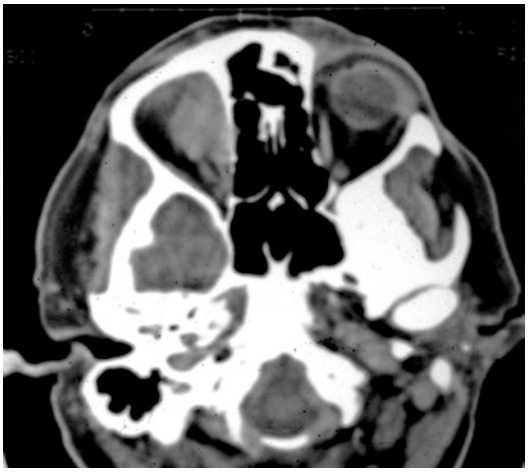

Fig. 15.3 Axial CT scan of patient in Fig. 15.2, showing superior orbital mass molding to the orbital wall

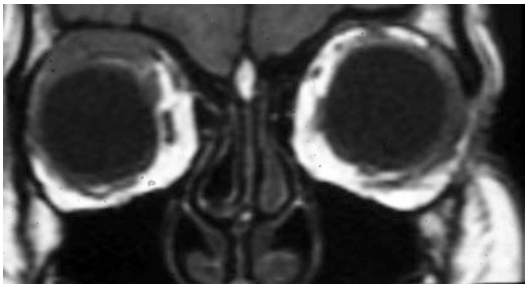

Fig. 15.4 Coronal MRI scan (T1-weighted image) demonstrating bilateral orbital involvement

cent to the optic nerve), or diffuse choroidal thickening. Fluorescein (FA) and indocyanine green angiography (ICG) are useful in suspected cases of uveal involvement. ICG demonstrates a characteristic pattern of focal hypocyanescence corresponding to clinically observed choroidal infiltrates. These foci may represent regions of choroidal non-perfusion secondary to space-occupying choroidal infiltration by lymphoma cells. ICG is superior to FA in visualizing the choroidal circulation and is therefore preferred for confirming the diagnosis and extent of disease burden [23]. When performed, FA may show early hyperfluorescence, hypofluorescent spots corresponding clinically observed choroidal infiltrates, choroidal folds, or a normal angiogram.

Staging Procedures

OAL can occur in the setting of systemic lymphoma; therefore when the disease presents at an ocular site, initial staging is performed. This includes a thorough physical examination, ideally performed by a medical oncologist with expertise in lymphoproliferative disorders. Invasive staging has been replaced by the use of high-resolution contrast-enhanced imaging techniques: CT of the chest, abdomen, and pelvis (or full-body positron-emission tomography) and MRI of the brain and orbits. Imaging of the neck is performed if cervical nodes are palpated or suspected to be enlarged. Laboratory evaluation includes complete blood count (CBC), hepatic enzymes, and serum lactate dehydrogenase (LDH). Although part of the formal staging process for systemic lymphoma, bone marrow aspiration and biopsy may have low yield in OAL in the absence of cytopenia or radiographic evidence of systemic disease.

An understanding of the staging process is important for multidisciplinary management of OAL. While newer staging systems exist, a modified version of the Ann Arbor system continues to be used in some centers. Lymphoma types are divided into low-grade or high-grade based on their expected clinical behavior. Low-grade (indolent) lymphoma (EMZL, FL, LPL) are divided into two stages, while high-grade lymphoma (DLBCL, MZL) is divided into three stages (Table 15.3). The Ann Arbor staging system has several deficiencies for characterizing OAL, particularly, as it results in a disproportionate staging distribution. Two-thirds of primary OAL present as a localized mass, which are classified as stage 1E [3, 7, 19]. Overall rates for initial staging are 60–80% for IE, 4–25% for IIE, and 16–18% for Stages III and IV combined [1, 24]. Studies using criteria of extra-orbital disease showed Stages III and IV rates of 22–36% at diagnosis [18, 19]. The disproportionate number of cases staged as IE precludes the ability to differentiate the majority of OAL from one another in terms of disease extent within the ocular adnexal structures. This in turn can have important prognostic implications.

Table 15.3 Staging of OAL by Ann Arbor and tumor-node-metastasis systems

Ann Arbor system	
Indolent lymphomas: EMZL, FL, LPL	
Stage I	Localized disease (Ann Arbor [AA] I, IE and II, IIE)
Stage II	Disseminated disease (Ann Arbor [AA] III and IV)
Aggressive lymphomas: DLBCL, MCL	
Stage I	Localized or extranodal disease (Ann Arbor [AA] I or IE)
Stage II	Two or more nodal sites; three or more extranodal sites
Stage III	Stage II with additional poor prognostic features
Tumor-node-metastasis system[a]	
T classification	
TX	Lymphoma extent not specified
T0	No evidence of lymphoma
T1	Conjunctival lymphoma alone
T2	Orbital lymphoma with or without conjunctival involvement
T3	Preseptal eyelid lymphoma with or without conjunctival/orbital disease
T4	Orbital and extra-orbital lymphoma with invasion of adjacent structures (bone, sinus, brain)
N classification	
NX	Lymph node involvement not assessed
N0	No evidence of lymph node involvement
N1	Involvement of lymph node regions superior to the mediastinum
N1a	Involvement of a single lymph node region superior to the mediastinum
N1b	Involvement of two or more lymph node regions superior to the mediastinum
N2	Involvement of lymph node regions of the mediastinum
N3	Diffuse or disseminated involvement of peripheral and central lymph node regions
M classification	
M0	No evidence of involvement of other extranodal sites
M1a	Noncontiguous involvement of tissue or organs (parotids, liver, spleen, kidney, breast)
M1b	Lymphomatous involvement of the bone marrow
M1c	Both M1a and M1b involvement

EMZL extranodal marginal zone lymphoma, *FL* follicular lymphoma, *MCL* mantle cell lymphoma, *LPL* lymphoplasmacytic lymphoma, *DLBCL*, diffuse large B-cell lymphoma, *E* extranodal disease

[a]Modified from the American Joint Committee on Cancer (AJCC) eighth edition TNM-based staging manual for OAL

More recently, a tumor-node-metastasis (TNM)-based staging system for primary OAL has been developed under the guidance of the American Joint Committee on Cancer (AJCC) [25]. This system addresses many of the deficiencies of the Ann Arbor system and more precisely defines disease extent. The ultimate goal of TNM-based staging is to facilitate future studies aimed at identifying clinical and histopathologic features of OAL of prognostic significance and to assess treatment outcomes. TNM staging continues to be evaluated in regard to its prognostic significance for OAL [26].

Differential Diagnosis

The differential diagnosis for OAL is extensive. It includes inflammatory lesions (Fig. 15.5), benign lymphoproliferative lesions (Fig. 15.6), epithelial tumors, lightly melanocytic tumors, infectious lesions, and lacrimal gland lesions (ectopic tissue). In the orbit and eyelid, masses including metastases, dacryoadenitis, chalazion, inflammation, and other benign and malignant tumors must be considered.

Pathologic Features

Pathologic analysis can identify obvious lymphomas but cannot reliably differentiate lymphoma types (Fig. 15.7). Recent data has shown that using the current WHO classification, 76% of lesions previously classified as RLH are now reclassified as lymphomas. This is due to the recognition that a small number of malignant lymphocytes, whose presence is indicative of lymphoma, can be overshadowed by surrounding normal or reactive lymphoid cells.

The common immunophenotypic expressions of OAL subtypes are shown in Table 15.1. Immunophenotyping can be carried out qualitatively on tissue sections or quantitatively on dispersed cells (flow cytometry). The use of intact tissue allows localization of marker expression, which can be critical for establishing the correct diagnosis. For example, overexpression of

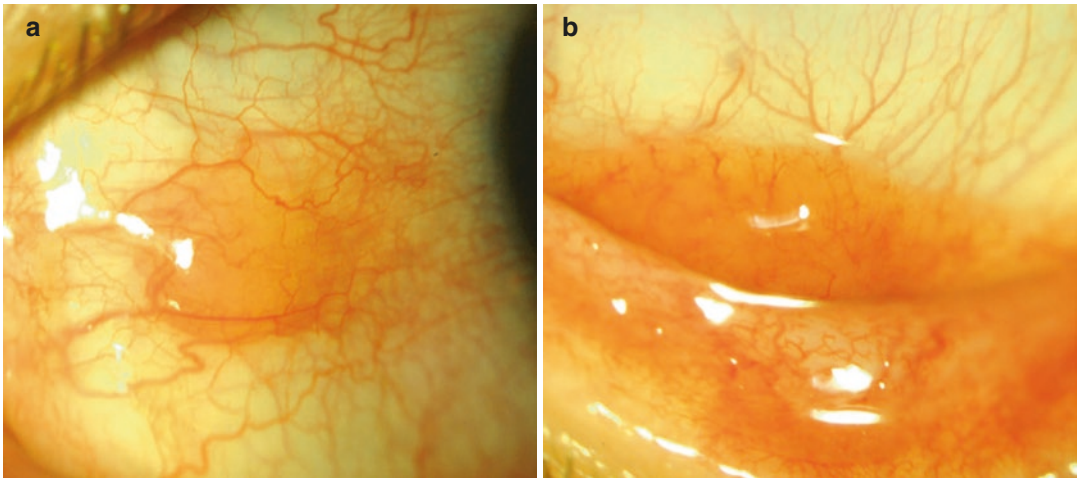

Fig. 15.5 Bulbar (**a**) and forniceal (**b**) idiopathic inflammatory conjunctival granuloma simulating ocular adnexal lymhoma

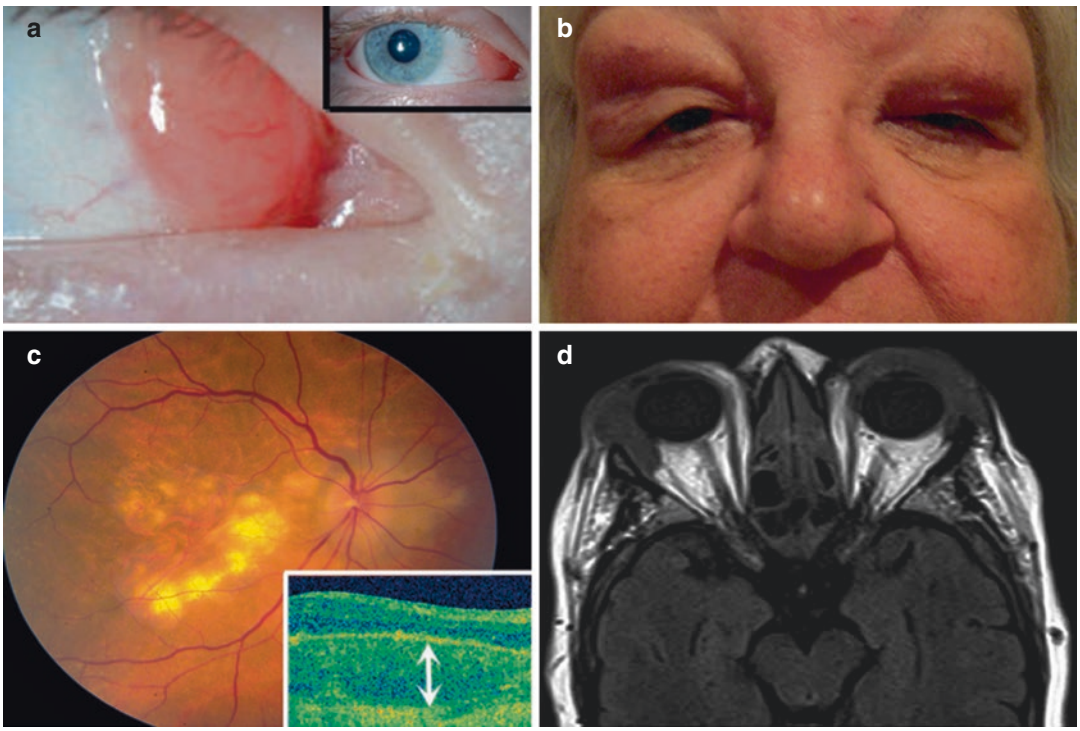

Fig. 15.6 Clinical presentations of reactive lymphoid hyperplasia (RLH). Salmon patch lesion of the right eye which was biopsy-confirmed RLH. Inset shows the lesion on the bulbar conjunctiva was limited to the medial canthal region (**a**). Facial photograph of patient with bilateral RLH of the lacrimal gland demonstrates fullness of both orbits and cheeks (**b**). Fundus photograph of the right eye of the same patient reveals creamy choroidal lesions consistent with uveal RLH (**c**). The inset demonstrates choroidal thickening observed on OCT (arrow). The left fundus and OCT revealed similar findings. MRI of the same patient demonstrates bilateral lacrimal gland swelling (**d**). (Reprinted from Stacy et al. [27]. With permission from Elsevier)

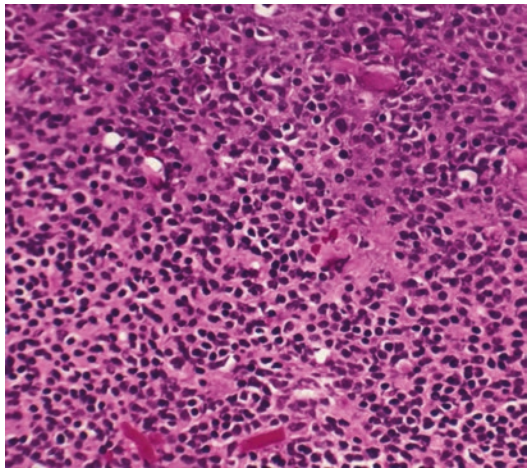

Fig. 15.7 Photomicrograph of monomorphic lymphocytes typical of EMZL-type ocular adnexal lymphoma (H&E, Original magnification ×100)

cytoplasmic Bcl-2 is not seen in normal follicular structures and is consistent with follicular lymphoma (Fig. 15.8) [27]. Immunohistochemistry may not detect critically important cells when sampling effect limits their presence. Flow cytometry, in contrast, does not give anatomic information but can accurately assign the immunophenotype of involved cells in very small samples.

Molecular genetics analysis of OAL is important in two ways. Identification of overexpressed heavy chain gene rearrangements is indicative of clonality which confirms malignancy. Tumor cells can be analyzed for translocations, which can be suggestive of a specific lymphoma subtype (Table 15.4). Translocation of the MALT gene with API2 [t(11;18)(q21;q21)] is of specific interest as its presence is generally associated with

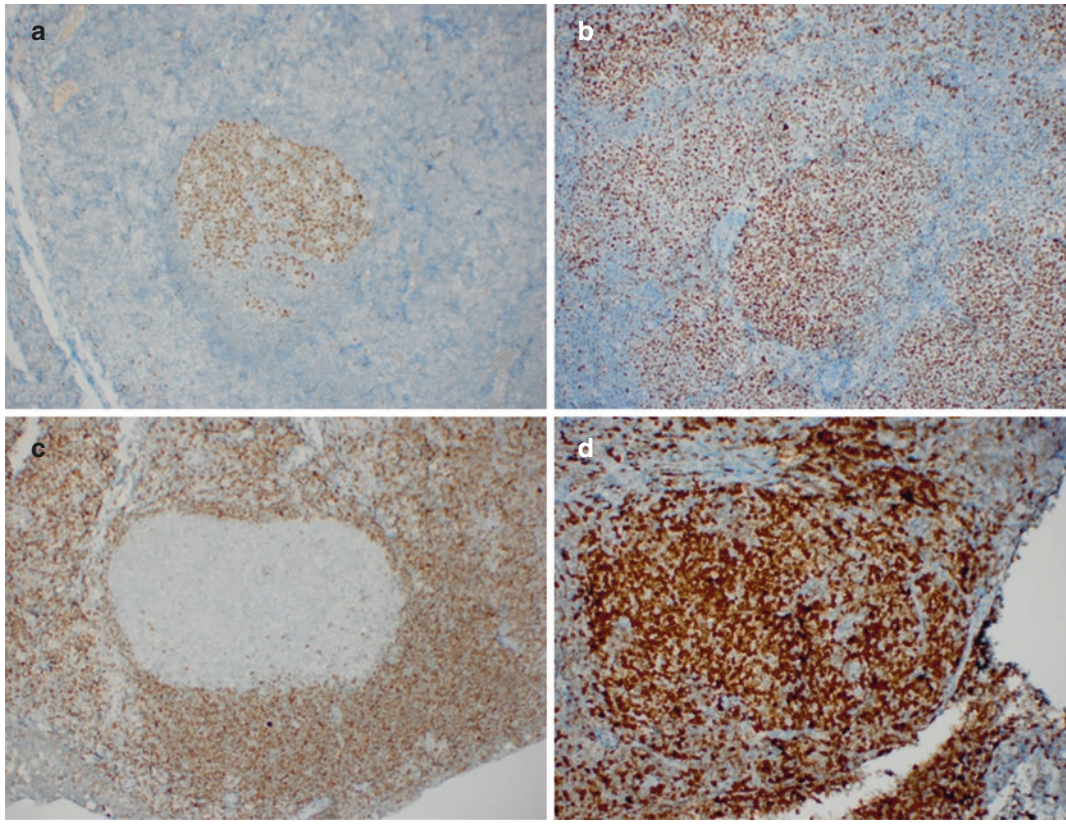

Fig. 15.8 Immunohistochemical characterization of RLH and follicular lymphoma (FL); Bcl-6 stains B cells within follicles of RLH (**a**). Follicles of FL are also positive for Bcl-6 (**b**). The follicles of RLH are negative for Bcl-2 (**c**). Follicles of FL are positive for BCL-2 (**d**). Follicles in RLH are positive for CD10 (**e**). Follicles of FL are also positive for CD10 but with more interfollicular staining than RLH (**f**) (immunoperoxidase reactions, 200×). (Reprinted from Stacy et al. [27]. With permission from Elsevier)

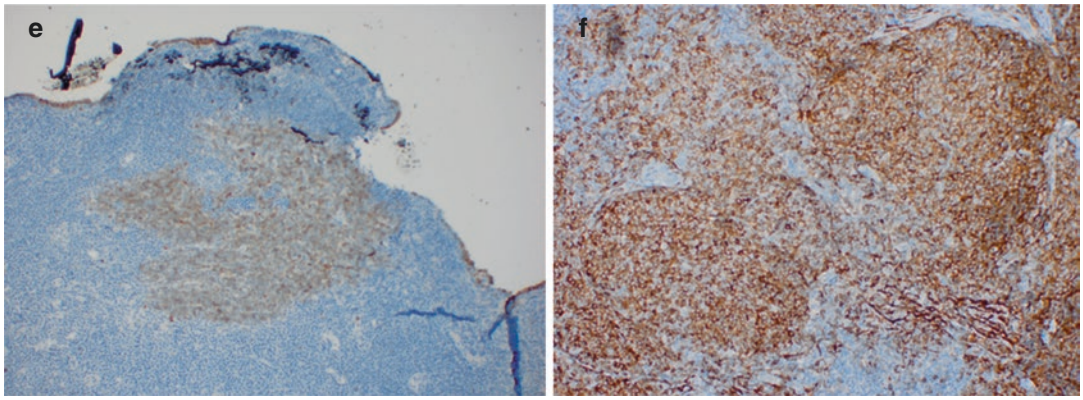

Fig. 15.8 (continued)

Table 15.4 Common translocations observed in OAL

Type	Genetic change	Mechanism	Frequency	Proto-oncogene
EMZL	t(11;18)(q21;q21)	Fusion Transcript deregulation	50% Rare	API2/MLT Bcl-10
FL	t(14;18)(q32;q21)	Transcript deregulation	80–90%	Bcl-2
MCL	t(11;14)	Transcript deregulation	70%	Bcl-1 (encodes cyclin D1)
LPL	T(9;14)(p13;q32)	Transcript deregulation	50%	PAX-5
DLBCL	Der (3)(q27)	Transcript deregulation		Bcl-6

EMZL extranodal marginal zone lymphoma, *FL* follicular lymphoma, *MCL* mantle cell lymphoma, *LPL* lymphoplasmacytic lymphoma, *DLBCL* diffuse large B-cell lymphoma

more aggressive disease [28]. The expansion of tools for lymphocyte characterization has paradoxically increased the chances for contradictory or incomplete characterizations using newer criteria. In such situations, the wisdom of an experienced hematopathologist is ideal, although some lesions will remain unclassifiable.

Rare Variants

There are several rare variants and simulating conditions of OAL such as Langerhans cell histiocytosis (LCH), Rosai-Dorfman disease, T-cell lymphoma, T-cell/natural killer (NK)-cell lymphoma (lethal midline granuloma), and Burkitt lymphoma that we have included in this review.

Langerhans Cell Histiocytosis

LCH is characterized by a proliferation of Langerhans cells and inflammatory cells that generally affects children and young adults. The disease may be localized or it may affect multiple systems including the skin, bone, lungs, and lymphatics. Ophthalmic disease is observed in 10–23% of cases and most often manifests as a solitary lesion within the orbit; however, intraocular involvement in the form of an atrophic chorioretinopathy has been reported [29]. Confirmation of diagnosis is made by biopsy, which demonstrates numerous histiocytes, giant cell formation, and eosinophilic granulocytes. Transmission electron microscopy (TEM) reveals characteristic intracytoplasmic Birbeck granules.

Rosai-Dorfman Syndrome

Also labeled as sinus histiocytosis with massive lymphadenopathy is a benign form of idiopathic histiocytosis that typically affects children and young adults. The majority of individuals (approximately 80%) develop painless cervical lymphadenopathy [30]. Extranodal involvement

may affect multiple systems including the respiratory tract, skin, bones, visceral organs, and the central nervous system. The disease has multiple ophthalmic manifestations including lesions within the orbit, eyelid, and lacrimal apparatus. Compressive optic neuropathy, uveitic glaucoma, serous retinal detachment, and marginal corneal infiltrates can occur. Ocular adnexal involvement occurs in approximately 10% of patients with extranodal disease [31].

T-Cell Lymphoma

In rare cases, OAL can be of T-cell origin. In a review of 353 individuals with OAL, only a single case (0.3%) was of T-cell lineage [7]. As with B-cell neoplasms, a heterogeneous group of T-cell lymphomas can involve the ocular adnexal structures (Fig. 15.9). Most T-cell lymphomas affecting the ocular adnexal structures are aggressive and carry a poor prognosis.

Most non-B-cell lymphomas are an extension of the malignant stage of mycosis fungoides or a secondary manifestation of systemic T-cell lymphoma. In a series of seven individuals with OAL of T-cell origin, three cases were peripheral T-cell lymphomas (PTCL) demonstrating positivity for CD3, CD8, and βF1 and negativity for CD56. Two cases were positive for CD3 and CD30 while negative for CD56 and were classified as anaplastic large-cell lymphomas of T-cell type (T-ALCL) [32]. The remaining two cases were positive for CD3 and CD56 and negative for βF1. These two cases were positive for Epstein-Barr virus (EBV) by in situ hybridization, consistent with T-cell/natural killer (NK)-cell lymphoma of nasal type (also referred to as lethal midline granuloma) [32].

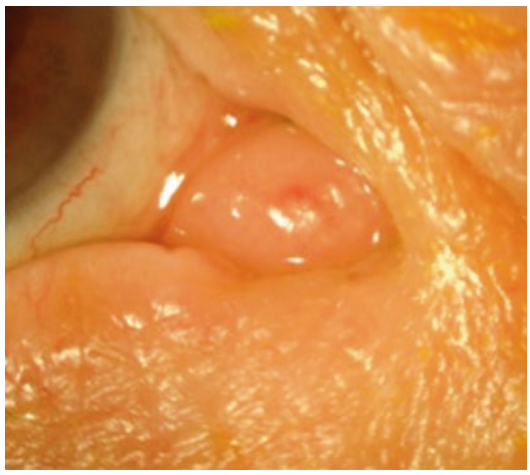

Fig. 15.9 T-cell lymphoma of the caruncle in a patient with slowly progressive mycosis fungoides

Burkitt Lymphoma

Burkitt lymphoma is a rare entity associated with translocation between chromosomes 8 and 14 affecting c-myc [33]. Three forms, all of which may affect the orbit, have been described. The African type frequently involves the orbits and maxillary bones and is associated with the presence of antibodies against Epstein-Barr virus (EBV) antigens [33]. The non-African type usually affects lymph nodes, bone marrow, and viscera. The third form affects immunocompromised individuals and is associated with acquired immunodeficiency syndrome (AIDS) (Fig. 15.10). Recent review of 16 immunocompetent individuals with sporadic orbital Burkitt lymphoma revealed a median age at diagnosis of 12 years [34]. Presenting symptoms included proptosis, ophthalmoplegia, and eyelid edema. Fourteen (88%) in this series had systemic involvement [34]. Biopsy of orbital lesions reveals a characteristic "starry-sky" appearance associated with Burkitt lymphoma. Prognosis is guarded for this extremely aggressive lymphoma as significant mortality (54%) is observed within 1 year of presentation [34].

Treatment

The treatment of OAL is an area of controversy, progress, and change. Currently OAL treatment depends on whether the disease is localized or systemic. Local disease can be effectively treated with radiotherapy alone. Systemic disease is frequently treated in a manner similar to other indolent lymphomas, typically using rituximab or

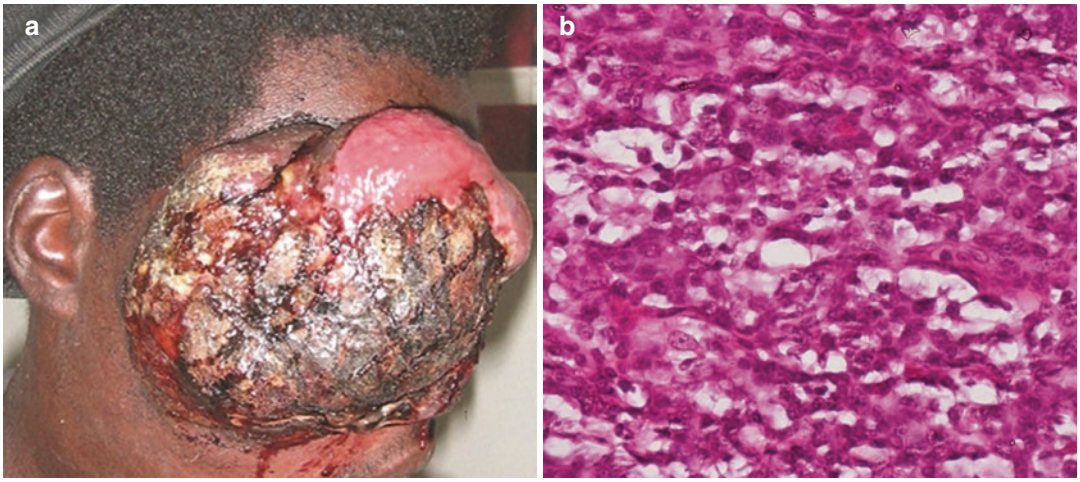

Fig. 15.10 A 24-year-old Haitian man presented with rapidly progressive right eye proptosis (**a**). An exenteration was performed, and the tissue sample was sent to the pathology laboratory, which revealed the characteristic "starry-sky" appearance of a Burkitt lymphoma (**b**). The patient expired shortly after due to complications from systemic involvement. (Reprinted from Giuliari et al. [35]. With permission from Creative Commons License: https://creativecommons.org/licenses/by/3.0/)

other immunotherapies alone, or in combination with cytotoxic chemotherapy. With the recognition that the vast majority of OAL are of the EMZL/MALT type and that there may be an infectious basis for this subgroup of OAL, there is a possibility of deferring cytotoxic modalities. A second controversy is whether to treat BRL and indolent OAL. In recent years, there has been a paradigm shift in the management of indolent systemic lymphoma. Rather than up-front treatment and systemic imaging surveillance repeated at regular intervals, many patients are now being monitored with a "watch and wait" approach. In the absence of symptoms, treatment for indolent systemic lymphoma can be deferred. It may be reasonable then to apply this strategy to asymptomatic cases of RLH and low-grade OAL. A survey of treatment modalities follows.

Surgery

Surgery has been reported to be successful in managing certain cases of highly localized OAL and has been recommended for Stage I MALT systemic lymphoma in some sites. Its applicability remains dubious for most OAL due to the diffuse nature and frequent juxtaposition of OAL to sensitive ocular tissues. Surgery should therefore be reserved for localized, isolated lesions of the conjunctiva [1].

Cryotherapy

Cryotherapeutic ablation of OAL has limited use in the management of OAL. It has resulted in variable success due to debulking the tumor without complete elimination of malignant tissue. It may have application in a limited number of patients with conjunctival OAL who are unable to receive other treatment modalities.

Radiation

Historically, external beam radiation (EBRT) has been the most frequently used modality for treatment of OAL. Analysis of this modality is confounded by small patient numbers in most series, the use of early and inaccurate classification schemes, short follow-up times, and apparent lack of ophthalmic follow-up. Complications were detected at a rate of up to 50% higher when close ophthalmic follow-up was performed.

Both electron and photon irradiation have been successfully employed in OAL. Dosage is based on the tumor grade or type [18, 19]. Typical doses are 24–30 Gy for low-grade OAL and 30–40 Gy for high-grade OAL [36]. In a recent review of 77 eyes with OAL treated with radiation alone (mean follow-up of 38 months), highly fractionated EBRT with a mean dose of 25 Gy was found to be effective, providing high local control and low risk of visually significant complications [37]. These findings are consistent with results from a phase III randomized trial [38] and guidelines from the International Lymphoma Radiation Oncology Group recommendations for extranodal lymphoma of all sites (Fig. 15.11) [39]. The role of lens shielding to decrease cataract formation remains controversial, with some studies showing no effect on local recurrence and others showing high recurrence rates [36]. While radiation studies frequently emphasize the ability to obtain local control, the effect of this modality on the overall course and prognosis is less clear. Even Stage IV-EA disease showed good local control, though survival was significantly lower. Multiple studies revealing higher rates of delayed systemic recurrence suggest that longer follow-up is necessary for accurate assessment of treatment effect [19].

More recently, there has been interest in treating OAL using ultra-low-dose radiotherapy, or the so-called "boom-boom" therapy, based on the success of this regimen for indolent systemic lymphoma. This entails delivering a total dose of 4 Gy in two 2 Gy fractions. In one series of 22 patients with OAL (86% with low-grade EMZL or follicular lymphoma), there was an overall response rate of 100% (86% had a complete response and 14% had a partial response) [40]. Further studies are needed to assess the role of ultra-low-dose irradiation for OAL.

Chemotherapy

Since OAL frequently presents as localized disease (Stage IE), chemotherapy is rarely used, with the exception of aggressive DLBCL (Fig. 15.12). The review of chemotherapy used in lymphoma is beyond the scope of this chapter.

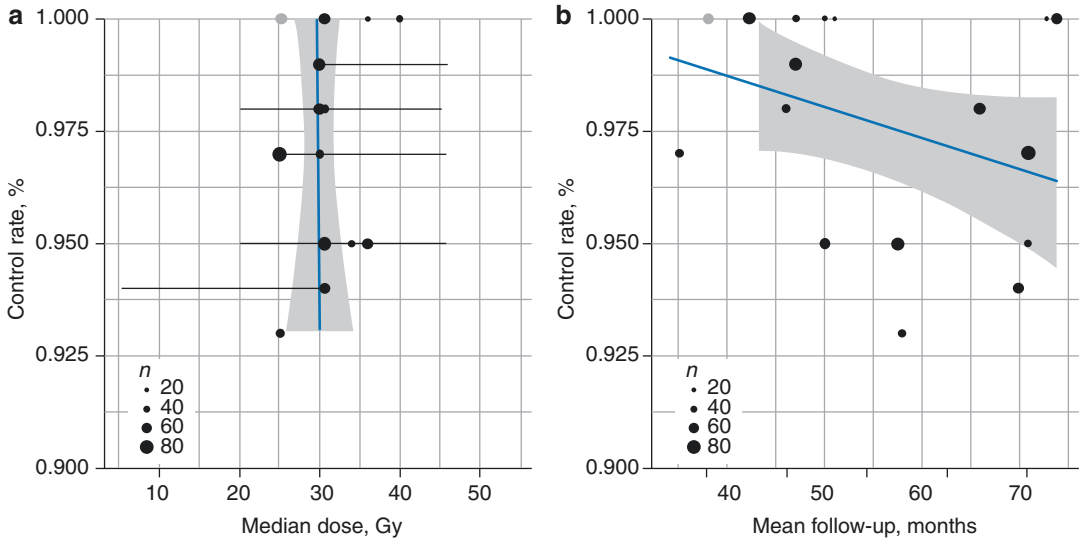

Fig. 15.11 Published studies. Association between median dose and control rate. The x-axis shows the radiation dose in Gy. Points represent the median dose reported in a study, and the whiskers represent the range of radiation dose in the study. The size of the point corresponds to the number of subjects in the study. The y-axis is the reported local control rate of the study (**a**). Association between mean follow-up duration (months) and control rate. The x-axis represents the reported follow-up time of the study, and the y-axis is the reported control rate. The size of the point represents the number of subjects in the study. The blue line represents the line of best fit weighted by the number of subjects in the study. The gray areas represent the standard error associated with the line of best fit (**b**) (Adapted from Yahalom J et al. [39])

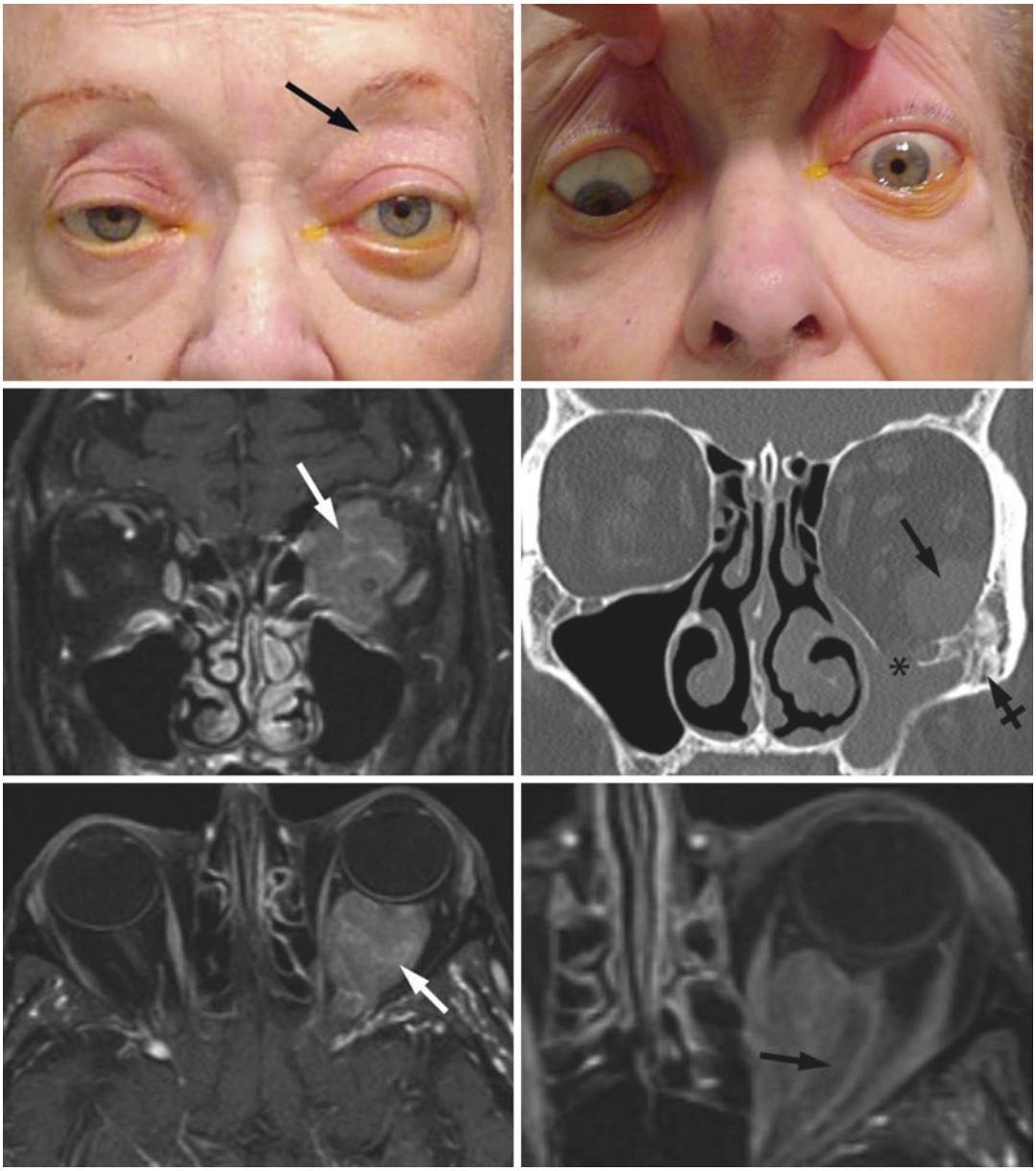

Fig. 15.12 Clinical and radiographic features of diffuse large B-cell lymphoma of the orbit. Top left: patient with mass in the left upper orbit (arrow) producing mild, non-congestive proptosis. Top right: mass effect caused limited eye movements and infraduction of the left globe. Middle left: typical location of an orbital lymphoid tumor (arrow) in the superior and superonasal regions of the orbit. There is no bone erosion. Middle right: an unusual inferotemporal tumor (arrow) has created adjacent bone changes (crossed arrow). An old inferior, post-traumatic orbital floor fracture (*) explains the absence of clinical proptosis. Bottom left: an intraconal, retrobulbar mass (arrow) is accompanied by moderate proptosis. Bottom right: in the same patient portrayed in the bottom left, axial CT reveals that the tumor encases the optic nerve (arrow) asymmetrically, with a more prominent component nasally. The patient had a decline in visual acuity and an afferent pupillary defect. (Reprinted from Stacy et al. [41]. With permission from Elsevier)

Standard chemotherapy for OAL when it is part of more advanced disease is that of standard systemic lymphoma regimens using single-agent rituximab alone or in combination with cyclophosphamide, doxorubicin, vincristine, and prednisone (CHOP), the alkylating agent chlorambucil, and, more recently, bendamustine which has dual properties of an alkylating agent and a purine analogue. While some have used systemic corticosteroids for tumor suppression of OAL, steroids offer ineffective long-term control.

Immunotherapy

Interferon (IFN-alpha) has been used rarely for OAL despite its long-standing use in systemic lymphoma. One report of five cases showed 80% initial complete response with short-term follow-up [42]. One patient with Stage IIA disease died of systemic lymphoma at 1 year. More data regarding local and systemic efficacy are needed prior to acceptance of this modality.

Antilymphocyte antibodies are a recent form of lymphoma treatment. The most commonly used is rituximab, an anti-CD-20 monoclonal antibody, which leads to destruction of B cells using mechanisms of complement and antibody-mediated destruction as well as induction of apoptosis. These antibodies are effective when used alone but also significantly increase the remission rates when used in combination with chemotherapy. While standardly administered as an intravenous infusion, intralesional injection of rituximab (50 mg/1 ml) for low-grade OAL has shown promise in early studies [43]. Most recently, subcutaneous formulations (1400 mg) of rituximab have shown similar efficacy and safety profile compared to intravenous delivery for systemic follicular lymphoma [44]. The role of subcutaneous rituximab for OAL has yet to be established.

Antimicrobial Treatment

A recent development in OAL management is based on the IMM model of lymphomagenesis. There is increasing evidence of the role of chronic infection in OAL. Both *C. psittaci* and *H. pylori* have been implicated [11, 12]. Follow-up data from *C. psittaci* detection studies have suggested a therapeutic effect following antibiotic therapy with doxycycline, presumably by eradication of the infection which underlies lymphomagenesis. Other studies have shown an effect in small numbers of patients using anti-*H. pylori* triple therapy [45]. Overall, antibiotic treatment regimens have shown variable results by study group and geographic location. Larger studies are needed to clarify the role of antibiotics in treatment of OAL.

Prognosis

Prognosis of OAL is evaluated in three ways: local control, progression to systemic involvement, and death from lymphoma. While certain anatomic sites, such as orbital involvement, are presently assigned a higher TNM stage and have traditionally been associated with a poorer prognosis (in comparison to conjunctival lymphoma), the lymphoma subtype is probably a better indicator of prognosis. Validation of newer staging protocols will provide future evidence in this regard. Excellent local control has been reported using external beam radiation. Among OAL, EMZL has a quantitatively better prognosis than other tumor types with regard to spread of tumor and lymphoma-related death; however, the risk ratio is similar among indolent forms including EMZL, LPL, and FCL. The mortality ranges are EMZL, 0–20%; DLBCL, 25–75%; FL, 20–37%; MCL, 38–100%; and LPL, 14–100%. Extraorbital spread can occur in over 45% of EMZL cases after a mean follow-up of 63 months, suggesting that long-term follow-up is needed [1,

18, 19]. A recent large, single-center report of long-term outcomes of patients with primary low-grade OAL found that age <60 years was associated with improved progression-free survival and that while individuals with indolent disease may survive decades without treatment, up to 4% of OAL may transform to more aggressive variants [46].

Future Research

Our evolving ability to characterize OAL on a molecular level will increase potential for developing newer and less toxic therapies. Recent advances in next-generation sequencing have allowed for more comprehensive genomic profiling of OAL. In one series of 36 samples, 53% harbored a potentially actionable mutation [47]. Ultimately, this personalized medicine approach may facilitate the discovery of therapeutic targets and guide future clinical trials.

References

1. Coupland SE, Hellmich M, Auw-Haedrich C, et al. Prognostic value of cell-cycle markers in ocular adnexal lymphoma: an assessment of 230 cases. Graefe's archive for clinical and experimental ophthalmology = Albrecht von Graefes Archiv fur klinische und experimentelle. Fortschr Ophthalmol. 2004;242(2):130–45.
2. Cohen VM, Sweetenham J, Singh AD. Ocular adnexal lymphoma. What is the evidence for an infectious aetiology? Br J Ophthalmol. 2008;92(4):446–8.
3. Hatef E, Roberts D, McLaughlin P, et al. Prevalence and nature of systemic involvement and stage at initial examination in patients with orbital and ocular adnexal lymphoma. Arch Ophthalmol. 2007;125(12):1663–7.
4. Bayraktar S, Bayraktar UD, Stefanovic A, et al. Primary ocular adnexal mucosa-associated lymphoid tissue lymphoma (MALT): single institution experience in a large cohort of patients. Br J Haematol. 2011;152(1):72–80.
5. Shields JA, Bakewell B, Augsburger JJ, et al. Classification and incidence of space-occupying lesions of the orbit. A survey of 645 biopsies. Arch Ophthalmol. 1984;102(11):1606–11.
6. Spraul CW, Grossniklaus HE. Analysis of 24,444 surgical specimens accessioned over 55 years in an ophthalmic pathology laboratory. Int Ophthalmol. 1997;21(5):283–304.
7. Ferry JA, Fung CY, Zukerberg L, et al. Lymphoma of the ocular adnexa: a study of 353 cases. Am J Surg Pathol. 2007;31(2):170–84.
8. Knowles DM, Jakobiec FA, McNally L, et al. Lymphoid hyperplasia and malignant lymphoma occurring in the ocular adnexa (orbit, conjunctiva, and eyelids): a prospective multiparametric analysis of 108 cases during 1977 to 1987. Hum Pathol. 1990;21(9):959–73.
9. Ye H, Liu H, Attygalle A, et al. Variable frequencies of t(11;18)(q21;q21) in MALT lymphomas of different sites: significant association with CagA strains of H pylori in gastric MALT lymphoma. Blood. 2003;102(3):1012–8.
10. Takada S, Yoshino T, Taniwaki M, et al. Involvement of the chromosomal translocation t(11;18) in some mucosa-associated lymphoid tissue lymphomas and diffuse large B-cell lymphomas of the ocular adnexa: evidence from multiplex reverse transcriptase-polymerase chain reaction and fluorescence in situ hybridization on using formalin-fixed, paraffin-embedded specimens. Modern pathology : an official journal of the United States and Canadian Academy of Pathology. Inc. 2003;16(5):445–52.
11. Ferreri AJ, Guidoboni M, Ponzoni M, et al. Evidence for an association between Chlamydia psittaci and ocular adnexal lymphomas. J Natl Cancer Inst. 2004;96(8):586–94.
12. Chan CC, Smith JA, Shen DF, et al. Helicobacter pylori (*H. pylori*) molecular signature in conjunctival mucosa-associated lymphoid tissue (MALT) lymphoma. Histol Histopathol. 2004;19(4):1219–26.
13. Dagklis A, Ponzoni M, Govi S, et al. Immunoglobulin gene repertoire in ocular adnexal lymphomas: hints on the nature of the antigenic stimulation. Leukemia. 2012;26(4):814–21.
14. Harris NL, Jaffe ES, Stein H, et al. A revised European-American classification of lymphoid neoplasms: a proposal from the International Lymphoma Study Group. Blood. 1994;84(5):1361–92.
15. Swerdlow S, Campo E, Harris NL, et al. WHO classification of tumours of haematopoietic and lymphoid tissues. Revised 4th edition. World Health Organization; Lyon, France: IARC; 2017.
16. Aronow ME. Ocular adnexal lymphoma: evidence-based treatment approach. Int Ophthalmol Clin. 2015;55(1):97–109.
17. Yen MT, Bilyk JR, Wladis EJ, et al. Treatments for ocular adnexal lymphoma: a report by the American Academy of Ophthalmology. Ophthalmology. 2018;125(1):127–36.
18. Fung CY, Tarbell NJ, Lucarelli MJ, et al. Ocular adnexal lymphoma: clinical behavior of distinct World Health Organization classification subtypes. Int J Radiat Oncol Biol Phys. 2003;57(5):1382–91.
19. Jenkins C, Rose GE, Bunce C, et al. Histological features of ocular adnexal lymphoma (REAL classification) and their association with patient morbidity and survival. Br J Ophthalmol. 2000;84(8):907–13.

20. Stafford SL, Kozelsky TF, Garrity JA, et al. Orbital lymphoma: radiotherapy outcome and complications. Radiother Oncol: J Eur Soc Therapeutic Radiol Oncol. 2001;59(2):139–44.
21. Fuller ML, Sweetenham J, Schoenfield L, et al. Uveal lymphoma: a variant of ocular adnexal lymphoma. Leuk Lymphoma. 2008;49(12):2393–7.
22. Aronow ME, Portell CA, Sweetenham JW, et al. Uveal lymphoma: clinical features, diagnostic studies, treatment selection, and outcomes. Ophthalmology. 2014;121(1):334–41.
23. Saatci AO, Arikan G, Ozcan MA, et al. Indocyanine green angiographic features of systemic non-Hodgkin's lymphoma and bilateral choroidal involvement. Ophthalmic surgery, lasers & imaging : the official journal of the International Society for Imaging in the. Eye. 2006;37(3):236–9.
24. McKelvie PA, McNab A, Francis IC, et al. Ocular adnexal lymphoproliferative disease: a series of 73 cases. Clin Exp Ophthalmol. 2001;29(6):387–93.
25. Coupland SE, White VA, Rootman J, et al. A TNM-based clinical staging system of ocular adnexal lymphomas. Arch Pathol Lab Med. 2009;133(8):1262–7.
26. Aronow ME, Portell CA, Rybicki LA, et al. Ocular adnexal lymphoma: assessment of a tumor-node-metastasis staging system. Ophthalmology. 2013;120(9):1915–9.
27. Stacy RC, Jakobiec FA, Schoenfield L, et al. Unifocal and multifocal reactive lymphoid hyperplasia vs follicular lymphoma of the ocular adnexa. Am J Ophthalmol. 2010;150(3):412–26 e1.
28. Liu H, Ye H, Dogan A, et al. T(11;18)(q21;q21) is associated with advanced mucosa-associated lymphoid tissue lymphoma that expresses nuclear BCL10. Blood. 2001;98(4):1182–7.
29. Thanos A, Vavvas D, Young LH, et al. Choroidal neovascular membrane formation and retinochoroidopathy in a patient with systemic langerhans cell histiocytosis: a case report and review of the literature. Case Rep Ophthalmol. 2012;3(1):128–35.
30. Rosai J, Dorfman RF. Sinus histiocytosis with massive lymphadenopathy: a pseudolymphomatous benign disorder. Analysis of 34 cases. Cancer. 1972;30(5):1174–88.
31. Zimmerman LE, Hidayat AA, Grantham RL, et al. Atypical cases of sinus histiocytosis (Rosai-Dorfman disease) with ophthalmological manifestations. Trans Am Ophthalmol Soc. 1988;86:113–35.
32. Coupland SE, Foss HD, Assaf C, et al. T-cell and T/natural killer-cell lymphomas involving ocular and ocular adnexal tissues: a clinicopathologic, immunohistochemical, and molecular study of seven cases. Ophthalmology. 1999;106(11):2109–20.
33. Ruf IK, Rhyne PW, Yang H, et al. Epstein-barr virus regulates c-MYC, apoptosis, and tumorigenicity in Burkitt lymphoma. Mol Cell Biol. 1999;19(3):1651–60.
34. Baker PS, Gold KG, Lane KA, et al. Orbital burkitt lymphoma in immunocompetent patients: a report of 3 cases and a review of the literature. Ophthal Plast Reconstr Surg. 2009;25(6):464–8.
35. Giuliari GP, Sadaka A, Cortez MA, et al. Orbital Burkitt's lymphoma: an aggressive presentation. Case Rep Ophthalmol Med. 2012;2012:354043.
36. Uno T, Isobe K, Shikama N, et al. Radiotherapy for extranodal, marginal zone, B-cell lymphoma of mucosa-associated lymphoid tissue originating in the ocular adnexa: a multiinstitutional, retrospective review of 50 patients. Cancer. 2003;98(4):865–71.
37. Platt S, Al Zahrani Y, Singh N, et al. Extranodal marginal zone lymphoma of ocular adnexa: outcomes following radiation therapy. Ocul Oncol Pathol. 2017;3(3):181–7.
38. Lowry L, Smith P, Qian W, et al. Reduced dose radiotherapy for local control in non-Hodgkin lymphoma: a randomised phase III trial. Radiother Oncol. 2011;100(1):86–92.
39. Yahalom J, Illidge T, Specht L, et al. Modern radiation therapy for extranodal lymphomas: field and dose guidelines from the International Lymphoma Radiation Oncology Group. Int J Radiat Oncol Biol Phys. 2015;92(1):11–31.
40. Pinnix CC, Dabaja BS, Milgrom SA, et al. Ultra-low-dose radiotherapy for definitive management of ocular adnexal B-cell lymphoma. Head Neck. 2017;39(6):1095–100.
41. Stacy RC, Jakobiec FA, Herwig MC, et al. Diffuse large B-cell lymphoma of the orbit: clinicopathologic, immunohistochemical, and prognostic features of 20 cases. Am J Ophthalmol. 2012;154(1):87–98.
42. Blasi MA, Gherlinzoni F, Calvisi G, et al. Local chemotherapy with interferon-alpha for conjunctival mucosa-associated lymphoid tissue lymphoma: a preliminary report. Ophthalmology. 2001;108(3):559–62.
43. Demirci H, Kauh CY, Rajaii F, et al. Intralesional rituximab for the treatment of recurrent ocular adnexal lymphoma. Ophthal Plast Reconstr Surg. 2017;33(3S. Suppl 1):S70–S1.
44. Davies A, Merli F, Mihaljevic B, et al. Efficacy and safety of subcutaneous rituximab versus intravenous rituximab for first-line treatment of follicular lymphoma (SABRINA): a randomised, open-label, phase 3 trial. Lancet Haematol. 2017;4(6):e272–e82.
45. Abramson DH, Rollins I, Coleman M. Periocular mucosa-associated lymphoid/low grade lymphomas: treatment with antibiotics. Am J Ophthalmol. 2005;140(4):729–30.
46. Desai A, Joag MG, Lekakis L, et al. Long-term course of patients with primary ocular adnexal MALT lymphoma: a large single-institution cohort study. Blood. 2017;129(3):324–32.
47. Cani AK, Soliman M, Hovelson DH, et al. Comprehensive genomic profiling of orbital and ocular adnexal lymphomas identifies frequent alterations in MYD88 and chromatin modifiers: new routes to targeted therapies. Mod Pathol. 2016;29(7):685–97.

Malignant Orbital Tumors

16

Bhupendra C. K. Patel

Introduction

Malignant orbital tumors represent a broad spectrum of tumors which include primary tumors, secondary tumors (extension from adjacent structures), and metastatic tumors. In addition, orbital inflammation and infection may clinically simulate an orbital neoplasm (Chap. 7). In a recent survey of 1264 consecutive patients with suspected orbital tumor referred to an ophthalmic oncology center, 36% were malignant tumors [1]. The percentage of malignant tumors increases with age, due to higher incidence of lymphoma and metastasis in the older age groups [1].

Malignant tumors of vascular (Chap. 8), neural (Chap. 11), fibrous, and osseous origin are rare in the orbit. Rhabdomyosarcoma is the most frequent primary malignant orbital tumor in children (Chap. 17), and lymphoproliferative disorders including lymphoma are most frequent in older adults (Chap. 15). Malignant orbital tumors may also arise from the lacrimal gland (Chap. 13) and lacrimal sac (Chap. 14). The details of clinical examination (Chap. 1), clinical evaluation (Chap. 2), and imaging techniques (Chap. 5) supplement contents of this review. Malignant orbital tumors not covered under other chapters are reviewed herein.

B. C. K. Patel (✉)
Division of Facial Cosmetic and Reconstructive Surgery, University of Utah, Salt Lake City, UT, USA
e-mail: bhupendra.patel@hsc.utah.edu

C. J. Hwang et al. (eds.), *Clinical Ophthalmic Oncology*,
https://doi.org/10.1007/978-3-030-13558-4_16

Esthesioneuroblastoma

Introduction

Esthesioneuroblastoma is a tumor of neural crest origin that arises from the sensory olfactory epithelium and can invade the cribriform plate, the ethmoid sinuses, and the orbit. Most esthesioneuroblastomas seen in the orbit have invaded the orbit secondarily [2]. Approximately 25% of newly diagnosed esthesioneuroblastomas will present with orbital extension. The peak incidence is in the second to third decades. They are frequently mistaken for other small-cell tumors. Males and females are equally affected and have age peaks at 20 and 50 years.

Clinical Features

When confined to the nasal cavity or paranasal sinus, patients will have nasal obstruction, bloody nasal discharge, and headache. Three-quarters of patients with olfactory esthesioneuroblastoma have ophthalmic symptoms such as periorbital pain, epiphora, decreased vision, and diplopia. The most common ophthalmic signs include eyelid edema and proptosis. Ptosis and cranial nerve palsies may also be present.

Diagnostic Evaluation

CT scans show an isodense homogenous tumor in the nasal cavity and ethmoid sinus, often with orbital extension [3]. Esthesioneuroblastomas are classified according to their location: Group A tumors are confined to the nasal cavity, group B tumors affect the nasal cavity and one or more paranasal sinuses, and group C tumors extend into the cranium or orbit. Histologically, the hallmark of diagnosis is the presence of rosettes of the neuroblastoma cells, but histology is variable widely. These tumors are often mistakenly labelled as undifferentiated carcinoma.

Treatment

The prognosis is best for group A (75% survival at 5 years) and worst for group C (less than 45% survival at 5 years). Treatment consists of aggressive craniofacial resection with adjunctive radiotherapy and chemotherapy. Esthesioneuroblastoma is characterized by extended remissions and multiple recurrences. Local recurrence occurs in 50–75% of patients and metastases in 20–30%.

Malignant Peripheral Nerve Sheath Tumor

Introduction

This rare tumor may develop de novo, following radiotherapy, or secondary to plexiform neurofibroma. About 50% of patients with malignant peripheral nerve sheath tumors are associated with neurofibromatosis [4].

Clinical Features

These tumors are seen in the fourth and fifth decades, except in patients with neurofibromatosis when it occurs in the teens. Patients present with proptosis and globe displacement. Periorbital pain, hypoesthesia, ptosis, and visual loss frequently occur.

Diagnostic Evaluation

CT imaging shows an irregular, nodular, poorly defined mass. There may be bone destruction or enlargement of the superior orbital fissure. The supraorbital nerve is more commonly affected. T1-weighted MRI shows a heterogeneous signal isointense with muscle and hypointense to fat. T2-weighted sequence shows a signal that is hyperintense to both muscle and fat [5]. Ultrasound may show cystic spaces within the tumor. Histopathologically, the tumors can resemble fibrosarcomas with long fascicles of spindle cells forming a herringbone pattern. Immunostaining for S-100 protein, Leu-7, and myelin basic protein confirms nerve sheath differentiation.

Treatment

In cases of orbital involvement, exenteration is often needed. Ancillary chemotherapy and radiotherapy have been used but do not appear to improve survival. Recurrences are typical and often grow rapidly. Sometimes, recurrences are seen after many years. Most patients with orbital disease develop intracranial extension or pulmonary metastases [6].

Alveolar Soft Part Sarcoma

Introduction

This is a rare tumor, believed to be of myogenic origin [7]. It occurs mostly in the lower extremities and buttocks. Head and neck region is the site of primary tumor in only 10% of cases. The mean age at presentation is 20–30 years. Females are affected three times more frequently than males.

Clinical Features

Proptosis and globe displacement develop rapidly over 4–6 months. Apical tumors cause visual loss, orbital congestion, and ocular motility disturbances. Sensory nerve involvement causes pain [8]. Anterior masses may present as eyelid lumps with dilated epibulbar vessels.

Diagnostic Evaluation

CT imaging shows a moderately well-defined mass, usually involving the superior orbit with marked contrast enhancement owing to tumor hypervascularity. Tumor necrosis results in a central area of low attenuation. Histopathology shows large, round, or polygonal cells with large nuclei and prominent nucleoli.

Treatment

Wide surgical resection is mandatory. For recurrences or large tumors, orbital exenteration is necessary. The role of chemotherapy and radiotherapy has not definitively been determined [9]. Tumors localized to the orbit carry a better prognosis than alveolar soft part sarcoma developing in the lower extremities and buttocks. The tumor-related mortality is about 15% over 10 years for orbital alveolar soft part sarcoma.

Osteosarcoma

Introduction

Osteosarcoma, also called osteogenic sarcoma, is the most common primary malignant neoplasm of the bone. Most cases arise de novo but may arise secondary to Paget's disease, fibrous dysplasia, radiation therapy, giant cell tumor, or osteoblastoma [10]. Osteosarcoma is also seen as a second tumor in patients with familial retinoblastoma, even in the absence of a history of radiotherapy [11]. Although it may affect any of the orbital bones, the maxillary bone is the most frequent orbital site of the tumor.

Clinical Features

Most patients present with chronic symptoms, of at least several months to a year. Presentations include proptosis, dysesthesias, and diplopia. However, patients may present with rapid-onset painful proptosis and sudden decrease in vision.

Diagnostic Evaluation

CT imaging shows a mixed lytic and sclerotic mass with indistinct margins. The appearance depends upon the predominance of osseous, cartilaginous, or fibrous tissue components. Bone destruction and calcification with new bone formation often occurs. The sunray appearance is said to be a classic finding radiographically but is only seen in about 25% of cases.

Treatment

Management of osteosarcoma involves preoperative chemotherapy, resection, and continuation of the chemotherapy. Radiotherapy may be used as an adjunctive treatment for residual tumor. The prognosis of osteosarcoma involving the orbital bones remains poor. It is rare for a patient to survive 5 years following treatment (15–20%).

Malignant Fibrous Histiocytoma

Fibrous histiocytoma is the most common mesenchymal orbital tumor in adults, seen most commonly in middle-aged adults [12]. They may be benign, locally aggressive, or malignant. Patients present with proptosis, a mass effect, decreased vision, double vision, pain, eyelid swelling, and ptosis (Fig. 16.1). Malignant fibrous histiocytoma or myxofibrosarcoma may arise de novo or follow orbital radiotherapy, especially in children with the germline mutation of retinoblastoma. Malignant fibrous histiocytoma requires exenteration. Although metastases are rare, the tumor shows local infiltrative features with a tendency to local recurrence.

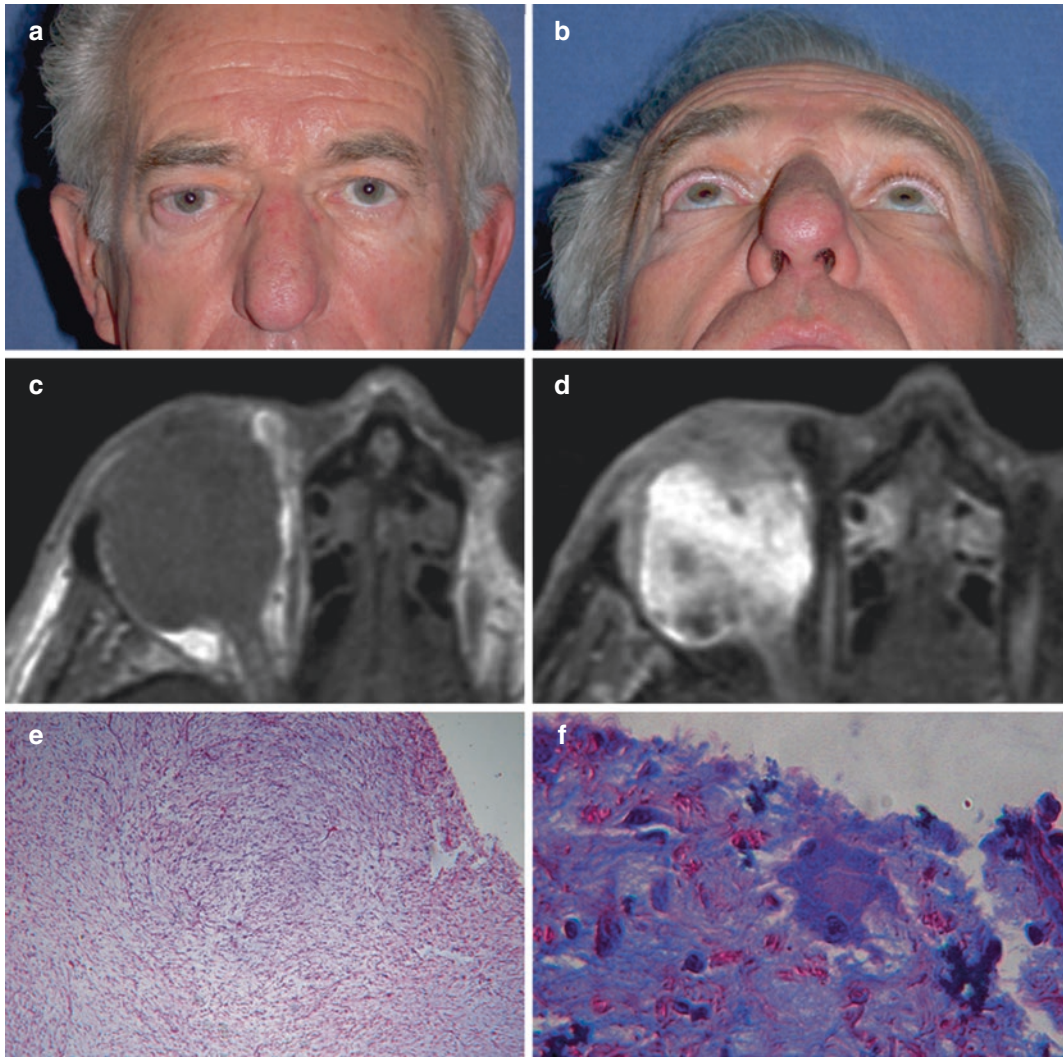

Fig. 16.1 Malignant histiocytoma or myxofibrosarcoma. A 75-year-old male with onset of double vision over 2 months and limitation of ocular movements in all fields of gaze. Note hypoglobus (**a**) and proptosis (**b**) on the right side. MRI shows a right superior orbital mass (**c**) which enhances irregularly with gadolinium (**d**). On histopathology, storiform or cartwheel-like growth pattern is seen (**e**). Note Touton giant cell (**f**). Exenteration was performed and the patient is recurrence-free at 4 years

Leiomyosarcoma

Introduction

Leiomyosarcomas are usually seen as radiation-induced tumors following orbital irradiation in children. They arise from the smooth muscle in blood vessels, Muller's muscle, and smooth muscle precursor cells decades after the radiation [13, 14].

Clinical Features

Patients present with progressive painless proptosis. The duration of symptoms varies from 6 weeks to 18 months. Globe proptosis and displacement are seen. Patients develop motility disturbance and visual loss. Anterior lesions may be palpable as a firm mass [15].

Diagnostic Evaluation

A heterogeneously dense, well-defined, lobulated mass is seen within the orbit on CT scans. The borders may mold around the globe. Destruction of the adjacent bone may be seen. Histopathology may show well-differentiated or poorly differentiated tumors with multinucleated giant cells [16].

Treatment

Most cases require aggressive resection with extended orbital exenteration, including adjacent bones. Local or small tumors may be treated with local resection and adjunctive radiotherapy. Systemic metastases require chemotherapy. Local resection alone is associated with 60% local recurrence within 3 years. Most patients progress to develop metastases to the lungs, liver, kidney, and brain.

Liposarcoma

Introduction

Liposarcoma is common soft tissue sarcoma in adults, but it rarely arises within the orbit [17]. Very rarely, liposarcoma may metastasize to the orbit [18].

Clinical Features

There are no specific clinical features diagnostic of liposarcoma. In a series of five cases, diplopia and proptosis were most frequent clinical findings (Fig. 16.2) [19].

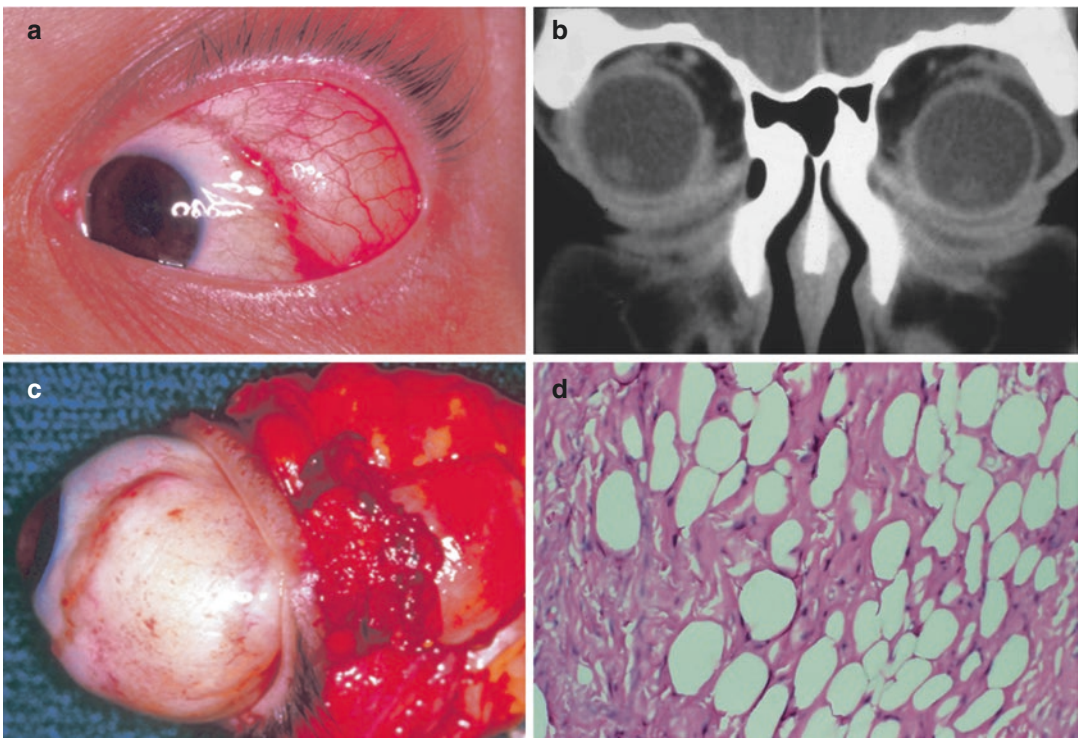

Fig. 16.2 Liposarcoma. A 45-year-old male presents with left retrobulbar pain and a mass in the superotemporal fornix (**a**). CT scan shows a superotemporal mass with the consistency of fat (**b**). Gross specimen of exenteration although some patients can be managed with local excision (**c**). Low-grade liposarcoma with vacuolated and signet ring cells (**d**)

Diagnostic Evaluation

CT scan appearance of fat density enclosed by a radiodense pseudocapsule can lead to an initial impression of a cyst [19]. MRI will confirm presence of fat within the lesion (hyperintense signals in T1-weighted images) [19]. Liposarcoma should be considered in the differential diagnosis of any unusual mesenchymal tumor in the orbit [17].

Treatment

Limited resection followed by radiation may be adequate treatment in well-differentiated tumors without invasion into orbital structures [20]. In some cases, despite exenteration and radiation, delayed local recurrence has been observed [21]. Regional or distant metastases are uncommon [19].

Secondary Orbital Tumors

Introduction

Secondary orbital tumors represent contiguous orbital extension of a primary ocular, conjunctival, eyelid, sinus, or intracranial tumor. Basal cell carcinoma, squamous cell carcinoma, melanoma, and sebaceous cell carcinoma of the eyelid may secondarily invade the orbit because of late presentation, incomplete excision (sebaceous cell carcinoma), rapid and aggressive growth, or perineural spread (squamous cell carcinoma and melanoma).

Clinical Features

Basal Cell Carcinoma

Basal cell carcinoma invasion of the orbit is most often seen medially with extraocular muscle restriction and fixation of the tumor to the adjacent bone (Fig. 16.3) [22].

Squamous Cell Carcinoma

Squamous cell carcinoma tends to spread along fascia and fatty planes relatively rapidly compared to basal cell carcinoma (Fig. 16.4). Perineural invasion may occur and is associated with pain or ophthalmoplegia [23]. Squamous cell carcinoma is capable of metastasis to regional preauricular or submandibular lymph nodes. Squamous cell carcinoma of the conjunctiva may also invade the orbit.

Melanoma

Multiple recurrences of conjunctival melanoma associated with primary acquired melanosis may lead to orbital extension. On rare occasions, uveal melanoma may extend into the orbit (Fig. 16.5).

Sebaceous Carcinoma

Sebaceous carcinoma is more prevalent in Asian populations. About one-third of epithelial malignancies invading the orbit are sebaceous carcinoma. This tumor tends to spread to the lymphatic system and subsequently to the lung, liver, brain, or skull.

Merkel Cell Carcinoma

Merkel cell carcinoma is an eyelid neoplasm that may arise in the eyelid or periocular region. They demonstrate rapid growth with a bulging, red appearance with overlying telangiectatic vessels in the elderly (Fig. 16.6). The diagnosis is confirmed by the characteristic immunocytochemical and electron microscopic features. The tumor is associated with local recurrence and satellite lesions, regional nodal metastases, and distant metastases in about half of patients. Orbital invasion is associated with tumor recurrence and may lead to intracranial spread.

Diagnostic Evaluation

Careful assessment of extraocular muscle function is necessary in patients with periorbital malignancies. Medial spread of a tumor will often present with restriction of gaze followed by double vision. CT scans will reveal an irregular, often lobulated, well-defined mass extending from the preseptal to the postseptal space. Spread down the nasolacrimal duct and along the extraocular muscles may be seen.

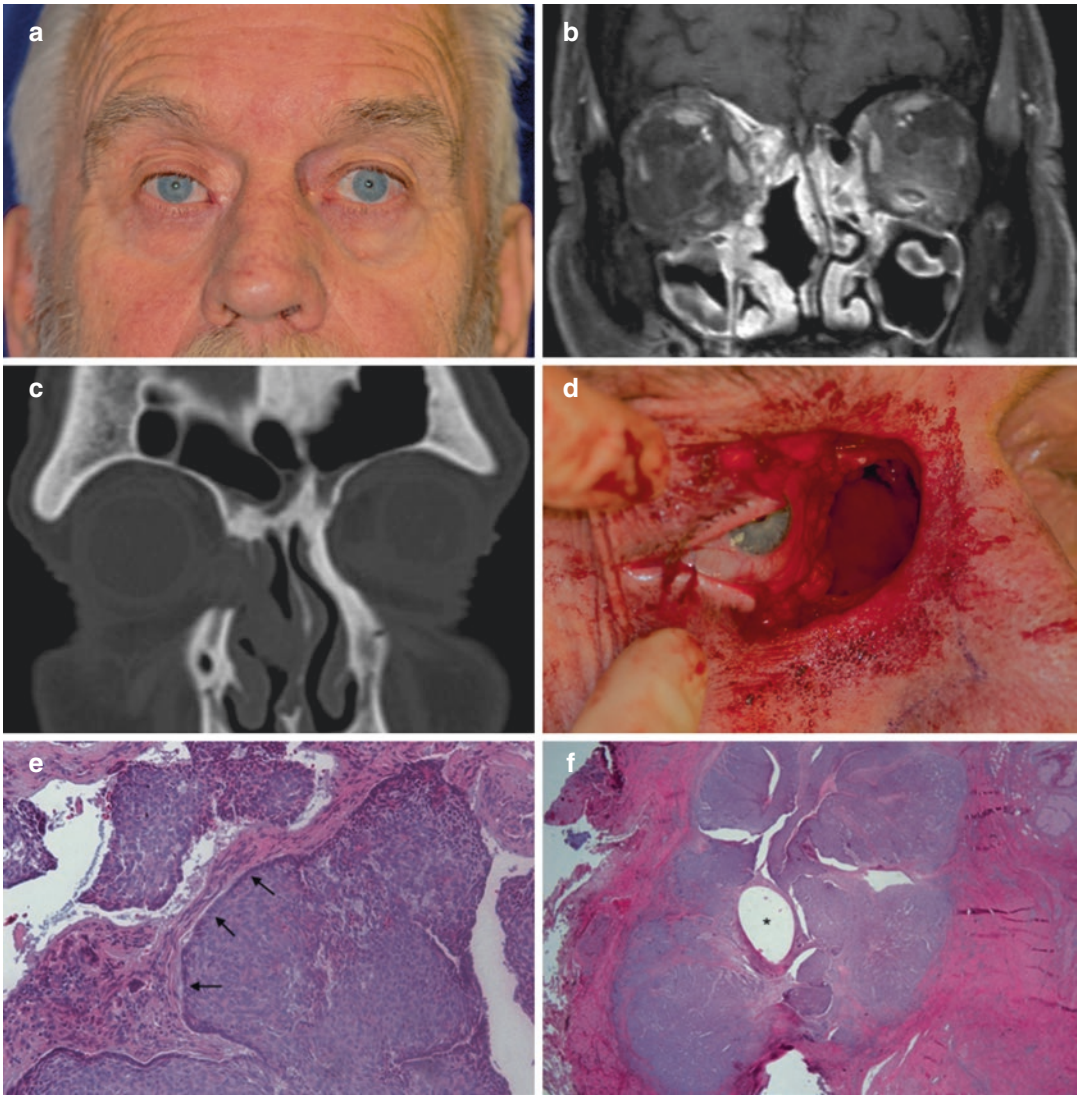

Fig. 16.3 Basal cell carcinoma invading the orbit: treated with globe preservation. A 72-year-old male presents with double vision and medial canthal scarring with dystopia, 2 years after resection of a medial canthal basal cell carcinoma (**a**). MRI scans show invasion of the tumor into the anterior third of the orbit with spread along the medial rectus muscle to the middle of the orbit (**b**). CT scans show bony invasion of tumor into the anterior ethmoids (**c**). Globe-preservation resection of tumor with frozen section controls performed (**d**). Patient is alive with no recurrence 5 years after surgery. H/E-stained frozen section; note the palisading nuclei (**e**, arrows 100×). The tumor surrounded the nasolacrimal duct (**f**, asterisk 20×)

Treatment

For orbital basal cell carcinoma, a globe-sparing resection may be attempted. However, the more aggressive basal cell carcinomas and squamous cell carcinomas may require aggressive resection with free borders and may need an exenteration.

Sebaceous carcinomas need a radical resection and lymph node dissection. Radiotherapy may control local disease if the patient is unable to undergo surgery. When conjunctival malignant melanoma spreads into the orbit, exenteration with nodal resection may be required. Treatment of Merkel cell carcinoma consists of aggressive

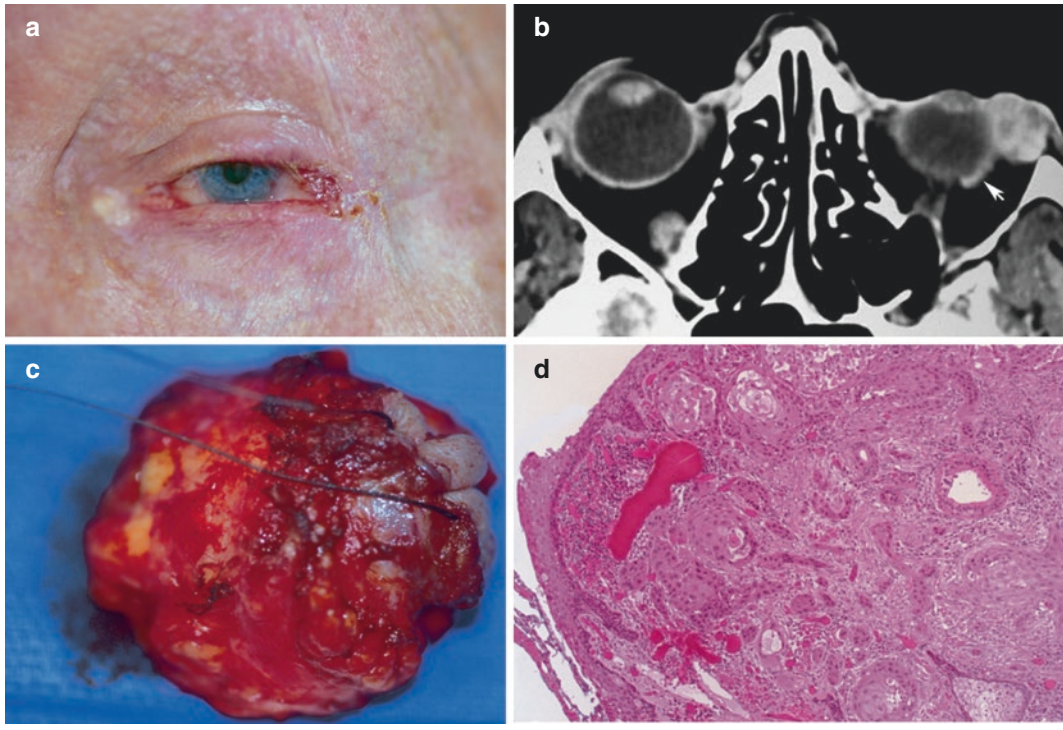

Fig. 16.4 Extension of squamous cell carcinoma into the orbit. A 71-year-old male with a 5-year history of multiple resections of left lower lid squamous cell carcinoma (**a**). CT scan shows an irregular but lobulated, well-defined density involving the tissues anterior to the orbital septum and extending into the retroseptal space (**b**, arrow). Mohs resection was attempted, but the deep tumor could not be removed necessitating exenteration (**c**). On histopathology, islands of squamous cells with dyskeratosis and keratin whorls were observed (**d**)

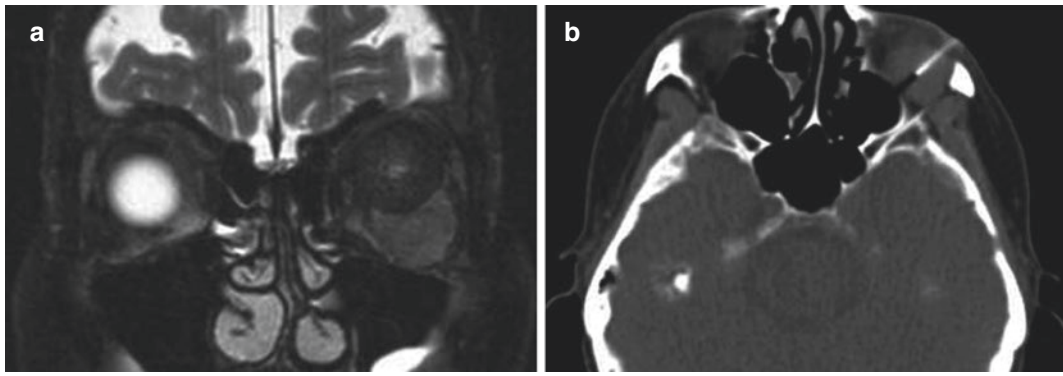

Fig. 16.5 Secondary melanoma. Orbital melanoma following enucleation for a large uveal melanoma. Histopathology of the globe was negative for extrascleral extension. MRI (T2) showing partially vascularized orbital implant with an orbital mass (**a**). The clinical diagnosis was confirmed by CT-guided fine needle aspiration biopsy (**b**)

surgical excision with wide margins and postoperative radiotherapy.

Mutation in the patched 1 gene (PTCH1) has been implicated in BCC, and overexpression of epidermal growth factor receptor (EGFR) has been shown in SCC. Vismodegib, an inhibitor of smoothened, which is activated upon binding of hedgehog to Ptc, has been shown to significantly

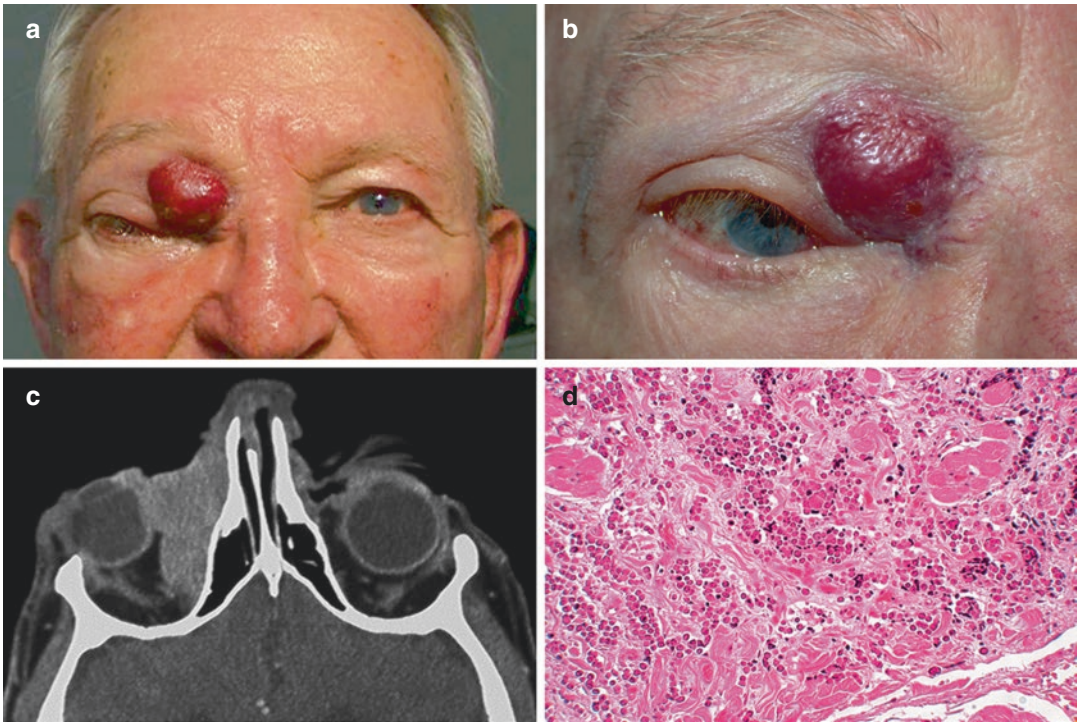

Fig. 16.6 Merkel cell carcinoma. A 78-year-old gentleman with a right medial canthal lesion initially biopsied elsewhere and diagnosed as basal cell carcinoma (**a**). He was referred after "recurrence." Note typical building reddish lesion with overlying vascularity (**b**). CT scan showed diffuse tumor with orbital invasion but without bone involvement (**c**). Note relatively large cells with uniformly staining eosinophilic cytoplasm (**d**)

decrease BCC tumor size or even produce complete resolution, especially in cases of basal cell nevus syndrome. Similarly, EGFR inhibitors have been shown to significantly decrease SCC tumor size in cases of locally advanced and metastatic disease. Vismodegib has been used to reduce bulky eyelid and periocular basal cell carcinomas in patients with the basal cell nevus syndrome. Similarly, erlotinib (EGFR inhibitor) has been shown to be useful in patients with SCC when the patient is not a candidate for surgery because of advanced disease of the orbit. Targeted therapy using hedgehog pathway and EGFR inhibitors shows significant promise in treatment of orbital and periocular BCC and cutaneous SCC, respectively. Such targeted therapy may be appropriate for patients who are not good candidates for surgery [24].

Orbital Metastases: Adults

Introduction

Approximately 8% of all orbital neoplasia are metastatic in origin. Breast cancer (Fig. 16.7), lung cancer (Fig. 16.8), prostate cancer, and melanoma are the most frequent primary tumors in adults that metastasize to the orbit (Fig. 16.9). In approximately 10% of cases, the primary tumor remains unidentified. In the majority of cases (75%), a diagnosis of preexisting primary tumor is known (Fig. 16.10), but in about 25% of cases, the orbital tumor is the first presentation (Fig. 16.11) [25]. We have noticed that metastatic tumors to the extraocular muscles (lung, carcinoid, lymphoma) will often give a posterior

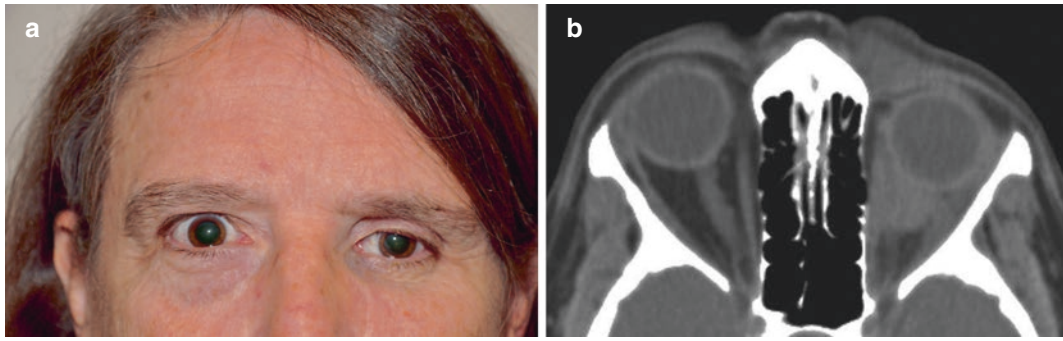

Fig. 16.7 Metastatic breast carcinoma. Orbital enophthalmos is evident on clinical examination (**a**) and CT scan (**b**). Note orbital mass in the affected left orbit

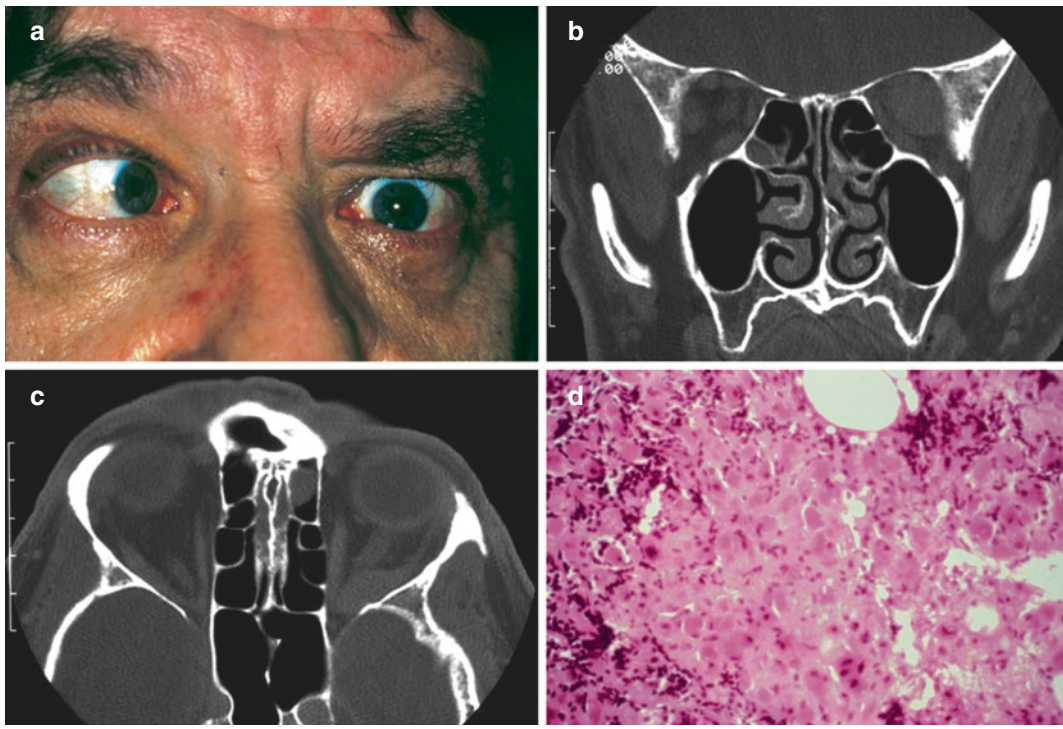

Fig. 16.8 Metastatic lung carcinoma. A 55-year-old male smoker presented with marked limitation of left eye abduction, slight left enophthalmos, and decrease of vision to counting fingers in the left eye (**a**). Coronal (**b**) and axial (**c**). CT scans show a homogenous posterior lateral rectus mass with compression of the optic nerve. The muscle is infiltrated with mixed small/large malignant cells with minimal cytoplasm and hyperchromatic nuclei (**d**)

muscle thickening, sometimes with what we have called the "Arabian vase sign" similar to the ancient Arabian vases which had a narrow neck with a wide base (and Geoff Rose has referred to as the "Amphora" sign, referring to the Greek vases). When such a sign is seen on radiology, we believe it is mostly due to malignancy (Fig. 16.12).

Clinical Features

Patients have more rapid onset of symptoms compared to other types of orbital neoplasia. Proptosis and motility disturbances are the most common presenting symptoms and signs. Pain is noted early in the course of the disease.

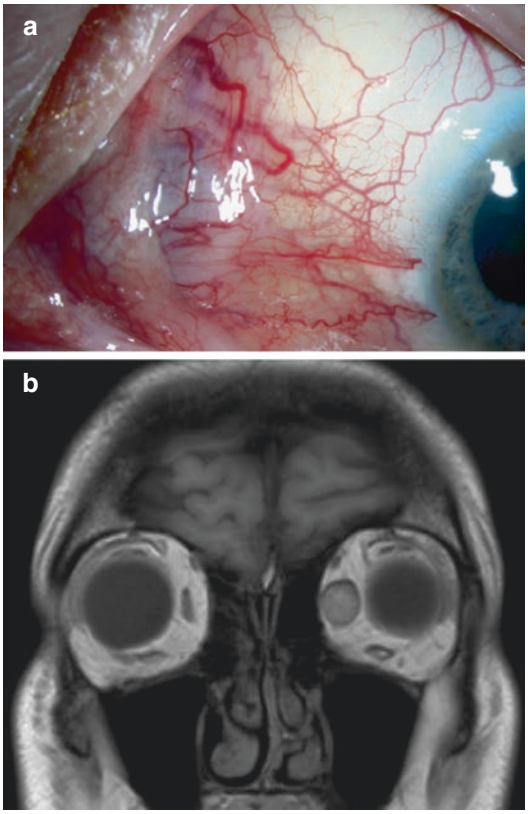

Fig. 16.9 Metastatic skin melanoma. Acute onset of painful proptosis and diplopia with congestion and bluish prominence of the medial rectus muscle insertion (**a**). MRI confirmed thickening of the medial rectus muscle (**b**). The patient had widespread metastatic cutaneous melanoma

Other symptoms and signs include a palpable mass, blepharoptosis, and decreased vision. Enophthalmos is present in 10% of cases (most being metastasis from breast cancer). Clinical presentation of orbital metastatic disease can be categorized into mass effect, infiltrative (causing diplopia, enophthalmos), functional (neurological deficits), inflammatory (pain, chemosis, swelling), or silent (discovered on imaging or at surgery with no symptoms or signs) (Table 16.1) [26].

Diagnostic Evaluation

CT imaging may show a mass, bony changes (hyperostosis-prostate or hypostatic-thyroid), enlargement of muscle, or diffuse orbital tissue enlargement. Open orbital biopsy or needle biopsy confirms the diagnosis.

Treatment

Management may include radiotherapy, hormonal therapy, chemotherapy, or surgery. In some patients, control of local disease may limit progressive orbital pain, corneal exposure, and vision loss.

Orbital Metastases: Children

Introduction

Neuroblastoma, Ewing's sarcoma, Wilms' tumor, testicular embryonal sarcoma, ovarian sarcoma, and renal embryonal sarcoma may cause metastases to the orbit in children.

Neuroblastoma

Neuroblastoma is the second most common (after rhabdomyosarcoma) orbital malignancy of childhood, and it accounts for 8–10% of all childhood malignancies. Neuroblastoma arises from embryonic neural crest tissue of the postganglionic sympathetic nervous system. The most common site for primary tumor is in the abdomen, but the thorax, neck, or pelvis may also be affected. The tumor presents anytime in the first two decades although the vast majority present before the age of 3 years [27].

There is a sudden and rapid progression of proptosis, which may be unilateral or bilateral and accompanied by edema, ecchymosis, and ptosis. The differential diagnosis includes orbital cellulites, rhabdomyosarcoma, Ewing's sarcoma, medulloblastoma, and Wilms' tumor and lymphangioma. The superolateral orbit is most commonly involved.

There is a combination of bone and soft tissue involvement. There may be evidence of bone destruction with evidence of other cranial metastases. The patient may have Horner's syndrome, opsoclonus, myoclonus, and metastases to the

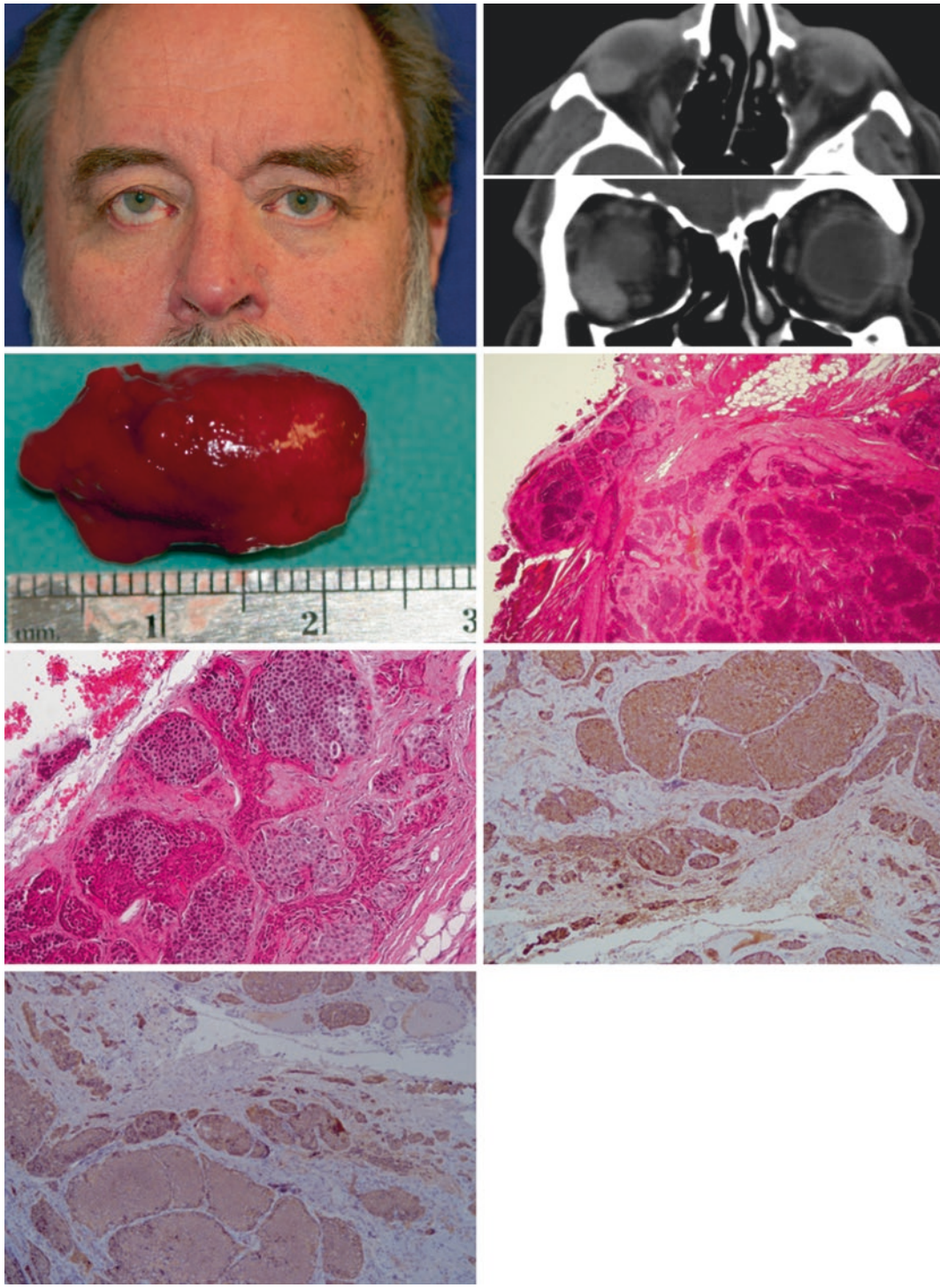

Fig. 16.10 Carcinoid tumor metastatic to the orbit. A 63-year-old male with a history of the carcinoid syndrome presented with double vision. Right proptosis and hyperglobus (**a**). Right inferolateral orbital mass causing hyperglobus and proptosis (**b**). Gross appearance after resection (**c**). The bulk of the lesion is made up of a cellular infiltrate that has a nesting pattern to it (**d**, H&E 4×). The cells themselves have a large nucleus with pleomorphism, nucleoli formation, and clumped chromatin. There are also scattered mitotic figures (**e**, H&E 20×). The tumor was positive for chromogranin (**f**, 10×) and synaptophysin (**g**, 10×) confirming neuroendocrine origin

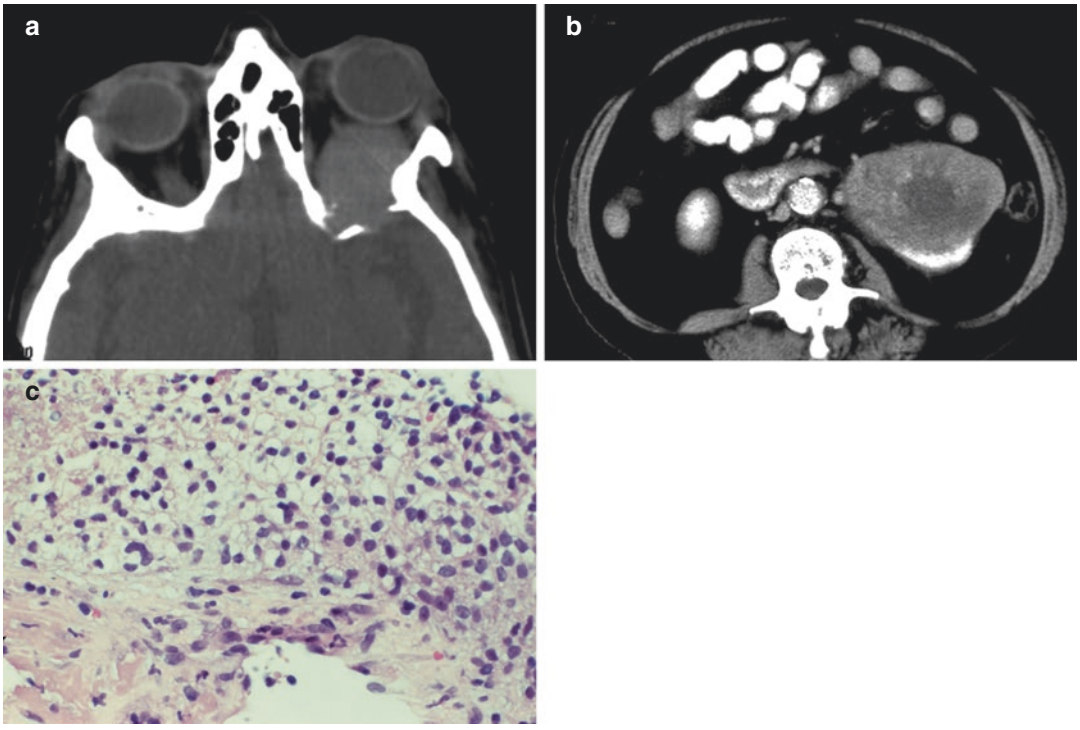

Fig. 16.11 Metastatic renal carcinoma. A 63-year-old female presented with proptosis, diplopia, and decreased vision in the left eye (**a**). Axial CT scans show a circumscribed homogenous orbital mass with bone destruction. Evaluation for primary tumor revealed a large mass replacing the right kidney (**b**). Fine needle aspiration biopsy of the kidney confirmed a clear cell renal carcinoma (**c**)

Fig. 16.12 Metastatic lung adenocarcinoma. A 65-year-old male (nonsmoker) presented with unintentional weight loss and increasing double vision in upgaze with limitation of right upgaze (**a**). Initial MRI scans (T2) from an outside facility showed mild right inferior rectus thickening posteriorly (**b**). These scans were performed 2 months after the first ones clearly showing an increasing mass in the posterior inferior rectus showing what we have described as the "Arabian vase sign" of muscle thickening posteriorly as seen in the ancient Arabian vases. We have seen these in numerous metastatic tumors to the extraocular muscles (lung cancer, carcinoid) and also with lymphoma, which tends to be more diffuse (**c**). Ultrasound (left) shows thickened inferior rectus muscle, and the FDG PET/CT scan shows markedly increased FDG activity in the tumor in the inferior rectus indicative of malignancy (**d**). A lung mass was found which had a needle aspiration biopsy which showed an adenocarcinoma

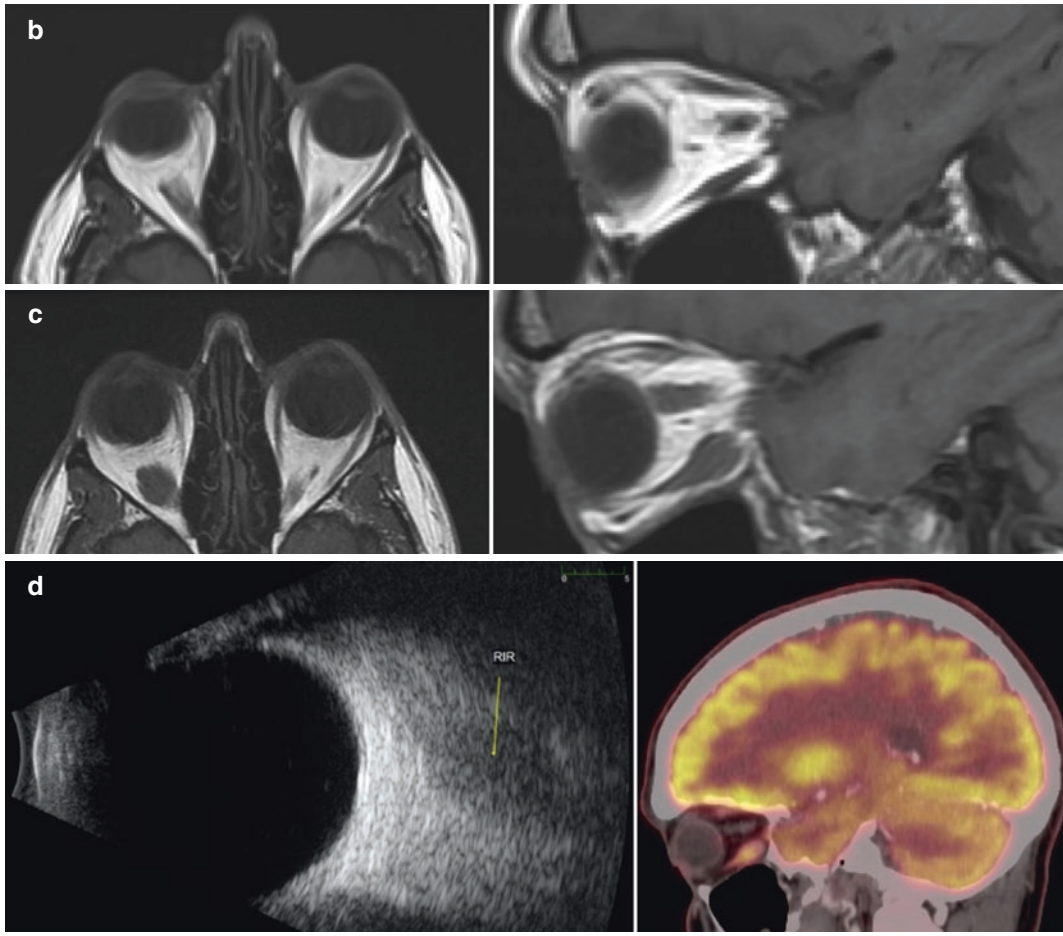

Fig. 16.12 (continued)

Table 16.1 Clinical features of orbital metastatic disease

Category	Feature
Mass effect	Visible or palpable mass
Infiltrative	Diplopia, exophthalmos, enophthalmos
Functional	Neurological deficits
Inflammatory	Pain, chemosis, swelling
Silent	Discovered on imaging or at surgery with no symptoms or signs

Based on data from Ref. [26]

iris or choroids. Aggressive combination chemotherapy and total body irradiation are used, but the prognosis remains poor. Prognosis depends upon the patient's age, the tumor stage, and histopathologic classification. More recently, new gene mutations have been found in familial and sporadic neuroblastoma cases which show poor outcomes [28].

Ewing's Sarcoma

Ewing's sarcoma is a highly malignant, small, round cell tumor of primitive mesenchymal cells in the bone marrow. These tumors may present as metastatic tumors or primary soft tissue orbital tumors [29]. Primitive neuroectodermal tumor of the orbit closely resembles Ewing's sarcoma [29]. The maxilla and the mandible are more commonly affected than the orbit. This tumor usually presents in the second decade of life. Orbital tumors present with rapidly progressing proptosis with or without orbital hemorrhage. The involved bone has a moth-eaten appearance. Treatment includes radiotherapy and chemotherapy along with local

resection. These tumors are quite radiosensitive. The 5-year survival rate is 80% with surgery, radiation, and chemotherapy. Second primary osteogenic sarcoma may occur, so long-term follow-up is necessary. Prognostic factors found to be associated with survival include presence of metastasis at presentation, size of tumor (more than 8 cm diameter), and axial skeletal tumors [30].

References

1. Shields JA, Shields CL, Scartozzi R. Survey of 1264 patients with orbital tumors and simulating lesions: the 2002 Montgomery Lecture, part 1. Ophthalmology. 2004;111(5):997–1008.
2. Laforest C, Selva D, Crompton J, et al. Orbital invasion by esthesioneuroblastoma. Ophthal Plast Reconstr Surg. 2005;21(6):435–40.
3. Loevner LA, Sonners AI. Imaging of neoplasms of the paranasal sinuses. Magn Reson Imaging Clin N Am. 2002;10(3):467–93.
4. Lyons CJ, McNab AA, Garner A, et al. Orbital malignant peripheral nerve sheath tumors. Br J Ophthalmol. 1989;73:731–8.
5. Bhargava R, Parham DM, Lasater OE, et al. MR differentiation of benign and malignant peripheral nerve sheath tumors: use of the target sign. Pediatr Radiol. 1997;27:124–9.
6. Erzurum SA, Melen O, Lissner G, et al. Orbital malignant peripheral nerve sheath tumors. Treatment with surgical resection and radiation therapy. J Clin Neuroophthalmol. 1993;13:1–7.
7. Ordonez NG, Mackay B. Alveolar soft-part sarcoma: a review of the pathology and histogenesis. Ultrastruct Pathol. 1998;22:275–92.
8. Jordan DR, MacDonald H, Noel L, et al. Alveolar soft-part sarcoma of the orbit. Ophthalmic Surg. 1995;26:269–70.
9. Sherman N, Valvilala M, Pollock R, et al. Radiation therapy for alveolar soft-part sarcoma. Med Pediatr Oncol. 1994;22:380–3.
10. Mark RJ, Sercarz JA, Tran L, et al. Osteogenic sarcoma of the head and neck. The UCLA experience. Arch Otolaryngol. 1991;117:761–6.
11. Abramson DH, Ronner HJ, Ellsworth RM. Second tumors in non-irradiated bilateral retinoblastoma. Am J Ophthalmol. 1979;87:624–7.
12. Jacobiec FA, Howard GM, Jones IS, et al. Fibrous histiocytomas of the orbit. Am J Ophthalmol. 1974;77:333–45.
13. Folberg R, Cleaseby G, Flanagan JA, et al. Orbital leiomyosarcoma after radiation therapy for bilateral retinoblastoma. Arch Ophthalmol. 1983;101:1562–5.
14. Font RL, Jurco S III, Brechner RJ. Postradiation leiomyosarcoma of the orbit complicating bilateral retinoblastoma. Arch Ophthalmol. 1983;101:1557–61.
15. Kaltreider SA, Destro M, Lemke BN. Leiomyosarcoma of the orbit. A case report and review of the literature. Ophthal Plast Reconstr Surg. 1987;3:35–41.
16. Jakobiec FA, Howard G, Rosen M, et al. Leiomyoma and leiomyosarcoma of the orbit. Am J Ophthalmol. 1975;80:1028–42.
17. Cai YC, McMenamin ME, Rose G, et al. Primary liposarcoma of the orbit: a clinicopathologic study of seven cases. Ann Diagn Pathol. 2001;5:255–66.
18. Tehrani AH, Heegaard S, Prause JU, et al. Liposarcoma metastatic to the orbit. Eur J Ophthalmol. 2003;13:108–12.
19. Jakobiec FA, Rini F, Char D, et al. Primary liposarcoma of the orbit. Problems in the diagnosis and management of five cases. Ophthalmology. 1989;96:180–91.
20. Costas A, Castro P, Munoz JM. Primary orbital liposarcoma: case report and review of the literature. Int J Oral Maxillofac Surg. 2001;30:170–2.
21. Cockerham KP, Kennerdell JS, Celin SE, et al. Liposarcoma of the orbit: a management challenge. Ophthal Plast Reconstr Surg. 1998;14:370–4.
22. Howard GR, Nerad JA, Carter KD, et al. Clinical characteristics associated with orbital invasion of cutaneous basal cell and squamous cell tumors of the eyelid. Am J Ophthalmol. 1992;113:123–33.
23. Reifler DM, Hornblass A. Squamous cell carcinoma of the eyelid. Surv Ophthalmol. 1986;30:349–65.
24. Goldberg RA, Rootman J, Cline RA. Tumors metastatic to the orbit: a changing picture. Surv Ophthalmol. 1990;35:1–24.
25. Yin VT, Pfeiffer ML, Esmaeli B. Targeted therapy for orbital and periocular basal cell carcinoma and squamous cell carcinoma. Ophthal Plast Reconstr Surg. 2013;29(2):87–92.
26. Goldberg RA, Rootman J. Clinical characteristics of metastatic orbital tumors. Ophthalmology. 1990;97:620–4.
27. Levy WJ. Neuroblastoma. Br J Ophthalmol. 1957;41(1):48–53.
28. Ahmed AA, Zhang L, Reddivalla N, et al. Neuroblastoma in children: update on clinicopathologic and genetic prognostic factors. Pediatr Hemat. 2017;34(3):165–85.
29. Dutton JJ, Rose JG Jr, DeBacker CM, et al. Orbital Ewing's sarcoma of the orbit. Ophthal Plast Reconstr Surg. 2000;16(4):292–300.
30. Bosma SE, Ayu O, Fiocco M, et al. Prognostic factors for survival in Ewing sarcoma: a systematic review. Surg Oncol. 2018;27(4):603–10.

Orbital Rhabdomyosarcoma

17

Julian D. Perry and Bhupendra C. K. Patel

Introduction

Rhabdomyosarcoma (RMS) represents the most common orbital malignancy in children, and patients with this disease often present to the ophthalmologist. RMS is usually diagnosed at age 7–8 years. The incidence is about four to seven cases per million [1]. Because current therapeutic regimens offer an excellent chance for curing isolated orbital disease, prompt diagnosis and treatment are essential. Much of the success in reducing the morbidity and mortality over the past three decades has been through the collaborative efforts of the Intergroup Rhabdomyosarcoma Studies (IRS) formulated in the 1970s. Treatment of RMS with multiple modalities has transformed the dismal 25% 3-year life expectancy of the 1960s to overall survival (OS) rates of higher than 90% today [2, 3]. With such success, clinicians now have the opportunity to focus on minimizing the serious late sequelae of aggressive therapy.

At present, RMS is generally classified based on the histologic and biologic features of the tumor which help determine the treatment regimen. The two major subtypes are embryonal rhabdomyosarcoma (ERMS) and alveolar rhabdomyosarcoma (ARMS). The embryonal type is the most common and tends to occur in the head and neck region of infants and young children. This type typically shows less-aggressive behavior and provides a better prognosis. The morphological embryonal variants, such as spindle cell and botryoid type, are also highly curable. The alveolar type tends to affect older children and occurs more commonly in the extremities and trunk. It grows faster and requires more intensive treatment than ERMS.

Anaplastic rhabdomyosarcoma (formerly called pleomorphic RMS) is an uncommon type that occurs mostly in adults but may rarely occur in childhood.

Etiology

Most cases of RMS are sporadic occurrences, and its cause is still unknown. There is a slight predilection for males, with a 1.3–1.5:1 male to female ratio [4, 5]. No recognizable environmental, infectious, or biochemical influence in the pathogenesis of RMS exists; however, the malignancy has occurred secondarily in patients after radiotherapy for retinoblastoma and squamous cell carcinoma [6]. Epidemiological studies

J. D. Perry
Department of Ophthalmology and Oculofacial Plastic Surgery, Cole Eye Institute, Cleveland Clinic, Cleveland, OH, USA

B. C. K. Patel (✉)
Division of Facial Cosmetic and Reconstructive Surgery, University of Utah, Salt Lake City, UT, USA
e-mail: bhupendra.patel@hsc.utah.edu

C. J. Hwang et al. (eds.), *Clinical Ophthalmic Oncology*,
https://doi.org/10.1007/978-3-030-13558-4_17

Table 17.1 Familial cancer predisposition syndromes associated with RMS [13]

Li-Fraumeni syndrome (TB53)
Neurofibromatosis type 1 (NF1)
Beckwith-Wiedemann syndrome (11p15 genes)
Costello syndrome (HRAS)
Noonan syndrome
Hereditary retinoblastoma syndrome (RB1)
Nevoid basal cell carcinoma syndrome (PTCH)
Rubinstein-Taybi syndrome (CREMMP)

Reprinted from Xia et al. [13]. With permission from Taylor & Francis

suggest that genetic predisposition may play an important role in RMS [7–12] (Table 17.1).

RMS is rare in adulthood. For that reason, the tumor may be thought to be an infection, inflammatory, or vascular in origin [14–16]. Orbital RMS is more often alveolar and has high tendency to invade the surrounding bone and to extend intracranially, especially in the adult group and even after treatment with radiochemotherapy [17, 18]. The prognosis of adult rhabdomyosarcoma is poor. More than 60% of adult patients have regional or distant metastasis at the initial diagnosis [19, 20].

Pathogenesis

Although RMS was once believed to arise from extraocular muscles, it is now accepted that the tumor originates from undifferentiated mesenchymal cells possessing the capacity to differentiate into striated muscle. Molecular genetic studies indicate that RMS arises by a distinct multistep process of molecular alterations. In addition to the primary mutations (PAX3/PAX7-FKHR gene fusions in ARMS and 11p15.5 allelic loss in ERMS), genetic alterations of other oncogenes and tumor suppressor genes occur as secondary events which may selectively collaborate with the primary alterations. These molecular changes result in high levels of exclusive products of the abnormal chromosome and ultimately contribute to tumorigenic behavior [21].

Table 17.2 Presenting symptoms of orbital rhabdomyosarcoma

Proptosis	80–100%
Globe displacement	80%
Eyelid and conjunctival swelling	60%
Blepharoptosis	30–50%
Palpable mass	25%
Pain	10%

Clinical Features

The clinical features depend on the primary location. Most tumors are extraconal (37–87% of cases), and more than two thirds of cases occupy the anterior or mid-orbit [22].

Symptoms

Orbital RMS is an aggressive tumor, and it commonly presents as rapidly progressive unilateral proptosis with periorbital soft tissue swelling: usually the history is one of proptosis or swelling developing within 2–4 weeks. Lack of recognition and a confusing history of minor periorbital trauma often delay diagnosis (Table 17.2).

Signs

Patients typically have nonaxial proptosis. The most typical location of the tumor is the superonasal quadrant of the orbit, and about half of embryonal rhabdomyosarcomas occur in this location, which causes hypoglobus, exoglobus, and/or blepharoptosis. Abnormal extraocular motility is common. More anteriorly located tumors within the conjunctiva or eyelid tissues may produce periorbital soft tissue changes as eyelid edema, erythema, and conjunctival chemosis. The presentation often masquerades as an infectious or inflammatory process. Fundoscopic examination may show choroidal folds or optic disc edema with posterior orbital lesions (Table 17.3).

Table 17.3 Signs of orbital RMS

Proptosis/hypoglobus
Palpable mass
Lid edema or erythema
Chemosis, exposure keratopathy
Optic neuropathy or disc edema
Choroidal folds

Diagnostic Evaluation

Imaging

When suspicion of RMS occurs, imaging should proceed urgently. Both computed tomography (CT) and magnetic resonance (MR) imaging can play a major role for provisional diagnosis, preoperative evaluation, staging, and follow-up. Each modality has different advantages. Computed tomography shows bony destruction with aggressive lesions better than MR imaging, and serial CT imaging studies may better show bone healing in response to treatment. Conversely, MR imaging demonstrates soft tissue extension better, especially intracranial and cavernous sinus involvement. MR imaging typically requires sedation or general anesthesia for younger patients to avoid motion artifact.

On CT imaging, RMS typically appears as a well-circumscribed, extraconal, homogeneous mass with isodensity relative to extraocular muscle (Fig. 17.1). Calcification usually presents only in association with adjacent bony destruction. Heterogeneous areas may be seen in areas of tumor necrosis or hemorrhage. Signs of periorbital soft tissue swelling are expected, whether the tumor invades into the preseptal area or not. Contrast-enhanced studies show moderate to marked generalized enhancement. Bony erosion can be seen in 30–40% of cases, especially in larger-sized tumors [22, 23].

On MR imaging, orbital RMS exhibits isointensity relative to muscle and brain parenchyma on T1-weighted studies and shows hyperintensity to these tissues on T2-weighted studies. Orbital structures may be encased by tumor extension.

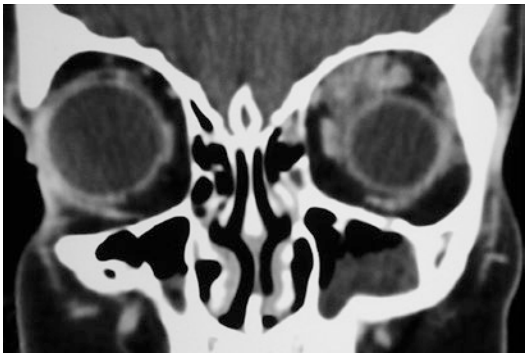

Fig. 17.1 Coronal computed tomographic imaging study of an alveolar rhabdomyosarcoma demonstrates a moderately well-defined superior nasal quadrant lesion that is isodense to the extraocular muscles. Adjacent bony destruction, although common in rhabdomyosarcoma, is not demonstrated in this study

Moderate to marked uniform enhancement is seen on contrast-enhanced images (Fig. 17.2). In suspected paranasal sinus invasion, MR imaging can help differentiate trapped mucous secretion from tumor extension. Paranasal sinus invasion is seen in approximately 20% of cases [22].

Tissue Diagnosis: Biopsy

Prompt open biopsy is preferred over fine-needle aspiration, which may provide inadequate tissue for pathological and immunohistochemical studies (Fig. 17.3). The decisions for excisional versus incisional biopsy depend upon factors such as tumor site, size, adjacent orbital structures, extension, and visual function. Surgery should remove as much tumor load as possible but generally preserve visual structures and function, as RMS carries a reasonable prognosis with adjuvant treatment. Whereas it was accepted that a simple biopsy to confirm the diagnosis was sufficient to commence the accepted treatment regimes, it is now recognized that the surgeon plays a vital role in the outcome of this condition. The surgeon should try to remove as much tumor as safely possible: this improves survival.

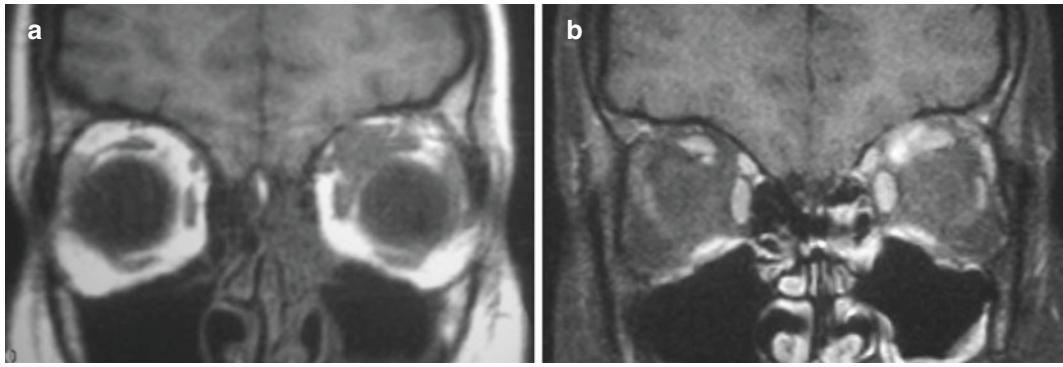

Fig. 17.2 T1-weighted MR imaging study shows the lesion is isointense to the extraocular muscles and hypointense to the orbital fat (**a**). Gadolinium-DTPA enhancement shows moderate enhancement (**b**)

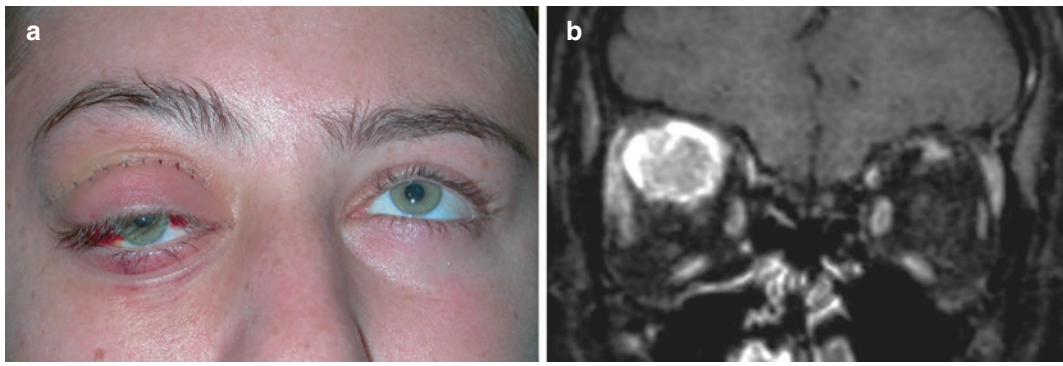

Fig. 17.3 Clinical appearance after orbital biopsy via anterior orbitotomy (**a**) for enhancing superior orbital mass (**b**)

Metastasis tends spread hematogenously rather than via a lymphatic route. The lung and bone represent the most common metastatic targets of this disease. Spread to local lymph nodes occurs uncommonly, typically from more commonly anteriorly located tumors. Palpable nodes require biopsy with cytological confirmation for staging. Orbital RMS requires a full systemic and metastatic evaluation performed by the pediatric oncologist [24].

Salient Diagnostic Findings

Histology

Differentiation from other spindle-cell tumors may present a significant challenge to the pathologist.

Light Microscope

Embryonic RMS is composed of small round cells to elongated or spindle-shaped cells which display various degrees of myogenic differentiation (Fig. 17.4). In abundant eosinophilic cytoplasm, bundles of actin and myosin filaments may produce cross-striations with Masson trichrome staining which is seen in 20–60% of tumors [22, 25].

Alveolar RMS tumor cells are small with a round nuclei and scant cytoplasm. Thin fibrovascular septae separate the tumor into round or ovoid spaces in a pattern reminiscent of lung alveoli (Fig. 17.5).

Immunohistochemistry

Numerous immunohistochemical markers identify the skeletal muscle-specific expression in an

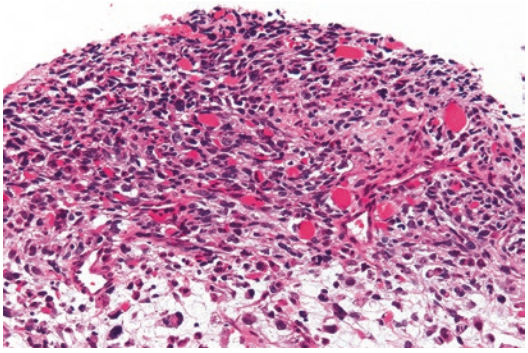

Fig. 17.4 Embryonal rhabdomyosarcoma with a combination of numerous small, primitive cells and larger cells with rhabdomyoblastic differentiation. The rhabdomyoblasts demonstrate eccentric nuclei and abundant densely pink cytoplasm (hematoxylin and eosin, 20×) (Courtesy of Thomas Plesec, MD, Cleveland, Ohio)

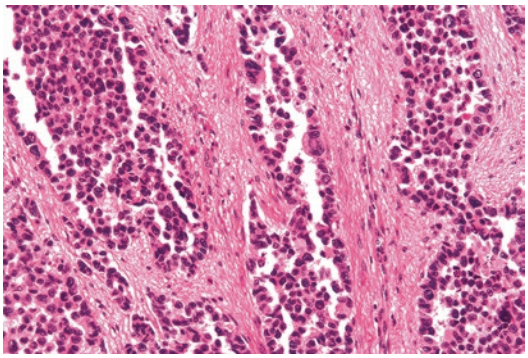

Fig. 17.5 Alveolar rhabdomyosarcoma with its characteristic nested or "alveolar" growth pattern. The nests are often lined by a single layer of malignant cells with discohesive cells lining the central zones (Courtesy of Thomas Plesec, MD, Cleveland, Ohio)

RMS tumor (Fig. 17.6). Desmin provides high sensitivity for tumors with skeletal differentiation, but it is not specific for RMS because it may also stain smooth muscle cells and occasionally myofibroblasts. Muscle-specific actin is seen in some cases of RMS. Vimentin staining assists in ruling out other small round cell tumors of childhood. Antibodies to myogenin and MyoD1 show high expression in more primitive cells (97% sensitivity when combined) [26] but only faintly stain differentiated cell types. Caveolin-3 is a new marker that appears highly sensitive and specific for more differentiated RMS tumors and may help to detect residual tumor following chemotherapy. Table 17.4 lists commonly used stains. Unfortunately these stains are not reliable for subtyping RMS tumor [27].

Molecular Analysis

Due to significant genetic differences between RMS types, cytogenetic studies assist in classifying the primary orbital tumor cells and detecting early disease recurrence.

Alveolar RMS cases often contain a unique chromosome translocation between the FKHR(FOX01A) gene on chromosome 13 either with the PAX3 gene on chromosome 2t(2;13)(q35;q14) or with the PAX7 gene on chromosome 1t(1;13)(p36;q14), which generates PAX3-FKHR and PAX7-FKHR fusion products, respectively. Approximately 20–30% of alveolar RMS cases, however, lack these specific translocations (Fig. 17.7) [13, 26]. In contrast to the alveolar type, embryonal RMS does not show recurrent structural chromosome rearrangements; rather, it often displays aneuploidy (a frequent allelic loss at chromosome 11p15.5 and a frequent chromosome gain of chromosome 8).

Differential Diagnosis

Orbital RMS should be considered in the differential diagnosis of any child with proptosis and subacute edema. The rapidly progressive course and associated inflammatory signs can suggest both benign and malignant etiologies. Malignancies that can simulate RMS include neuroblastoma, leukemia or other metastases, lymphoma, and other sarcomas. Nonmalignant diseases include orbital cellulitis, dacryocystitis, idiopathic orbital inflammation, lymphangioma, capillary hemangioma, and dermoid cyst (Table 17.5).

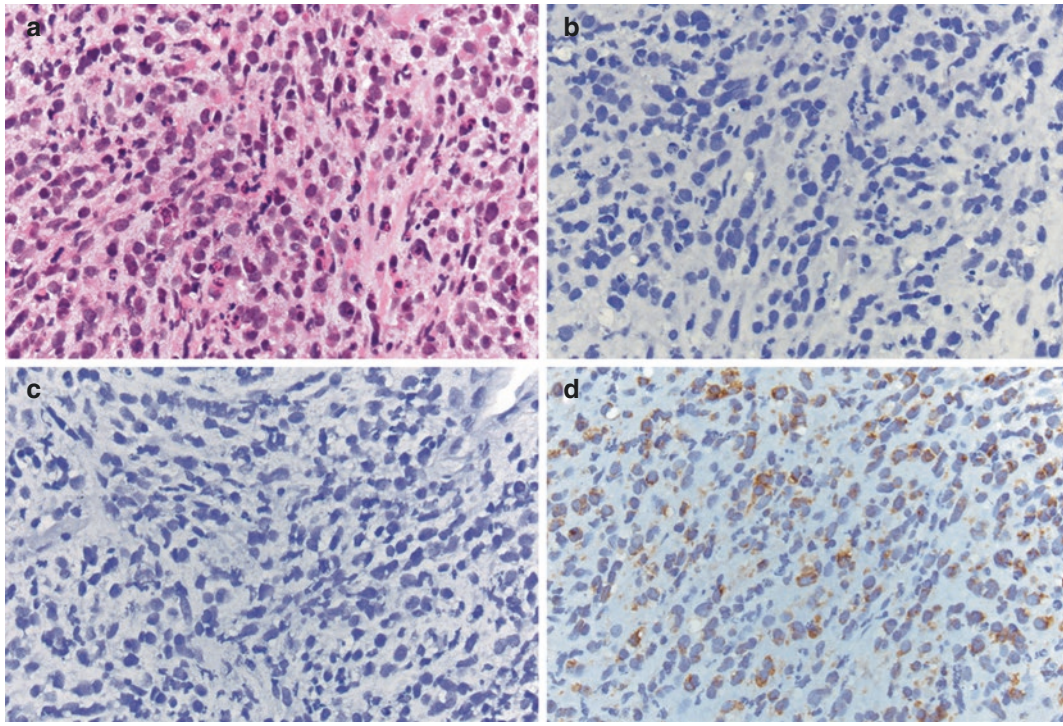

Fig. 17.6 Rhabdomyosarcoma (immunohistochemistry). This tumor is composed predominantly of small primitive cells with innumerable apoptotic bodies engendering a wide differential diagnosis, including carcinoma, lymphoma, and Ewing sarcoma in addition to rhabdomyosarcoma (**a**, hematoxylin and eosin, 20×). Leukocyte common antigen stain (LCA or CD45) is negative, which argues against lymphoma (**b**). Cytokeratin AE1/AE3 is a broad-spectrum keratin that is positive in most carcinomas. In this case, it is negative (**c**). Desmin is a sensitive marker of muscle differentiation, which is positive in this case (**d**). Myogenin (not pictured) is more specific for skeletal muscle differentiation, and it is also positive in this case (Courtesy of Thomas Plesec, MD, Cleveland, Ohio)

Table 17.4 Immunohistochemical markers of rhabdomyosarcoma

Desmin
Myoglobin
Myogenin
MyoD1
Vimentin
Caveolin-3
Muscle-specific actins

Treatment

Current IRS treatment protocols for orbital RMS now consist of combined multimodal therapy including surgery (incisional or excisional biopsy, surgical debulking, or complete gross excision) followed by combinations of multiagent chemotherapy and/or radiation. Surgical margins, histology, and patient age contribute to the risk and regimen treatment stratification necessary to optimize outcome. We run a tumor board with active participation by the surgeon, oncology, radiation oncology, radiology, and pathology to ensure clear understanding of the staging of the disease and clearance margins of the tumor resection [28].

Surgery

The surgical margin outcome determines the grouping classification assignment and influences the radiotherapy and chemotherapy regimen (Table 17.6). Therefore, the initial surgery should debulk as much tumor as possible with care to preserve vital orbital structures.

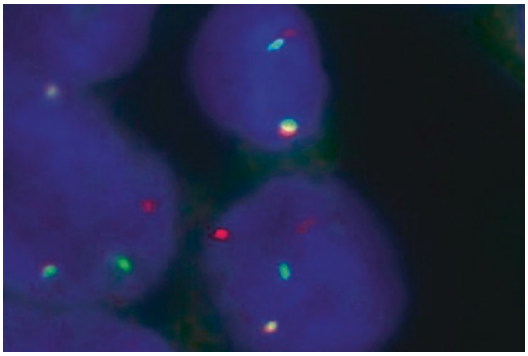

Fig. 17.7 Rhabdomyosarcoma (FISH). Dual-color break-apart fluorescence in situ hybridization (FISH) assay for the detection of FOXO1 (13q14) rearrangements. Two blue- stained nuclei each demonstrate evidence of a FOXO1 translocation as well as an intact chromosome. Split red and green signals indicate the translocation involving the FOXO1 gene, whereas, when the gene is intact, the red and green signals are closely apposed and combine to create a yellow signal (Courtesy of Thomas Plesec, MD, Cleveland, Ohio)

Table 17.5 Imaging helps distinguish lesions that may clinically simulate orbital RMS

Benign lesion	Imaging characteristics
Subperiosteal hemorrhage	MRI: changing signal intensity of hemorrhage evolution, may present fluid level of blood product
Orbital cellulitis	Occur with adjacent paranasal sinusitis
	Contrast enhancement in distinguishing sinus secretion from enhanced tumor invasion, especially in MRI finding
	No bony erosion
Complicated dermoid cyst	Mostly located near zygomaticofrontal suture
	Cystic lesion with adjacent long-standing bone change effect
Lymphangioma	Reveal blood level in the larger cystic spaces "fluid-fluid level"
Malignant lesion	
Langerhans cell histiocytosis	Moth-eaten osteolytic lesion, arise in bone as origin
Chloroma (granulocytic sarcoma)	Frequent bilateral orbital lesion
Lymphoma	Lacrimal gland involvement
	Encase the globe
Metastasis of neuroblastoma	No definite clue
	Need tissue diagnosis or finding of primary tumor

Table 17.6 IRSG grouping system

Group	Definition
I	Localized tumor, completely removed with pathologically clear margins, and no regional LN involvement
II	Localized tumor, grossly removed with (a) microscopically involved margins, (b) involved grossly resected regional LN, or (c) both
III	Localized tumor, with gross residual disease after grossly incomplete removal or biopsy only
IV	Distant metastases present at diagnosis

Well-circumscribed, accessible lesions may allow for complete gross excision. More commonly, surgery results in significant gross residual tumor in order to preserve ocular function. The surgical approach to a RMS should preserve orbital periosteum, which may act as a barrier to local spread. These tumors will often have a pseudo-capsule: we find it helpful to perform a "traction and blunt separation" technique using a broad Freer elevator and avoid the "piece-meal" approach.

Chemotherapy

At present, all RMS patients receive some form of adjunctive chemotherapy. The regimen depends on the histologic type and grouping of the tumor (Table 17.7). The standard regimen is a combination of vincristine, actinomycin D, and cyclophosphamide (VAC). High-risk patients are considered for more additional treatment as topotecan or irinotecan. Some patients with low-risk disease may receive only VA.

Radiotherapy

The radiotherapy is essential for most cases except for completely resected localized lesions (group I). The radiation dose depends predominantly on the residual disease after the primary surgical resection. Low-dose radiation (40 Gy) for ERMS group II provides local tumor control rates of at least 90%. For group III patients, radiation doses are more commonly 50 Gy. Modern

Table 17.7 Orbital RMS: modified IRSG study V treatment protocol

	Risk (protocol)	Group	Age	XRT	Chemo treatment
ERMS	Low risk	I		–	VA
		II a		40 Gy	
		III		50 Gy	
		II b		40 Gy	VAC
		II c		40 Gy	
		III + node positive		50 Gy	
	Intermediate risk	IV	Age < 10 year old	Local and distant RT	VAC ± Topo
	High risk		Age ≥ 10 year old		CPT-11 + VAC
ARMS	Intermediate risk	I, II, III		Local and distant RT	VAC + Topo
	High risk	IV			CPT-11 + VAC

ERMS embryonal, botryoid, or spindle-cell rhabdomyosarcoma, *ARMS* alveolar rhabdomyosarcoma, undifferentiated sarcoma, *XRT* radiotherapy, *VAC* vincristine, actinomycin D, cyclophosphamide, *Topo* topotecan, *CPT-11* irinotecan

Table 17.8 Late ocular sequelae of radiation therapy for orbital RMS [29]

Cataract	82 %
Impaired vision in the treated eye	70 %
Orbital hypoplasia and asymmetry	59 %
Dry eyes	30 %
Ptosis/enophthalmos	28 %

Reprinted from Raney et al. [29]. With permission from John Wiley & Sons

radiotherapy techniques, including intensity-modulated radiotherapy (IMRT), fractionated stereotactic radiotherapy (FSRT), and proton radiotherapy, which deliver high doses to a definite target, may maintain outcomes while decreasing radiation-related side effects.

Follow-Up

After treatment, patients require serial comprehensive ocular examinations that measure visual acuity, proptosis, and extraocular motility. Examinations should evaluate for sequelae of radiation treatment, such as cataract, retinopathy, and keratopathy (Table 17.8). Imaging studies should document new baseline status and residual tumor size. Follow-up should be every 3–4 months for the first year, then every 4–6 months for several years thereafter, and subsequently on a yearly basis with periodic orbital imaging. Secondary biopsy offers low yield with significant risk and should be reserved for patients with clinical indications of recurrence and changes on serial imaging studies [24].

Prognosis

In general, RMS's outcome depends on primary site, tumor size, local extension, presence of nodal and distal metastases, and histologic subtype including molecular analysis.

Isolated orbital involvement carries the best prognosis of all primary RMS locations, with an overall survival rate of 96% and eye preservation rate of 86% [29]. Five-year survival rates for ERMS increased during the period from 1976 to 2000 (60.9–73.4%, respectively), whereas there was no significant improvement for 5-year survival rates of ARMS (40.1 and 47.8%, respectively). Children who present between age 1 and 10 have a more favorable prognosis than infants or young adults. Histologic examination and molecular analysis contribute significantly to prognosis. For the more favorable embryonal tumors, prognosis improves with evidence of genetic hyperploidy. In contrast, less favorable alveolar tumors fare even worse with evidence of tetraploid DNA content [30]. Karyotype detection of chromosomal translocations indicates alveolar morphology, with the t(2;13) PAX3-FKHR fusion gene faring worse than those bear-

ing t(1;13) PAX7-FKHR fusion gene [31]. In the rare instances where orbital disease is refractory to standard treatment, aggressive secondary surgery yields 3-year survival rates up to 70% [32]. Patients with metastatic disease may benefit from myeloablative treatment with stem cell support. Survivors of previous treatment protocols now show the unfortunate side effects of radiotherapy, with over 70% of eyes suffering some degree of vision loss [29]. Other common late sequelae include cataracts and facial hypoplasia.

Nonrhabdomyosarcoma Soft Tissue Sarcomas (NRSTS) (Fig. 17.8a–d)

Unlike rhabdomyosarcomas, NRSTS have no distinguishing immunohistochemical features and are therefore difficult to classify. Recent advances in molecular genetic analyses may help classify these ubiquitous tumors better. More is known about NRSTS outside the orbit: survival in patients with NRSTS appears to be based on tumor invasiveness and size, age at diagnosis, primary tumor site, resection margins, initial resectability, and response to radiation and chemotherapy. NRSTS are poorly responsive to chemotherapy and are also not especially responsive to radiotherapy. Surgery is the mainstay of treatment with or without adjuvant therapy. Wide resection of the primary tumor with tumor-free margins greater than 1 cm is the surgical goal for tumors outside the orbit. NRSTS are uncommon in the orbit but are beginning to be recognized. Complete surgical resection is the most important prognostic factor for extra-orbital NRSTS, and the same probably applies to orbital NRSTS. These tumors present without cross-striations, only focal staining for muscle markers, and lack of TFE3 and FOXO1 gene rearrangements, which differentiates the lesion from orbital rhabdomyosarcoma.

Because of the rarity of NRSTS arising in the orbit, there is little precedent available to guide treatment. Surgical resection (as complete as possible) is important, and chemoradiation therapy is administered [33, 34].

Future Research

New Proposed Classification

Individuals with the PAX7 translocation are younger and have longer event-free survival than those with the PAX3 translocation in the ARMS group, and they seem to respond as well as the ERMS group. Adding chromosomal translocation and specific gene expression profiles to a risk-adapted classification scheme may allow some patients to receive less intensive treatment.

Improving the Standard Treatment

Chemotherapy and Radiation: The currently "ARST0331 protocol" study from IRS V for patients with low-risk ERMS, including most of the orbital RMS patients, is ongoing. The objectives are to maintain excellent survival rates while decreasing radiotherapy doses, decreasing the duration of vincristine and actinomycin D chemotherapy, and adding a total cumulative dose of cyclophosphamide. Limiting the use of these modalities should lower the risk of secondary malignancies and myelosuppression.

Gene and Signaling Pathway Study: Molecularly targeted agents (IGF1R inhibition, antiangiogenic approaches, and mTOR inhibition) are currently under investigation in combination with chemotherapy for patients with recurrent or metastatic RMS to provide less toxic systemic treatments and control the development of this malignant tumor as a vaccine therapy [21, 35].

Conclusion

RMS represents the most common childhood orbital malignancy. Despite recent advancements in treatment, it remains a potentially fatal disease, and current treatment regimens continue to carry significant morbidity. As the management of orbital RMS becomes increasingly complex, close collaboration between the ophthalmic surgeon, pediatric oncologist, and the radiation oncologist becomes necessary to optimize outcome.

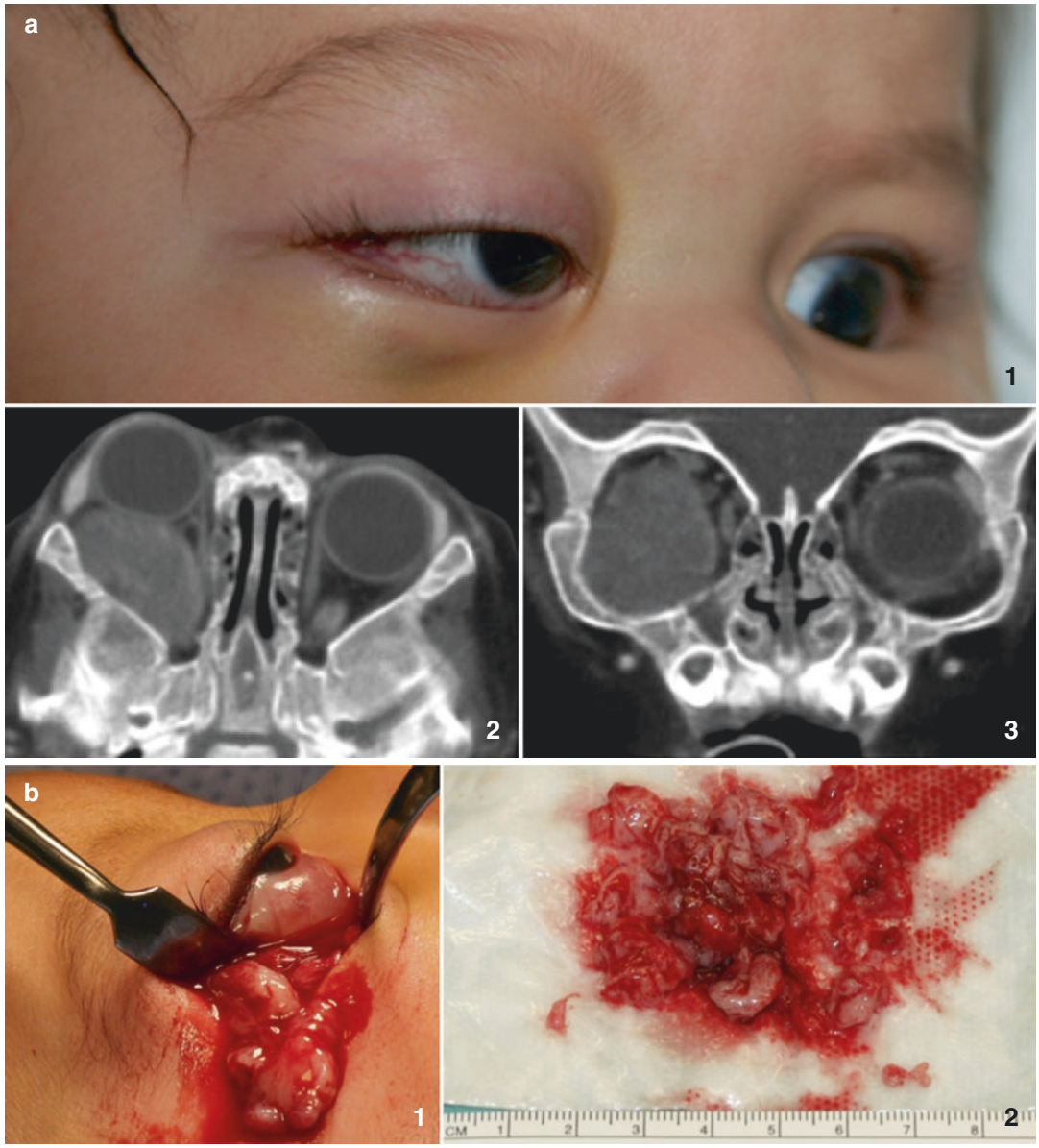

Fig. 17.8 (**a**-1) External photograph demonstrates axial proptosis of the right eye with mild periorbital ecchymosis. (**a**-2,3) Axial and coronal post-contrast CT of the orbits CT of the orbits demonstrates a heterogeneously enhancing intraorbital mass, producing marked proptosis and deformation of the right globe. (**b**-1) Intraoperative photo showing tumor in lateral orbit during excisional biopsy. (**b**-2) Gross tumor specimen. (**c**-1) Hematoxylin and eosin stain × 100 demonstrating patternless sheets of undifferentiated tumor cells. (**c**-2) Hematoxylin and eosin stain × 200 shows brisk mitotic activity and prominent nucleoli. (**c**-3,4) Immunostains for myogenin (**c**-2) and desmin (**c**-3) reveal scattered positive cells, but the majority of the tumor did not stain with these antibodies. (**d**-1,2) Axial T1 weighted post-contrast orbital MRI pretreatment (**d**-1) and posttreatment (**d**-2) demonstrating significant reduction in tumor size after chemoradiation for his first recurrence with a small nodular lesion temporal to the right optic nerve (**d**-2). (**d**-3) 1 month postoperative photo showing reduction in proptosis and periorbital edema

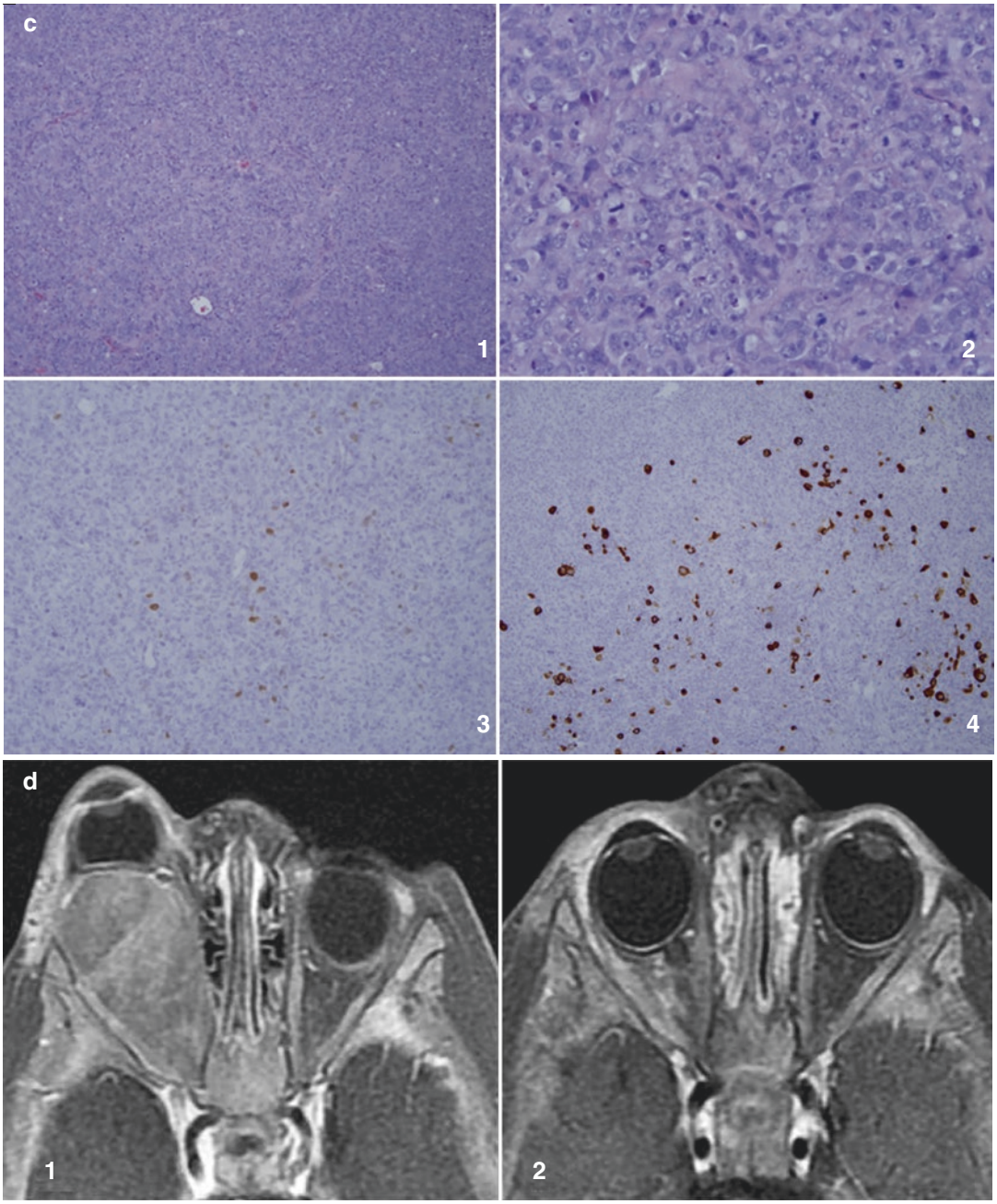

Fig. 17.8 (continued)

Fig. 17.8 (continued)

References

1. Young JL Jr, Ries LG, Silverberg E, et al. Cancer incidence, survival, and mortality for children younger than age 15 years. Cancer. 1986;58:598–602.
2. Friedrich P, Ortiz R, Strait K, et al. Pediatric sarcoma in Central America: outcomes, challenges, and plans for improvement. Cancer. 2012;119(4):871–9.
3. Howard GM, Casten VG. Rhabdomyosarcoma of the orbit in brothers. Arch Ophthalmol. 1963;70:319–22.
4. Dagher R, Helman L. Rhabdomyosarcoma: an overview. Oncologist. 1999;4(1):34–44.
5. Shields CL, Shields JA, Honavar SG, et al. Clinical spectrum of primary ophthalmic rhabdomyosarcoma. Ophthalmology. 2001;108(12):2284–92.
6. Hasegawa T, Matsuno Y, Niki T, et al. Second primary rhabdomyosarcomas in patients with bilateral retinoblastoma: a clinicopathologic and immunohistochemical study. Am J Surg Pathol. 1998;22(11):1351–60.
7. Gripp KW. Tumor predisposition in Costello syndrome. Am J Med Genet C Semin Med Genet. 2005;137C(1):72–7.
8. Gripp KW, Lin AE, Stabley DL, et al. HRAS mutation analysis in Costello syndrome: genotype and phenotype correlation. Am J Med Genet A. 2006;140:1):1–7.
9. Kerr B, Delrue MA, Sigaudy S, et al. Genotype-phenotype correlation in Costello syndrome: HRAS mutation analysis in 43 cases. J Med Genet. 2006;43(5):401–5.
10. Moschovi M, Touliatou V, Papadopoulou A, et al. Rhabdomyosarcoma in a patient with Noonan syndrome phenotype and review of the literature. J Pediatr Hematol Oncol. 2007;29(5):341–4.
11. Samuel DP, Tsokos M, DeBaun MR. Hemihypertrophy and a poorly differentiated embryonal rhabdomyosarcoma of the pelvis. Med Pediatr Oncol. 1999;32(1):38–43.
12. Trahair T, Andrews L, Cohn RJ. Recognition of Li Fraumeni syndrome at diagnosis of a locally advanced extremity rhabdomyosarcoma. Pediatr Blood Cancer. 2007;48(3):345–8.
13. Xia SJ, Pressey JG, Barr FG. Molecular pathogenesis of rhabdomyosarcoma. Cancer Biol Ther. 2002;1(2):97–104.
14. Singh AD, Traboulsi EI, Reid J, et al. Orbital cyst: prenatal diagnosis. Ophthalmology. 2009;116:2042–42.e2.
15. Eghtedari M, Farsiani AM, Bordbar MR. Congenital orbital rhabdomyosarcoma. Ocul Oncol Pathol. 2018;4:165–9.
16. Ahmad TY, Al Houri HN, Al houri AN, et al. Aggressive orbital rhabdomyosarcoma in adulthood: a case report in a public hospital in Damascus, Syria. Avicenna J Med. 2018;8(3):110–3.
17. Kaliaperumal S, Tiroumal S, Rao V. Orbital rhabdomyosarcoma: a case series. Indian J Cancer. 2007;44:104–7.
18. Garduño-Vieyra L, Hernandez-Da Mota SE, Gonzalez CR, et al. Rhabdomyosarcoma in an elderly patient. A case report. Rev Mex Oftalmol. 2017;91:73.
19. Wu TH, Huang JS, Wang HM, et al. Long-term survivors of adult rhabdomyosarcoma of maxillary sinus following multimodal therapy: case reports and literature reviews. Chang Cung Med J. 2010;33:466–71.
20. Joo JH, Han JS, Choi SM, et al. One-year survivor of adult alveolar rhabdomyosarcoma of themaxillary sinus with orbital extension: case report. Medicine. 2018;97(35):e11866.
21. Belyea B, Kephart JG, Blum J, et al. Embryonic signaling pathways and rhabdomyosarcoma: contributions to cancer development and opportunities for therapeutic targeting. Sarcoma. 2012;2012:406239.
22. Chung EM, Smirniotopoulos JG, Specht CS, et al. From the archives of the AFIP: pediatric orbit tumors and tumor-like lesions: nonosseous lesions of the extraocular orbit. Radiographics. 2007;27(6):1777–99.
23. Mafee MF, Pai E, Philip B. Rhabdomyosarcoma of the orbit. Evaluation with MR imaging and CT. Radiol Clin N Am. 1998;36(6):1215–27. xii.

24. Shields JA, Shields CL. Rhabdomyosarcoma: review for the ophthalmologist. Surv Ophthalmol. 2003;48(1):39–57.
25. Napolitano L, Howard J. Electron microscopic observations on non-specific lead staining in the small intestine of the cat after lipid or carbohydrate feeding. Anat Rec. 1968;160(1):25–35.
26. Davicioni E, Anderson MJ, Finckenstein FG, et al. Molecular classification of rhabdomyosarcoma–genotypic and phenotypic determinants of diagnosis: a report from the Children's Oncology Group. Am J Pathol. 2009;174(2):550–64.
27. Fine SW, Lisanti MP, Argani P, et al. Caveolin-3 is a sensitive and specific marker for rhabdomyosarcoma. Appl Immunohistochem Mol Morphol. 2005;13(3):231–6.
28. Dasgupta R, Fuchs R, Rodeberg D. Rhabdomyosarcoma. Semin Pediatr Surg. 2016;25:276–83.
29. Raney RB, Anderson JR, Kollath J, et al. Late effects of therapy in 94 patients with localized rhabdomyosarcoma of the orbit: report from the Intergroup Rhabdomyosarcoma Study (IRS)-III, 1984–1991. Med Pediatr Oncol. 2000;34(6):413–20.
30. Pappo AS, Crist WM, Kuttesch J, et al. Tumor-cell DNA content predicts outcome in children and adolescents with clinical group III embryonal rhabdomyosarcoma. The Intergroup Rhabdomyosarcoma Study Committee of the Children's Cancer Group and the Pediatric Oncology Group. J Clin Oncol. 1993;11(10):1901–5.
31. Sorensen PH, Lynch JC, Qualman SJ, et al. PAX3-FKHR and PAX7-FKHR gene fusions are prognostic indicators in alveolar rhabdomyosarcoma: a report from the Children's Oncology Group. J Clin Oncol. 2002;20(11):2672–9.
32. Lawrence W Jr, Anderson JR, Gehan EA, et al. Pretreatment TNM staging of childhood rhabdomyosarcoma: a report of the Intergroup Rhabdomyosarcoma Study Group. Children's Cancer Study Group. Pediatric Oncology Group. Cancer. 1997;80(6):1165–70.
33. Adesina OO, Zaugg BE, Dries DC, et al. Undifferentiated nonrhabdomyosarcoma soft tissue sarcoma of the orbit. Ophthalmic Plasti Reconstr Surg. 2017;33(3):e57–60.
34. De Niro JE, Cham EM, Silkiss RZ. Undifferentiated sarcoma of the orbit with angiomyxoid features. J Pediatr Ophthalmol Strabismus. 2014;51:e4–7.
35. Gosiengfiao Y, Reichek J, Walterhouse D. What is new in rhabdomyosarcoma management in children? Paediatr Drugs. 2012;14(6):389–400.

Enucleation for Ocular Tumors

18

Bhupendra C. K. Patel and Julian D. Perry

Introduction

Many studies over the past decade report a trend toward fewer enucleations, suggesting that improved treatments prevent end-stage eye disease. Interestingly, however, the incidence of enucleation for neoplasia has not decreased despite the more widespread use of globe-sparing techniques, such as chemotherapy and brachytherapy [1].

Enucleation represents the surgical removal of the globe from the orbit. The term "primary enucleation" is used to designate the first and the only treatment modality for an ocular tumor without any prior or adjunctive therapy. The goal of enucleation surgery for ocular malignancy is to prevent further local orbital spread of disease and to reduce the risk of regional spread and distant metastasis. For over a century, enucleation has played a major role in the treatment of ocular malignancy. In addition to eradicating malignancy, enucleation should also form the structural foundation to restore cosmesis and improve quality of life after what amounts to a devastating amputation to many patients (Table 18.1).

Table 18.1 Goals of enucleation

Remove malignancy with clear margins
Provide a healthy and comfort orbital socket without further complications
Restore quality of life and cosmesis

Indications

The procedure is considered for extensive malignant ocular tumor refractory to other treatments, too advanced for more conservative therapies, or in patients who elect the procedure over other options. Surgery is generally reserved for advanced tumors that destroy visual function, cause intractable pain, or are unlikely to respond to further nonsurgical therapy (Fig. 18.1).

The Collaborative Ocular Melanoma Study (COMS) includes the following indications for primary enucleation for choroidal melanoma:

- A medium-sized tumor (2.4–10 mm in thickness or up to 16 mm in basal diameter) with poor vision (<20/400) or no potential for visual recovery, with consideration of the functional status of the other eye and patient preference
- A large-sized tumor (more than 10 mm in thickness or more than 16 mm in basal diameter) with neovascular glaucoma, optic nerve invasion, blind painful eye, localized extrascleral extension, or patient preference

B. C. K. Patel (✉)
Division of Facial Cosmetic and Reconstructive Surgery, University of Utah, Salt Lake City, UT, USA
e-mail: bhupendra.patel@hsc.utah.edu

J. D. Perry
Department of Ophthalmology and Oculofacial Plastic Surgery, Cole Eye Institute, Cleveland Clinic, Cleveland, OH, USA

C. J. Hwang et al. (eds.), *Clinical Ophthalmic Oncology*,
https://doi.org/10.1007/978-3-030-13558-4_18

Fig. 18.1 As the preoperative external appearance is usually normal, presence of intraocular tumor should be confirmed by indirect ophthalmoscopy before proceeding (Reprinted from Perry et al. [2]. With permission from Elsevier)

The indications for secondary enucleation for choroidal melanoma include failure of conservative therapy and ocular pain from radiation-related complications, such as neovascular glaucoma.

For medium-sized tumors, patients choose a treatment option based on the expectation for vision preservation and the risk of radiation complications, since no survival or long-term quality of life advantages exist for one treatment over the other [3]. For large melanomas, no difference in survival exists between pre-radiation enucleation and primary enucleation [3–5]. The functional status of the fellow eye and patient preference represent important factors in the decision-making process.

For intraocular tumors with limited extrascleral or orbital invasion, enucleation alone risks transecting the orbital component of the tumor and leaving residual disease within the orbit. Modified enucleation with partial tenonectomy or lateral orbitotomy with or without adjuvant therapy has theoretical advantages and avoids exenteration; however, current evidence does not suggest improved survival for any particular technique in these instances [6–9].

For retinoblastoma, enucleation is considered for extensive unilateral disease and neovascular glaucoma or for an eye with advanced disease with no hope for useful vision. Eyes harboring other ocular tumors that fail to respond to conventional therapy or that develop secondary complications leading to a blind, painful eye may be considered for enucleation [10].

When the fundus cannot be visualized, it is important to obtain an ultrasound prior to performing an evisceration to exclude an intraocular tumor. If there is an intraocular mass, the proposed evisceration should be converted to an enucleation.

Preoperative Preparation

Preoperative consideration should be given to the decision for the procedure itself, the type of anesthesia, and the implant used to restore orbital volume after globe removal. Preoperative counseling provides information about advantages, disadvantages, alternatives, risks, and potential complications of enucleation, the orbital implant, and the prosthesis. Genetic counseling should be provided in cases where such information is available. Patients should be made aware that they may develop unexpected symptoms after enucleation, including strain with reading, changes in depth perception, visual hallucinations, and even depression and other unexpected consequences [11, 12]. The surgeon should encourage the patient to volunteer such symptoms and help provide them instruction on how to adapt the loss of an eye. All patients losing an eye meet with our clinical psychologist. For those patients that wish to, an appointment is made to meet the ocular prosthetician.

Given the psychological issues surrounding the loss of an eye, general anesthesia is often preferred over sedation. General anesthesia may allow for better analgesia and hemostasis. Local anesthesia with supplemental monitored intravenous sedation may be more suitable in selected cases, such as those associated with medical risk factors for complications of general anesthesia [13]. In these cases, a supraorbital nerve, an infraorbital nerve, and a modified van Lint block may enhance patient comfort.

The ideal orbital implant should not only restore orbital volume and couple extraocular muscle movement to the prosthesis; it should also maximize biologic compatibility and minimize complications and cost.

Current orbital implants can be classified as integrated or nonintegrated (Chap. 21). Nonintegrated implants are solid, with no capacity for tissue ingrowth or direct attachment to the surrounding orbital tissues. They become encapsulated over time. Extraocular muscle movement is coupled to prosthesis movement by the shape of the implant as it conforms to a concavity within the prosthesis. Nonintegrated orbital implant materials include polymethylmethacrylate (PMMA) and silicone which are spherical.

In contrast, integrated orbital implants contain pores and channels to allow for fibrovascular ingrowth, so the implant may accept a drilled-in motility peg to better couple implant movement to prosthesis movement. These implants are currently made from hydroxyapatite, porous polyethylene, and bioceramic materials. The rectus muscles are sutured directly to the implant or to an overlying wrapping material. Wrapping materials include donor sclera, autogenous fascia, and polyglycolic acid mesh; wrapping materials may increase infection rates and delay fibrovascular ingrowth [14]. Pegging rates have decreased significantly over the last decade, as surgeons have encountered complications from pegging, including mucous discharge, and excessive motility revealing the prosthesis edges. Serious complications from pegging, such as exposure, extrusion, and infection, can occur that may result in loss of the implant. Current pegging rates are under 10% [15]. For unpegged implants, nonintegrated and integrated implants may provide similar motility when they are implanted using similar surgical techniques [16, 17]. As the use of integrated implants adds morbidity and additional cost without clear benefit in unpegged cases, some surgeons are using traditional nonintegrated, solid implants with increasing frequency [18, 19]. There is a tendency to insert porous implants without being covered with sclera or other materials. When such implants need to be removed (exposure, infection, replacement of size, etc.), this causes unnecessary extensive trauma to the orbits because of extensive adhesions and ingrowths of the orbital tissues to the porous implant. Covered implants, especially those covered with sclera, are easier to remove with less trauma. History also keeps on repeating itself with multifaceted (four-breasted) implants being created to try to achieve a pseudo-coupling with the prosthesis. Of course, erosions over the mounds are bound to occur, and one sacrifices volume by using non-spherical implants. There is a reason why the eyeball was designed (or evolved!) to be round: replace like with like! Similarly, oval implants have been created to try to replace volume loss caused by enucleation. We feel it is wiser to use a correctly calculated spherical implant than a shape that is not round.

Most adult patients require at least a 20–22 mm spherical implant to replace 4.2–5.6 ml in volume, respectively, and to leave 2–2.5 ml for a prosthesis. Proper implant size leads toward a better aesthetic result and decreases socket complications. Alternatively, orbital implant size can be determined preoperatively or intraoperatively by using sizing algorithms (Table 18.2).

Given the smaller but growing orbital volume of pediatric patients (less than 5 years of age), determining suitable implant size can present challenges. Some surgeons suggest replacing 70% of the enucleated eye volume with an implant and the remainder with the prosthesis. An implant 2 mm less in diameter than the axial length of the enucleated specimen or 1 mm less than the axial length of contralateral eye can be considered, which typically calls for implant sizes of 18–20. These algorithms tend to improve outcome and produce less socket complications

Table 18.2 Algorithm for implant size

Axial length[a] − 2 mm (− 1 mm in hyperopia)
[a]A-scan of the fellow eye, axial length (mm) = distance from the anterior cornea to the anterior aspect of the posterior sclera + 1 mm

Based on data from Ref. [20].

Table 18.3 Pediatric implant size (axial length − 2 mm = implant diameter)

Axial length/volume, mm/ml	Implant size/volume, mm/ml	% volume, implant	Prosthetic volume, ml	% volume, prosthesis
16/2.1	14/1.4	67	0.7	33
18/3.0	16/2.1	70	0.9	30
20/4.2	18/3.0	71	1.2	29
22/5.6	20/4.2	75	1.4	25
24/7.2	22/5.6	78	1.6	22

Based on data from Ref. [21]

(Table 18.3) [21]. In general, the largest implant that can be placed without undue wound tension should be used.

Technique

While enucleation techniques vary, certain principles apply. Whether employing general or local anesthesia, analgesia and improved hemostasis may be achieved with a retrobulbar or peribulbar block consisting of 3–4 ml of 1 % lidocaine with 1:100,000 epinephrine and 8.4% sodium bicarbonate in a 1:10 ratio with 50 units per 10 ml of hyaluronidase. An additional 1 ml of the same solution can be injected beneath the conjunctiva. Penetration or perforation of the eye with the needle must be avoided during the block (Fig. 18.2).

Blunt Westcott scissors are used to create a 360-degree peritomy. Conjunctiva and the Tenon layer are dissected from underlying sclera using Stevens scissors. Stevens scissors bluntly dissect each oblique quadrant, and each rectus muscle is isolated on a muscle hook. The Tenon layer attachments to each rectus muscle are lysed, and the muscle is secured on a double armed 6-0 polyglactin 910 suture through its insertion. Each muscle is disinserted from the globe using blunt Westcott scissors or Abley scissors.

The inferior oblique muscle insertion is identified and isolated with a muscle hook in the inferotemporal quadrant. The inferior oblique muscle may be cauterized prior to transection in order to minimize bleeding. The superior oblique muscle is identified in the superomedial quadrant and cut. Some surgeons secure the oblique muscles for later suturing to the implant.

After muscle disinsertion, some surgeons inject 2.5 cc of anesthetic solution into the sub-Tenon space of each oblique quadrant using a blunt irrigation tip. This may improve analgesia and hemostasis and displace the globe anteriorly to facilitate access to the optic nerve and reduce the risk of globe injury from the enucleation scissors.

A muscle hook is swept against the ocular surface to identify any remaining attachments that require dissection, and a small incision is created in the posterior Tenon layer using Stevens scissors. A long curved hemostat may be introduced through the posterior Tenon layer incision to clamp the optic nerve in order to maintain hemostasis. The hemostat is inserted with the blades closed to palpate and strum the optic nerve prior to clamping. A hemostat or locking toothed forceps secures the medial rectus muscle stump to assist in gently retracting and elevating the globe. The optic nerve is transected using enucleation scissors, and the globe is removed using the hemostat or forceps on the medial rectus stump. Some surgeons do not clamp the optic nerve because the clamp may diminish the space to apply the enucleation scissors and because clamping may introduce crush artifact to the optic nerve aspect of the specimen. After transection of the nerve, the optic nerve stump is cauterized with bipolar cautery under direct visualization using malleable retractors. Thermal trauma of the orbital soft tissues may cause a loss of orbital volume, so cautery should be minimized and performed only in the area of the optic nerve stump under direct visualization. The posterior orbit can be packed with anesthetic-soaked gauze for a few minutes: this usually reduces the need for extensive cautery.

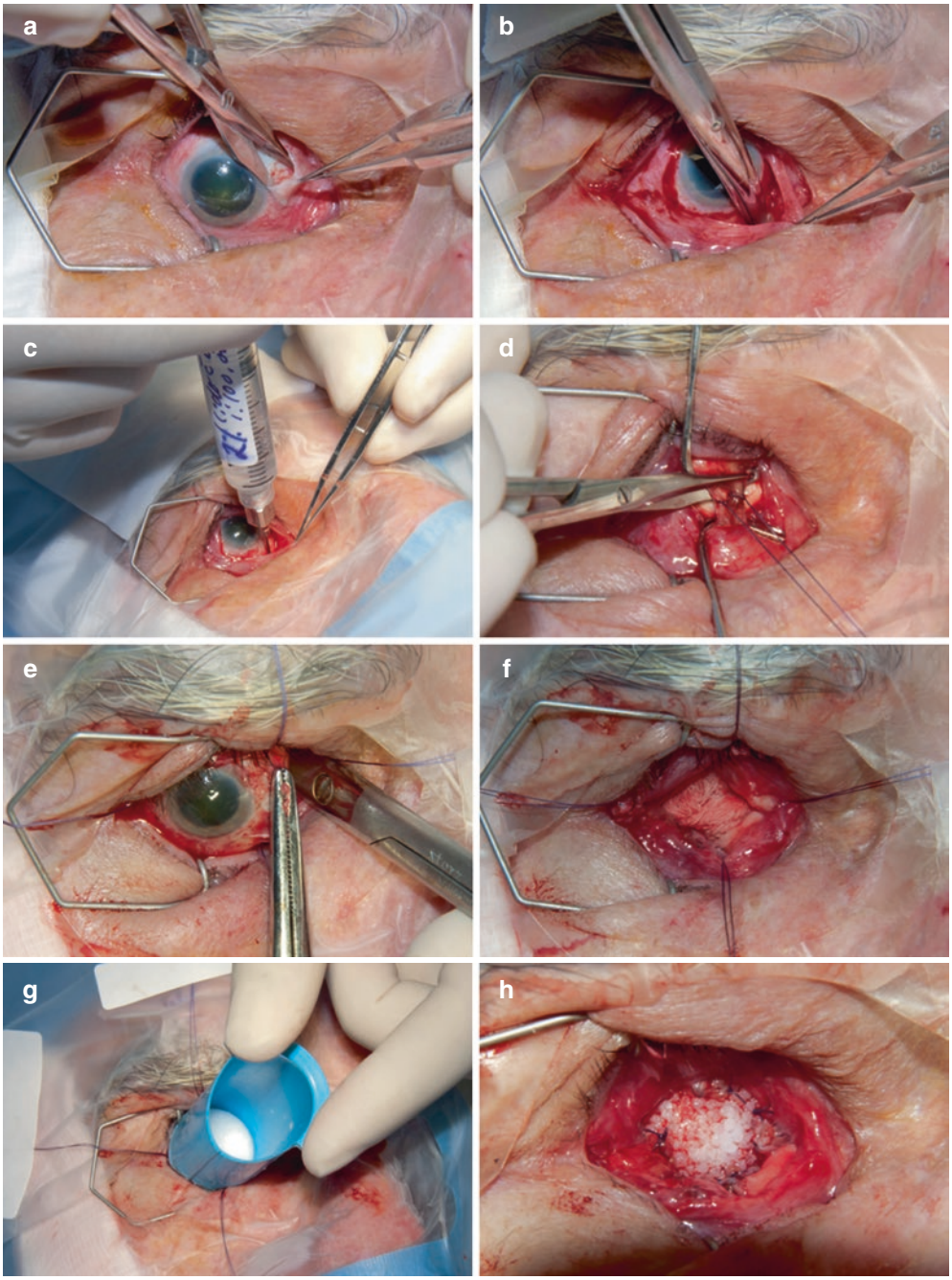

Fig. 18.2 Conjunctival peritomy (**a**) is followed by quadrantic dissection (**b**) and injection of local anesthetic (50:50 mixture of 2% lignocaine with 1 in 100,000 epinephrine and 0.5% bupivacaine) for hemostasis and postoperative analgesia (**c**). Recti muscle is then hooked and disinserted after tagging with 5–0 vicryl suture (**d**). Using a straight artery clamp applied to the medial rectus muscle stump with forward traction and slightly curved enucleation scissor inserted through the medial aspect, the optic nerve is identified by "strumming" (**e**). After resection of the optic nerve and delivery of the globe, the orbit is packed with a wet gauze (**f**). After 5–10 min hemostasis can be usually achieved by this method. A 22 mm unwrapped polyethylene implant is being inserted (**g**). All recti insertions are sutured to the implant in anatomical position (**h**) followed by meticulous closure of Tenon's layer (**i**) and conjunctiva (**j**). After insertion of a conformer, heavy patch is applied (**k**) (Reprinted from Perry et al. [2]. With permission from Elsevier)

Fig. 18.2 (continued)

An injector (Carter implant introducer) or a periosteal elevator with modest posterior digital pressure is used to place the implant. For wrapped implants, windows are created just posterior to each rectus muscle attachment. Direct attachment of the vertical rectus muscles to each other may lead to fornix insufficiency. Porous polyethylene allows for direct suturing of the rectus muscles to the implant according to the manufacturers, but the limitation of later removal atraumatically should be noted as discussed above. For unwrapped solid implants, suturing each rectus muscle to the adjacent rectus muscle suture using a 4-0 polyglactin 910 suture creates a physiologic attachment of the extraocular muscles over the implant with a diameter of approximately 10 mm. The anterior Tenon layer is closed using a running 4-0 polyglactin 910 suture. The conjunctiva is closed using a running 6-0 plain gut suture or 6-0 or 7-0 polyglactin 910 suture.

Antibiotic ointment and a small plastic conformer are placed into the socket, and temporary tarsorrhaphy is performed by suturing the upper and lower eyelids to each other with a suture through the lid margin. A pressure patch is placed up to 1 week (Fig. 18.3) although some patients prefer to remove the patch within 24 hours.

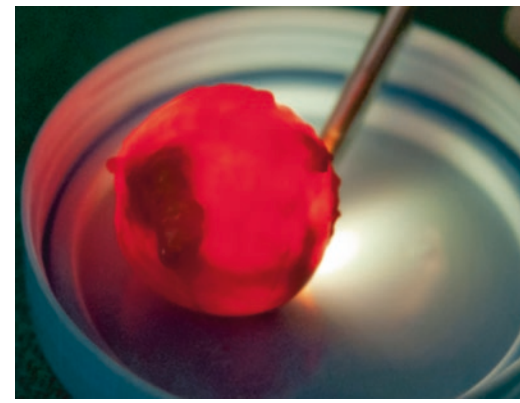

Fig. 18.3 Enucleated globe should be examined to document the length of the optic nerve stump and presence or absence of gross extraocular extension. Using transillumination, tumor can be easily located in preparation to retrieve fresh tissue for diagnostic, prognostic, or research purposes (Reprinted from Perry et al. [2]. With permission from Elsevier)

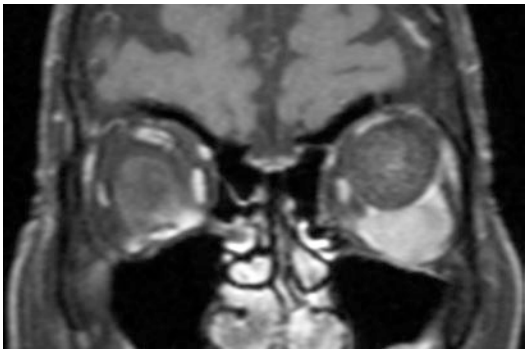

Fig. 18.4 Three years after an eventful enucleation for all large choroidal melanoma, this patient presented with displacement of the prosthesis. MRI (T1, post contrast, fat suppressed) showed enhancing orbital mass. Orbital recurrence of melanoma was confirmed by orbital fine-needle aspiration biopsy. Review of histopathology of the enucleated globe revealed evidence of extension into vortex vein without extrascleral or orbital extension

Table 18.4 Perioperative and immediate postoperative complications

Pain that prolonged hospitalization	1–2%
Hemorrhage	1%
Eyelid swelling	4%

Based on data from Ref. [25]

Table 18.5 Long-term complications of enucleation

Structure	Complication
Ocular surface	Chronic discharge, pyogenic granuloma, giant papillary conjunctivitis, conjunctival cyst
Implant	Exposure, extrusion, migration, infection, volume insufficiency
Eyelid	Laxity, malposition (ectropion, entropion, blepharoptosis)
Fornix	Foreshortening, socket contraction
Optic nerve	Phantom eye syndrome (visual hallucination and phantom eye pain)

Results and Complications

Tumor Recurrence

In choroidal melanoma, tumor recurrence after enucleation is 1.1–14.6%, and it can present up to 20 years following surgery. Patients with extrascleral extension discovered clinically, at surgery, or in the pathology laboratory, should receive periodic orbital imaging, such as CT scan, MR imaging, or positron-emission tomography (PET) scan (Fig. 18.4) [22, 23].

Complications

Despite advances in operative techniques and improvements in orbital implants, postoperative complications continue to occur. Complication rates of 4–28% have been reported [24, 25].

In the early postoperative period, local complications common to all surgeries, such as pain, swelling, and hemorrhage, may occur (Table 18.4). Early conjunctival wound dehiscence may also occur [26]. While conjunctival wound dehiscence may occur more commonly in patients with a history of preoperative radiation (8% vs. 4%) [24], this complication is often the result of poor technique. Proper implant sizing, posterior implant placement, and efforts to minimize wound tension minimize this complication. Early infection is uncommon and occurs equally between radiated and non-radiated eyes. Long-term complications can involve the surface, implant, eyelid, or the fornices (Table 18.5).

Significant overlap exists between these complications, and many can be avoided with proper surgical technique and implant sizing and placement. In the COMS large tumor trial, patients who received pre-enucleation radiation had an overall complication rate of 8%, whereas patients who did not receive radiation had a complication rate of 4% [25].

Additional complications of pegged implants include chronic discharge, visible prosthesis edges on extreme gaze, peg malposition, peg cracking, and an audible peg click [27]. Reports on overall complication rates vary widely for porous and nonporous implants and for pegged and unpegged implants. However, general trends among the various implant choices exist. While porous implants may not extrude as often as solid implants because of fibrovascular ingrowth, they likely incur a higher exposure rate versus silicone implants, and nearly all exposures will ultimately require surgical repair. Reported exposure rates

range from 0 to 33.3% for porous implants [28, 29]. A recent survey revealed an overall exposure rate of only 3%, with the vast majority of events occurring with porous implants rather than solid implants [27]. A meta-analysis of exposure rates of enucleation implants demonstrated a 1.3% rate with silicone, a 4.9% rate with coralline hydroxyapatite, and an 8.1% rate with porous polyethylene [30]. For pegged implants, all complication rates are greater, including pyogenic granuloma formation (14%), exposure (6%), infection (5%), and peg malposition (5%) [27].

Most exposed and extruded implants are chronically infected and will require surgical intervention to remove the avascular portion of the implant (and possibly the entire implant) and place vascularized tissue over the new/revised implant. Free mucous membrane implants placed directly over the exposed implant without removing the avascular and chronically infected portion rarely survive. Tarsoconjunctival flaps may be placed over the exposure after debriding the implant, but these flaps may produce fornix foreshortening. Dermis fat grafts may be placed over the debrided implant as well, but survival will depend upon the underlying vascularity. Volume insufficiency can be addressed with deep orbital wedge implants or replacement of a small implant with a larger one. Injections of hyaluronic acid filler substances and free fat grafts have also been used to augment orbital volume. Fornix insufficiency can be addressed with free mucous membrane grafts or allografts. Dermis fat grafts can simultaneously address volume and conjunctival insufficiency.

Phantom eye syndrome is increasingly recognized to be frequent and persistent even several years after enucleation. Visual hallucination and phantom eye pain (penetrating, shooting, or superficial) may be present in 42 and 23% of cases, respectively [31].

Postoperative Pain Control

Traditionally, surgeons have injected the orbit prior to surgery and at the end of surgery with a mixture of lidocaine and bupivacaine. This usually gives adequate anesthesia postoperatively for up to 7 hours. Some surgeons have delivered local anesthesia via an orbital catheter after surgery [32]. Most patients require oral narcotic analgesics for several days after surgery. The combination of the effects of the anesthesia, the pressure created by postoperative swelling, and the pain also contribute to postoperative nausea.

Liposomal bupivacaine (Exparel, Pacira Pharmaceuticals, Parsippany, NJ, USA) is an extended-release liposomal formulation of bupivacaine administered by injection and has been Food and Drug Administration approved for postsurgical local anesthesia. The duration of action is up to 72 hours (bupivacaine has an analgesic effect of up to 7 hours). Liposomal bupivacaine has been successfully used in breast surgery and orthopedic surgery [33, 34]. Of late, we give a bupivacaine retrobulbar injection at the start of surgery, followed by a retrobulbar injection of a mixture of 50% liposomal bupivacaine (13.3 mg/ml) and 50% bupivacaine 0.25% with 1:200,000 epinephrine, where the surgical facility formulary allows us to access to the liposomal bupivacaine. Like other authors [35], we have found a decrease in the need for oral narcotic analgesics. We do prescribe hydrocodone/acetaminophen (5 mg/300 mg) but have them convert to ibuprofen or naproxen as quickly as possible. Overall, for enucleation and evisceration, this use of liposomal bupivacaine has improved postoperative pain control, but this comment is only based on five patients to date (all following enucleation).

Side effects (more than 5%) of bupivacaine alone include headache, nausea, constipation, and vomiting. With liposomal bupivacaine, the side effects include nausea, constipation, vomiting, flatulence, pruritis, and urinary retention [36].

Costs must always be considered by all physicians: this also applies to the choice of implants in the case of enucleation and evisceration. The approximate cost per dose of liposomal bupivacaine is $ 300 and that for bupivacaine is $1–$3 (these are wholesale costs to hospitals). Indirect savings can accrue from reduced postoperative need for opiate analgesics and shorter inpatient

stay for certain procedures. As the price difference is substantial, authors have, quite correctly, suggested that proper comparative studies need to be completed prior to routinely using liposomal bupivacaine for procedures.

Alternative Technique of Enucleation

When performing an enucleation with retinoblastoma, it is important to obtain a long piece of optic nerve, especially when preoperative imaging indicates spread of tumor down the optic nerve. In many of these eyes, the tumor us large and the globe enlarged, which can make getting a long piece of the optic nerve difficult. We have been sent patients where the optic nerve has been transected during enucleation and the tumor extends beyond the cut end of the nerve. This necessitates further surgery to remove the optic nerve posteriorly and irradiation to the socket. The other concern with eyes which are full of tumor is the risk of a partial enucleation which has been reported when the posterior part of the globe is transected instead of the optic nerve: this happens because the globe is full of tumor and the resection posteriorly is being performed blindly.

In order to overcome these risks and problems, we have applied our superomedial skin crease approach to the optic nerve to these patients. Essentially, the enucleation proceeds as a normal enucleation until the extraocular muscles have been detached from the globe. At this point, a superomedial skin crease incision is made, and the optic nerve is visualized. Through this approach, it is possible to cut the optic nerve so as to obtain a long optic nerve segment. This approach also ensures that the risk of transecting the globe is negated. Once the globe is delivered, the skin crease incision is closed, and the enucleation is completed in the standard fashion. Using this technique, we have routinely been able to obtain optic nerve lengths in excess of 10 mm when enucleating for retinoblastomas and been able to safely enucleate globes full of tumor.

Follow-Up

An anophthalmic socket patient requires lifelong follow-up, with the aim to address three major issues: comfort (a healthy socket with adequate structure allows for comfortable retention of an ocular prosthesis), cosmesis (symmetry of eyelid position, prosthesis projection, soft tissue contour, and prosthetic movement is never perfect but can be maximized with additional surgery or revision of the prosthesis if needed; aging changes and the altered ligamentous structures after enucleation often produce cosmetic issues that may benefit from additional surgery), and disease recurrence (follow-up should include examination of the eye socket for signs of disease recurrence in addition to evaluating socket fornices, volume, implant, and eyelid position) [37].

Conclusion

Enucleation still represents the treatment of choice for a variety of ocular malignancies and tumors. Enucleation removes malignancy with clear margins to reduce metastasis and improve survival and allow for the comfortable retention of an ocular prosthesis to restore cosmesis. Understanding the principles of enucleation surgery should improve functional and aesthetic results while minimizing complications.

References

1. Setlur VJ, Parikh JG, Rao NA. Changing causes of enucleation over the past 60 years. Graefes Arch Clin Exp Ophthalmol. 2010;248(4):593–7.
2. Perry JD, Singh AD, Mehta MP. Enucleation for choroidal melanomas. In: Ryan SJ, editor. Retina. St. Louis: Elsevier; 2011.
3. Melia M, Moy CS, Reynolds SM, et al. Quality of life after iodine 125 brachytherapy vs enucleation for choroidal melanoma: 5-year results from the Collaborative Ocular Melanoma Study: COMS QOLS report no. 3. Arch Ophthalmol. 2006;124(2):226–38.
4. Jampol LM, Moy CS, Murray TG, et al. The COMS randomized trial of iodine 125 brachytherapy for choroidal melanoma: IV. Local treatment failure and enucleation

in the first 5 years after brachytherapy. COMS report no. 19. Ophthalmology. 2002;109(12):2197–206.
5. Fine SL, Hawkins BS. The investigators' perspective on the collaborative ocular melanoma study. Arch Ophthalmol. 2007;125(7):968–71.
6. De Potter P, Shields JA, Shields CL, et al. Modified enucleation via lateral orbitotomy for choroidal melanoma with orbital extension: a report of two cases. Ophthal Plast Reconstr Surg. 1992;8(2):109–13.
7. Fusetti S, Parrozzani R, Urban F, et al. Modified enucleation for choroidal melanoma with large extrascleral extension. Orbit. 2010;29(2):70–5.
8. Singh AD, Jacques R, Rundle PA, et al. Combined enucleation and orbitotomy for choroidal melanoma with orbital extension. Eye (Lond). 2006;20(5):615–7.
9. Blanco G. Diagnosis and treatment of orbital invasion in uveal melanoma. Can J Ophthalmol. 2004;39(4):388–96.
10. Moshfeghi DM, Moshfeghi AA, Finger PT. Enucleation. Surv Ophthalmol. 2000;44(4):277–301.
11. Amaro TA, Yazigi L, Erwenne C. Depression and quality of life during treatment of ocular bulb removal in individuals with uveal melanoma. Eur J Cancer Care (Engl). 2010;19(4):476–81.
12. Coday MP, Warner MA, Jahrling KV, et al. Acquired monocular vision: functional consequences from the patient's perspective. Ophthal Plast Reconstr Surg. 2002;18(1):56–63.
13. Yen KG, Elner VM, Musch DC, et al. Periocular versus general anesthesia for ocular enucleation. Ophthal Plast Reconstr Surg. 2008;24(1):24–8.
14. Gayre GS, Lipham W, Dutton JJ. A comparison of rates of fibrovascular ingrowth in wrapped versus unwrapped hydroxyapatite spheres in a rabbit model. Ophthal Plast Reconstr Surg. 2002;18(4):275–80.
15. Viswanathan P, Sagoo MS, Olver JM. UK national survey of enucleation, evisceration and orbital implant trends. Br J Ophthalmol. 2007;91(5):616–9.
16. Custer PL, Kennedy RH, Woog JJ, et al. Orbital implants in enucleation surgery: a report by the American Academy of Ophthalmology. Ophthalmology. 2003;110(10):2054–61.
17. Colen TP, Paridaens DA, Lemij HG, et al. Comparison of artificial eye amplitudes with acrylic and hydroxyapatite spherical enucleation implants. Ophthalmology. 2000;107(10):1889–94.
18. Perry JD, Tam RC. Safety of unwrapped spherical orbital implants. Ophthal Plast Reconstr Surg. 2004;20(4):281–4.
19. Wells TS, Harris GJ. Direct fixation of extraocular muscles to a silicone sphere: a cost-sensitive, low-risk enucleation procedure. Ophthal Plast Reconstr Surg. 2011;27(5):364–7.
20. Kaltreider SA, Lucarelli MJ. A simple algorithm for selection of implant size for enucleation and evisceration: a prospective study. Ophthal Plast Reconstr Surg. 2002;18(5):336–41.
21. Kaltreider SA, Peake LR, Carter BT. Pediatric enucleation: analysis of volume replacement. Arch Ophthalmol. 2001;119(3):379–84.
22. Shields JA, Augsburger JJ, Dougherty MJ. Orbital recurrence of choroidal melanoma 20 years after enucleation. Am J Ophthalmol. 1984;97(6):767–70.
23. Asensio Sanchez VM, Alonso M, Sierra JM. Positron emission tomography in the diagnosis of orbital relapse of choroidal melanoma. Arch Soc Esp Oftalmol. 2005;80(2):113–5.
24. Tataru CP, Pop MD. Enucleation in malignant choroidal melanoma – results in 15 years of using a new material in the prosthesis of the orbital cavity. J Med Life. 2012;5(2):185–8.
25. The Collaborative Ocular Melanoma Study (COMS) randomized trial of pre-enucleation radiation of large choroidal melanoma III: local complications and observations following enucleation COMS report no. 11. Am J Ophthalmol. 1998;126(3):362–72.
26. Sami D, Young S, Petersen R. Perspective on orbital enucleation implants. Surv Ophthalmol. 2007;52(3):244–65.
27. Su GW, Yen MT. Current trends in managing the anophthalmic socket after primary enucleation and evisceration. Ophthal Plast Reconstr Surg. 2004;20(4):274–80.
28. Nunery WR, Heinz GW, Bonnin JM, et al. Exposure rate of hydroxyapatite spheres in the anophthalmic socket: histopathologic correlation and comparison with silicone sphere implants. Ophthal Plast Reconstr Surg. 1993;9(2):96–104.
29. Nunery WR, Cepela MA, Heinz GW, et al. Extrusion rate of silicone spherical anophthalmic socket implants. Ophthal Plast Reconstr Surg. 1993;9(2):90–5.
30. Custer PL, Trinkaus KM. Porous implant exposure: incidence, management, and morbidity. Ophthal Plast Reconstr Surg. 2007;23(1):1–7.
31. Rasmussen ML. The eye amputated - consequences of eye amputation with emphasis on clinical aspects, phantom eye syndrome and quality of life. Acta Ophthalmol. 2010;88 Thesis 2:1–26.
32. Merbs SL, Grant MP, Iliff NT. Simple outpatient postoperative analgesia using an orbital catheter after enucleation. Arch Ophthalmol. 2004;122:349–52.
33. Butz DR, Shenaq DS, Rundell VL, et al. Postoperative pain and length of stay lowered by use of exparel in immediate implant-based breast reconstruction. Plast Reconstr Surg Glob Open. 2015;3:e391.
34. Surdam JW, Licini DJ, Baynes NT, et al. The use of exparel (liposomal bupivacaine) to manage postoperative pain in unilateral total knee arthroplasty patients. J Arthroplast. 2015;30:325–9.
35. Ang MJ, Silkiss RZ. The use of long-acting liposomal bupivacaine (exparel) for postoperative pain control following enucleation or evisceration. Ophthalmic Plast Reconstr Surg. 2018;34(6):599.
36. Noviasky J, Pierce DP, Whalen K, et al. Bupivacaine liposomal versus bupivacaine: a comparative review. Hosp Pharm. 2014;49(6):539–43.
37. Shields CL, Shields JA. Retinoblastoma management: advances in enucleation, intravenous chemoreduction, and intra-arterial chemotherapy. Curr Opin Ophthalmol. 2010;21(3):203–12.

19 Orbital Exenteration

Elad Ben Artsi, Suresh Sagili, and Raman Malhotra

Introduction

Orbital exenteration is defined as removal of all the orbital contents including the periorbita and eyelids. The aim of exenteration is to achieve local control of disease extending to the orbit while preserving normal tissues whenever possible to optimize surgical rehabilitation. The procedure can vary from subtotal (sometimes termed as anterior or partial) exenteration, for anteriorly located tumors, to total or complete exenteration. Either type could be with or without eyelid sparing. If the bone of the orbit is invaded, an "extended" exenteration is required that includes resection of the diseased bone. The ethmoids, maxillary wall, and zygomatic bone are commonly resected in extended orbital exenteration.

Indications

Orbital invasion by periocular cutaneous malignant tumors (basal cell carcinoma, sebaceous gland carcinoma, squamous cell carcinoma, and melanoma) remains the most common indication for orbital exenteration [1–3]. Other indications include tumors arising in the conjunctiva, orbit, globe, or paranasal sinuses.

Eyelid Malignant Tumors

Basal cell carcinoma (BCC) is the most common malignant skin tumor accounting for approximately 90% in most series [4, 5], squamous cell carcinoma (SCC) and sebaceous gland carcinoma (SGC) each comprising approximately 4–6% of cases. The reported incidence of orbital invasion by periocular cutaneous BCC and SCC is 1.6–2.5 and 5.9%, respectively [6, 7]. Recurrent tumor, large tumor, medial canthal location, infiltrative and morpheic histologic growth patterns, perineural invasion, and patient's age are known risk factors for orbital invasion by all above eyelid tumors [8]. Orbital invasion usually presents as mass effect (globe displacement, ptosis) or signs of tissue infiltration (restricted ocular motility, enophthalmos, immobile eyelids, fixation of the tumor to bone) [6].

Once the diagnosis of orbital invasion is made, the treatment modality should be individualized and chosen with consideration of the extent of orbital involvement, visual function, and the patient's general health. Exenteration may be combined with adjunctive radiotherapy in cases in which margins are not clear or in high-risk aggressive tumors with perineural invasion (PNI).

E. B. Artsi (✉) · R. Malhotra
Corneo-Plastic Unit, Queen Victoria Hospital, East Grinstead, UK

S. Sagili
Ophthalmology Department, The Royal Shrewsbury Hospital, Shropshire, UK

C. J. Hwang et al. (eds.), *Clinical Ophthalmic Oncology*, https://doi.org/10.1007/978-3-030-13558-4_19

Although orbital invasion by BCC has been traditionally managed by exenteration, an alternative conservative (non-exenterating) excision may be considered in selected cases in early stages of anterior orbital invasion [6]. In selected cases, when there is only anterior orbital involvement or in patients with a single eye, local excision (Fig. 19.1) with or without radiotherapy and close follow-up with regular scans (preferably magnetic resonance imaging, MRI) is a possible alternative option (globe-sparing excision). Madge et al. reported a 20 case series of medial canthal BCCs, complicated by anterior orbital invasion and managed using globe-sparing surgical techniques rather than exenteration [6]. There was one recurrence in this series in a patient with previously recurrent disease. Surgical technique involved en bloc excision of visible tumor plus a clinically tumor-free margin. The bone was removed as part of an en bloc specimen in five patients. The lacrimal sac was removed in every patient. Frozen-section histologic examination was used for margin control in eight patients (40%) and rapid paraffin in nine patients (45%). A combination of techniques (frozen section then paraffin, Mohs' surgery then paraffin section) was used in three patients to address cutaneous and then deeper orbital margins, respectively. The decision to exenterate or to pursue a conservative surgical excision should be made after a full discussion with the individual patient and taking into consideration the level of vision in each eye.

Recently, Sagiv et al. [9] reported their experience with neoadjuvant use of vismodegib (Erivedge, Genentech, given orally at 150 mg daily) followed by globe-preserving surgery in eight patients with locally advanced (T4 per American Joint Committee on Cancer (AJCC) 8th edition) BCC. Patients were treated for a median of 14 months. All final surgical margins were negative for tumor. Five patients

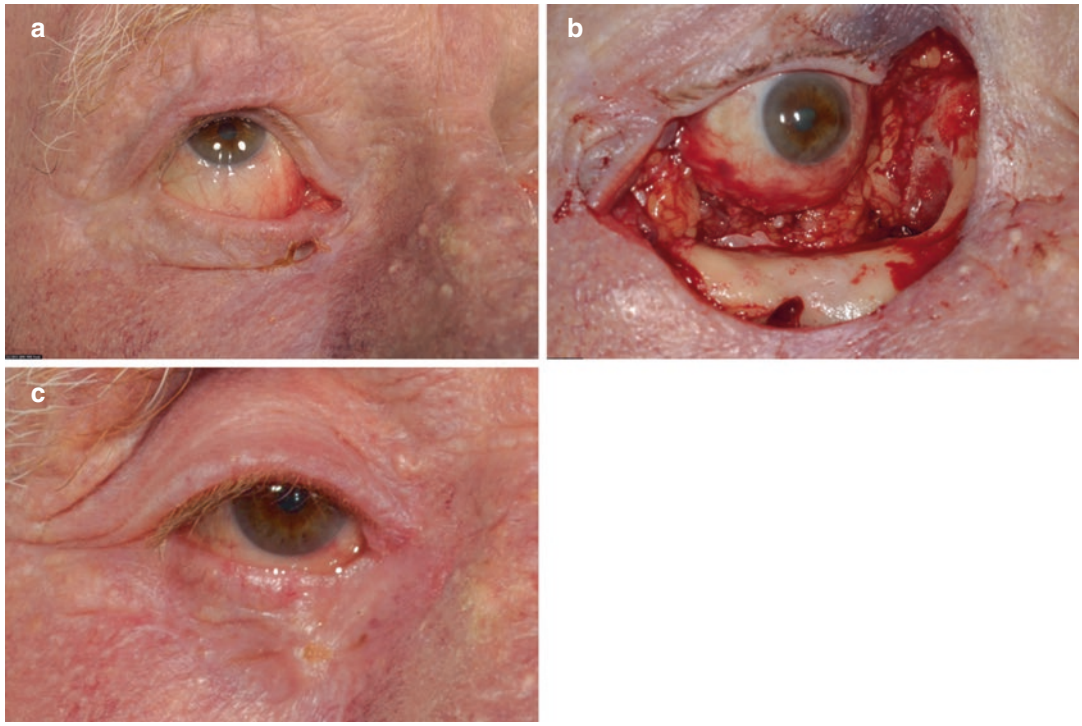

Fig. 19.1 Recurrent lower eyelid BCC invading the anterior orbit (**a**). Anterior orbitectomy was performed (globe sparing) to excise the tumor along with anterior orbital tissue and lacrimal sac with periosteum (**b**). The defect was closed using a midline forehead pericranial periosteal flap and skin graft. Appearance 4 months later (**c**)

demonstrated complete response to vismodegib with no residual BCC found on histology. After a mean follow-up of 18 months (range, 6–43) from surgery, all patients were off vismodegib and without evidence of disease.

Orbital invasion has been reported in 6–45% of SGC cases; orbital exenteration with or without adjuvant radiotherapy may help reduce the potential for metastasis and improve survival [10–12]. The presence of conjunctival intraepithelial (pagetoid) spread in SGC of eyelids has been reported to traditionally carry a higher likelihood for requiring orbital exenteration [13].

Conjunctival Malignant Tumors

The most common conjunctival tumors that require exenteration are melanoma and squamous cell carcinoma. McKelvie et al. reported orbital invasion in 15% of cases with conjunctival squamous cell neoplasia and performed orbital exenteration in all these cases [14]. Conjunctival squamous cell carcinoma, particularly the rare variants, mucoepidermoid or spindle cell carcinomas, tends to invade the orbit, and in such cases, orbital exenteration generally achieves tumor control [15]. The advent of topical chemotherapy brought a paradigm shift in the management of ocular surface squamous neoplasia with only advanced invasive lesions requiring exenteration. Miller et al. presented 38 patients with advanced conjunctival SCC with 47% invading the orbit. Of the treated patients (n = 35), 28% underwent exenteration, while the rest were treated with local excision. The recurrence rate of exenterated patients was lower than those who had had local excision (20% vs 52%, respectively) although that was not statistically significant. None of the recurrent cases after local excision needed further exenteration in a mean follow-up of 2 years [16].

Shields et al. [17] recommended orbital exenteration in extensive recurrent conjunctival melanoma and in cosmetically unacceptable or non-resectable neoplasm without demonstrable metastasis. In cases of advanced conjunctival melanoma, they recommended an eyelid-sparing exenteration, which provides more rapid healing of the socket. In recent years however, adjunctive brachytherapy and topical chemotherapy have been reported to achieve high rates of local tumor control in conjunctival melanoma, obviating the need for exenteration [18].

Intraocular Malignant Tumors

The management of choroidal melanoma with extrascleral extension has been a subject of controversy with some authors proposing orbital exenteration whenever extrascleral extension is demonstrated and others reporting it to be of no value in increasing survival [17, 19]. Although extrascleral extension of choroidal melanoma is associated with an increased risk of metastasis, there has been no clinically significant difference noted in survival probabilities of patients undergoing early exenteration compared to enucleation alone, on extended follow-up [19, 20]. Poor prognosis in these patients is due to the increased risk of metastasis associated with extrascleral extension. Anterior extrascleral extension can be treated by local resection with enucleation or scleral reinforcement after local radiation therapy. Advanced extension may be dealt with by enucleation with resection of all visible orbital melanoma followed by radiation [21].

Exenteration as a first-line treatment in the management of extraocular retinoblastoma is obsolete [22]. Retinoblastoma invading the orbit can now be managed with combination therapy consisting of neoadjuvant chemotherapy followed by enucleation, subtotal exenteration, or complete exenteration, depending on the orbital tumor response to the neoadjuvant treatment. Honavar et al. suggested consolidation of this regimen with external beam radiotherapy and further adjuvant chemotherapy and reported dramatic improvement of mortality rate [23].

Orbital Malignant Tumors

The primary modality of treatment of orbital rhabdomyosarcoma is combined radiotherapy

and chemotherapy. Orbital exenteration may be indicated in cases of incomplete tumor regression or in cases of recurrence after treatment with chemotherapy and radiotherapy [24].

Malignant epithelial tumors of the lacrimal gland have traditionally been treated with orbital exenteration or extended orbital exenteration with resection of the adjacent bony wall when needed, followed by radiotherapy. Nevertheless, patients still experienced local-regional recurrence and distant relapse and death with a 5-year survival of approximately 50%. In recent years eye-preserving surgery followed by adjuvant radiotherapy for lacrimal gland carcinoma has gained in popularity. Woo et al. reported 37 patients with a median follow-up time of 53 months (4-217) who underwent eye-preserving surgery followed by adjuvant radiotherapy for lacrimal gland carcinoma. For the entire cohort, the 5-year recurrence-free, disease-free, and overall survival rates were 44.8%, 72.9%, and 87.4%, respectively [25].

Paranasal Sinus Malignant Tumors

Present studies often categorize the orbital invasion into erosion of the bony orbital wall (grade I), involvement of the orbital periosteum (grade II), and penetration beyond the orbital periosteum and involvement of the orbital soft tissues (grade III) [26]. For low- and middle-grade orbital involvement, most authors recommend preservation of the orbit plus radiotherapy. High-grade orbital involvement poses more controversies. Recently, Safi et al. compared exenteration of the orbit with preservation of the orbit plus radiotherapy for grade III orbital invasion of sinonasal malignancies. Exenteration of the orbit was associated with a significantly better 5-year overall survival rate (65.5%) than preservation of the orbit (14%) [27].

As the eyelids are rarely involved by tumors arising from paranasal sinuses, an eyelid-sparing exenteration can usually be performed in these cases.

Miscellaneous Diseases

Orbital exenteration has been reported in the management of advanced or poorly controlled benign orbital disease associated with chronic periorbital pain and no functional vision [28]. In these cases, an eyelid-sparing exenteration can be performed.

Preoperative Preparation

A multidisciplinary team approach is necessary in planning the management of cases with malignant tumors invading the orbit. A maxillofacial or head and neck surgeon, plastic surgeon, neurosurgeon, pathologist, radiologist, oncologist, and prosthetician (anaplastologist) may be involved in the management of these cases. As it is a disfiguring procedure with prolonged rehabilitation, preoperative counseling is important in deciding on the timing and best surgical approach.

The surgical technique is dependent upon the location and extent of the tumor. The eyelids may be preserved in tumors placed posteriorly within the orbit and in selected cases with periocular skin involvement. If macroscopic changes suspicious of bone invasion are identified at the time of surgery, frozen-section examination of the periorbita may be helpful in identifying tumor infiltration. If it is positive, an extended exenteration (Fig. 19.2) is required with wide margin removal of adjacent bone up to normal-looking bone cortex. The resected bone should be sent for decalcification and pathological analysis.

Computerized tomography (CT) scanning should be performed to evaluate the bony details of the orbit. The image acquisition protocol should include fine cuts (1–3 mm), coronal and axial views with bone, and soft tissue windows. MRI with contrast is required to identify the extent of tumor invasion into and beyond the orbit. MRI with contrast is also useful in helping to identify perineural invasion. Antiplatelet agents should be discontinued preoperatively if considered appropriate. Arrangements should be made for cross-matched blood in patients with low hemoglobin levels. A pathologist should be con-

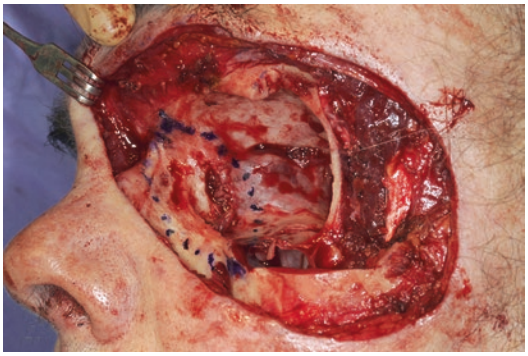

Fig. 19.2 Extended exenteration with partial excision of lateral orbital wall and temporalis muscle. The lacrimal sac fossa and medial maxilla surrounding this area are outlined for excision based upon radiological evidence of extension into the proximal nasolacrimal duct

sulted in advance for the potential need for frozen-section evaluation of cutaneous resection margins. The anesthetist should be warned that the dissection and excision of the orbital apex can provoke the oculocardiac reflex, inducing a severe bradycardia and, occasionally, brief asystole.

Technique

General anesthesia is preferable due to potential for inadequate analgesia during posterior excision with the use of regional and local anesthesia combined with intravenous sedation. In all cases, adjunctive regional anesthesia, 5–10 ml of 0.5% bupivacaine with 1:200,000 units of adrenaline, is given as a peribulbar injection. In addition, a further 10–12 ml of 0.5% bupivacaine with 1:200,000 units of adrenaline is given as a series of subcutaneous injections around the orbital margin and as specific nerve blocks around the supratrochlear, supraorbital, infratrochlear, anterior ethmoidal, infraorbital, zygomaticofacial, and zygomaticotemporal nerves.

Total Exenteration (Including the Eyelids)

The skin incision is marked around the orbital margin. The eyebrow is normally preserved unless involved in the malignant tumor. The eyelid margins are sutured together with a 4-0 silk suture. Skin and subcutaneous tissues are incised using a No. 15 blade, and the dissection is carried down to the periosteum of the orbital rim. Hemostasis is achieved with a bipolar cautery. The periosteum at the orbital margin is then incised with a No. 15 blade (Fig. 19.3). The periosteum is elevated from the margins of the orbit, and subperiosteal dissection into the orbit is carried out using a periosteal elevator. Malleable retractors such as Davis brain spatulas, Bernstein nasal, or Sewell orbital retractors are placed around the orbit to retract the soft tissues (Fig. 19.3). The periosteum is elevated from the orbital walls, beginning superotemporally in a spiral configuration, circumnavigating the anterior orbit before continuing the dissection more posteriorly. The periosteum should be kept intact to avoid any prolapse of orbital fat. Periosteal elevation along the orbital roof should be performed carefully to avoid the risk of damage to the dura mater through dehiscences in the bone (Fig. 19.4). The use of monopolar cautery should be avoided along the orbital roof and apex as it can result in cerebrospinal fluid leak in the presence of bony defects. The dissection is then continued inferotemporally and the lateral canthal tendon is incised. The zygomaticotemporal and zygomaticofacial vessels are cauterized, and the dissection is then continued across the floor of the orbit. Bleeding from the bone can be managed with bone wax. The subperiosteal dissection then continues from the superolateral orbit toward the superomedial orbit. The supraorbital and supratrochlear vessels are cauterized using bipolar cautery.

At the medial canthus, the angular vessels are cauterized using bipolar cautery, and the medial canthal tendon is incised. The subperiosteal dissection is then carried along the lacrimal fossa beyond the posterior lacrimal crest. The proximal nasolacrimal duct (NLD) is incised at the entrance of its foramen, and hemostasis is usually achieved using both monopolar and bipolar cauteries.

The periorbita is carefully raised from the medial orbital wall, avoiding fracture of the lamina papyracea. The anterior and posterior

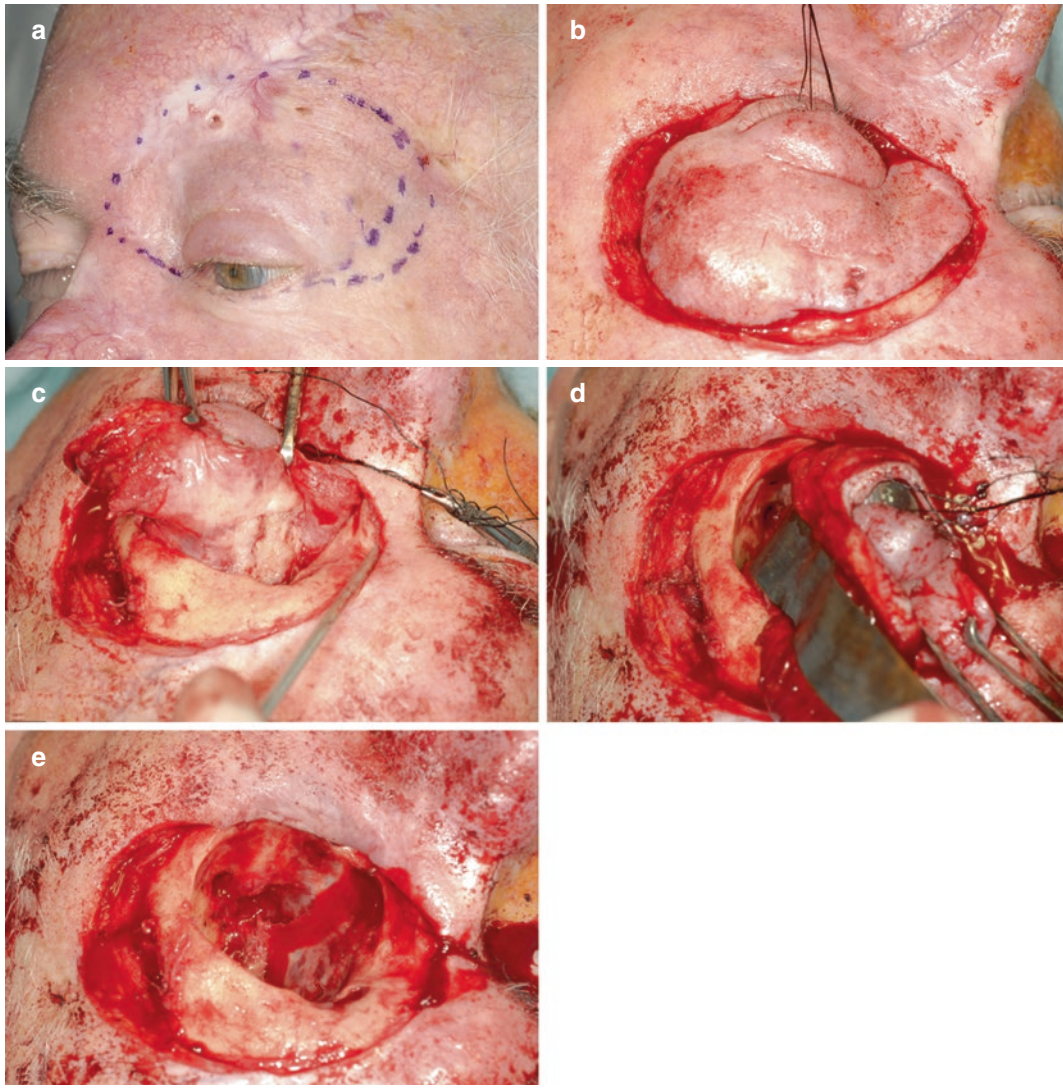

Fig. 19.3 Skin incision is marked for total exenteration (**a**), and skin, subcutaneous tissue, and periosteum are incised (**b**). Periosteum is elevated (**c**) from the margins of the orbit, and subperiosteal dissection into the orbit is carried out along the lateral wall of the orbit (**d**). Exenterated orbit (**e**)

ethmoidal vessels are identified at their respective foramina and are cauterized. Once the dissection has approached the apex of the orbit, a curved clamp is placed deeply within the orbit, just anterior and close to the apex enclosing the muscles, nerves, and vessels. Tissues anterior to the clamp are excised. Intracranial arterial avulsion during orbital exenteration has been reported due to variable communications between the ophthalmic artery and other intracranial vascular structures [29]. Therefore, judicious traction on orbital apical soft tissue should be used during exenteration to minimize the risk of intracranial injury. Where macroscopic or radiological evidence of bone involvement exists, the affected bone is removed with rongeurs or a saw (extended exenteration). The skin and muscle are approximated medially and laterally at the orbital rim to reduce the skin aperture before assessing the defect to reconstruct.

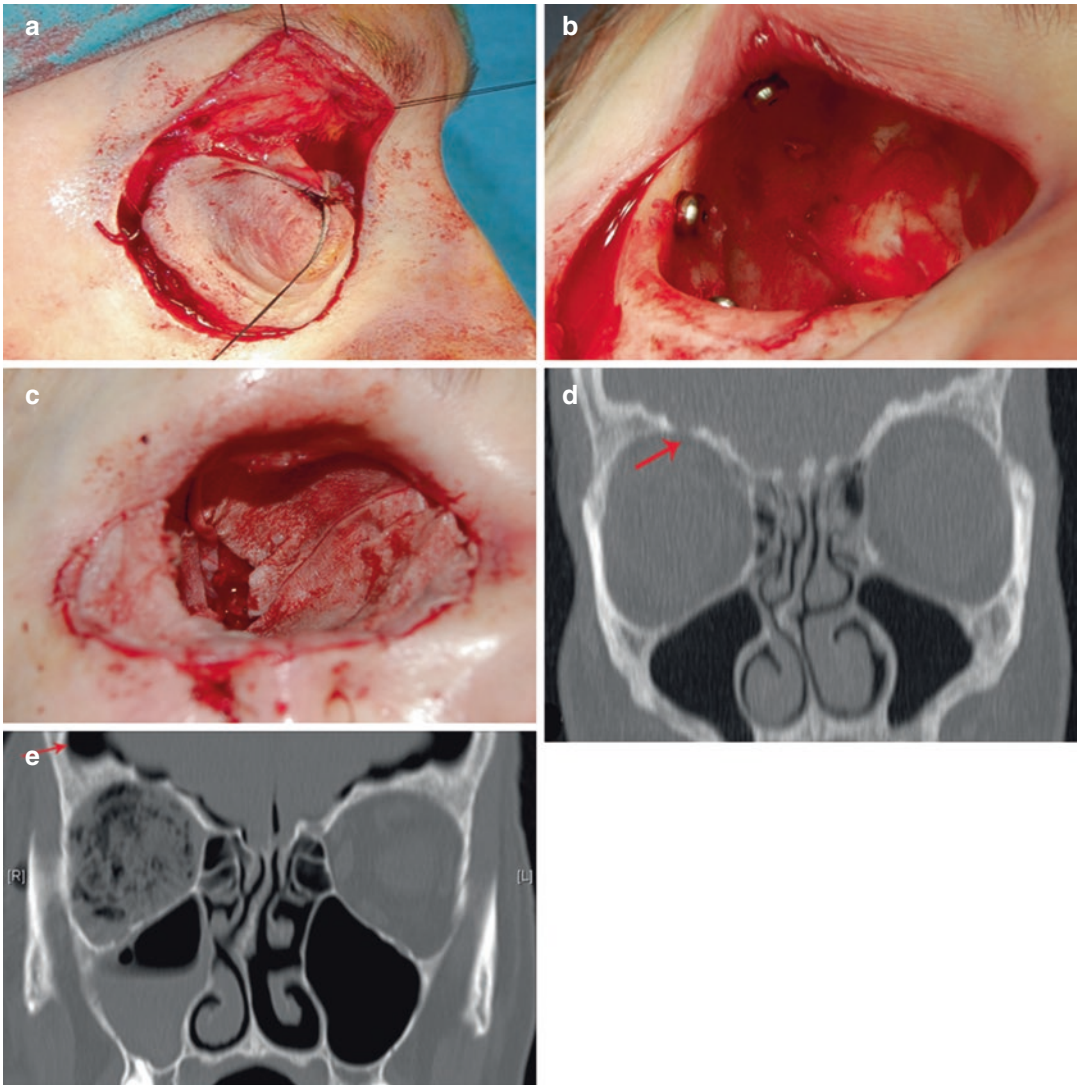

Fig. 19.4 Orbital exenteration was performed for a lower eyelid sebaceous gland carcinoma invading the orbit (**a**). Osseointegration (**b**) was performed at the time of exenteration, and the socket was lined with split-thickness skin graft (**c**). Breach in the thin orbital roof occurred during surgery in a thin aspect of the orbital roof that can be seen in the preoperative CT scan (**d**, arrow), which resulted in CSF leak and a pathognomonic pneumocranium (**e**, arrow) postoperatively

Total Exenteration (Eyelid Sparing)

Incisions are made 1 mm from the lashes in the upper and lower lids (Fig. 19.5). Dissection is preferably deep to the orbicularis muscle, but it can be at a more superficial level between the skin and orbicularis muscle if tumor clearance would be compromised by a deeper level of dissection. At the orbital rim, the periosteum is incised 360°, and the exenteration proceeds as described for total exenteration above. The skin–muscle flaps preserved from the eyelids are sutured together (Fig. 19.5). A drain may be placed in the socket; however, this is not usually necessary. Antibiotic ointment is instilled. A simple dressing is placed over the skin lining of the socket, and a pressure bandage is applied.

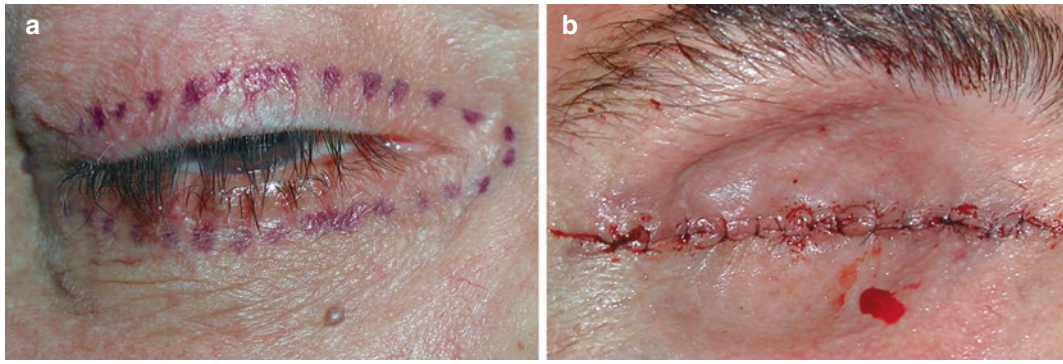

Fig. 19.5 Sub- and supraciliary skin incision marked for eyelid-sparing exenteration (**a**). The skin–muscle flaps preserved from the eyelids are sutured together after exenteration (**b**)

Healing is significantly shorter following eyelid-sparing exenteration. The socket deepens relatively quickly postoperatively in order to allow fitting of a prosthesis.

Subtotal Exenteration

In subtotal exenteration, at least a quadrant of the orbit or the apical orbital tissues posterior to the globe are preserved [2]. Available intra-orbital tissue planes to guide the extent of the subtotal exenterations are the globe itself, orbital septum, eyelid retractors, and extraocular muscles. Subtotal exenteration can be further classified into eyelid-sparing or non-eyelid-sparing exenteration. Eyelid-sparing exenteration can be either conjunctiva-sparing or not conjunctiva-sparing. Preserving normal orbital tissue was reported to result in shortened recovery time, facilitates the reconstruction of the exenterated socket, reduces complications, and optimizes cosmesis.

Eyelid- and Conjunctiva-Sparing Exenteration

Conjunctiva-sparing exenteration has been reported by Goldberg et al. [2] and may be suitable in selected cases, taking into consideration the location of the tumor (localized invasion in one quadrant of the orbit) and biological behavior of the disease process. Looi et al. described an eyelid- and conjunctiva-sparing exenteration procedure with temporalis muscle transfer and dermis fat graft [30]. They reserved this procedure for selected cases with histologically benign orbital lesions that exhibit local aggressive clinical behavior or for malignant lesions with no significant conjunctival, eyelid, lacrimal gland, or posterior orbit involvement.

Preservation of eyelids and the conjunctiva allows early rehabilitation and fitting of an ocular prosthesis (prosthetic shell). The basic requirements for a conjunctiva-sparing exenteration socket to maintain a prosthetic shell are (1) orbital tissue volume to support the prosthesis, (2) a mucous membrane surface with fornices to accommodate the prosthesis, and (3) eyelids to hold the prosthesis within the socket [2].

A limbal peritomy is performed, and the dissection is carried out in the subconjunctival plane to the orbital rim. A subperiosteal dissection is then carried out posteriorly into the orbit, thus preserving the uninvolved conjunctiva. Goldberg et al. recommended preserving approximately 50% of the conjunctival surface and then using a mucous membrane-free graft (buccal mucosa, hard palate mucosa, or nasal turbinate mucosa) to reconstruct the residual defect in the fornix [2]. A dermis fat graft is sutured to the deep orbital remnants to augment the orbital volume.

Reconstruction of the Orbital Cavity

Orbital reconstruction can be divided into three groups: *local*, healing by secondary intention

(laissez-faire), split-thickness skin graft, or dermis fat graft; *locoregional*, advancement flaps, regional pedicle flaps, temporalis muscle transfer, frontalis rotational flap, or temporoparietal fascial flap; and *distal*, microvascular free flaps.

Local Reconstruction Techniques

Laissez-Faire

The traditional approach after excision is to allow healing by spontaneous granulation and epithelialization [31]. If the socket is to be left to heal by secondary intention or if a split-thickness skin graft is used (see below), antibiotic ointment is instilled, and either an Aquacel® dressing (ConvaTec Ltd) or an Allevyn Cavity® dressing (manufactured by Smith & Nephew United, Inc. of Largo, FL) is placed into the socket, and a sterile dressing (eye pads) is applied [32]. The purpose of a deep cavity dressing is to provide an antibacterial role and stimulus for granulation and hemostasis. To this effect, a cheaper alternative for a deep cavity dressing

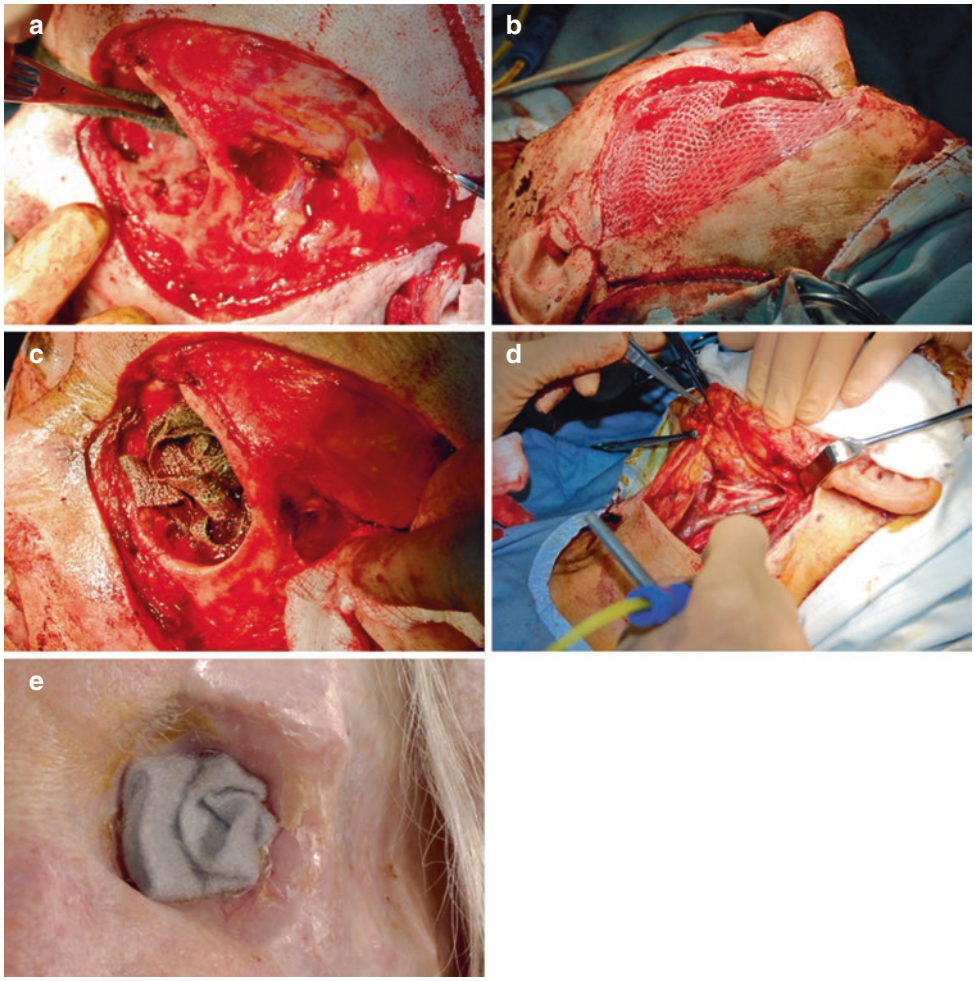

Fig. 19.6 Orbital exenteration defect (**a**), following excision of a large 8 cm diameter malignant melanoma of the eyelid (Breslow thickness greater than 4 mm and Clark's level V). Neck dissection was performed at the same time (**b**). The socket was dressed with Whitehead's varnish soaked in ribbon gauze and allowed to heal by laissez-faire (**c**). The temple defect was covered with a fenestrated split-thickness skin graft (**d**). This patient remains alive and well 4 years since excision (**e**)

(Fig. 19.6) in individuals without a history of iodine sensitivity is the traditional Whitehead's varnish (compound iodoform paint BPC). It consists of iodoform, benzoin, starch, natural balsams, and solvent ether. In addition to its disinfectant action, the iodoform provides some anesthesia when applied to mucous membranes and has been shown to reduce pain on split-thickness skin graft donor sites [33, 34]. Another alternative is Medihoney® (Comvita, Paengaroa, NZ). Medihoney® is an antibacterial wound gel that contains 80% antibacterial honey (800 mg/g). It is made up of honey derived mainly from the group of plants known as *Leptospermum*. Bhatt et al. showed that in over half of the patients Medihoney® was used on, it appeared to contribute in healing the chronically static sockets within 1–2 months following commencement of treatment [32].

The dressing is removed 5–6 days postoperatively. The socket is cleaned and dressed daily for 2 weeks, and the frequency of the wound care is gradually reduced. The wound can be left exposed and camouflaged with a plastic eye shield (Cartella shield) once the discharge has ceased. Complete healing of the socket can take up to 3–4 months. An orbital prosthesis is fitted when the socket has completely healed. Laissez-faire is an easier, quicker option that allows recurrences to be detected potentially early (an advantage in the past before improved imaging became available) and provides a comparable color match to the surrounding skin when granulation is complete. Historically, this was considered particularly useful in the elderly patients not suitable for more lengthy reconstructive procedures. The disadvantages of secondary healing of an exenterated orbit include the need for regular dressing changes, delayed healing, potentially greater likelihood of persistent sino-orbital fistulas, prolonged postoperative socket care, and delayed facial rehabilitation. The delayed healing might delay, in turn, the optimal timing for adjuvant radiation, needed in many cases with advanced diseases [1]. The Manchester orbital exenteration wound assessment tool (MOEWAT) has been reported to be useful in tracking changes in wound healing, postoperatively [35]. MOEWAT uses eight parameters as indices for the assessment and tracking of wound progress and wound healing (body mass index, bone exposure, wound appearance, fistula/sinus, exudates, wound margin, pain, and conjunctive therapies). More recently MOEWAT was modified to allow grading of clinical photographs, and was found to be successful in monitoring wound healing in exenterated sockets, with good inter-observer agreement [36].

Split-Thickness Skin Graft

Split- or full-thickness skin grafts can be used for reconstruction when an open cavity is desired; when there is no need to isolate the orbital cavity from the sinonasal, oral, or intracranial cavities; and when radiation therapy is not given preoperatively. A split-thickness skin graft is preferred and provides the greatest coverage. It is usually harvested from the thigh with a dermatome and placed directly onto the bone in order to line as much of the socket as possible (Fig. 19.7). The edges of the graft are usually sutured to the skin edges around the socket. The use of a skin graft shortens the healing period. It helps reduce undue wound contracture and maintains a deeper socket in comparison to that usually achieved by secondary healing in order to enable easy fitting of an orbital prosthesis. It also facilitates easy examination of the socket where the possibility of tumor recurrence may exist. This approach however requires a separate donor site. The skin graft may fail in patients who are at risk of poor healing, including diabetic patients, and those who have previously received radiotherapy.

Split-thickness skin grafts may be used in conjunction with and placed over pericranial periosteal flaps. A large periosteal flap may be harvested from the forehead and placed directly over the bony cavity and, in particular, any bony defect of the orbital roof or medial wall. Pericranial periosteal flaps, being a vascular structure, help accelerate the take of split-thickness skin grafts and also osseointegration, thus reducing the time taken for prosthetic rehabilitation (Fig. 19.7) [37].

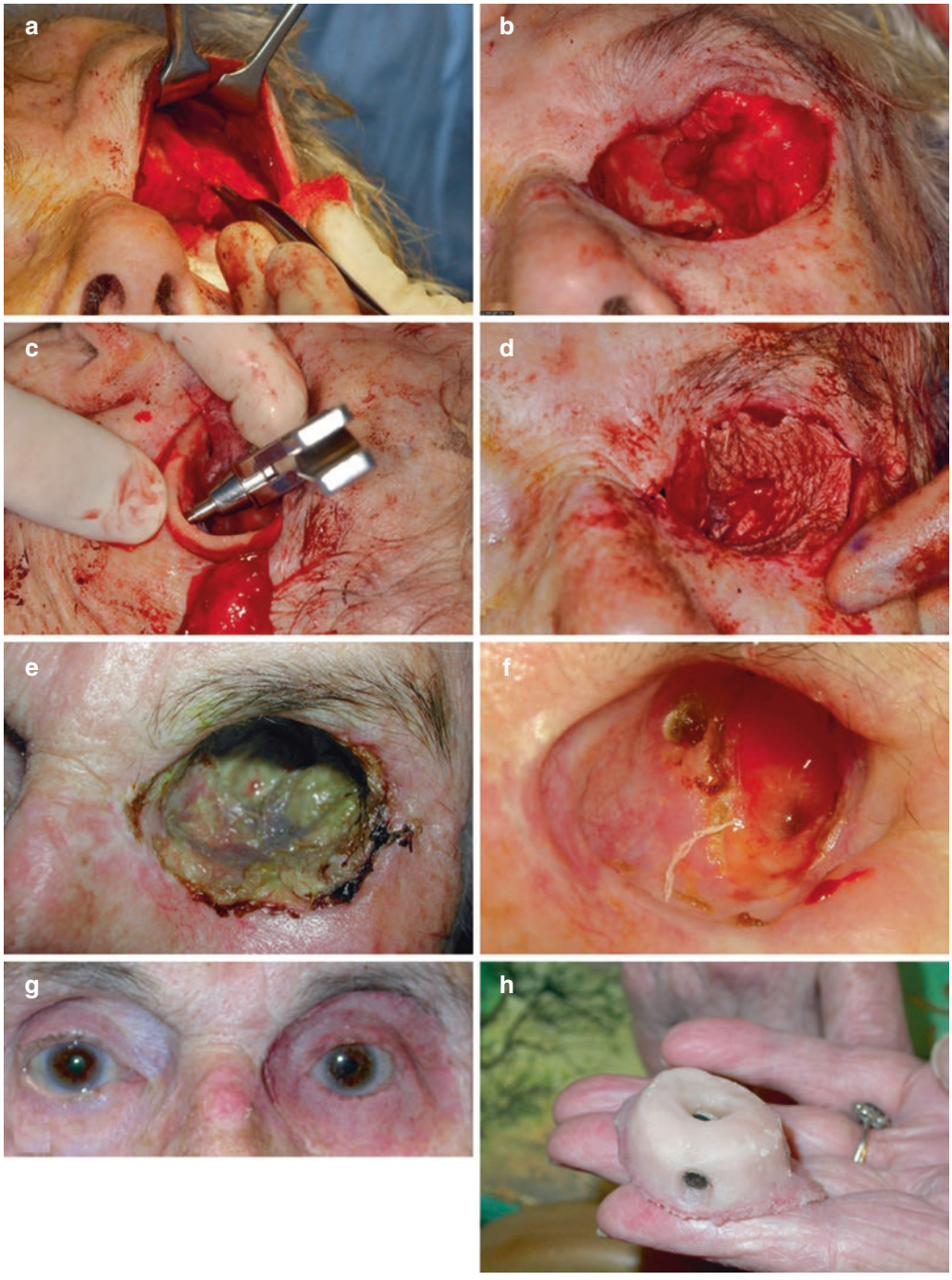

Fig. 19.7 This patient had previously undergone orbital radiotherapy for an incompletely excised basal cell carcinoma which subsequently recurred, requiring exenteration. Pericranial flap fashioned from the forehead to line the exenterated orbit (**a**, **b**). Osseointegrated implants inserted at the time of exenteration (**c**). Split-thickness skin graft placed over the pericranial flap to line the orbit (**d**). Three weeks post exenteration with split-thickness skin graft placed over a pericranial flap (**e**). Nine months later, the socket has still not healed completely and there is incomplete keratinization (**f**). Prosthesis covering the exenterated left orbit (**g**). Magnets cast into the posterior surface of the prosthesis (**h**)

Dermis Fat Graft

A dermis fat graft from the abdominal wall can be used to fill the defect after subtotal eyelid-sparing exenteration. The remaining eyelid skin is closed over the graft. The dermis fat graft derives its blood supply from any residual posterior orbital tissues and the eyelid skin and orbicularis muscle anteriorly. Alternatively, a myocutaneous flap may also be advanced over the graft to provide further blood supply to the dermis fat graft [38].

Locoregional flaps and microvascular free flaps provide early rehabilitation. These act as effective barriers for separating the orbit from adjacent structures particularly if an extended orbital exenteration is performed. A locoregional and even distal free flap is of potential benefit in patients receiving postoperative adjunctive radiation therapy. In addition to providing soft tissue coverage over the orbital bones, locoregional flaps and microvascular free flaps allow isolation of the orbit from the nasal cavity, paranasal sinuses, and cranial cavity to help prevent fistulas. Locoregional flaps have the advantage of being derived from areas anatomically adjacent to the orbit and require less socket care than for sockets managed by laissez-faire or split-thickness skin grafts [31].

Locoregional Reconstruction Techniques

Cheek Advancement Flap

Our preferred technique of direct closure with cheek advancement is a modification of the cervicofacial flap and offers a one-stage, reliable, and safe method of reconstruction following orbital exenteration [39]. Reconstruction of the exenterated orbit using cheek advancement represents an evolution of the flap repair described by Robin Beare in 1969 [40]. This technique was later reported by Mercer [41] as the "cervicofacial" flap. This is of particular benefit in cases of neglected tumor where the patient is reluctant or unable to attend regular hospital appointments, and thus rehabilitation with minimal postoperative intervention is necessary. Subcutaneous cheek dissection (thus avoiding injury to the facial nerve) to a level just below the oral commissure and 2–3 cm below the angle of the mandible is performed. The cheek flap is fixed with deep sutures to the inferior orbital rim using 4-0 Vicryl® sutures and where periosteum is not present, using the infraorbital canal as a bone tunnel and a point for deep fixation of the cheek (Fig. 19.8). This simple cheek advancement avoids creating a secondary defect, and because it involves less dissection and additional skin incisions in comparison to a cervicofacial or other regional flaps, it is an easier procedure to perform with fewer facial scars. It may pull the brow inferiorly; however, this is not a problem if a prosthesis is being fitted and may be corrected by way of a direct supra-brow lift with insertion of the excised skin as a graft, directly below the brow hair. Extensive dissection into the cervical region is avoided, and it can be used in conjunction with additional methods such as pericranial or skin transposition flaps. It does not preclude osseointegration if required either at the time of repair or at a later date, and as such, we would recommend it as a useful option in repairing the exenterated orbit. Other locoregional options include a cheek fasciocutaneous V-Y flap [42] or the use of a galeal flap [43], pericranial flap [37], local transposition skin flaps from the forehead, and temporalis muscle flap.

Temporalis Muscle Transfer

The temporalis fascia and muscle are split, and the muscle is released from the zygomatic arch and lateral orbital rim. The temporalis muscle flap is then transposed into the orbit through a bony opening made in the lateral wall and covered by a skin graft or remnant eyelids [44]. This procedure adds volume to the orbit and covers small bony defects and any dural tears. Disadvantages include contour problems in the temporal fossa and, rarely, compromised mastication.

Temporal myocutaneous flap based on the superficial temporal artery is rotated deep to the tissues of forehead and below the supraorbital rim into the orbit [31]. The donor site defect is closed with a full-thickness skin graft or direct closure. An advantage of this flap is its applica-

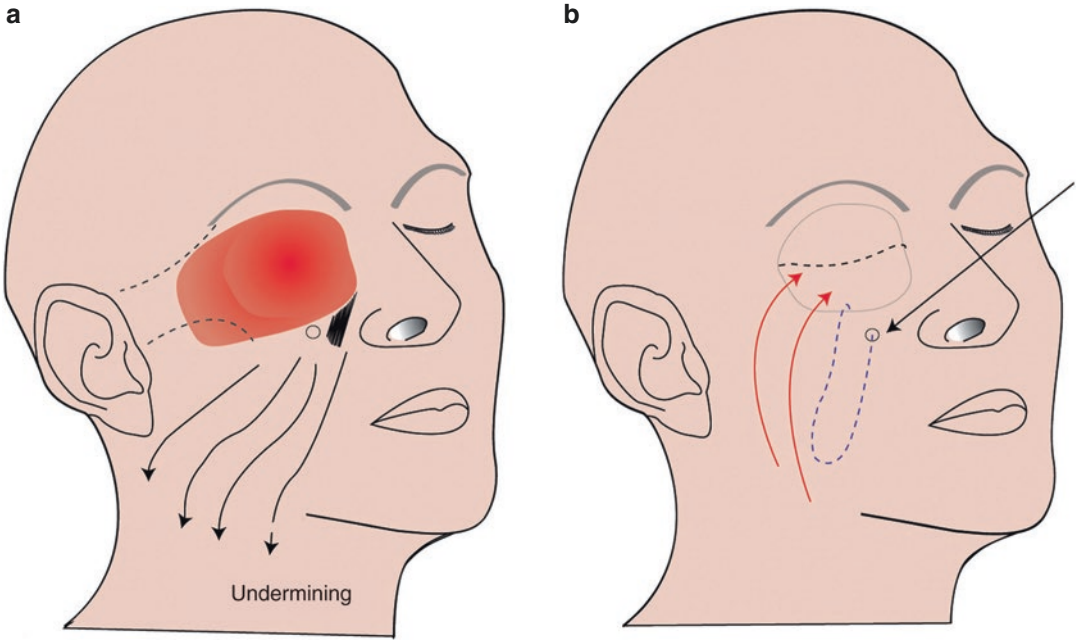

Fig. 19.8 Following total exenteration, subcutaneous cheek dissection (to avoid injury to the facial nerve) is carried out to a level just below the oral commissure and 2–3 cm below the angle of the mandible (**a**). To facilitate sufficient vertical advancement of the cheek flap, a point for deep fixation of the flap is created using deep sutures to the inferior orbital rim using 4-0 Vicryl® sutures and, where periosteum is not present, using the infraorbital canal as a bone tunnel (**b**, arrow). The cheek flap is padded with the cheek supported upward for 3–7 days

tion to make the socket deformity shallower in a patient not keen on wearing a prosthesis. However, the procedure leaves a secondary depression in the temple. The temporal branch of the facial nerve may also be damaged, resulting in a brow ptosis.

Distal Reconstruction Technique (Free Flap)

A microvascular free flap is particularly useful for the reconstruction of large defects from an extended exenteration. Microvascular free-tissue transfer is a technique that involves the harvest of the patient's own soft tissues and/or bone from remote anatomical sites. These flaps, along with their defined vasculature, are then used to reconstruct the defect. Blood supply to the flap is reestablished at the reconstructed site by anastomosis of the artery and vein to recipient vessels (the superficial temporal artery and vein).

Commonly used microvascular flaps include the rectus abdominis free flap [45], latissimus dorsi, radial forearm, or lateral arm flap [31].

A free flap can help minimize the severe cosmetic disfigurement of an extended exenteration with exposed sinus cavities. Unlike a locoregional flap, free flaps are not limited by the flap size or pedicle length and provide ample volume to fill the orbital defect while minimizing the morbidity associated with local flaps. They also have the advantage of providing healthy tissue in the case of previously irradiated sites. However, these procedures are difficult to perform and extremely time-consuming. There is a risk of flap failure and donor site morbidity. If the flap is too bulky, as can occasionally be the case, it may prevent the successful wearing of an orbital prosthesis. Cavity obliteration techniques were traditionally considered to hamper clinical surveillance of the operative site; however, imaging techniques have advanced reducing the likelihood of missing a recurrence.

Novel Technique

Patel et al. recently reported the usage of an INTEGRA® (Integra Life Sciences Corporation, Plainsboro, NJ) dermal regeneration matrix in a two-stage rapid exenteration reconstruction. INTEGRA® dermal regeneration templates are a synthetic bilayer porous matrix of fibers of cross-linked bovine tendon collagen and glycosaminoglycan covered with thin polysiloxane that function as a scaffold for regrowth of neodermis consisting of blood vessels and dermal skin cells. INTEGRA® grafts have been used in patients with thermal injuries and significant scar contractures and in reconstruction of defects created by tumor excision, with marked success in regenerating dermal skin, causing less scarring, and earlier rehabilitation. In the reported case, the INTEGRA® graft was sutured immediately after an extended orbital exenteration to cover the defect. Three weeks after the initial surgery, the INTEGRA® graft was found to be well integrated and vascularized. Thinned full-thickness skin grafts were sutured over the INTEGRA® matrix. Adjuvant radiotherapy began 5 weeks after initial exenteration with a fully epithelized exenterated socket. The patient had no complications after a total of 47 weeks follow-up [46].

Complications (Table 19.1)

Table 19.1 Complications following exenteration

Intraoperative	Hemorrhage
	Exposure of dura
	CSF leak
	Intracranial arterial avulsion
Postoperative	Fistula formation into the paranasal sinuses, the nose, or the nasolacrimal duct
	Infection (bacterial/fungal)
	Orbital abscess
	Graft necrosis/eschar formation
	Nonhealing ulcers
	Chronic discharge and exposed bone
	Cerebrospinal fluid leak and pneumocranium

Intraoperative Persistent Hemorrhage

Persistent hemorrhage may occur either at the orbital apex or at the proximal nasolacrimal duct. In order to reduce venous congestion and venous bleeding, the simple measure of elevating the operating table head by 10–15° in the reverse Trendelenburg position should be considered, remembering uncommon but significant complications such as venous air embolism and cerebral hypoperfusion. Other relevant considerations for encouraging venous drainage are keeping the head straight (without kinks), avoiding ties around the neck and avoiding venodilation causing hypercapnia by means of adequate ventilation.

With regard to arterial bleeding – several systemic steps are worth coordinating with the anesthetist. Controlled hypotension – a key factor in reduction of intraoperative bleeding – should be initiated. It is defined as a reduction of the systolic blood pressure to 80–90 mmHg or a reduction of mean arterial pressure (MAP) to 50–65 mmHg or by 30% of baseline.

MAP and heart rate – another key player in manipulating arterial bleeding – were found to be significantly lower in general anesthetic patients ventilated by laryngeal mask airways (LMA) contributing to a better quality of operative field during surgery. This may be attributed to decreased sympathetic stimulation associated with the insertion of an LMA compared with endotracheal intubation.

Induction of total intravenous anesthesia with propofol or remifentanil, rather than inhalational anesthesia with isoflurane or sevoflurane, decreases intraoperative heart rate and induces less significant peripheral vasodilation, thus reducing intraoperative bleeding as well [47].

Intraoperative hemostasis, after applying preoperative measures discussed above, is further achieved by careful surgical technique. In general, respecting tissue planes, cautious ligation, and cautery of known blood vessels and utilizing good illumination are all substantial practices for minimizing bleeding. If spontaneous clot fails to form, a reasonable next step would be to apply

pressure or compression with sterile cotton gauze at the bleeding site. A bipolar cautery or monopolar cautery can then be used to cauterize any bleeding vessels. However, it is important to avoid the use of monopolar cautery along the orbital roof as it can cause a CSF leak in the presence of a bony defect. Adrenaline-soaked packs can also be applied to cause vasoconstriction. Bleeding from the bone can be controlled by application of bone wax, and the bleeding caused by emissary vessels can be controlled by dry bone drilling. Excessive hemorrhage following the transaction of the orbital tissues at the orbital apex may be managed by clamping of the residual stump, by use of bipolar cautery, and by applying pressure. Injudicious use of monopolar cautery should be avoided at the orbital apex. For persistent cavity bleeds, it is useful to consider the application of hot packs at approximately 50 °C. This is a traditional practice in maxillofacial and head and neck surgery. Since the last century, hot-water irrigation has been used in obstetrics to reduce predelivery and post-delivery bleeding [48]. Hot-water irrigation is also well established as an effective treatment modality for intractable posterior epistaxis [49, 50]. The mechanism behind its effectiveness remains unclear; however, based upon rabbit studies, hot-water nasal irrigation above 46 °C achieved vasodilation and mucosal edema with subsequent narrowing of the intranasal lumen. Severe changes, including epithelial necrosis, occurred with temperatures beyond 52 °C [51]. It is also possible that an increase in temperature may increase the speed of the clotting cascade.

Management of Cerebrospinal Fluid (CSF) Leak

The reported incidence of CSF leaks during orbital exenteration varies between 0.6% and 16.7% [52]. De Conciliis noted that dural exposure occurred in 20.5% of exenterations and 30.8% of extended exenterations which included excision of one or more orbital walls [53]. Furthermore, in that study, 60% of CSF leaks and 75% of dural exposures occurred in extended exenterations involving resection of one or more orbital walls. De Conciliis et al. were able to predict dural exposure in 50% of the cases based on clinical data and CT findings [53]. Hence, preoperative evaluation is invaluable in predicting and preparing for management of CSF leaks, helping to alert the surgeon to proceed with caution where pathology has infiltrated or thinned posterior or superior bone (Fig. 19.4). A temporary CSF leak may also be seen at the time of cutting the optic nerve at the apical stump [52].

Diagnosis of a CSF leak at the time of surgery can be made when leakage of clear fluid is seen in areas at high risk for encountering dura. However, when CSF and blood are mixed together, diagnosis may be difficult. CSF separates from blood when placed on filter paper and produces a ring or *halo* sign. This is not however exclusive to CSF and can lead to false-positive results. Glucose content can be analyzed rapidly; however, this is also unreliable as glucose in CSF cannot be distinguished from that in blood, tears, or nasal secretions. Hence, measuring glucose from the discharge is generally of little value in the preoperative setting. Beta-2 transferrin assay is a marker protein specific to CSF. It has high sensitivity and specificity, can be performed rapidly, and is the test of choice if available. Primary repair with 5-0 or 6-0 polyglactin or braided nylon should be performed to create a watertight seal when there is adequate exposure, and the edges of the dural laceration can be readily apposed. An onlay graft, commonly a layer of fat, a pericranium flap, temporalis muscle, or fascia, may then be placed over the exposed dura to further ensure a watertight barrier [54]. Flaps may be particularly useful in patients with a history of radiation [55]. Other reported materials include mucosal grafts and free cartilage from the ear or nasal septum [55]. TISSEEL fibrin glue (Baxter Healthcare Corp., Deerfield, IL) has been used with favorable results in CSF leaks to the orbit [56]. Although often used in conjunction with an onlay graft to further seal the repair, using an adhesive alone has also been reported to be adequate in very small dural defects without tissue loss [52]. Cyanoacrylate glue applied to a dry surgical field has also been effective in closure of CSF leaks. Bone wax has also

been described in situations where the leak arises from the depth of a relatively small bony defect [57]. The aim is to fill the bone defect preventing CSF leakage into the orbit while the dura seals itself. However, bone wax should be used with caution as Bolger et al. reported three cases of CSF leaks that were associated with bone wax [58]. Large fistulas can be managed with a pericranial flap or a temporalis muscle flap [59]. CSF leaks identified postoperatively can be managed conservatively. A pneumocranium on CT scan is pathognomonic (Fig. 19.4e). Conservative management includes avoiding straining activities such as nose-blowing or coughing, use of stool softeners, and elevating the head to reduce CSF pressure. Prophylactic antibiotics are often used in cases of CSF leaks; however, their use remains controversial. Surgical repair should be considered when the leak does not settle conservatively [52].

Management of Sino-Orbital Fistula

The incidence of sino-orbital fistulas ranges from 5% to 23% and commonly involves the ethmoid sinus. The risk factors for developing sino-orbital fistulas are prior radiotherapy, sinus disease, and intraoperative penetration of the sinus. Fistulas occur more commonly in sockets left to granulate and are less common in sockets lined by skin graft [60]. Late presentation of fistulas may be due to bony erosion from tumor recurrence, and orbital examination and imaging should be considered. Nonhealing fistulas can cause symptoms of malodorous discharge, crusting, wound breakdown, hypernasal speech, infection, and inability to use an ocular prosthesis. Small asymptomatic fistulas can be managed conservatively with socket hygiene, and small symptomatic fistulas can be closed directly. Large fistulas are repaired with grafts or flaps. Commonly used grafts include skin, mucous membrane, temporalis muscle/fascia, fascia lata, or pericranium. Commonly used flaps include skin flaps, myocutaneous flaps, free flaps, and pericranial flaps [61]. Pericranial flap is our preferred option as it is flexible, thin, and vascular and acts as a tough barrier between the orbit and sinus. The use of uncinate flaps and middle turbinate flaps has also been described to close fistulas from the nasal side [62]. Al-Hity et al. reported a significant reduction of sino-orbital fistula formation in cases in which polydioxanone (PDS) foil (Johnson & Johnson Inc., New Brunswick, NJ) was applied to line the medial wall of the orbit as a preventative measure [63].

Management of Other Complications

Infections in the orbit can be treated with topical and/or systemic antibiotics. Graft necrosis can be either managed conservatively (allowed to granulate) or treated with a repeat skin graft. Chronic nonhealing ulcers can be debrided and treated with a skin graft or flap. Yassur et al. have reported the use of becaplermin gel (recombinant human platelet-derived growth factor) for the treatment of chronic orbital ulcer after exenteration [64].

Cosmetic Rehabilitation

Rehabilitation usually involves a prosthesis; however, patients may prefer to wear a patch or dark glasses. An essential part of the surgical decision-making process is the reconstruction and rehabilitation of the exenterated socket. Whenever feasible, a decision should be made before surgery as to whether the patient will wear a patch, an oculofacial prosthesis, or an ocular prosthesis (prosthetic shell). Oculofacial prosthesis can be mounted on the glasses (Fig. 19.9), fixed with tissue glue, or attached by magnets or clips to titanium osseointegrated implants (Fig. 19.7g, h). Spectacle-mounted prostheses prevent the spectacles ever being removed in public. Patients often lose confidence with these methods and tend to abandon their prosthesis for a patch [2]. Notwithstanding, a survey of 125 medical students who graded patient appearance following reconstruction of exenterated orbits, according to comfort of interaction, visceral reaction to the reconstruction, and perceived patient social interaction and health, demonstrated a significant preference to prosthesis-wearing patients. The authors

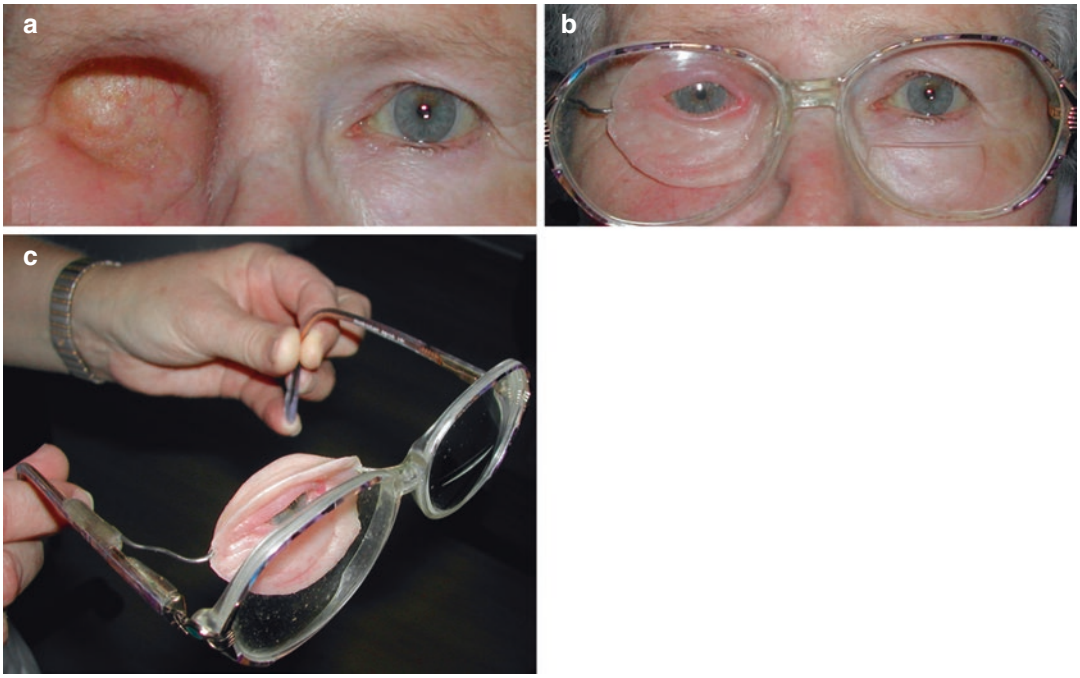

Fig. 19.9 Spectacle-mounted prosthesis (**b**, **c**) as a simple option for cosmetic rehabilitation of the exenterated orbit (**a**)

acknowledged that novel solutions such as 3-D printers may reduce the orbital prosthesis cost and increase the accuracy of the fit, increasing patient's motivation to wear them [65].

Titanium Osseointegrated Implants

Nerad et al. first described osseointegrated implants as a means of fixing oculoplastic prosthesis [66]. This was described as a two-stage procedure (first, insertion of the titanium implants and, second, placement of the transcutaneous abutments). Transcutaneous abutments were traditionally placed 4 months after the insertion of titanium implants, under local anesthesia. A series of bars or magnetic devices are then attached to the abutments, which allow firm fixation of the prosthesis. The insertion of titanium implants was not performed at the time of exenteration because of the risk of skin graft necrosis, when placed over an avascular structure (titanium). However, this can now be performed at the time of exenteration [67]. Cameron et al. [37] described the use of pericranial graft to facilitate the placement of osseointegrated implants at the time of exenteration. The pericranial flap, being a highly vascular tissue, improves the take of a split-skin graft. This technique allows reliable alignment of the prosthesis and good retention. Removal and reattachment of the prosthesis by the patient are also relatively easy. The prosthesis can be made light in weight. The edge of the prosthesis can also be made to blend with the surrounding skin more easily, and the cosmetic results can be excellent for the carefully selected patient. The ideal patient is relatively young, highly motivated, and with good hygiene, will comply with long-term aftercare of the implants, and will attend long-term follow-up appointments. This technique is time-consuming and expensive, however. The implants must be kept meticulously clean to avoid inflammation or infection. There is a small risk of losing the implants in previously irradiated orbits [66].

Ocular Prosthesis (Prosthetic Shell)

A prosthetic shell can be fitted in a selected group of patients where the eyelids and conjunctiva are spared during orbital exenteration. The basic requirements for a conjunctiva-sparing exenteration socket to maintain a prosthetic shell are orbital tissue volume to support the prosthesis, a mucous membrane surface with fornices to accommodate the prosthesis, and eyelids to hold the prosthesis within the socket [2]. If approximately 50% of the patient's conjunctival surface can be saved, then a mucous membrane-free graft (buccal mucosa, hard palate mucosa, or nasal turbinate mucosa) can be used to reconstruct the fornix. If split-thickness skin is used instead, then the patient may be bothered by persistent discharge and a smelly "mixed socket."

Prognosis

The success of the surgery depends on obtaining tumor-free margins at the time of surgery. It is not always possible to achieve complete clearance of a tumor with exenteration, and incomplete clearance has been reported in up to 38% of total and 17% of subtotal exenterations by Goldberg et al. [2]. The lower percentage of incomplete clearance with subtotal exenteration in this study was due to the fact that the cases with locally invasive malignancy were treated with subtotal exenteration and the cases with widespread tumor invasion were treated with total exenteration.

Bartley et al. reported an 88.6% survival at 1 year and a 56.8% survival at 5 years in patients with no residual tumor after exenteration [11]. Their reported 1-year survival was 55.0%, and the 5-year survival was 25.8% in patients with metastasis or residual tumor after exenteration. Rahman et al. reported an overall survival of 93% at 1 year, 57% at 5 years, and 37% at 10 years [20]. They reported that achieving tumor-free margins after exenteration did not influence the long-term survival. Hence, the presence of clear surgical margins should not be regarded as an indication of cure as clear excision margins may prevent local recurrence, but they do not always prevent micrometastasis to lymph nodes or distant organs.

More recently, Wong et al. reported the highest 5-year survival rate in 73 exenterated patients within a study period of 13 years in a tertiary care center. Survival rates at 1 year, 5 years, and 10 years were 88%, 64%, and 38%, respectively. Their results strengthened previous studies that showed no statistically significant difference in survival rates when cleared margin cases were compared with non-cleared cases. The authors' findings indicated that the histology diagnosis is more relevant to prognosis than surgical margins, by showing that deaths in the BCC group occurred at almost half the rate of those in the non-BCC disease group (mainly SCC, sebaceous cell carcinoma, and malignant melanoma) [68]. Micrometastasis are exceedingly rare in BCC tumors [69]; BCC perineural invasions are rare as well [70]; hence complete excision of these tumors might serve as a stronger indication for cure.

Perineural invasion is associated with increased incidence of incomplete clearance and recurrence resulting in worse prognosis particularly in squamous cell carcinoma and lacrimal gland adenoid cystic carcinoma. In cases of tumor-positive margins, other treatment modalities such as radiation or chemotherapy may play a role in prolonging survival. Williams et al. reported a 5-year survival of 50% in patients with radiological (CT/MRI) evidence of perineural invasion, compared with 86% survival in patients with no radiological evidence of perineural invasion [71].

References

1. Zhang Z, Ho S, Yin V, et al. Multicentred international review of orbital exenteration and reconstruction in oculoplastic and orbit practice. Br J Ophthalmol. 2018;102(5):654–8. https://doi.org/10.1136/bjophthalmol-2017-310681.
2. Goldberg RA, Kim JW, Shorr N. Orbital exenteration: results of an individualized approach. Ophthal Plast Reconstr Surg. 2003;19:229–36.
3. Ben Simon GJ, Schwartz RM, Douglas R, et al. Orbital exenteration: one size does not fit all. Am J Ophthalmol. 2005;139:11–7.
4. Tyers AG. Orbital exenteration for invasive skin tumors. Eye. 2006;20:1165–70.

5. Howard GR, Nerad JA, Carter KD, et al. Clinical characteristics associated with orbital invasion of cutaneous basal cell and squamous cell tumors of the eyelid. Am J Ophthalmol. 1992;113:123–33.
6. Madge SN, Khine AA, Thaller VT, et al. Globe-sparing surgery for medial canthal basal cell carcinoma with anterior orbital invasion. Ophthalmology. 2010;117:2222–8.
7. Donaldson MJ, Sullivan TJ, Whitehead KJ, et al. Squamous cell carcinoma of the eyelids. Br J Ophthalmol. 2002;86:1161–5.
8. Gerring RC, Ott CT, Curry JM, et al. Orbital exenteration for advanced periorbital non-melanoma skin cancer: prognostic factors and survival. Eye. 2017;31(3):379–88. https://doi.org/10.1038/eye.2016.218.
9. Sagiv O, Nagarajan P, Ferrarotto R, et al. Ocular preservation with neoadjuvant vismodegib in patients with locally advanced periocular basal cell carcinoma. Br J Ophthalmol. 2018. https://doi.org/10.1136/bjophthalmol-2018-312277
10. Xu Y, Li F, Jia R, et al. Updates on the clinical diagnosis and management of ocular sebaceous carcinoma: a brief review of the literature. Onco Targets Ther. 2018;11:3713–20. https://doi.org/10.2147/OTT.S162073.
11. Bartley GB, Garrity JA, Waller RR, et al. Orbital exenteration at the Mayo Clinic 1967–1986. Ophthalmology. 1989;96:468–73.
12. Cook BE Jr, Bartley GB. Treatment options and future prospects for the management of eyelid malignancies: an evidence-based update. Ophthalmology. 2001;108:2088–98.
13. Chao AN, Shields CL, Krema H, et al. Outcome of patients with periocular sebaceous gland carcinoma with and without intraepithelial invasion. Ophthalmology. 2001;108:1877–83.
14. McKelvie PA, Daniell M, McNab A, et al. Squamous cell carcinoma of the conjunctiva: a series of 26 cases. Br J Ophthalmol. 2002;86:168–73.
15. Shields JA, Shields CL, Demirci H, et al. Experience with eyelid-sparing orbital exenteration: the 2000 Tullos O. Coston lecture. Ophthalmic Plast Reconstr Surg. 2001;17:355–61.
16. Miller CV, Wolf A, Klingenstein A, et al. Clinical outcome of advanced squamous cell carcinoma of the conjunctiva. Eye (Lond). 2014;28(8):962–7. https://doi.org/10.1038/eye.2014.79.
17. Shields JA, Shields CL. Massive orbital extension of posterior uveal melanoma. Ophthal Plast Reconstr Surg. 1991;7:238–51.
18. Damato B, Coupland SE. An audit of conjunctival melanoma treatment in Liverpool. Eye (Lond). 2009;23:801–9.
19. Kersten RC, Tse DT, Anderson RL, et al. The role of orbital exenteration in choroidal melanoma with extrascleral extension. Ophthalmology. 1985;92:436–43.
20. Rahman I, Maino A, Cook AE, et al. Mortality following exenteration for malignant tumors of the orbit. Br J Ophthalmol. 2005;89:1445–8.
21. Lin KL, Tena LB, Finger PT. Orbital brachytherapy for extrascleral extension of choroidal melanoma. Br J Ophthalmol. 2006;90:1438–9.
22. Meel R, Radhakrishnan V, Bakhshi S. Current therapy and recent advances in the management of retinoblastoma. Indian J Med Paediatr Oncol. 2012;33:80–8.
23. Honavar SG, Manjandavida FP, Reddy VAP. Orbital retinoblastoma: An update. Indian J Ophthalmol. 2017;65(6):435–42. https://doi.org/10.4103/ijo.IJO_352_15.
24. Raney B, Huh W, Hawkins D, et al., for the Soft Tissue Sarcoma Committee of the Children's Oncology Group, Arcadia, CA. Outcome of patients with localized orbital sarcoma who relapsed following treatment on Intergroup Rhabdomyosarcoma Study Group (IRSG) Protocols-III and -IV, 1984–1997: a report from the Children's Oncology Group. Pediatr Blood Cancer. 2013;60(3):371–6. https://doi.org/10.1002/pbc.24289.
25. Woo KI, Sagiv O, Han J, et al. Eye-preserving surgery followed by adjuvant radiotherapy for lacrimal gland carcinoma. Ophthal Plast Reconstr Surg. 2018;1:570. https://doi.org/10.1097/IOP.0000000000001106.
26. Nazar G, Rodrigo JP, Llorente JL, et al. Prognostic factors of maxillary sinus malignancies. Am J Rhinol. 2004, 18(4):233–8. http://www.ncbi.nlm.nih.gov/pubmed/15490570. Accessed 30 July 2018.
27. Safi A-F, Behn L, Rothamel D, et al. Therapy of sinonasal malignancies invading the orbit-orbital exenteration versus preservation of the orbit plus radiotherapy. J Craniomaxillofac Surg. 2017;45(2):258–61. https://doi.org/10.1016/j.jcms.2016.11.013.
28. Rose GE, Wright JE. Exenteration for benign orbital disease. Br J Ophthalmol. 1994;78:14–8.
29. Gonzalez LF, Bilyk JR. Intracranial arterial avulsion during orbital exenteration. Orbit. 2012;31:190–3.
30. Looi A, Kazim M, Cortes M, et al. Orbital reconstruction after eyelid- and conjunctiva-sparing orbital exenteration. Ophthal Plast Reconstr Surg. 2006;22:1–6.
31. Levin PS, Ellis DS, Stewart WB, et al. Orbital exenteration. The reconstructive ladder. Ophthal Plast Reconstr Surg. 1991;7:84–92.
32. Cooper J. Wound management following orbital exenteration surgery. Br J Nurs. 2009;18(6):S4.
33. Stanley D, Emerson DJ, Daley JC. Whitehead's varnish and Jelonet–a better dressing for skin graft donor sites than Jelonet alone. Ann R Coll Surg Engl. 1988;70:369–71.
34. Lim M, Lew-Gor S, Sandhu G, et al. Whitehead's varnish nasal pack. J Laryngol Otol. 2007;121:592–4.
35. Cooper J. The MOEWAT as a proposed method of evaluating orbital exenteration wounds. J Wound Care. 2011;20(478):480–3.
36. Cooper J, Dharmasena A, Malik R, et al. Reliability and effectiveness of the manchester orbital exenteration wound assessment tool: inter-observer agreement. Orbit. 2015;34(3):127–31. https://doi.org/10.3109/01676830.2015.1014506.
37. Cameron M, Gilbert PM, Mulhern MG, et al. Synchronous reconstruction of the exenterated orbit

with a pericranial flap, skin graft and osseointegrated implants. Orbit. 2005;24:153–8.
38. Shore JW, Burks R, Leone CR Jr, et al. Dermis-fat graft for orbital reconstruction after subtotal exenteration. Am J Ophthalmol. 1986;102:228–36.
39. Sira M, Malhotra R. Reconstruction of orbital exenteration defects by primary closure using cheek advancement. Br J Ophthalmol. 2013;97(2):201–5.
40. Beare R. Flap repair following exenteration of the orbit. Proc R Soc Med. 1969;62:1087–90.
41. Mercer DM. The cervicofacial flap. Br J Plast Surg. 1988;41:470–4.
42. Moretti E, Ortiz S, Gómez García F, et al. Complete mobilization of the cheek zone for orbit exenteration. J Craniofac Surg. 2005;16:823–8.
43. Zwahlen RA, Grätz KW, Obwegeser JA. The galea fascia flap in orbital reconstruction: innovative harvest technique. Eur J Surg Oncol. 2006;32:804–7.
44. Reese AB, Jones IS. Exenteration of the orbit and repair by transplantation of the temporalis muscle. Am J Ophthalmol. 1961;51:217–27.
45. Pryor SG, Moore EJ, Kasperbauer JL. Orbital exenteration reconstruction with rectus abdominis microvascular free flap. Laryngoscope. 2005;115:1912–6.
46. Patel SY, Tamboli DA, Mancini R. Two-stage rapid exenteration reconstruction to allow early radiation therapy for an aggressive orbital cancer. Int Ophthalmol. 2018;38(2):833–6. https://doi.org/10.1007/s10792-017-0525-3.
47. Sia DIT, Chalmers A, Singh V, et al. General anaesthetic considerations for haemostasis in orbital surgery. Orbit. 2014;33(1):5–12. https://doi.org/10.3109/01676830.2013.842250.
48. Hansen TB. Hot water irrigation to obtain haemostasis [Danish]. Bull Midwifes (Copenh). 1890;3:8–10.
49. Novoa E, Schlegel-Wagner C. Hot water irrigation as treatment for intractable posterior epistaxis in an outpatient setting. J Laryngol Otol. 2012;126:58–60.
50. Stangerup S, Dommerby H, Siim C, et al. New modification of hot-water irrigation in the treatment of posterior epistaxis. Arch Otolaryngol Head Neck Surg. 1999;125:686–90.
51. Stangerup SE, Thomsen HK. Histological changes in the nasal mucosa after "hot-water-irrigation": an animal experimental study. Rhinology. 1996;34:14–7.
52. Limawararut V, Valenzuela AA, Sullivan TJ, et al. Cerebrospinal fluid leaks in orbital and lacrimal surgery. Surv Ophthalmol. 2008;53:274–84.
53. de Conciliis C, Bonavolonta G. Incidence and treatment of dural exposure and CSF leak during orbital exenteration. Ophthal Plast Reconstr Surg. 1987;3:61–4.
54. Ebersold MJ. Five things oculoplastic surgeons should know about neurosurgery. Ophthal Plast Reconstr Surg. 2000;16:247–9.
55. Massoud VA, Fay A, Yoon MK. Cerebrospinal fluid leak as a complication of oculoplastic surgery. Semin Ophthalmol. 2014;29(5–6):440–9. https://doi.org/10.3109/08820538.2014.959187.
56. Goldberg RA, Weinberg DA, Shorr N, et al. Maximal, threewall, orbital decompression through a coronal approach. Ophthalmic Surg Lasers. 1997;28:832–43.
57. Graham SM, Brown CL, Carter KD, et al. Medial and lateral orbital wall surgery for balanced decompression in thyroid eye disease. Laryngoscope. 2003;113:1206–9.
58. Bolger WE, Tadros M, Ellenbogen RG, et al. Endoscopic management of cerebrospinal leak associated with the use of bone wax in skull-base surgery. Otolaryngol Head Neck Surg. 2005;132:418–20.
59. Schaefer SD, Soliemanzadeh P, Della Rocca DA, et al. Endoscopic and transconjunctival orbital decompression for thyroid-related orbital apex compression. Laryngoscope. 2003;113:508–13.
60. Rahman I, Cook AE, Leatherbarrow B. Orbital exenteration: a 13 year Manchester experience. Br J Ophthalmol. 2005;89:1335–40.
61. Mehta V, Alon EE, Buchbinder D, et al. Novel use of unilateral galeopericranial flaps for closure of sino-orbital cutaneous fistulas. Laryngoscope. 2011;121:777–81.
62. Limawararut V, Leibovitch I, Davis G, et al. Sino-orbital fistula: a complication of exenteration. Ophthalmology. 2007;114:355–61.
63. Al-Hity A, Gregory ME, Kemp EG. The intraoperative use of polydioxanone foil to reduce the risk of sino-orbital fistula formation in orbital exenteration. Orbit. 2018;37(2):140–4. https://doi.org/10.1080/01676830.2017.1383463.
64. Yassur I, Hirschbein MJ, Karesh JW. Clinicopathologic reports, case reports, and small case series: 0.01% becaplermin gel for the treatment of a chronic orbital ulcer after exenteration. Arch Ophthalmol. 2001;119:1858–9.
65. Kuiper JJ, Zimmerman MB, Pagedar NA, et al. Perception of patient appearance following various methods of reconstruction after orbital exenteration. Orbit. 2016;35(4):187–92. https://doi.org/10.1080/01676830.2016.1176207.
66. Nerad J, Carter KD, LaVelle WE, et al. The osseointegration technique for the rehabilitation of the exenterated orbit. Arch Ophthalmol. 1991;109:1032–8.
67. Greig AV, Jones S, Haylock C, et al. Reconstruction of the exenterated orbit with osseointegrated implants. J Plast Reconstr Aesthet Surg. 2010;63:1656–65.
68. Wong JCL, Thampy R, Cook A. Life expectancy following orbital exenteration. Br J Ophthalmol. 2015;99(1):1–4. https://doi.org/10.1136/bjophthalmol-2013-304436.
69. Weiss GJ, Korn RL. Metastatic basal cell carcinoma in the era of hedgehog signaling pathway inhibitors. Cancer. 2012;118(21):5310–9. https://doi.org/10.1002/cncr.27532.
70. Wu A, Sun MT, Huilgol SC, et al. Histological subtypes of periocular basal cell carcinoma. Clin Exp Ophthalmol. 2014;42(7):603–7. https://doi.org/10.1111/ceo.12298.
71. Williams LS, Mancuso AA, Mendenhall WM. Perineural spread of cutaneous squamous and basal cell carcinoma: CT and MR detection and its impact on patient management and prognosis. Int J Radiat Oncol Biol Phys. 2001;49:1061–9.

Principles of Orbital Surgery

20

David H. Verity and Geoffrey E. Rose

Introduction

Over the past 55 years, the management of orbital disease has increasingly been recognised as a discipline in its own right. While in the early 1940s orbital surgery was considered to lie firmly within the realm of the neurosurgeon [1], access to orbital pathology is now achieved almost exclusively through periorbital incisions within skin tension lines or the conjunctiva itself. However, where disease extends beyond the bony confines of the orbit into the cranium, pterygopalatine fossa, or paranasal sinuses, multidisciplinary management with a neurosurgeon and maxillofacial or head-and-neck surgeon may be required. This chapter covers special preoperative, intraoperative, and postoperative considerations in patients undergoing orbital surgery and illustrates a series of practical approaches to the orbital contents.

Anatomical Limitations: The 'Conoid of View' in Orbital Surgery

The bony orbit is tetrahedral in shape, its walls protecting the orbital soft tissues whose volume is about 28 ml. Unless the bony wall(s) are displaced or removed, all surgical approaches to the orbit are limited by the anterior orbital opening (generally less than 3 cm) and the extent to which the globe can be displaced. Thus, for a lesion in the orbital apex, the surgeon's maximum *theoretical* binocular 'conoid of view' is about 50° by 30°, although in reality is narrower because the soft tissues obscure the operative field even further, with the operative view becoming monocular in the depths of the surgical field. Thus, the wider the 'conoid' of view, the wider the stereoscopic surgical. Wider access is therefore desirable for deeper-placed pathology and can be achieved either by placing the incision closer to the lesion (e.g. using a lateral canthotomy for lateral lesions) or by displacing the orbital wall laterally (as is performed in a bone-swinging lateral orbitotomy).

Orbital Surgery: Risks to Visual Functions

Operating within the confined space of the bony orbit carries significant risks of injury to the delicate soft tissues contained within it [2].

D. H. Verity (✉)
Adnexal Service, Moorfields Eye Hospital, London, UK
e-mail: david.verity@nhs.net

G. E. Rose
Adnexal Service, Moorfields Eye Hospital, London, UK

NIHR Biomedical Centre, Institute of Ophthalmology, London, UK

C. J. Hwang et al. (eds.), *Clinical Ophthalmic Oncology*,
https://doi.org/10.1007/978-3-030-13558-4_20

While impairment of motor and facial sensory nerves can be reversible, visual loss due to ischaemic optic neuropathy – presumed due to vasospasm – rarely recovers. This risk depends upon both the difficulty of surgical access and the space available for tissue displacement while operating. Although risk 'zones' are discussed (Tables 20.1 and 20.2), the surgeon's experience is also a significant factor across all zones, with more posterior lesions presenting the greatest challenge and requiring greater expertise.

Surgery for lesions alongside the globe in the anterior one-third of the orbit, where the conoid of view is wide, carries significantly less risk for iatrogenic nerve damage (Table 20.1) than for surgery in the posterior third of the orbit (Table 20.2), where the conoid of view is restricted and structures are viewed more obliquely. These considerations frequently influence management, with a judicious 'wait and watch' approach being acceptable for some posterior lesions suspected of being benign and where the natural history (and risk to vision) remains uncertain (such as venous malformations).

Table 20.1 Risks of surgery in the anterior third of the orbit

1. General risks:
Visual loss (low)
Diplopia
2. Specific risks:
Orbital roof: Sensory changes corresponding to frontal nerve and/or supratrochlear nerve, CSF leak
Superonasal quadrant: Sensory changes, diplopia (injury to trochlea or superior oblique tendon)
Medial orbit: Risk to lacrimal outflow apparatus (watery eye), risk of medial orbital wall fracture
Orbital floor: Sensory changes (infraorbital nerve)
Lateral orbit: Mydriasis (causing photophobia, early presbyopia), reduced aqueous tear production (rare)

Table 20.2 Risks of surgery in the middle and posterior thirds of the orbit

Irreversible visual loss, partial or complete
Diplopia
Ptosis
Periocular paraesthesia or anaesthesia

Preoperative Counselling

The risks to sight, ocular alignment, and periocular sensation must be discussed with all patients prior to surgery. Unlike other areas of ophthalmology (such as cataract surgery), the risks cannot be quantified with great precision due to wide variation between patients in the extent and severity of disease and in orbital soft tissue and bony anatomy. However, certain risks are associated with the location of surgery (Table 20.3). For example, approaches to the orbital roof carry a small risk of injury to the frontal nerve, a minute risk to vision and ocular alignment, and a miniscule risk of CSF leak. Similarly, surgery in the anterior superomedial quadrant risks injury to the trochlea and thus secondary diplopia. In contrast, the surgical risk is much greater for posterior lesions, where the conoid of view is narrower and the space for tissue manipulation is limited. For apical lesions whose behaviour and imaging suggest a 'benign' pathology (such as an apical cavernous hemangioma), the patient may safely be monitored with periodic documentation of visual functions, and intervention is only considered if and when there is clear evidence of progression. Where the history, clinical behaviour, or imaging indicates a malignant process, however, the risks of surgery may be outweighed by those of *not* operating, that is, by the risk of regional or systemic spread of an undiagnosed malignant neoplasm.

Table 20.3 Perioperative risks in orbital surgery

Compromised visualization of orbital structures
Fat prolapse into the surgical field
Orbital hemorrhage
Tissue injury:
Manipulation of the orbital tissues and thermal injury from diathermy (both increasing the risk of postoperative visual loss due to vasospasm at the orbital apex [2])
Sustained pressure on the globe and ocular ischemia
Ocular surface exposure

Perioperative Medical and Anaesthetic Considerations

Orbital surgery can be performed with local and regional blocks under deep sedation (especially for more anterior procedures, such as lacrimal gland biopsy). However, unless the risks are considered unacceptable, the use of general anaesthesia is often preferred as it permits better control of systemic blood pressure during surgery. In all patients, pre-existing medical conditions, including systemic hypertension, hypo- or hyperthyroidism, and diabetes, should be as well controlled as possible, and patients should be assessed by an anaesthetist familiar with the specific anaesthetic requirements for orbital surgery. Preoperative investigations will be determined by the medical history of the patient and the nature of the proposed surgery but will often include a full blood count, urea and electrolytes, thyroid function tests, clotting studies, and an ECG.

When medically appropriate, hypotensive anaesthesia improves the operative field by reducing arterial and venous bleeding: this can be achieved with either a volatile anaesthetic agent (e.g. isoflurane or sevoflurane) or with total intravenous anaesthesia (TIVA) using a combination of propofol and remifentanil. There is much evidence to support the use of TIVA: it often confers a smooth recovery from anaesthesia and also is associated with a lower incidence of postoperative nausea and vomiting. These qualities of TIVA are highly desirable for orbital surgery, where a postoperative surge in orbital perfusion pressure can be hazardous and particularly where day-case surgery is being performed [3]. Remifentanil is a powerful, extremely short-acting synthetic opiate that not only prevents intraoperative coughing (without the need for intraoperative muscle relaxants) but also reduces the hypertensive response to pain [4]. As remifentanil is rapidly metabolised on ceasing the infusion (with a context-sensitive half-life of about 3 min), it is essential that an intraoperative analgesic is also given, with intravenous paracetamol usually being the first choice. The perioperative use of platelet-inhibiting anti-inflammatory analgesics such as diclofenac and ibuprofen is controversial and, considering the risks of orbital haemorrhage, is best avoided. Reduced perioperative bleeding in craniofacial surgery has been reported with the use of the antifibrinolytic drug tranexamic acid (TXA) [5] and should be strongly considered (both peri- and postoperatively) in orbital surgery for vascular lesions or more posterior pathology. Finally, consideration should be given to the position of the patient during surgery, with a 15° head-up reverse Trendelenburg position preferred by these authors for both orbital and lacrimal surgeries.

Postoperative pain, also a risk factor for hypertension and, thereby, for orbital haemorrhage (which can be severe), should be pre-empted with longer-acting perioperative opiates, such as morphine or fentanyl. Regional infiltration with a long-acting local anaesthetic, such as bupivacaine, should also be considered where possible as it further reduces the need for postoperative analgesia and, therefore, the risk of postoperative nausea and vomiting. Finally, where surgery involves placement of an orbital implant – for example, after ocular evisceration or enucleation or with fracture repairs – parenteral dexamethasone, in combination with a 5HT-3 receptor antagonist (such as ondansetron), should also be used to reduce the incidence of nausea, vomiting, and secondary hypertension.

Numerous drugs affect hemostasis and carry a significant risk of hemorrhage in orbital surgery [6]. These include antiplatelet agents (typically for cardiovascular indications), numerous variants of nonsteroidal medications, certain antidepressants [7], and herbal remedies and spices (including garlic extracts) [8]. The orbital surgeon should document a thorough drug history as well as seek the advice of a physician before discontinuing such drugs prior to surgery (Table 20.4).

Table 20.4 Antiplatelet agents, warfarin, and orbital surgery

Antiplatelet agent	Minimum cessation prior to surgery
All versions of amino-salicylic acid (ASA):	4 weeks
Nonsteroidal medications	3 weeks
Other antiplatelet drugs (e.g. clopidogrel)	2 weeks
Warfarin – Target INR for orbital surgery is <1.5	3–4 days
Herbal remedies	4 weeks
Spices containing ajoenes (garlic, ginger, gingko, ginseng)	4 weeks

Depending on the indication, cessation of antiplatelet agents and warfarin can cause significant comorbidity, and, in certain circumstances, a low molecular weight heparin may need to be given over the perioperative period [9]. Irrespective of the other risk factors for haemorrhage, a surgeon should always consider placing a vacuum drain for 12–24 h when operating on all but the most anterior of orbital lesions.

The Six Essential Orbitotomies: An Overview

The six approaches described here (Table 20.5) permit access to each region of the orbit. When disease is ill-defined or straddles different areas, combinations of these approaches may aid in visualisation and dissection. While the approach can often be determined preoperatively, if inadequate access is afforded by the initial approach, additional adjoining approaches can be added. The choice of orbitotomy is largely determined by the location and depth of the access required: for example, where incisional biopsy is intended, a trans-lid approach (either via the upper lid skin crease or inferior conjunctiva) is often adequate. In contrast, to increase the surgeon's conoid of view for intact excision of a deeper lesion, it might be necessary to utilise a lower lid swinging flap or bone-swinging lateral orbitotomy, these approaches giving wider access to the orbital depths.

Anterior Orbitotomy: Upper Eyelid Skin-Crease Approach

The upper two-thirds of the orbit are readily accessible through the upper eyelid approach, this healing with no visible scar and providing access as far back as the superior orbital fissure and orbital apex (Fig. 20.1). Surgery involves an incision through the upper lid skin crease, dividing the orbicularis muscle along the length of the incision and placing the skin/muscle flaps on traction (a 2/0 silk suture is convenient for this). For lacrimal gland masses, the incision is placed in the lateral aspect of the skin crease and – with blunt dissection of the suborbicularis plane – the arcus marginalis is exposed at the superolateral orbital rim. With a Desmarres retractor elevating the incision edge and brow tissues and a 16 mm malleable retractor displacing the lacrimal gland and orbital septum inferomedially, the arcus marginalis is opened for about 15–20 mm immediately inferior to the lateral orbital rim, this exposing the preaponeurotic fat pad and the outer face of the orbital lobe of the lacrimal gland. The latter is readily mobilised from its fossa (unless there has been marked chronic inflammation), and a large specimen may be harvested from its external surface using an E11 blade. Haemostasis is achieved by applying diathermy directly to the cut surfaces, the gland is repositioned within the orbit, orbital fat re-draped in the region, and the skin closed with a running 6/0 nylon suture or, in a child, with an 8/0 soluble suture. A topical ocular antibiotic is applied and a non-adherent dressing applied with firm padding for 12–24 h – a drain being unnecessary. The patient should be evaluated 10–14 days postoperatively with review of the histopathology and, in the adult, removal of the non-absorbable surface suture.

Frequently, biopsy of the lacrimal gland is inappropriately performed via the superolateral conjunctival fornix, this considered to be more straightforward than the orbitotomy approach described above. However, such surgery is always to be avoided because it carries a *major* risk of dry eye due to inadvertent injury to the lacrimal ductules, and moreover, the palpebral lobe is often spared by underlying disease process.

For non-lacrimal masses, the orbital septum should be opened near the lesion and a few millimetres below the arcus marginalis, to avoid damage to the levator apparatus. Access to the orbital *roof* is achieved by spreading the connective tissue septa *above* the preaponeurotic fat pads with

Table 20.5 The six principle approaches to the orbit

1. Upper eyelid skin-crease approach
2. Swinging lower eyelid approach (two variants)
3. Lateral canthotomy approach
4. Bone-swinging lateral orbitotomy
5. Transconjunctival retrocaruncular approach
6. Conjunctival peritomy approach

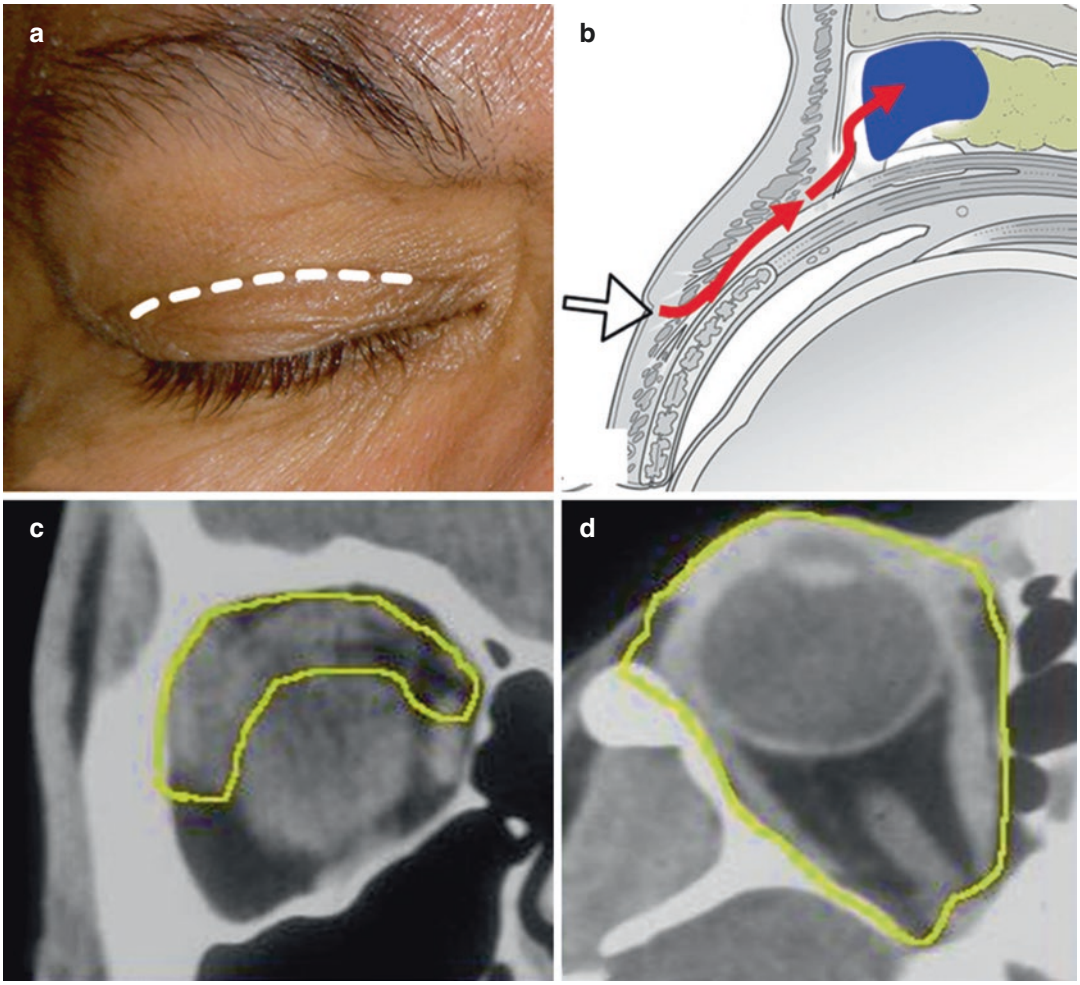

Fig. 20.1 Anterior orbitotomy – upper eyelid skin-crease approach incision (dotted line) (**a**). Schematic route to the postseptal space. Arrow demonstrates skin crease (**b**) and areas of the orbit that can be reached by this approach (**c** and **d**)

blunt-ended scissors, taking care to avoid injury to the frontal neurovascular complex. In contrast, gentle blunt dissection *beneath* the preaponeurotic fat pads and across the surface of the levator muscle provides access to the levator complex or to the upper intraconal space (for lesions lying above or medial to the optic nerve) [10].

Using blunt-ended scissors to open up the soft tissues and placing 16 mm malleable retractors either side of the scissors, the orbital depths are exposed after applying diathermy to the tissue septa overlying the area of interest. This manoeuvre is repeated several times, with the assistant gently retracting the surrounding tissues to maintain a clear view of the area in question. Where the intention is to excise intact a well-defined mass, any adjacent bridging vascular pedicles are divided after diathermy until the entire surface of the mass has been cleared from adjacent tissues and can be removed without tissue-drag. For incisional biopsy of an ill-defined lesion, the mass is gripped firmly (crush artefact being minimised by avoiding repeated grasping) and a large biopsy obtained either with an E11 blade or with tissue scissors. After obtaining hemostasis, a vacuum drain is placed for all surgery within the deep orbit – this reduces serum accumulation at the orbital apex and, thereby, minimizes the risk of

visual loss; the drain trocar is passed through the eyebrow to avoid a visible scar.

Anterior Orbitotomy: Swinging Lower Eyelid Approach

Although the inferior two-thirds of the orbit can be reached by several routes, the previously popular 'tear-trough' skin incision is now obsolete due to the evident lower lid scar, the risks of fistula formation, and the risk of lower eyelid retraction due to adhesions to the underlying bone. Although the subciliary blepharoplasty incision remains a reliable approach where skin reduction is required during orbital surgery, the conjunctival approach often gives wider exposure with less tissue manipulation while avoiding the above risks.

Thus, the contemporary approach to the lower two-thirds of the orbit is the lower lid swinging flap [11, 12], of which there are two types (Fig. 20.2). The first is the 'high' flap, this providing immediate access to the *preseptal* plane and thence to the inferior orbital rim, from which exceptional access is gained to the orbital floor and medial wall. The second, giving wide access

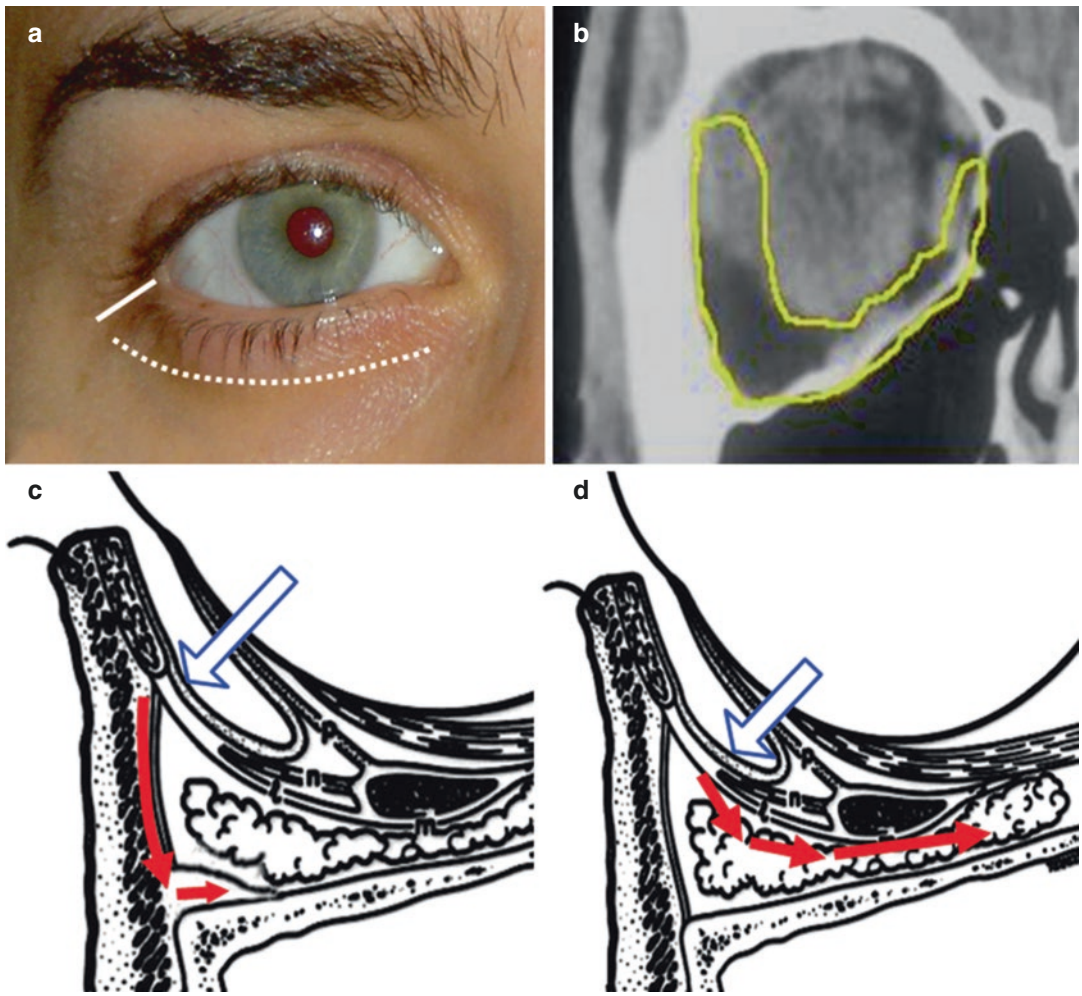

Fig. 20.2 Anterior orbitotomy – swinging lower eyelid approach. Figure showing lateral canthotomy and conjunctival incision (**a**, dotted line) and the area of the orbit that can be reached (**b**). The 'high' (**c**, arrow) and 'low' (**d**, arrow) variants are shown

to the extraconal and intraconal spaces, is the 'low' flap, in which the conjunctival incision is placed low in the depths of the inferior fornix. This incision directly enters the *postseptal* extraconal fat, from which – with gentle tissue spreading and the use of retractors – the orbital contents can be reached. Understanding the fundamental difference between these two approaches and their rationale (these not developed in the original description) [12] is essential when planning an approach through the lower eyelid.

The 'High' Variant of the Swinging Lower Eyelid Approach

For both variants, the lower lid is first disconnected from the lateral orbital rim using a slightly downward-directed lateral canthotomy and cantholysis. The conjunctiva is then opened along its full horizontal extent at a millimetre below the tarsus, taking care to avoid inadvertent injury to the canaliculus. The cornea is protected by approximating the cut edge of the inferior conjunctiva to the upper lid margin with a widely spaced 4/0 nylon loop on a bow; this suture also keeps the septum taut and aids subsequent opening of the preseptal (post-orbicularis) plane. After separating the septum and orbicularis, the inferior orbital rim and suborbicularis fat pad (just below the rim) are exposed with firm sweeps of a cotton bud and the periosteum opened at the orbital rim to expose the inferior extraperiosteal space. A 16 mm malleable retractor is used to raise the periosteum off the floor, taking care to diathermy and divide the artery that crosses from the infraorbital canal to the orbit.

Such an approach is typically used for the repair of orbital fractures; exposure of the whole medial orbital wall is readily achieved, and the conjunctival incision can be continued into the retrocaruncular line and temporary division of the origin of the inferior oblique muscle where necessary. After closure of the orbital periosteum with interrupted 5/0 soluble sutures, the lower eyelid swinging flap is repaired in a layered fashion using a 6/0 soluble suture; this involves a single suture to close the lateral aspect of the conjunctiva, alignment of the grey line and lash lines, suturing of the cut end of the lower tarsus to the upper limb of the canthal tendon, closure of the orbicularis muscle, and finally closure of the skin.

The 'Low' Variant of the Swinging Lower Eyelid Approach

The postseptal route offered by the 'low' lower lid swinging flap affords good access to the lateral, inferior, and even medial extraconal space, allowing the orbital surgeon to remove large tumours from these regions. Masses overlying an expanded inferior orbital fissure can be debulked as far posteriorly as the pterygopalatine fossa, and intraconal lesions can be excised after entering the intraconal fat space between the inferior and lateral recti, these muscles being the most widely spaced. This route also permits access to tumours of the optic nerve; for example, in cases of a painful, blind exophthalmos due to an optic nerve tumour (without intracranial extension), the entire intraorbital portion of the nerve may be removed with this versatile approach. Similarly, the more oblique approach to the inferior rectus (as compared with a conjunctival approach which gives an 'end-on' view of the muscle) markedly facilitates representative biopsy of the belly of this muscle [13].

Anterior Orbitotomy: Lateral Canthotomy Approach

Exposure of the lateral half of the orbit can be achieved through a lateral canthotomy incision, this having several advantages over other approaches including a short operative time, no perceptible scar, and no disruption of the attachments of the upper or lower limbs of the lateral canthal tendon (Fig. 20.3). This approach is particularly useful where a diffuse process, such as lymphoma or idiopathic inflammation, involves multiple tissues and where biopsy of muscle, fat, and lacrimal gland is required [14].

In this approach, the outer canthus is divided horizontally to the orbital rim and traction sutures placed through the upper and lower eyelids. The

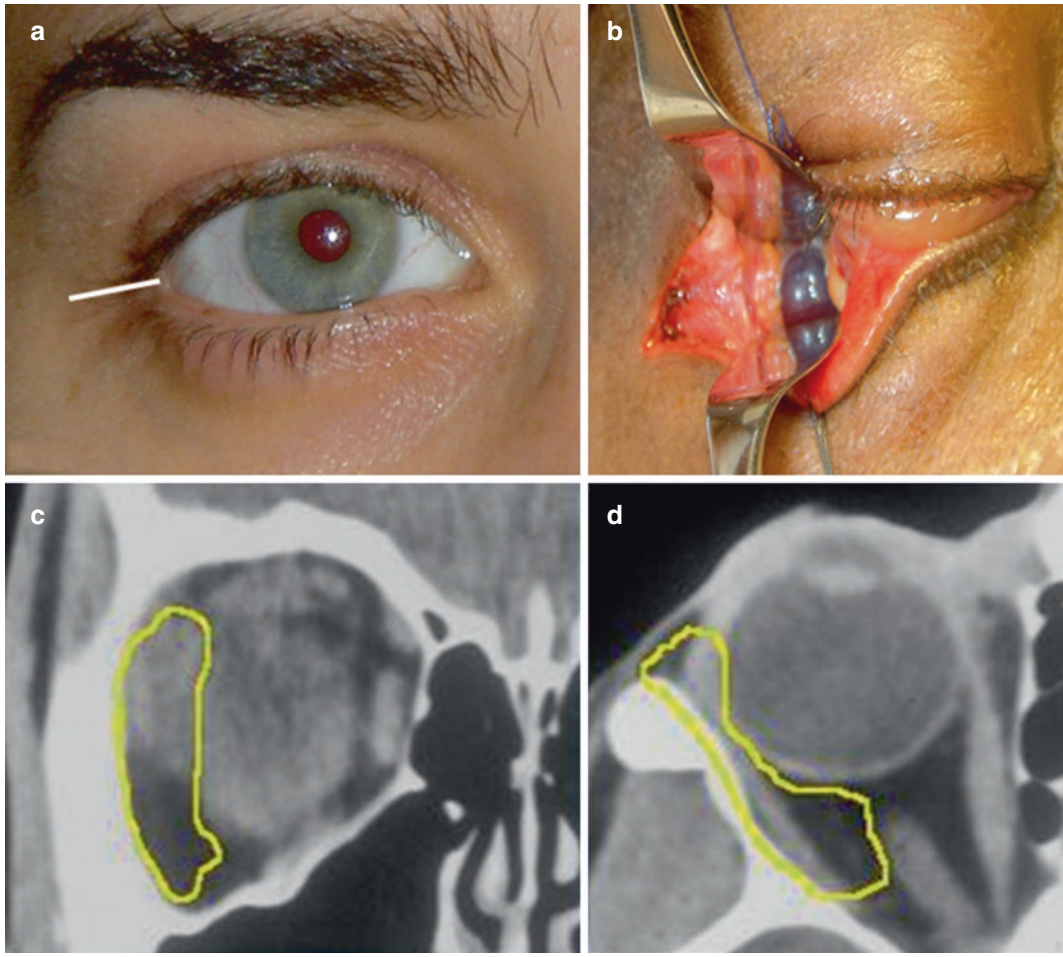

Fig. 20.3 Anterior orbitotomy: lateral canthotomy approach. Skin incision (**a**). Patient undergoing removal of a vascular lesion (note superior and inferior placement of paddle retractors (**b**) and areas of the orbit that can be reached through this approach (**c**, **d**)

tissues are spread and retracted to expose the lateral extraperiosteal fat plane, with division of the lower forniceal conjunctiva further enhancing access if required. The incision is readily closed with 6/0 soluble sutures aligning the lid margins and uniting the upper and lower limbs of the tendon and skin closure with the same suture.

Lateral Orbitotomy with Bone Mobilization

In the lateral orbitotomy approach, the surgical 'conoid of view' is significantly widened by swinging the lateral orbital wall outwards on the temporalis muscle, thereby shortening the surgical path length and improving access to the orbital apex (Fig. 20.4). With increasing usage of the 'low' lower lid swinging flap, the need to use this approach for the removal of retrobulbar lesions has declined significantly. However, lateral orbitotomy remains an important approach for removal of large lacrimal gland pleomorphic adenomas (where the wider exposure reduces the risk of tumour disruption during isolation of the posterior pole of the gland) and for removing lesions tightly wedged into the orbital apex (where the approach reduces surgical path length and improves tumour visualisation). Although past techniques were based on the Stallard-

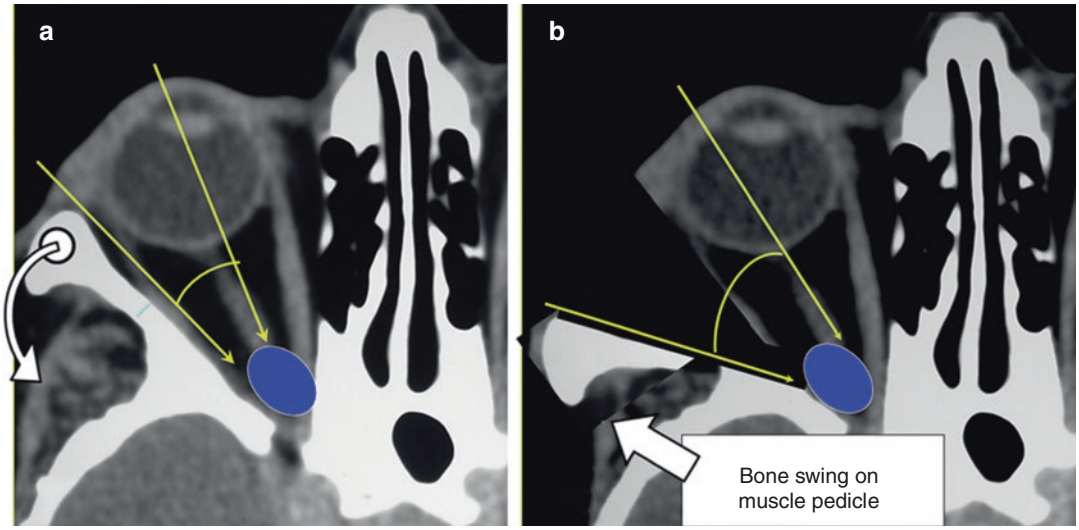

Fig. 20.4 Lateral orbitotomy with bone mobilization. Schematic showing bone mobilisation on a temporalis flap (**a**), thereby reducing the surgical path length and widening the 'conoid of view' (arrows) of the orbital apex (**b**). Arrows demonstrate the 'conoid of view' with each approach

Table 20.6 Advantages of the extended upper lid skin-crease lateral orbitotomy approach compared to previous brow approaches

The surgeon can plan a skin-crease incision approach and extend this intraoperatively into a lateral orbitotomy approach if necessary
Excellent access to the superior and lateral orbit [11]
Shorter, aesthetically acceptable incision than a sub-brow incision
No thinning of the brow hairs
Less brow soft-tissue atrophy

Wright extended brow incision [12, 15], an upper lid skin-crease incision with infero-lateral extension across the horizontal raphe is now the preferred approach (Table 20.6) [16]. Furthermore, the previous techniques with lateral wall removal (i.e. separation form the underlying temporalis muscle) risked ischaemic necrosis of the bone, whereas the contemporary method of swinging the bone on a temporalis muscle flap avoids this risk, retains the good access, and speeds the surgical closure.

Surgery involves extending a lateral two-thirds upper eyelid skin-crease incision for about 10–15 mm into the *infero*-lateral rhytid. The periosteum is incised widely at about 6–7 mm outside the rim, from the lateral one-third of the upper rim to the level of the inferior orbital rim. The periosteum is then raised off the bone in an anterior direction, over the lateral orbital rim, and posteriorly across the lateral orbital wall taking care to diathermy and divide the zygomaticotemporal perforating vessels.

Using a high-frequency oscillating saw, two parallel anteroposterior cuts are made through the lateral wall, the upper cut being at the level of the superficial temporal line and the lower just above the level of the zygomatic arch. Two 10–15 mm relieving incisions are made as 'extensions' of these bony cuts – one being upwards to mobilise the superficial temporal fascia and the other inferiorly into the temporalis muscle – to create a 'muscle hinge' upon which the bone can later be out-fractured. A pair of 2 mm drill holes is placed in the rim either side of each of the osteotomies, and the same drill is used to 'score' the internal face of the lateral wall about 1 cm behind the rim, this creating a fault line which aids subsequent out-fracturing of the rim. With a large retractor placed between the lateral wall and periosteum to protect the orbital contents, the lateral rim is out-fractured on the temporalis muscle hinge and the ragged bone edge of the lateral

orbital wall cropped backwards both to increase access to the orbital apex and to ease repositioning of the mobilised rim at the end of surgery. Venous haemorrhage from the exposed sphenoidal marrow space, if significant, can be treated with bone wax, and access to the orbit is then gained by opening the periosteum behind the arcus marginalis.

This approach is commonly performed for intact excision of large pleomorphic adenomas (Chap. 13) of the lacrimal gland (this diagnosis strongly suggested on clinical and radiological grounds) (Table 20.7 and Fig. 20.5) or for resection of small apical masses or very large intraconal tumours. It can also be used in concert with a pterional neurosurgical approach for wide debulking of orbito-cranial sphenoid wing meningiomas. Following meticulous haemostasis, the laterally displaced bone fragment is swung back into position and secured with 4/0 absorbable sutures passed through each pair of drill holes. A vacuum drain is placed after bone-swinging lateral orbitotomy, with the drain passing out through the lateral eyebrow. The periosteum and deep tissues are closed, in layers, with the same 4/0 soluble suture and the skin incision closed with a running 6/0 nylon suture along its length.

Table 20.7 Clinical and radiological features of pleomorphic adenoma

Gradually progressive lid fullness and hypoglobus
Painless (pain implying malignant transformation)
Hard palpable mass in the lacrimal fossa
CT characteristics
Well-defined lesion
Indentation of the globe
Smooth expansion of the lacrimal gland fossa
Preservation of cortical bone

Transconjunctival Retrocaruncular Approach to the Medial Orbit

The transconjunctival retrocaruncular (transcaruncular) approach provides excellent access to the medial orbit, ethmoid sinuses, the medial half of the orbital floor, and the extraconal structures within the medial part of the orbit (Fig. 20.6) [17]. The approach leaves the lacrimal sac undisturbed, is rapid, and leaves no visible scar and as such is vastly superior to the previously popular Lynch incision. It is particularly valuable where an infero-medial orbital decompression is required for compressive optic neuropathy but is also useful for draining medial orbital collections, for removing medial orbital masses, and for the newly described procedure to correct exotropias where standard strabismus surgery has failed [18].

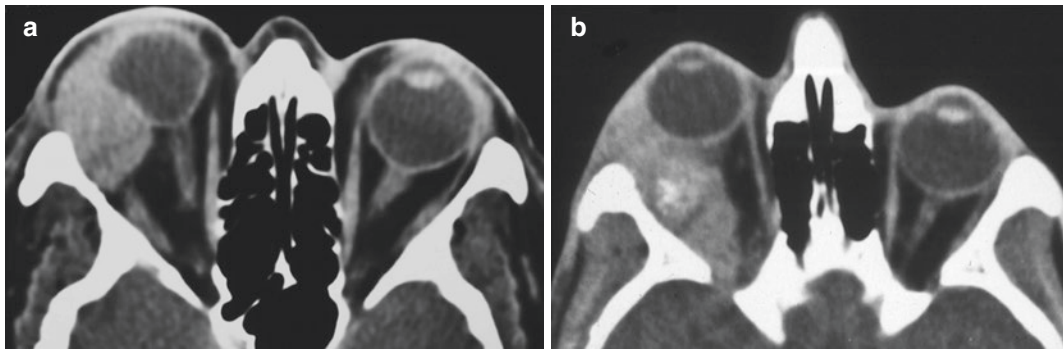

Fig. 20.5 Computed tomography (CT) is the imaging of first choice for investigating the patient with orbital disease. A well-defined solid lesion is shown which indents the globe (**a**) which, taken with the clinical history of a gradually enlarging painless mass, is most likely to be a pleomorphic adenoma that requires intact excision – either through a skin-crease orbitotomy or through a bone-swinging lateral orbitotomy. In contrast, a pervasive lesion which cloaks the globe (without indentation) and which has spread along the lateral orbital wall and invaded the superior ophthalmic fissure. With an acute history of painful lid swelling and exophthalmos, this lesion is likely to be a malignant lacrimal gland neoplasm and requires urgent biopsy through an upper lid skin-crease orbitotomy (**b**)

The medial ends of the eyelids are retracted with 2/0 silk sutures, and discrete points of diathermy are applied to the conjunctiva on the back edge of the caruncle and continued in an arc about 5 mm superiorly and 10–15 mm inferiorly along the fornices. These points define an incision mark at a safe distance from the two canaliculi; the conjunctiva is then opened along this line with tissue scissors, and with the lacrimal sac protected by an 11 mm malleable retractor, the posterior lacrimal crest is exposed by blunt dissection with the scissors directed 45° postero-medially, and the lateral orbital soft tissues gently held laterally with a 16 mm malleable retractor. The plane of dissection remains intraperiosteal for removing or biopsying lesions in the medial orbit. For access to the ethmoid air cells (for medial wall decompression or fracture repair), the extraperiosteal space should be entered about 5 mm posterior to the posterior lacrimal crest, and the medial periosteum is reflected laterally with a 16 mm retractor. This approach affords good access of the orbital apex, from the ethmoidal neurovascular bundles superiorly down to the orbital floor medial to the infraorbital nerve. To prevent fat prolapse, the conjunctival incision should be closed with two 7/0 absorbable sutures, one at the upper and one at the lower border of the caruncle.

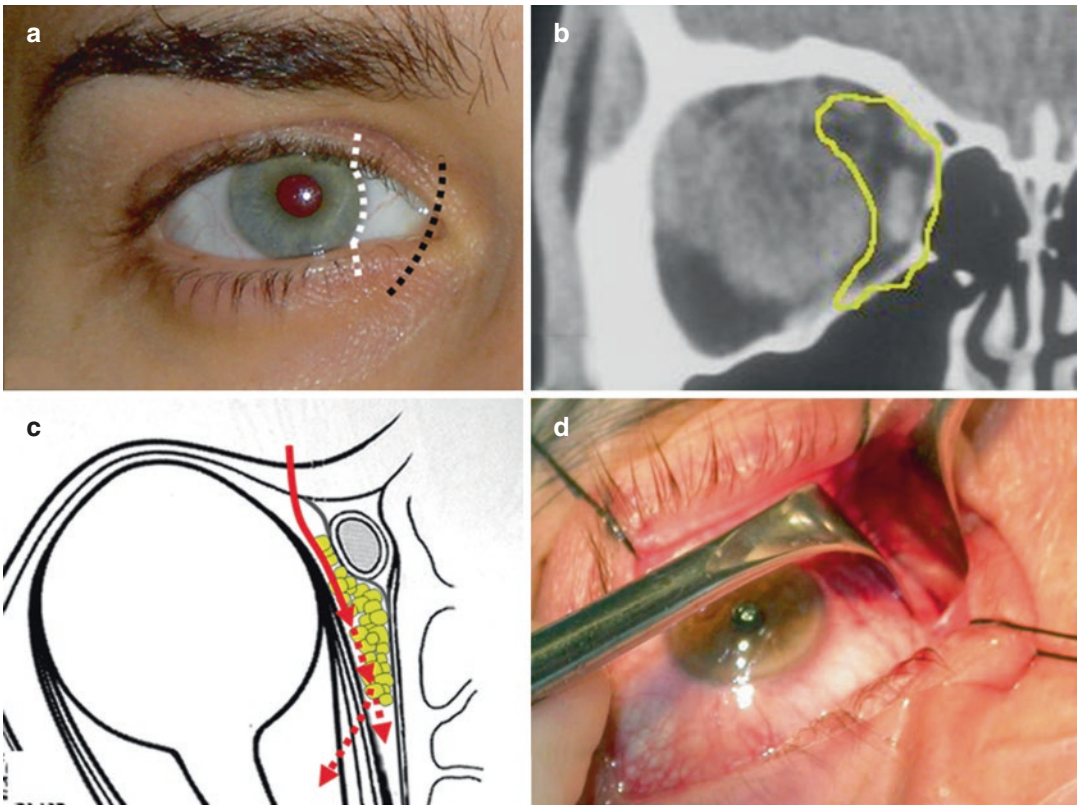

Fig. 20.6 Conjunctival approaches to the orbit. Image showing a peritomy approach (white dotted line) and a retrocaruncular transconjunctival approach (**a**, black dotted line). The region which can be accessed is shown (**b**), while the schematic (**c**) shows the surgical path taken by the retrocaruncular approach. The lids are separated with traction sutures, while two paddle retractors are placed within the medial orbit, one retracting the globe laterally and the other protecting the lacrimal sac (**d**)

The Conjunctival Peritomy Approach

Although this approach might appear to be easier than those described previously, the view of deep orbital structures tends to be much more oblique ('end-on') than that achieved with the eyelid approaches, this often leading to biopsies of inadequate size, biopsies with marked crush artefact, or non-representative samples from the periphery of the true pathology. Despite these limitations, however, the transconjunctival peritomy can still be useful for masses abutting the globe or for retrobulbar lesions [19]. Access to the parabulbar space is achieved through a conjunctival peritomy of up to 180° (with radial relieving incisions to improve access further), and the deep retrobulbar space is reached by fenestrating the posterior Tenon's fascia at the appropriate site. The peritomy is readily closed with 2 or 3 tacking 8/0 soluble sutures at the limbus.

Early Postoperative Management and Counselling

Several manoeuvres may reduce accumulation of fluid and inflammatory mediators deep in the orbit. A vacuum drain may be positioned within the orbital depths, the operated orbit padded moderately firmly, and the patient nursed in a semi-recumbent position. Good postoperative blood pressure control and adequate prevention of coughing, retching, or straining may minimise the risk of postoperative haemorrhage. With surgery in the mid-orbit or apex, intraoperative parenteral glucocorticoids reduce the exudation of inflammatory mediators and offer neuroprotection. A rapidly tapering postoperative course of oral steroid can also be given. Intraoperative and postoperative antibiosis may be used for prolonged procedures and surgeries involving the paranasal sinus cavities to reduce the risk of infection.

In over 30 years of experience, the authors have never seen mydriasis or visual loss caused by a *painless* acute haemorrhage [2]: the only instance of acute haemorrhage causing optic neuropathy (interestingly, due to palpebral artery haemorrhage after eyelid surgery) was associated with both extreme and increasing pain that could not be ignored. Our current recommendation is, therefore, to monitor the patient for severe and increasing pain for 12 h after surgery, rather than the conventional teaching of frequent monitoring of pupillary reactions and vision. Arterial orbital haemorrhage can lead to a 'rock-hard' orbit and optic nerve ischemia, and in such cases, any sutured closure should be released as a matter of urgency, the hematoma drained, and – if necessary – the operative site re-explored to perform diathermy haemostasis and for placement of a corrugated drain.

The orbital vacuum drains are removed once they have stopped draining, this typically being within 8–12 h in most patients. Unless there is any suggestion of slow postoperative orbital bleeding, the anticoagulated patient can restart anticoagulants a day or two after surgery.

Following discharge, usually 1 day after surgery, patients are encouraged to pursue all normal activities, with the exception of vigorous sports, heavy lifting, or inverted yoga positioning – all of which significantly increase orbital venous pressure and which should, therefore, be avoided for 2–3 weeks. In addition, patients are advised not to fly or dive for about 10–14 days after *any* orbital (or lacrimal) surgery involving the paranasal sinuses, this including repair of orbital floor fractures or decompression of the medial wall or orbital floor.

Patients are advised that, following deep orbital surgery, eyelid swelling, ptosis, and diplopia are not uncommon and can take weeks or months to settle fully. The risk of significant diplopia – and its potential impact on lifestyle and livelihood – should be clearly discussed at the outset and surgery planned accordingly. Certain self-employed patients considering aesthetic orbital decompression might reasonably opt for lateral wall decompression alone to minimise the risk of incapacitating short-term diplopia, but the risk of residual exophthalmos, and thus the need for further orbital decompression, should be clearly understood before surgery.

Summary

The surgical principles in managing orbital disease include a detailed understanding of the preoperative surgical risks (such as uncontrolled hypertension or thyrotoxicosis, antiplatelet agents, and herbal remedies), obtaining dedicated orbital imaging (with CT being preferred, except where there is optic nerve disease or intracranial extension of disease), determining whether an incisional biopsy or intact excision is required, and providing comprehensive preoperative counselling to the patient (Table 20.8). With the six fundamental orbitotomies described, it is possible to deal with all solely orbital disease, with almost no need to resort to dated approaches such as lid-split orbitotomy or the bicoronal flap approach. Where disease straddles the craniofacial compartments, however, such patients are best treated by surgeons familiar with periorbital surgery, and this can involve more extensive approaches (such as midfacial degloving, lateral rhinotomy, or bicoronal flap) – with the most complex cases often involving different surgeons with overlapping areas of expertise [20, 21].

Table 20.8 Orbital disease: Principles of surgical management

The preoperative medical risks for surgery should be recognised and treated
Dedicated orbital imaging – typically CT – is required to determine the location and extent of disease
The decision to biopsy a lesion or excise a mass intact is determined on the basis of the history, as well as the clinical and imaging characteristics:
Biopsy:
Pervasive lesions
Lesions straddling surgical boundaries
Where complete excision poses an unacceptable risk to vision
Intact excision:
Well-defined lesions
Probable pleomorphic adenoma (this based on the history and CT findings)
Thorough explanation of the surgical risks to visual functions, these based on preoperative morbidity, location of lesion, and surgical approach
Sound knowledge of the six key orbitotomy approaches and their indications
Maximise width of access (conoid of view)
Minimise surgical path length
Meticulous haemostasis and careful tissue handling
Prompt recognition and treatment of early postoperative haemorrhage

References

1. Dandy W. Results following the transcranial attack of orbital tumours. Arch Ophthalmol. 1941;25:191–6.
2. Rose GE. The "devil's touch"; visual loss and orbital surgery. A synopsis of the Mustardé lecture, 2006. Orbit. 2007;26:147–58.
3. Chatterjee S, Rudra A, Sengupta S. Current concepts in the management of postoperative nausea and vomiting. Anesthesiol Res Pract. 2011;2011:748031. https://doi.org/10.1155/2011/748031.
4. Thompson JP, Rowbotham DJ. Remifentanil–an opioid for the 21st century. Br J Anaesth. 1996;76:341–3.
5. Murpy GR, Glass GE, Jain A. The efficacy and safety of tranexamic acid in cranio-maxillofacial and plastic surgery. J Craniofac Surg. 2016;27:374–9.
6. Hass AN, Penne RB, Stefanyszyn MA, et al. Incidence of postblepharoplasty orbital haemorrhage and associated visual loss. Ophthal Plast Reconstr Surg. 2004;20:426–32.
7. Saraghi M, Golden L, Hersh EV. Anesthetic considerations for patients on antidepressant therapy – part II. Anesth Prog. 2018;65:60–5.
8. Wong WW, Gabriel A, Maxwell GP, et al. Bleeding risks of herbal, homeopathic, and dietary supplements: a hidden nightmare for plastic surgeons? Aesthet Surg J. 2012;32:332–46.
9. Douketis JD, Spyropoulos AC, Spencer FA, et al., American College of Chest Physicians. Perioperative management of antithrombotic therapy: antithrombotic therapy and prevention of thrombosis, 9th ed: American College of Chest Physicians evidence-based clinical practice guidelines. Chest. 2012;141:e326S–50.
10. Pelton RW, Patel BC. Superomedial lid crease approach to the medial intraconal space: a new technique for access to the optic nerve and central space. Ophthal Plast Reconstr Surg. 2001;17:241–53.
11. De Riu G, Meloni SM, Gobbi R, et al. Subciliary versus swinging eyelid approach to the orbital floor. J Craniomaxillofac Surg. 2008;36:439–42.
12. McCord CD Jr, Moses JL. Exposure of the inferior orbit with fornix incision and lateral canthotomy. Ophthalmic Surg. 1979;10:53–63.
13. Mombaerts I, Rose GE, Verity DH. Diagnosis of enlarged extraocular muscles: when and how to biopsy. Curr Opin Ophthalmol. 2017;28:514–21.
14. Hamed-Azzam S, Verity DH, Rose GE. Lateral canthotomy orbitotomy: a rapid approach to the orbit. Eye (Lond). 2018;32:333–7.
15. McNab AA, Wright JE. Lateral orbitotomy – a review. Aust N Z J Ophthalmol. 1990;18:281–6.

16. Harris GJ, Logani SC. Eyelid crease incision for lateral orbitotomy. Ophthal Plast Reconstr Surg. 1999;15:9–16.
17. Shorr N, Bayliss HI, Goldberg RA, et al. Transcaruncular approach to the medial orbit and orbital apex. Ophthalmology. 2000;107:1459–63.
18. Hull S, Verity DH, Adams GG. Periosteal muscle anchoring for large angle incomitant squint. Orbit. 2012;31:1–6.
19. Cho KJ, Paik JS, Yang SW. Surgical outcomes of transconjunctival anterior orbitotomy for intraconal orbital cavernous hemangioma. Korean J Ophthalmol. 2010;24:274–8.
20. Saeed P, van Furth WR, Tanck M, et al. Surgical treatment of sphenoorbital meningiomas. Br J Ophthalmol. 2011;95:996–1000.
21. Shriver EM, Ragheb J, Tse DT. Combined transcranial-orbital approach for resection of optic nerve gliomas: a clinical and anatomical study. Ophthal Plast Reconstr Surg. 2012;28:184–91.

Orbital Implants

21

David R. Jordan and Stephen R. Klapper

Introduction

Removal of an eye may be indicated due to the presence of a malignant tumor, following severe penetrating trauma, or because of degenerative changes resulting from end-stage ocular disease. Loss of binocular visual function with reduced peripheral field and loss of depth perception may result in difficulties with activities of daily living and impose various vocational restrictions [1–6]. Individuals may experience a sense of facial disfigurement and poor self-esteem as a result of the lost body part [3, 4, 6]. Because eye contact and facial appearance are an essential part of human interaction, it is important for the anophthalmic patient to maintain a natural, normal appearing prosthetic eye.

Characteristics of the ideal anophthalmic socket include [7]:

1. A centrally placed, well-covered, buried implant of adequate volume, fabricated from a bioinert material that transmits motility from the implant to the overlying prosthesis.
2. A socket lined with healthy conjunctiva and fornices deep enough to retain the prosthesis and permit horizontal and vertical excursions of the artificial eye.
3. Normal eyelid and eyelash position, appearance, and tone.
4. A supratarsal eyelid fold that is symmetric with that of the contralateral eyelid.
5. A comfortable ocular prosthesis that looks similar to the sighted, contralateral globe and in the same horizontal and anterior-posterior plane.

Currently, no surgical procedure satisfies all of the above criteria. Over the past three decades, there have been numerous developments and refinements in anophthalmic socket surgery with respect to implant material and design, implant wrapping, implant-prosthesis coupling, and socket volume considerations. Successful anophthalmic surgery is achieved when the anophthalmic patient obtains a painless, noninflamed eye socket with adequate volume restoration and an artificial eye that looks and moves almost as naturally as a normal eye.

Historical Perspective

In 1884, P. H. Mules inserted a hollow glass sphere into the scleral cavity following removal of the intraocular contents [8]. A year later W. A.

D. R. Jordan (✉)
Department of Ophthalmology, University of Ottawa Eye Institute and the Ottawa Hospital, Ottawa, ON, Canada

S. R. Klapper
Klapper Eyelid and Facial Surgery, Carmel, IN, USA

C. J. Hwang et al. (eds.), *Clinical Ophthalmic Oncology*,
https://doi.org/10.1007/978-3-030-13558-4_21

Frost introduced a similar implant into Tenon's capsule following an enucleation procedure [9, 10]. The Mules sphere revolutionized anophthalmic socket surgery by replacing lost orbital volume with a buried orbital implant. Complications including migration, extrusion, and implant shattering became evident as use of these novel implants increased [9, 11]. Sponge, rubber, paraffin, ivory, wool, cork, bone, cartilage, silver, gold and many other buried orbital implant materials were utilized with little success over the next several decades [10]. The idea of coupling an orbital implant to the overlying prosthetic eye to improve motility was first reported in 1945 (Rudemann) and was followed by several other unique designs that allowed direct attachment of the orbital implant (via a peg) to an overlying prosthetic eye [9, 12]. Unfortunately, with time and increased use, their complications became more evident, and most coupled implants eventually extruded due to chronic infection [9, 12, 13]. By the 1950s completely buried implants gained wide acceptance [9–11]. A variety of implant designs attempting to indirectly couple the buried implant to an overlying prosthetic eye by modifying the anterior implant surface, a type of quasi-integration, became available (e.g., Iowa implant, Allen implant), as did paired magnets in the implant and prosthetic eye [11, 14–17]. Despite initial acceptance, prosthetic fitting and implant exposure problems plagued these designs [4, 14–18]. Many surgeons returned to simpler spherical buried implants associated with a lower risk of socket complications [9–11]. By 1989 spherical implants made of silicone, polymethylmethacrylate (PMMA), or glass were the implants most widely used by ophthalmic plastic surgeons [18].

Porous Orbital Implants

Hydroxyapatite Implants

In an effort to design a biocompatible, integrated orbital implant, Perry (1991) introduced coralline (sea coral) hydroxyapatite (HA) spheres (Bio-Eye, Integrated Orbital Implants, San Diego, CA) [19]. The HA implants (FDA approved in 1989) represented a new generation of buried, biointegrated spheres with a regular system of interconnecting pores that allowed host fibrovascular ingrowth (Fig. 21.1) [19, 20]. Implant fibrovascularization theoretically was thought to reduce the risk of migration, extrusion, and infection [20]. The HA implant also allowed secure attachment of the extraocular muscles, which was suggested to potentially improve implant motility [19, 20]. By drilling into the HA implant, inserting a peg, and coupling the peg to the prosthetic eye, an improved range of movement and fine darting eye movements (seen during conversation) were possible, permitting a naturally appearing artificial eye.

Although HA implants represented a significant advance in anophthalmic surgery, experience with HA over the last few decades has

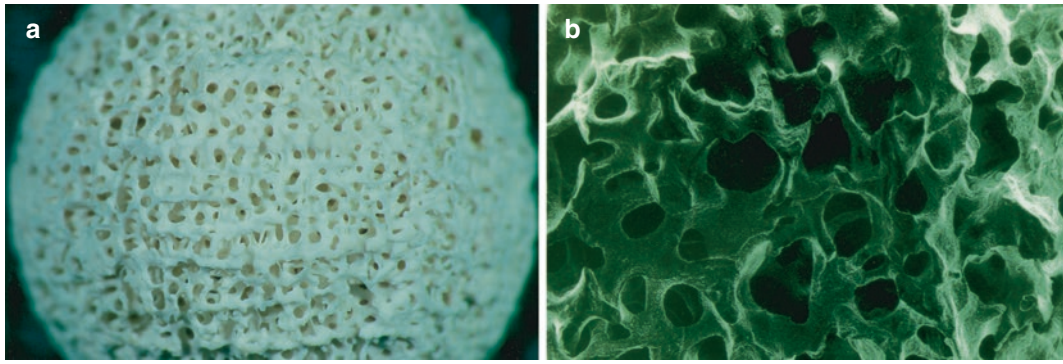

Fig. 21.1 The porous architecture of the Bio-Eye™ hydroxyapatite implant is well visualized (**a**). Scanning electron microscopy illustrating the porous architecture of a Bio-Eye™ (**b**, 222 × 10)

expanded our understanding of its limitations. Reported complications are not uncommon and include implant exposure, conjunctival thinning, socket discharge, pyogenic granuloma formation, implant infection, and persistent pain or discomfort [21–27].

The introduction of HA as an orbital implant significantly raised the costs associated with enucleation, evisceration, and secondary orbital implant procedures. The Bio-Eye™ HA implant cost is much higher ($825–$985 US) than traditional silicone or polymethylmethacrylate (PMMA) spherical implants ($30–$60 US). Additional expenses associated with HA placement include an implant wrap material, assessment of implant vascularization with a confirmatory magnetic resonance (MR) imaging study, a secondary drilling procedure with peg placement, and prosthesis modification. In the search for porous orbital implants with a reduced complication profile and diminished surgical and postoperative costs, numerous alternative implant materials have been introduced worldwide.

Synthetic Porous Polyethylene Implants

Synthetic porous polyethylene (MEDPOR®, Stryker Craniomaxillofacial, Kalamazoo, Michigan, 49002, USA) implants were introduced over two decades ago (MEDPOR®, Porex Surgical Inc., Newnan, GA, USA) for use in the orbit and have been widely accepted as an alternative to the Bio-Eye™ HA [28–31]. Porous polyethylene implants although less biocompatible than HA are typically well tolerated by orbital soft tissue [32]. They have a smoother surface than HA implants which permits easier implantation and potentially less irritation of the overlying conjunctiva following placement (Fig. 21.2). These implants have a high tensile strength yet are malleable which allows sculpting of the anterior surface of the implant. Although the rectus muscles may be sutured directly to the implant, many surgeons may find this challenging without predrilled holes and prefer to use wrapping material to facilitate extraocular muscle attachment. Porous polyethylene implants are available in spherical, egg, conical, and mounded shapes (quad-implant) [29–31]. The anterior surface can also be manufactured with a smooth, nonporous surface to potentially minimize irritation of the overlying tissue (e.g., MEDPOR® smooth surface tunnel implant, SST™) while retaining a larger pore size posteriorly to facilitate fibrovascular ingrowth. The addition of Bioglass (US biomaterials Corp, Alachua, FL, USA) to the MEDPOR® implant may help stimulate early vascular ingrowth and reduce complications such as exposure, migration, and extrusion [33]. The MEDPOR® implant costs vary depending upon

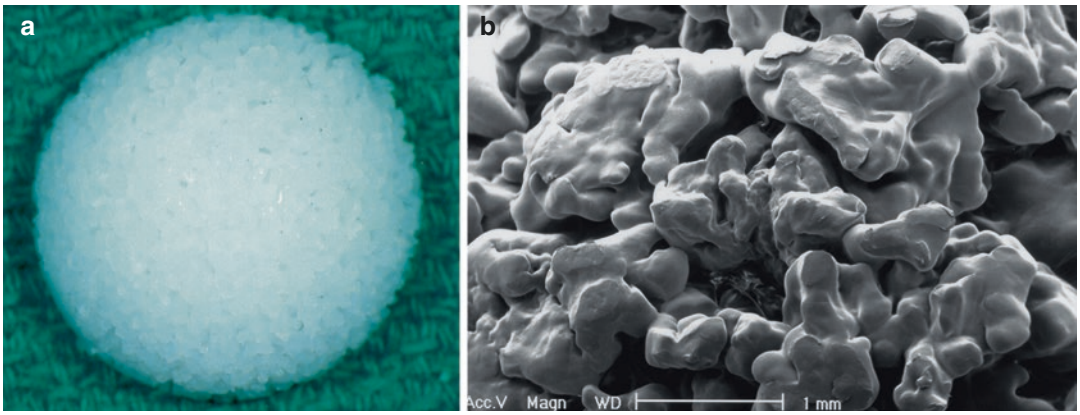

Fig. 21.2 On gross examination, the porous polyethylene implant appears to have more of a channel system than pores (**a**). Scanning electron microscopy of a porous polyethylene implant (222 × 10) illustrating the smooth surface of the architecture as well as the channel system (**b**)

what model is used and the quantity purchased ($600–$777 US).

Synthetic Hydroxyapatite Implants

Synthetic HA implants developed by FCI (Issy-les-Moulineaux, Cedex, France) have an identical chemical composition to that of the Bio-Eye™, although scanning electron microscopy (SEM) has revealed decreased pore uniformity and interconnectivity and the presence of blind pouches [34]. Central implant fibrovascularization in a rabbit model still appears to occur in a similar manner in both the Bio-Eye™ and FCI_3 implants [35]. The synthetic FCI_3 implant has gained in popularity in many parts of the world over the past 20 years; however, it is not yet available in the United States. The problems and complications associated with the synthetic FCI_3 implant are similar to that of the Bio-Eye™ [36]. It is typically less expensive than the Bio-Eye.

Other forms of HA implants in use around the world include the Chinese HA and the Brazilian HA implants [37, 38]. Although less expensive than the Bio-Eye™, these implants have impurities or poor porous structure that make them inferior products [37, 38]. Other implant designs continue to be developed, some of which offer little added value while others have only been in use for a short time and their advantages/disadvantages have not been elucitated [39, 40].

Bioceramic Implants

Aluminum oxide (Al_2O_3) is a ceramic implant biomaterial that has been used in orthopedic surgery and dentistry for more than 30 years. Spherical and egg-shaped Bioceramic Orbital Implants (FCI, Issy-Les-Moulineaux, Cedex, France) have been available in North America for over 15 years. Aluminum oxide is a porous, inert substance and has been suggested as a standard reference material in studies of implant biocompatibility [41]. These implants permit host fibrovascular ingrowth similar to the Bio-Eye™ [42, 43]. Human fibroblasts and osteoblasts proliferate more rapidly on aluminum oxide than HA suggesting it is a more biocompatible substance than HA [32, 41]. The Bioceramic implant is lightweight and has a uniform pore structure and excellent pore interconnectivity (Fig. 21.3a, b) [34]. The microcrystalline structure is smoother than the rough- surfaced Bio-Eye™ (Fig. 21.3c). Although sockets with the aluminum oxide implants may initially be quieter than those with HA, the same complications as other porous implants (e.g., primarily exposure) may be seen [44]. Long term follow-up is important with any porous implant as late complications (years after implantation) are known to occur [44–47]. As with most of the other available porous orbital implants, aluminum oxide implants are less expensive than the Bio-Eye™ ($460–$495 US).

Porous Versus Nonporous Implants

Although porous orbital implants for use following enucleation and evisceration had been tried and discarded several decades ago, a new era in anophthalmic socket surgery began with the introduction of coralline hydroxyapatite (HA) by Dr. A. Perry (discussed earlier) [19].

In 1989, HA accounted for only 1.5% of implants used, but by 1992 it had become the anophthalmic orbital implant of choice [18]. Over the next several years, additional porous implants (e.g., synthetic hydroxyapatite, porous polyethylene, aluminum oxide) entered the marketplace and were widely promoted as reviewed earlier in this chapter [48]. Implant companies often portrayed their porous implant as better than their competitor, frequently with little scientific support. Marketing slogans, such as "the original, the leader, the total solution," "take a closer look at a better material," and "the best choice for implantation candidates," became common at oculoplastic surgery meetings and in ophthalmic plastic surgery journals [49]. During this same time period, we and many others reported our experience with a variety of porous orbital implants including their problems and complications [21–28, 36, 44, 46, 47, 50–52]. It

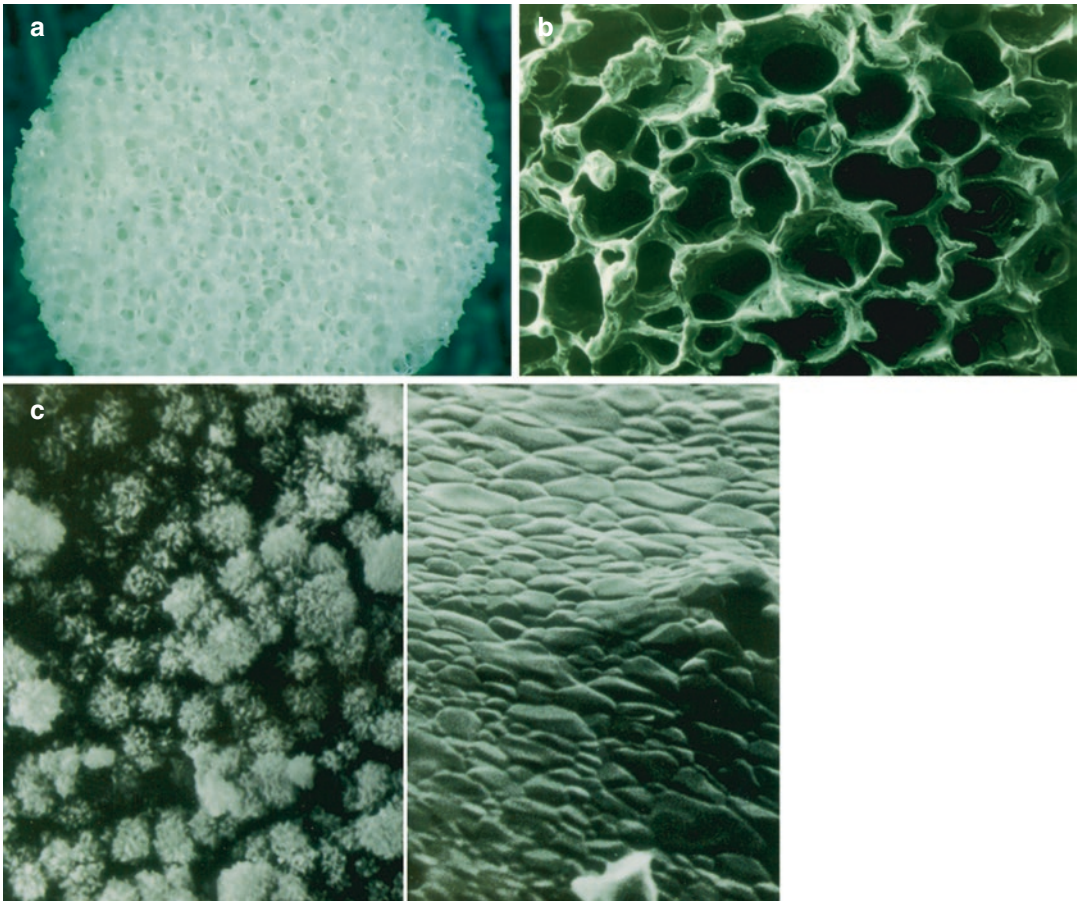

Fig. 21.3 The porous architecture of an aluminum oxide (Bioceramic) implant is well visualized (**a**). Scanning electron microscopy illustrating the more uniform porous architecture of the aluminum oxide orbital implant (**b**, 222 × 10). On high-power scanning electron microscopy (230×10^3), the solid component of the Bio-Eye™ (**c**, left half of photo) has a rough-appearing microcrystalline structure compared to the smooth microcrystalline structure of the aluminum oxide (Bioceramic) implant (**c**, right)

remained difficult to determine whether one porous implant was truly superior than another [23, 28, 36, 44, 46, 47, 50, 51]. However, it became clear that all porous implants had potential complications including conjunctival thinning, implant exposure, pyogenic granulomas, socket discharge, implant infection, persistent pain and discharge, as well as pegging issues [12–23, 28, 44, 46, 50, 51]. With time, some surgeons began to question the use of porous implants and advocated a return to nonporous spheres because of their overall low complication rate [52–55]. Spirited debate centered on multiple questions including the following: which porous implant is the best, should they be wrapped, which wrap is the best, should they be pegged, which peg system is the best, who should be pegged, when should pegging be done, are porous implants truly advantageous, do they have a lower migration rate, do they have a lower extrusion rate, is there resistance to infection, and is there any motility advantage? [56].

With respect to implant migration, an early enucleation technique by Frost-Lange involved imbricating the extraocular muscles over unwrapped polymethylmethacrylate (PMMA) or silicone spheres [57]. It is now well established that this technique leads to *superotemporal* implant migration in 16% or more of patients over 8–10 years, so it has largely been abandoned [50,

58–60]. Nunnery, Wells, and others have shown that attaching the rectus muscles in their normal anatomic position to nonporous spheres (e.g., PMMA, silicone) results in a very low *superotemporal* migration rate (0–1.3%) and is stable over many years [59–61]. Reports of *superotemporal* migration with porous orbital implants are not significantly different (0.5–1.7%) [18, 53]. However, if one considers *anterior migration* of porous implants, the overall rate of implant migration may be higher with porous implants as this type of implant migration is seldom discussed. *Anterior migration* manifests as implant exposure. These cases are often grouped with other cases of implant exposure that may be due to a variety of other factors (e.g., inadequate or poor closure, infection, mechanical or inflammatory irritation from the rough anterior surface of the porous implant, delayed ingrowth of fibrovascular tissue with subsequent tissue breakdown, and pressure points from a poorly fit prosthesis) [36]. *Anterior migration* is most often secondary to improper seating of the porous implant. Porous implants have a rough surface and drag tissue inward as they are placed into the orbit; this "Velcro" effect makes implantation technically more demanding [54]. A tissue glide or wrap may help avoid the posterior drag of anterior tissue [62]. The overlying tissue may be closed successfully over the implant, but with time the tissues dragged inward may try to return to their original relaxed position – a natural restitution of tissue (cactus syndrome) [62]. As this occurs, a gradual migration of the implant anteriorly with progressive conjunctival thinning and eventual tissue breakdown over the anterior implant surface (exposure) occurs [62]. Fibrovascular ingrowth has not been shown to diminish implant exposure risk [61]. Thus, there is little evidence that implant migration is less with porous orbital implants; it may actually be more common if one also considers anterior implant migration.

With respect to implant extrusion, when nonporous implants become exposed, they typically extrude from the socket [51, 52]. When porous orbital implants become exposed, the fibrovascular ingrowth helps retain them within the orbit, often preventing complete extrusion. Although porous implant exposures can be surgically repaired by a variety of techniques, large, recurrent, or persistent exposures may require implant removal which essentially is a delayed extrusion (iatrogenic). Rather than ask whether porous orbital implants have a decreased extrusion rate, it is more prudent to ask whether they have a "decreased exposure rate." [59]. Implant exposure is the most frequent and challenging problem associated with porous orbital implants [52]. Reported exposure rates for nonporous spherical implants (e.g., PMMA/silicone) are typically low (0–3%) [18, 23, 52, 59–61]. Exposure rates for porous orbital implants are also generally low but can vary from 0% to 50% [18, 44, 47, 52, 53, 61]. Custer et al. reviewed pooled data and found a 6.6% exposure rate in 3012 porous orbital implants compared to 2.9% in 615 nonporous implants [52]. More recently, Wladis et al. reported that rates of exposure (and extrusion) are generally comparable between porous and nonporous implants, suggesting the choice of implant may not result in a dramatic difference in this complication [61]. Thus, there is little evidence that porous implants have a reduced extrusion or exposure rate, and in fact, it may be higher [52, 53]. Porous implant exposures can occur anytime, and with the longer the follow-up, the greater the number of exposures [46, 51, 52].

With respect to infection, nonporous implants (e.g., PMMA/silicone) have been shown to have a low infection rate (0–1%) [18, 60, 61]. Unpegged porous orbital implants also have a low infection rate (0–2%) [36, 44, 46, 47, 53, 61]. Pegging porous implants is associated with an increased number of complications, one of which is infection and has been reported in up to 20% of pegged orbital implants in one study [46, 51]. Fibrovascular ingrowth has not been shown to afford protection against infection [61]. Thus, there is little evidence to support the suggestion that porous orbital implants have a reduced infection rate; it appears to be similar to nonporous implants and potentially higher with a peg [46, 51].

With respect to enhanced motility, peg placement has been shown to improve horizontal gaze movements in the artificial eye [20, 63–65]. There is also a more natural movement to the prosthesis because of the fine darting eye movements retained with direct coupling to a peg [20,

54]. However, without a peg in place, there is no proven motility advantage of porous over nonporous implants [52, 61, 63–65].

As with innovative implant designs from the past (e.g., Mules, Rudemann, Cutler), the initial wave of enthusiasm with porous implants has been tempered as an increasing number of surgeons recognizing that the touted advantages have little scientific data to support them and that these implants are associated with numerous risks and complications that may be challenging to manage [18, 21, 23, 36, 46–52]. Porous implants may not be the presumptive "gold standard" as often marketed [49], and continued research is essential to develop improved materials and techniques to further minimize the complications associated with anophthalmic surgery.

Implant Selection

There continues to be little consensus regarding orbital implant material and design preference [60]. Surgeons have their own preferences regarding porous versus nonporous implants, spherical versus shaped implants, wrapped versus unwrapped implants, and pegged versus unpegged implants. Implant cost, surgery center and hospital budgets, and marketing pressures also play a role in implant selection.

When deciding upon an implant to use, these authors divide the various implants into three useful categories:

1. Porous spheres that may potentially be pegged (HA – coralline or synthetic, porous polyethylene (MEDPOR®), aluminum oxide (Bioceramic))
2. Quasi-integrated implants (Universal implant, Durette implant, Quad MEDPOR®)
3. Standard nonporous sphere (polymethymethacrylate, silicone)

Ophthalmic surgeons currently favor the use of porous implants even though unpegged porous implants have no apparent advantage over nonporous spheres [53, 61, 63, 65–67]. The decision to use a porous or nonporous implant is up to the surgeon and his/her patient. Porous implants are not for every patient [54, 55]. If the patient is healthy and roughly between the ages of 15 and 70 years, a porous implant (e.g., aluminum oxide implant) that can potentially be pegged is initially considered [43, 44]. Those with chronic systemic disease (e.g., collagen vascular disease, autoimmune disorders, diabetes mellitus, peripheral vascular disease) or who use immunosuppressive medication (e.g., prednisone, methotrexate, etc.) or have undergone prior socket radiation are generally poor candidates [50, 51]. Porous orbital implants are also not for every ophthalmic surgeon [54, 55]. Implantation requires experience and skill to appreciate technical nuances critical for a successful outcome. We *only* consider porous implant use in healthy, adult patients wanting maximal prosthetic motility (pegging) and willing to accept the potential increased risk of complications. Ideally, the patient *should* live within a reasonable travel distance to maintain regular follow-up visits so that any minor implant problems can be promptly addressed. Continued follow-up (typically every 1–2 years) is essential for porous implants (pegged or unpegged) as small problems (e.g., implant exposure) can often be handled within the office/minor room setting before they develop into a more extensive problem (e.g., implant infection), requiring additional surgery and potentially implant removal [44, 46]. If there is no plan to peg, a nonporous implant (sphere or mounded) may be preferred. Nonporous spherical implants can be used efficiently and effectively during a primary procedure such as enucleation or evisceration; the surgical techniques required can be mastered by most ophthalmic surgeons. Direct anatomic fixation of the rectus muscles to a solid silicone sphere or a wrapped PMMA sphere provides implant stability and good prosthesis movement [60]. Motility results are similar to that of nonpegged porous implants [60, 61, 63–65]. Nonporous implants are inexpensive, and in a health care era in which the global expense of a patient's anophthalmic socket rehabilitation should be considered, a cost-conscious primary procedure with a low incidence of complications may be desirable [60].

A quasi-integrated implant such as the Universal or Durette (PMMA) and the

MEDPOR® Quad mounded implant are alternative considerations to the porous or nonporous spherical implants as the mounded surface of the implant potentially offers improved motility over a standard sphere as a result of the partial coupling that occurs between the mounds on the implant and the posterior surface of the prosthesis [31]. Correct implant placement is technique sensitive and may require considerable surgeon experience with enucleation and secondary implant placement.

In a young child (less than 5 years), a wrapped nonporous sphere (PMMA, silicone) centered within the muscle cone and connected to the four rectus muscles and the inferior oblique muscle or a PMMA mounded implant (Universal or Durette) is preferred. Implant exchange with a porous orbital implant that can potentially be pegged is considered at a later age (roughly > 15 years). An additional factor to consider in children undergoing eye removal is the need for further growth of the orbit. Eighty percent of adult orbital volume is reached around 5 years of age, with adult volume achieved by 12–14 years [68, 69].

Orbital soft tissue volume is a critical factor in continued orbital and facial bone growth, and thus adequate socket volume replacement following enucleation or evisceration surgery is important. The ocular prosthesis is also believed to be an important factor that helps minimize orbital growth retardation and prevent significant periorbital asymmetries following enucleation or evisceration. Autogenous dermis-fat grafts are an alternative to the above described orbital implants in children under 5 years of age for volume replacement. These grafts may undergo hypertrophy and help stimulate orbital bone growth [70, 71].

Socket Volume Considerations

Removal of an eye following enucleation or evisceration creates an orbital soft tissue volume deficiency. Insufficient volume replacement often results in an abnormally deep superior sulcus, upper eyelid ptosis, and enophthalmos and may require a larger than desirable prosthesis (the "anophthalmic socket syndrome") [72–77].

The ideal implant volume may be estimated either preoperatively from the axial length of the eye or intraoperatively by determining the volume of fluid the enucleated eye displaces in a graduated cylinder [72, 75–78]. Several authors have reported that the variability of axial length and globe volume can be significant with globe volumes varying between 6.9 and 9.0 mL [75–77]. Calculated implant volumes can be greater than 22 mm in some instances. Implants larger than 22 mm may be unavailable, are difficult to insert in the socket, frequently limit socket excursion, have a higher exposure rate, and hinder fitting of an acceptable custom prosthesis [72, 77, 78].

Ideally, 70–80% of the volume of an individual's normal globe should be replaced with the orbital implant [75]. This generally allows for a prosthetic volume that is approximately 2 mL [72]. Larger prostheses often result in progressive lower eyelid laxity and malposition due to the weight of the prostheses on the eyelid. Larger prostheses may also have limited socket excursion [72].

In most adults, 20–22 mm spherical implants are typically used following enucleation and 18–20 mm implants following evisceration. In pediatric patients slightly smaller implants (16–18 mm) may be sufficient, depending on the patient's age and orbital development. Individualization of the implant size is important in optimizing orbital volume replacement and in achieving the best possible esthetic result [74, 75, 77, 78].

Orbital Implant Wrapping

Placement of an HA implant or Bioceramic implant within the soft tissue of the eye socket is facilitated by a smooth wrapping material which diminishes tissue drag and facilitates precise anatomic fixation of the rectus muscles to the implant surface [19, 62]. Implant wraps may also provide a barrier function over the spiculated porous implant surface [19, 45] although there is some debate as to whether exposure is truly minimized by an avascular implant covering [79–81]. Suggested advantages of placing an unwrapped implant include simplification of the procedure, decreased operating room time, reduced cost,

elimination of a second surgical site for harvesting autogenous wrap, avoidance of a possible barrier to fibrovascular ingrowth, and decreased risk of disease transmission [79–81].

Human donor sclera was historically the first choice of implant wrapping material for most orbital surgeons [19, 20]. The use of human donor material, however, carries the risk of transmission of viruses (e.g., HIV, hepatitis B or C) and other pathogens (prions) that may be responsible for a variety of degenerative disorders (e.g., Creutzfeldt-Jakob disease) [82, 83]. Although we are not aware of any reports of disease transmission from donor sclera, segments of the human immunodeficiency virus (HIV)-1 genome have been identified in preserved human sclera [82, 84]. Creutzfeldt-Jakob disease (prion) transmission from dural and corneal transplants has been reported [85–87]. In addition, seronegative organ and tissue donors may transmit HIV [88]. Many eye banks also charge a substantial fee to provide donor sclera.

Specially processed human donor pericardium, fascia lata, and sclera are marketed (Biodynamics International (USA), Inc., Tampa, FL) as safe alternative implant wraps to preserved human donor tissues. These wraps have the convenience of a long (up to 5 years) shelf life; however, they are currently priced at levels that may exceed the cost of the implant itself.

Processed bovine pericardium (Peri-Guard® or Ocu-Guard™ Supple, Bio Vascular Inc., Saint Paul, MN, USA) is FDA approved and also available as an implant wrap material [89, 90]. Although there have been only few cases of bovine spongiform encephalopathy (BSE) in American cattle to date, reports of infected cattle in Alberta, Canada, have surfaced in the past decade, and the potential for the disease to occur with possible prion transmission still exists [83].

Autologous temporalis fascia [91], fascia lata [92], rectus abdominis sheath [93], and posterior auricular muscle complex graft [94] have been tried as orbital implant wrapping materials. Use of these tissues requires a second operative site, prolonged operative time, and a potentially increased risk of morbidity.

Microporous expanded polytetrafluoroethylene (e-PTFE) (Gore-Tex, W. L. Gore & Associates, Flagstaff, AZ) has also been advocated as an implant wrapping material (Oculo-Plastik, Montreal, Quebec, Canada); however, complications with its use have made it undesirable [95–97].

Undyed polyglactin 910 mesh (Vicryl mesh, Ethicon, Somerville, NJ, USA) is a bioabsorbable synthetic material and is our preference as a wrapping material for porous orbital implants [98, 99]. Vicryl mesh eliminates the risk of infectious disease transmission, does not require a second surgical site, is readily available, is simple to use, and is inexpensive. Vicryl mesh-wrapped HA implants have been shown to permit rapid implant fibrovascularization in an animal model and may provide a potential advantage of permitting fibrovascular ingrowth over the entire implant surface unlike implants completely wrapped in sclera [99–101]. We have reported a 2.1% incidence of implant exposure in 187 consecutive patients receiving Vicryl mesh-wrapped HA orbital implants [102]. The addition of a small scleral cap (13–15 mm) over the anterior surface of the Vicryl mesh-wrapped implant may reduce implant exposure even further [45]. Oestreicher et al. [26] also reported a low exposure incidence using a similar bioabsorbable wrapping material composed of polyglycolic acid (Dexon mesh style No. 8, non-stretch, medium-weight closed tricot, Davis & Geck, Manati, Puerto Rico). Despite our success with polyglactin 910 mesh as an implant wrap material, some surgeons continue to believe that it is associated with a higher rate of implant exposure [51, 103]. It remains the view of these authors that high exposure rates with Vicryl mesh-wrapped implants are a technique-related problem that can be significantly minimized with correct implant insertion and meticulous tension-free wound closure. We also now routinely place a 13–15 mm diameter cap of donor sclera over the anterior surface of the mesh-wrapped implant as added insurance against implant exposure [45].

Pegging Porous Orbital Implants

Motility peg placement improves horizontal gaze movements in the artificial eye [66]. Despite the improved motility, many surgeons and patients elect to avoid peg placement due to the satisfac-

tory results without pegging and the possibility of pegging-related complications [60, 104–109]. Complications with implant pegging may include discharge, recurrent pyogenic granulomas, implant exposure around the peg, implant infection, tissue overgrowth, peg dislocation, audible clicking, and various fitting problems [104]. Refitting the prosthesis, scleral patch grafting, peg removal, and occasionally implant removal may be required [104].

Although the use of pegging has declined dramatically over the past few years, a precise and meticulous technique [110] in the appropriately selected individual can yield a successful outcome. Johnson [111] and others [45, 46] have also shown largely positive results, validating the efficacy of pegging porous orbital implants (e.g., hydroxyapatite, Bioceramic) with minimal risk of significant complications.

Proper care of the artificial eye and regular follow-up visits with the ocularist and ophthalmic plastic surgeon are important. Watching for small problems (e.g., exposure around the peg) and management of these minor issues at an early stage can often avoid more serious problems with the peg and implant later. If the patient is unlikely, unable, or unwilling to adhere to timely follow-up visits, pegging should be avoided. The authors do not think children (less than age 15 years), older adults (over the age of 70 years), or individuals of any age with a chronic illness (diabetes mellitus, collagen vascular disease, autoimmune disorder, peripheral vascular disease, or immunosuppression) should be considered for pegging.

Peg systems were generally designed for peg placement once fibrovascularization of the implant has been completed. Drilling into an avascular area of the implant may predispose the implant to infection [112]. Gadolinium-enhanced MR imaging is currently the recommended method of assessing the extent of implant vascularization [113]. Fibrovascular ingrowth may occur at varying rates in different patients. Implant drilling and peg insertion are generally deferred until 10–12 months following HA implant placement.

Several titanium peg systems used to be available for the various porous orbital implants. The only system available at this time is the P-K titanium peg for the Bio-Eye™ and supplied by Integrated Orbital Implants (11230 Sorrento Valley Road, Suite 135, San Diego, CA, 92121). Titanium is more biocompatible and better tolerated by human soft tissue than the original peg systems made of polycarbonate [114]. The once available FCI peg system utilized a hydroxyapatite-coated titanium sleeve [109]. The HA coating potentially allowed for stronger interface bonding with the orbital fibroblasts than the uncoated P-K system supplied for use with the Bio-Eye™. The MEDPOR® Motility Coupling Post (MCP) which is also no longer available was a titanium screw that could be screwed directly into porous polyethylene implants [115, 116]. Some authors used to advocate primary placement of the MCP at the time of implant insertion; however, this practice was controversial, and most surgeons deferred implant pegging for more than 6 months after implant placement [18, 21].

Summary

Anophthalmic surgery is no longer simply about replacing a diseased eye with an orbital implant. Ophthalmic surgeons and ocularists are increasingly focused on restoring a patient's appearance and prosthetic motility to as near normal as possible. Evisceration surgery is favored by many surgeons because of the simplicity of the technique, minimal disruption to the socket anatomy, and excellent cosmetic results. Enucleation is still required in patients with known or potentially occult ocular malignancies as well as blind, painful, and/or unsightly eyes with opaque media and unknown or poorly documented past ocular histories [117].

References

1. Coday MP, Warner MA, Jarling KV, et al. Acquired monocular vision, functional consequences form the patients perspective. Ophthalmic Plast Reconstr Surg. 2002;18:55–63.
2. Bohman E, Roed Rassmussen ML, Dafgard Kopp E. Pain and discomfort in the anophthalmic socket. Curr Opin Ophthalmol. 2014;25:455–60.

3. Rasmussen ML, Ekholm O, Prause JU, et al. Quality of life of eye amputated patients. Acta Ophthalmol. 2012;90:435–40.
4. Ahn JM, Lee SY, Yoon JS. Health related quality of life and emotional status of anophthalmic patients in Korea. Am J Ophthalmol. 2010;149:1005–11.
5. Masdottir S, Sahlin S. Patient satisfaction and results after evisceration with a split-sclera technique. Orbit. 2007;26:241–7.
6. McBain HB, Ezra DG, Rose GE, et al. The psychological impact of living with an ocular prosthesis. Orbit. 2014;33:33–9.
7. Jordan DR, Klapper SR, Mawn LA. Chapt 36: The anophthalmic socket and complications. In: Fay A, Dolamn P, editors. Diseases and disorders of the orbit and ocular adnexa. Edinburgh: Elsevier; 2017. p. 657–75.
8. Mules PH. Evisceration of the globe, with artificial vitreous. Trans Ophthalmol Soc UK. 1885;5:200–6.
9. Gougelmann HP. The evolution of the ocular motility implant. Int Ophthalmol Clin. 1970;10(4):689–711.
10. Kelley JJ. History of ocular prosthesis. Int Ophthalmol Clin. 1970;10(4):713–9.
11. Luce CM. A short history of enucleation. Int Clinics North America Int Ophthalmol Clin. 1970;10:681–7.
12. Cutler NL. A positive contact ball and ring implant for use after enucleation. Arch Ophthalmol. 1947;37:73–8.
13. Beard C. Remarks on historical and newer approaches to orbital implants. Ophthalmic Plast Reconstr Surg. 1995;11(2):89–90.
14. Allen JH, Allen L. A buried muscle cone implant: development of a tunneled hemispherical type. Arch Ophthalmol. 1950;43:879–90.
15. Allen LH, Ferguson EC III, Braley AE. A quasi integrated buried muscle cone implant with good motility and advantages for prosthetic fitting. Trans Am Acad Ophthalmol Otolaryngol. 1960;64:272–8.
16. Spivey BE, Allen LH, Burns CA. The Iowa enucleation implant: a ten year evaluation of techniques and results. Am J OPhthalmol. 1969;67:171–81.
17. Jordan DR, Anderson RL, Nerad JA, et al. A preliminary report on the universal implant. Arch Ophthalmol. 1987;105:1726–31.
18. Hornblass A, Biesman BS, Eviator JA. Current techniques of enucleation: a survey of 5,439 intraorbital implants and a review of the literature. Ophthalmic Plast Reconstr Surg. 1995;11:77–88.
19. Perry AC. Advances in enucleation. Ophthal Clin North Am. 1991;4:173–82.
20. Dutton JJ. Coralline hydroxyapatite as an ocular implant. Ophthalmology. 1991;98:370–7.
21. Nunery WR, Heinz GW, Bonnin JM, et al. Exposure rate of hydroxyapatite spheres in the anophthalmic socket: histopathologic correlation and comparison with silicone sphere implants. Ophthalmic Plast Reconstr Surg. 1993;9:96–104.
22. Goldberg RA, Holds JB, Ebrahimpour J. Exposed hydroxyapatite orbital implants: report of six cases. Ophthalmology. 1992;99:831–6.
23. Buettner H, Bartley GB. Tissue breakdown and exposure associated with orbital hydroxyapatite implants. Am J Ophthalmol. 1992;113:669–73.
24. Kim YD, Goldberg RA, Shorr N, et al. Management of exposed hydroxyapatite orbital implants. Ophthalmology. 1994;101:1709–15.
25. Remulla HD, Rubin PAD, Shore JW, et al. Complications of porous spherical orbital implants. Ophthalmology. 1995;102:586–93.
26. Oestreicher JH, Liu E, Berkowitz M. Complications of hydroxyapatite orbital implants: a review of 100 consecutive cases and a comparison of Dexon mesh (polyglycolic acid) with scleral wrapping. Ophthalmology. 1997;104:324–9.
27. Jordan DR, Brownstein S, Jolly SS. Abscessed hydroxyapatite orbital implants: a report of two cases. Ophthalmology. 1996;103:1784–7.
28. Blaydon SM, Shepler TR, Neuhaus RW, et al. The porous polyethylene (Medpor) spherical orbital implant: a retrospective study of 136 cases. Ophthalmic Plast Reconstr Surg. 2003;19:364–74.
29. Karesh JW, Dresner SC. High density porous polyethylene (Medpor) as a successful anophthalmic implant. Ophthalmology. 1994;101:1688–96.
30. Rubin PAD, Popham J, Rumeldts S, et al. Enhancement of the cosmetic and functional outcomes of enucleation with the conical orbital implant. Ophthalmology. 1998;105:919–25.
31. Anderson RL, Yen MT, Lucci LM, et al. The quasi-integrated porous polyethylene orbital implant. Ophthalmic Plast Reconstr Surg. 2002;18:50–5529.
32. Mawn LA, Jordan DR, Gilberg S. Proliferation of human fibroblasts in vitro after exposure to orbital implants. Can J Ophthalmol. 2001;36:245–51.
33. Ma Y, Schou KR, Maloney-Schou M, et al. The porous polyethylene/Bioglass spherical orbital implant: a retrospective study of 170 cases. Ophthalmic Plast Reconstr Surg. 2011;27:21–7.
34. Mawn L, Jordan DR, Gilberg S. Scanning electron microscopic examination of porous orbital implants. Can J Ophthalmol. 1998;33:203–9.
35. Jordan DR, Munro SM, Brownstein S, et al. A synthetic hydroxyapatite implant: the so-called counterfeit implant. Ophthalmic Plast Reconstr Surg. 1998;14(4):244–9.
36. Jordan DR, Bawazeer A. Experience with 120 synthetic hydroxyapatite implants (FCI_3). Ophthalmic Plast Reconstr Surg. 2001;17:184–90.
37. Jordan DR, Pelletier C, Gilberg SM, et al. A new variety of hydroxyapatite: the Chinese Implant. Ophthalmic Plast Reconstr Surg. 1999;15(6):420–4.
38. Jordan DR, Hwang I, McEachren TM, et al. Brazilian hydroxyapatite implant. Ophthalmic Plast Reconstr Surg. 2000;16:363–9.
39. Jordan DR, Brownstein S, Gilberg S, et al. Investigation of a bioresorbable orbital implant. Ophthalmic Plast Reconstr Surg. 2002;18:342–8.
40. Klett A, Guthoff R. Deckung von Orbitaimplantaten mit muskelgestielter autologer sklera. Ophthalmologe. 2003;100:449–52.

41. Christel P. Biocompatibility of alumina. Clin Orthop. 1992;282:10–8.
42. Jordan DR, Mawn L, Brownstein S, et al. The bioceramic orbital implant: a new generation of porous implants. Ophthalmic Plast Reconstr Surg. 2000;16:347–55.
43. Jordan DR, Gilberg S, Mawn LA. The bioceramic orbital implant: experience with 107 implants. Ophthalmic Plast Reconstr Surg. 2003;19:128–35.
44. Jordan DR, Klapper SK, Gilberg SM, et al. The bioceramic implant: evaluation of implant exposures in 419 implants. Ophthalmic Plast Reconstr Surg. 2010;26:80–2.
45. Wang JK, Lai PC, Liao SL. Late exposure of the bioceramic orbital implant. Am J Ophthalmol. 2009;147:162–70.
46. Karslioglu SK, Buttanri IB, Fazil K, et al. Long-term outcomes of pegged and unpegged bioceramic orbital implants. Ophthalmic Plast Reconstr Surg. 2012;28:264–7.
47. Jordan DR, Gilberg SM, Bawazeer A. The coralline hydroxyapatite orbital implant (Bio-Eye™): experience with 170 Patients. Ophthalmic Plast Reconstr Surg. 2004;20(1):69–71.
48. Jordan DR. Anophthalmic orbital implants. Ophthal Clinics North Am. 2000;13(4):587–608.
49. Integrated Orbital Implants, Inc. advertisement. Ophthalmic Plast Reconstr Surg. 2017;33:2:1.
50. Jordan DR, Brownstein S, Faraji H. Clinicopathologic analysis of 15 explanted hydroxyapatite implants. Ophthalmic Plast Reconstr Surg. 2004;20(4):285–90.
51. Jordan DR, Chan S, Mawn L, et al. Complications associated with pegging hydroxyapatite orbital implants. Ophthalmology. 1999;106:505–12.
52. Custer PL, Trinkhaus KM. Porous implant exposure: incidence, management and morbidity. Ophthalmic Plast Reconstr Surg. 2007;23:1:1–7.
53. Su GW, Yen MT. Current trends in managing the anophthalmic socket after primary enucleation and evisceration. Ophthalmic Plast Reconstr Surg. 2004;20(4):274–80.
54. Goldberg RA. Who should have hydroxyapatite orbital implants? Arch Ophthalmol. 1995;113:566–7.
55. Codere F. Hydroxyapatite implants: a rational approach. Can J Ophthalmol. 1995;30:235–7.
56. Jordan DR. Porous orbital implants; are they advantageous and anyone still pegging? American Society of Ophthalmic Plastic and Reconstructive Surgery meeting, Fairmont, Waterfront Hotel, Vancouver, British Columbia, June 23–25, 2017.
57. Allen L. The argument against imbricating the rectus muscles over spherical orbital implants after enucleation. Ophthalmology. 1983;90:1116–20.
58. Trichopoulos N, Augsberger JJ. Enucleation with unwrapped porous and nonporous orbital implants: a 15-year experience. Ophthal Plast Reconst Surg. 2005;21(5):331–6.
59. Nunery WR, Cepela MA, Heinz GW, et al. Extrusion rate of silicone spherical anophthalmic socket implants. Ophthalmic Plast Reconstr Surg. 1993;9:290–4.
60. Wells ST, Harris GJ. Direct fixation of extraocular muscles to a silicone sphere: a cost-sensitive, low risk enucleation procedure. Ophthalmic Plast Reconstr Surg. 2011;27:364–7.
61. Wladis EI, Aakalu VK, Sobel RK, et al. Orbital implants in enucleation surgery; a report by the American Academy of Ophthalmology. Ophthalmol 2017; 2017. pii: S0161–6420(17)32438–7. https://doi.org/10.1016/j.ophtha.2017.08.006. [Epub ahead of print].
62. Sagoo MS, Rose GE. Mechanisms and treatment of extruding intraconal implants. Arch Ophthalmol. 2007;125(12):1116–620.
63. Custer PL, Trinkaus KM, Fornoff J. Comparative motility of hydroxyapatite and alloplastic enucleation implants. Ophthalmology. 1999;106:513–6.
64. Guillinta P, Vasani SN, Granet DB, et al. Prosthetic motility in pegged and unpegged integrated porous orbital implants. Ophthalmic Plast Reconstr Surg. 2000;19:119–22.
65. Colen TP, Paridaens DA, Lemij HG, et al. Comparison of artificial eye amplitudes with acrylic and hydroxyapatite spherical enucleation implants. Ophthalmology. 2000;107:1889–94.
66. Guillinta P, Vasani SN, Granet DB, et al. Prosthetic motility in pegged versus unpegged integrated porous orbital implants. Ophthalmic Plast Reconstr Surg. 2000;19:119–22.
67. Custer PL, Kennedy RH, Woog JJ, et al. Orbital implants in enucleation surgery, a report by the American Academy of Ophthalmology. Ophthalmology. 2003;110:2054–61.
68. Bentley RP, Sgouros S, Natarajan K, et al. Normal changes in orbital volume during childhood. J Neurosurg. 2002;96:742–6.
69. Yago K, Furuta M. Orbital growth after unilateral enucleation in infancy without an orbital implant. Jpn J Ophthalmol. 2001;45:648–52.
70. Heber KL, Katowitz JA, Low JE. Unilateral dermis-fat graft implantation in the pediatric orbit. Ophthalmic Plast Reconstr Surg. 1998;14:81–8.
71. Mitchell KT, Holster DA, White WL. The autogenous dermis-fat orbital implant in children. J AAPOS. 2001;5:367–9.
72. Kaltreider SA. The ideal ocular prosthesis: analysis of prosthetic volume. Ophthalmic Plast Reconstr Surg. 2000;16:388–92.
73. Kaltreider SA, Lucarelli MJ. A simple algorithm for selection of implant size for enucleation and evisceration. Ophthalmic Plast Reconstr Surg. 2002;18:336–41.
74. Custer PL, Trinkaus KM. Volumetric determination of enucleation implant size. Am J Ophthalmol. 1999;128:489–94.
75. Thaller VT. Enucleation volume measurement. Ophthalmic Plast Reconstr Surg. 1997;13:18–20.
76. Kaltreider SA, Jacobs JL, Hughes MO. Predicting the ideal implant size before enucleation. Ophthalmic Plast Reconstr Surg. 1999;15(3):37–43.
77. Trichopoulas N, Augsburger JJ. enucleation with unwrapped porous and non-porous implants: a 15

year experience. Ophthalmic Plast Reconstr Surg. 2005;21:331–6.
78. Perry JD. Hydroxyapatite implants (letter). Ophthalmology. 2003;110:1281.
79. Long JA, Tann TM, Bearden WH, et al. Enucleation: is wrapping the implant necessary for optimal motility. Ophthalmic Plast Reconstr Surg. 2003;19(3):194–7.
80. Suter AJ, Molteno AC, Becin TH, et al. Long term follow-up of bone derived hydroxyapatite orbital implants. Br J Ophthalmol. 2002;86:1287–992.
81. Nunery WR. Risk of prion transmission with the use of xenografts and allografts in surgery. Ophthalmic Plast Reconstr Surg. 2003;17:389–94.
82. Seiff SR, Chang JS Jr, Hurt MH, et al. Polymerase chain reaction identification of human immunodeficiency virus-1 in preserved human sclera. Am J Ophthalmol. 1994;118:528–9.
83. Long CJ, Heckman JG, Neunderfer B. Creutzfeldt-Jakob disease via dural and corneal transplants. J Neurol Sci. 1998;160:128–39.
84. Hogan RN, Brown P, Heck E, et al. risk of prion disease transmission from ocular donor tissue transplantation. Cornea. 1999;18:2–11.
85. Heckman JG, Lang CJ, Petruch F, et al. Transmission of Creutzfeldt-Jakob disease via a corneal transplant. J Neurol Neurosurg Psychiatry. 1997;63:388–90.
86. Simonds RJ, Holmberg SD, Hurwitz RL, et al. Transmission of human immunodeficiency virus type 1 from a seronegative organ and tissue donor. N Engl J Med. 1992;326:726–32.
87. Arat YO, Shetlar DJ, Boniuk M. Bovine pericardium versus homologous sclera as a wrapping for hydroxyapatite orbital implants. Ophthalmic Plast Reconstr Surg. 2003;19:189–93.
88. Gayre GS, DeBacker CM, Lipham W, et al. Bovine pericardium as a wrapping for orbital implants. Ophthalmic Plast Reconstr Surg. 2001;17:381–7.
89. Pelletier C, Gilberg S, Jordan DR. Use of Temporalis fascia for management of exposed hydroxyapatite implants. Ophthalmic Plast Reconstr Surg. 1998;198-203(1998):14.
90. Naugle TC Jr, Fry CL, Sabatier RE, et al. High leg incision fascia lata harvesting. Ophthalmology. 1997;104:1480–8.
91. Kao SCS, Chen S. The use of rectus abdominis sheath for wrapping of the hydroxyapatite orbital implants. Ophthalmic Surg Lasers. 1999;30:69–71.
92. Naugle TC Jr, Lee AM, Haik BG, et al. Wrapping hydroxyapatite orbital implants with posterior auricular muscle complex grafts. Am J Ophthalmol. 1999;128:495–501.
93. Karesh JW. Polytetrafluoroethylene as a graft material in ophthalmic plastic and reconstructive surgery: an experimental and clinical study. Ophthalmic Plast Reconstr Surg. 1987;3:179–85.
94. Choo PH, Carter SR, Crawford JB, et al. Exposure of expanded polytetrafluoroethylene-wrapped hydroxyapatite orbital implant: a report of two patients. Ophthalmic Plast Reconstr Surg. 1999;15:77–8.
95. Kao L. Polytetrafluoroethylene as a wrapping material for a hydroxyapatite orbital implant. Ophthalmic Plast Reconstr Surg. 2000;16:286–8.
96. Jordan DR, Allen LH, Ells A, et al. The use of vicryl mesh (polyglactin 910) for implantation of hydroxyapatite orbital implants. Ophthalmic Plast Reconstr Surg. 1995;11:95–9.
97. Jordan DR, Ells A, Brownstein S, et al. Vicryl-mesh wrap for the implantation of hydroxyapatite orbital implants:an animal model. Can J Ophthalmol. 1995;30:241–6.
98. Klapper SR, Jordan DR, Punja K, et al. Hydroxyapatite implant wrapping materials: analysis of fibrovascular ingrowth in an animal model. Ophthalmic Plast Reconstr Surg. 2000;16:278–85.
99. Gayre GS, Lipham W, Dutton JJ. A comparison of rates of fibrovascular ingrowth in wrapped versus unwrapped hydroxyapatite spheres in a rabbit model. Ophthalmic Plast Reconstr Surg. 2002;18:275–28.
100. Jordan DR, Klapper SR, Gilberg SM. The use of vicryl mesh in 200 porous orbital implants. Ophthalmic Plast Reconstr Surg. 2003;19:53–61.
101. Custer PL. Enucleation: past, present, and future. Ophthalmic Plast Reconstr Surg. 2000;16:316–21.
102. Custer PL. Reply to Dr. D.R. Jordan's letter on polyglactin mesh wrapping of hydroxyapatite implants. Ophthalmic Plast Reconstr Surg. 2001;17:222–3.
103. Edelstein C, Shields CL, DePotter P, et al. Complications of motility peg placement for the hydroxyapatite orbital implant. Ophthalmology. 1997;104:1616–21.
104. Lin CJ, Lio SL, Jou JR, et al. Complications of motility peg placement for porous hydroxyapatite orbital implants. Br J Ophthalmol. 2002;86:394–6.
105. Jordan DR. Spontaneous loosening of hydroxyapatite peg sleeves. Ophthalmology. 2001;108:2041–4.
106. Cheng MS, Lio SL, Lin L. Late porous polyethylene implant exposure after motility coupling post placement. Am J Ophthalmol. 2004;138:420–4.
107. Lee SY, Jang JW, Lew H, et al. Complications in motility peg placement for hydroxyapatite orbital implants in anophthalmic socket. Jpn J Ophthalmol. 2002;46:103–7.
108. Jordan DR, Klapper SR. A new titanium peg system for hydroxyapatite orbital implants. Ophthalmic Plast Reconstr Surg. 2000;16:380–7.
109. Johnson RLC, Ramstead CL, Nathoo N. Ophthalmic Plast Reconstr Surg. 2011;27:74–5.
110. Ainbinder DJ, Haik BG, Tellado M. Hydroxyapatite orbital implant abscess: histopathologic correlation of an infected implant following evisceration. Ophthalmic Plast Reconstr Surg. 1994;10:267–70.
111. Klapper SR, Jordan DR, Ells A, et al. Hydroxyapatite orbital implant vascularization assessed by magnetic resonance imaging. Ophthalmic Plast Reconstr Surg. 2003;19:46–5.
112. Cook S, Dalton J. Biocompatibility and biofunctionality of implanted materials. Alpha Omegan. 1992;85:41–7.

113. Choi JC, Iwamoto MA, Bstandig S, et al. Medpore motility coupling post: a rabbit model. Ophthalmic Plast Reconstr Surg. 1999;15:190–201.
114. Rubin PAD, Fay AM, Remulla HD. Primary placement of motility coupling post in porous polyethylene orbit implants. Arch Ophthalmol. 2000;118:826–32.
115. Hsu WC, Green JP, Spilker MH, et al. Primary placement of a titanium motility post in a porous polyethylene orbital implant. Ophthalmic Plast Reconstr Surg. 2003;16:370–9.
116. Tawfik HA, Dutton JJ. Primary peg placement in evisceration with the spherical porous polyethylene orbital implant. Ophthalmology. 2004;111:1401–6.
117. Timothy NH, Feilich DE, Linberg JV. Perspective: evisceration versus enucleation, the oculariists standpoint. Ophthalmic Plast Reconstr Surg. 2003;19(6):417–20.

Orbital Prostheses

22

Paul Tanner and Bhupendra C. K. Patel

Introduction

An increase in the average life span has resulted in an increased incidence of malignant skin tumors of the face and eyelids. This has led to the increase in the rate of exenteration. Orbital exenteration includes the removal of the globe, extraocular muscles, adipose tissue, and optic nerve to the optic foramen (Chap. 18) [1, 2]. Traditionally, exenterations in ophthalmology are divided into four types based upon the 1971 Meyer and Zaoli's classification [3] and based upon the extent of destruction involved in the surgery:

- Type I: palpebral skin and *conjunctiva* are spared.
- Type II: only the palpebral skin is spared, and the eyeball and its appendages are removed with the *conjunctiva*.
- Type III: both eyelids are removed with orbital contents.
- Type IV: the eyeball, eyelids, and appendages of the eye are removed with the involved bone structures.

P. Tanner
Huntsman Cancer Hospital, University of Utah, Salt Lake City, UT, USA

B. C. K. Patel (✉)
Division of Facial Cosmetic and Reconstructive Surgery, University of Utah, Salt Lake City, UT, USA
e-mail: bhupendra.patel@hsc.utah.edu

C. J. Hwang et al. (eds.), *Clinical Ophthalmic Oncology*,
https://doi.org/10.1007/978-3-030-13558-4_22

However, as clear margins of tumor resection are sought with modern oncological approaches, exenteration may extend to other facial structures including the forehead, cheeks, nose, and lower face, requiring the creation of the field of anaplastology (Gr kana, anew; plastos, molded; logy, the study of) with a particular emphasis on facial prosthetic design.

An external facial prosthesis for orbital exenteration is called an orbital prosthesis when solely involving the soft tissue of the orbit. An upper facial prosthesis restores the orbit in addition to portions of the frontal or zygomatic bones. A hemifacial prosthesis restores the orbit in addition to portions of the nose or maxillary bone. Orbital, upper facial, and hemifacial external prostheses will all be referred to as orbital prostheses in this chapter [4, 5].

Pre-exenteration Decision-Making

Not all oncology or trauma patients receive a realistic prosthesis for an exenterated orbit even though the prosthesis is the most natural reconstructive method. Availability and access to quality orbital prostheses are important for the patient to decide between an eye patch or orbital prosthesis. When a patient is presented for an orbital exenteration, the patient should be informed of the available reconstruction options. It must be clearly understood that the eye cannot be surgically reconstructed and the

loss of the eye will result in the loss of depth perception, smaller field of view, and other issues related to monocular vision [6]. If possible, the patient also needs to know before the exenteration about long-term care and cleaning related to the surgery. The surgery can result in exposed sinuses and mucosa which can result in excessive exudate or dryness and bleeding of the mucosa.

Any patient likely to undergo exenteration should meet with a facial prosthetist (vocationally known as an anaplastologist or epithetist). Patients will benefit by knowing that there are others who have experienced similar circumstances [7]. Other patients can serve as emotional support and can comfort and assure the newly diagnosed patient that life can return to normal, albeit with a few modifications. It is also beneficial to see photographs of other patients that have had orbital exenterations so that they can be more informed of the surgical defect and the reconstructive options. Realistic results may be presented to patients based upon knowledge of the degree of surgical resection that is likely, with the proviso that each prosthesis is by necessity distinct. Of course, patients should be informed that the eye will not move or blink.

The objectives of the healthcare providers are to relieve the patient from pain, provide the best care, and return the patient to a normal lifestyle as quickly as possible. If a prosthesis is chosen as the method of reconstructing the orbit, the type of retention of the prosthesis should be determined prior to surgery when possible [8, 9]. Of course, the patient can re-evaluate this decision at any time. Regarding retention of orbital prostheses, there are several options (Table 22.1). We prefer to make orbital prostheses that can be retained by undercuts in the remaining anatomy [10]. The orbital prosthesis can be fabricated to be air-filled and pop into place if it is shaped properly. Adhesives can assist in the retention of prostheses if proper materials and fitting techniques are used (Fig. 22.1) [11].

Table 22.1 Retention methods for orbital prostheses

More common -> <– Less common	**Type of retention of orbital prostheses**	**Considerations**
	Anatomical	The surface of the prosthesis adjacent to mucosa must be glossy
	Adhesive	Edges of the prosthesis must be strong
	Magnets with oral obturator	Must be as lightweight as possible
	Osseointegrated titanium implants	Soft tissue reduction around implants. Abutments must be short. Magnets, ball/socket, and bar/clip systems can be attached to the bone-anchored implants
	Eyeglasses	Frames must be acrylic

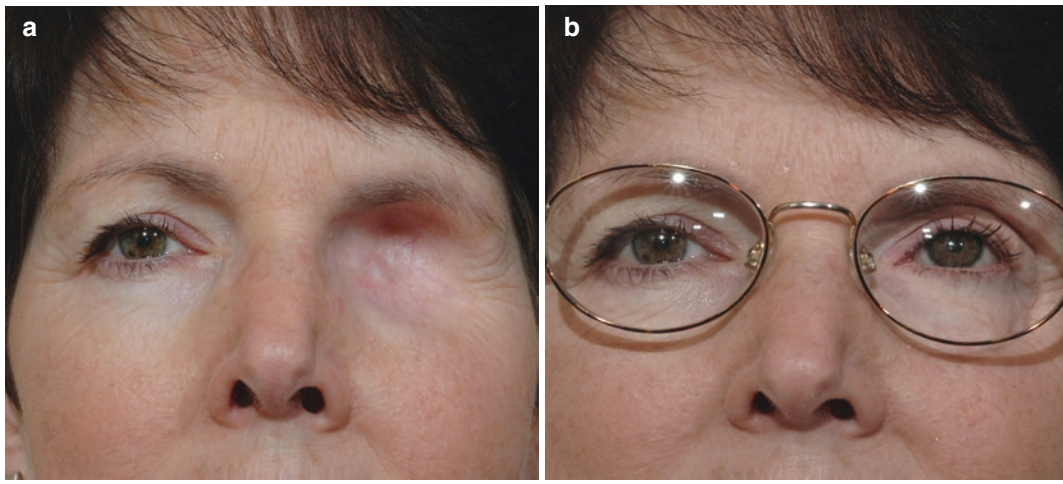

Fig. 22.1 (**a**, **b**) Orbital prosthesis with adhesive retention

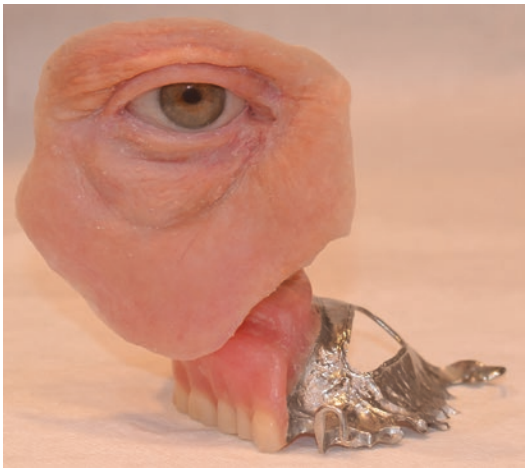

Fig. 22.2 Midfacial prosthesis with magnetic connection to oral obturator

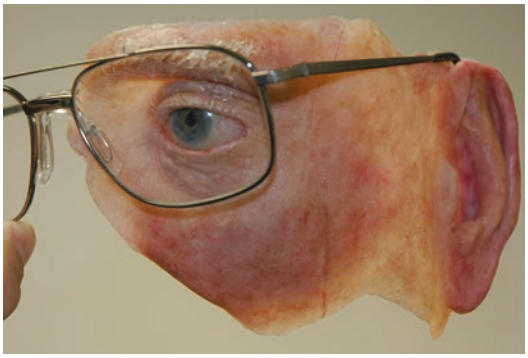

Fig. 22.3 Attachment of silicone prosthesis to eyeglasses for unusually large defects

When the sinus is obliterated and the patient receives an oral obturator, magnets can connect the orbital prosthesis to the oral obturator (Fig. 22.2). Retention with eyeglasses can be invaluable when resections larger than the orbit are required and there are no other available means of retention (Fig. 22.3) [12–14]. Osseointegrated implants can be used for retention but can complicate the fabrication of orbital prostheses and have the potential of skin irritation and infection [15–18]. Magnets, ball/socket, and bar/clip systems can be attached to bone-anchored implants (Fig. 22.4) [19]. Patients have the potential to lose an implant if inadequate placement of implants is achieved; there is poor bone quality or in the presence of inadequate soft

Fig. 22.4 (**a**, **b**) Orbital prosthesis with osseointegrated implant retention using magnets

tissue management around the transcutaneous abutments [20]. The surgeon and prosthetist need to actively plan the type of retention that will be chosen so that proper surgical and prosthetic procedures may be performed: this lowers the risk of losing an implant [21, 22]. The chosen retention method may need to be changed after surgery, depending upon multiple factors. Osseointegrated implants should not be placed by the surgeon unless the facial prosthetist is involved in surgical planning and is present during the surgery [23, 24].

Intraoperative Considerations

During surgery, bone spurs need to be flattened or smoothed to avoid tender or painful areas. If there is an option to spare the eyelids during the exenteration, the authors recommend removing the eyelashes and tacking and packing the eyelid to the superior wall of the orbit. Care should be taken to leave the eyebrow in the proper location – perhaps even fixing it in place early in the surgery. Ideally, a skin graft should line the orbital cavity: this will greatly expedite rehabilitation. With more extensive exenterations, the sinuses and nasal cavity present some challenges for patients. If the nasal cavity is exposed, drying of the mucosa with subsequent bleeding can occur and can also significantly affect speech.

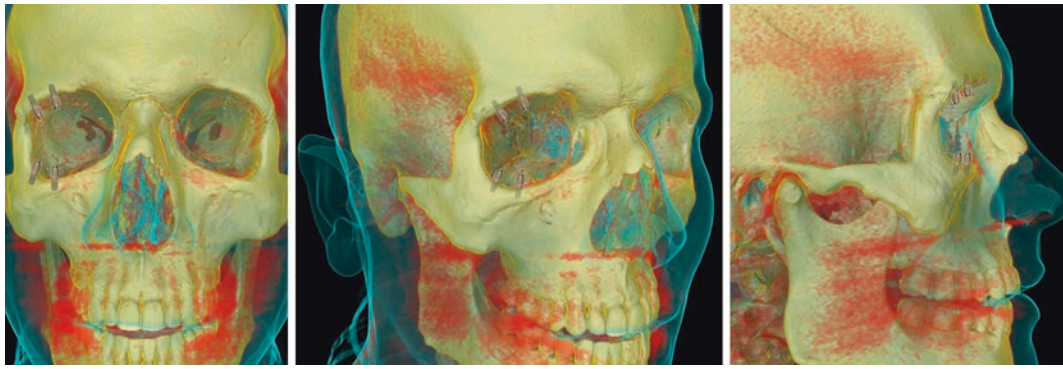

Fig. 22.5 Location and angulation of osseointegrated implants for orbital prosthesis retention

Exposed sinuses result in weeping which becomes emotionally exhausting for patients.

Free flaps are often used to cover the exenterated orbit [25] and may or may not include bone. When a free flap is used, the orbit is usually too shallow for a prosthesis. If a prosthesis were to be made for a bulky free flap, the prosthesis would by necessity need to be made very thin: the orbital prosthesis would appear to be proptotic. It is better to wait a few months and revise the flap by removing the adipose tissue. During this time, the muscle atrophies. Osseointegrated implants could be placed during this revision if implants are the desired method of retention [26].

Osseointegrated implants are one of the least preferred methods of retention for an orbital prosthesis because of the limited space of the cavity of the orbit, soft tissue irritation, and fabrication challenges. However, if osseointegrated implants are the desired form of retention for the patient and a free flap is not used for reconstruction, the implants can be placed during the initial surgery. Implants should be placed more than 1 centimeter apart. Two potential implant sites are in the frontal bone lateral to the frontal sinus and supraorbital foramen and medial to the frontozygomatic suture. Two more potential implant sites are in the zygoma inferior to the frontozygomatic suture and lateral to the maxillozygomatic suture. Care should be taken to avoid the zygomaticofacial foramen. At least three implants are required for adequate retention and long-term survival of the implants. The implants should be placed perpendicular to the plane of the bone and should be targeted to the most cortical bone available. The bone along the lateral rim of the orbit may need to be reduced. The angulation of each implant must be vertical (Fig. 22.5). If angled improperly, the implants and abutments will protrude from the orbit. In order to cover poorly angled implants, the prosthesis would give the appearance of being proptotic. Angled abutments can be used as a work around for select malpositioned implants, although this is not ideal. The most superolateral implant usually interferes with the eye component of the orbital prosthesis and is the most important to angle inward into the cavity of the orbit. Adipose tissue near the implants should be removed: ideally, within 1 centimeter of the implant, there should be the periosteum and integumentary tissues, with as little adipose tissue as possible. Debulking the soft tissue around the implants will decrease the amount of exudate around the implants. Three-millimeter-long transcutaneous abutments are ideal.

Postoperative Considerations

Most patients choose to wear a flesh-colored bandage or an eye patch after surgery. Orbital exenterations often leave a surgical defect larger than a conventional eye patch and thus require a custom eye patch. The professional that makes the orbital prosthesis should be able to fashion a custom eye patch in any color. An eye patch can help

the defect heal and facilitate cleaning by maintaining a humid environment. When a sinus or nasal cavity is exposed by the exenteration, the exudate can be removed with long cotton-tipped swabs or water flushes while showering with a 50 or 100 mL syringe.

During this waiting period, the patient should also procure eyeglasses to protect the remaining eye and correct the eyesight as needed. Eyeglasses should be comfortable, be lightweight, have photochromic lenses (to function as sunglasses as well), have a gradient tint from the top to the middle portion of the lens, and have bifocal amplification if desired. The frame of the eyeglasses should be dark or bold colored to draw attention to the glasses rather than the immobile eye and the orbital prosthesis that does not blink. Eyeglasses can be crucial for an imperceptible prosthesis.

Patients can begin the prosthesis fabrication a few weeks after the ablative surgery when skin grafts or flaps are deemed to be stable and healthy. The patient and providers should mutually determine the best time to begin fabrication of the orbital prosthesis. Edema can remain for months to even years, and the fit of the prosthesis may need to be adjusted because the prosthesis is not retained properly. Refitting may also be needed in some patients. When working with transcutaneous implants, the prosthetist should begin the work 7–10 days after surgery to allow for adequate healing time. If rushed, the prosthesis may aggravate the soft tissue surrounding the implants and prolong the healing process.

Prosthesis Fabrication

The state of the art in orbital prosthesis fabrication is a unique blend of technology, artistry, and craftsmanship that allows the patient to have a prosthesis fabricated in as few as five appointments that have an average duration of 90 min (Table 22.2). When a patient travels a long distance, a prosthesis can be fabricated in as little as a few days. Technology, coupled with skilled and experienced prosthetists, has evolved the fabrication process to have shorter and fewer appointments so that the logistics and duration of appointments is not burdensome for patients. This trend is expected to continue.

Before the patient is healed from surgery, the eye component of the prosthesis can be fabricated [27]. The process of making the eye component is similar to the process described in the chapter regarding ocular prostheses, but there is no fitting involved. The process of fabricating the eye for an orbital prosthesis begins with measurements of the remaining eye. Notable is the diameter of the iris and the average size of the pupil. There are techniques that exist for creating the illusion of a dilating pupil [28]. Average eye measurements are used for replicating the anterior half of the eye [29]. However, if there is inadequate space between the defect and the desired location of the cornea of the prosthesis, a flatter shape will need to be made. After the eye component is fabricated, an impression of the orbit is obtained with a silicone material. The impression material, which has the consistency of honey and the flow of toothpaste, solidifies into a rubber within 5 min. A plaster-like gypsum-based material is cast into the rubber impression and, when removed, results in a stone duplicate of the patient's anatomy. This stone model becomes the foundation for the positioning of the eye and modeling of the prosthesis [30, 31]. Eyeglasses for the patient can help determine the position of the eye and the location of the edges of the prosthesis, but a modified manual pupilometer is essential to position the eye (Fig. 22.6) [32]. When the position and gaze of the eye are satisfactory, the eyelids can be sculpted. After all the sculpting and texturing, the wax model is adapted to the movements of the soft tissues of the patient. The edges of the prosthesis should also align with the junctions of the aesthetic units of the face [33]. The stone model derived from the impression of the patient can no longer be used after fitting. A gypsum-based mold is created in 2–3 parts that encompasses the wax model [34]. Silicone is pigmented to replicate the epidermis and dermis and applied to the mold in layers [35]. Artistry and color acuity are of utmost importance in this step. The quantity of pigment changes the translucency of the silicone, while

Table 22.2 Blend of technology, artistry, and craftsmanship in orbital prosthesis fabrication

Fabrication steps	Materials and methods	Technological assistance
	Make mold for the eye component if not standard shape	
Re-evaluate retention method and paint the iris (patient is present)	Approximate the iris color and bond to a clear piece of plastic resembling the cornea	Using photography and photo-editing software, the iris can be replicated fairly well. Seal the photo print and bond to plastic cornea
	Include the cornea plastic (with the iris) while casting the sclera portion of the prosthesis. Remove 1 mm off the surface of the sclera, and remove the anterior portion of the cornea until 1 mm away from the iris	
Eye fabrication and impression (patient is present)	Provide detail and enhance the color of the iris. Apply reddish fibers and yellow and blue/gray to the sclera	
	Raise the skin of the brow with tape, and obtain an impression of the cavity of the orbit with vinyl polysiloxane or equivalent	Use photogrammetry to obtain a 3D surface scan with color
	A gypsum compound is mixed with water and poured into the impression	
Position the eye		By digitally merging an existing CT scan with the plaster cast, the X, Y, and Z axes of the eye prosthesis can be determined
Eye positioning and rough sculpting (patient is present)	Using a modified manual exophthalmometer and calipers (Fig. 22.6), we can approximate the X, Y, and Z axes of the eye by positioning the eye with clay and affixing it with wax	Verify the location of the eye in person, and make minor adjustments to the clay and wax
Patient is present: Sculpting and fitting	When hand-sculpting, start with the eyelids. Patients may already be fatigued, and it may be apparent in the shape of their eyelids. Hand-sculpting may require 1–3 appointments. When the shape and texture are mutually determined by the patient and prosthetist, the prosthesis needs to be fit to the patient. Ideally, the prosthesis should be as small and lightweight as possible while crossing the least amount of aesthetic units of the face. The edge of the prosthesis should also align the borders of the aesthetic units. The size, fit, and location of the edge of the prosthesis will determine the fit, function, and aesthetics of the prosthesis	By digitally merging a CT scan or photogrammetry composition, the absent tissue of the orbit can be restored and 3D printed. After duplicating in wax, the shape can be verified and fitted in person. Large surface texture is added
Mold making	The eye component is indexed, and typically a gypsum-based mold is made of two or three parts around the wax model	Although not presently done by the author, the probability of scanning the wax model and creating a machined or 3D-printed mold is highly likely in the future
Internal coloring	Silicone is pigmented to match the color of the dermis, superficial vessels, and epidermis	Photospectroscopy can be used to measure the reflectance intensity of the pigments relative to the light source to analyze the turbidity/translucency and color of the prosthesis relative to the adjacent and contralateral skin
Patient is present: Painting and delivery	Enhancing the color in the prosthesis is often required for an accurate color match. The external pigmentation is sealed, and the surface texture of the final sealing coat is modified to appear to have a satin finish	

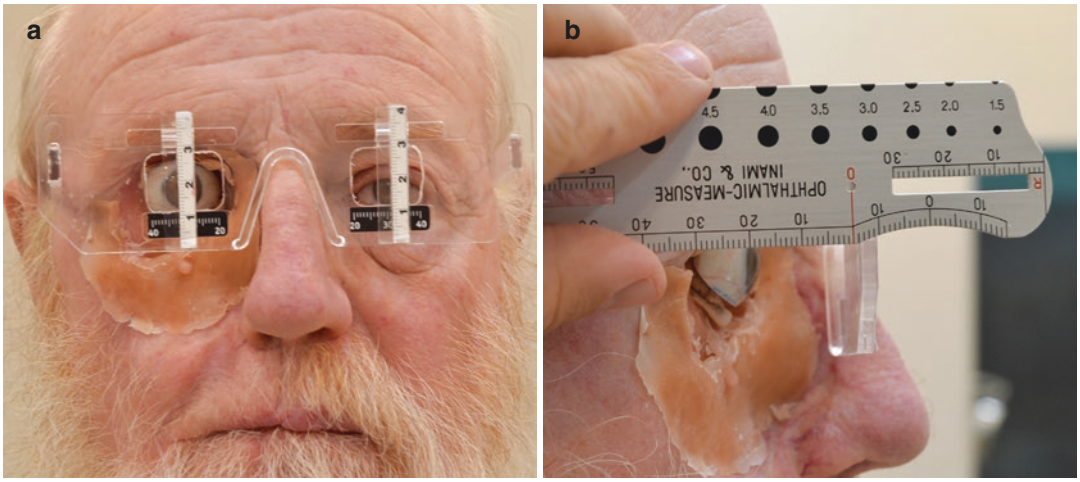

Fig. 22.6 (**a**, **b**) The use of manual pupilometer to approximate the position of the eye in the orbital prosthesis

the composition of pigments determines the colors [36]. After the silicone catalyzes, the prosthesis can be removed from the mold to be carefully trimmed and prepped for external painting to enhance certain colors. In theory, the only colors that should be enhanced are reds and browns that replicate the superficial vessels and melanin pigment in the epidermis. The colors replicating the dermis should already be part of the prosthesis. A sealing coat of a silicone adhesive is used to bond the external painting to the prosthesis and finish the surface texture of the prosthesis to match the specular and diffuse reflectance ratio of the skin of the patient [37].

Using an Orbital Prosthesis

An orbital prosthesis is expected to last approximately 2 years. If surgery was recent and edema continues to recede, a new prosthesis likely needs to be made in less than 2 years to accommodate the change in the fit and resulting function of the prosthesis. If tissues are well healed after several years, a prosthesis may last longer than 2 years if the prosthesis is made with quality materials. Patients are expected to return at least annually to assess the fit and function of the prosthesis. Red-colored pigments tend to fade faster than other colors and may need to be enhanced annually.

Microbes are always present on prostheses but should not be permanently attached. Permanently attached microbes will appear as black- or cream-colored spots in the silicone [38]. If microbes are visible and are in the silicone, the patient should be referred back to the prosthetist for a replacement prosthesis. Patients should routinely wash the prosthesis with soap and water. The prosthesis should have no odor if it is adequately washed. Hair conditioner or any other product containing polysiloxanes or dimethicones (silicone oils) should not come in contact with the prosthesis. Hair dyes should also not come in contact with the prosthesis because the dyes cause discoloration.

Smoking nicotine or other substances can cause significant yellowing/browning of the prosthesis in a short amount of time. There are no known materials that facial prosthetists can use to deter this effect. However, acetoxy and oxime cure silicones are known to discolor much faster than platinum cure silicones. For this reason, a platinum cure adhesive is preferred, rather than an acetoxy cure adhesive, to seal the external painting to the prosthesis.

If the retention of the prosthesis is with osseointegrated implants, care should be taken to remove visible exudate with a soft instrument such as a cotton-tipped swab. If a patient is too aggressive with cleaning, the microbiome is

adversely affected and may lead to chronic inflammation and hypertrophic scarring [38, 39]. A toothbrush with sharp bristles or any other sharp object should not be used. Skin reactions are minimized with little but adequate care in removing the dried exudate after bathing [39].

Historical Review and Advances in Realistic Prostheses

External orbital prostheses were first documented by Ambroise Paré, a prominent French barber surgeon known for conceptualizing and inventing not only surgical techniques and instruments but prosthetics as well. In the mid-1500s, Paré designed many prosthetic devices including legs, noses, and eyes. The hypoblephara eye prosthesis that Paré conceptualized had a wire that wrapped around the head and positioned the prosthetic eye on top of the atrophic eye (Fig. 22.7) [40, 41]. Before this, prosthetic eyes were used in the Middle East and Egypt and made from clay, wood, ivory, wax, glass, leather, and metals [42–44]. In 1894, facial prostheses were made of a hard, black, opaque rubber material called vulcanite which was invented for car tires [45]. After the turn of the century, a gelatin glycerin formula was individualized and given to each patient with a metal mold. Patients would cast their own prosthesis each week. It is unknown how common this was and how it was attached to the skin. Several metals such as silver, copper, aluminum, gold, and tin were used to make prostheses [46]. Metal prostheses were made by taking a life cast of the patient, shaping wax to fill the absent anatomy, and then using an electroplating process to deposit dissolved metal cations onto the surface of the wax with an electrical current. An American artist named Anna Coleman Ladd drew a lot of attention to this process when she used her artistic skills with the American Red Cross and fabricated approximately 185 metal masks for French soldiers wounded in World War I in Paris [47–49] (Fig. 22.8 of a French soldier).

Rigid plastics such as phenolic and cellulose plastics, polymethyl methacrylate (commonly known as acrylic), and vinyl and styrene plastics were exciting new materials in the early twentieth century because of their translucent qualities. Simultaneously, flexible but less durable materials such as latex and plasticized polyvinyl chloride (commonly known as plastisol in screen printing shirts) were tried [50, 51]. By the mid-1900s, most facial prostheses were made with polymethyl methacrylate, rubber latex, and plasticized polyvinyl chloride. In the 1940s, a super elastic and translucent material called polydimethylsiloxane, commonly known as silicone rubber, was invented. In the 1960s, surgeons were using silicone rubbers as subdermal implants to augment the face, and prosthetists started using them

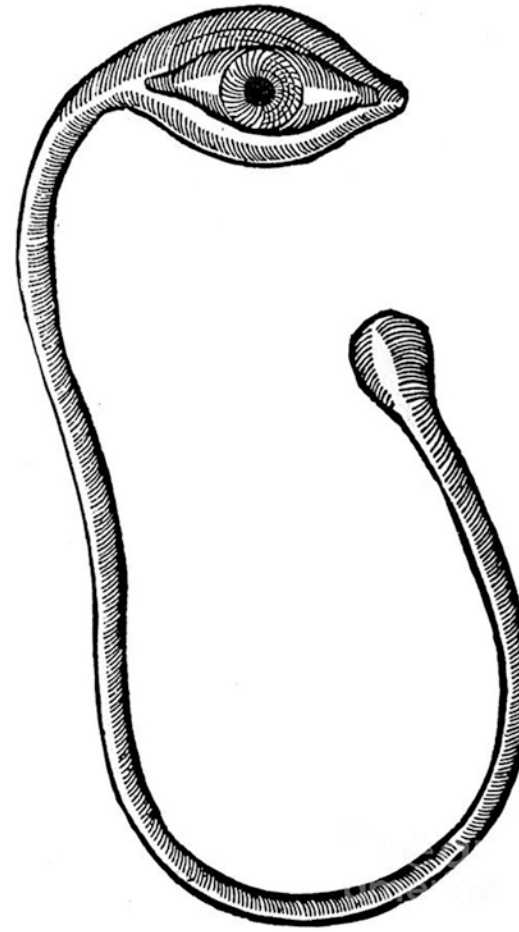

Fig. 22.7 The hypoblephara eye prosthesis of Ambroise Paré (mid-1500s)

Fig. 22.8 (**a**, **b**) Orbital prosthesis made by Anna Coleman Ladd for a French soldier circa 1913. (WWI soldier facial reconstruction documentation photograph, circa 1920/American Red Cross, photographer. Anna Coleman Ladd papers, circa 1881–1950. Archives of American Art, Smithsonian Institution)

Fig. 22.9 Orbital prosthesis made of rigid plastic (polymethyl methacrylate) in 1980

for facial prosthetics [52, 53]. Silicones evolved to have incredible elongation and tear properties since the 1940s. Silicone rubber is the predominant material for facial prostheses today, but there are some prosthetists that make prostheses with acrylic plastic because silicones may not be accessible in all areas of the world and silicones are not as durable (Fig. 22.9). Thermoplastic polyurethanes have great elongation and tear properties and could also be used if fabrication methods evolve with three-dimensional printing. The commercialization and open-source nature of three-dimensional printing have lowered the cost and facilitated the fabrication of custom shapes with thermoplastic materials. Soon, prosthetists will have many more materials and methods for fabricating facial prosthetics.

Research efforts have also been made at making the eye component of the orbital prosthesis move simultaneously with the contralateral side by attaching a tracking camera to the eyeglasses frame and using electromagnetics to quickly control movements [54, 55]. Efforts have also been made to enable blinking of the upper eyelid [55]. Practical working models have yet to be created though. There are also several efforts to create bionic eyes, enabling optic nerve stimulation and low-resolution sight [56, 57]. The future is bright for those in need of orbital prostheses. Methods and materials are evolving. The aim is to create an orbital prosthesis that moves, blinks, and perhaps have some vision with optic nerve stimulation. The next frontier in orbital and facial prosthetics may well be in the promising fields of artificial intelligence and robotics.

References

1. Tyers AG. Orbital exenteration for invasive skin tumours. Eye. 2006;20:1165–70.
2. Nassab RS, Thomas SS, Murray D. Orbital exenteration for advanced periorbital skin cancers: 20 years experience. J Plas Recon Aesth Surg. 2007;60:1103–9.
3. Radici M, Bicciolo G, Palma O, Bozza F. Il massiccio facciale. In: De Campora E, Marzetti F, editors. La chirurgia oncologica della testa e del collo. Pisa: Pacini Editore; 1996. p. 345–81.
4. Kesting MR, Koerdt S, Rommel N, et al. Classification of orbital exenteration and reconstruction. J Cranio-Maxillo-Facial Surg. 2017;45:467–73.
5. Sophie JY, Dierks EJ, Over LM, et al. Prosthetic reconstruction of the orbit/globe. Oral Maxillofacial Surg Clin N Am. 2012;24:697–712.
6. Doan BD. A psychologist's perspective on clinical practice in anaplastology. J Facial Somato Pros. 1997;3(2):89–94.
7. Herzmann K, Schwenke J, Eckelt. Psychocial issues in the treatment and rehabilitation of patients with oral and head and neck cancer. J Facial Somato Pros. 1997;3(1):23–32.
8. Bulbulian AH. Reconstruction of the orbit and the eye. In: facial prosthesis. Philidelphia: WB Saunders Company; 1945. p. 141–8.
9. Cobein MV, Coto NP, Crivello O Jr, et al. Retention systems for extraoral maxillofacial prosthetics implants: a critical review. Br J Oral Max Surg. 2017;55:763–9.
10. McKinstry RE, Retention and facial Prosthetics. In: McKinstry RE. Fundamentals of facial prosthetics. Arlington: ABI Professional Publications; 1995. 24–25.
11. Wachter R, Lauer G, Schilli W, et al. Difficulties in the epithetic treatment of orbital defects after irradiation. J Facial Somato Pros. 1997;3(1):39–54.
12. Leeming B, Renk A. A method of attaching an orbital prosthesis to spectacle frames. J Facial Somato Pros. 1997;3(1):33–8.
13. Thomas KF. Spectacle considerations. In: Prosthetic rehabilitation. London: Quintessence Publishing Co., Ltd; 1994. p. 163–7.
14. Wuebolt GE, Patel BC, Silver JH, et al. Brow-supported spectacle frames for nasal bridge reconstruction and other deformities. Arch Ophthalmol. 1993 Feb;111(2):162–3.
15. Greig AVH, Jones S, Haylock C, et al. Reconstruction of the exenterated orbit with Osseointegrated implants. J Plas Recon Aesth Surg. 2010;63:1656–65.
16. Nerad JA, Carter KD, LaVelle WE, et al. The Osseointegration technique for the rehabilitation of the exenterated orbit. Arch Ophthalmol. 1991 Jul;109:1032–8.
17. Tjellström A, Jansson K, Brånemark P-I. Craniofacial defects. In: Advanced osseointegration surgery: applications in the maxillofacial region. London: Quintessence Publishing Co., Ltd; 1992. p. 304–6.
18. DeSerres JJ, Budden CR, Wolfaardt JF, et al. Long-term follow-up of Osseointegrated orbital prosthetic reconstruction. J Craniofac Surg. 2017;28(8):1901–5.
19. Becker H, Franz-Hausmann D, Trainer D, et al. Clinical experiences using different extraoral implant systems after orbital exenteration. J Facial Somato Pros. 2000;6(1):11–8.
20. Toljanic JA, Eckert SE, Roumanas E, et al. Osseointegrated craniofacial implants in the rehabilitation of orbital defects: an update of a retrospective experience in the United States. J Pros Dent. 2005;94(2):177–82.
21. Rangert B. Biomechanical considerations for implant-supported orbital prostheses. J Facial Somato Pros. 1996;2(1):43–50.
22. Schwipper V, Tilkorn H. Combined extra- and intraoral defects: their repair by reconstructive surgery and dental and facial prostheses. J Facial Somato Pros. 2000;6(1):29–38; Leeming B, Renk A, Olberding S, Sigel K, Möhler H. Microbiological flora around percutaneous craniofacial implants. J Facial Somato Pros. 1999;5(1):35–40.
23. Tanner PB, Mobley SR. External auricular and facial prosthetics: a collaborative effort of the reconstructive surgeon and anaplastologist. Facial Plast Surg Clin of N Am. 2006;14:137–45.
24. Özçelik TB, Tanner PB. A surgical guide for craniofacial implant placement for an implant-retained auricular prosthesis. J Prosthet Dent. 2010;103:253–5.
25. Eaton LD. Functional and cosmetic alloplastic reconstruction of the eye socket, orbit and midface. J Ophthalmic Pros. 2001;6(1):31–42.
26. Schwenzer N. Bonegrafting and sigittal implantation to support an orbital prosthesis. J Facial Somato Pros. 1997;3(2):43–8.
27. Gully NJ. Fabrication of an ocular prosthesis using a custom jig. J Facial Somato Pros. 1997;3(1):13–8.
28. Harwin F. Creating the illusion of a dilating pupil. J Ophthalmic Pros. 2000;5(1):29–36.
29. Oyster CW. Ocular geometry and topography. In: The human eye: structure and function. Boston: Sinauer Associates, Inc; 1999. p. 96.
30. Clarke CD. Orbital prosthetics. In: Prosthetics. Butler: The Standard Arts Press; 1965. p. 117–32.
31. Thomas KF. Orbital prostheses. In: Prosthetic rehabilitation. London: Quintessence Publishing Co., Ltd; 1994. p. 69–78.
32. Bergstöm K. Prosthetic procedures for orbital defects: technique and case study. J Facial Somato Pros. 1996;2(1):27–36.
33. Chepeha DB, Wang SJ, Marentette LJ, et al. Restoration of the orbital aesthetic subunit in complex mid facial defects. Laryngoscope. 2004;114(10):1706–13.
34. Morgan NA, Asher ES. Simple two-piece mold-making technique for orbital prostheses. J Facial Somato Pros. 2002;8(1):1–8.
35. Erb RA. Intrinsic and extrinsic coloration of prostheses. In: McKinstry RE, editor. Fundamentals of facial

prosthetics. Arlington: ABI Professional Publications; 1996. p. 161–8.
36. Tanner PB, Leachman S, Boucher K, et al. Depigmented skin and phantom color measurements for realistic prostheses. Skin Res Technol. 2013;0:1–5.
37. Zahouani H, Vargiolu R. Skin line morphology: tree and branches. In: Agache P, Humbert P, editors. Measuring the skin. Berlin: Springer; 2004. p. 40–59.
38. Spinelli G, Asher E. Microbial growth on midfacial prostheses: identification, treatment, and prevention. J Facial Somato Pros. 2003;9(2):81–92.
39. Reisberg D, Viana M. Soft tissue response to percutaneous implants: a literature review. J Facial Somato Pros. 2000;6(2):73–80.
40. Conroy BF. A brief sortie into the history of cranio-oculofacial prosthetics. Facial Plast Surg. 1993;9(2):89–115.
41. Snyder C. Ambroise Paré and ocular prosthesis. Arch Ophthalmol. 1963;70(1):130–2.
42. Enoch JM. History is the light on the path to (the) future: the Burnt City, and the first known artificial eye. Hindsight. 2007;38(3):58–67.
43. Wilson RP. Artificial eyes in ancient Egypt. Surv Ophthalmol. 1972;16(5):322–31.
44. Reisberg DJ, Habakuk SW. A history of facial and ocular prosthetics. Adv Ophthalmic Plast Reconstr Surg. 1990;8:11–24.
45. Tetamore FLR. Deformities of the face and orthopedics. NY: Brooklyn; 1984.
46. Bulbulian AH. Materials that may be used in the construction of a prosthetic restoration. In: Facial prosthesis. Philidelphia: WB Saunders Company; 1945. p. 21–8.
47. Alexander C. Faces of war. Smithsonian Magazine. 2007. https://www.smithsonianmag.com/arts-culture/faces-of-war-145799854/ Video: http://www.smithsonianmag.com/videos/category/history/about-face/. Accessed April 2018.
48. Kazanjian VH. De la prothèse dan le traitment des lésions des parties molles de la bouche et de la face. Restauration Maxillo-Fac. 1918;2:345–82.
49. Desfosses P. L'Oeuvre de Madame Ladd. Presse Méd. 1918;1:345–6.
50. Bulbulian AH. Use of plastics in facial Prosthetics. In: Facial prosthesis. Philidelphia: WB Saunders Company; 1945. p. 141–8.
51. Bulbulian AH. Prevulcanized latex and methods of compounding it for use in making latex restorations. In: Facial prosthesis. Philidelphia: WB Saunders Company; 1945. p. 149–56.
52. Wainstock MA, Metz HH. Rehabilitation of the orbit after exenteration for malignancy. J Int Coll Surg. 1965 Sep;44:289–97.
53. Cantor R, Curtis TA, Rozen RD. Orofacial prosthetic rehabilitation. Arch Otolaryngol. 1968 May;87(5):559–61.
54. Miranda E, Habakuk S. Artificial movement as applied to prostheses of the orbit: a literature review. J Facial Somato Pros. 2000;6(2):95–108.
55. Klein M, Menneking H, Hasenpusch M, et al. A new orbital prosthesis with a mobile upper eyelid. J Facial Somato Pros. 1999;5(1):11–8.
56. Lewis PM, Ayton LN, Guymer RH, et al. Advances in implantable bionic devices for blindness: a review. ANZ J Surg. 2016;86:654–9.
57. Ong JM, Cruz L. The bionic eye: a review. Clin Exp Ophthalmol. 2012;40:6–17.

Ocular Prostheses

23

Kuldeep Raizada, Bhupendra C. K. Patel, and Paul Tanner

Introduction

The loss (enucleation, evisceration) or absence (microphthalmos, anophthalmos) of an eye is devastating to the individual and to the family. Whereas the raison d'etre of the ophthalmologist, preservation of vision, cannot be exercised in such circumstances, a refined ocularist, imbued with kindness, artistry, imagination, and, above all, patience, is a prized asset to a reconstructive team. Such an artist who is able to master the art of fabrication and fitting of a prosthetic eye is able to rehabilitate a patient psychologically and cosmetically.

Historical Perspective

The earliest known prosthetic eye (c. 2700–2300 BCE) was found in Shahr-e Sukhteh (The Burnt City) in modern day Southeast Iran. It is thought it was made of bitumen paste which was covered with a thin layer of gold and engraved with a central iris, from which lines would radiate out like the rays of the sun. The Seated Scribe (2600–2350 BCE; of the Old Kingdom, 4th Dynasty is from Saqqara, north of the alley of the sphinxes, Serapeum, Egypt) (Fig. 23.1) is a painted limestone statue of a scribe portrayed at work, which is unusual in Egyptian statuary [1]. Sons of Didufri (4th Dynasty) were represented in this position, so it is thought that this may represent a member of the royal family. The most remarkable aspect about the statue is the face, in particular the eyes. The eyes consist of a piece of red-veined white magnesite, in which a piece of slightly truncated rock crystal was placed. The front part of the crystal was carefully polished. The back side was covered with a layer of organic material, creating the color of the iris and also probably serving as an adhesive. The entire eye was then held in the socket by two large copper clips welded on the back. A line of black paint defines the eyebrows. The hands, fingers, and fingernails are sculpted with a remarkable delicacy. When viewed live (at the Louvre, Paris), the eyes look like they were only recently minted. A modern ocularist would be proud to be the designer of such prosthetic eyes!

The eye was a symbol of life to the ancient world, particularly in Egypt, where bronze and precious stone eyes were placed on the deceased. The Romans decorated statues with artificial eyes

K. Raizada
International Prosthetic Eye Center, Hyderabad, Telangana State, India

B. C. K. Patel (✉)
Division of Facial Cosmetic and Reconstructive Surgery, University of Utah, Salt Lake City, UT, USA
e-mail: bhupendra.patel@hsc.utah.edu

P. Tanner
Huntsman Cancer Hospital, University of Utah, Salt Lake City, UT, USA

C. J. Hwang et al. (eds.), *Clinical Ophthalmic Oncology*, https://doi.org/10.1007/978-3-030-13558-4_23

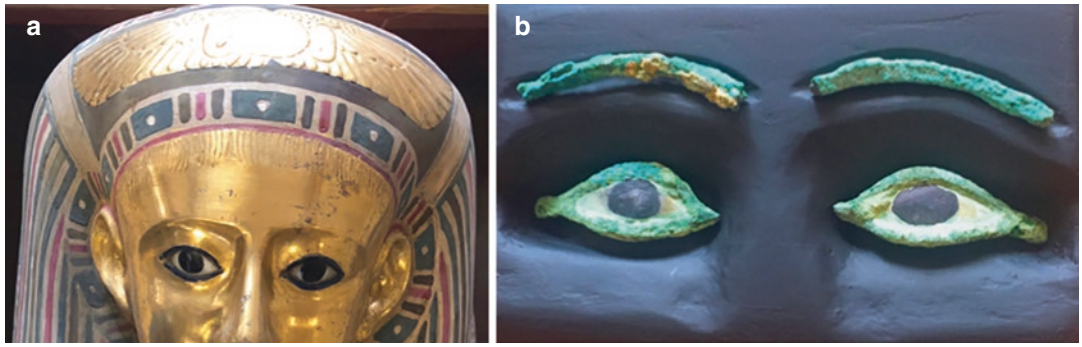

Fig. 23.1 The eye was the symbol of life in the ancient world. In Egypt, bronze, silver, gold, and precious stones were used for eyes of the deceased (**a**). Bronze Egyptian eyes c 600–300 BCE (**b**)

made of silver. Prosthetic eyes worn outside the socket were made by Egyptian and Roman priests (around 500 BCE) who made the prosthesis from painted clay: these eyes would be attached to a cloth and worn around the head. The Greeks called this type of prosthesis "ekblepharon." As with most things that evolved over time, it is difficult to trace the inventor of the artificial eye.

It has been suggested that the ancient Egyptians and Indians knew how to fashion prosthetic eyes. The Seated Scribe may be the oldest example of three-dimensional eyes. Whereas the Seated Scribe does not confirm that they used these remarkable prosthetic eyes in humans as well as statues, it certainly shows their ingenuity and suggests possibilities.

Ambroise Paré (1510–1590) described an external prosthetic eye that was fastened to the end of a metal rod which bent around the back of the head to hold the eye in place: this was illustrated in his 1614 textbook (published posthumously). Paré is also credited with the first prosthetic eye (1561) worn inside the socket (termed "hypoblephara"), although there is evidence that similar prosthetic eyes made from wood and ivory had been used previously [2–5]. Subsequent sixteenth-century prosthetic eyes worn inside the socket were made from gold or silver with colored enamel coating. By the late sixteenth century, Venetian glassblowers were making more realistic prosthetic eyes from glass. Although fragile, and uncomfortable to wear, they were beautifully made by skilled glassblowers, who, nevertheless, kept their methods secret.

Fig. 23.2 Collection of glass eyes manufactured in Germany

Subsequently, similar glass eyes were also produced in Augsburg near Munich in the sixteenth century (Fig. 23.2) [6].

In Britain, an advertisement for prosthetic eyes appeared in "Merlin's Ephemeris" in 1681 with the proclamation that William Boyse of London was "the only English operator in glass and the most expert in making artificial eyes so exact as not to be distinguished from the natural." The missive went on to claim that the eye could be "worn with much ease and so curious that they have the motion of the natural eye, being exactly made to the colour or bigness of the same, which renders them very ornamental and commodious, the like of which was never made in England" [7–9].

In the 1700s, Auguste Boissonneau made artificial eyes in Paris: they could be purchased by mail order or by appointment in Paris. His thin enamels were designed to be worn over an atrophied eye. Dr. Heister of Nuremberg in 1752 recorded that he preferred glass eyes to metal eyes because metal eyes repelled tear fluid and lost their brightness. Friedrich Philipp Ritterich (1787–1866), a doctor and teacher at the University of Leipzig, was appalled at the cost of artificial eyes from Paris and advocated for the establishment of a glass eye industry in Germany. He organized classes in glassblowing techniques and established a free glass eye service at the Leipzig Eye Institute where glass eyes were custom manufactured for individual patients. This was the first time glass eyes were fitted and supplied to individual patients rather than being sold from stock.

By the mid-nineteenth century, the center of glass eye manufacture had moved to Germany. In 1832, Ludwig Muller-Uri, a glassblower who made dolls' eyes at the famous Lauscha Glass factory in Sonneberg, developed the cryolite glass eye which was more durable than previous glass eyes.

In response to the increase in the number of enucleations being carried out following the introduction of anesthesia and asepsis, Herman Snellen, a Dutch eye surgeon, developed the "reform" eye in 1880: this was a hollow glass eye with rounded edges. This resulted in a more full prosthesis rather than the earlier shell-like glass eyes. This facilitated the restoration of socket volume and improved wearing comfort.

In 1885 in England, Philip Henry Mules implanted a glass sphere into the scleral cavity of an eye following an evisceration. This was the first attempt at restoring lost orbital volume, thereby giving better movement to the overlying prosthetic eye.

A major advance in the prosthetic eye construction was the introduction of polymethyl methacrylate (PMMA) by ICI in 1930. Dentists adapted this into a medical grade PMMA to replace the vulcanite rubber which had been used till then for denture bases. Like many advances in plastic surgery, the Second World War ushered in the next development: the war brought a shortage of glass eyes from Germany, thereby forcing British Royal Navy dental technicians to investigate the use of PMMA for prosthetic eyes. Fritz W. Jardon, a German dental technician who immigrated to the United States in 1932, and the Royal Navy technicians are both credited for developing the PMMA prosthetic eye. PMMA was more durable than glass, and its working properties enabled prosthetic eyes to be custom made for the first time from an impression of the patient's socket. In the latter half of the twenty-first century, PMMA eyes by and large supplanted the 350-year-old glass eyes. A professional change was ushered in by these changing techniques: until the introduction of PMMA, all glass prosthetic eyes and shells were made and fitted by members of the optometry profession. Dental technicians, who were more familiar with the new PMMA technology, then took over the manufacture of prosthetic eyes, at least in the United Kingdom and established a new discipline of maxillofacial prosthetics.

Since World War II, there are two main schools of training for ocularists. The US school is centered on the American Society of Ocularists which was established in 1958. The English school is rooted in dental technology. Both schools now produce very skilled ocularists. Design and manufacture of ocular prostheses continues to be an intricate art form even though technology now allows many steps to be mechanized.

Psychological Aspects of Loss of an Eye

Most major institutions now have clinical psychologists who are immensely helpful to patients who may be losing an eye. There are several useful publications, like "My Fake Eye" for children, which help prepare children and adults during this period. More recently, physicians have begun to appreciate the importance of organizing meetings with the ocularist prior to surgery to remove an eye. Patients need careful guidance by surgeon and ocularist alike. Furthermore, when they have concerns about the

appearance or fit of a prosthetic eye, careful attention needs to be paid, as we have found that most patients will bring this up because they are getting comments from strangers and become even more self-conscious. Whenever surgical management can improve the appearance and fit of a prosthesis, we always discuss it in detail and are always willing to consider it: much more so than we would with minor or moderate changes in a binocular patient [10, 11].

Surgical Aspects of Importance to the Ocularist

The choice of the implant, the implant size, its placement, gentle tissue handling, attention to creation of fornices with adequate conjunctival lining, proper upper and lower eyelid positioning, and correction of any laxity are all important parts of the surgical planning and execution. Two-thirds of the lost volume of an eyeball should ideally be replaced by an implant and no more than one-third of the volume by the prosthesis [12]. To that end, accurate sizing of orbital implants is of paramount importance. In most adult sockets, a 20 or 22 mm implant is likely adequate. In children, at least a 20 mm implant is placed [13]. The implant should be centered. After an enucleation, careful suturing of the extraocular muscles, around the implant, is important. The more recent technique of inserting uncovered porous implants creates adhesions to the implant along the track of the muscles and also adhesions of the orbital fat: this makes subsequent removal of the implant, should the need arise, very traumatic. In cases undergoing evisceration, the aim should be to remove the contents of the globe with posterior sclerotomies to allow the placement of the appropriately sized implant with proper anterior overlapping closure of the sclera and tenons and conjunctival closure without tension. When implants are covered with sclera, there is no advantage to using porous implants over nonporous implants [14]. When smooth implants have the extraocular muscles imbricated in front of the implant, it increases the risk of supero-temporal dislocation of the implant over time [15]. To help decrease the risk of displacement and improve motility, implants can be covered with sclera with the extraocular muscles sutured to the sclera. In patients who have sustained trauma, the lacrimal system should be evaluated for obstruction.

Referral to the Ocularist

When referring patients to the ocularist:

- A pre-surgical visit to the ocularist should be arranged if possible.
- A preoperative photograph of the face and the two eyes is useful for the ocularist to know what the appearance of the eye was prior to surgery. Photographs from years past may be useful when there is an evolving and changing disease process or in the presence of anophthalmos or microphthalmos.
- The aim should be to fit the patient with a prosthetic eye within 6–8 weeks of surgery. The ocularist should be familiar with a systematic approach to examining the socket before a prosthesis is made and during subsequent visits.
- A detailed history of the patient, including prior irradiation, other surgeries, and exact diagnosis, should be conveyed to the ocularist.
- A detailed operative report should be submitted to the ocularist, including details of the implant type and size, what it was covered with, muscle attachments (to insertion points, imbrication, etc.), details of any fornix reconstruction or eyelid reconstruction, and presence of any tarsorrhaphy.
- An outline of future care of the patient: will the patient need irradiation or other surgical intervention following the fitting of the prosthesis?

Materials Used to Make Prosthetic Eyes

For more than 300 years, glass was the preferred prosthetic material used. Owing to difficulty in

molding and because of its fragility, glass is used rarely today. However, there are still parts of Europe where glass eyes are made.

Most modern ocular prostheses are made using polymethyl methacrylate (PMMA). The material is inert in nature and is easy to mold, making it the material of choice. Silicone was used for making ocular prostheses but is now rarely used because of a lack of proper expertise and also because of the hydrophobic nature of the material. However, silicone is used for making facial prostheses as it is nonreactive, molds easily, and can be used to match skin texture and color.

Fabrication of an Ocular Prosthesis (Fig. 23.3)

The following steps are involved in the fabrication of an ocular prosthesis [16, 17].

1. Examination by the ocularist. Even though an attempt is made to make a prosthesis 6–8 weeks after surgery, it is first important to examine the socket to assess the healing and presence of sutures, fornices, lid position, chemosis, pain, cysts, and scarring and also to assess the surrounding structures.
2. Taking an impression: Patients are often anxious about the first step of taking an impression. The patient should be reassured that taking an impression is not uncomfortable. The normal contralateral eye is kept open with fixation on a predetermined point. The impression is taken with the patient sitting in a chair: topical anesthetic is instilled, and the molding material known as alginate (usually hydrophilic colloid) is prepared with a spatula in a rubber bowl. The mixture is placed in a syringe. The molding shell (which is also called an impression tray) is placed on the socket with the patient looking down so that the shell is first inserted under the upper eyelid, followed by the lower eyelid. With the eyes then in primary gaze, the syringe is attached to the shell, and the molding mate-

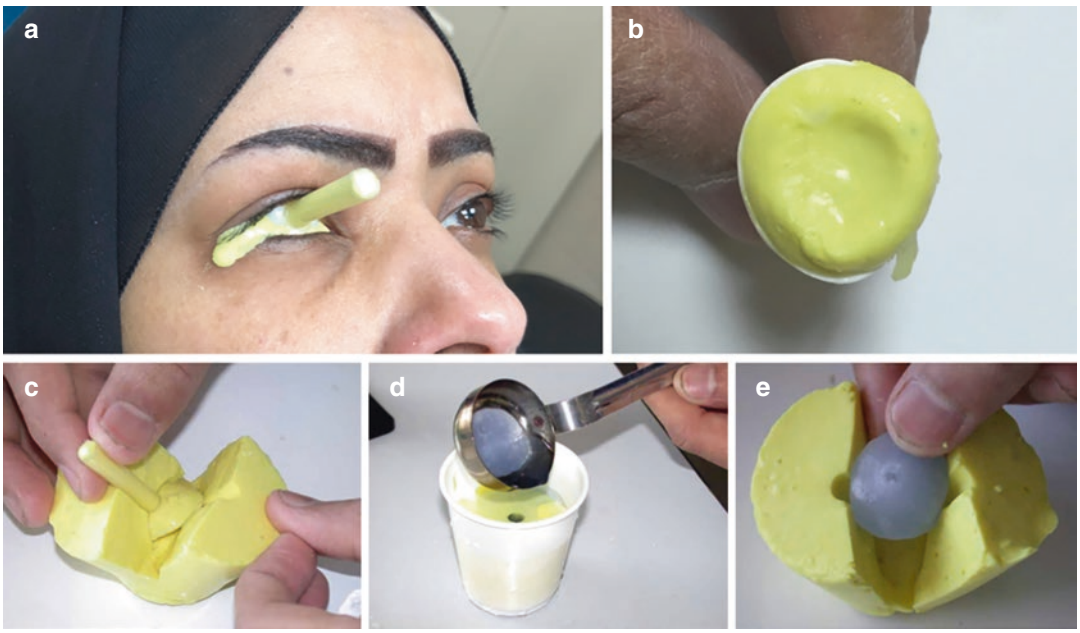

Fig. 23.3 Taking of the impression with the impression tray in situ with alginate (**a**). Removal of the impression shows the three-dimensional imprint of the socket (**b**). Shows duplication of the shape in an alginate mold (**c**). Pouring of wax into the alginate mold to make the wax prototype (**d**). Wax prototype achieved after cooling the wax at room temperature (**e**)

rial is injected gently. The molding mixture fills the socket with the impression material and sets (gels) in about 2 minutes with the consistency of a hard-boiled egg. With the upper and lower eyelids gently retracted, the shell handle is rocked side to side and removed from the socket. The impression is then immersed in water.

3. Molding the impression into the wax model: half a cup of distilled water is taken and mixed thoroughly with one spoonful of alginate. This paste is then poured in a plastic cup and into the rear surface of the impression. The alginate hardens in 2–3 minutes. The alginate mold is cut along the lines drawn on the impression tray. The carving wax is heated in a steel bowl till it becomes liquid. The molten wax is poured into the alginate mold and allowed to harden. An exact replica of the socket impression is now created.
4. Centration of the iris: centration of the iris and marking the corneal plane are essential to achieve symmetry of the two eyes. Various methods are used to achieve this symmetry.
   (a) *Using the interpupillary distance (IPD)*: Once the wax model has been made, wax solvent is used to smooth the surface. This wax model is inserted in the patient's socket. After making it symmetrical with respect to its position and plane, the interpupillary distance is marked with a nontoxic marker.
   (b) *Using Hirschberg's test*: In absence of gross asymmetry of the orbit, the base for the ocular prosthesis can be made in white acrylic and inserted into the socket. The light reflex is kept at the center of the model.
   (c) *Using iris corneal buttons*: This is the most difficult of the various methods described. However this gives the best cosmetic result. The iris button is inserted in the wax model using the carving wax and hot metal spatula, and symmetry is achieved by trial and error.
   (d) *Using the Peg*: The 18 mm stem frees up a hand to mark the center of the iris.
   (e) *Freehand drawing*: On the white acrylic base, based on the ocularist's judgment, a circle is marked in the center corresponding to the fellow eye.
5. Fabrication of the iris and pupil to match the fellow eye: Once the wax model is finished, a two-piece mold in the dental stone is prepared (Fig. 23.4). There are several ways to create an iris corneal component to integrate into an eye prosthesis (Fig. 23.5).
   (a) *Iris corneal disc system*: This is a two-piece system where the iris disc (sized 10 mm through 13.5 mm) and cornea button are selected with proper three-dimensional pupil (sizes 2–7 mm). The iris disc is hand painted (1200–1500 brush strokes) using dry earth pigment or oil pigments, copying colors of the opposite

Fig. 23.4 Fabrication of two-piece mold in the dental stone

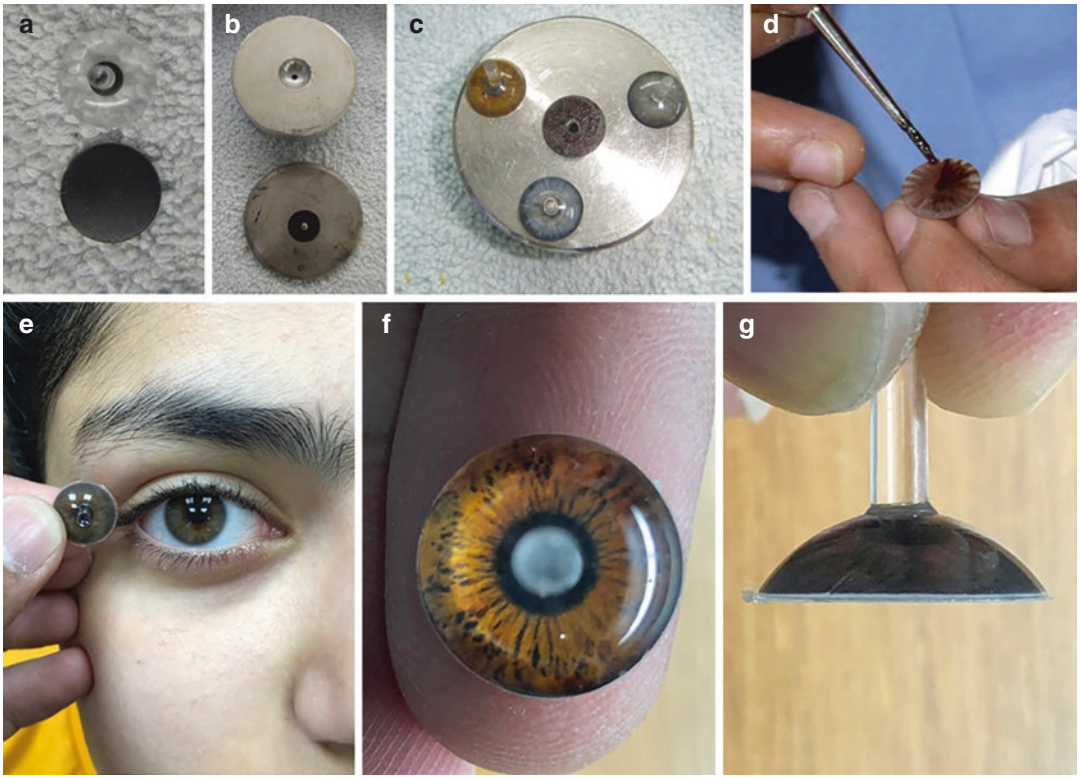

Fig. 23.5 Methods of centering the iris. Using the metal iris button (**a**–**c**), plastic stem (**d**) corneal reflex method over the shape prepared in scleral white PMMA (**e**). The iris button with pupil and the black iris disc system (**f**). The reverse-painting method: painting over the back of the clear iris button **g**)

eye to reproduce anatomy of the stroma and the collarette. The iris is later glued with pre-defined pupil size and corneal button.

(b) *Molding into a metal die*: One can paint over tin foil and transfer over the corneal mold.

(c) *Reverse painting*: Those with an artistic eye and knowledge of the anatomy of the iris and also an understanding of colors can reverse-paint. (Fig. 23.5).

(d) *Digital iris buttons*: Using a high-resolution camera, a high-definition image of the iris is printed and glued or molded into the iris die.

(e) *Colored buttons*: These are pre-defined base colors, one can use which can be modified.

6. Preparing the white base: The white base of the PMMA is poured into the molds and cured at 110°C and at 4 bar pressure for 25 minutes. Once cured, it is removed from the mold; the edges are trimmed and polished and inserted into the patient's socket (Fig. 23.6). While doing so we reconfirm the size, plane, and angle of the iris in the white base. The corneal button is exposed, and the process of tinting is begun. Cotton rayon threads are used to give the appearance of blood vessels (Fig. 23.7). Dry, fine Earth-colored pigments are used to achieve a close match for the sclera to the opposite eye (Fig. 23.8). Once it is ensured that the exact color matching has been achieved, the base of the prosthesis is kept in the oven at 85°C for 30 minutes. This cures the colors to saturation levels and prevents any

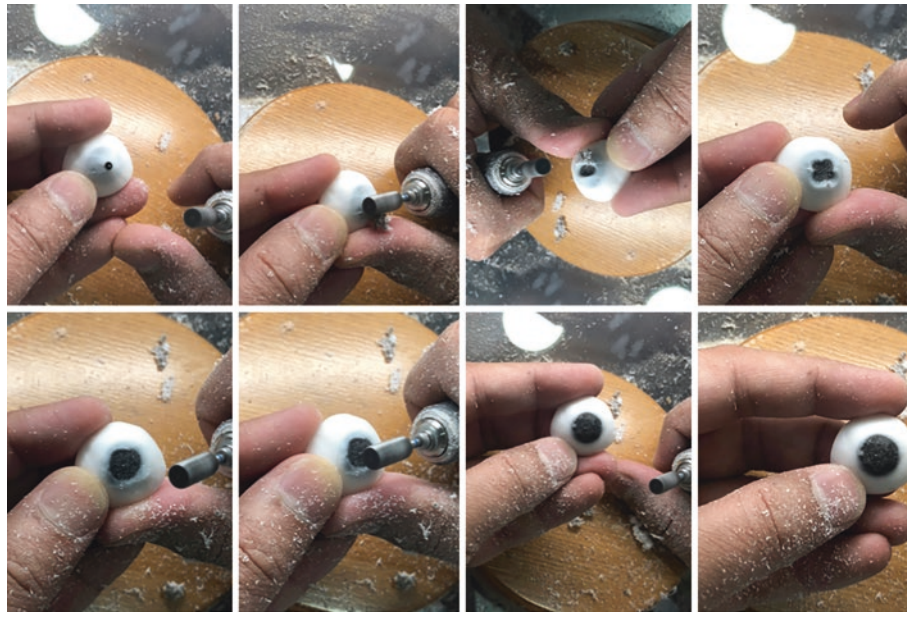

Fig. 23.6 Shows trimming of the "flesh" from the scleral shape. The stem is trimmed from the scleral shape. The plastic over the corneal button is removed. An "X"-shaped cut on the surface is made. The remainder of the plastic is then removed uniformly over the rest of the surface

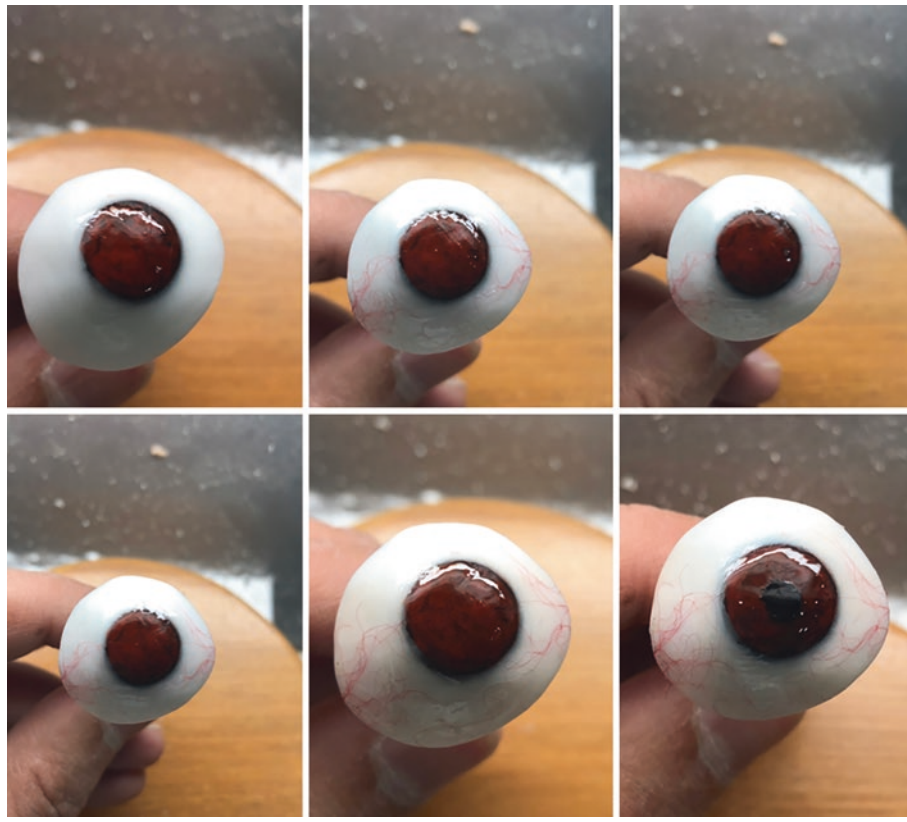

Fig. 23.7 Cotton rayon threads are used to mimic blood vessels

Fig. 23.8 Further tinting of the sclera with color pigments to achieve a balanced color to match the fellow eye, feathering of the limbus to make it look more natural, and adjustment of the pupil size give a realistic product

future fading. Once the artwork is completed, the shell is put back into mold, and a layer of clear acrylic is polymerized on the front surface, thereby encapsulating the pigmentation and adding proper anterior curvature. This completes the fabrication process (Fig. 23.9). After trimming and polishing, the final prosthesis may need minor adjustments by removing or adding PMMA in different places, thereby improving lid opening and closure, and correct eyelid malpositions as needed.

7. Final evaluation of the following is performed to assess for comfort, stability, vertical and horizontal positions, motility, iris and scleral colors, iris position, iris size, pupil size, and anterior and posterior curvature (Fig. 23.10).

Instructions on socket hygiene and prosthetic care are given along with the technique of removal and insertion of the final prosthetic eye.

Fig. 23.9 Polishing of the surfaces and edges together with careful inspection of the front and back surfaces under magnification to remove residual irregularities leaves a final shiny, smooth product

Fig. 23.10 Appearance before (left panel) and after fitting with a custom ocular prosthesis (right panel)

Fig. 23.10 (continued)

The Ideal Prosthesis

There are two main questions that patients raise about their prostheses: "How will it look?" And "will my prosthesis move?" A less common question asked is, "will my pupil dilate and constrict?" The appearance is where the fit and the artistry of the ocularist come in. The anteroposterior thickness should be no more than 7 mm. The prosthesis should be light with minimal pressure being exerted on the orbital tissues. It should have reasonable movement in all fields of gaze and should correct the volume deficit so as to match the appearance of the fellow eye. In the presence of an ideal socket (deep fornices, volume loss less than 4.2 ml, centered orbital implant, quiet, smooth conjunctiva, good lid positions, no sulcus deformity or socket contracture, and minimal lagophthalmos), such an ideal prosthesis will fit and look its best. Of course, individual socket differences may require the use of the modified impression technique as described by Allen [15].

Prosthetic Mobility

Prosthetic mobility is a very understandable concern of patients. It is important to point out to patients that the prosthesis will not move as well as their native eye. Most adults will adapt to move the head rather than the eyes when looking in particular directions, whereas children may not do so. Therefore, most adults will move their eyes within a range of about 30° to the right or left. A well-sized and properly placed (central) implant with attachment of the extraocular muscles will give very satisfactory transmission of movement to the prosthesis. An inferiorly displaced or supero-temporally displaced implant will give suboptimal motility. Pegs are only rarely used now due to problems with exposure and granuloma formation.

Advances and Modifications of Prostheses

(a) In the presence of ptosis, a ptosis crutch can be built upon a prosthesis as has been in use for several decades now [18]. When built upon solid prostheses, this adds weight which is borne by the lower eyelid which invariably leads to lower eyelid laxity over time. This led to the creation of hollow prosthetic devices [16], where two separate pieces are made which are then joined, thereby allowing reduction in the overall weight of the prosthesis by as much as 26%. This type of hollow prostheses cannot be designed when the prosthesis is very thin. Modern advances include the development of the volume-displacement technique which allows the weight to be shifted from the lower part to the upper portion of the prosthesis, thereby relieving pressure on the lower eyelid [19].

(b) Studies have shown that the anophthalmic socket often suffers from deficient tear pro-

duction. Kelly from Philadelphia designed the self-lubricating ocular prosthesis [20]. This type of prosthesis has a chamber that holds the lubricant, an exit hole and a releasable cap covering the chamber. During a normal blink, lubricant is drawn out of the chamber, thereby lubricating the prosthesis. The chamber can be cleaned with a contact lens solution cleaner, and the chamber may be refilled with lubricant. This type of prosthesis is useful in the very dry irradiated anophthalmic sockets and other dry anophthalmic sockets which can make it impossible to tolerate a prosthesis.

(c) We developed a digital technique which allowed the quick fabrication of a prosthesis which could be used immediately after surgery so the patient does not have to wear a clear conformer [21]. This technique used photography of the opposite iris with incorporation of a high-resolution print by lamination onto a shell. Modern advances in digital technology now allow the creation of stable and reproducible colors. In the United Kingdom, a company now makes 3D-printed eye prostheses with starch and laminate with acrylic resins, but these are not used to make custom eye prostheses.

(d) At Moorfields Eye Hospital, with Nigel Sapp and Richard Collin, we also developed a bank of colored conformers after studying the range of iris colors in our population in London. These were designed with a drain hole in the middle which served as a pupil. A prosthesis can be selected from a bank of different colored prosthesis to be used immediately after surgery. This bank of prosthetic shells, with some modifications, is still used at Moorfields Eye Hospital [22, 23]. Our system has been replicated in other parts of the world with varying degrees of success, although different types of iris-printed and iris-painted conformers are now commercially available.

(e) In the presence of loss of the upper and/or lower eyelids which cannot be reconstructed, an acrylic eyelid with eyelashes can be made and attached to the prosthesis giving very acceptable cosmetic results (http://www.jahrling.com/Result/Case5-3.htm).

Care for Ocular Prostheses, Eyelids, and Socket

(a) Eyelids will often build up secretions on the lashes and along the lid margins overnight. Therefore in the mornings, the eyelids can be cleaned with baby shampoo (which has a neutral pH and will not sting). A warm facecloth will soften the secretions by wiping from the outside in toward the nose. If one wipes outward, the prosthesis can rotate or fall out of the socket. Most prosthesis wearers will also need to wipe secretions from the prosthesis or lids three to five times a day.

(b) Cleaning the prosthesis: Never clean the prosthesis with a cloth, abrasive soap, or toothpaste. A mild soap or baby shampoo is best: clean by gently washing between soapy fingers. All soap must be rinsed from the prosthesis before reinsertion.

(c) As the prosthesis is made of an acrylic plastic, it should never be soaked in alcohol, gasoline, or bleach. A prosthesis should never be sterilized in an autoclave. In the office, a prosthesis can be disinfected in a cold sterilization medium such as Cidex (Johnson & Johnson).

(d) Lubricants: Normal artificial tears usually do not work well with prosthetic eyes. There are a number of support sites (e.g., http://www.losteye.com) where patients exchange their experiences. Vitamin E oil, Clerz 2, alo vera-based oils, silicone oils such as Ocusil & Sil Oph Eye Drops, and others have been found to be useful for lubrication of the prosthesis.

Long-Term Care

Most modern prostheses are durable, unlike glass prostheses. Most ocularists will polish the prosthesis every 6 months or if they become pitted or scratched. As the socket changes, it is sometimes necessary to modify the size of the prosthesis.

Most patients will be seen every 6 months by the ocularist and once a year by the surgeon. This allows for assessment of the socket and optimization of the prosthesis. Over time, most sockets develop changes of the post enucleation socket syndrome (deeper upper sulcus, ptosis or retraction of the upper lid, lower lid laxity, shallowing of the inferior fornix). Over time, granulomas, cysts, erosions, or changes in lid position are also addressed.

Future Research and Advances

The art of making prosthetic eyes continues to evolve [24–26]. A number of researchers are working on prostheses with the ability to change pupil size; however, a perfect model is yet to be crafted.

Motility also continues to be a challenge. Attempts have been made to attach the extraocular muscles to the fornices to improve the movement of the prosthesis with promising early results.

3D printing with refinements holds promise. Work is ongoing on how to use 3D printing to acquire shapes and directly print with biocompatible resins [27].

References

1. Patel BCK, Singh A, Dua H. The seated scribe 2600–2350 BC. The old Kingdom, 4th Dynasty. From Saqquara, north of the valley of the sphinzes, Serapeum, Egypt. Br J Ophthalmol. 2008;92(6):739.
2. Handley N. Artificial eyes and the artificialisation of the human face. In: Timmermann C, Anderson J, editors. Devices and designs: medical technologies in historical perspective. Basingstoke: Palgrave; 2006. p. 97–111.
3. Wilson RP. Artificial eyes in ancient Egypt. Surv Ophthalmol. 1972;16(5):322–31.
4. Enoch JM. History is the light on the path to (the) future: the Burnt City, and the first known artificial eye. Hindsight. 2007;38(3):58–67.
5. Conroy BF. A brief sortie into the history of cranio-oculofacial prosthetics. Facial Plast Surg. 1993;9(2):89–115.
6. Martin O, Clodius L. The history of the artificial eye. Ann Plast Surg. 1979;3(2):168–71.
7. Reisberg DJ, Habakuk SW. A history of facial and ocular prosthetics. Adv Ophthalmic Plast Reconstr Surg. 1990;8:11–24.
8. Roman F. The history of artificial eyes. Br J Ophthalmol. 1994;78(3):222.
9. Danz W. Ancient and contemporary history of artificial eyes. Adv Ophthalmic Plast Reconstr Surg. 1990;8:1–10.
10. Slonim MD, Martino MD. Eye was there: a patient's guide to coping with the loss of an eye (Kindle Locations 1080–1094). Bloomington: AuthorHouse; 2011. Kindle Edition.
11. Kohlhaas M, Schulz D. Functional and cosmetic relevance of primary orbital implants. Klin Monatsbl Augenheilkd. 2003;220(6):418–22.
12. Kaltreider SAMD. The ideal ocular prosthesis: analysis of prosthetic volume. Ophthalmic Plast Reconstr Surg. 2000;16(5):388–92.
13. Thaller VT. Enucleation volume measurement. Ophthalmic Plast Reconstr Surg. 1997;13(1):18–20.
14. Sadiq SA, Mengher LS, Lowry J, et al. Integrated orbital implants – a comparison of hydroxyapatite and porous polyethylene implants. Orbit. 2008;27(1):37–40.
15. Allen L. The argument against imbricating the rectus muscles over spherical orbital implants after enucleation. Ophthalmology. 1983;90:1116–20.
16. Allen L, Webster HE. Modified impression method of artificial eye fitting. Am J Ophthalmol. 1969;67(2):189–218.
17. Jahrling ER. The making of a hollow prosthetic eye. J ASO. 1986;17:31–3.
18. Cohen PR. A modification of the ptosis crutch. Opt J Rev Optom. 1946;83(7):26.
19. Raizada K, Raizada D. Volume displacement technique: lower lid laxity in anophthalmic sockets. J Ophthalmol Vis Sci. 2016;1(1):1010.
20. Kelly KV. The SLP, self-lubricating prosthesis, 25th ed. Am Soc Ocul. 1994;1994:26–30.
21. Patel BCK. The interim cosmetic shell: a new technique. Ruedemann Lecture, American Society of Ophthalmic Plastic and Reconstructive Surgeons and American Society of Ocularists, Las Vegas, November 17, 2006.
22. Patel BC, Sapp NA, Collin R. Standardized range of conformers and symblepharon rings. Ophthalmic Plast Reconstr Surg. 1998;14(2):144–5.
23. Patel BC, Sapp NA, Collin JR. Cosmetic conformers. Ophthalmic Surg Lasers. 1997;28(2):171–3.
24. Raizada K, Rani D. Ocular prosthesis. Cont Lens Anterior Eye. 2007;30(3):152–62.
25. Shome D, Honavar SG, Raizada K, et al. Implant and prosthesis movement after enucleation: a randomized controlled trial. Ophthalmology. 2010;117(8):1638–44.
26. Raizada K, Shome D, Honavar SG. New measurement device and technique for assessing implant and prosthetic motility. Ophthalmic Plast Reconstr Surg. 2007;23(1):59–60.
27. He Y, Xue GH, Fu JZ. Fabrication of low cost soft tissue prostheses with the desktop 3D printer. Sci Rep. 2014;4:6973.

Index

C. J. Hwang et al. (eds.), *Clinical Ophthalmic Oncology*,
https://doi.org/10.1007/978-3-030-13558-4